# PERIÓDICO TCHÊ QUÍMICA

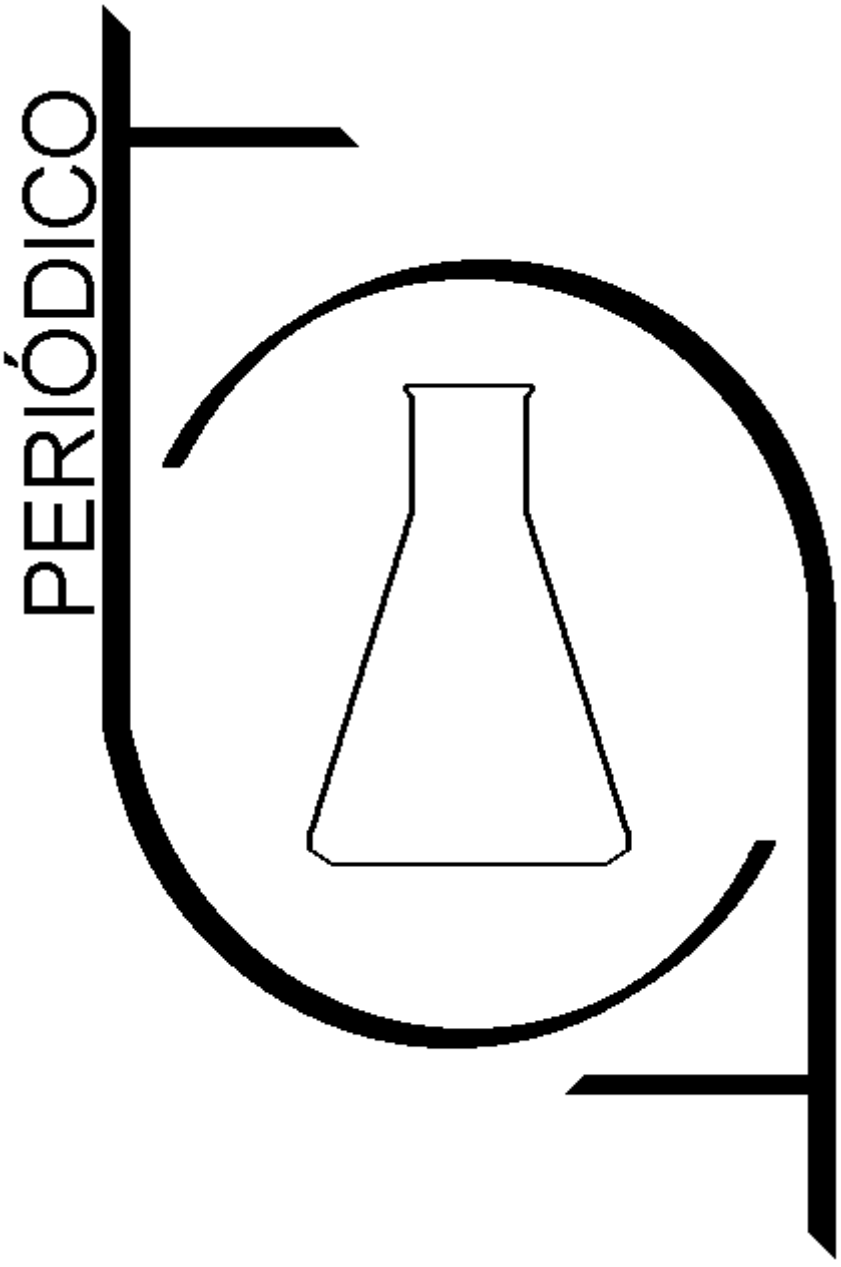


Volume 18 - Número 37 - 2021 ISSN 2179-0302

**Órgão de divulgação científica e informativa**

**www.periodico.tchequimica.com**

# PERIÓDICO TCHÊ QUÍMICA

ISSN - 1806-0374 (Impresso) - ISSN - 2179-0302 (Online)

**Volume 18** **Número 37 – 2021** **ISSN 2179 - 0302**

Órgão de divulgação científica e informativa.

**Dados Internacionais de Catalogação na Publicação (CIP)**

Periódico Tchê Química: órgão de divulgação científica e informativa [recurso eletrônico] / Grupo Tchê Química – Vol. 1, n. 1 (Jan. 2004)- . – Porto Alegre: Grupo Tchê Química, 2005 - Semestral.
Sistema requerido: Adobe Acrobat Reader.
Modo de acesso: World Wide Web:
<http://www.tchequimica.com>

Descrição baseada em: Vol. 14, n. 28 (ago. 2017).
ISSN 1806-0374
ISSN 2179-0302
1. Química. I. Grupo Tchê Química.

CDD 540

**Bibliotecário Responsável**
Ednei de Freitas Silveira
CRB 10/1262

## Welcome to the TCHÊ QUÍMICA JOURNAL

*International multidisciplinary scientific journal*

*The Tchê Química Journal publishes original research papers, review articles, short communications (scientific publications), book reviews, forum articles, technical reports, articles on chemical education, interviews, announcements or letters. Articles suitable for publication in the Tchê Química Journal are those that cover the traditional fields of* ***Chemistry, Physics, Mathematics, Biology, Pharmacy, Medicine, Engineering and Agriculture****. We are especially interested in those submissions that are highly relevant to theoretical and* ***applied contributions in the area of chemistry and related disciplines.***

# PERIÓDICO TCHÊ QUÍMICA

Volume 18 Número 37 – 2021 ISSN 2179 - 0302

**Órgão de divulgação científica e informativa.**

**Periódico Tchê Química**

ISSN - 1806-0374 (Print)
ISSN - 2179-0302 (Online)

LCCN: 2010240735

Divulgação *on-line* em
http://www.periodico.tchequimica.com
http://www.journal.tchequimica.com
http://www.tchequimica.com

Esta revista é indexada e resumida em CAS, EBSCO, Index Copernicus, EJL, Latindex, Web of Science (ESCI), OAJI.net, CAB Abstracts, ROAD, EuroPub, e Sumários..


**Missão**

O Periódico Tchê Química (PTQ) publica artigos de pesquisa originais, artigos de revisão, notas curtas (publicações científicas), revisões de livros, artigos de fórum, editoriais e entrevistas. Pesquisadores de todos os países são convidados a publicar nas páginas do PTQ.

A responsabilidade sobre os artigos é de exclusividade dos autores.


**Correspondências**
Rua Anita Garibaldi, 359/603.
Bairro Mon't Serrat. CEP: 90450-001
Porto Alegre – RS. Brasil.
Skype: tchequimica
www.periodico.tchequimica.com
tchequimica@tchequimica.com

# Índice

PERIÓDICO TCHÊ QUÍMICA
ERRATUM

# O PAPEL DA VITAMINA D COMO UM NOVO MARCADOR NA INFERTILIDADE DAS MULHERES

# THE ROLE OF VITAMIN D AS A NEW MARKER ON THE WOMEN INFERTILITY

# دور فيتامين D كعلامة دالة جديدة لعقم النساء

MOHAMMED, Najla Salim[1]; AL-JAWADI, Zena Abdul Monim[2]*

[1,2] University of Mosul, College of Science, Department of Chemistry, Mosul, Iraq.

** Corresponding author*
*e-mail: zena_aljawadi@uomosul.edu.iq*

Received 25 Aug. 2020; received in revised form 10 October 2020; accepted 30 October 2020

- Paper originally published in November 2020 (vol.17 (n°36) - available for downaload at www.periodico.tchequimica.com)

Original version

Page: 1101

Item: ***2.1.3 Blood Collection***

Two groups were tested for blood over 12-hour fasting (values for 5ml), early follicular cycles (cycle days two or three) for estrogen (E2), progesterone, follicle-stimulating hormones (FSH) and lutein's hormone (LH) and vitamin D. Luteal prolactin (cycle day 21). Into the test tube (gel and clot activator tube for serum separation) by drawing (5ml), and centrifuged for serum separation within an hour of blood collection, and the serum was stored in a deep freezer at a temperature of 70°C for subsequent analysis. Samples were analyzed in batches of 100 to be omitted between analytical variations. Samples were permitted to reach room temperature before the study.

- The temperature to be considered (line 11 in the original file published) is **-20°C** instead of **70°C**. The corrected paragraph is shown below.

**Corrected version**

Page: 1101

Item: ***2.1.3 Blood Collection***

Two groups were tested for blood over 12-hour fasting (values for 5ml), early follicular cycles (cycle days two or three) for estrogen (E2), progesterone, follicle-stimulating hormones (FSH) and lutein's hormone (LH) and vitamin D. Luteal prolactin (cycle day 21). Into the test tube (gel and clot activator tube for serum separation) by drawing (5ml), and centrifuged for serum separation within an hour of blood collection, and the serum was stored in a deep freezer at a temperature of **-20°C** for subsequent analysis. Samples were analyzed in batches of 100 to be omitted between analytical variations. Samples were permitted to reach room temperature before the study.

PERIÓDICO TCHÊ QUÍMICA
ARTIGO ORIGINAL

# ESTUDANDO A SUBLIMAÇÃO DE DIÓXIDO DE CARBONO

# STUDYING THE SUBLIMATION OF CARBON DIOXIDE

# ИССЛЕДОВАНИЕ ПРОЦЕССА СУБЛИМАЦИИ ДИОКСИДА УГЛЕРОДА

NEVEROV, Evgeniy N.[1]*; KOROTKIY, Igor A.[1]; KOROTKAYA, Elena V.[1]; RASSHCHEPKIN, Aleksandr N.[1]

[1]Kemerovo State University, Russian Federation.

** Corresponding author*
*e-mail: neverov42@mail.ru*

Received 23 November 2020; received in revised form 27 December 2020; accepted 03 February 2021

## RESUMO

**Introdução.** A utilização de gelo seco em unidades de resfriamento e armazenamento requer o ajuste da intensidade de sublimação devido aos requisitos de uso prudente do $CO_2$ para manter as condições térmicas pré-estabelecidas. **Objetivo.** Ao projetar um ciclo de dióxido de carbono, é essencial considerar a influência dos gradientes térmicos na adsorção e dessorção do dióxido de carbono. **Métodos**. Vários testes foram realizados para estudar a produção e sublimação do dióxido de carbono; os teste tiveram como objetivo definir a relação da temperatura do período de sublimação do gelo seco, a densidade do $CO_2$ prensado, a umidade do ambiente e a concentração. **Resultados e Discussão.** De acordo com os dados dos testes, houve uma relação linear entre a intensidade de sublimação e a temperatura do ar ambiente nas condições especificadas. O efeito da condensação de umidade na taxa de sublimação pareceu mais fraco do que o esperado, pois a quantidade de umidade na superfície dos espécimes era insignificante. A troca de calor foi intensificada pela queda da geada e a expansão da superfície relacionada. No entanto, muita umidade congelou sem atingir a superfície do gelo seco, e a camada formada de gelo formou uma superfície de isolamento térmico, e a sublimação sob essa camada foi menos intensa. A influência direta da sublimação veio da pressão na qual um espécime específico foi formado; no entanto, a pressão de 75 kN foi ótima. **Conclusão**. Apesar das maiores perdas de peso durante o armazenamento, a diferença na energia gasta é mais crítica do que 90 kN. O fator não menos importante foi a temperatura de armazenamento do dióxido de carbono. O tempo máximo de sublimação de um cilindro de 55 g formado a 75 kN e armazenado a -80 °C foi de 135 horas, muito maior do que com parâmetros semelhantes, mas a -60 °C. Dito isso, a quantidade de energia gasta para operar uma câmara fria foi praticamente idêntica.

**Palavras-chave**: *dióxido de carbono, sublimação de $CO_2$, $CO_2$, taxa de sublimação, unidades de resfriamento, aplicação de $CO_2$.*

## ABSTRACT

**Background:** The utilization of dry ice in cooling and storage units requires adjusting the intensity of sublimation due to the requirements of prudently using $CO_2$ to maintain preset thermal conditions. **Aim:** When designing a carbon dioxide cycle, it is essential to consider the influence of thermal gradients on the adsorption and desorption of carbon dioxide. **Methods:** tests were conducted to study the production and sublimation of carbon dioxide. The testes were aimed to define the temperature relation of the dry ice sublimation period, the density of pressed $CO_2$, and the humidity of the environment and concentration. **Results and Discussion**: According to the obtained test data, there was a linear relationship between the sublimation intensity and the ambient air temperature in the specified conditions. The effect of moisture condensation on the sublimation rate appeared weaker than expected, for the amount of moisture on the surface of the specimens was insignificant. The heat exchange was intensified by the fall of hoarfrost and the related surface expansion. However, much moisture froze out without reaching the dry ice surface, and the formed layer of ice formed a heat insulation surface, and the sublimation under that layer was less intensive. The direct influence of sublimation came from the pressure at which a specific specimen was formed; however, 75 kN pressure was optimal. **Conclusion:** Despite higher weight losses during the storage, the difference in spent energy is more critical than 90 kN. The factor no less important was the carbon dioxide storage temperature. The maximal sublimation time of a 55 g cylinder formed at 75 kN and stored at – 80°C was 135 hours, much higher than at similar parameters but at -60°C. That said, the amount of energy spent on operating a low-temperature chamber was almost identical.

**Keywords**: *carbon dioxide, $CO_2$ sublimation, $CO_2$, sublimation rate, cooling units, application $CO_2$.*

## АННОТАЦИЯ

**Введение:** При применении сухого льда в установках охлаждения и хранения, возникает необходимость регулирования интенсивности процесса сублимации вызванная требованиями рационального использования $CO_2$ с целью поддержания заданных температурных условий. **Цель:** При расчете углеродного цикла важно учесть влияние градиентов температуры на механизмы абсорбции и десорбции диоксида углерода. **Методы:** Для определения зависимости продолжительности сублимации сухого льда от температуры, плотности прессованного $CO_2$, а также влажности окружающей среды и концентрации нами был проведен ряд экспериментов по исследованию процессов получения и сублимации диоксида углерода. **Результаты и Обсуждения:** Согласно полученным экспериментальным данным, зависимость интенсивности процесса сублимации от температуры окружающего воздуха, при указанных выше условиях имеет линейный характер. Влияние конденсации влаги на скорость сублимации оказалось меньшим, чем ожидалось, т.к. объем ее на поверхности образцов незначителен. Выпадение инея и увеличение в связи с этим поверхности привело к интенсификации теплообмена. Однако, значительная часть влаги вымерзала, не доходя до поверхности сухого льда, а образующийся слой рыхлого инея являлся как бы теплоизоляцией и сублимация под ним протекала менее интенсивно. Прямое влияние на процесс сублимации оказывало давление, при котором был сформирован конкретный образец, однако серия экспериментов показала, что давление в 75 кН является оптимальным. **Заключение:** Несмотря на несколько большие потери массы в процессе хранения в сравнении с давлением в 90 кН разность в количестве затрачиваемой энергии более важна. Не менее важным фактором является и температура хранения диоксида углерода, максимальное время сублимации цилиндра массой 55 гр, сформированного при давлении 75 кН и хранившегося при минус 80°С составило 135 часов. Что значительно выше чем при схожих параметрах, но при минус 60°С. При этом затраты энергии на работу низкотемпературной камеры практически идентичны.

**Keywords**: *диоксид углерода, сублимация $CO_2$, скорость сублимации, холодильные установки, применение $CO_2$.*

## 1. INTRODUCTION

The development of technologies of applying carbon dioxide in various phase states has become an increasingly topical issue over recent years. The scope of using this gas is not confined to alimentary technologies; it is also applied in phytopharmaceuticals, cosmetics, resin, and bitumen fractionation, biofuel production, esterification, bitumen modification, production of new biomaterials, and extraction of transuranium and rare earth elements (Yoosook and Maneeintr, 2018). At present, scientists have already found out that it is possible to use carbon dioxide to intensify the extraction and desorption of valuable components from raw material and intensify homogenization, cold sterilizing, and detartration, and hypothermic preservation.

Because of its high efficiency, the utilization of carbon dioxide in various process cycles is a topical issue. It has been established that the reserves of $CO_2$ in the form of frozen crystalline hydrates amount to 1.5 trillion tons, i.e., are twice as high as the content of $CO_2$ in the atmosphere (Neverov, 2016; Neverov *et al.,* 2019; Aldamatov, and Grinyuk, 2018; Amokrane *et al*., 2018; ).

Carbon dioxide is not toxic but a negatively affecting substance due to the registered increase in its concentration in the Earth's atmosphere and its influence on climate change.

The accumulation of carbon dioxide in the atmosphere due to anthropogenic and natural influences will inevitably change the gas exchange between the world ocean waters and the near-surface layer of the atmosphere. Steps are being taken to control $CO_2$ emissions from power engineering, industrial, and transport facilities.

In 2019 the natural produced amounts of carbon dioxide were 432.5 thousand tons, equivalent to 4.6 billion rubles. The growth rate was 1% of the natural amount and 2% of the total worth. According to various data, the domestic consumed amount of carbon dioxide has remained stable in recent years and reached 420 to 430 thousand tons (Korotkaya and Kireev, 2016; Sparks *et al.,* 2008; Zhai *et al*., 2005; Belozerov *et al.,* 2011).

A group of specialists from the Kemerovo University has elaborated a technology of re-using carbon dioxide that is a by-product obtained at alcohol-processing and other alimentary industry enterprises (Neverov and Grinyuk, 2018; Grinyuk *et al*., 2018; Evans and James, 2008; Repice and Stumpf, 2007).

The utilization of dry ice in cooling and

storage units makes it necessary to control the intensity of sublimation due to the requirements of prudently using $CO_2$ to maintain preset thermal conditions. When designing a carbon cycle, it is essential to consider the influence of thermal gradients on the adsorption and desorption of carbon dioxide (Dyshlyuk *et al.,* 2018; Ruhe, 2007).

There is currently no reliable method of calculating the heat and mass exchange at the sublimation of dry ice. The need for this method stems from the requirements on the sustainable storage and utilization of dry ice as a coolant.

In machine-free chilling units with dry ice, the intensity of sublimation must be regulated for maintaining target temperature conditions in a well-minded manner. The process begins right after extracting the slab from the ice generator or under the dry ice press and continues through the ice transport and storage phases.

Sublimation appears due to difference in the partial pressures (concentrations) of carbon dioxide steam near the ice surface and the ambient medium. Rapid sublimation results in forming a boundary layer of saturated carbon dioxide steam above the solid phase surface; the partial pressure of this steam corresponds to the surface temperature of the ice in sublimation. Sublimation requires heat supply. Depending on the conditions, heat may be obtained from the ambient medium and the dry ice simultaneously, making the dry ice surface colder and produces a significant temperature gradient inside the ice.

If to imagine that the sublimation will spread from the half-limited batch surface into the unlimited air environment, the thermal balance for the sublimation can be preset proceeding from the consideration of the quasi-stationary process at the dry ice-air phase boundary.

The dry ice sublimation temperature depends on the conditions in which it is kept. If a dry ice cake is surrounded by carbon dioxide, the sublimation temperature at normal pressure will be 78.9°C. If the sublimation at this pressure spreads into the air, the sublimation temperature will drop. In this case, it depends on the tension of saturated carbon dioxide steam (concentration) in the boundary layer. The tension of $CO_2$ steam and the boundary layer thickness is defined by the heat and weight exchange conditions between dry ice and the air. The dependence of the dry ice sublimation temperature on the temperature of the ambient medium and the concentration of $CO_2$ in it can be defined analytically and graphically. (Neverov and Grinyuk, 2018; Grinyuk *et al*., 2018; Evans and James, 2008; Repice and Stumpf, 2007)

## 2. MATERIALS AND METHODS

### 2.1 Test environment

The dry ice temperature depended on the conditions of the process. It was equal to 78.9 °C only in a particular case, which corresponds to the ambient medium concentration at p = 1 AA. The temperature could be lower at this same pressure but at a lower concentration of $CO_2$. It did not seem possible to use the sublimation calculation expressions in practice, for the specialized literature provides no data about the dry ice sublimation coefficient.

Tests were conducted to define the temperature relation of the dry ice sublimation period, the density of pressed $CO_2$, and the humidity of the environment and the concentration. The tests were conducted at the atmospheric pressure and temperatures from -80 to -20°C.

### 2.2 Equipment description

During the tests, temperatures and humidity were maintained using a two-step automated cascade chilling unit. A 0.2 × 0.15 m thermally insulated box with the test specimens was placed in the chamber. Figure 1 illustrates the test bench layout.

(A)

(B)

(C)

***Figure 1.*** Test bench layout, (A) – thermally insulated box with $CO_2$; (B) – top view of the low-temperature chamber with the container installed; (C) – low-temperature chamber.

**2.3 Dry ice producing process**

The sublimation rate depends on the properties of the environment and the orientation of the limiting dry ice surfaces. The tests were conducted on dry ice obtained using the equipment, illustrated by Figure 2, to produce and supply carbon dioxide snow with a bulk density of 1.25 to 1.35 kg/dm² at seven to eight.

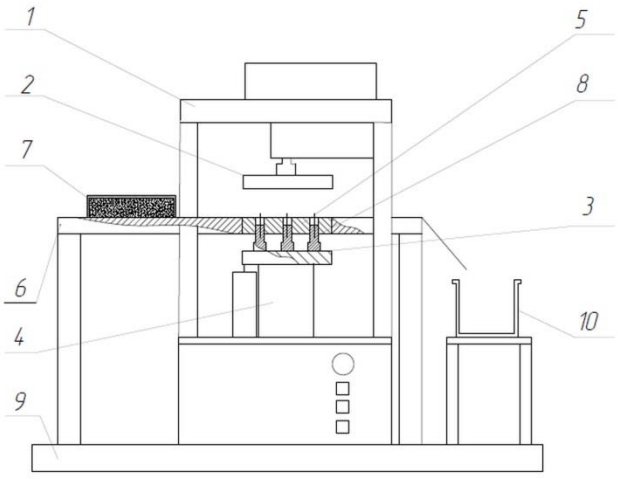


***Figure 2.*** Device for producing dry ice

1- press; 2- upper plate; 3- lower plate; 4 - loading device; 5 – matrix; 6 – table; 7 – box with carbon dioxide snow on it; 8 - punch stamps; 9 - baseplate.

The device operated as described: the container (7) with guide plates on its side surfaces was filled in advance with carbon dioxide and fixed in the sleds on Table 6. In the course of dosing, the box moved along matrix (5), which results in the openings being filled with the $CO_2$ snow. Then the container returned to the initial position, and the upper plate of the press (1) was lowered with the help of a handle until touching the matrix. Then the load was applied via lower plate (3) and punch stamps (8) to carry out the pressing in the matrix; thus, strong carbon dioxide cakes (11) of target size were formed that depend on the chosen matrix. The matrix and punch stamps can be replaced depending on the requirements of the final product. After the pellets were formed, the upper plate went up to the initial position, and the lower plate went up too. Thus the punch stamps pushed out the ready-made pellet to the matrix surface. The pellet was knocked to undertank (10) by the container with carbon dioxide that begins moving to the matrix for the openings to be filled with another portion of the $CO_2$ snow.

The bottom plate was returned to its original position to fill the device with carbon dioxide, and the cycle was repeated (Korotkaya and Kireev, 2016).

The cylindrical samples were obtained using special-purpose copper thin-walled cylindrical press dies installed in the device matrix and filled with the carbon dioxide snow produced in the device. A dry ice cake was formed using a press machine to generate 90, 75, 50, and 25 kN pressures. After it was taken out from the die, the cylinder was weighed and placed in the chamber for storage. That way, a dry ice sample of any shape could be obtained. The cylindrical samples were 30 mm in diameter, 45±3 mm in height, and weighed 50±3 g. The cylinder shape and size were accepted proceeding from the condition of approximating a self-similar process.

Since the cylinder shape was distorted during the sublimation (the cylinder became an ellipsoid by the end of the test), only those test readings were considered that corresponded to the geometrical similarity condition and steady-state mode. The cylinder geometric surface was conventionally taken for the sublimation surface; in reality, however, the sublimation took place not only from the surface but also in the dry ice zone of small depth, which was also considered in the

course of the study. The dry ice used in the tests had been produced with carbon dioxide snow production and supply at 7 to 8 atmospheres and had a bulk weight of 1.25—1.35 kg/dm$^2$. The production of $CO_2$ snow in these devices relied on the aftercooling of liquid carbon dioxide. In (Grinyuk *et al.,* 2018). the aftercooling of $CO_2$ was conducted through the washers with a throttle opening of 1 mm in diameter. The snow formation occurred in the cones with angles (α) from 3 to 16°, which allowed identifying the influence of the cone angle on the production of solid carbon dioxide. For the truncated cone layout, see Figure 1. For the geometric data on the cones, see Table 1.

***Table 1****. Geometric data on the cones*

| no. | D, mm | d, mm | l, mm | α,° | β,° |
|---|---|---|---|---|---|
| 1 | 42 | 50 | 80 | 3 | 87 |
| 2 | | 60 | | 6 | 84 |
| 3 | | 65 | | 8 | 82 |
| 4 | | 70 | | 10 | 80 |
| 5 | | 75 | | 12 | 78 |
| 6 | | 86 | | 16 | 74 |

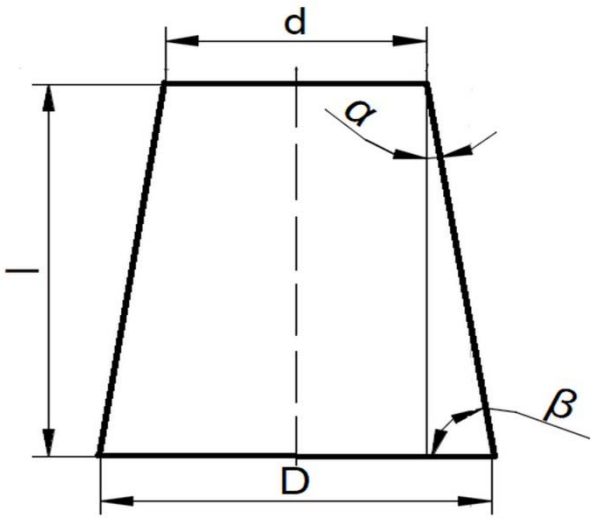


***Figure 3.*** Truncated cone

**2.4 Solid $CO_2$ producing process**

Figure 5 shows a diagram of the device for the production of solid $CO_2$. The device was equipped with plates on the external surface of the $CO_2$ feeding unit for reducing the losses of carbon dioxide snow being produced and increasing the filling of the die's internal space with it. The device also had a choke flange with a T-shaped opening intended to increase the amount of $CO_2$ snow at the throttling of liquid carbon dioxide. In these flanges, the conversion of carbon dioxide to a snow-like state was more intensive for the flow of liquid $C0_2$ changed its motion route, which led to an additional pressure drop: in this case, according to Bernoulli's equation, liquid $CO_2$ flows faster through the openings (Neverov and Korotkikh, 2019; Korotkov and Novikov, 2018; Frankel and Finley, 2008; Houska *et al.,* 2011; Koster, 2005; Maier and Wilson, 2006). Also, the opening configuration allowed splitting the flow in two, increasing the amount of snow output.

All of the device parts were made of stainless steel (see Figure 5). Nozzle (1) was connected to one of its sides to the pipeline feeding liquid carbon dioxide through the solenoid valve (13), controlled by a time relay (15). In contrast, on the other side, it had a guiding indentation for centering choke flange (2). This flange had a T-shaped opening. The nozzle was connected to $C0_2$ feeding tool (6) inside the body (7) through coupling nut (3) with a key outward profile. Inside the body (7), the external surface of $C0_2$ feeding unit (6) had plates (4) fixed using unit (5). These plates had grooves, where splines (10) are installed and fixed in (6) with the help of a pin. The slide bars on the external surface of the splines (10) were designed to move along the guides on the inner surface of the nut (5). Nut (5) moved along the guides using a flexible member (14) with the help of a stepper (12). The plates were returned and fitted in out-of-action mode with the help of springs (11). The motion of the plates along the horizontal axis was restricted using limiter (9) with contact switch (8).

**2.5 Carbon dioxide snow production process**

The operational principle of the carbon dioxide snow production device is described below. When $CO_2$ feeding unit (6) was put into the die (7), switch (8) contacts with the mold's surface, and a signal was transferred to stepper (12) that moves nut (5) by mean of flexible member (14). Nut (5) overcomed the action of spring (11) to put pressure on the edges of plates (4) that expanded from the opposite side; concurrently, the signal to open the solenoid valve (13) came from the time relay (15). Liquid carbon dioxide was supplied to choke flange (2), passes through the T-shaped opening, and was throttled and released into the mold's internal cavity through the feeding unit (6).

Having covered the time relay period, valve (13) closed to occlude the flow of liquid $C0_2$ to choke flange (2). Concurrently, the time relay switched off stepper (12) and spring (11) ensured the tight-fitting of plates (4) to the body of unit (6)

in the initial position.

### 2.6 Measurements

The weight of a dry ice cylinder was determined using a precision class II PCE BS 3000 touch-sensitive balance with a sensitivity of 0.1. The balance was calibrated before the procedure.

The relative humidity and temperature were measured using a DV2TC-5T-5P-AK measurement set designed for use in climatic thermal chambers. Together with an IVA-6B2-K temperature and humidity converter, it allows measuring and registering temperatures from -70 to +60℃ (with an inaccuracy of ± 0,2℃) and humidity of 0 to 99,9% (with an inaccuracy of ±0,5%).

The sample compression pressure was determined using the measurement set of a PM-MG4 test machine (the limits of the main relative error in force measurements are ±1%), designed for force generation and measurements in mechanical testing in construction, research and development work, and also in construction laboratories.

According to Paterson lab clocks, the sublimation period was determined with the annual limit of the main absolute error of measurement from +20 to − 20 seconds. (Wang *et al.*, 2020; Xu *et al.,* 2019).

The methods and experimental equipment make it possible to control all the necessary parameters with high accuracy.

## 3. RESULTS AND DISCUSSION

Carbon dioxide was throttled through washers with rectangular and T-shaped orifices of 0.5 to 2 mm in diameter, which allowed determining the influence of the orifice configuration on the carbon dioxide production in solid.

The first series of tests were conducted at the temperature of the bottle with liquid carbon dioxide of 19 °C. For the results of the dependence of the amount of $CO_2$ snow on the orifice diameter, see Figure 6.

As shown by analyzing the dependencies, the largest amount of snow was produced using the T-shaped orifices of 1.5 mm in diameter. This diameter is optimal for converting liquid $CO_2$ to solid. This is explained by the fact that the orifice of 1.5 mm in diameter creates an optimal difference in the pressure generated by the liquid carbon dioxide in the bottle and the atmospheric pressure. In this case, liquid consumption relation to the output of $CO_2$ (Figure 7) is 23.9 % (0.9/0.215 kg/kg).

If the washers with rectangular orifices are used, the maximal amount of snow is produced at the orifice diameter of 1.3 mm, though the snow output is much lower and equal to 17.1 % (0.85/0.145 kg/kg).

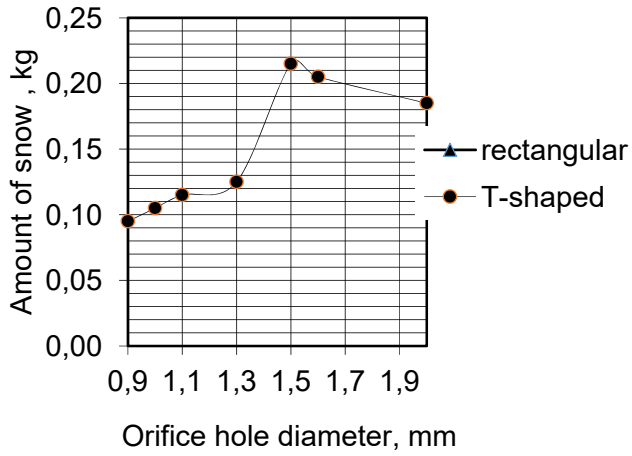


***Figure 6***. Snow output at liquid carbon dioxide temperature t = 19°C

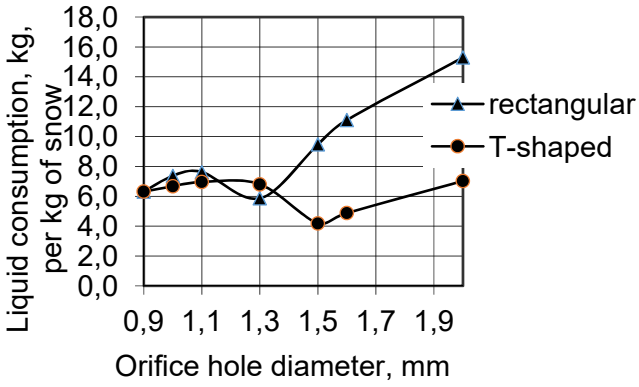


***Figure 7***. Reduced consumption of $CO_2$ at liquid carbon dioxide temperature t = 19 °C.

Thus, the conversion of carbon dioxide to snow through T-shaped orifices is more intensive because the flow of liquid $CO_2$ changes the motion path, which means an additional pressure drop is attended by an increase in the flow speed through the orifices (Bernoulli's equation). Also, the orifice configuration allows splitting the flow in two, increasing the output of snow.

The clear advantage of the choke flanges with T-shaped orifices allowed us to give up using their counterparts with rectangular orifices in subsequent tests.

The next series of tests consisted of studying the influence of lower temperatures in bottles with carbon dioxide on the output of $CO_2$: a bottle with carbon dioxide was put for the purpose in a chilling room and cured there at -2, -18, and -26°C for 8 to 12 hours.

For the results of the test at the bottle temperature of -2 °C, see Figure 8. The analysis of the dependences allows concluding that an increase in the orifice hole diameter is attended by the trend for a constant increase in the output of carbon dioxide snow.

However, the analysis of the dependence of 1 kg of liquid $CO_2$ consumed per kg of snow on the orifice hole diameter (Figure 9) allows concluding that the optimal orifice diameter at this temperature is 1.1 mm for the relation of the liquid consumption to the output of $CO_2$ is maximal and, in this case, equal to 40 % (0.60/0.24 kg/kg).

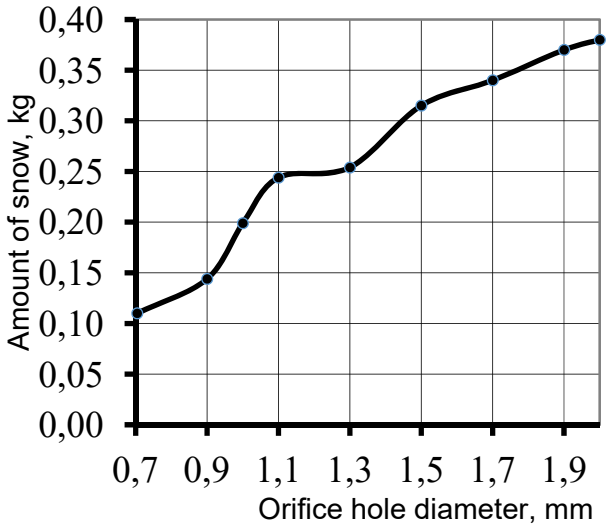


***Figure 8***. Snow output characteristic at liquid carbon dioxide temperature t = –2 °C.

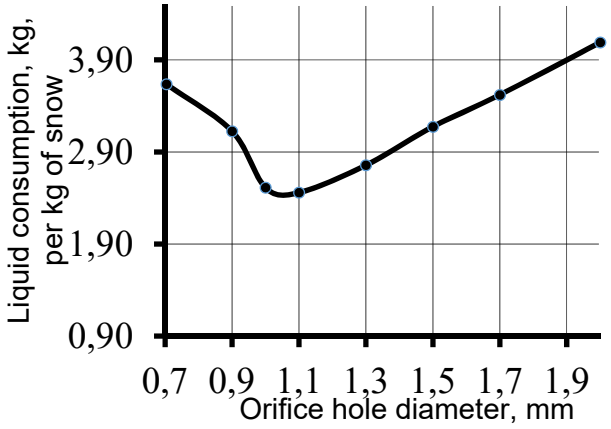


***Figure 9***. Reduced consumption of $CO_2$ at liquid carbon dioxide temperature t = –2 °C.

The trend for the reduction in the orifice hole diameter persisted with a further drop in the liquid carbon dioxide temperature. Thus it was established that at -18 and -26 °C it was expedient to use the choke flange with a diameter of 0.6 and 0.4 mm, respectively. In this case, the respective output of $CO_2$ is 54.8% (0.31/0.17 kg/kg) and 59.6 % (0.24/0.143 kg/kg).

Thus the drop in the liquid carbon dioxide temperature before throttling allows increasing the output of $CO_2$ snow; however, when choosing thermostatic control conditions, it is necessary to consider the issue's economic dimension that has to do with the costs of reducing the bottle temperature. The next phase of the generalization of the results in the manner most fitting for practical use.

Therefore, we combined the main parameters of carbon dioxide snow production and presented them in a nomograph. The nomograph in Figure 10 allows determining the orifice hole diameter concerning the liquid carbon dioxide temperature at the maximal output of $CO_2$ snow.

The liquid carbon dioxide temperature values are plotted along the Y-axis, whereas the T-shaped choke orifice diameters are plotted along the X-axis.

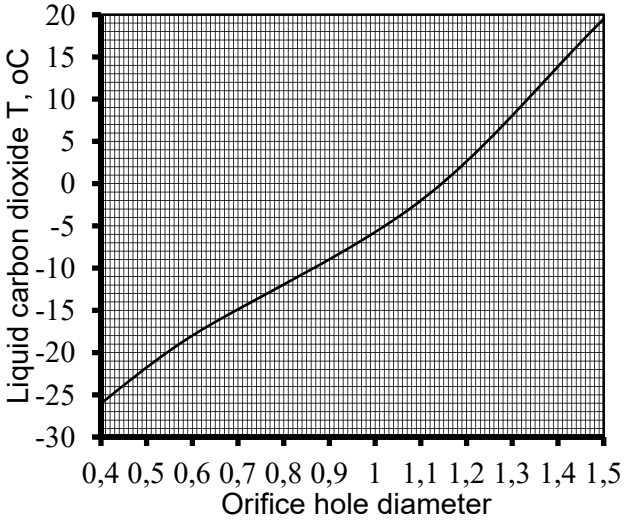


***Figure 10***. Nomograph for selecting orifice hole diameter

The nomograph is used as follows: knowing the liquid carbon dioxide temperature, draw a straight line parallel to the X-axis until the intersection with the line that shows the optimal output of $CO_2$ snow. The numerical value is determined along the Y-axis.

For example, we take that the liquid $CO_2$ temperature is 0ºC and find the recommended orifice plate hole diameter of 1.14 mm that will ensure the maximal output of $CO_2$ snow.

While analyzing the dependence, it should be noted that the production of carbon dioxide snow in the snow-formative flare fitting is divided into several phases. Phase one has to do with the Bernoulli equation for the stream of carbon dioxide passes through the washer with a throttle opening of 1 mm in diameter, where the gas or liquid flow rate rises (dynamic pressure $\frac{\rho v^2}{2}$ rises); at this same moment, however, the static pressure drops; therefore, with a reduction in the cross-section of the stream due to a rise in speed, that is, dynamic pressure, static pressure/drops.

Then, the stream goes into the cone and, with the growth of the angle of the snow-formative cone, the formed snow-mass increases to 0.175 kg, in which case the cone angle is 12°; thus, the pressure rise in front of the cone increases the speed along the whole snow-formative cone. In the expanding part, the stream slows down, and the pressure rises. The optimal cone angle is 12°. At this angle, the maximal pressure is generated to convert as much carbon dioxide as possible to a snow-like state.

For example, in the first series of tests at a liquid carbon dioxide temperature of 10±1 °C, the ratio of the liquid consumption to the output of $CO_2$ snow is 25% (0.175/0.7 kg/kg), in which case the optimal cone angle is 12°.

The following tests were made at a liquid carbon dioxide temperature of 10±1°C. With the growth in the angle of the snow-formative cone, the formed snow-mass rises to 0.18 kg, in which case the optimal cone angle is 120.

In this case, the liquid consumption ratio to the output of $CO_2$ snow is 30% (0.18/0.6 kg/kg). A drop in the temperature of liquid $CO_2$ before throttling increases the output of carbon dioxide snow.

The third series of the tests were conducted at a liquid carbon dioxide temperature of 0±1°C, in which case the ratio of the liquid consumption to the output of $CO_2$ snow is 30.9% (0.17/0.55 kg/kg). The optimal cone angle was also 12°.

The following group of tests was conducted at a liquid carbon dioxide temperature of - 10±1°C, in which case the optimal solution is also the cone with an angle of 12°. In this case, the liquid consumption ratio to the output of $CO_2$ snow is 31.25 % (0.25/0.8 kg/kg).

According to the analysis of the dependencies from Figure 2, the largest amount of snow was produced at -10 °C, while using the cone with an angle of 12°.

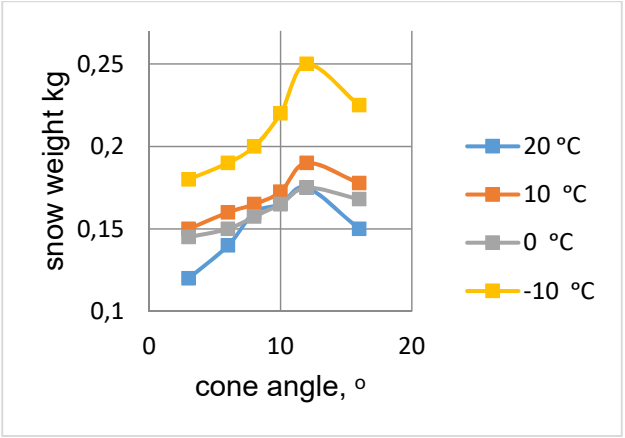


***Figure 4***. The output of snow-like $CO_2$ at different angles of the snow-formative cone

Thus, a drop in the carbon dioxide temperature before throttling allows increasing the output of $CO_2$ snow while selecting the optimal angle in the snow-formative flare fitting means an additional increase in the output of carbon dioxide snow. However, thermal control conditions should be chosen, considering the economic aspect of the issue, linked with the expenses on cooling liquid carbon dioxide.

During the test, the samples were placed in a thermally insulated box installed in the chilling unit chamber. The first series of tests were conducted at a chamber air temperature of -78±2 °C and relative humidity of 20%. In the design period, the concentration of $CO_2$ in the chamber did not exceed 20%. For the test results, see Figure 11A.

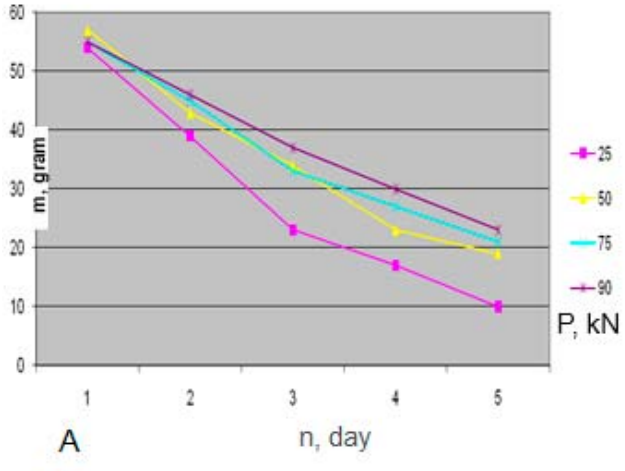

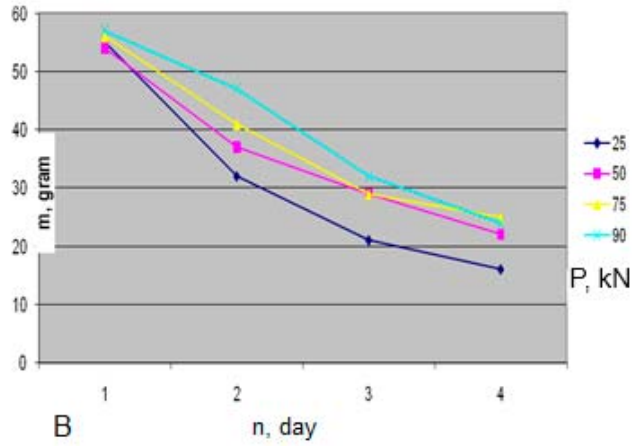


***Figure 11.*** Dependence of the dry ice sublimation intensity on the ambient air temperature at chamber air temperatures of -78±2 °C (A) and -60±2 °C (B)

The sample pressed at 25 kN is sublimated more intensively because the heat exchange involves most of the carbon dioxide snow surface. In the samples pressed at higher pressures, the inter-fraction distance is much shorter, inhibiting the convective heat exchange and reducing specimen weight losses.

For the study similar to the first one but conducted in the chamber at -60 °C, see Figure 11b: it confirms the regularities discovered in the first series of the tests. In that case, however, the sublimation was more than twenty hours shorter, which was because it occurred at higher temperatures.

Sublimation results from the difference in partial pressure between the carbon dioxide steam near the ice surface and the $CO_2$ steam in the environment; also, if the sublimation is rapid, a layer of saturated carbon dioxide steam forms above the solid-phase surface of the interface layer of saturated $CO_2$ the partial pressure of which corresponds to the surface temperature of the ice exposed to sublimation.

The sublimation process required a supply of heat. Depending on the conditions, heat can be borrowed from the environment, which cools down the ice surface and results in a significant thermal gradient inside the ice.

The dry ice temperature depends on the conditions in which the process develops. If the dry ice cake is surrounded by carbonate acid gas, the sublimation temperature at normal pressure will reach -78.9°C. In contrast, if the sublimation of ice into the air occurs at the same pressure, the sublimation temperature will be much lower, in which case it depends on the tension (concentration) of the carbon dioxide steam in the interface layer. The carbon dioxide steam tension and the interface layer thickness are determined by the heat and mass exchange conditions between the ice and the air.

The effects of evaluating the sublimation rate of carbon dioxide cylinders formed at various pressures and deposited in the chamber at -40±2 and 20±2°C, as in Figures 12A and 12B, respectively.

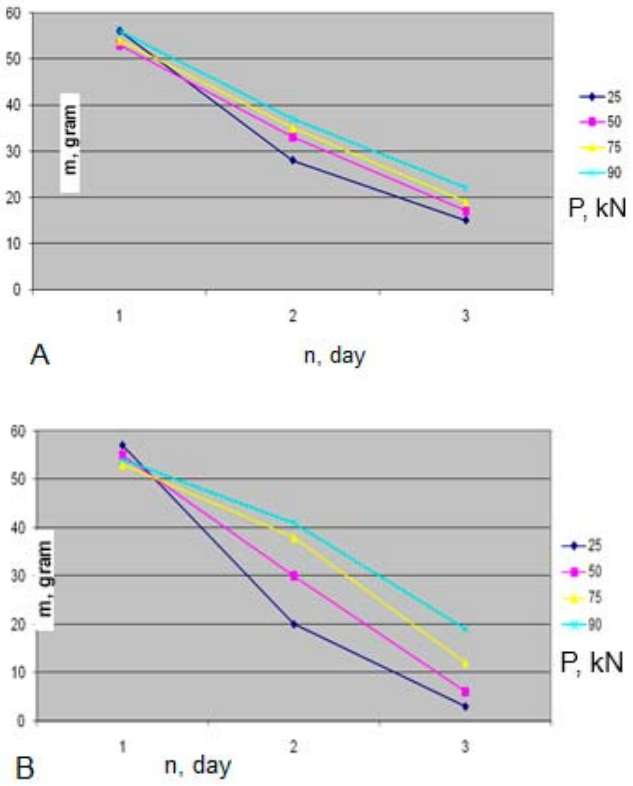


***Figure 12.*** Dependence of the dry ice sublimation in the chamber on the ambient air temperature at an in-chamber air temperature of -40±2 °C (A) and -20°C (B)

As seen from the plot, the average weight losses observed in the tests are much more significant than in the first two test series. Thus, the sublimation period at -40 and -20°C was, respectively, by 100 and 150 % shorter than in the first series of the tests. The weight losses were linear and amounted to about 20 g per 24 hours. This can be explained by the fact that the heat was supplied by convection and beam emissions; the latter provided 20 and up to 45% of the total heat supplied at the test chamber wall temperature of -78 and -20°C, respectively. Because of the low heat capacitance (C = 900 (J/(kg·K)) and weak heat conductance (λ=138 W/(m·K)) of the dry ice cake, the heat supplied to

its surface, especially when the cake is small, cannot have any significant influence on the process.

As a general matter, the convective and radiation supply from the ambient medium may take place and produce by test, allowing mutually controlling them. The sublimation intensity as the average integral quantity on the surface characterizes separate sublimation conditions. It can be defined by weighing a cake, in which case the conductive heat supply comes from the same batch of dry ice due to a drop in the ice surface temperature during sublimation.

The sublimation intensity at enforced air convection is much higher than at free convection. The dry ice surface cools down with an increase in the convection rate. This can be explained by the fact that convective heat supply took place and heat supply by irradiation. As already noted earlier, the heat supply due to the condensation of moisture from the air on the dry ice surface cannot significantly affect the process either.

## 4. CONCLUSIONS

According to the test data, there is a linear relation between the sublimation intensity and the ambient air temperature in the above-specified conditions.

It was observed that the largest output of $CO_2$ snow is produced using choke flanges with T-shaped holes. The effective orifice hole diameters have been determined that allow producing the maximal output of $CO_2$ snow at the optimal liquid carbon dioxide consumption at throttling temperatures of 26 to 19 $^oC$. It has also been established that the pre-throttling drop in the liquid carbon dioxide temperature allows increasing the output of $CO_2$ snow.

The condensation of moisture appears to have a weaker influence on the sublimation rate than expected. The heat exchange was intensified by the fall of hoarfrost and, as a result, the expansion of the surface. However, much moisture froze out without reaching the dry ice surface, and the formed layer of mellow ice would form a kind of heat insulation, and the sublimation under that layer was less intensive. The direct influence of sublimation came from the pressure at which a particular specimen was formed; however, the 75 kN pressure was optimal, as shown by the tests. Despite somewhat more significant weight losses during the storage, the difference in the amount of spent energy is more critical than 90 kN. The factor no less important is the carbon dioxide storage temperature. The maximal sublimation period of a 55 g cylinder formed at 75 kN and stored at – 80 °C was 135 hours, which is much higher than at similar parameters but at -60 °C. That said, the energy amounts spent on running a low-temperature chamber are almost identical.

However, it can be assumed that no complete analogy can be drawn between the heat and the mass exchange during the sublimation of dry ice into the air at various temperatures because sublimation inhibits heat exchange as a result of the fact that the streams of heat and mass are directed toward one another, and the contraction of dry ice allows making this effect weaker.

## 5. REFERENCES


1. Aldamatov, N. E.; Grinyuk, A. N. (2018). Cooling of rabbit meat with snow-like carbon dioxide during its transportation in a heat-insulated container *Food innovations in biotechnology. Proceedings of the VI international conference. Conf. Students, postgraduates, and young scientists.* Turkey, Kemgu, 1, pp. 84-89.
2. Amokrane, B. A.; Provost, E.; Dalmazzone, D.; Osswald, V.; Clain, P.; Delahaye, A.; Fournaison, L. (2018). Kinetic study of $CO_2$ hydrates crystallization: Characterization using FTIR/ATR spectroscopy and contribution modeling of equilibrium/non-equilibrium phase-behavior. *Chemical Engineering Science*, 192, 371-379. DOI: 10.1016/j.ces.2018.07.050.
3. Belozerov, G. A.; Tvorogova, A. A.; Andreev, S. P.; Mednikova, N.M. (2011). Development of cold chain in Russia: collection. *Proceeding 23rd IIR International Congress of Refrigeration*. pp. 2315-2320.
4. Dyshlyuk, L. S.; Sukhikh, S. A.; Ivanova, S. A.; Smirnova, I. A.; Subbotina, M. A.; Pozdnyakova, A. V.; Neverov, E. N.; Garmashov, S. Y. (2018). Prospects for the use of cedar nuts in dairy industry products.*Food and Raw Materials*, 2, 264-280.
5. Evans, J.; James, S. J. (2008). A review of the performance of domestic refrigeration. *Journal of Food Engineering*, 87(1), 2-10.
6. Frankel, E. N.; Finley, J. W. (2008). How to standardize the multiplicity of methods to evaluate natural antioxidance. *J. Agric.*

*Food Chem.,* 56, 4901–4908.
7. Grinyuk, A. N.; Shakhobiddinov, B. B.; Pereverzev, R. . (2018). On the production of snow-like carbon dioxide. *Chemistry, chemical technologies, and ecology: science, production, education. International scientific and practical conference and school of young scientists,* DSU publishing House, Makhachkala, Russia, pp. 221–222.
8. Houska, M.; Kazilova, L.; Landfeld, A. (2011). Time Temperature Histories Of Perishable Foods During Shopping Transport And Home Refrigerated Storage. *Proceedings of ICR-2011*, Prague, Czech Republic, ID-102.
9. Korotkaya, E. V.; Kireev, V. V. (2016). Energy efficiency analysis of the sea buckthorn (hippophae rhamnoides) fruits quick freezing. *Foods and Raw Materials*, 4(1), 110–120.
10. Korotkov, P. S.; Novikov, E. V. (2018). Freezing of Turkey meat in the apparatus with carbon dioxide recycling Food innovations in biotechnology. *Materials of the VI international conference. Conf. Students, postgraduates and young scientists,* Turkey, Kemgu, 1, pp. 178-182.
11. Koster, G. J. (2005). Carbon dioxide as refrigerant; why, and when beneficial. *IIR Conference: Ammonia Refrigerating Systems, Renewal, and Improvement,* Ohrid, North Macedonia.
12. Maier, D.; Wilson, D. (2006). Carbon dioxide for use as a refrigerant. *Proc. IIR-IRHACE Conference, Innovative Equipment and Systems for Comfort and Food Preservation,* University of Auckland, New Zealand, pp. 305-311.
13. Neverov, E. N.; Grinyuk, A. N. (2018). The use of carbon dioxide for the transport of rabbit meat. *Achievements in the field of engineering research. International Conference on Intelligent Solutions for Agriculture*, 151, pp. 825–829.
14. Neverov, E. N.; Korotkiy, I. A; Korotkih, P. S.; Lifenceva, L. V. (2019) The Method of Carbon-Dioxide Recovery. *Fish-Processing Industry. IOP Conf. Ser.: Earth Environ.* Sci. 224 012039.
15. Neverov, E. N. (2016). The use of carbon dioxide for the cold processing of fish. *Bulletin of the Krasnoyarsk State Agrarian University*, 4, 125–131.
16. Neverov, E. N.; Korotkikh, P. S. (2019). Investigation of the heat transfer process during trout cooling using carbon dioxide.*Technique and technology of food production*, 3, 383-389.
17. Repice, C.; Stumpf, A. (2007). Energy Efficiency in Transport Refrigeration. *IIR Congress,* Beijing, China.
18. Ruhe, X. (2007). Refrigeration transportation, energy consumption, and food supply in China. *IEA Heat Pump Centre Newsletter*, 2.
19. Sparks, L. D.; Hernandez, R.; Antonio Estévez, L. A. (2008). Evaluation of density-based models for the solubility of solids in supercritical carbon dioxide and formulation of a new model. *Chemical Engineering Science*, 63(17), 4292-4301. DOI: 10.1016/j.ces.2008.05.031.
20. Wang Y. N., Pfotenhauer J. M., Qiu L. M., Zhi X. Q., Jiang X. B. (2020). Experimental study of carbon dioxide desublimation and sublimation process on low-temperature surface*. IOP Conf. Ser.: Mater. Sci. Eng*., 755, 012157. DOI: 10.1088/1757-899X/755/1/012157
21. Xu Y., Tannert T., Hesse U. (2019). A table-top demonstration unit for CO2-sublimation cycles. *Proceedings of the 25th IIR International Congress of Refrigeration*: Montréal, Canada, August 24-30., 483, 30026422
22. Yoosook, H; Maneeintr, K. (2018). Chemical Engineering Transactions 63 217. *Intergovernmental Panel on Climate Change (IPCC) 2005 IPCC Special report on carbon dioxide capture and storage*. Cambridge, United Kingdom: University Press.
23. Zhai, S.; Su, H.; Taylor, R.; Slater, N. K. N. (2005). Pure ice sublimation within vials in a laboratory lyophiliser; comparison of theory with experiment. *Chemical Engineering Science,* 60(4), 1167-1176. DOI: 10.1016/j.ces.2004.09.078.

**FIGURES**

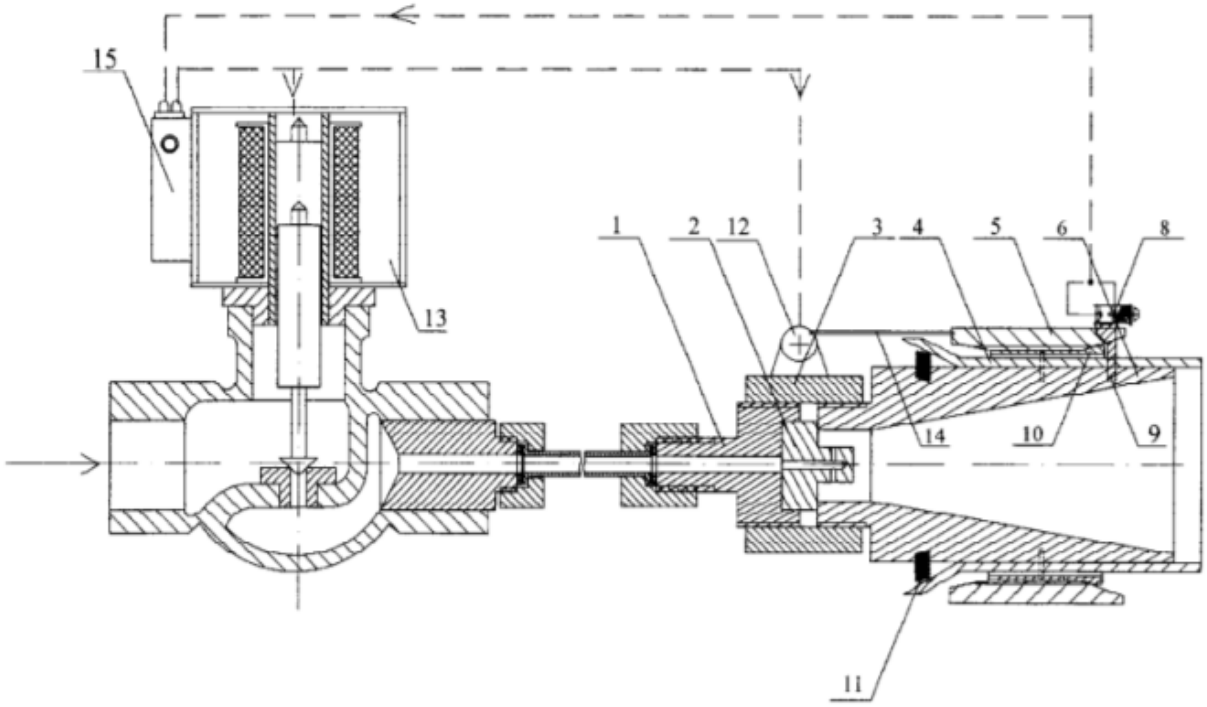


***Figure 5***. Carbon dioxide snow production unit layout
1 – nozzle; 2 – choke flange; 3 – coupling nut; 4 – plates; 5 – auxiliary unit; 6 – $C0_2$ feeding tool; 7– body; 8 – contact switch; 9 – limiter; 10 – splines; 11 – springs; 12 – stepper; 13 – solenoid valve; 14 – flexible member; 15 – time relay.

PERIÓDICO TCHÊ QUÍMICA
ARTIGO ORIGINAL

# ADSORÇÃO DE METAIS PESADOS A PARTIR DE UMA SOLUÇÃO MULTIMETAIS POR PELLETS DE ZEÓLITAS DE BENTONITA-CAOLIM: REGRESSÃO LINEAR E NÃO LINEAR E ANÁLISE DE ERROS

# HEAVY METAL ADSORPTION FROM A MULTIMETAL SOLUTION BY BENTONITE-KAOLIN-ZEOLITE PELLETS: LINEAR AND NONLINEAR REGRESSION, AND ERROR ANALYSIS

# ADSORCIÓN DE METALES PESADOS DE UNA SOLUCIÓN MULTIMETÁLICA USANDO PELLETS DE BENTONITA-CAOLÍN-ZEOLITA: REGRESIÓN LINEAL Y NO LINEAL, Y FUNCIONES DE ERROR

CARBONEL-RAMOS, Dalia Elisa[1*]; CHIRINOS, Hugo David[2]; AGARWAL, Madhu[3].

[1,2] National University of Engineering, Faculty of Environmental Engineering, Peru

[3] Department of Chemical Engineering, Malaviya National Institute of Technology Jaipur, India

** Correspondence author*
*e-mail: dcarbonelr@uni.pe*

Received 18 January 2020; received in revised form 05 February 2021; accepted 10 February 2021

## RESUMO

**Introdução:** A poluição por metais pesados tem grandes impactos na saúde e nos ecossistemas; tecnologias de remediação podem reduzir custos para resolver esses problemas. Os metais pesados representam um sério problema no meio ambiente principalmente por sua tendência a persistir, bioacumular e biomagnificar na cadeia trófica. Remover esses compostos tóxicos das águas residuais ainda é uma tarefa desafiadora. **Objetivo:** A capacidade de remoção de metais pesados foi analisada usando pelotas adsorventes feitas com bentonita natural, caulim e zeólita. Este estudo descreve o equilíbrio de adsorção e cinética de remoção de metal usando análise de regressão linear e não linear. Os mecanismos de adsorção também foram analisados. **Métodos:** A qualidade do ajuste dos dados de equilíbrio de adsorção foi testada com as quatro formas linearizadas da equação de Langmuir, bem como os modelos de Freundlich, Temkin e Dubinin-Radushkevich. Para escolher o modelo de melhor ajuste com maior confiabilidade, cinco funções de erro foram utilizadas: $R^2$, $X^2$, SSE, ABS e ARE. Para a cinética de adsorção os modelos de Pseudo Primeira Ordem, Pseudo Segunda Ordem e Elovich foram estudados com análise de regressão linear e não linear. **Resultados e Discussão:** A linearização tipo I da isoterma de Langmuir deu o melhor ajuste para os três metais, com capacidades máximas de adsorção para chumbo, cobre e cádmio de 7,27, 1,45 e 0,28 mg/L respectivamente. Os resultados mostram que a Pseudo Segunda Ordem com regressão linear melhor ajustada para dados de chumbo e cobre e o modelo Pseudo Primeira Ordem com regressão linear para cádmio. **Conclusões:** A regressão não linear foi considerada melhor para se ajustar aos modelos de equilíbrio de adsorção e a regressão linear para se ajustar aos modelos cinéticos. Os principais mecanismos responsáveis pela adsorção no sistema são pensados para ser a troca iônica entre grupos funcionais e cátions, e atração de carga superficial relacionada às forças de Van der Waals.

**Palavras-chave**: Aluminossilicatos; peletização; tratamento de água poluída.

## ABSTRACT

**Background:** Heavy metal pollution has significant impacts on health and ecosystems; remediation technologies can reduce the cost to solve these problems. Heavy metals present a severe problem in the environment, mainly for their tendency to persist, bioaccumulate and biomagnification in the trophic chain. Removing these toxic compounds from wastewater remains a challenging task. **Aim:** Heavy metal removal capacity was analyzed using adsorbent pellets made with natural bentonite, kaolin, and zeolite. This study describes the equilibrium adsorption and kinetics of metal removal by using linear and nonlinear regression analysis. Adsorption mechanisms were also analyzed. **Methods:** The goodness of fit of the adsorption equilibrium data was tested with the four linearized forms of the Langmuir equation, as well as the Freundlich, Temkin, and Dubinin-Radushkevich models. To choose the best-fit model with greater reliability, five error functions were used: $R^2$, $X^2$, SSE, ABS, and ARE. For adsorption kinetics the Pseudo First Order, Pseudo Second Order and Elovich models were studied with linear and nonlinear regression analysis. **Results and Discussion:** Type I linearization of the Langmuir isotherm

showed the best fit for the three metals, with maximum adsorption capacities for lead, copper, and cadmium of 7.27, 1.45 and 0.28 mg/L, respectively. The results show that Pseudo Second Order with linear regression best fitted for lead and copper data and Pseudo First Order model with linear regression for cadmium. **Conclusions:** Nonlinear regression was found better to fit adsorption equilibrium models and linear regression to fit kinetics models. The main mechanisms responsible for adsorption in the system are thought to be ion exchange between functional groups and cations and surface charge attraction related to Van der Waals forces.

**Keywords**: Alluminosilicates; pelletization; wastewater treatment.

## RESUMEN

**Antecedentes:** La contaminación con metales pesados tiene graves impactos en la salud y los ecosistemas, las tecnologías de remediación pueden reducir los costos asociados a la resolución de estos problemas. Los metales pesados son un problema ambiental principalmente por su tendencia a ser persistentes, bioacumularse y biomagnificarse en la cadena trófica. Remover estos compuestos tóxicos de las aguas residuales continúa siendo un reto. **Objetivo:** La capacidad de remoción de metales pesados se analizó empleando adsorbentes hechos con bentonita, caolín y zeolita natural. Este estudio describe la cinética y parámetros de remoción de metales usando el análisis de regresión lineal y no lineal. **Métodos:** El ajuste de datos al equilibrio de adsorción se comparó con las cuatro formas linearizadas de la ecuación de Langmuir, así como con los modelos de Freundlich, Temkin y Dubinin-Radushkevich. Para escoger el modelo de mejor ajuste con mayor confiabilidad, se aplicaron cinco funciones de error: $R^2$, $X^2$, SSE, ABS y ARE. Para la cinética de adsorción se estudiaron los modelos de Pseudo Primer Orden, Pseudo Segundo Orden y Elovich con análisis de regresión lineal y no lineal. **Resultados y discusiones:** La linearización Tipo I de la isoterma de Langmuir fue la de mejor ajuste para los tres metales, con capacidades máximas de adsorción para plomo, cobre y cadmio de 7.27, 1.45 y 0.28 mg/L respectivamente. Los resultados muestran que el modelo de Pseudo Segundo Orden con regresión lineal fue el de mejor ajuste para plomo y cobre, y que el modelo de Pseudo Primer Orden con regresión lineal fue el de mejor ajuste para el cadmio. **Conclusiones:** La regresión no lineal se ajustó mejor a los modelos de equilibrio de adsorción y la regresión lineal a los modelos cinéticos. Se podría inferir que los principales mecanismos responsables de la adsorción del sistema son el intercambio iónico entre grupo funcionales y cationes, y la atracción por carga superficial relacionada con las fuerzas de Van der Waals.

**Palabras clave**: Aluminosilicatos; peletización; tratamiento de aguas residuales.

## 1. INTRODUCTION:

Heavy metal pollution has major impacts on health and ecosystems, and applying prevention technologies could reduce the costs associated with alleviating these problems. Heavy metals have toxic characteristics that aggravate the environmental pollution problem, i.e. persistence, bioaccumulation, and biomagnification (Kurniawan, Ismadji, Soetaredjo, and Ayucitra, 2014). Thus, how effectively and intensely remove undesired metals from wastewater is a serious and challenging task. Various technology proposed to remove heavy metals i.e., chemical precipitation, ion exchange, membrane filtration, electrochemical treatment. Chemical precipitation, used as a primary treatment, generates large amounts of hazardous waste. Membrane technologies (i.e., electrodialysis, reverse osmosis) gives excellent potential in the treatment process but high installation, maintenance, and energy costs (Renu, Agarwal, and Singh, 2017). Adsorption has many advantages compared to other treatments (Zhao, Xu, Zhang, Rong, and Zeng, 2016); it is a simple and economical treatment process that can remove heavy metals and a wide range of other contaminants (Worch, 2012).

Among the available adsorbents, clays, zeolites, and aluminosilicates are classified as the promising ones for heavy metals removal from aqueous systems. This is partly because of their great cation exchange capacity, low cost, high availability, high specific surface area, selectivity and regeneration capacity (Ismadji, Soetaredjo, and Ayucitra, 2015; Kurniawan *et al*., 2014; Novikova and Belchinskaya, 2016).

Evaluation of the goodness of fit to any model and determination of the parameters will enable the possible adsorption mechanisms to be understood. This is best done using regression analysis, either linear or nonlinear depending on their mathematical nature. In linear regression, the experimental data are adjusted to the to the linear expression of the model. In nonlinear regression, the parameters come from the nonlinear form of the model, and linearization, and linearization is not needed (Foo and Hameed, 2010).

Linear regression is one of the most

commonly used methods, despite the non-linearity of the kinetic and isothermal models and the linear analysis (Gusain, Srivastava, Sillanpää, and Sharma, 2016). On the other hand, nonlinear regression is a powerful tool for analyzing scientific data – the errors generated in linear adjustment are reduced (Ghaffari *et al*., 2017; Khalid, Kazmib, Habibc, Jabeena, and Shahzadd, 2015).

The objective of this study was to examine the adsorption of lead, copper and cadmium on bentonite, kaolin and zeolite pellets and describe the kinetic of metal removal and parameters by using linear and nonlinear regression analysis. Adsorption mechanisms were also defined in this work.

## 2. MATERIALS AND METHODS:

### 2.1. Clay characterization

The kaolin, bentonite and zeolite all came from natural deposits – the kaolin and bentonite from Cajamarca in northern Peru, and the zeolite from New Mexico (Hydro Source).

The aluminosilicates were characterized by spectrometry before pelletization and FTIR analysis was done on the pellets. Adsorbent pellets were ground in an agate mortar. Subsequently about 100 mg of adsorbent powder was analyzed at room temperature (20.3 ºC) and 66% of relative humidity. The analysis was made using a Perkin Elmer Frontier MIR spectrometer, with a $4cm^{-1}$ resolution and a KBr pressed disc technique.

### 2.2. Reagents

The metallic reagents – lead nitrate ($Pb(NO_3)_2$), copper sulfate pentahydrate ($CuSO_4.5H_2O$), and standard cadmium solution (1,000 mg/L) – were supplied by Merck Laboratories. Multimetallic solutions were prepared by diluting the reagents in distilled water, and the pH was adjusted with $H_2S0_4$ or KOH. Standard solutions for lead, copper, and cadmium were elaborated in four different concentrations, diluting standard stock solutions of 1000 mg/L concentration. This allowed obtaining the calibration curve. After adsorption and without further filtration, heavy metal concentrations were measured with an atomic absorption spectrometer (Model AA-700, Shimadzu), using an acetylene/air flame. The detection limit of the mentioned equipment for the three metals was between 0.001 mg/L and 0.009 mg/L. Wavelength measures for lead, copper and cadmium were 217 nm, 324.8 nm, and 228.8 nm, respectively. The slit width for all metals was 0.7 nm.

### 2.3. Pelletization

The dried clays and zeolites were screened to a particle size below 33 µm. Each pellet contained 67% zeolite, 29% bentonite, and 4% kaolin. The pellets were made using an adapted form of the method described in Miranda *et al.* (2015). The zeolite, bentonite, and kaolin powder mix were made into a paste with distilled water and then kneaded and passed through a manual extruder to form pellets 5 ± 0.1 mm long x 2 mm diameter. These were dried and calcined following Ciosek *et al.* (Ciosek, Luk, Warner, and Warner, 2016). The pellets were oven-dried at 105 °C for 18 hours and then calcined at 600 °C for 6 hours, increasing the temperature at 5 °C/min.

### 2.4. Adsorption tests

#### *2.4.1 Adsorption column*

Adsorption was evaluated in a column using a system similar to that described by Salem and Sene (Salem and Akbari Sene, 2012). A total of 300 mL aliquots of the solution were circulated at 20 mL/min using a peristaltic pump. Experiments were conducted at different parameters, i.e., circulation time, pH, and initial heavy metals concentration.

These were dried and calcined following recommendations by Ciosek *et al.* (2016). The pellets were oven-dried at 105 °C for 18 hours and then calcined at 600 °C for 6 hours, increasing the temperature at 5 °C/min.

#### *2.4.2 Removal efficiency and adsorption capacity*

Removal efficiency ($\%R_{em}$) was determined using Equation 1:

$$\%R_{em} = \frac{C_o - C_e}{C_o} \cdot 100 \qquad \text{(Eq. 1)}$$

where $C_o$ (mg/L) and $C_e$ (mg/L) represent the initial and final concentrations of the heavy metals.

The equilibrium adsorption capacity, $Q_e$, (mg/g) was found with Equation 2:

$$Q_e = \frac{Co - C_e}{m} \cdot V \qquad \text{(Eq. 2)}$$

where $C_e$ (mg/L) is the equilibrium concentration, m the total mass of adsorbent (g) and V the

volume (L) of solution.

### 2.5. Equilibrium and kinetic studies

Adsorption equilibrium tests were performed with 300 mL of multimetallic solution, an adsorbent dose of 15 g/L and pH 4.5 ± 0.5, for 160 minutes. Initial lead and copper concentrations were between 1.5 and 30 mg/L, and cadmium between 0.5 and 15 mg/L. The data were fitted to the Langmuir, Freundlich, Temkin, and Dubinin-Radushkevich (D-R) models.

The Langmuir model (Equation 3) was the first equation proposed to describe adsorption:

$$Q_e = \frac{Q_{max} \cdot K_L \cdot C_e}{1 + K_L \cdot C_e} \qquad \text{(Eq. 3)}$$

where $Q_e$ (mg/g) is the amount of solute adsorbed onto the adsorbent surface in equilibrium conditions, $Q_{max}$ (mg/g) the maximum removal capacity of the adsorbent, and $K_L$ (L/mg) and $C_e$ (mg/L) the parameters of affinity and equilibrium concentration of the solute. The separation factor, $R_L$, is calculated using Equation 4:

$$R_L = \frac{1}{1 + b \cdot C_o} \qquad \text{(Eq. 4)}$$

where $C_o$ (mg/L) is the initial concentration and b the intercept of the nonlinear equation.

The Freundlich isotherm (Equation 5) is also one of the very early empirical adsorption equations:

$$Q_e = K_F \cdot C_e^{1/n} \qquad \text{(Eq. 5)}$$

where $K_F$ ((mg/g).(L/mg)^(1/n)) indicates the adsorption capacity of the adsorbent and n the system's heterogeneity.

The Temkin model is represented in Equation 6:

$$Q_e = B_T \cdot \ln(A_T \cdot C_e) \qquad \text{(Eq. 6)}$$

where $A_T$ and $B_T$ are equilibrium binding and parameter constants.

The D-R model is expressed in Equation 7:

$$Q_e = Q_{max} \cdot e^{-\beta\varepsilon^2} \qquad \text{(Eq. 7)}$$

β indicates the average sorption of free energy E (kJ/mol).

To analyze the adsorption kinetics, 500 mL portions of multimetallic solution were prepared, with initial Cu and Pb concentrations of 15 mg/L, and 5 mg-Cd/ L, an adsorbent dose of 10 g/L and pH 4 ± 0.5. Samples of the treated solution were taken between minutes 10 and 300. The pseudo first order (PFO), pseudo second order (PSO) and Elovich models were all analyzed. The PFO model (Equation 8) was proposed by Lagergren:

$$Q_t = Q_e(1 - \exp(k_1 \cdot T)) \qquad \text{(Eq. 8)}$$

where $k_1$ (1/min) and $Q_e$ (mg/g) are parameter constants.

The PSO model, developed by Ho and McKay, is shown in Equation 9:

$$Q_t = \frac{Q_e^2 \cdot k_2 \cdot T}{1 + Q_e \cdot k_2 \cdot T} \qquad \text{(Eq. 9)}$$

where $k_2$ (g.mg^-1.min^-1) is the equation parameter.

Zeldowitsch developed the Elovich model (Equation 10):

$$Q_t = \frac{1}{Q_t} \ln((1 + Q_e \cdot k_e \cdot T) \qquad \text{(Eq. 10)}$$

where $k_e$ (1/min) is the desorption constant.

### 2.6 Statistical analysis

For linear regression, the data were plotted according to the linearized form of each model (Table 1). It is noted that the Langmuir model can be linearized in four ways. The intercept and slope values on the graph were calculated, and the parameters for each equation were determined.

***Table 1.*** *Linear expressions of Langmuir model*

| Langmuir model | Linearization |
|---|---|
| Type I | $\frac{1}{Q_e} = \frac{1}{Q_{max} \cdot K_L} \cdot \frac{1}{C_e} + \frac{1}{Q_{max}}$ |
| Type II | $\frac{C_e}{Q_e} = \frac{1}{Q_{max} \cdot K_L} + \frac{Ce}{Q_{max}}$ |
| Type III | $Q_e = Q_{max} - \frac{1}{K_L} \cdot \frac{Q_e}{C_e}$ |

| | |
|---|---|
| Type IV | $\frac{Q_e}{C_e} = KLQ_{max} - KLQ_e$ |

The nonlinear regression was optimized using the Excel Solver plug-in, with the GRG algorithm. Goodness of fit was measured on the basis of five different error functions (Table 2).

***Table 2.*** *Error functions*

| Function name | Error function |
|---|---|
| Sum of square errors- SSE | $SSE = \sum_{i=1}^{n} (y_{i,exp} - y_{i,mod})^2$ |
| Coefficient of determination – $R^2$ | $R^2 = 1 - \frac{\sum_{i=1}^{n}(y_{i,exp} - y_{i,mod})^2}{\sum_{i=1}^{n}(y_{i,exp} - \overline{y_{i,exp}})^2} = 1 - \frac{SSE}{SST}$ |
| Sum of absolute errors - ABS | $ABS = \sum_{i=1}^{n} \lvert y_{i,exp} - y_{i,mod} \rvert$ |
| Chi square – $X^2$ | $x^2 = \sum_{i=1}^{n} \frac{(y_{i,exp} - y_{i,mod})^2}{y_{i,mod}}$ |
| Average relative error - ARE | $ARE = \frac{100}{n} \sum_{i=1}^{n} \left\lvert \frac{y_{i,exp} - y_{i,mod}}{y_{i,mod}} \right\rvert$ |

## 3. RESULTS AND DISCUSSION:

### 3.1 Adsorbent characterization

Table 3 shows the chemical composition of the bentonite, kaolin and zeolite adsorbents. The three minerals consist mainly of silica and alumina, with lesser amounts of calcium, magnesium, sodium and potassium oxides. This confirms the potential of these materials for use as adsorbents (Uddin, 2017). The sodium and potassium oxides concentrations, and the magnesium and calcium oxides represent the feldspar content (Krupskaya *et al*., 2019). The ignition loss values indicate that these materials have low carbonaceous matter and high mineral content (Uddin, 2017).

***Table 3.*** *Chemical composition of the clays and zeolite*

| Element | Bentonite | Kaolin | Zeolite |
|---|---|---|---|
| $SiO_2$ | 62.63% | 44.60% | 65.91% |
| $Al_2O_3$ | 17.10% | 36.09% | 10.60% |
| $Fe_2O_3$ | 3.53% | 3.43% | 3.03% |
| CaO | 2.61% | 1.29% | 2.52% |
| MgO | 0.61% | 0.35% | 0.18% |
| $Na_2O$ | 0.99% | 0.30% | 3.77% |
| $K_2O$ | 0.07% | 0.19% | 0.14% |
| $TiO_2$ | 0.53% | 1.42% | 0.17% |
| $P_2O_5$ | 0.03% | 0.03% | 0.07% |
| Loss off ignition | 11.80% | 12.30% | 13.60% |

Figure 1 shows the FTIR analysis in the spectrum range between 400 and 4000 $cm^{-1}$. No peaks were observed in the first region of the spectrum, between the 3500 and 1600 $cm^{-1}$ bands, attributed to surface and internal hydroxyl group vibrations. The curve is flat from 2842.60 to 1626 $cm^{-1}$, a region attributed to the adsorption of water in aluminosilicates (Hofmeister and Bowey, 2006). In the last region there is higher band intensity, this corresponds to the vibration of the oxygen bonds with aluminum or silicon. For the latter, the peaks are at 1023.04 $cm^{-1}$ (from T-O junctions where T can be either aluminum or silicon) and six peaks in the range 874.79 and 447.00 $cm^{-1}$ (corresponding to the T-O-T vibrations) (Madejová, Gates, and Petit, 2017).

### 3.2 Langmuir linearization

Langmuir model can be linearized in four different types of equations (Table 1), giving different results according to the formula used. Table 4 shows the equation parameters and error functions for each type of Langmuir linearization – the values vary independently, increasing or reducing the error. Langmuir equation types I and II are those most used because the results of the adjusted equations have less error (Armagan and Toprak, 2013). Table 4 shows that equations types I and IV were the ones with the least error.

The type I Langmuir equation obtained the highest $R^2$ and lowest ABS and ARE for the three metals studied. Type II Langmuir equation represents the smallest $X^2$ and lowest SSE for lead and copper. Type III equation shows the lowest SSE for cadmium, and type IV equation shows, the lowest ABS for copper and cadmium. From Table 4, it can be concluded that the type I Langmuir equation had the better fit to data.

These results show the complexity of estimating isothermal parameters using linearization techniques (Armagan and Toprak, 2013). For example, the $R^2$ linearization values for

each type (Table 4) and the other three models (Table 5) are all different. For lead and copper, the Langmuir equations types II, III, and IV $R^2$ values suggest that the Freundlich model gives the best fit. For cadmium, taking into account only Langmuir types II, III, and IV $R^2$ values, the Temkin isotherm would be the best fit.

### 3.3 Equilibrium isotherms

Table 5 compares the error functions of equilibrium models with linear and nonlinear regression, allowing the model to fit the data better. The $X^2$ value for 0.95 probability and 6 degrees of freedom is 1.64; all values are less than or equal to 1 (Table 5).

When changing from linear to nonlinear analysis, the values changed in all cases, except with $R^2$ of Temkin, and only for cadmium with $X^2$. The latter is to be expected given the low variation and concentrations of the data. Długosz and Banach (Długosz and Banach, 2018) obtained similar results in their study of copper adsorption on vermiculite; the Temkin model's $R^2$ was the same linear and nonlinear analyses.

The tendency is that nonlinear regression analysis reduces the error difference between experimental and expected data (Table 5). Comparing the error function values obtained with linear and nonlinear regression shows that four error functions ($X^2$, SSE, ABS, and ARE) indicate that the Temkin model had the worst fit to the experimental data. Regarding the error function variation from linear to nonlinear analysis, $R^2$ increased, and ABS and ARE decreased in all cases. This supports the findings of several authors who confirm that nonlinear regression analysis gives better results (Rostami, Pourzamani, Bina, and Karimi, 2019).

The differences between experimental data and the linear expressions of isotherms may be due to problems in the transformation from a nonlinear form, which is how adsorption models are expressed and formulated to a linear one. This changes the experimental error and the normality assumption in the least-squares. In linear regression the linearity of the points is assumed but not tested, and the slope and intercept of the best fit are predicted. The linear method assumes that the scattered points around this straight line have a Gaussian distribution and that the error distribution is the same for each value of "x". However, this rarely occurs in adsorption equilibrium models, where the distribution error is altered by transforming the data to linear form. In the linear method "y" is predicted for the corresponding "x" and only the error distribution along the "y" axis is considered, without taking into account its correspondence on the "x" axis (Armagan and Toprak, 2013). This yields different error values and parameters depending on how the data are linearized. For this reason, as well as on the evidence of the results from this study, nonlinear regression is considered the best method for determining equilibrium model adsorption parameters.

The linear regression error functions show that the Temkin model had the lowest $R^2$, and the highest SSE and ABS. For lead, the Langmuir model had the highest $R^2$, and the lowest SSE and ABS, while, for copper, the Freundlich model had the highest $R^2$ and lowest SSE (0.95 and 5.22), and the Langmuir model the highest $R^2$ and lowest ABS (0.98 and 0.48). Cadmium had higher and lowered $R^2$ and $X^2$ in the Temkin model with linear regression, but four error functions indicate that the Langmuir model best represents the data. For lead, R2, SSE, and ABS values confirm that the Langmuir isotherm is the best fit, while $R^2$ and ABS confirm the same for copper.

Error functions in the linear regression confirm that the Langmuir model best fits the lead, copper, and cadmium adsorption data, followed by the Freundlich model. Similar studies in which linear and nonlinear regression have been compared have had better results with linear analysis of the Langmuir model (Mallakpour and Rashidimoghadam, 2019), and sometimes with Freundlich, Temkin and D-R models (Batool, Akbar, Iqbal, Noreen, and Bukhari, 2018).

Figure 2 shows the Langmuir, Freundlich, Temkin, and D-R experimental data and nonlinear regression curves models. It is notorious the better fit of data to Langmuir and Freundlich models for the three metals.

Table 6 shows the parameters and $R^2$ values for each model for linear and nonlinear analyses, and the great variation between the Langmuir linear and nonlinear parameters model for lead, copper and cadmium is evident.

#### *3.3.1 Langmuir*

The error function analysis for lead, copper and cadmium in the nonlinear regression indicates that the Langmuir model best describes the experimental data. Other authors have obtained similar results with heavy metal adsorption onto clays (K. Abu-Hawwas, M. Ibrahim, and M. Musleh, 2018; Mu'azu, Bukhari, and Munef, 2020). The maximum adsorption capacities predicted by the Langmuir model for lead, copper, and

cadmium are 7.27, 1.45, and 0.68 mg/g, respectively. The best fit by the Langmuir model means that the process occurs in a monolayer and that each active site houses an adsorbate molecule, characteristics typical of physisorption (Ismadji *et al*., 2015).

The parameter $K_L$ measures the adsorption intensity between the adsorbate and adsorbent (Ismadji *et al*., 2015). In this study its value was highest for cadmium and lowest for lead, implying that cadmium molecule adhesion at the interface is stronger than that of copper and lead. The separation factor, $R_L$, indicates the viability of adsorption (Ismadji *et al*., 2015). Table 6 observed that this factor was reduced from a linear to a nonlinear regression; however, for the three metals, the ranges remained lower than 1, indicating that the adsorption is viable.

### *3.3.2 Freundlich*

In the Freundlich model, the parameter $K_F$ is related to multilayer adsorption capacity, and n indicates adsorption intensity, which varies with interface heterogeneity (Ismadji *et al*., 2015). The value of n enables understanding of the process and the system's complexity; magnitudes between 1 and 10 are considered favorable, but values exceeding 10 indicate irreversible conditions. Nonlinear regression for lead, copper, and cadmium yielded values of 1.09, 3.30, and 6.09, respectively, showing that the process is viable, with adsorption tending to be most substantial for cadmium, then copper, and finally lead. $K_F$ also indicates the sorption capacity of the adsorbent (Ismadji *et al*., 2015). It was highest for copper, followed by lead and cadmium. These results agree with Bahabadi *et al.* (Bahabadi, Farpoor, and Mehrizi, 2017). They studied adsorption on clays and zeolites and concluded that natural adsorbents had a greater affinity for copper than zinc and cadmium.

The nonlinear analysis of $R^2$ showed that the Freundlich model is second in order adjustment for lead and cadmium, and third for copper. Similar results were reported by Soleimani and Siahpoosh (Soleimani and Siahpoosh, 2015) in relation to copper adsorption with nanoclays. While the Freundlich model is not the best to describe the data, the values of $R^2$, between 0.968 and 0.986, indicate that the equation may be applicable. This can be attributed to the fact that active sites can be characterized as monolayer or multilayer, and the interface as heterogeneous (Padmavathy and Murali, 2017).

### *3.3.3 Temkin*

Low $Q_t$ values for the three metals studied indicate that adsorption is physical. The $A_T$ value decreased in the order Cd>Cu>Pb, indicating that cadmium has the highest binding energy of the three to the adsorbent. This corroborates the results from the Freundlich and Langmuir models.

According to the nonlinear $R^2$, the Temkin model had the lowest fit for lead, copper, and cadmium. This behavior is common in adsorption studies (Salmani *et al*., 2019). The results agree with the data fit to the Langmuir model, indicating the predominance of physisorption. The Temkin isotherm is more appropriate for describing chemisorption (Ahmedzeki, Rashid, Alnaama, Alhasani, and Abdulhussain, 2013; Gao *et al*., 2013).

### *3.3.4 D-R*

The D-R model helps to distinguish between physical and chemical adsorption using the value of E. When this is below 8 kJ/mol, adsorption is physical; between 8 and 16 kJ/mol ion exchange and chemical mechanisms predominate; and above 16 kJ/mol, particle diffusion governs the reaction (Sadeghalvad, Khosravi, and Azadmehr, 2016). Table 6 shows that E is reduced when transferring from linear to nonlinear analysis, except below 8 kJ/mol, where values were maintained, indicating physical adsorption. This corroborates the findings from the three other models.

For lead and cadmium, the nonlinear $R^2$ places this model third in order of adjustment, consistent with several studies showing lower $R^2$ values with this equation (Mosai and Tutu, 2019; Nikolic, Jeffry Robert, and Girish, 2019).

## 3.4 Kinetics

Experimental data were compared with three equations that consider surface reaction kinetics as a critical step: the PFO, PSO, and Elovich models. The linear regressions for the three, and their respective equations, are shown in Figure 3.

When changing from linear to nonlinear regression (Table 7) the error functions all vary except $X^2$ in the PFO model and $X^2$ and $R^2$ in the PSO model for lead. Variations are expected when moving between linear and nonlinear models – e.g., López-Luna *et al.* (López-Luna *et al*., 2019) had similar outcomes in a study of arsenic and manganese adsorption.

Having five error functions to select the best fit increases the reliability of the results. For 9 degrees of freedom and p 0.95, $X^2$ is 3.33. Table 7 shows no data exceeded this limit, even for p 0.99 ($X^2$ is 2.09). A comparison shows that SSE, ABS, and ARE for lead, copper, and cadmium are higher in the Elovich equation.

When changing from linear to nonlinear regression concerning error function, $R^2$ increased in all cases, except for the PSO model for lead. $X^2$ decreased for copper and cadmium in all three models, but for lead, it remained the same in the PFO and PFO models and increased in the Elovich model. SSE decreased in all cases, and ARE was reduced in the PFO model for lead, and in the Elovich model for both lead and copper.

The error function analysis seems to indicate error reduction with nonlinear regression. However, the optimal parameter values for cadmium could not be found for the PFO model when performing nonlinear regression and some parameter values suggested during optimization were very low (Table 8). The Elovich nonlinear parameters, $Q_e$, are much lower than both the linear and experimental parameters, which means that nonlinear regression cannot be applied successfully to the Elovich model. Moreover, the lead and copper error functions and parameters are similar in the linear and nonlinear regressions. The Elovich model's inapplicability and the small difference between linear and nonlinear regression for lead and copper meant that kinetic analysis was preferred using linear regression. Other authors have reported similar results (Açikyildiz, Gürses, Güneş, and Yalvaç, 2015). Nonlinear regression for kinetic models demands specific and previous expertise and takes longer (Açıkyıldız *et al.*, 2015).

The best fit for cadmium was the PFO model in linear and nonlinear regression (Table 7). Lead and copper showed best fits with the PSO model with linear regression, and this was maintained in nonlinear regression for lead. Other authors have also reported good correlations with these models (Milenković *et al*., 2013) and a poorer fit with the Elovich equation (Yousefi *et al*., 2018).

Figure 4 shows linear regression curves of the PFO, PSO, and Elovich models.

#### *3.4.1 PFO*

The PFO model is widely used to describe the heavy metal adsorption but the adsorption capacity predicted is usually below the experimental one (Dotto, Salau, Piccin, Cadaval, and de Pinto, 2017). The $Q_e$ values for lead, copper, and cadmium are 0.95, 0.94, and 0.85 mg/g, respectively. Those for lead and copper are lower than the experimental maxima for both linear and nonlinear regressions.

In the case of cadmium, in both linear and nonlinear regressions, the error functions indicate that the PFO model is the best fit. In this model, it is assumed that the adsorption rate is directly proportional to the adsorbate concentration and that the limiting step is diffusion at the adsorption surface (Ho and McKay, 1999). Although it is most common that the PSO model gives the best fit to the data in heavy metal adsorption, other researchers have reported similar results (Mejia Miranda, Laverde, Avella, and Peña Ballesteros, 2015).

#### *3.4.2 PSO*

Ho and McKay (1999) suggested that, if metal ion adsorption fits the PSO model, the process limiting step could be chemisorption. This would involve adsorbate-adsorbent electron exchange, although physical interactions could also be the cause.

In both linear and nonlinear regression analysis, lead fits the PSO model best, and the same is true for copper in linear regression. Several heavy metal adsorption studies with bentonite and zeolite, have shown a better fit to the PSO model (Melichová and Ľuptáková, 2016; Mu'azu *et al*., 2020). The results seem to indicate that chemisorption could control lead and copper adsorption.

#### *3.4.3 Elovich*

The calculated adsorption capacity of metals was lower than the experimental one due to this the Elovich equation for linear and non linear regression was not suitable to describe adsorption capacity of three metals.

Although the model has been reported to adjust better at very low concentrations (López-Luna *et al*., 2019), it is usual for this equation to have a lower adjustment of data than the PFO PSO models (Schwantes *et al*., 2016).

### 3.5 Adsorption mechanisms

After selecting the appropriate adsorbent in terms of cost, efficiency, selectivity and kinetics, the second most important step for effective adsorption is to identify the predominant

mechanisms and elucidate the interactions occurring at the interface.

Adsorption mechanisms can be classified into physisorption, ion exchange, chemisorption, and precipitation. Physisorption includes processes like surface adsorption, Van der Waals interactions and hydrogen bonding (Crini, Lichtfouse, Wilson, and Morin-Crini, 2018). Ion exchange involves replacing interchangeable cations (i.e. Na+, K+, $Ca^2$+ and $Mg^2$+) at the interface, and is usually fast and reversible (Shaban and Abukhadra, 2017), but also between the aluminosilicate Al(OH) and Si(OH) groups and the metal ions (Burakov *et al*., 2018). Chemisorption usually involves electrostatic interactions, covalent bonds, and complex formation, while precipitation can be micro- or surface-, or via proton displacement (Crini *et al.*, 2018). Several authors agree that the above are all likely mechanisms in natural adsorbents (Al-Jlil and Latif, 2013; Alexander, Ahmad Zaini, Surajudeen, Aliyu, and Omeiza, 2018).

The analysis carried out in the investigation did not cover complex formation or surface precipitation in the adsorbent; for this reason, it is unknown if these mechanisms also play an important role in adsorption.

Adsorption equilibrium and kinetics analysis indicate the predominance of physisorption in the system. Therefore, it can be deduced that the main mechanisms responsible for adsorption are: ion exchange between functional groups and cations and surface charge attraction related to Van der Waals forces.

## 4. CONCLUSIONS:

Nonlinear regression was found better to fit adsorption equilibrium models and linear regression to fit kinetics models. The Langmuir isotherm gave the best fit to the experimental data with maximum adsorption capacities for lead, copper, and cadmium of 7.27, 1.45, and 0.28 mg/L, respectively. The Freundlich isotherm also had high correlation values ($R^2$ between 0.968 and 0.986), indicating that active sites can be characterized as mono or multilayer, and the adsorption surface as heterogeneous. The lead and copper data were better adjusted to the PSO model, and the cadmium data to the PFO model.

## 5. ACKNOWLEDGMENTS:

This research was made with funding from the Faculty of Environmental Engineering of the National University of Engineering in Peru (Grant Number RD 038-2018).

## 6. REFERENCES:

1. Açikyildiz, M., Gürses, A., Güneş, K., and Yalvaç, D. (2015). A comparative examination of the adsorption mechanism of an anionic textile dye (RBY 3GL) onto the powdered activated carbon (PAC) using various the isotherm models and kinetics equations with linear and nonlinear methods. *Applied Surface Science*. https://doi.org/10.1016/j.apsusc.2015.07.021
2. Ahmedzeki, N. S., Rashid, H. A., Alnaama, A. A., Alhasani, M. H., and Abdulhussain, Z. (2013). Removal of 4-nitro-phenol from wastewater using synthetic zeolite and kaolin clay. *Korean Journal of Chemical Engineering*, *30*(12), 2213–2218. https://doi.org/10.1007/s11814-013-0165-x
3. Al-Jlil, S. A., and Latif, M. S. (2013). Evaluation of equilibrium isotherm models for the adsorption of Cu and Ni from wastewater on bentonite clay. *Materiali in Tehnologije*.
4. Alexander, J. A., Ahmad Zaini, M. A., Surajudeen, A., Aliyu, E. N. U., and Omeiza, A. U. (2018). Insight into kinetics and thermodynamics properties of multicomponent lead(II), cadmium(II) and manganese(II) adsorption onto Dijah-Monkin bentonite clay. *Particulate Science and Technology*. https://doi.org/10.1080/02726351.2016.1276499
5. Armagan, B., and Toprak, F. (2013). Optimum isotherm parameters for reactive azo dye onto pistachio nut shells: Comparison of linear and nonlinear methods. *Polish Journal of Environmental Studies*.
6. Bahabadi, F. N., Farpoor, M. H., and Mehrizi, M. H. (2017). Removal of Cd, Cu and Zn ions from aqueous solutions using natural and Fe modified sepiolite, zeolite and palygorskite clay minerals. *Water Science and Technology*. https://doi.org/10.2166/wst.2016.522
7. Batool, F., Akbar, J., Iqbal, S., Noreen, S., and Bukhari, S. N. A. (2018). Study of

Isothermal, Kinetic, and Thermodynamic Parameters for Adsorption of Cadmium: An Overview of Linear and Nonlinear Approach and Error Analysis. *Bioinorganic Chemistry and Applications*. https://doi.org/10.1155/2018/3463724

8. Burakov, A. E., Galunin, E. V., Burakova, I. V., Kucherova, A. E., Agarwal, S., Tkachev, A. G., and Gupta, V. K. (2018). Adsorption of heavy metals on conventional and nanostructured materials for wastewater treatment purposes: A review. *Ecotoxicology and Environmental Safety*, *148*, 702–712. https://doi.org/10.1016/j.ecoenv.2017.11.034
9. Ciosek, A. L., Luk, G. K., Warner, M., and Warner, R. A. (2016). An Innovative Design of a Clay-Zeolite Medium for the Adsorption of Total Phosphorus from Wastewater. *Water Environment Research*, *88*(2), 131–142. https://doi.org/10.2175/106143015X14338845155787
10. Crini, G., Lichtfouse, E., Wilson, L. D., and Morin-Crini, N. (2018). *Adsorption-Oriented Processes Using Conventional and Non-conventional Adsorbents for Wastewater Treatment*. https://doi.org/10.1007/978-3-319-92111-2_2
11. Długosz, O., and Banach, M. (2018). Kinetic, isotherm and thermodynamic investigations of the adsorption of Ag+ and Cu2+ on vermiculite. *Journal of Molecular Liquids*, *258*, 295–309. https://doi.org/10.1016/j.molliq.2018.03.041
12. Dotto, G. L., Salau, N. P. G., Piccin, J. S., Cadaval, T. R. S., and de Pinto, L. A. A. (2017). Adsorption Kinetics in Liquid Phase: Modeling for Discontinuous and Continuous Systems. In *Adsorption Processes for Water Treatment and Purification* (pp. 53–76). https://doi.org/10.1007/978-3-319-58136-1_3
13. Foo, K. Y., and Hameed, B. H. (2010). Insights into the modeling of adsorption isotherm systems. *Chemical Engineering Journal*, *156*(1), 2–10. https://doi.org/10.1016/j.cej.2009.09.013
14. Gao, Y., Chen, N., Hu, W., Feng, C., Zhang, B., Ning, Q., and Xu, B. (2013). Phosphate Removal from Aqueous Solution by an Effective Clay Composite Material. *Journal of Solution Chemistry*, *42*(4), 691–704. https://doi.org/10.1007/s10953-013-9985-x
15. Ghaffari, H. R., Pasalari, H., Tajvar, A., Dindarloo, K., Goudarzi, B., Alipour, V., and Ghanbarneajd, A. (2017). Linear and nonlinear two-parameter adsorption isotherm modeling: a case-study. *Int. J. Eng. Sci.*, *6*(9), 01–11.
16. Gusain, D., Srivastava, V., Sillanpää, M., and Sharma, Y. C. (2016). Kinetics and isotherm study on adsorption of chromium on nano crystalline iron oxide/hydroxide: linear and nonlinear analysis of isotherm and kinetic parameters. *Research on Chemical Intermediates*, *42*(9), 7133–7151. https://doi.org/10.1007/s11164-016-2523-x
17. Ho, Y. ., and McKay, G. (1999). Pseudo-second order model for sorption processes. *Process Biochemistry*, *34*(5), 451–465. https://doi.org/10.1016/S0032-9592(98)00112-5
18. Hofmeister, A. M., and Bowey, J. E. (2006). Quantitative Infrared Spectra of Hydrosilicates and Related Minerals. *Monthly Notices of the Royal Astronomical Society*, *367*(2), 577–591. https://doi.org/10.1111/j.1365-2966.2006.09894.x
19. Ismadji, S., Soetaredjo, F. E., and Ayucitra, A. (2015). *Clay Materials for Environmental Remediation*. https://doi.org/10.1007/978-3-319-16712-1
20. K. Abu-Hawwas, J., M. Ibrahim, K., and M. Musleh, S. (2018). Characterization of Jordanian Porcelanite Rock with Reference to the Adsorption Behavior of Lead Ions from Aqueous Solution. *Oriental Journal of Chemistry*, *34*(2), 663–674. https://doi.org/10.13005/ojc/340208
21. Khalid, A., Kazmib, M. ., Habibc, M., Jabeena, S., and Shahzadd, K. (2015). Kinetic and equilibrium modelling of copper biosorption. *Journal of Faculty of Engineering and Technology*, *22*(1), 131–145.
22. Krupskaya, V., Novikova, L., Tyupina, E., Belousov, P., Dorzhieva, O., Zakusin, S., … Belchinskaya, L. (2019). The influence

of acid modification on the structure of montmorillonites and surface properties of bentonites. *Applied Clay Science*, *172*, 1–10. https://doi.org/10.1016/j.clay.2019.02.001

23. Kurniawan, A., Ismadji, S., Soetaredjo, F. ., and Ayucitra, A. (2014). Natural clays/clay minerals and modified forms for heavy metals removal. In R. S. of Chemistry (Ed.), *Heavy Metals in Water: Presence, Removal and Safety* (First Edit, p. 380). Cambridge, United Kingdom.

24. López-Luna, J., Ramírez-Montes, L. E., Martinez-Vargas, S., Martínez, A. I., Mijangos-Ricardez, O. F., González-Chávez, M. del C. A., … Vázquez-Hipólito, V. (2019). Linear and nonlinear kinetic and isotherm adsorption models for arsenic removal by manganese ferrite nanoparticles. *SN Applied Sciences*, *1*(8), 950. https://doi.org/10.1007/s42452-019-0977-3

25. Madejová, J., Gates, W. P., and Petit, S. (2017). *IR Spectra of Clay Minerals*. https://doi.org/10.1016/B978-0-08-100355-8.00005-9

26. Mallakpour, S., and Rashidimoghadam, S. (2019). Poly(vinyl alcohol)/Vitamin C-multi walled carbon nanotubes composites and their applications for removal of methylene blue: Advanced comparison between linear and nonlinear forms of adsorption isotherms and kinetics models. *Polymer*, *160*, 115–125. https://doi.org/10.1016/j.polymer.2018.11.035

27. Mejia Miranda, C., Laverde, D., Avella, V., and Peña Ballesteros, D. Y. (2015). Adsorción de iones Ni(II) sobre una arcilla bentonítica peletizada. *Revista ION*, *28*(2), 61–68. https://doi.org/10.18273/revion.v28n2-2015005

28. Melichová, Z., and Ľuptáková, A. (2016). Removing lead from aqueous solutions using different low-cost abundant adsorbents. *Desalination and Water Treatment*, *57*(11), 5025–5034. https://doi.org/10.1080/19443994.2014.999713

29. Milenković, D., Milosavljević, M., Marinković, A., Đokić, V., Mitrović, J., and Bojić, A. L. (2013). Removal of copper(II) ion from aqueous solution by high-porosity activated carbon. *Water SA*, *39*(4). https://doi.org/10.4314/wsa.v39i4.10

30. Mosai, A. K., and Tutu, H. (2019). The effect of crop exudates and EDTA on cadmium adsorption by agricultural podsolic soil: implications on groundwater. *International Journal of Environmental Science and Technology*, *16*(7), 3071–3080. https://doi.org/10.1007/s13762-018-1927-0

31. Mu'azu, N. D., Bukhari, A., and Munef, K. (2020). Effect of montmorillonite content in natural Saudi Arabian clay on its adsorptive performance for single aqueous uptake of Cu(II) and Ni(II). *Journal of King Saud University - Science*, *32*(1), 412–422. https://doi.org/10.1016/j.jksus.2018.06.003

32. Nikolic, M., Jeffry Robert, R., and Girish, C. R. (2019). The Adsorption of Cadmium, Nickel, Zinc, Copper and Lead from Wastewater using Tea Fiber Waste. *Journal of Engineering and Applied Sciences*, *14*(20), 7743–7755. https://doi.org/10.36478/jeasci.2019.7743.7755

33. Novikova, L., and Belchinskaya, L. (2016). Adsorption of Industrial Pollutants by Natural and Modified Aluminosilicates. In *Clays, Clay Minerals and Ceramic Materials Based on Clay Minerals*. https://doi.org/10.5772/61678

34. Padmavathy, K., and Murali, A. (2017). Adsorption of hexavalent chromium (Cr (VI)) from wastewater using novel chitosan/halloysite clay nanocomposite films. *Indian Journal of Chemical Technology*, *24*(6), 593–600.

35. Renu, Agarwal, M., and Singh, K. (2017). Heavy metal removal from wastewater using various adsorbents: a review. *Journal of Water Reuse and Desalination*, *7*(4), 387–419. https://doi.org/10.2166/wrd.2016.104

36. Rostami, M., Pourzamani, H., Bina, B., and Karimi, H. (2019). Linear and nonlinear isotherm modeling of nitrate removal from aqueous solution by alternating current electrocoagulation. *International Journal of Environmental Health Engineering*, *8*(1), 2. https://doi.org/10.4103/ijehe.ijehe_9_17

37. Sadeghalvad, B., Khosravi, S., and Azadmehr, A. R. (2016). Nonlinear isotherm and kinetics of adsorption of

copper from aqueous solutions on bentonite. *Russian Journal of Physical Chemistry A*, *90*(11), 2285–2291. https://doi.org/10.1134/S00360244161100 30

38. Salem, A., and Akbari Sene, R. (2012). Optimization of zeolite-based adsorbent composition for fabricating reliable Raschig ring shaped by extrusion using Weibull statistical theory. *Microporous and Mesoporous Materials*, *163*, 65–75. https://doi.org/10.1016/j.micromeso.2012. 06.026
39. Salmani, M. H., Sahlabadi, F., Eslami, H., Ghaneian, M. T., Balaneji, I. R., and Zad, T. J. (2019). Removal of Cr(VI) oxoanion from contaminated water using granular jujube stems as a porous adsorbent. *Groundwater for Sustainable Development*, *8*, 319–323. https://doi.org/10.1016/j.gsd.2018.12.001
40. Schwantes, D., Gonçalves, A. C., Coelho, G. F., Campagnolo, M. A., Dragunski, D. C., Tarley, C. R. T., … Leismann, E. A. V. (2016). Chemical Modifications of Cassava Peel as Adsorbent Material for Metals Ions from Wastewater. *Journal of Chemistry*, *2016*, 1–15. https://doi.org/10.1155/2016/3694174
41. Shaban, M., and Abukhadra, M. R. (2017). Geochemical evaluation and environmental application of Yemeni natural zeolite as sorbent for Cd2+ from solution: kinetic modeling, equilibrium studies, and statistical optimization. *Environmental Earth Sciences*, *76*(8), 310. https://doi.org/10.1007/s12665-017-6636-3
42. Soleimani, M., and Siahpoosh, Z. H. (2015). Ghezeljeh nanoclay as a new natural adsorbent for the removal of copper and mercury ions: Equilibrium, kinetics and thermodynamics studies. *Chinese Journal of Chemical Engineering*, *23*(11), 1819–1833. https://doi.org/10.1016/j.cjche.2015.08.02 4
43. Uddin, M. K. (2017). A review on the adsorption of heavy metals by clay minerals, with special focus on the past decade. *Chemical Engineering Journal*, *308*, 438–462. https://doi.org/10.1016/j.cej.2016.09.029
44. Worch, E. (2012). *Adsorption technology in water treatment* (W. de Gruyter, ed.). Beriln.
45. Yousefi, T., Abas Mohsen, M., Mahmudian, H. R., Torab-Mostaeidi, M., Moosavian, M. A., and Aghayan, H. (2018). Removal of Pb(II) by Modified Natural Adsorbent; Thermodynamics and Kinetics Studies. *J. Water Environ. Nanotechnol*, *3*(3), 265–272. https://doi.org/10.22090/jwent.2018.03.00 7
46. Zhao, M., Xu, Y., Zhang, C., Rong, H., and Zeng, G. (2016). New trends in removing heavy metals from wastewater. *Applied Microbiology and Biotechnology*, *100*(15), 6509–6518. https://doi.org/10.1007/s00253-016-7646-x

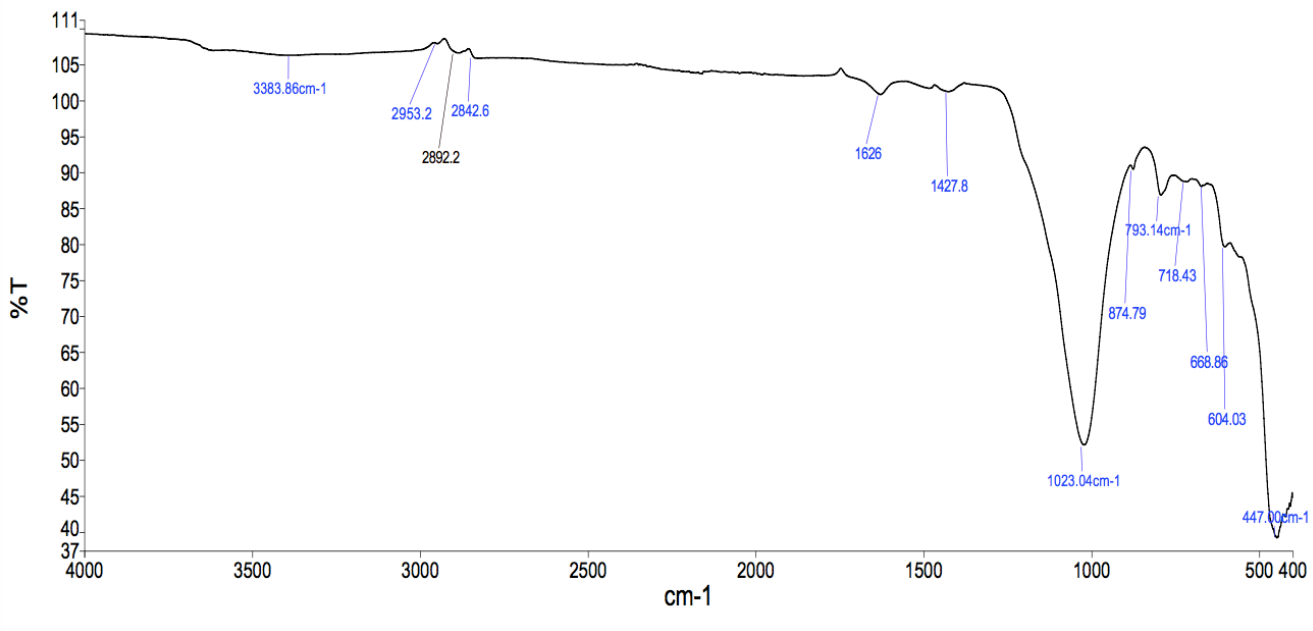


***Figure 1.*** *FTIR spectra of adsorbent pellets*

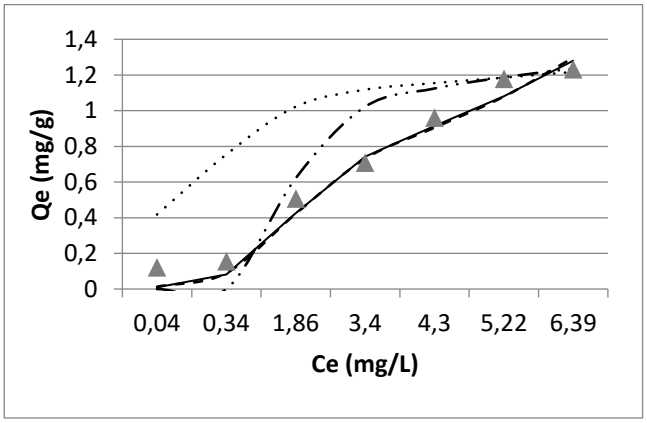


***(a)***

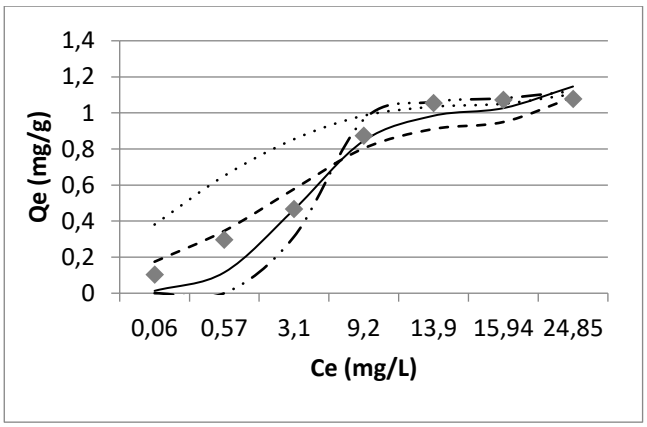


***(b)***

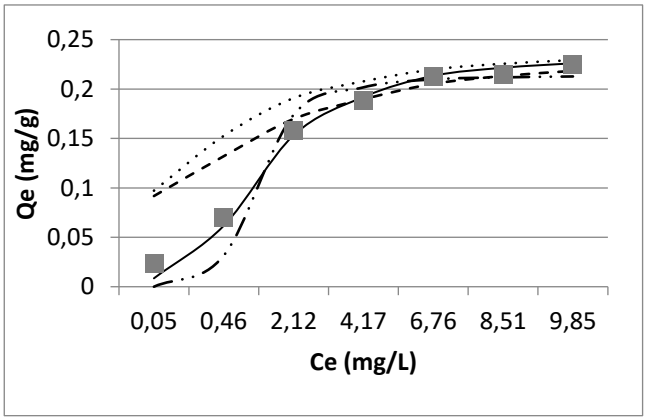


***(c)***

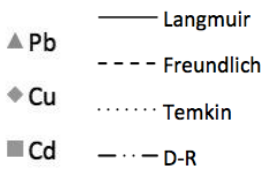


***Figure 2.*** *Adsorption equilibrium curves with nonlinear regression for lead (a), copper (b), and cadmium (c)*

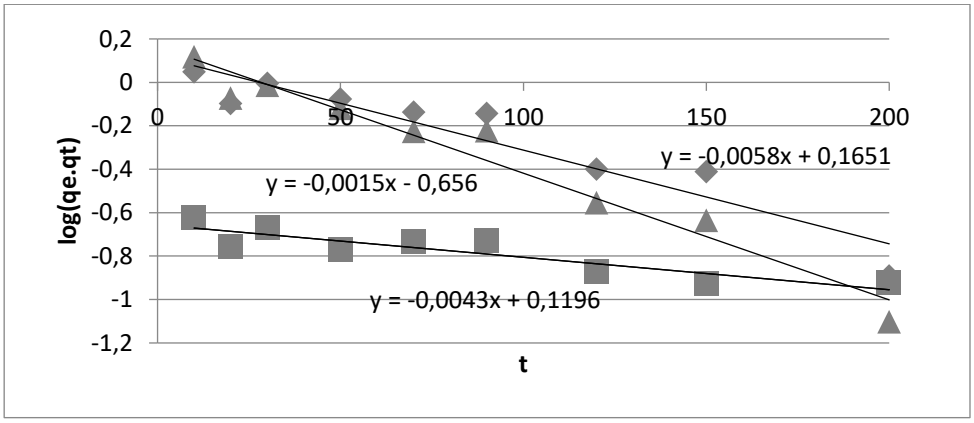


**(a)**

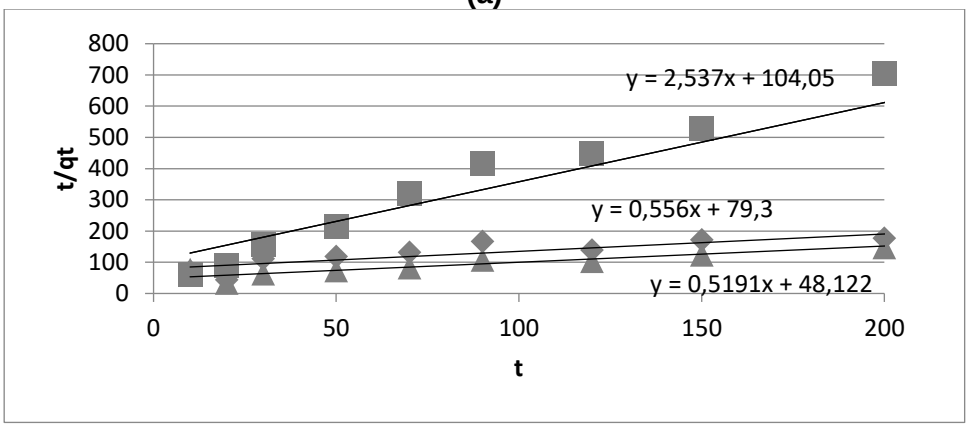


**(b)**

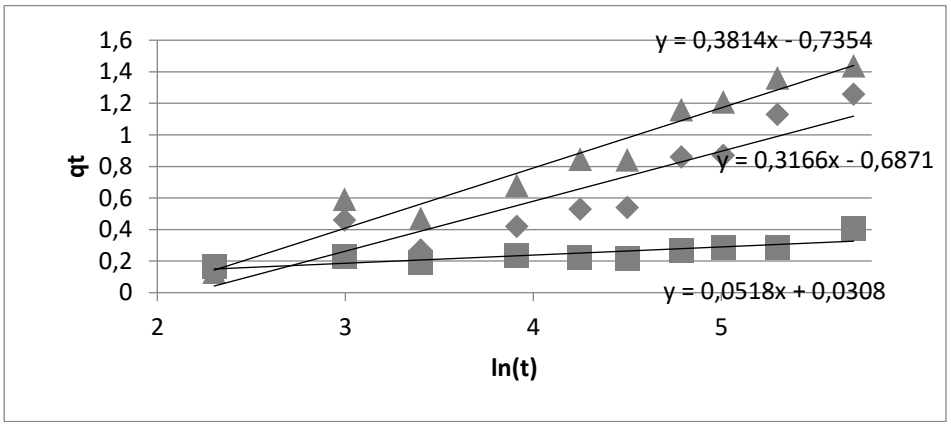


**(c)**

▲ Pb

◆ Cu

■ Cd

**Figure 3.** *Linear regression of PFO (a), PSO (b), and Elovich (c) models*

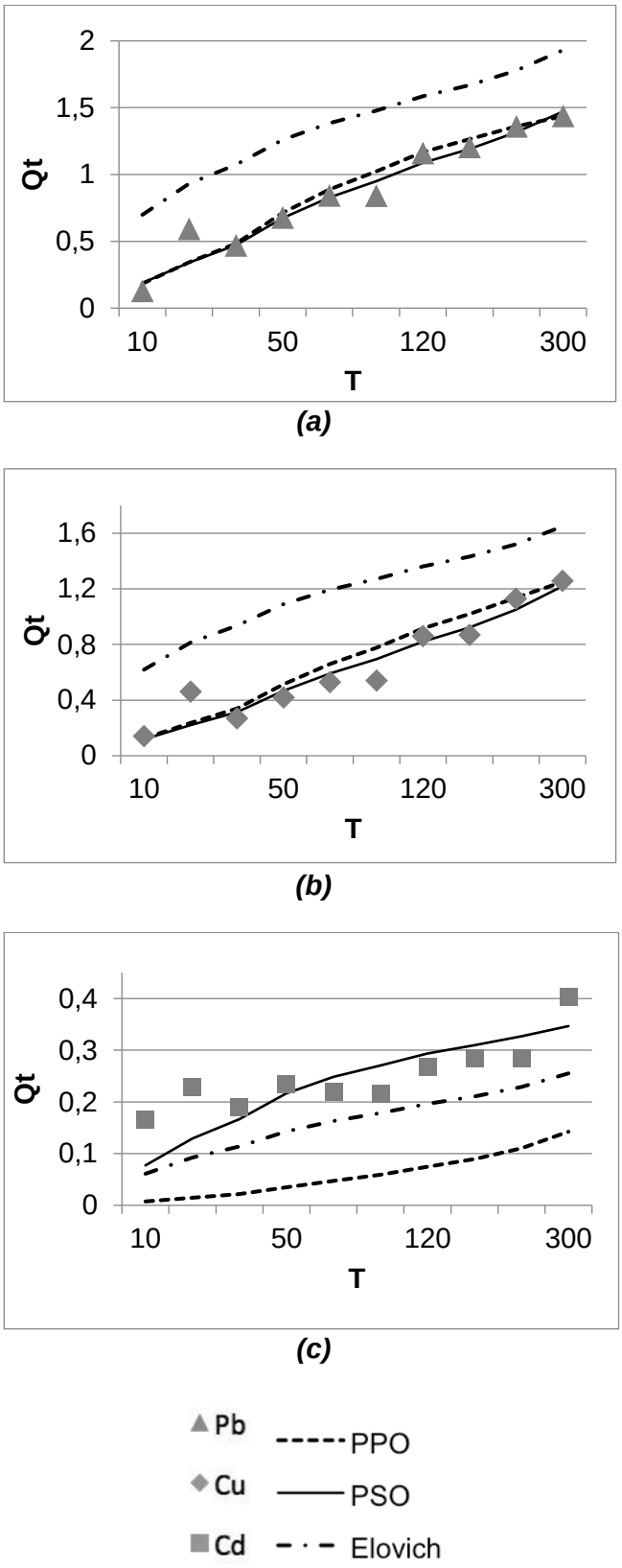


***Figure 4.*** *Linear regression curves of kinetic models for lead (a), copper (b), and cadmium (c)*

***Table 4.*** *Adsorption parameters and error functions for Langmuir equations type I, II, III and IV*

| Model | Parameters | Pb | Cu | Cd |
|---|---|---|---|---|
| Langmuir Type I | $Q_{max}$ (mg/g) | 1.59 | 1.18 | 0.24 |
| | $K_L$ (L/mg) | 0.38 | 0.43 | 1.07 |
| | $R^2$ | 0.924 | 0.943 | 0.991 |
| | $X^2$ | 1.000 | 1.000 | 1.000 |
| | SSE | 15.420 | 14.847 | 0.641 |
| | ABS | 0.720 | 0.499 | 0.046 |
| | ARE | 25.179 | 21.776 | 10.743 |
| Langmuir Type II | $Q_{max}$ (mg/g) | 0.55 | 0.74 | 0.18 |
| | $K_L$ (L/mg) | 6.68 | 2.64 | 2.92 |
| | $R^2$ | 0.585 | 0.754 | 0.915 |
| | $X^2$ | 0.971 | 0.754 | 0.915 |
| | SSE | 8.937 | 0.998 | 1.000 |
| | ABS | 2.180 | 10.802 | 0.539 |
| | ARE | 47.347 | 1.543 | 0.187 |
| Langmuir Type III | $Q_{max}$ (mg/g) | 0.87 | 0.92 | 0.21 |
| | $K_L$ (L/mg) | 3.79 | 1.85 | 2.26 |
| | $R^2$ | 0.663 | 0.800 | 0.941 |
| | $X^2$ | 0.981 | 0.999 | 1.000 |
| | SSE | 12.921 | 13.107 | 0.603 |
| | ABS | 1.582 | 1.057 | 0.114 |
| | ARE | 51.532 | 26.926 | 13.996 |
| Langmuir Type IV | $Q_{max}$ (mg/g) | 1.16 | 1.03 | 0.22 |
| | $K_L$ (L/mg) | 1.42 | 1.18 | 1.83 |
| | $R^2$ | 0.793 | 0.853 | 0.960 |
| | $X^2$ | 0.994 | 0.999 | 1.000 |
| | SSE | 15.597 | 14.423 | 0.625 |
| | ABS | 1.249 | 0.824 | 0.092 |
| | ARE | 46.458 | 25.498 | 13.377 |

***Table 5.*** *Equilibrium models error functions of with linear and nonlinear regression*

| Model | | Lead | | Copper | | Cadmium | |
|---|---|---|---|---|---|---|---|
| | | **Linear** | **Nonlinear** | **Linear** | **Nonlinear** | **Linear** | **Nonlinear** |
| Langmuir | $R^2$ | 0.585 | 0.987 | 0.754 | 0.981 | 0.915 | 0.999 |
| | $X^2$ | 0.971 | 1 | 0.998 | 1 | 1 | 1 |
| | SSE | 8.937 | 15.168 | 10.802 | 14.275 | 0.539 | 0.638 |
| | ABS | 2.18 | 0.494 | 1.543 | 0.482 | 0.187 | 0.04 |
| | ARE | 47.347 | 25.354 | 29.728 | 24.127 | 17.385 | 12.043 |
| Freundlich | $R^2$ | 0.953 | 0.986 | 0.962 | 0.968 | 0.954 | 0.987 |
| | $X^2$ | 0.893 | 1 | 0.826 | 1 | 0.986 | 1 |
| | SSE | 6.311 | 15.183 | 5.223 | 13.59 | 0.177 | 0.640 |
| | ABS | 3.312 | 0.502 | 3.756 | 0.577 | 1.042 | 0.158 |
| | ARE | 65.454 | 24.455 | 75.963 | 20.839 | 95.393 | 56.663 |
| Temkin | $R^2$ | 0.783 | 0.783 | 0.912 | 0.912 | 0.972 | 0.972 |
| | $X^2$ | 0.783 | 0.701 | 0.293 | 0.958 | 0.897 | 0.999 |
| | SSE | 0.025 | 18.922 | 27.379 | 15.843 | 1.33 | 0.693 |
| | ABS | 32.24 | 2.036 | 4.432 | 1.2 | 1.174 | 0.231 |
| | ARE | 239.701 | 24.455 | 166.445 | 70.823 | 193.188 | 67.984 |
| D-R | $R^2$ | 0.553 | 0.925 | 0.609 | 0.974 | 0.8 | 0.973 |
| | $X^2$ | 0.553 | 0.998 | 0.988 | 0.998 | 0.99 | 1 |
| | SSE | 0.963 | 17.147 | 8.695 | 14.791 | 0.192 | 0.640 |
| | ABS | 8.226 | 0.883 | 2.105 | 0.703 | 0.981 | 0.108 |
| | ARE | 53.653 | 49.691 | 39.471 | 35.56 | 88.828 | 25.697 |

***Table 6.*** *Lead, copper and cadmium isotherm models linear and nonlinear parameters*

| Model | Parameters | Pb | | Cu | | Cd | |
|---|---|---|---|---|---|---|---|
| | | **Linear** | **Nonlinear** | **Linear** | **Nonlinear** | **Linear** | **Nonlinear** |
| Langmuir Type I | $Q_{max}$ (mg/g) | 1.59 | 7.27 | 1.18 | 1.45 | 0.24 | 0.26 |
| | $K_L$ (L/mg) | 0.38 | 0.03 | 0.43 | 0.15 | 1.07 | 0.68 |
| | $R_L$ | 0.55-0.94 | 0.10-0.58 | 0.14-0.81 | 0.05-0.59 | 0.10-0.79 | 0.07-0.70 |
| | $R^2$ | 0.923 | 0.987 | 0.943 | 0.981 | 0.991 | 0.999 |
| Freundlich | $K_F$(mg/g).(L/mg)$^{(1/n)}$ | 0.14 | 0.24 | 2.47 | 0.41 | 0.004 | 0.15 |
| | N | 2.04 | 1.09 | 0.08 | 3.30 | 2.31 | 6.09 |
| | $R^2$ | 0.953 | 0.986 | 0.962 | 0.968 | 0.954 | 0.987 |
| Temkin | $B_T$ (J/mol) | 0.22 | 0.16 | 0.18 | 0.12 | 0.04 | 0.03 |
| | $A_T$ (L/g) | 704.12 | 354.66 | 525.05 | 398.13 | 1561.52 | 974.9 |
| | $R^2$ | 0.783 | 0.783 | 0.912 | 0.912 | 0.972 | 0.972 |
| D-R | β(mol$^2$/kJ$^2$) | 0.03 | 0.67 | 0.04 | 2.67 | 0.04 | 0.23 |
| | $Q_{max}$(mol/g) | 0.48 | 1.35 | 0.55 | 1.15 | 0.02 | 0.22 |
| | E(kJ/mol) | 4.07 | 0.86 | 3.48 | 0.43 | 3.68 | 1.47 |
| | $R^2$ | 0.553 | 0.925 | 0.609 | 0.974 | 0.800 | 0.973 |

***Table 7.*** *Kinetic model error functions of with linear and nonlinear regression*

| Model | | Pb | | Cu | | Cd | |
|---|---|---|---|---|---|---|---|
| | | **Linear** | **Nonlinear** | **Linear** | **Nonlinear** | **Linear** | **Nonlinear** |
| PFO | $R^2$ | 0.942 | 0.950 | 0.899 | 0.942 | 0.843 | 0.892 |
| | $X^2$ | 1.000 | 1.000 | 1.000 | 0.984 | 0.240 | 0.000 |
| | SSE | 34.156 | 30.888 | 21.290 | 14.093 | 0.974 | 0.613 |
| | ABS | 0.645 | 1.015 | 0.986 | 2.375 | 1.890 | 2.492 |
| | ARE | 17.444 | 17.174 | 27.637 | 45.993 | 85.162 | 102.999 |
| PSO | $R^2$ | 0.950 | 0.950 | 0.918 | 0.940 | 0.625 | 0.680 |
| | $X^2$ | 1.000 | 1.000 | 1.000 | 0.933 | 1.000 | 0.999 |
| | SSE | 32.915 | 32.522 | 19.736 | 12.459 | 2.192 | 1.539 |
| | ABS | 0.605 | 0.662 | 0.778 | 2.977 | 0.461 | 0.965 |
| | ARE | 14.923 | 15.298 | 20.320 | 53.996 | 23.784 | 46.472 |
| Elovich | $R^2$ | 0.950 | 0.952 | 0.862 | 0.939 | 0.702 | 0.892 |
| | $X^2$ | 0.989 | 1.000 | 0.972 | 0.045 | 1.000 | 0.000 |
| | SSE | 50.355 | 32.278 | 33.483 | 8.032 | 1.903 | 0.613 |
| | ABS | 5.066 | 0.965 | 5.410 | 4.883 | 0.333 | 2.491 |
| | ARE | 127.619 | 31.310 | 165.581 | 80.483 | 13.577 | 102.983 |

***Table 8.*** *Kinetic models parameters and coefficients of determination*

| Model | Parameters | Pb | | Cu | | Cd | |
|---|---|---|---|---|---|---|---|
| | | **Linear** | **Nonlinear** | **Linear** | **Nonlinear** | **Linear** | **Nonlinear** |
| PFP | $Q_e$ (mg/g) | 1.46 | 1.46 | 1.32 | 1.32 | 0.22 | 0.67 |
| | $k_1$ (1/min) | 0.01 | 1.00E-02 | 0.01 | 4.14E-03 | 3.45E-03 | 7.61E-08 |
| | $R^2$ | 0.942 | 0.950 | 0.899 | 0.942 | 0.843 | 0.889 |
| PSO | $Q_e$ (mg/g) | 1.93 | 1.93 | 1.80 | 1.80 | 0.39 | 0.30 |
| | $k_2$ (g.mg$^{-1}$*min$^{-1}$) | 5.60E-03 | 5.43E-03 | 3.90E-03 | 1.48E-03 | 0.06 | 0.05 |
| | $R^2$ | 0.950 | 0.950 | 0.918 | 0.940 | 0.625 | 0.680 |
| Elovich | $Q_e$ (mg/g) | 0.20 | 0.05 | 0.19 | 2.29E-03 | 0.05 | 6.10E-07 |
| | $k_e$ (1/min) | 2.62 | 2.61 | 3.16 | 3.15 | 19.31 | 0.03 |
| | $R^2$ | 0.950 | 0.952 | 0.862 | 0.939 | 0.702 | 0.892 |

PERIÓDICO TCHÊ QUÍMICA
ARTIGO ORIGINAL

# MITIGAÇÃO DA TOXICIDADE DE ALUMÍNIO EM MUDAS DE *GLYCYRRHIZA GLABRA* L. USANDO SILÍCIO

# MITIGATING ALUMINUM TOXICITY IN SEEDLINGS OF *GLYCYRRHIZA GLABRA* L. USING SILICON

# بهبود سمیت آلومینیوم در گیاهچه‌های *GLYCYRRHIZA GLABRA* L. با استفاده از سیلیکون

YAZDANI, Mojtaba[1]; SAADATMAND, Sara[2]*; ENTESHARI, Shekoofeh[3]; HABIBOLAHI, Saeed[4];

[1,2] Department of Biology, Science and Research Branch, Islamic Azad University, Tehran, Iran

[3] Department of Biology, Payame Noor University, Tehran, Iran

[4] Department of Chemistry, Payame Noor University, Tehran, Iran

** Corresponding author*
*e-mail: saadatmand.srbiau@gmail.com*

Received 19 November 2020; received in revised form 08 February 2021; accepted 14 February 2021

## RESUMO

**Introdução:** O silício é um elemento benéfico para a planta, com papel primordial no aumento da resistência da planta à toxicidade de metais pesados e considerando a importância da fitorremediação para remover metais pesados de solos contaminados. Pode ser usado para a aplicação exógena para aliviar os efeitos nocivos dos metais pesados na planta. **Objetivo:** Este estudo teve como objetivo investigar o papel do silício no equilíbrio dos efeitos destrutivos do alumínio em *Glycyrrhiza Glabra* L. **Métodos:** as mudas foram cultivadas em sistema hidropônico com solução nutritiva Long Ashton; as mudas com 15 dias de idade foram expostas ao silício (0, 0,5, 1,5 mM) por 110 dias e, posteriormente, estressadas por interações de cloreto de alumínio ($AlCl_3.6H_2O$; 0, 100, 250 e 400 M). **Resultados e Discussão:** os efeitos interativos do silício melhoraram significativamente as consequências negativas da toxicidade do alumínio. A combinação de Si 1,5 mM e Al 400 µM produziu a maior biomassa na parte aérea (45,67 g). O simples efeito do Si 1,5 mM (12,14 g) proporcionou o maior peso seco da parte aérea. Por outro lado, a maior quantidade de massa fresca e seca de raiz (12,52 e 3,22 g, respectivamente) foi observada em Si 1,5 mM. Entre os tratamentos, Si 0,5 mM + Al 100 µM apresentou a maior altura do caule (38 cm) entre os tratamentos de interação. Da mesma forma, os pigmentos fotossintéticos afetados pelo silício, Al 250 µM + Si 1,5 mM apresentaram o maior teor de clorofila a (1,91 µg / g FW), enquanto Al 400 + 1,5 mM indicou o maior aumento na clorofila b (0,78 µg / g FW) entre os efeitos de interação. Este tratamento, ao produzir 0,663 µg/g FW, rendeu o maior teor de carotenóides. Os maiores teores de prolina na parte aérea e nas raízes (69,54 e 81,46 µg/g FW, respectivamente) foram observados na interação de Al 400 µM e Si 1,5 mM. Além disso, observou-se que esse tratamento apresentou a maior concentração de catalase (1,22 U/mg proteína). O menor conteúdo de malondialdeído foi marcado em Si 1,5 mM + Al 100 µM (0,702 nM/g FW). **Conclusões:** no geral, *Glycyrrhiza Glabra* L. parece ter alto potencial de fitorremediação de Al, que pode ser aprimorado com a aplicação exógena de um nível moderado de silício.

**Palavras-chave**: *estresse abiótico, MDA, prolina, alcaçuz, metais pesados.*

## ABSTRACT

**Background:** Silicon is a beneficial element for the plant, with the primary role in increasing plant resistance to heavy metals' toxicity and considering the importance of phytoremediation to remove heavy metals from contaminated soils. It could be used for the exogenous application for alleviating the harmful effects of heavy metals on the plant. **Aim:** This study aimed to investigate the role of Silicon in balancing the destructive effects of aluminum on *Glycyrrhiza glabra* L. **Methods:** the seedlings were grown under a hydroponic system using Long Ashton nutrient solution; the 15-day-old seedlings were exposed to Silicon (0, 0.5, 1.5 mM) for 110 days and afterward stressed by interactions of aluminum chloride ($AlCl_3.6H_2O$; 0, 100, 250, and 400 M). **Result and Discussion:** the interactive effects of Silicon significantly ameliorated the negative consequences of aluminum toxicity. The combination of Si 1.5 mM and Al 400 µM produced the highest biomass in shoots (45.67 g). The

simple effect of Si 1.5 mM (12.14 g) made the highest shoot dry weight. On the other hand, the highest quantity of root fresh and dry weight (12.52 and 3.22 g, respectively) was observed in Si 1.5 mM. Among the treatments, Si 0.5 mM + Al 100 µM had the most stem height (38 cm) among interaction treatments. Similarly, photosynthetic pigments affected by Silicon, Al 250 µM + Si 1.5 mM had the highest content of chlorophyll a (1.91 µg/g FW), while Al 400 + 1.5 mM indicated the most increase in chlorophyll b (0.78 µg/g FW) among interaction effects. This treatment by producing 0.663 µg/g FW yielded the highest carotenoid content. The highest proline content in shoots and roots (69.54 and 81.46 µg/g FW, respectively) were observed in the interaction of Al 400 µM and Si 1.5 mM. Additionally, this treatment was observed to have the highest concentration of catalase (1.22 U/mg protein). The lowest malondialdehyde content was marked in Si 1.5 mM + Al 100 µM (0.702 nM/g FW). **Conclusion:** overall, *Glycyrrhiza Glabra* L. seems to have high Al phytoremediation potential that can be enhanced with the exogenous application of a moderate Silicon level.

***Keywords****: abiotic stress, MDA, proline, licorice, heavy metals*

**چکیده**

**پیشنه تحقیق:** سیلیکون عنصری مفید برای گیاه است که مهمترین نقش آن افزایش مقاومت گیاه به سمیت فلزات سنگین است. با توجه به اهمیت گیاه پالایی برای حذف فلزات سنگین از خاک‌های آلوده، این می‌تواند برای اعمال خارجی روی گیاهان و کاهش اثرات منفی فلزات سنگین استفاده گردد. **هدف:** این بررسی مطالعه نقش سیلیکون در توازن اثرات مخرب آلومینیوم بر نهال‌های *Glycyrrhiza glabra* L. را دنبال نمود. **روش‌ها:** نهال‌ها تحت سیستم هیدروپونیک و محلول تغذیه‌ای لانگ اشتون پرورش یافتند؛ نهال‌های پانزده روزه به مدت 110 روز در معرض سطوح مختلف سیلیکون (1/5، 0/5، 0 میلی مول ) قرار گرفتند، سپس با اثرات منفرد و متقابل کلرید آلومینیوم (400، 250، 100، 0 میکرومول) مورد استرس قرار گرفتند. **نتایج و بحث:** اثرات متقابل سیلیکون به طور قابل توجهی تاثیرات منفی سمیت آلومینیوم را بهبود بخشید. اثر متقابلAl 400µM + Si 1/5 mM بیشترین میزان تولید توده زیستی را داشته است (67/45 گرم). در حالیکه اثر ساده Si 1/5 mM (12/14 گرم) بیشترین وزن خشک شاخساره را داشت. از سوی دیگر، بیشترین وزن تر و خشک ریشه (12/52 و 3/22 گرم) در Si 1/5 mM مشاهده گردید. نهال‌های تیمار شده با Al 100µM + Si 0/5 mM از بالاترین ارتفاع (38 سانتی متر) برخوردار بودند. به طور مشابه، رنگدانه های فتوسنتزی نیز تحت تأثیر سیلیکون قرار گرفتند که در آنها اثر متقابل Al 250µM + Si 1/5 mM با 1/91 µg/g FW بیشترین مقدار کلروفیل a را دارا بود، در حالیکه، Al 400µM + Si 1/5 mM بیشترین میزان افزایش میزان کلروفیل b را در میان اثرهای متقابل به همراه داشت (0/78 µg/g FW). این تیمار با تولید 0/663 µg/g FW، بیشترین میزان محتوای کارتنوئید را داشته است. بیشترین پرولین در ساقه و ریشه (به ترتیب 81/46 و 69/54 µg/g FW) در اثر متقابل Al 400µM + Si 1/5 mM مشاهده گردید، همچنین بیشترین میزان فعالیت آنزیم کاتالاز (1/22 U/mg protein) در این تیمار مشاهده گردید. کمترین میزان مالون دی آلدئید در همین تیمار متقابلAl 100µM + Si 1/5 mM مشاهده شد (0/702 nM/g FW). **نتیجه‌گیری:** به طور کلی، به نظر می رسد که *Glycyrrhiza glabra* L. دارای پتانسیل بالایی برای گیاه پالایی آلومینیوم برخوردار است که می تواند با اعمال خارجی سیلیکون افزایش یابد.

***کلیدواژه:*** *تنش غیرزیستی، پرولین، MDA، شیرین بیان، فلزات سنگین*

---

## 1. INTRODUCTION:

Various physical, chemical, and biological approaches have been proposed to refrain from contaminated areas with heavy metals and other pollutants, mostly cost-intensive and inefficient. One of the detoxification methods and the reduction of toxic substances, including heavy metals in the contaminated environments, is utilizing accumulating plants in so-called phytoremediation (Lombi *et al.*, 2001; Ali *et al.*, 2013; Mahar *et al.*, 2016). An approach for removing heavy metals and other pollutants from soil and water systems. This procedure utilizes plant species that can uptake and accumulate heavy metals in their tissues, and they can grow at a concentration of 10 to 100 times that of plants crop tolerant of accumulating. One of the benefits of phytoremediation in this way is the preservation of the soil building and fertility after harvesting heavy metals and finally is a reliable alternative solution to energy-intensive and cost-effective engineering methods (Ghosh and Singh, 2005; Chehregani *et al.*, 2009; Jabeen *et al.*, 2009; Mahar *et al.*, 2016). Phytoremediation is a cost-effective, environmental, and scientific technique, especially for developing countries. Unfortunately, despite this potential, some countries, such as Iran, have not received the attention it deserves as a commercial technology (Rafia and Sehrish, 2008). The effect and efficiency of hyperaccumulator plant species to a large extent depends on the plant characteristics, including growth rate, high biomass, tolerance range, and accumulation of heavy elements from the soil (Barceló and Poschenrieder, 1990). The application of ameliorating treatments can enhance biomass production in soils contaminated with heavy elements. Such treatments play an essential role in increasing

phytoremediation efficiency (Das *et al.*, 1997). An ideal plant species for the phytoremediation process should have a high biomass production rate, high absorption capacity, high rate of reproduction, and fast-growing and resistance to unfavorable environmental conditions(Marrugo-Negrete *et al.*, 2016).

Aluminum (Al) is one of the critical factors limiting the growth and production of plants found in acidic soils around the world(Kochian *et al.*, 2004). Today, about 51 percent of the arable lands are occupied by acidic soils, and Al toxicity is one of the main problems in these soils (Singh *et al.*, 2017). Due to the high acidity of the subsoil, the toxicity of Al reduces the penetration depth of plant roots, increases sensitivity to drought and nutrient deficiency (Foy, 1988; Zuh *et al.*, 2009). Accumulation of Al at the cellular and ultrastructural parts leads to changes in leaves, heightens diffusion resistance, decreases in stomatal function, a decline in photosynthesis, reduces number and leaf size, and finally, reduction in aerial biomass (Shen *et al.*, 2014). Because stressful environmental conditions disrupt plants' biochemical processes, plant stress can be considered a tool to study and understand the mechanisms of tolerance in the plant (Rehmus *et al.*, 2014). The high growth rate and covering the ground under the aerial parts in the early stages of growth are advantageous for plant species growing in heavy metal polluted soils. Therefore any factor that delays or delays the germination of seeds or reduces the growth of roots and stems delays land cover uniformity, which eventually reduces plant yield (Nagy *et al.*, 2004; B. Ali *et al.*, 2008). Thus, the cultivation of plants for phytoremediation purposes in Al contaminated soils can be highly limiting. Treating plants with compounds such as Si to alleviate adverse effects of Al during critical growth stages as seedling stages can be helping plants in the successful establishment.

In soil solution, Silicon exists as dissolved silica and absorbed by plants in the form of monosilicic acid ($H_4SiO_4$). This element composes 28% of the Earth crust as the second most abundant element after oxygen, 47%. Although Si is not an essential element for plant growth and development, the beneficial effects of Si on the plant under stress conditions have been reported (Liang *et al.*, 2005; Guntzer *et al.*, 2012; Emamverdian *et al.*, 2018). One of the benefits of Si application is the increased tolerance of some plant species to heavy metal toxicity is heavy (Samuels *et al.*, 1993). Si is deposited in the endoderm and reduces cadmium transport via apoplast or Intercellular open spaces (Abu-Muriefah, 2015). It is a mitigating agent of toxic effects caused by heavy metals and various types of environmental stresses as salinity, drought, and frost stress. Another positive influence of Si was found to the increase in light-receiving efficiency that with accumulation in the cell walls of the xylem increases plant resistance against heavy metal elements (Corrales *et al.*, 1997; Liang *et al.*, 2005; Kim *et al.*, 2014; Emamverdian *et al.*, 2018). This element stimulates the plant antioxidant system, the formation of complexes with heavy metals, and metal transferring of heavy ions to organs such as plant cell vacuoles reduces heavy metals' stress and toxicity. Si deficiency in the soil, photosynthetic pigments such as chlorophyll-a, reduces the photosynthesis rate (Wang *et al.*, 2004; Song *et al.*, 2011; Torabi *et al.*, 2015).

*Glycyrrhiza glabra* L. or licorice is one of the oldest medicinal plants with more than two thousand years of medicinal application of its roots(Wittschier *et al.*, 2009). Research on the healing properties of this plant has proven its impacts on subacute liver disorders, chronic hepatitis B and C, infectious hepatitis, and hemophilia. Preventing HIV replication and hindering immune system disorders in patients with AIDS are also among the therapeutic properties of this plant (Jalilzadeh-Amin *et al.*, 2015; Dastagir and Rizvi, 2016; Karkanis *et al.*, 2018). Expansion of the use of this plant and study strategies for its large-scale production is required. Considering the phytoremediation ability of licorice, studying possible approaches to improve seed germination and growth at early stages are critically in demand. Propagation via seed in this plant is an economically viable method.

This study aimed to investigate whether the application of Si can alleviate the toxic impacts of Al on seedlings of licorice further to evaluate its potentials as a phytoremediator of Al.

## 2. MATERIALS AND METHODS:

### 2.1. Medium preparation and sowing seeds

Healthy and vigor seeds of licorice were procured from PakanBazr Co. (Isfahan, Iran). Licorice seeds were first disinfected with 10% bleach (20 minutes) and 70% alcohol (60 seconds). After washing with distilled water, they were cultured in a soil mixture of perlite and irrigated with distilled water for one week. After germination and emergence of 2 to 3 leaves, seedlings were irrigated with Long Ashton nutrient solution (half concentration). After two weeks,

healthy seedlings were selected and transferred to the hydroponic culture medium and fed with complete Long Ashton nutrient solution(Smith *et al.*, 1983). The hydroponic culture medium consisted of 1.5-liter dark plastic containers filled with Long Ashton nutrient solution and Si and Al treatments (Figure 1). The solution inside the containers was stirred continuously and changed every five days. The pH conditions of all nutrient solutions were considered to be 5.5. Each container contained two seeds, which were viewed as a total of one replicate (Figure 1). Plants were placed in the greenhouse controlled environment with a light period of 16 hours of light and 8 hours of darkness and day and night temperature 16±2 and 24±2, respectively. Light intensity of 250 µmol $m^{-2}s^{-1}$ was maintained at wavelengths of 400 to 700 nm. To prepare the Long Ashton nutrient solution, first stock solutions of macro and microelements were prepared then an appropriate amount was taken from them to make the nutrient solution.

**2.2. Application of treatments**

The 15-day-old licorice seedlings were exposed to different levels (0, 0.5, and 1.5 Mm) of sodium metasilicate ($Na_2SiO_3.5H_2O$) for 110 days, after which they stressed by simple and interaction effects of various concentrations of aluminum chloride ($AlCl_3.6H_2O$), zero, 100, 250, and 400 µM. At the end of each experiment, one of the two plants in each container was randomly selected to measure morphological traits. The second plant was immediately frozen in liquid nitrogen and transferred to a -20 °C freezer for assays that required fresh material.

**2.3. Determining biomass production**

Parameters of biomass production were recorded by measuring stem height and fresh shoot and root weight using digital calipers and scale. Then to obtain the dry weight of shoot and root, the samples placed in paper bags were put at 70 °C in the oven, where they dried for 48 hours.

**2.4. Determination of photosynthetic pigments**

To determine the amount of Chlorophyll-b, a, and carotenoids, the protocol previously detailed by Lichtenthaler (1987) was used, in which 0.5 g of green tissue of leaves with 10 ml of 80% acetone was pulverized. Then samples were centrifuged for 10 minutes at 6,000 rpm. The amount of chlorophyll-a in the absorption spectrum is 663, chlorophyll b at 645, and the carotenoid absorption spectrum at a wavelength of 470 nm with UV-Visible Spectrophotometer (Model -Cary50) analyzed. To set the device, acetone 80% was used. Concentrations of pigments using euqations 1, 2 and 3, in milligrams per gram of fresh weight (FW) of the sample, were calculated.

Chlorophyll a = (19.3 × A663 - 0.886 × A645) V / 100W mg.g-1 FW

(Eq. 1)

Chlorophyll b = (19.3 × A645 - 3.6 × A663) V / 100W mg.g-1 FW

(Eq. 2)

Carotenoids = 100 (A470) - 3.27 (mg chl. a) - 104 (mg chl. b) /227 mg.g-1 FW

(Eq. 3)

In the above equations, A is the wavelength (nm) read by the device, V volume (mL) of the filtered solution after centrifuge, and FW fresh weight of the sample per gram of fresh tissue.

**2.5. Extraction and measurement of proline**

The proline content of stems was estimated by a method described by Bates *et al.* (1973). To prepare the reagent of Ninhydrin, 30 ml of glacial acetic acid mixed with 20 ml of 6 M phosphoric acid stir gently until completely dissolved. The solution was stable at 4 °C for 24 h. To measure the proline content, 0.5 g of fresh leaf tissue was homogenized in 10 ml of sulfosalicylic acid 3%. The obtained extract was filtered using Whatman No. 2, 2 ml of the extract was mixed with 2 ml of the Ninhydrin reagent and 2 ml of glacial acetic acid placed for one hour in a 100 $^{o}$C hot water bath. Then the experiment ended by placing the tubes in an ice bath. Then 4 ml of toluene were added to the contentes of each tube and shaken for 30 seconds; Toluene is perfect to complete dissolve of proline. Therefore, there is no need for another centrifugation. The upper layer of the solution that includes toluene and proline was separated from the aqueous phase. The absorption of the remaining phase of the solution was measured by spectrophotometer at a wavelength of 520 nm and the proline concentration expressed in mg per gr fresh weight.

**2.6. Malondialdehyde assay**

To measure membrane lipid peroxidation, malondialdehyde (MDA) concentration was

measured by Heath and Packer (1968) method. In this method, 0.1 g of leaf tissue was extracted with the help of 2 ml of 5% trichloroacetic acid (TCA) solution by sonicator for 30 seconds at four °C. The resulting extract was centrifuged at room temperature at 12000 rpm for 15 min. At 532 nm, the absorption of the supernatant was measured. The absorption of other non-specific pigments was determined at 600 nm and subtracted from the adsorption at 532 nm.

#### 2.7. Catalase assay

The activity of this enzyme was measured using Nakano and Asada (1981) method. An amount of 0.1 g of the frozen leaf sample was extracted in 3 ml of 25 mM sodium phosphate buffer with pH = 6.8. The resulting homogenates were centrifuged at 15,000 rpm at four °C. The supernatant was used to measure catalase activity. The reaction mixture consisted of 2.5 mL of 25 mM sodium phosphate buffer at pH = 6.8, 0.5 mL of 10 mM H2O2, and 100 µl of enzyme extract, then read at 290 nm by spectrophotometer and expressed as per µg of protein of enzymatic activity.

#### 2.8. Statistical analysis

The experiment was performed in a completely randomized factorial design with four replicates, and each replicated had two sub-samples. The main factors were Si (A), and Al (B) and the interaction of concentrations of factors A and B. Analysis of means carried out employing the SPSS package (version 26; IBM, US). Using the Duncan test, the differences among treatments were evaluated at the level of 5%.

## 3. RESULTS AND DISCUSSION:

The most expected effect of heavy metals on plants often involves growth inhibition(Gajewska and SkŁodowska, 2010). Exogenous application of Si limits the harmful effects of Al (Singh *et al.*, 2011; Emamverdian *et al.*, 2018). Measuring growth parameters has often been critical in showing heavy metals' influence on biomass production(Wang and Zhou, 2005; Gajewska and SkŁodowska, 2010). According to Figure 3, where means are compared at the probability level of 5% of the Duncan test, application of Si treatment, particularly at 1.5 mM, can effectively limit the adverse effects of Al toxicity. In plants exposed to various levels of Al stress and moderate or high levels of Si managed to increase fresh stem weight (Figure 2 and Figure 3a). However, the interaction of Si mM 1.5 and Al 400 µM produced 45.67 g biomass in shoots but was not statistically significant compared to the other treated plants. But plants under Al 400 µM treatment indicated the lowest quantity of fresh shoot weight (36.08 g) statistically significant at 5% of the Duncan test. The simple effect of Si 1.5 mM (12.14 g) produced higher shoot dry weight, which had no statistically significant difference with Si 0.5 mM and control (Figure 3b). The shoot dry weight followed a pattern in which the values declined as the concentration of Al increased. Si 1.5 mM had the highest quantity of fresh root weight (12.52 g) while Al 400 µM alone with 5.98 g showed the lowest root fresh weight, which both produced a significant difference in control. The interaction of Al 100 and Si 1.5 with 10.58 g had the highest root fresh weight among the interactions (Figure 3c; 2.61g). When it came to root dry weight, a similar pattern to root fresh weight was observed (Figure 3d). In the case of the shoot fresh weight/dry weight ratio, in general, the simple effect of Al in all concentrations had the higher ratios where Al 400 µM with 11.44 showed the highest ratio (Figure 3e), with a significant difference with control. An analogous paradigm was observed for root fresh weight/dry weight ratio in which the single effect of Al had a higher ration, however, the combination of Al 400 µM and Si 0.5 Mm indicated a high ratio (Figure 3f). Among the treatments, Si 0.5 mM and Al 100 µM, the stem height of 38 cm found to be the highest among interaction treatments, a similar pattern was observed in other interaction effects (Figure 3g).

The fundamentals of the physiological impact of Al toxicity still is an open question (Ryder *et al.*, 2003). Prabagar *et al.* (2011) studied the effect of Al toxicity on cell suspension cultures of Norway spruce observed growth inhibition due to necrosis of cells resulting from deformation of subcellular like creating several small size vacuoles most likely from the Golgi body. Enhanced aggregation of Al through the root system and consequently generating adverse physiological modification have often been associated with Al toxicity (Corrales *et al.*, 1997; Prabagar *et al.*, 2011). This previous evidence can explain the decrease of fresh and dry weight in stem and root. Additionally, Si application and its adverse effects on Al uptake have been proposed in several other studies (Prabagar *et al.*, 2011; Shahnaz *et al.*, 2011; Singh *et al.*, 2011; Pontigo *et al.*, 2017). In agreement with the results of this study, Singh *et al.* (2011) similarly indicated the positive impacts on Al-stressed seedlings of rice. Possible mechanisms suggested for ameliorating the influence of Si on Al toxicity involve lowering the chance of availability of sites for Al to bind in

the cellular wall, decreased possibility of formation of Al-plasma member bonds. Finally, discharging exudates by roots makes apoplastic presence Al difficult (Cocker *et al.*, 1998). Thus, the application of Si along with Al possibility positively impacted one of those above mechanisms. Additionally, the mitigation influence of Si on Al-stressed plant can be associated with decrementing the quantity of available phytotoxic Al in nutrition media. For instance, reducing Al in the media due to adding Si has been correlated with the development and formation of nonfunctional biological compounds known as hydroxyl aluminum silicate (Wang *et al.*, 2004).

Photosynthetic pigments are highly critical for photosynthesis apparatuses. In comparison, they are significantly vulnerable to the stress imposed by toxic doses of heavy metal ions (Ozyigit *et al.*, 2013; Paunov *et al.*, 2018). In this study, exogenous application of Si 0.5 and 1.5 mM improved the chlorophyll content in the plant exposed to Al stress (Figure 4a). In the interaction of Al 250 µM and Si 1.5 mM, stressed plants had the highest quantity of chlorophyll a by 1.91 µg/g FW among the interaction effect, which did not significantly differ from the other treatments at $p < 0.05$ level. The combination and single effects of Al 400 µM treatment generated the lowest values for chlorophyll a where Al 400 µM concentration with 0.836 indicated to be the lowest. Again, an exact similar trend was observed for chlorophyll b except that the interaction and simple effects of Al 400 µM yielded higher values (Figure 4b). Among the consequences of Si and Al, the interaction of Al 400 µM with Si 1.5 mM could increase chlorophyll b content (0.78 µg/g FW) to a statistically significant level ($p < 0.05$) (Figure 4b). In treatments that plants exposed to Al only, by increasing Al concentration, the content of chlorophyll a and chlorophyll b experienced a significant reduction. Similar patterns reflect the importance of Si against toxic ions of heavy metals, especially Al, as its possibly due to the preventative effects of Si on Al uptake (Guntzer *et al.*, 2012; Pontigo *et al.*, 2017; Liu *et al.*, 2018). An interesting pattern was observed in the reaction of carotenoid accumulation to Al stress and Si application. Al 400 µM interaction with Si 1.5 by producing 0.663 µg/g FW carotenoid had a notable difference in compared with other interaction effects and was statistically significant ($p < 0.05$). However, Al 400 µM indicated the lowest carotenoid 0.263 µg/g FW among all treatments (Figure 4c).

The enzymatic and non-enzymatic antioxidants such as catalase (CAT), $\alpha$-tocopherol, carotenoids, and proline collectively play a significant role in plants stressed by heavy metals(Anjum *et al.*, 2016; Rao *et al.*, 2016). Besides being a nosmolyte to protect plant cells against osmotic stress imposed by a toxic heavy metal ion, proline is a vital energy source for plants that they can rely on to swift recovery from stress (Jain et al., 2001). Enzymatic and non-enzymatic antioxidants preserve plant cells from the negative consequences of heavy metal stress, mainly by scavenging reactive oxygen species (ROS). This process is through intercellular mechanisms in different organs, including cytosol, mitochondria, chloroplast, apoplast, and peroxisomes (Nwugo and Huerta, 2008; Foyer and Noctor, 2011; Hasanuzzaman *et al.*, 2012; Emamverdian *et al.*, 2018). In the present study, the amount of proline in the stem and roots under $AlCl_3.6H_2O$ treatment was stressed, which positively affected the concentration of $AlCl_3.6H_2O$ and Si treatment used (1.5 mM). Interaction of Al 250 and 400 µM and Si 1.5 mM in stem by 72.14 and 81.46 µg/g FW and had the highest quantity of proline content (Figure 5a) with statistically significant differences with the rest of the treatments at $p < 0.05$. The proline content of roots also had a similar trend in which Al 400 µM and Si 0.5 and 1.5 mM in the root by 69.22 and 69.54 µg/g FW produced the highest statistically significant values (Figure 5b). Proline, known to have cytosolic activities and quenching ROSs, has enabled this compound to increase almost in all the possible conditions that plant faces abiotic and biotic stress (Hayat *et al.*, 2012; X. Liang *et al.*, 2013; Kavi and Sreenivasulu, 2014). This is possibly why the proline content significantly increased by increasing the concentration of Al, and the positive influence of Si also can be witnessed. These results indicate the importance of proline biosynthesis in plants under Al stress and the importance of Si to intensify its production. The ratio of proline in shoot/root was mainly increased by enhancement of Al concentrations. Additionally, the highest ratios were found in treatments; Al 250 and 400 µM in combination with 1.5 mM (1.35 and 1.17, respectively, Figure 5c).

Catalase is localized in a specific cellular organ, peroxisomes. Its primary responsibility is to eradicate the H2O2 generated by the SOD reaction; therefore, it is crucial for survival plants when exposed to Al stress (Racchi, 2013). The stress-induced by Al increased enzymatic antioxidant content, CAT in both stem and root (Figure 5d). It seems the addition of both Si (0.5 and 1.5 Mm) and Al (100, 250, and 400 µM) combined or alone increased CAT by increasing in concentration. Si 1.5 mM alone with 1.61 U/mg

protein had the highest value among all treatments, also amongst the interaction effects, Al 400 µM and Si 1.5 were observed to have the highest concentration of CAT (1.22 U/mg protein). Simultaneously, the simple impact of Al 250 µM by having a value of 0.44 U/mg protein showed the lowest concentration of CAT.

Accumulation of ROS is highly expected in plants exposed to heavy metal stress because of the important role of ROS in signaling Al stress to initiate defense mechanisms. Plants also have potent antioxidant mechanisms to scavenge the ROS when it reaches an excessive level(Yamamoto *et al.*, 2003; Achary *et al.*, 2012; Huang *et al.*, 2014); in this study, significant enhancement in CAT by increasing the concentration of Al which means that *G.glabra* has a robust antioxidant system. However, the introduction of Si to Al treated plants caused a notable reduction in CAT, as Torabi *et al.* (2015) analogously reported a decrease in CAT activity of *Borago officinalis* L. when exposed to salinity. Similarly, Kim *et al.* (2014)observed a reduction in CAT activity in salt-stressed rice plants. The effect mechanisms of Si on the antioxidant defense system is poorly understood. But the addition of Si is often reported to increase antioxidant enzymes, particularly CAT (Kachout *et al.*, 2009; Shi *et al.*, 2010; Hajiboland and Cheraghvareh, 2014; Adrees *et al.*, 2015).

Malondialdehyde is a damaging product of peroxidation of lipids of the cellular membrane. It is a reliable index of the degree of oxidative stress caused by heavy metal ions (Guo *et al.*, 2004). A dose-dependent behavior was observed in the effect of Si on MDA concentration (Figure 5e). In general, Si showed a notable influence on reducing lipid peroxidation rate. Still, in the interaction of Al (100, 250, and 400 µM) with Si treatments (0.5 and 1.5 Mm), the dominant effect of 1.5 mM in all Al concentration was vivid. The lowest lipid peroxidation was found to be in Si 1.5 (0.574 nM/g FW), which had a significant difference with the highest concentration of Al used in this study, 400 µM (1.31 nM/g FW) at $p < 0.05$. Among the interaction effects, Al 100 µM and Si 1.5 mM (0.702 nM/g FW) indicated the lowest MAD concentration. In a study conducted on rice, exposure to Al and the addition of Si led to a decrease in MDA content (Song et al., 2011), which later found out considerable enhancement in the quantity of proline and CAT due to Si addition. This possible can significant reduction in MDA by increasing the concentration of Si in our study.

Additionally, the result of this study is consistent with those of Shamsi *et al.* (2008), who observed a notable increase in MDA by rising in Al concentration. The positive effect of Si in interaction with Al on reducing MDA was observed in Borago officinalis L. (Shahnaz *et al.*, 2011). Similar results also have been reported in barley (Tamás *et al.*, 2003), tea (Ghanati *et al.*, 2005), and *Stipagrandis* and *Leymuschinensis* (X. Song *et al.*, 2016). Exogenous application of Si in rice by controlling metal transport prevents the uptake of Al, therefore, prevents the lipid peroxidation and ultimately reduces MDA content(Kim *et al.*, 2014).

## 4. CONCLUSIONS:

The results indicated that silicon-treated plants were to a significant extent protected from AlCl3.6H2O toxicity and produced higher biomass, suggesting that Silicon may increase plants' resistance to environmental stress (toxic ions). Improving the stressing situation for seedlings seems to be via increasing the proline content as a universal osmoprotectant and preventing lipids' oxidation. Finally, Silicon has reduced cell membrane vulnerability and improved the structure to deal with $AlCl_3.6H_2O$ stress in licorice and revealed some of the capability of Silicon to control the toxicity of $AlCl_3.6H_2O$. More comprehensive studies are required, exposing licorice to other heavy metal stresses and employing other ameliorating chemicals such as salicylic acid are recommended.

## 5. REFERENCES:


1. Abu-Muriefah, S. (2015). Effects of Silicon on membrane characteristics, photosynthetic pigments, antioxidative ability, and mineral element contents of faba bean (Vicia faba L.) plants grown under Cd and Pb stress. *International Journal of Advance Research in Biological Science,* 2, 1-17.
2. Achary, V. M. M.; Patnaik, A. R.; Panda, B. B. (2012). Oxidative biomarkers in leaf tissue of barley seedlings in response to aluminum stress. *Journal od Ecotoxicology and Environmental Safety,* 75, 16-26.
3. Adrees, M.; Ali, S.; Rizwan, M.; Zia-ur-Rehman, M.; Ibrahim, M.; Abbas, F.; Farid, M.; Qayyum, M. F., Irshad, M. K. (2015). Mechanisms of silicon-mediated alleviation of heavy metal toxicity in plants: a review. *Journal of Ecotoxicology and Environmental Safety,* 119, 186-197.

4. Ali, B.; Hasan, S.; Hayat, S.; Hayat, Q.; Yadav, S.; Fariduddin, Q.; Ahmad, A. (2008). A role for brassinosteroids in the amelioration of aluminium stress through antioxidant system in mung bean (Vigna radiata L. Wilczek). *Journal of Environmental and Experimental Botany,* 62, 153-159.

5. Ali, H.; Khan, E.; Sajad, M. A. (2013). Phytoremediation of heavy metals—concepts and applications. *Chemosphere,* 91, 869-881.

6. Anjum, N. A.; Khan, N. A.; Sofo, A.; Baier, M.; Kizek, R. (2016). Redox homeostasis managers in plants under environmental stresses. *Frontiers in Environmental Science,* 4, 35.

7. Barceló, J.; Poschenrieder, C. (1990). Plant water relations as affected by heavy metal stress: a review. *Journal of Plant Nutrition,* 13, 1-37.

8. Bates, L. S.; Waldren, R. P.; Teare, I. (1973). Rapid determination of free proline for water-stress studies. *Journal of Plant and Soil,* 39, 205-207.

9. Chehregani, A.; Noori, M.; Yazdi, H. L. (2009). Phytoremediation of heavy-metal-polluted soils: screening for new accumulator plants in Angouran mine (Iran) and evaluation of removal ability. *Journal of Ecotoxicology and Environmental Safety,* 72, 1349-1353.

10. Cocker, K. M.; Evans, D. E.; Hodson, M. J. (1998). The amelioration of aluminium toxicity by Silicon in wheat (Triticum aestivum L.): malate exudation as evidence for an in planta mechanism. *Journal of Planta,* 204, 318-323.

11. Corrales, I.; Poschenrieder, C.; Barceló, J. (1997). Influence of silicon pretreatment on aluminium toxicity in maize roots. *Journal of Plant and Soil,* 190, 203-209.

12. Das, P.; Samantaray, S.; Rout, G. (1997). Studies on cadmium toxicity in plants: a review. *Journal of Environmental pollution,* 98, 29-36.

13. Dastagir, G., Rizvi, M. A. (2016). Glycyrrhiza glabra L.(Liquorice). *Pakistan Journal of Pharmaceutical Sciences,* 29.

14. Emamverdian, A.; Ding, Y.; Xie, Y., Sangari, S. (2018). Silicon mechanisms to ameliorate heavy metal stress in plants. *Journal of BioMed Research International,* 2018.

15. Foy, C. D. (1988). Plant adaptation to acid, aluminum-toxic soils. *Communications in Soil Science and Plant Analysis,* 19, 959-987.

16. Foyer, C. H.; Noctor, G. (2011). Ascorbate and glutathione: the heart of the redox hub. *Journal of Plant Physiology,* 155, 2-18.

17. Gajewska, E.; SkŁodowska, M. (2010). Differential effect of equal copper, cadmium and nickel concentration on biochemical reactions in wheat seedlings. *Journal of Ecotoxicology and Environmental Safety,* 73, 996-1003.

18. Ghanati, F.; Morita, A.; Yokota, H. (2005). Effects of Aluminum on the Growth of Tea Plant and Activation of Antioxidant System. *Plant and Soil,* 276, 133-141.

19. Ghosh, M.; Singh, S. (2005). A review on phytoremediation of heavy metals and utilization of it's by products. *Asian Journal of Energy Environment* 6, 18.

20. Guntzer, F.; Keller, C.; Meunier, J.-D. (2012). Benefits of plant silicon for crops: a review. *Journal of Agronomy for Sustainable Development,* 32, 201-213.

21. Guo, T.; Zhang, G.; Zhou, M.; Wu, F.; Chen, J. (2004). Effects of aluminum and cadmium toxicity on growth and antioxidant enzyme activities of two barley genotypes with different Al resistance. *Journal of Plant and Soil,* 258, 241-248.

22. Hajiboland, R.; Cheraghvareh, L. (2014). Influence of Si supplementation on growth and some physiological and biochemical parameters in salt-stressed tobacco (Nicotiana rustica L.) plants. *Journal of Sciences, Islamic Republic of Iran,* 25, 205-217.

23. Hasanuzzaman, M.; Hossain, M. A.; da Silva, J. A. T.; Fujita, M. (2012). Plant response and tolerance to abiotic oxidative stress: antioxidant defense is a crucial factor. In *Crop stress and its management: Perspectives and strategies* (pp. 261-315): Springer.

24. Hayat, S.; Hayat, Q.; Alyemeni, M. N.; Wani, A. S.; Pichtel, J.; Ahmad, A. (2012). Role of proline under changing environments: a review. *Plant signaling & behavior,* 7, 1456-1466.

25. Heath, R. L.; Packer, L. (1968).

Photoperoxidation in isolated chloroplasts: I. Kinetics and stoichiometry of fatty acid peroxidation. *Archives of Biochemistry and Biophysics,* 125, 189-198.

26. Huang, W.; Yang, X.; Yao, S.; LwinOo, T.; He, H.; Wang, A.; Li, C.; He, L., biochemistry. (2014). Reactive oxygen species burst induced by aluminum stress triggers mitochondria-dependent programmed cell death in peanut root tip cells. *Journal of Plant Physiology,* 82, 76-84.
27. Jabeen, R.; Ahmad, A.; Iqbal, M. (2009). Phytoremediation of heavy metals: physiological and molecular mechanisms. *The Botanical Review,* 75, 339-364.
28. Jalilzadeh-Amin, G.; Najarnezhad, V.; Anassori, E.; Mostafavi, M.; Keshipour, H. (2015). Antiulcer properties of Glycyrrhiza glabra L. extract on experimental models of gastric ulcer in mice. *Iranian Journal of Pharmaceutical Research: IJPR,* 14, 1163.
29. Kachout, S. S.; Mansoura, A.; Leclerc, J.; Mechergui, R.; Rejeb, M.; Ouerghi, Z. (2009). Effects of heavy metals on antioxidant activities of Atriplex hortensis and A. rosea. *Journal od Food, Agriculture and Environment,* 7, 938-945.
30. Karkanis, A.; Martins, N.; Petropoulos, S.; Ferreira, I. C. (2018). Phytochemical composition, health effects, and crop management of liquorice (Glycyrrhiza glabra L.): A medicinal plant. *Journal of Food Reviews International,* 34, 182-203.
31. Kavi Kishor, P. B.; Sreenivasulu, N. (2014). Is proline accumulation per se correlated with stress tolerance or is proline homeostasis a more critical issue? *Plant, Cell & Environment,* 37, 300-311.
32. Kim, Y. H.; Khan, A. L.; Waqas, M.; Shim, J. K.; Kim, D. H.; Lee, K. Y.; Lee, I. J. (2014). Silicon application to rice root zone influenced the phytohormonal and antioxidant responses under salinity stress. *Journal of Plant Growth Regulation,* 33, 137-149.
33. Kochian, L. V.; Hoekenga, O. A.; Pineros, M. A. (2004). How do crop plants tolerate acid soils? Mechanisms of aluminum tolerance and phosphorous efficiency. *Annual Review of Plant Biology,* 55, 459-493.
34. Liang, X.; Zhang, L.; Natarajan, S. K.; Becker, D. F. (2013). Proline mechanisms of stress survival. *Antioxidants & redox signaling,* 19, 998-1011.
35. Liang, Y.; Si, J.; Römheld, V. (2005). Silicon uptake and transport is an active process in Cucumis sativus. *New Phytologist,* 167, 797-804.
36. Lichtenthaler, H. K. (1987). Chlorophylls and carotenoids: pigments of photosynthetic biomembranes. In *Methods in Enzymology* (Vol. 148, pp. 350-382). Academic press.
37. Liu, G.; Huang, Y.; Zhai, L. (2018). Impact of nutritional and environmental factors on inflammation, oxidative stress, and the microbiome. *BioMed research international,* 2018.
38. Lombi, E.; Zhao, F.; Dunham, S.; McGrath, S. (2001). Phytoremediation of heavy metal–contaminated soils: Natural hyperaccumulation versus chemically enhanced phytoextraction. *Journal of Environmental Quality,* 30, 1919-1926.
39. Mahar, A.; Wang, P.; Ali, A.; Awasthi, M. K.; Lahori, A. H.; Wang, Q.; Li, R.; Zhang, Z. (2016). Challenges and opportunities in the phytoremediation of heavy metals contaminated soils: a review. *Journal of Ecotoxicology and Environmental Safety,* 126, 111-121.
40. Marrugo-Negrete, J.; Marrugo-Madrid, S.; Pinedo-Hernández, J.; Durango-Hernández, J.; Díez, S. (2016). Screening of native plant species for phytoremediation potential at a Hg-contaminated mining site. *Journal of Science of the total environment,* 542, 809-816.
41. Nagy, N. E.; Dalen, L. S.; Jones, D. L.; Swensen, B.; Fossdal, C. G.; Eldhuset, T. D. (2004). Cytological and enzymatic responses to aluminium stress in root tips of Norway spruce seedlings. *New Phytologist,* 163, 595-607.
42. Nakano, Y.; Asada, K. (1981). Hydrogen peroxide is scavenged by ascorbate-specific peroxidase in spinach chloroplasts. *Journal of Plant Cell Physiology,* 22, 867-880.
43. Nwugo, C. C.; Huerta, A. (2008). Effects of silicon nutrition on cadmium uptake, growth and photosynthesis of rice plants exposed to low-level cadmium. *Journal of*

*Plant and Soil,* 311, 73-86.

44. Nwugo, C. C.; Huerta, A. J. (2008). Effects of silicon nutrition on cadmium uptake, growth and photosynthesis of rice plants exposed to low-level cadmium. *Journal od Plant and Soil,* 311, 73-86.
45. Ozyigit, I.; Vardar, F.; Yaşar, Ü.; Akinci, S. (2013). Long-Term Effects of Aluminum and Cadmium on Growth, Leaf Anatomy, and Photosynthetic Pigments of Cotton. *Communications in Soil Science and Plant Analysis,* 44, 3076-3091.
46. Paunov, M.; Koleva, L.; Vassilev, A.; Vangronsveld, J.; Goltsev, V. (2018). Effects of Different Metals on Photosynthesis: Cadmium and Zinc Affect Chlorophyll Fluorescence in Durum Wheat. *International Journal of Molecular Sciences,* 19, 787.
47. Pontigo, S.; Godoy, K.; Jiménez, H.; Gutiérrez-Moraga, A.; Mora, M. d. l. L., Cartes, P. (2017). Silicon-mediated alleviation of aluminum toxicity by modulation of Al/Si uptake and antioxidant performance in ryegrass plants. *Journal of Frontiers in Plant Science,* 8, 642.
48. Prabagar, S.; Hodson, M. J.; Evans, D. E. (2011). Silicon amelioration of aluminium toxicity and cell death in suspension cultures of Norway spruce (Picea abies (L.) Karst.). *Journal of Environmental and Experimental Botany,* 70, 266-276.
49. Racchi, M. L. (2013). Antioxidant defenses in plants with attention to Prunus and Citrus spp. *Journal of Antioxidants,* 2, 340-369.
50. Rafia, A.; Sehrish, H. (2008). Photochemistry of light harvesting pigments and some biochemical changes under aluminium stress. *Pakistan Journal of Botany,* 4, 779-784.
51. Rao, N. S.; Shivashankara, K. S.; Laxman, R. (2016). *Abiotic stress physiology of horticultural crops*. Springer.
52. Rehmus, A.; Bigalke, M.; Valarezo, C.; Castillo, J. M.; Wilcke, W. (2014). Aluminum toxicity to tropical montane forest tree seedlings in southern Ecuador: response of biomass and plant morphology to elevated Al concentrations. *Journal of Plant and Soil,* 382, 301-315.
53. Ryder, M.; Gérard, F.; Evans, D. E.; Hodson, M. J. (2003). The use of root growth and modelling data to investigate amelioration of aluminium toxicity by Silicon in Picea abies seedlings. *Journal of Inorganic Biochemistry,* 97, 52-58.
54. Samuels, A.; Glass, A.; Ehret, D.; Menzies, J. (1993). The effects of silicon supplementation on cucumber fruit: changes in surface characteristics. *Annals of Botany,* 72, 433-440.
55. Shahnaz, G.; Shekoofeh, E.; Kourosh, D.; Moohamadbagher, B. (2011). Interactive effects of Silicon and aluminum on the malondialdehyde (MDA), proline, protein and phenolic compounds in Borago officinalis L. *Journal of Medicinal Plants Research,* 5, 5818-5827.
56. Shamsi, I.; Wei, K.; Zhang, G.; Jilani, G.; Hassan, M. (2008). Interactive effects of cadmium and aluminum on growth and antioxidative enzymes in soybean. *Biologia Plantarum,* 52, 165-169.
57. Shen, X.; Xiao, X.; Dong, Z.; Chen, Y. (2014). Silicon effects on antioxidative enzymes and lipid peroxidation in leaves and roots of peanut under aluminum stress. *Acta Physiologiae Plantarum,* 36, 3063-3069.
58. Shi, G.; Cai, Q.; Liu, C.; Wu, L. (2010). Silicon alleviates cadmium toxicity in peanut plants in relation to cadmium distribution and stimulation of antioxidative enzymes. *Journal of Plant Growth Regulation,* 61, 45-52.
59. Singh, S.; Tripathi, D. K.; Singh, S.; Sharma, S.; Dubey, N. K.; Chauhan, D. K.; Vaculík, M. (2017). Toxicity of aluminium on various levels of plant cells and organism: a review. *Journal of Environmental and Experimental Botany,* 137, 177-193.
60. Singh, V. P.; Tripathi, D. K.; Kumar, D.; Chauhan, D. K. (2011). Influence of exogenous silicon addition on aluminium tolerance in rice seedlings. *Biological Trace Element Research,* 144, 1260-1274.
61. Smith, G.; Johnston, C.; Cornforth, I. (1983). Comparison of nutrient solutions for growth of plants in sand culture. *New phytologist,* 94, 537-548.
62. Song, A.; Li, P.; Li, Z.; Fan, F.; Nikolic, M.; Liang, Y. (2011). The alleviation of zinc toxicity by Silicon is related to zinc transport and antioxidative reactions in

rice. *Journal of Plant and Soil,* 344, 319-333.

63. Song, X.; Wang, Y.; Lv, X. (2016). Responses of plant biomass, photosynthesis and lipid peroxidation to warming and precipitation change in two dominant species (Stipa grandis and Leymus chinensis) from North China Grasslands. *Ecology and evolution,* 6, 1871-1882.

64. Tamás, L.; Huttová, J.; Mistrík, I. (2003). Inhibition of Al-induced root elongation and enhancement of Al-induced peroxidase activity in Al-sensitive and Al-resistant barley cultivars are positively correlated. *Journal of Plant and Soil,* 250, 193-200.

65. Torabi, F.; Majd, A.; Enteshari, S. (2015). The effect of Silicon on alleviation of salt stress in borage (Borago officinalis L.). *Soil science,* 61, 788-798.

66. Wang, M.; Zhou, Q. (2005). Single and joint toxicity of chlorimuron-ethyl, cadmium, and copper acting on wheat Triticum aestivum. *Journal of Ecotoxicology and Environmental Safety,* 60, 169-175.

67. Wang, Y.; Stass, A.; Horst, W. J. (2004). Apoplastic binding of aluminum is involved in silicon-induced amelioration of aluminum toxicity in maize. *Plant Physiology,* 136, 3762-3770.

68. (2009). Aqueous extracts and polysaccharides from liquorice roots (Glycyrrhiza glabra L.) inhibit adhesion of Helicobacter pylori to human gastric mucosa. *Journal of Ethnopharmacology,* 125, 218-223.

69. Yamamoto, Y.; Kobayashi, Y.; Devi, S. R.; Rikiishi, S., Matsumoto, H. (2003). Oxidative stress triggered by aluminum in plant roots. In *Roots: The Dynamic Interface between Plants and the Earth* (pp. 239-243). Springer.

70. Zhu, M.-h.; Cai, M.; Wu, S.; Li, F.; Liu, P.; Wang, Z. (2009). Effect of Phosphorus on Element Uptake and Transportation in Buckwheat under Aluminum Stress. *Journal of Soil Water Conservation,* 2.

***Figure 1.*** *15 and 30-day-old seedlings (left and right, respectively) of G. glabra in containers containing Long Ashton media.*


***Figure 2.*** *Effect of different levels of Al (100, 250, and 400 µM in combination with Si (1.5 Mm) on G. glabra seedlings.*

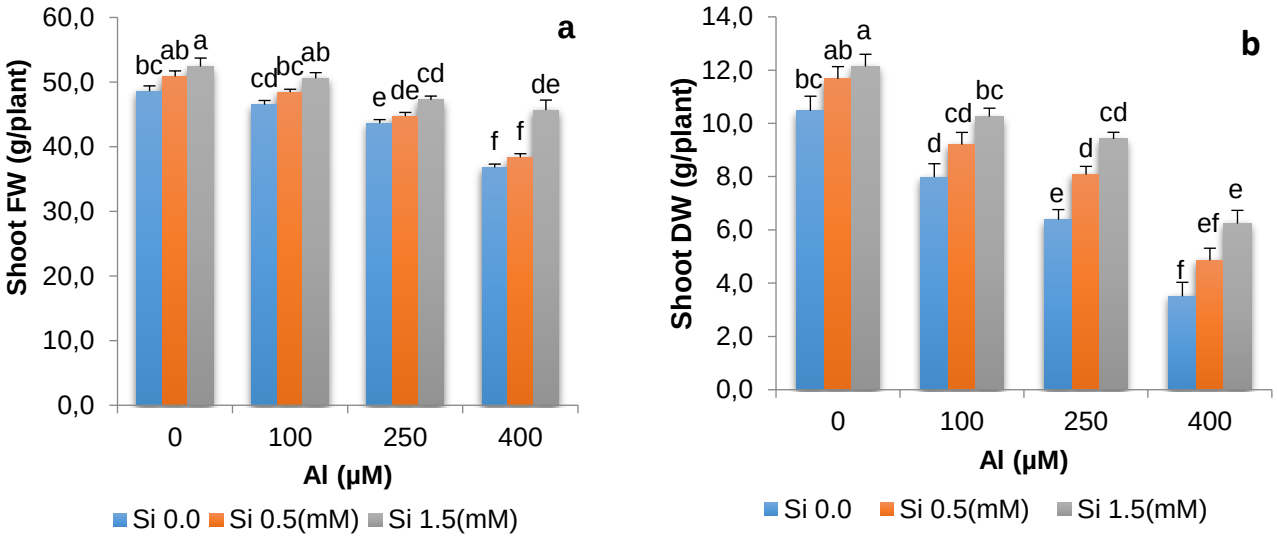

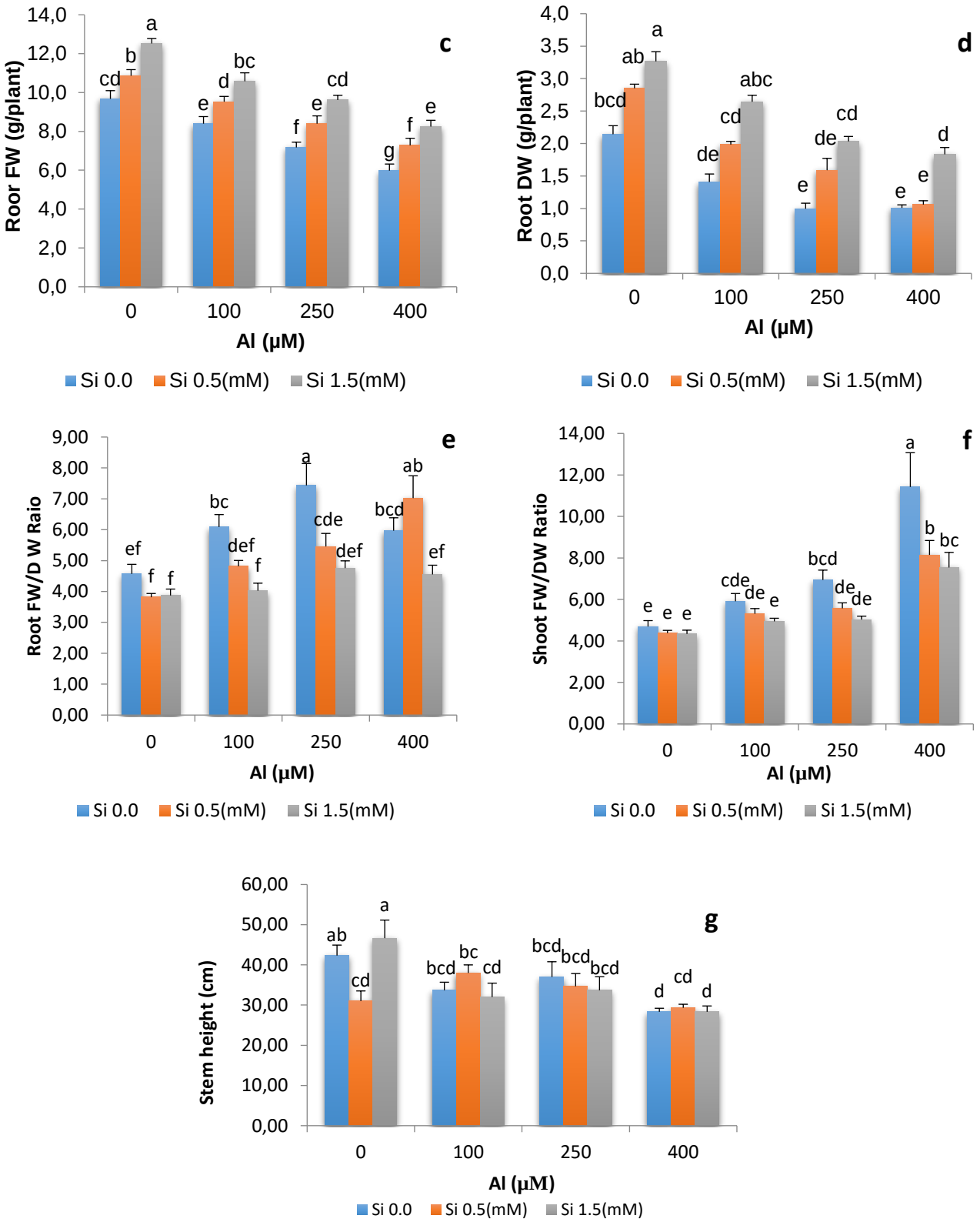


***Figure 3.*** *Effect of different concentrations of Al (0, 100, 250 and 400 µM) and Si (0, 0.5 and 1.5 Mm) and their interaction on shoot fresh weight (a), shoot dry weight (b), root fresh weight (c), root dry weight (d), root FW/DW (e), shoot FW/DW (f), and stem height (g). Columns with non-common letters indicate a significant difference between treatments based on the Duncan test (p <0.05).*

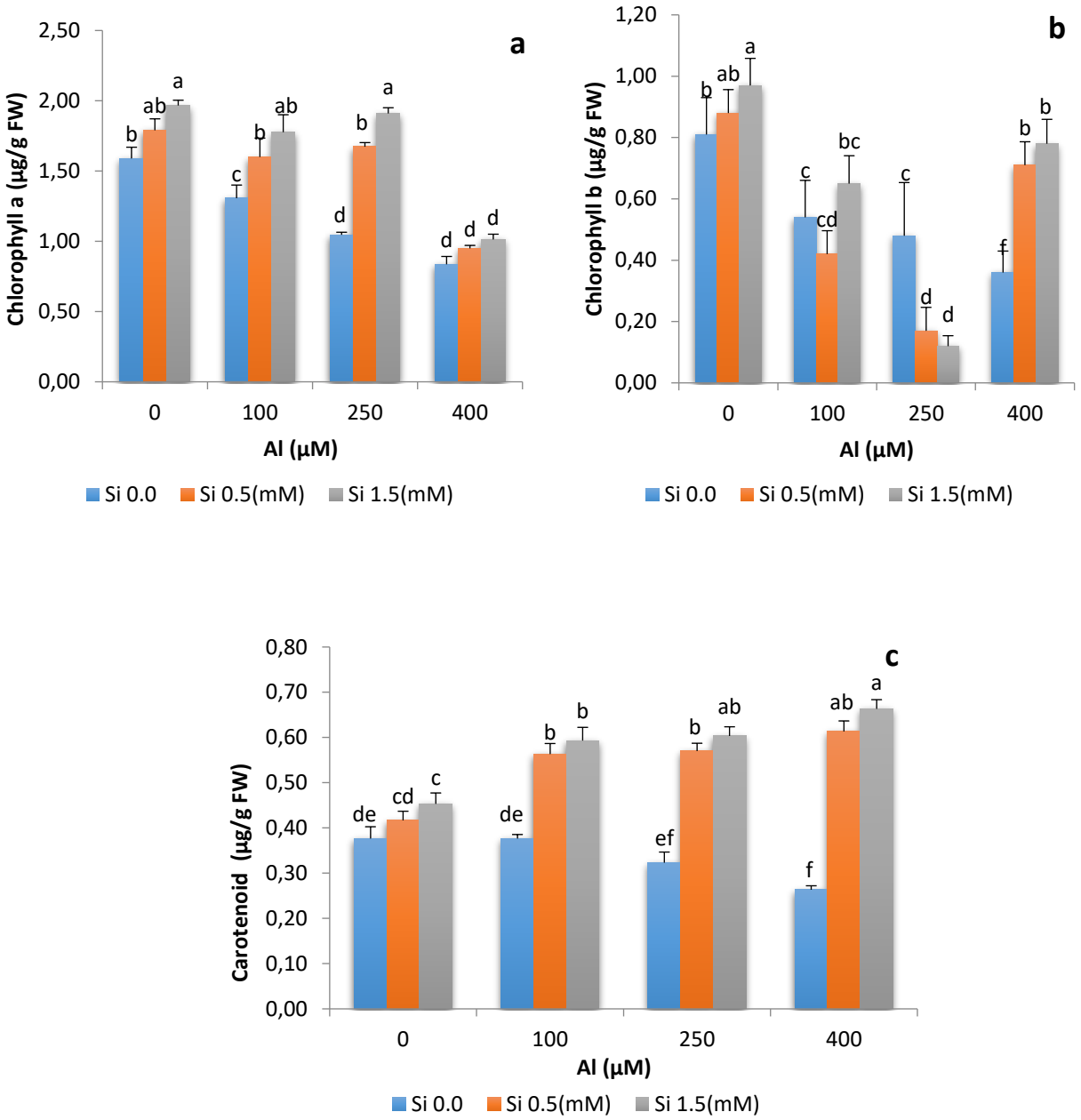


***Figure 4.*** *Effect of different concentrations of Al (0, 100, 250 and 400 µM) and Si (0, 0.5 and 1.5 Mm) and their interaction on contents of Chlorophyll a (a), Chlorophyll b (b) and Carotenoid (c). Columns with non-common letters indicate a significant difference between treatments based on the Duncan test (p <0.05).*

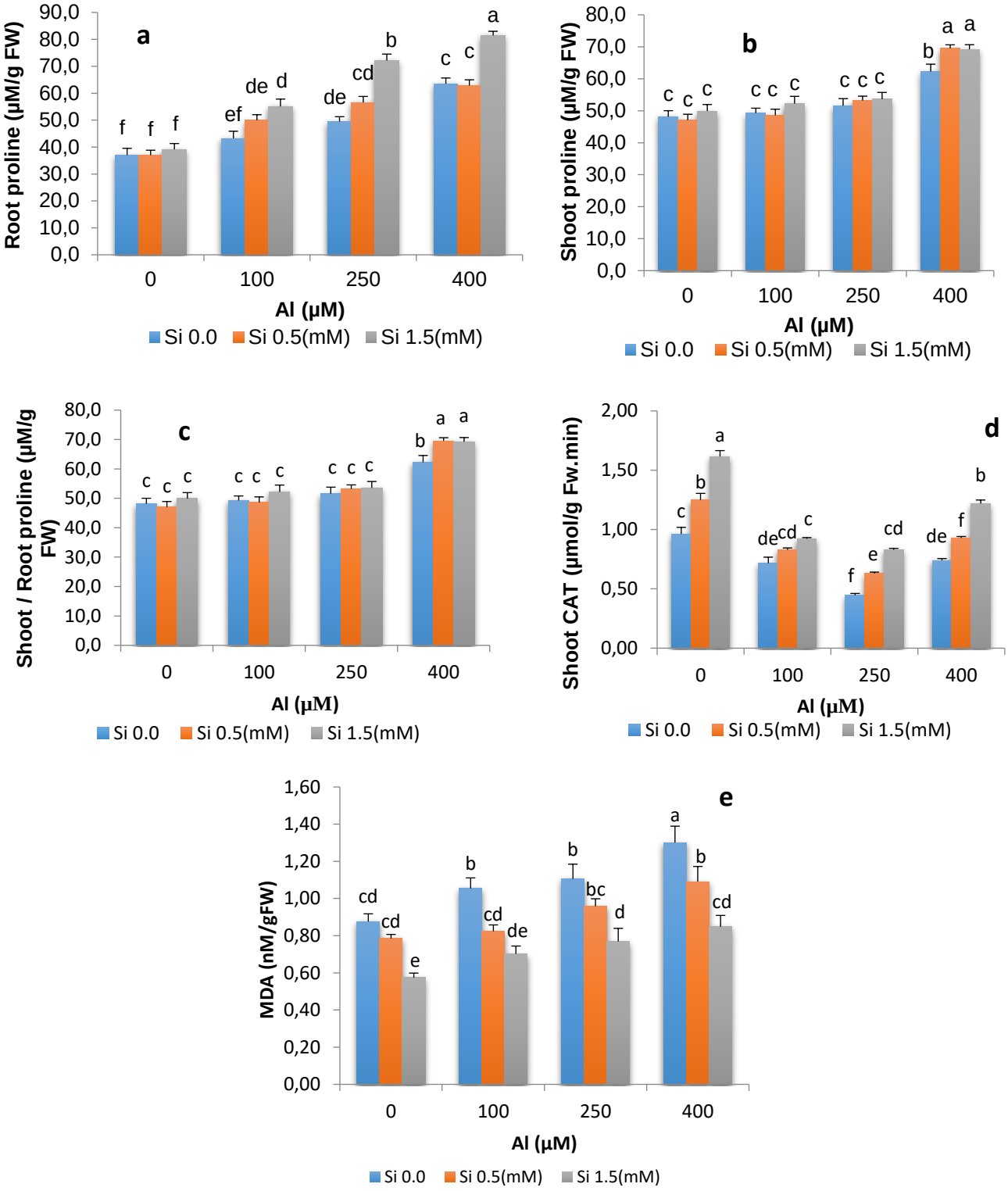


***Figure 5.*** *Effect of different concentrations of Al (0, 100, 250 and 400 µM) and Si (0, 0.5 and 1.5 Mm) and their interaction on contents of proline in root (a), and stem (b), root/shoot proline ration (c) CAT enzyme content in root (d) and MDA (e). Columns with non-common letters indicate a significant difference between treatments based on the Duncan test (p <0.05).*

PERIÓDICO TCHÊ QUÍMICA
ARTIGO ORIGINAL

# DETERMINANTES DO DIABETES MELLITUS GESTACIONAL

# DETERMINANTS OF GESTATIONAL DIABETES MELLITUS

# DETERMINAN DIABETES MELITUS GESTASIONAL

DEVI, Yuli Puspita[1]; ABDILLAH, Rumaisah[2]; MUTHMAINNAH, Muthmainnah[3*];

[1] Universitas Indonesia, Faculty of Public Health, Department of Biostatistics. Indonesia.

[1,2] Universitas Airlangga, Faculty of Public Health, Department of Biostatistics and Population Study. Indonesia.

[3] Universitas Airlangga, Faculty of Public Health, Health Promotion and Behavior Sciences. Indonesia.

** Corresponding author*
*e-mail: muthmainnah@fkm.unair.ac.id*

Received 08 February 2021; received in revised form 20 February 2021; accepted 28 February 2021

## RESUMO

**Introdução:** O Diabetes Mellitus Gestacional (DMG) é um distúrbio de tolerância à glicose que aparece pela primeira vez durante a gravidez. DMG pode causar uma variedade de complicações obstétricas e perinatais para mulheres grávidas e seus fetos. A prevalência de GDM na cidade de Surabaya em 2015 era de 2,29%, passando para 3,88% em 2018. **Objetivo.** O objetivo deste estudo foi analisar os determinantes (história familiar de diabetes mellitus, IMC, história de peso ao nascer, paridade e idade da gestante) que influenciam no DMG. **Métodos:** Esta pesquisa é um estudo analítico com abordagem observacional. O desenho da pesquisa foi realizado por meio de um estudo de caso-controle. O número de amostras neste estudo foi de 36 pessoas, 6 casos e 30 pessoas como controles, e foram retiradas aleatoriamente. A fonte de dados veio de dados secundários (prontuários de mulheres grávidas) no Centro de Saúde de Mulyorejo Surabaya. A análise utilizada neste estudo foi um teste de regressão logística simples. **Resultados e Discussão:** A análise mostrou que houve efeito da história familiar de diabetes mellitus (p = 0,035) sobre a incidência de DMG. A paridade é uma variável potencial (p = 0,077) na incidência de DMG. Enquanto isso, IMC, história de peso ao nascer e idade materna não tiveram efeito sobre a incidência de DMG. **Conclusões:** Mulheres grávidas com histórico familiar de diabetes que não estão em equilíbrio com um bom estilo de vida podem ter complicações quando experimentam o DMG.

**Palavras-chave**: *História Familiar de DM, Paridade, Diabetes Mellitus Gestacional (DMG).*

## ABSTRACT

**Background:** Gestational Diabetes Mellitus (GDM) is a glucose tolerance disorder that first appears during pregnancy. GDM can cause a variety of obstetric and perinatal complications for pregnant women and their fetuses. The prevalence of GDM in the city of Surabaya in 2015 amounted to 2.29%, increasing to 3.88% in 2018. **Aim:** The purpose of this study was to analyze the determinants (family history of diabetes mellitus, BMI, history of birth weight, parity, and the age of the pregnant woman) that influence the GDM. **Methods:** This research is an analytical study with an observational approach. The research design was carried out using a case-control study. In this study, the number of samples was 36 people, 6 cases, and 30 people as controls, and were taken randomly. The data source obtained from secondary data (medical records of pregnant women) at Mulyorejo Health Center Surabaya. The analysis used in this study was a simple logistic regression test. **Results and Discussion:** The result showed an effect of a family history of diabetes mellitus (p = 0.035) on the incidence of GDM. Parity was a potential variable (p = 0.077) on the incidence of GDM. Meanwhile, BMI, history of birth weight, and mother's age did not affect the incidence of GDM. **Conclusion:** Pregnant women with a family history of diabetes who are not balanced with maintaining a good lifestyle can experience complications of developing GDM.

**Keywords**: *History of DM in the Family, Parity, Gestational Diabetes Mellitus (GDM).*

## ABSTRAK

**Latar Belakang:** Diabetes Melitus Gestasional (DMG) adalah gangguan toleransi glukosa yang pertama kali muncul selama kehamilan. DMG dapat menyebabkan berbagai komplikasi kebidanan dan perinatal bagi ibu hamil dan janinnya. Prevalensi DMG di Kota Surabaya pada tahun 2015 sebesar 2,29% meningkat menjadi 3,88% pada

tahun 2018. **Tujuan:** Tujuan penelitian ini adalah untuk menganalisis determinan (riwayat diabetes melitus dalam keluarga, IMT, riwayat berat bayi lahir, paritas, dan usia ibu hamil) yang mempengaruhi kejadian DMG. **Metode:** Penelitian ini merupakan penelitian analitik dengan pendekatan observasional. Desain penelitian dilakukan dengan menggunakan studi kasus kontrol. Jumlah sampel dalam penelitian ini berjumlah 36 orang, 6 kasus dan 30 orang sebagai kontrol, dan diambil secara acak. Sumber data berasal dari data sekunder (rekam medis ibu hamil) di Puskesmas Mulyorejo Surabaya. Analisis yang digunakan dalam penelitian ini adalah uji regresi logistik sederhana. **Hasil dan Diskusi:** Hasil analisis dalam studi ini menunjukkan ada pengaruh riwayat keluarga diabetes mellitus (p = 0,035) terhadap kejadian DMG. Paritas merupakan variabel potensial (p = 0,077) terhadap kejadian DMG. Sedangkan BMI, riwayat berat badan lahir, dan umur ibu tidak berpengaruh terhadap kejadian DMG. **Kesimpulan:** Ibu hamil dengan riwayat keluarga diabetes yang tidak seimbang dengan mempertahankan gaya hidup yang baik dapat mengalami komplikasi berkembangnya DMG.

**Kata kunci**: *Riwayat DM dalam Keluarga, Paritas, Diabetes Melitus Gestasional (DMG).*

## 1. INTRODUCTION:

Gestational Diabetes Mellitus (GDM) is a glucose tolerance disorder that first appears during pregnancy (American Diabetes Association, 2004). The GDM condition applies to women who have never previously detected diabetes and are diagnosed with an increase in glucose during pregnancy or as a result of pregnancy. The International Diabetes Federation estimates in its research results that 20.9 million or 16.2% of live births by women in 2015 had some form of hyperglycemia in pregnancy. These hyperglycemia forms account for 85.1% of cases due to gestational diabetes mellitus (International Diabetes Federation, 2015). The prevalence of gestational diabetes mellitus in Indonesia is 1.9% -3.6% in general pregnancies (Soewondo and Pramono, 2011). The prevalence of GDM in Surabaya as described by the Dr. Soetomo General Hospital in 2015 was 2.29% (Sholehudin, 2015), increasing to 3.88% in 2018 (Brina, 2019).

Women with GDM are at high risk of developing type 2 diabetes after pregnancy (Bao *et al*., 2016). Other risk factors can occur in pregnant women over 30 years of age, obesity (BMI> 30), excessive weight gain during pregnancy, which is more than 11-12 kg, there is a family history of DM, a history of GDM in a previous pregnancy, parity, multiparity, hypertension, history of stillbirth (death of a baby in the womb), history of giving birth to a baby with congenital abnormalities, glucosuria (excess sugar levels in urine) during pregnancy, history of giving birth to large babies (>4000 grams) (Ferrara, 2007). Obesity and other factors that promote insulin resistance appear to increase the risk of type 2 diabetes. Offspring of women with GDM have an increased risk of obesity, glucose intolerance, and Diabetes Mellitus. (Wahab *et al*., 2020).

The classification of GDM in pregnant women has been a matter of debate on the cut-off point or when the mother can be diagnosed with gestational diabetes mellitus (Koning *et al*., 2016). In simple terms, the classification of Diabetes Mellitus or Gestational Diabetes Mellitus can be done according to when the mother was diagnosed with diabetes. If the mother acquires diabetes before pregnancy, the classification is pregestational diabetes Mellitus; if the mother is diagnosed for the first time during pregnancy, she is classified as diabetes Mellitus.

The incidence of diabetes Mellitus at Mulyorejo Health Center was the 7th most disease category with 647 incidents. Women with GDM are often asymptomatic, so screening is important for detection. Screening in women with GDM also needs to be done 6 or 12 weeks after delivery. Carry out lifelong diabetes screening in women with a history of GDM at least once every three years (Garrison, 2015).

In a normal pregnancy, insulin resistance increases in mid-pregnancy and continues until birth (Kampmann *et al*., 2019). This is the reason why GDM can only be detected in the second and third trimesters of gestation. The impact caused by mothers with GDM is that they are at high risk of experiencing excess weight gain, preeclampsia, eclampsia, cesarean section, cardiovascular complications, and death. (Perkins *et al*., 2007). The factors that cause the incidence of GDM are history of GDM in a previous pregnancy, the history of diabetes mellitus (DM) in the family (parents, siblings, grandparents), multiparity, BMI, and age of pregnant women (Agussalim *et al*., 2018). Macrosomia is one of the high risks of neonatal mortality. Macrosomics is a condition in which the fetus is born outside a certain body weight, usually more than 4000g or 4500g, regardless of the gestational age of the fetus (Said and Manji, 2016). Previous macrosomic babies weighing 4.5 kg or more are also at risk for gestational diabetes (NICE, 2015). Likewise, mothers with GDM are at risk of giving birth to macrosomic babies (KC *et al.,* 2015).

Therefore, this study aimed to analyze the factors of the occurrence of GDM to do prevention early and minimize the incidence of complications and maternal death.

## 2. MATERIALS AND METHODS:

### 2.1. Study Design

This study was an analytical study with an observational approach. The research design was carried out with a case-control study. This study group samples were pregnant women registered at Primary Health Care of Mulyorejo Surabaya from 2017 to May 2018. The total sample in this study was 36 people, 6 people as cases and 30 people as controls, and was taken randomly. The data source comes from secondary data (medical records of pregnant women) at Primary Health Care of Mulyorejo Surabaya.

The sample was calculated using the sample size formula for case control studies with propotion value for diabetes cases (Bener *et al*., 2011). Calculate the sample size with a ratio of cases and controls 1: 5 as follows:

$$N = (1+1/c)\ p\ q\ (Z_{1-\alpha/2} + Z_{1-\beta})^2 / (p_1 - p_0)^2$$
$$N = (1+1/5)\ 0{,}759\ (0{,}241)\ (1{,}96 + 0{,}842)^2 / (0{,}8 - 0{,}718)^2 = 5{,}4409$$

The calculation results show the minimum case sample is 5.4409 then rounded to 6. Because it uses a ratio of 1: 5, the number of samples of cases was 6 and controls was 30.

### 2.2. Data Collection

Data collection techniques used secondary data taken through patient medical records by asking the mothers about their visit. The data categorized the factors that affect the health risks of pregnant women into two. The first was health status factors that contain family history of diabetes mellitus sufferers by asking the mother whether there is a family who has diabetes mellitus (Yes or No), BMI was calculated from the ratio of height and weight (<25: normal, 25-29.9: overweight, ≥30: obesity). The second one was the reproductive status factor which contains history of birth weight (<2500 grams; 2500-3900 grams; ≥4000 grams) the birth weight which was more than 4000 grams is considered a macrosomic baby, parity was indicated by how many children have been born of the mother (>2 or ≤2) and the age of the pregnant woman (<20 years; 20-35 years;>35 years).

### 2.3. Ethics

This study has received ethical approval from the Health Research Ethics Committee of the Faculty of Public Health, Airlangga University, with number 441-KEPK.

### 2.4. Data Analysis

The data analysis used in this research was a simple logistic regression test. The initial stage of this analysis was to use variables for candidate selection. All independent variables were analyzed using a simple logistic regression selection test. If an independent variable has p ≤0,250, it becomes a candidate and can be continued to the multivariable test. The next stage is to test to see the effect of the variables together using multiple logistic regression. The independent variable is said to significantly influence the dependent variable if the p-value is <0.05.

## 3. RESULTS AND DISCUSSION:

The results showed that 11 mothers had a history of DM in the family and 36.4% who had GDM, while 8% of other mothers had GDM but there was no family history of DM. Not all mothers who have a family history of DM can experience GDM or vice versa. This might be influenced by the aware attitude of the mother, who already knows that she has a risk factor for a family history of DM in maintaining her lifestyle, either from food or physical activity. On the other hand, mothers who do not have a family history of diabetes will not necessarily avoid GDM if they do not maintain their lifestyle. In this study, respondents were divided based on 3 categories, namely BMI <25 (normal), 25≤IMT≤ 29.9 (overweight), and BMI ≥30 (obesity). Based on the study results, the BMI of women before pregnancy was in the overweight category, namely 18 people. Mothers with GDM who had a BMI before pregnancy were in the overweight category of 22.2%, and a normal BMI of 13.3%. Mothers who did not have GDM but had BMI in the obesity category were 3 people. In this study, it was found that mothers experienced the majority of GDM events with BMI in the range of 25≤IMT≤ 29.9. Mothers who have a BMI who are overweight are more at risk of experiencing GDM.

It could also be observed that of the 6 mothers who experienced GDM, only one mother had a history of birth weight more than 4000 grams (macrosomia). Most mothers have a history of giving birth to babies with normal weight 2500-3900 grams. There were 11.8% of mothers who

had GDM with a history of giving birth to babies weighing between 2500-3900 grams. The results showed that mothers who had a history of giving birth to babies weighing ≥4000 grams had no risk of developing GDM because most mothers who had GDM had babies with a history of normal birth weight, and only one mother with a history of macrosomic babies.

The distribution of the parity variable showed that almost all pregnant women had parity ≤2. Mothers with GDM with parity ≤2 were 14.7% of the total 34. Mothers with GDM with parity> 2 were only one person. The results in this study only found 2 mothers with multiparity, while only one mother developed GDM. Most of these mothers with parity ≤2 were probably due to the family planning program run well by the government.

The distribution of mothers in this study showed that the mean age of mothers is in the range of 20-35 years. The results of the study were only three mothers aged> 35 years. Mothers who have GDM 5 people have an age range of 25 to 35 years and mother ages> 35 years. The results of this study indicate that mothers who were susceptible to GDM were those between 25-35 years of age. This might happen because she felt that she was still young, so she ignored her diet and lifestyle.

### 3.1 Health Status Factors

The health status factor is a factor that is an intermediate determinant of influencing pregnancy complications and death in the mother (McCarthy and Maine, 1992). Health status factors include the family history of DM and the body mass index (BMI) of a mother before pregnancy. The study respondents were 6 pregnant women with GDM and 30 pregnant women who did not experience GDM. The following is a discussion of health status factors that influence GDM.

#### *3.1.1 History of Diabetes Mellitus (DM) in the Family*

The results showed that 4 mothers had a history of DM in the family and experienced GDM, while the other 2 mothers had GDM, but there was no family history of DM. Based on the multiple logistic regression test results, it was found that significant results were that the family history of DM affects the incidence of GDM in pregnant women. The analysis results also obtained an OR value that indicates that a family history of DM in pregnant women has a 22,000 times chance of causing GDM compared to pregnant women who do not have a history of DM in the family. This study is in line with a previous study that mothers with a family history of DM have a 1.481 fold increased risk for GDM compared with no family history of DM (Zhu *et al*., 2017).

History has a very strong influence on the incidence of GDM, because according to a study about 50 percent of patients with type 2 diabetes have a parent who has diabetes, and more than a third of diabetes patients have a sibling with diabetes (Tandra, 2008). So when a mother has a family history of DM, the mother has a greater risk of experiencing GDM during pregnancy. Research by Cong Luat Nguyen, *et al* (2018) on the prevalence of GDM from January 2000 to December 2016 states that the prevalence of GDM varies across countries, including identification of pregnant women during the first and second trimesters. Besides that, it is influenced by several factors, one of which is genetic factors. As a result of this gestational diabetes mellitus, the impact will only be visible after a few years; if it is not handled now, it will trigger an increase in the incidence of GDM. Mothers with GDM are at high risk for excess body weight gain, preeclampsia, eclampsia, cesarean section, and cardiovascular complications to maternal death. Even in the world, the incidence is up to 1.3%. After giving birth, mothers with GDM are at risk of developing type 2 diabetes. For example, in India, it is stated that 6.3% of 811 pregnancies in the Indian Prima tribe of Arizona even occur recurrent GDM in the future. Meanwhile, babies born to mothers with gestational diabetes are at high risk for macrosomia, while the prevalence in pregnant women with a family history of diabetes is 1.5% (Sheen YJ, *et al.*, 2019).

#### *3.1.2 Body Mass Index (BMI) Before Pregnancy*

BMI before pregnancy is a major determinant of pregnancy outcome. Increased BMI was associated with an increased risk of preeclampsia, GDM, gestational hypertension, and cesarean delivery (Nelson *et al*., 2009). According to the National Health and Nutrition Examination Survey, 33.4% of women aged 20 to 34 were obese (body mass index (BMI) ≥30), and 58.4% were overweight (BMI ≥25)(Riley *et al*., 2018).

The results of statistical tests with simple logistic regression showed that the BMI of mothers before pregnancy did not significantly affect the incidence of GDM. This is contrary to research (Bener *et al*., 2011), which states that obesity was the most significant factor in the incidence of GDM.

The incidence of GDM is associated with the epidemic incidence of obesity in the past 6-8 years. The long-term impact of GDM is to increase the risk of obstetric complications of pregnancy such as hypertension, cesarean section, and increased risk of perinatal complications such as increased incidence of macrosomia, fetal miscarriage, neonatal complications (hypoglycemia, polycythemia, hyperbilirubinemia) (Takashi Sugiyama, 2011).

This study has interesting results where all mothers (3 people) who have a BMI before pregnancy in the obese category do not experience GDM. This may occur because of the many factors that can influence GDM. As the results of previous studies, it was found that 54.3% of the sample of pregnant women had a BMI in the overweight or obese category, and 32% of them had GDM (Pinheiro and Goldani, 2018). Lack of a physical activity can increase insulin resistance in pregnant women (Kampmann *et al*., 2019), mothers who regularly do physical activity can reduce their risk of developing GDM (Lin *et al*., 2020). A review study of several articles suggests that diet and physical activity interventions can help prevent GDM were inconsistent (Zhang *et al*., 2016). However, a previous review of five studies found that recreational physical activity in early pregnancy can reduce the risk of GDM by more than 20% (Tobias *et al*., 2011).

**3.2 Reproductive Status Factors**

Reproductive status is a factor that is an intermediate determinant of influencing pregnancy complications and maternal mortality (McCarthy and Maine, 1992). Reproductive status factors include the history of birth weight, parity, and maternal age. The study respondents were 6 pregnant women with GDM and 30 pregnant women who did not experience GDM. The following is a discussion of reproductive status factors that influence GDM.

***3.2.1 History of Birth Weight***

One of the agreed risk factors for GDM was a history of having given birth to a macrosomic baby in a previous pregnancy without an explanation for stillbirth or neonatal death (Shannon and Wong, 2010). Women with a history of delivering a macrosomic baby have a significantly increased risk of having another macrosomic baby in a subsequent pregnancy. For women with two or more macrosomic babies, the risk was even more significant (Aye *et al*., 2011). Delivering a baby weighing more than 3.5 kilograms was a significant predictor of T2DM development (Herath *et al*., 2017).

In this study only one mother with a history of giving birth to a macrosomic baby. According to the simple logistic regression results, there is no significant relationship between the history of birth weight and the incidence of GDM. In line with the previous study, only 3 mothers suffered from GDM out of 50 mothers who gave birth to macrosomic babies (Oroh *et al*., 2015). Macrosomia has many other causes besides diabetes mellitus, such as obesity, multiparity (Oroh *et al*., 2015). 79% of macrosomic babies were born again to mothers who were not glucose intolerant (Magenheim *et al*., 2007). Macrosomic babies born to mothers with diabetes are more at risk of hyperinsulinemia than macrosomic babies born to mothers with normal sugar levels (Siraj *et al*., 2020).

***3.2.2 Parity***

The multiple logistic regression test results showed that parity was not a variable affected ($p = 0.077$) on the incidence of GDM. Still, parity was a potential variable for the incidence of GDM. The distribution of the parity variable showed that almost all pregnant women had parity ≤2. Mothers with GDM who have parity> 2 are only one person.

Nurrahmani (2012) said that mothers with multiparity (more than 3) have a risk factor for diabetes mellitus in pregnancy, which is about 78% of women with multiparity (more than 3). This can happen because physiological changes affect carbohydrate metabolism due to the presence of the placental hormone lactogen that is resistant to insulin. So that insulin resistance is not only due to the due date of birth, but the hormones estrogen, progesterone, cortisol, and prolactin also affect insulin resistance. Cortisol levels in pregnant women will increase 3 times during pregnancy. So the need for insulin in pregnant women becomes high and weight gain in pregnant women is also quite easy. Besides, it is a risk factor for diabetes that is influenced by changes in the lifestyle of every human being will impact on changes in disease patterns that occur in society. In other research, several factors that are part of the lifestyle are reducing the consumption of junk food which is currently becoming very popular among children to adults, other factors such as a healthy diet, regular exercise, and other lifestyles can affect the lower risk of mothers getting diabetes in pregnancy (Irawan, 2010).

The incidence of GDM per 1000 persons per year was 3.69 in primiparous women and 4.12 in multiparous women (Almahmeed *et al*., 2017).

Women with multiparous have a higher risk of developing diabetes than women with primiparous. The odds ratio for multiparous was 1.33 times the chance of getting diabetes mellitus compared to women with primiparous. GDM had a relationship with multiparity (Huillca-Briceño and Varillas, 2016). Multiparous mothers were more likely to develop GDM than primiparous (Zhu *et al*., 2017).

#### *3.2.3 Age of Pregnant Women*

The distribution of mothers in this study shows that the mean age of mothers was in the range of 20-35 years. This is consistent with previous studies that out of 87 mothers who experienced GDM, 64 (73.6%) were aged 25 to 35 (Xu *et al*., 2017). Delivering a child after 30 years is a significant predictor of T2DM development (Herath *et al*., 2017).

According to the simple logistic regression test results, it was found that maternal age did not affect the incidence of GDM. This contradicts with the previous study, which stated that age was a risk factor for GDM. The risk of GDM will increase with age. With each increase in 1 year of age (between 17 and 46 years of age), the risk for GDM increases by 5.3% (Zhu *et al*., 2017). Although in this study age did not influence the incidence of GDM, it should be noted that six mothers experience GDM who are at risk for developing DM in the next 5 to 10 years. The ages of these mothers ranged from 30-50 years when experiencing DM. This incident showed that there will be a period of degenerative disease, in this case, DM was no longer experienced by the elderly only. Therefore, it is important to pay attention, especially in the prevention and screening of the incidence of GDM in pregnant women.

## 4. CONCLUSIONS:

Pregnant women with a family history of diabetes that is not matched by maintaining a good lifestyle can develop complications of GDM. Most of the mothers did not have a family history of DM even though most of the mothers BMI was in the range 25≤IMT≤29.9. The distribution of the history of birth weight for infants is mostly in the range 2500-3900 g. The majority of mothers have parity of not more than 2 children. The distribution of mother's age was mostly in the range of 20-35 years.

Based on the influence analysis results, it was found that the health status factor which was a determinant (had an influence) on the incidence of GDM was a family history of DM. The reproductive status factor, parity, is a potential factor to influence the incidence of GDM. Therefore, there were several inputs for stakeholders to be able to prevent the incidence of GDM in this study, namely as follows: Health screening (integrated ANC and laboratory health tests) must be done (prioritized) for pregnant women at Primary Health Care of Mulyorejo Surabaya who has a history of DM in families and multiparity.

Mothers need to maintain their health with regular consultations related to their pregnancy to health service centers, especially hospitals. Routinely carry out health screening after childbirth and maintain a healthier lifestyle so that the GDM incident does not develop into DM in the future.

## 5. ACKNOWLEGDMENTS:

The author would like to thank the Primary Health Care of Mulyorejo and Universitas Airlangga for permissions support and Lembaga Pengelola Dana Pendidikan (LPDP) for financial support.

## 6. REFERENCES:

1. Agussalim, Jacob, A. S., and Harliani. (2018). Risk Factors of Diabetes Mellitus Occurrence Gestasional. *Global Scientific Research Journal of Diabetes*, *1*(11), 1–8.
2. Almahmeed, B., Shah, B. R., Mukerji, G., Ling, V., Booth, G. L., and Feig, D. S. (2017). Effect of multiparity and ethnicity on the risk of development of diabetes: a large population-based cohort study. *Diabetic Medicine*, *34*(11), 1637–1645. https://doi.org/https://doi.org/10.1111/dme.13441
3. American Diabetes Association. (2004). Gestational Diabetes Mellitus. *Diabetes Care, 27*(1), S88-S90. https://doi.org/https://doi.org/10.2337/diacare.27.2007.S88
4. Aye, S. S., Miller, V., Saxena, S., and Farhan, M. (2011). Management of large-for-gestational-age pregnancy in non-diabetic women. *The Obstetrician and Gynaecologist*, *12*(4), 250–256.
5. Bener, A., Saleh, N. M., and Al-Hamaq, A. (2011). Prevalence of Gestational

Diabetes and Associated Maternal and Neonatal Complications in a Fast Developing Community: Global Comparisons. *International Journal of Women's Health*, *3*, 367–373. https://doi.org/10.1136/archdischild-2012-302724.0640

6. Brina, A. G. (2019). *Faktor Risiko Diabetes Melitus Gestasional di RSUD Dr. Soetomo Surabaya*. Universitas Airlangga.

*7. Ferrara, A. (2007).* Increasing prevalence of gestational diabetes mellitus: a public health perspective*. Diebetes Care. 30* (2):S141-S146*.*

8. Garrison, A. (2015). Screening, diagnosis and management of gestational diabetes mellitus. *American Family Physician*, *91*(7), 460–467. https://doi.org/10.1177/1753495X14536891

9. Herath, H., Herath, R., and Wickremasinghe, R. (2017). Gestational diabetes mellitus and risk of type 2 diabetes 10 years after the index pregnancy in Sri Lankan women - A community based retrospective cohort study. *PLoS ONE*, *12*(6), 1–14. https://doi.org/10.1371/journal.pone.0179647

10. Huillca-Briceño, A., and Varillas, M. R. (2016). Multiparity as a risk factor for gestational diabetes mellitus. *Revista Cubana de Obstetricia y Ginecologia*, *42*(2), 189–199.

11. International Diabetes Federation. (2015). *IDF Diabetes Atlas* (Seven).

*12. Irawan, D. (2010). Prevalensi dan Faktor Risiko Kejadian Diabetes Melitus Tipe 2 Di Daerah Urban Indonesia (Analisa Data Sekunder Riskesdes 2007). Thesis. Universitas Indonesia*

13. Kampmann, U., Knorr, S., Fuglsang, J., and Ovesen, P. (2019). Determinants of Maternal Insulin Resistance during Pregnancy: An Updated Overview. *Journal of Diabetes Research*, *2019*, 1-9. https://doi.org/10.1155/2019/5320156

14. KC, K., Shakya, S., & Zhang, H. (2015). Gestational diabetes mellitus and macrosomia: A literature review. *Annals of Nutrition and Metabolism*, *66*(2), 14–20. https://doi.org/10.1159/000371628

15. Koning, S. H., Hoogenberg, K., Lutgers, H. L., van den Berg, P. P., and Wolffenbuttel, B. H. R. (2016). Gestational Diabetes Mellitus: current knowledge and unmet needs. *Journal of Diabetes*, *8*(6), 770–781. https://doi.org/10.1111/1753-0407.12422

16. Lin, X., Yang, T., Zhang, X., and Wei, W. (2020). Lifestyle intervention to prevent gestational diabetes mellitus and adverse maternal outcomes among pregnant women at high risk for gestational diabetes mellitus. *Journal of International Medical Research*, *48*(12), 1–10. https://doi.org/10.1177/0300060520979130

17. Magenheim, R., Tabák, A., Lengyel, Z., Tóth, K. S., and Lévárdi, F. (2007). Is Previous Macrosomia a Risk Factor For Gestational Diabetes in The Era of General Screening. *International Journal of Obstetrics and Gynaecologi*, *114*(4), 512–513.

18. McCarthy, J., and Maine, D. (1992). A Framework for Analyzing the Determinants of Maternal Mortality. *Studies in Family Planning*, *23*(1), 23. https://doi.org/10.2307/1966825

19. Nelson, S. M., Matthews, P., and Poston, L. (2009). Maternal metabolism and obesity: Modifiable determinants of pregnancy outcome. *Human Reproduction Update*, *16*(3), 255–275. https://doi.org/10.1093/humupd/dmp050

20. Nguyen C.L., Pham N.M., Colin W.B., Duong D.V., and Andy H.Lee. (2018). Prevalance of Gestational Diabetes Mellitus in Eastren and Southeastern Asia: A Systematic Review and Meta-Analysis. *Journal of Diabetes Research*, *2018*, 1-10. https://doi.org/10.1155/2018/6536974

21. NICE. (2015). Diabetes in pregnancy: management from preconception to the postnatal period. Retrieved from https://www.nice.org.uk/guidance/ng3/resources/diabetes-in-pregnancy-management-of-diabetes-and-its-complications-from-preconception-to-the-postnatal-period-51038446021

22. Nurrahmani. (2012). Stop Diabetes Mellitus. Yogyakarta: Familia.

23. Oroh, A., Loho, M., and Mongan, S. (2015). Kaitan Makrosomia Dengan Diabetes Melitus Gestasional Di Bagian Obsgin BLU RSUP Prof. Dr. R. D. Kandou Manado Periode September 2012-September

2013. *Jurnal E-CliniC*, *3*(2). https://doi.org/10.35790/ecl.3.2.2015.8774

24. Perkins, J. M., Dunn, J. P., and Jagasia, S. M. (2007). Perspectives in gestational diabetes mellitus: A review of screening, diagnosis, and treatment. *Clinical Diabetes*, *25*(2), 57–62. https://doi.org/10.2337/diaclin.25.2.57

25. Pinheiro, T. V., and Goldani, M. Z. (2018). Maternal pre-pregnancy overweight/obesity and gestational diabetes interaction on delayed breastfeeding initiation. *PLoS ONE*, *13*(6), 1–11. https://doi.org/10.1371/journal.pone.0194879

26. Riley, L., Wertz, M., and McDowell, I. (2018). Obesity in pregnancy: Risks and management. *American Family Physician*, *97*(9), 559–561. https://doi.org/10.1258/om.2009.090009

27. Said, A. S., and Manji, K. P. (2016). Risk factors and outcomes of fetal macrosomia in a tertiary centre in Tanzania: A case-control study. *BMC Pregnancy and Childbirth*, *16*(1), 1–8. https://doi.org/10.1186/s12884-016-1044-3

28. Shannon, A., and Wong, C. K. (2010). Risk Factors Associated with Gestational Diabetes Mellitus. *International Journal Bioautomation*, *14*(1), 15–26. http://clbme.bas.bg/bioautomation/2010/vol_14.1/files/14.1_02.pdf

29. Sheen, Y. J., Hsu, C. C., Jiang. Y. D., Huang, C. N., Liu, J. S., Sheu, W. H. (2019). Trends in prevalence and incidence of diabetes mellitus from 2005 to 2014 in Taiwan. *Journal of the Formosan Medical Association, 118*(2), S66-S73.

30. Sholehudin, M. A. (2015). *Karakteristik Diabetes Melitus Pada Kehamilan di RSU dr. Soetomo Periode Januari-Desember 2015*. Universitas Airlangga.

31. Siraj, S., Raheem, M., Kamran, D. E. S., Khan, A. M., Parveen, N., and Qureshi, M. A. (2020). Serum insulin levels and anthropometric indices in macrosomic neonates; A comparative study between fetuses of diabetic and non-diabetic mothers. *Rawal Medical Journal*, *45*(3), 593–597.

32. Soewondo, P., and Pramono, L. A. (2011). Prevalence, characteristics, and predictors of pre-diabetes in Indonesia. *Medical Journal of Indonesia*, *20*(4), 283–294. https://doi.org/10.13181/mji.v20i4.465

33. Takashi Sugiyama. (2011). Management of Gestational Diabetes Mellitus. *Journal of the Japan Medical Association JMAJ*, *139*(10), 2089–2094.

34. Tandra, H. (2008). *Diabetes*. Gramedia Pustaka Utama.

35. Tobias, D. K., Zhang, C., Van Dam, R. M., Bowers, K., and Hu, F. B. (2011). Physical activity before and during pregnancy and risk of gestational diabetes mellitus: A meta-analysis. *Diabetes Care*, *34*(1), 223–229. https://doi.org/10.2337/dc10-1368

36. Wahab, R. J., Voerman, E., Jansen, P. W., Oei, E. H. G., Steegers, E. A. P., Jaddoe, V. W. V., and Gaillard, R. (2020). Maternal Glucose Concentrations in Early Pregnancy and Cardiometabolic Risk Factors in Childhood. *Obesity*, *28*(5), 985–993. https://doi.org/10.1002/oby.22771

37. Xu, X., Liu, Y., Liu, D., Li, X., Rao, Y., Sharma, M., and Zhao, Y. (2017). Prevalence and determinants of gestational diabetes mellitus: A cross-sectional study in China. *International Journal of Environmental Research and Public Health*, *14*(12), 1–13. https://doi.org/10.3390/ijerph14121532

38. Zhang, C., Rawal, S., and Chong, Y. S. (2016). Gestational diabetes mellitus and long-term consequences for mother and offspring: a view from Denmark. *Diabetologia*, *59*(7), 1396–1399. https://doi.org/10.1007/s00125-016-3985-5

39. Zhu, W. W., Yang, H. X., Wang, C., Su, R. N., Feng, H., and Kapur, A. (2017). High prevalence of gestational diabetes mellitus in Beijing: Effect of maternal birth weight and other risk factors. *Chinese Medical Journal*, *130*(9), 1019–1025. https://doi.org/10.4103/0366-6999.204930

***Table 1.*** *Multivariate logistic regression test for GDM risk factors (N=30)*

| Factors | | GDM | | Non-GDM | | p-value | |
|---|---|---|---|---|---|---|---|
| | | n | % | n | % | Selection of candidates | Multivariate test |
| History of DM in the Family | | | | | | .052* | .035** |
| | Yes | 4 | 36.4 | 7 | 63.6 | | |
| | No | 2 | 8.0 | 23 | 92 | | |
| BMI | | | | | | .808 | |
| | Normal | 2 | 13.3 | 13 | 86.7 | | |
| | Overweight | 4 | 22.2 | 14 | 77.8 | | |
| | Obesity | 0 | .0 | 3 | 100.0 | | |
| History of Birth Weight (grams) | | | | | | 1.000 | |
| | <2500 | 1 | 100.0 | 0 | .0 | | |
| | 2500-3900 | 4 | 11.8 | 30 | 88.2 | | |
| | ≥4000 | 1 | 100.0 | 0 | .0 | | |
| Parity | | | | | | .240* | .077 |
| | ≤2 | 5 | 14.7 | 29 | 85.3 | | |
| | > 2 | 1 | 50.0 | 1 | 50.0 | | |
| Age of mother (years old) | | | | | | .434 | |
| | <20 | 0 | .0 | 0 | .0 | | |
| | 20-35 | 5 | 15.2 | 28 | 84.8 | | |
| | > 35 | 1 | 33.3 | 2 | 66.7 | | |
| Total | | 6 | 16.7 | 30 | 83.3 | | |

Notes: *significant to a selection of candidates (<.25); **significant to multivariate test (<.05)

PERIÓDICO TCHÊ QUÍMICA
ARTIGO ORIGINAL

# METODOLOGIA DE SUPERFÍCIE DE RESPOSTA PARA OTIMIZAÇÃO DA ADSORÇÃO DE METAIS PESADOS EM UMA SOLUÇÃO MULTI-METAIS POR PELLETS DE ZEÓLITAS DE BENTONITA-CAOLIM

# RESPONSE SURFACE METHODOLOGY FOR OPTIMIZATION OF HEAVY METAL ADSORPTION IN A MULTIMETAL SOLUTION BY BENTONITE-KAOLIN-ZEOLITE PELLETS

# METODOLOGÍA DE SUPERFICIE DE RESPUESTA PARA LA OPTIMIZACIÓN DE LA ADSORCIÓN DE PELLETS DE BENTONITA-CAOLÍN-ZEOLITA EN UNA SOLUCIÓN MULTIMETÁLICA

CARBONEL-RAMOS, Dalia Elisa[1*]; CHIRINOS, Hugo David[2]; GOMÉZ-MARROQUÍN, Mery Cecilia[3]; AGARWAL, Madhu[4].

[1,2] Faculty of Environmental Engineering, National University of Engineering, Peru

[3] Faculty of Geological, Mining and Metallurgic Engineering, National University of Engineering, Peru

[4] Department of Chemical Engineering, Malaviya National Institute of Technology Jaipur, India

** Correspondence author*
*e-mail: dcarbonelr@uni.pe*

Received 22 September 2020; received in revised form 05 February 2021; accepted 10 February 2021

## RESUMO

**Introdução:** A contaminação das águas superficiais e subterrâneas com metais pesados é um grande problema ambiental. Os minerais de argila são porosos e eficientes para adsorver íons metálicos. Entre as tecnologias de tratamento disponíveis, a adsorção é a mais econômica, fácil de operar, escalonável e replicável para remediar metais pesados da solução aquosa. **Objetivo:** O objetivo desse estudo foi avaliar o desempenho de adsorção de pellets de argila de aluminossilicatos naturais, bentonita (29%), caulim (4%) e zeólita (67%) para remoção de metais pesados de soluções aquosas. **Métodos:** O efeito de condições operacionais ótimas, como tempo de contato, dose de adsorvente, pH e concentração inicial de metais pesados, foi estudado. Estudos cinéticos e de equilíbrio também foram realizados. Os adsorventes foram caracterizados usando análise de FTIR. **Resultados e Discussão:** Os valores ótimos para tempo de contato, dose do adsorvente, pH e concentração inicial de chumbo, cobre e cádmio foram; 240 min; 25 g/L; 4,3; e 4mg/L, 7 mg/L e 2 mg/L, respectivamente. A isoterma de Langmuir foi o modelo de isoterma mais bem ajustado para os três metais. A cinética de adsorção mostrou que a adsorção de chumbo e cobre seguiu o modelo de pseudo-segunda ordem, enquanto o cádmio se adequou ao modelo de pseudo-primeira ordem. A seletividade dos pellets para os íons metálicos foi da ordem de Pb> Cu> Cd. **Conclusões:** A nova combinação de pellets de bentonita-caulinita-zeólita funcionou bem no tratamento de águas residuais terciárias e foi utilizada com sucesso como um adsorvente natural em solução multimetal. Os resultados confirmaram que os grânulos de argila usados têm melhor capacidade de adsorção do que muitos outros estudos relatados. A capacidade de adsorção máxima pode ser aumentada ajustando a temperatura de calcinação e aplicando tratamentos químicos aos grânulos de argila antes da extrusão. A análise da superfície de resposta avaliou os valores ideais previstos para os quatro fatores operacionais.

**Palavras-chave**: Pelotas de argila; Adsorção; Solução multimetal; Análise de superfície de resposta

## ABSTRACT

**Background:** Heavy metals contamination of surface and groundwater is a major environmental problem. Clay minerals are porous and are efficient to adsorb metal ions. Amongst the available treatment technologies, adsorption is the most cost-effective, easy to operate, scalable, and replicable to remediate heavy metals from water solution. **Aim:** This study aimed to assess the adsorption performance of clay pellets of natural aluminosilicates, bentonite (29%), kaolin (4%) and zeolite (67%) to remove heavy metals from aqueous solutions. **Methods:** The effect of optimal operating conditions like contact time, adsorbent dose, pH, and heavy metals initial concentration has been studied. Kinetic and equilibrium studies were also performed. Adsorbents were

characterized using FTIR analysis. **Results and Discussion:** Optimum values for contact time, adsorbent dose, pH, and initial concentration of lead, copper, and cadmium were; 240 min; 25 g/L; 4.3; and 4mg/L, 7 mg/L and 2 mg/L, respectively. The Langmuir isotherm was the best-fitted isotherm model for the three metals. Adsorption kinetics showed that the lead and copper adsorption followed the pseudo-second-order model while cadmium suited with the pseudo-first-order model. The selectivity of the pellets towards the metal ions was in the order of Pb > Cu > Cd. **Conclusions:** The new combination of bentonite-kaolinite-zeolite pellets worked well in tertiary wastewater treatment and successfully utilized as a natural adsorbent in multimetal solution. The results confirmed that the used clay pellets have better adsorption capacity than many other reported studies. Maximum adsorption capacity can be further increased by adjusting the calcination temperature and applying chemical treatments to the clay pellets before extrusion. The response surface analysis evaluated the predicted optimal values for the four operating factors.

**Keywords**: *Clay pellets; Adsorption; Multimetal solution; Response surface analysis.*

## RESUMEN

**Antecedentes:** La contaminación por metales pesados en aguas superficiales y subterráneas es un grave problema ambiental. Entre las tecnologías disponibles de tratamiento para remover metales pesados de soluciones acuosas, la adsorción es la más rentable, fácil de operar, escalable y replicable. **Objetivo:** El objetivo de este estudio fue evaluar el rendimiento de adsorción de pellets de aluminosilicatos naturales de bentonita (29%), caolín (4%) y zeolita (67%) para eliminar metales pesados de soluciones acuosas. **Métodos:** Se estudió el efecto de las condiciones óptimas de funcionamiento, como el tiempo de contacto, la dosis de adsorbente, el pH y la concentración inicial de metales pesados. También se realizaron estudios cinéticos y de equilibrio. Los adsorbentes se caracterizaron mediante análisis FTIR. **Resultados y Discusión:** Los valores óptimos de tiempo de contacto, dosis de adsorbente, pH y concentración inicial de plomo, cobre y cadmio fueron; 240 min; 25 g/L; 4,3; y 4 mg/L, 7 mg/L y 2 mg/L, respectivamente. La isoterma de Langmuir fue el modelo de mejor ajuste para los tres metales. La cinética de adsorción mostró que el plomo y cobre se ajustaron mejor al modelo de pseudo-segundo orden, mientras que el cadmio se ajustó mejor al modelo de pseudo-primer orden. La selectividad de los pellets hacia los iones metálicos fue del orden de Pb> Cu> Cd. **Conclusiones:** Los pellets fabricados a partir de bentonita-caolín-zeolita demostraron ser efectivos como adsorbentes naturales en el tratamiento terciario de aguas residuales en una solución multimetálica. Los resultados confirman que los pellets usados tienen una mejor capacidad de adsorción que muchos otros estudios reportados. La capacidad máxima de adsorción podría aumentarse ajustando la temperatura de calcinación y aplicando tratamientos químicos a los adsorbentes antes de la extrusión.

**Palabras clave**: *Pellets de arcilla; Adsorción; Solución multimetálica; Análisis de superficie de respuesta*.

## 1. INTRODUCTION:

Heavy metal contamination of surface and groundwater is a major problem since the 1990s (UNEP, 2016). Agricultural runoffs contain high amounts of toxic inorganic and organic substances (Voulvoulis and Georges, 2016). Pesticides and fertilizers used in agriculture cause nonpoint-source pollution to surface water and groundwater. Natural geomaterials such as clay minerals and zeolites help control the release of fertilizers, pesticides, and herbicides (Manjaiah *et al*., 2019). Several studies explored the use of clay and zeolites to remediate toxic environmental pollutants (Calvo and Garcia-Lorenzo, 2018; Rao and Kashifuddin, 2016; Uddin, Ahmed, and Naushad, 2019).

Heavy metals are of special concern due to their toxic characteristics such as diffusion, persistence, toxic effects even at low concentration, bioaccumulation, and biomagnification. They can spread easily, which makes them ubiquitous, and they can be toxic at very low concentrations. The harmful effects of heavy metals can be long lasting and damage vital body organs. Various technologies have been implemented for the removal of heavy metals such as ion exchange (Dąbrowski, Hubicki, Podkościelny, and Robens, 2004), ultrafiltration and flocculation (Huang *et al*., 2016), membrane filtration (Alarifi *et al*., 2020), electrodialysis (Al-Shannag *et al*., 2015) and adsorption (Uddin and Nasar, 2020). Ion exchange is famous and commonly used for demineralization and disinfection of water. Although the ion-exchange system works well at low concentrations, yet the technique requires sophisticated equipment. Coagulation is a chemical procedure that is easy to operate and requires low maintenance but it generates large quantities of contaminated sludge. The membrane filtration process produces a pure effluent, but the energy demand is high as well as the operational and maintenance cost. Adsorption, however, shows the best performance

in terms of removal efficiency of aqueous pollutants compared to other methods. Adsorption is a low-cost, reliable, simple to install method which is easy to operate, demands fewer energy requirements; is adjustable, and easily replicable. Adsorption mechanism is generally being of weak physical adsorption or strong chemical adsorption. The physical adsorption process includes Van der Waals or electrostatic interaction between the surface of the adsorbent and targeted pollutants. Chemical adsorption is generally fast and involves chemical bonding between adsorbent and pollutants.

The use of clays and zeolites in the adsorption process for wastewater treatment has many advantages over other existing technologies. They are natural, less expensive, and provide significant benefits in the removal of metal ions. However, it is crucial to generate information that allows its application at the industrial level, such as operation conditions, equilibrium, and adsorption kinetics. To prepare the novel ionic liquid clay, Kakaei *et al*. recently modify raw clinochlore with triazole and triazolium ligands (Kakaei, Khameneh, Hosseini, and Moharreri, 2020). The prepared ecofriendly modified adsorbent was applied for the removal of lead, cobalt, and zinc ions. The catalyst material proved to be functional for heavy metal adsorption. In another study, single and mixed pillared clays were successfully utilized to remove inorganic pollutants from the water (Mnasri-Ghnimi and Frini-Srasra, 2019). In comparison, it was found that natural pillared clays had better adsorption properties for cadmium, cobalt, and copper metal ions. Recently, three different forms of raw attapulgite clay were prepared for the removal of cadmium and lead, and it was found that the adsorbent prepared by hydrothermal reaction and calcination was shown excellent adsorption properties while all the three adsorbents showed high adsorption for lead ions (Huang *et al*., 2020). Ravikumar and Udayakumar mixed *Moringa oleifera* seeds with bentonite clay and prepared a novel green clay composite for heavy metals removal (Ravikumar and Udayakumar, 2020). The natural zeolite of Kamchatka region, Russia was chosen to minimize the contents of heavy metals in the wastewater of the region (Belova, 2019). It was found that Yagodninsky deposit zeolites are very effective to extract several toxic metal ions from polluted water. The adsorption was in the row of $Cu^{2+}$> $Ni^{2+}$> $Co^{2+}$> $Fe^{2+}$. Pottery sludge consists of silica, alumina, iron oxide was applied for copper removal (Uddin, Rao, and Chandra Mouli, 2018). Glaze, which consists of clay minerals, boron, silica, fluxes, and melting agents, was proved to be an excellent adsorbent for copper (II) removal (Rao and Kashifuddin, 2012). So, there are many studies related to removing metal ions using clay adsorbents; however, adsorption in multi-metallic solutions with cylindrical shape pellets is not studied. This paper presents the first time use of clay pellets for tertiary wastewater treatment. The use of the pelletizing process reduces the cost, which makes this study attractive. From an economic point of view, the development of this material makes the removal of heavy metals from wastewater quite profitable.

Therefore, this study aimed to assess the adsorption performance of clay pellets of natural aluminosilicates, bentonite (29%), kaolin (4%) and zeolite (67%) to remove heavy metals from aqueous solutions.

## 2. MATERIALS AND METHODS:

The study was conducted in the Research Laboratory of the Environmental Engineering Faculty, National Engineering University, Peru. A third party laboratory present in the Science Faculty of the same university did some analysis.

### 2.1. Clay characterization

Kaolin and bentonite were obtained from a natural deposit in the city of Cajamarca, North Peru, while raw zeolite was obtained from Hydro Source, LLC. The analysis of the mineralogical composition of all the three aluminosilicates was done using spectrometry. Before adsorption, FTIR analysis was also conducted. Adsorbent pellets were ground in an agate mortar. Subsequently, about 100 mg of adsorbent powder was analyzed at room temperature (20.3 ºC) and 66% of relative humidity. The analysis was made using a Perkin Elmer Frontier MIR spectrometer, with a $4cm^{-1}$ resolution and a KBr pressed disc technique.

### 2.2. Reagents

Lead nitrate (Pb $(NO_3)_2$), copper sulfate pentahydrate ($CuSO_4$×5 $H_2O$), and cadmium nitrate (Cd $(NO_3)_2$) were acquired from Merck laboratory and used as metallic reagents. Multimetal solutions of lead (II), copper (II), and cadmium (II) were prepared by diluting the necessary amount of metal reagents in distilled water. Different molarities of $H_2SO_4$ and KOH were used to adjust the pH values.

Standard solutions for lead, copper, and cadmium were elaborated in four different concentrations, diluting standard stock solutions of

1000 mg/l concentration. This allowed obtaining the calibration curve. After adsorption and without further filtration, heavy metals concentrations were measured with an atomic absorption spectrometer (Model AA-700, Shimadzu), using an acetylene/air flame. The detection limit of the mentioned equipment for the three metals was between 0.001 mg/L and 0.009 mg/L. Wavelength measures for lead, copper and cadmium were 217 nm, 324.8 nm and 228.8 nm respectively. Slit width for all metals was 0.7 nm.

### 2.3. Pelletization

The method described in Miranda *et al*. was adapted for the preparation of pellets (Mejia Miranda, Laverde, Avella, and Peña Ballesteros, 2015). By using the dry and sieved material (particle size smaller than 33µm), aluminosilicates were mixed at a rate of 67% zeolite, 29% bentonite and 4% kaolin (based on the recommendation made by Salem and Akbari Sene (2012)). This mixture was moistened at a proportion of 42% (w/v). Pellets formed were dried at 100 °C and calcined at 600 °C in a furnace (Ciosek, Luk, Warner, & Warner, 2016).

### 2.4. Adsorption tests

#### *2.4.1 Adsorption*

Adsorption was done in a column system. 300 mL of multimetal solution was circulated using a peristaltic pump at the rate of 20 mL/min at different time intervals (45, 60, 120, 180, 240 and 300 minutes). The samples were taken for the measurement of adsorption efficiency. The effect of pH and contact time on the adsorption was also noted.

Removal efficiency percentage ($\%R_{em}$) was determined using Equation 1.

$$\%R_{em} = \frac{C_o - C_e}{C_o} \cdot 100 \qquad \text{(Eq. 1)}$$

Where $C_o$ (mg/L) and $C_e$ (mg/L) represent the initial and final concentrations of the heavy metals. The equilibrium adsorption capacity, $Q_e$ (mg/g), was found with Equation 2.

$$Q_e = \frac{Co - C_e}{m} \cdot V \qquad \text{(Eq. 2)}$$

Where $C_e$ (mg/L) is the equilibrium concentration, m the total mass of adsorbent (g) and V the volume (L) of solution.

### 2.5. Response Surface Methodology (RSM) design

RSM with a central composite rotatable design (CCRD) was applied to determine the optimum operating conditions. Four variables (contact time, adsorbent dose, pH and initial heavy metals concentration) with five levels were chosen to employ CCRD. Table 1 shows the matrix of the factors and their coded levels. Many authors have also used CCD to analyze the adsorption data critically. Recently, $2^n$ factorial design with 20 experimental runs was used to optimize the effect of pH, time, and initial concentration on the biosorption of chromium (Bayuo, Abukari, and Pelig-Ba, 2020). In another study, the CCD results were obtained for pH, adsorbent dosage, and initial concentration and the maximum experimental removal of $Cd^{2+}$ and $Pb^{2+}$ was 98.90% and 99.99%, respectively (Mohd Zahri *et al*., 2020). Sheydai *et al*. illustrated the effects of initial pH, dosage, sonication time and temperature on $Cu^{2+}$ ion removal efficiency using CCD (Sheydaei, Gasemsoltanlu, and Beiraghi, 2019). It was found that 97 % of $Cu^{2+}$ ions were adsorbed using natural clinoptilolite and the optimum condition was dosage: 500 mg/L, pH: 6, sonication time: 12 min and sonication temperature: 45°C. Another RSM method i.e., Box-Behnken Design (BBD) is also used to analyze the adsorption data. Chromium (VI) adsorptionby Litchi peel was statistically analysed by BBD, statistical hypothesis test, ANOVA and comparison of t-tests (Uddin and Salah, 2018). Adsorption capacity of plant bark towards lead ions was determined and optimized by BBD using dose, concentration, and temperature as independent variables (Khatoon, Uddin, and Rao, 2018).

The following quadratic model was constructed to explain the influence of adsorption factors (Equation 3):

$$y = \beta_0 + \sum_j \beta_j x_j + \sum_{i<j} \beta_{ij} x_i x_j + \sum_j \beta_{jj} x_j^2 + e \qquad \text{(Eq. 3)}$$

Where y is the response; βo is the intercept; βj, βij, βjj are the model coefficients; xj, xixj, $xj^2$ are the factors studied; and e the error. To determine the relevance of the model and the level of influence of the operating factors, the regression coefficients and the ANOVA method were determined.

### 2.6. Equilibrium and kinetic studies

Adsorption equilibrium tests were performed for 300 minutes with 300 mL of

multimetal solution using the adsorbent dose of 15 g/L at pH of 4.5 ±0.5. The initial concentration of lead and copper was between 1.5 mg/L and 30 mg/L, while for cadmium between 0.5 mg/L and 15 mg/L. Langmuir (Equation 4) and Freundlich (Equation 5) models were studied.

$$Q_e = \frac{Q_{max} \cdot K_L \cdot C_e}{1 + K_L \cdot C_e} \quad \text{(Eq. 4)}$$

Where $Q_e$ (mg/g) is the amount of solute adsorbed onto the adsorbent surface in equilibrium conditions, $Q_{max}$ (mg/g) is the maximum removal capacity of the adsorbent, $K_L$ (L/mg) and $C_e$ (mg/L) are the parameters of affinity and equilibrium concentration of the solute.

$$Q_e = K_F \cdot C_e^{1/n} \quad \text{(Eq. 5)}$$

$K_F$ $(L/mg)^{(1/n)}$ indicates the adsorption capacity of the adsorbent while n the heterogeneity of the system. The separation factor, $R_L$, was calculated using Equation 6.

$$R_L = \frac{1}{1 + b \cdot C_o} \quad \text{(Eq. 6)}$$

Where $C_o$ (mg/L) is the initial concentration and b is the intercept of the non-linear equation.

To analyze the adsorption kinetics, 500 mL of multimetal solutions were prepared, with the initial concentration of 15 mg/L for both Cu and Pb, while 5 mg/L for Cd with an adsorbent dose of 10 g/L and pH of 4 ±0.5. The pseudo-first-order model (PFO) (Equation 7) and pseudo-second-order model (PSO) (Equation 8) were then analyzed.

$$Q_t = Q_e(1 - \exp(k_1 \cdot T)) \quad \text{(Eq. 7)}$$

Where k1 (1/min) and Qe (mg/g) are the parameters of the model.

$$Q_t = \frac{Q_e^2 \cdot k_2 \cdot T}{1 + Q_e \cdot k_2 \cdot T} \quad \text{(Eq. 8)}$$

Where $k_2$ (g.mg^-1.min^-1) is the equation parameter.

## 3. RESULTS AND DISCUSSION:

### 3.1 Adsorbent characterization

Table 2 shows the chemical composition of bentonite, kaolin, and zeolite. The main components of the adsorbent are silica, alumina, iron, calcium and magnesium oxides; this confirms the potential of these materials to be used as adsorbent (Uddin, 2017). Alkaline oxides and alkaline earth concentrations represent the feldspar content (Krupskaya *et al*., 2019). Ignition loss values indicate that these adsorbents have low carbonaceous matter and high mineral content (Shehata, Geundi, Ashour, and Abobeah, 2016).

Figure 1 depicts the FTIR spectrum of the pellets used in the adsorption column in the range between 400 $cm^{-1}$ and 4000 $cm^{-1}$.

In the first region of the spectrum, no peaks in the curve were observed. The area between 3500 $cm^{-1}$ 1600 and $cm^{-1}$ represents the vibrations of surface and internal hydroxyl groups. From 2842.60 $cm^{-1}$ to 1626 $cm^{-1}$ region, the curve was flat which attributed the water adsorption in the aluminosilicate (Hofmeister and Bowey, 2006). The region related to the bonds between aluminum or silicon and oxygen found to has greater band intensity. For the latter peaks, especially at 1023.04 $cm^{-1}$ correspond to T-O bonds (where T can be aluminum or silicon) while other six peaks correspond to the T-O-T vibrations in the range of 874.79 $cm^{-1}$ to 447.00 $cm^{-1}$ (Madejová, Gates, and Petit, 2017).

### 3.2 RSM models and ANOVA (coefficients values)

Table 3 shows the full results (both experimental and predicted) of adsorption percentage (response) of lead, copper and cadmium for each coded and actual values. Results show that both lead and copper were removed up to the maximum level of 88%. In comparison, cadmium percentage removal was lower (78%). Table 4 shows the regression coefficients results of the response surface model for lead, copper and cadmium. The standard error, t value and probability were determined for each coefficient and intercept of the model.

The most significant coefficient for lead was of first and quadratic order, which can be sorted according to their significance as D^2 > intercept > C > C^2 > D > B^2. For copper, the first order, two-way interaction and quadratic order coefficients were significant. According to the significance, the order of relevance is D^2 > AB > A^2 > B^2 > D. For cadmium, only the first-order and quadratic factors A and D were significant; the order is D^2 > D > A > A^2. According to the significant coefficients, response surface equations were constructed which are shown in

the following equations:

%Rem Pb = 2.95E+02 - 7.73E+01 x C - 5.77E+00 x D + 4.87E-02 x B^2 + 6.90E+00 x C^2 + 1.43E-01 x D^2 (Eq. 9)

%Rem Cu = -2.88E+00 x D+ 1.15E-02 x AB + 7.84E-04 x A^2 + 9.09E-02 x B^2 + 4.60E-02 x D^2 (Eq. 10)

%Rem Cd = 4.84E-01 x A - 8.97E+00 x D - 6.56E-04 x A^2 + 3.74E-01 x D^2 (Eq. 11)

The adjusted $R^2$-square was found greater than 0.9 (0.9406, 0.9237, and 0.9121 for lead, copper, and cadmium, respectively), p and F values were also highly significant (36.09, 27.81, and 23.98 for lead, copper, and cadmium, respectively). The experimental data fitted the quadratic model very well. The adjusted regression coefficient values were very close to the initial regression coefficient. The difference of less than 0.04 indicated a good fit between the experimental and expected values. These results show that the constructed model analyzed the data very well. The significance of each factor was varied with every model (Equations 9, 10 and 11). The initial concentration of heavy metals found to be effective for all the three metals; time was significant in terms of copper and cadmium; the adsorbent dose was relevant for lead and copper while pH had the impact on lead removal, which can be explained by the selectivity of the solute for the active sites. It can be observed that because lead occupies the active sites faster, for this reason, the time had no such influence. Cadmium adsorption was lower, probably due to the competition with the lead and copper solutes in multimetal solution (Elkhatib, Mahdy, Sherif, and Elshemy, 2016).

### 3.3 Effect of operating conditions

To illustrate the combined effect of studied factors on the adsorption efficiency (response) and find the optimum values, response optimizer function in MINITAB 17 was used. The plot is shown in Figure 2. The optimization plot shows that the adsorption percentage of the studied metals augmented with the increase in time and dose, while it decreased with an increase in pH and concentration. The optimum conditions to get the maximum results can be noticed in the plot as the red color vertical line.

Moreover, linking the predicted values further validates the adequacy of the experimental data. It can be seen in Figure 3 that the actual values are much closer to the expected (predicted) ones, which confirms the statistical validation of the study.

#### *3.3.1 pH*

pH is one of the most important operating parameters in adsorption pH was evaluated between 4 and 6 (Glatstein and Francisca, 2015; Mahdi, Yu, and El Hanandeh, 2019). The effect of pH is visible in the percentage of copper removal. From a pH below 5.5, the efficiency was increased and reached close to 90%. For lead, the influence was not appreciated in the graph, although this factor was significant in the adsorption model. The analysis of the model contour curves allowed the identification and it was found that with a pH of less than 4.5, the lead removal efficiency was increased up to more than 90%. For cadmium, pH range between 4 and 6 did not affect the adsorption efficiency.

In the case of lead and copper, when the pH was more significant than 4.5, the adsorption efficiency was reduced, which can be understood that this is the maximum point of the pH curve. Hosseini *et al*. obtained similar results while analyzing the nickel adsorption in the raw zeolite between pH 2 and 5 (Hosseini, Khosravi, Tavakoli, Esmhosseini, and Khezri, 2015). The authors noted that the removal percentage was first increased and then decreased between 5 and 8. For cadmium, pH values greater than 6 did not affect the adsorption, but it was decreased with pH values under 4 (Akpomie and Dawodu, 2016). Despite the variations identified for lead and copper, response surface graphs indicate that pH between 4 and 6 had no major influence on the adsorption system. Other authors obtained similar results while studying the lead adsorption onto bentonite (Khan, Hegde, and Shabiimam, 2017; Zhu and Qin, 2017). This could mean that the adsorption mechanism that predominates in the system is ion exchange (Kyziol-Komosinska *et al*., 2015).

From this analysis, it was found that the optimum pH range was between 4 and 6. At an acidic pH, the density of positively charged active sites increases (Shi, Fang, Zhao, Sun, and Liang, 2015); this causes an electrostatic repulsion between the metal ions and the positive adsorption surface (Hu *et al*., 2015). As the pH increases, competition between metal and hydrogen ions reduced, leaving the adsorption sites free, which increased the metal removal (Hosseini *et al*., 2015). At pH values greater than 6, a reduction in efficiency may be due to the formation of complexes between metal and hydroxyl ions that precipitate in the adsorbent and cause greater

metal retention.

#### *3.3.2 Adsorbent dosage*

The dose evaluated was between 5 g/L and 25 g/L. It can be observed from Figure 2 that as the dose increases, the adsorption efficiency also rises. Similar results were obtained when analyzing copper, nickel, and zinc adsorption in bentonite (Esmaeili, Mobini, and Eslami, 2019), the optimal adsorbent doses for all the three metals were 22 g/L, 30 g/L, and 60 g/L, respectively.

For lead, an adsorption efficiency of 90% can be achieved with a dose of 17 g/L. The most efficient dose for 90% removal for copper and cadmium was 22 g/L. The lead had higher adsorption efficiency than copper and cadmium; when the lead was in solution, it had a greater affinity for active sites (Park *et al*., 2016). Copper and cadmium appeared to be more selective and require a greater amount of adsorbent to have more available active sites. As the adsorbent dose was increased, more adsorption sites were available; as the dose was reduced, so did the active sites.

#### *3.3.3 Heavy metal concentration*

Figure 2 shows that adsorption efficiency is higher at lower initial concentrations of the heavy metals. For lead, an efficiency higher than 80% was reached with an initial concentration of 6 mg/L. For copper and cadmium, 2 mg/L of initial concentration in the solution provided an efficiency greater than 70%. It is expected that a higher concentration of heavy metals will affect the adsorption due to the saturation of active sites at the interface (Drweesh *et al*., 2016). Khan *et al*. examined that the removal of lead onto the bentonite using the initial pH range of 1 mg/L to 180 mg/L and determined an optimal initial concentration of 35 mg/L) (Khan *et al*., 2017). Malima *et al*. reported an optimal initial concentration of 5 mg/L for cadmium adsorption using kaolin (evaluated between 5 mg/L and 25 mg/L (Malima *et al*., 2018). Naseef *et al*. analyzed copper adsorption using activated bentonite (Nassef, Mahmoud, Salah, and El-Taweel, 2017). The authors explained that the lower adsorption efficiency was at higher heavy metal concentrations due to the lesser availability of adsorption sites. This could have happened in the present study. Although higher initial heavy metals concentrations reduce adsorption efficiency, in turn, adsorption capacity is used to increase. By increasing the number of adsorbates in the solution, the concentration gradient is magnified; this gives the impulse to overcome the mass transfer resistance between the adsorbent and the adsorbate (Malima, Lugwisha, & Mwakaboko, 2018).

### 3.4 Comparison with other adsorbents

From the study of the response surface graphs and contour curves, optimal adsorption ranges were identified. Selected optimal values were obtained from the resolution of the equations constructed for each metal. In cadmium, to achieve a 70% removal, a very long time is required, compared to lead and copper.

Table 5 compares the optimal values selected in this study with other reported studies. The suggested optimal values for lead, copper, and cadmium found to be almost similar to those proposed in other reported studies. Despite this, the values obtained differed from each other, which shows that conditions were specific for each system according to the adsorbent characteristics, adsorbate type, and operating factors.

### 3.5 Equilibrium isotherms

Table 6 shows the parameters and coefficients of determination of each tested model. $R^2$ values indicated that the Langmuir model fits better with the experimental data for all the three metals studied. Other authors have obtained similar results in the adsorption of heavy metals with different clays (Abu-Hawwas, Ibrahim, and Musleh, 2018; Mu'azu, Bukhari, and Munef, 2020; Rao and Kashifuddin, 2016). The better fit to the Langmuir model suggests that the process occurred in monolayer formation, which is the typical physisorption characteristic. The maximum adsorption capacity predicted by the Langmuir model was 7.27 mg/g, 1.45 mg/g and 0.68 mg/g for lead, copper, and cadmium. KL parameter measures the adsorption intensity between adsorbate and adsorbent (Ismadji, Soetaredjo, and Ayucitra, 2015). In this case, values were higher for cadmium and lower for lead. The separation factor RL allows to know the viability of the adsorption; values between 0 and 1 indicate that adsorption is feasible (Chaudhry, Khan, and Ali, 2016; Ismadji *et al*., 2015). According to RL values, the present study shows feasible adsorption.

In the Freundlich model, parameter KF is related to the removal capacity in multilayers and n with the adsorption intensity, which varies with interface heterogeneity (Ismadji *et al*., 2015; Yang, Xu, Yu, and Zhang, 2016). The value of n allows

understanding the process and the complexity of the system. The magnitude of n value between 1 and 10 is considered favorable. In this study, the results show that the process is viable and that the adsorption tends to be stronger in cadmium, then copper and finally lead. The isotherm models were used to describe the data, the $R^2$ values, between 0.968 and 0.986 indicating sufficient adsorption. Padmavathy and Murali (Padmavathy and Murali, 2017) presented a similar result in chromium retention with clay nanocomposites. This can be attributed to the fact that active sites can be characterized as monolayer or multilayer and the interface as heterogeneous (Padmavathy and Murali, 2017).

#### 3.6 Kinetics

Relationship between adsorption efficiency and time is shown in Figure 4. In the case of lead and copper adsorption, it can be seen that after the four hours of adsorption, the system reached close to the equilibrium condition. Adsorption was slow at the start and then gradually increased until it began to show less variation due to the progressive occupation of adsorption sites (Meroufel and Zenasni, 2018).

In Table 7, the coefficient of determination indicates that the PSO model fitted more efficiently with lead and copper data while the PFO model suited well with cadmium data. Mu'azu *et al*. also observed a similar result and reported that the PSO model fitted well for copper and nickel adsorption onto bentonite (Mu'azu *et al*., 2020). Adsorbents based on bentonite and zeolite in lead solutions also fitted better with this formula (Melichová and Ľuptáková, 2016). Usually, in heavy metal adsorption, the kinetic data shows a better fit for the PSO model (Uddin and Fazul Rahaman, 2017). However, other researchers have noted the opposite outcomes in which the results of kinetics studies indicated that chemisorption could be the step that controls lead and copper adsorption (He, Gan, and Feng, 2017).

## 4. CONCLUSIONS:

Clay pellets have shown their reasonable adsorptive properties towards various metal ions. Despite having relatively low values of maximum adsorption capacity, this study proposes that the adsorption could be increased by adjusting the calcination temperature of pelletization and also by applying chemical treatments to clay pellets before extrusion. According to the results, the experimental adsorption data was fitted better with Langmuir isotherm, but Freundlich isotherm also had high correlation values ($R^2$ between 0.968 and 0.986). It can be concluded that the active adsorption sites can be characterized as monolayer or multilayer and the adsorption surface as heterogeneous. The kinetics study showed that after 300 minutes, adsorption efficiency began to stabilize for all three metals. Copper and lead data fitted well with the PSO model while cadmium with the PFO model. The response surface analysis allowed defining optimal values for the evaluated operating factors. For a multimetal solution, optimum values of the studied factors were 240 minutes of contact time, 25 g/L of adsorbent dose, pH 4.3, and initial heavy metal concentrations of 4 mg/L, 7 mg/L, and 2 mg/L of lead, copper, and cadmium, respectively.

## 5. ACKNOWLEDGMENTS:

This research was made with funding from the Faculty of Environmental Engineering of the National University of Engineering in Peru (Grant Number RD 038-2018).

## 6. REFERENCES

1. Abu-Hawwas, J. K., Ibrahim, K. M., and Musleh, S. M. (2018). Characterization of jordanian porcelanite rock with reference to the adsorption behaviour of lead ions from aqueous solution. *Oriental Journal of Chemistry*. https://doi.org/10.13005/ojc/340208
2. Aggour, Y., Diab, M., Hegazy, T., and Elmekkawy Halawia, S. (2015). Removal of cadmium, lead, zinc, copper and iron from their aqueous solution by kaolinite clay. *International Journal Of Advanced Research*, *3*(10), 1922–1934.
3. Akpomie, K. G., and Dawodu, F. A. (2016). Acid-modified montmorillonite for sorption of heavy metals from automobile effluent. *Beni-Suef University Journal of Basic and Applied Sciences*. https://doi.org/10.1016/j.bjbas.2016.01.003
4. Al-Makhadmeh, L., and Batiha, M. A. (2016). Removal of iron and copper from aqueous solutions using Jordanian kaolin and zeolitic tuff. *Desalination and Water Treatment*. https://doi.org/10.1080/19443994.2015.1110839
5. Alarifi, I. M., Kashif Uddin, M., Bilal Awan, A., Naushad, M., Alharbi, A. R., and

Asmatulu, R. (2020). *Synthesis of PAN-nanofibers for the separation of aqueous pollutants and performance of the net-zero energy water treatment plant*. https://doi.org/10.5004/dwt.2020.26064

6. Bayuo, J., Abukari, M. A., and Pelig-Ba, K. B. (2020). Optimization using central composite design (CCD) of response surface methodology (RSM) for biosorption of hexavalent chromium from aqueous media. *Applied Water Science*. https://doi.org/10.1007/s13201-020-01213-3
7. Belova, T. P. (2019). Adsorption of heavy metal ions (Cu2+, Ni2+, Co2+ and Fe2+) from aqueous solutions by natural zeolite. *Heliyon*. https://doi.org/10.1016/j.heliyon.2019.e02320
8. Calvo, J. P., and Garcia-Lorenzo, M. L. (2018). The contribution of industrial minerals to solving environmental issues. *Bulletin of the Geological Society of Greece*, *53*(1), 134. https://doi.org/10.12681/bgsg.18898
9. Chaudhry, S. A., Khan, T. A., and Ali, I. (2016). Adsorptive removal of Pb(II) and Zn(II) from water onto manganese oxide-coated sand: Isotherm, thermodynamic and kinetic studies. *Egyptian Journal of Basic and Applied Sciences*, *3*(3), 287–300. https://doi.org/10.1016/j.ejbas.2016.06.002
10. Ciosek, A. L., Luk, G. K., Warner, M., and Warner, R. A. (2016). An Innovative Design of a Clay-Zeolite Medium for the Adsorption of Total Phosphorus from Wastewater. *Water Environment Research*, *88*(2), 131–142. https://doi.org/10.2175/106143015X14338845155787
11. Dąbrowski, A., Hubicki, Z., Podkościelny, P., and Robens, E. (2004). Selective removal of the heavy metal ions from waters and industrial wastewaters by ion-exchange method. *Chemosphere*. https://doi.org/10.1016/j.chemosphere.2004.03.006
12. Drweesh, S. A., Fathy, N. A., Wahba, M. A., Hanna, A. A., Akarish, A. I. M., Elzahany, E. A. M., … Abou-El-Sherbini, K. S. (2016). Equilibrium, kinetic and thermodynamic studies of Pb(II) adsorption from aqueous solutions on HCl-treated Egyptian kaolin. *Journal of Environmental Chemical Engineering*, *4*(2), 1674–1684. https://doi.org/10.1016/j.jece.2016.02.005
13. Elkhatib, E., Mahdy, A., Sherif, F., and Elshemy, W. (2016). Competitive Adsorption of Cadmium (II) from Aqueous Solutions onto Nanoparticles of Water Treatment Residual. *Journal of Nanomaterials*, *2016*, 1–10. https://doi.org/10.1155/2016/8496798
14. Esmaeili, A., Mobini, M., and Eslami, H. (2019). Removal of heavy metals from acid mine drainage by native natural clay minerals, batch and continuous studies. *Applied Water Science*, *9*(4), 97. https://doi.org/10.1007/s13201-019-0977-x
15. Glatstein, D. A., and Francisca, F. M. (2015). Influence of pH and ionic strength on Cd, Cu and Pb removal from water by adsorption in Na-bentonite. *Applied Clay Science*, *118*, 61–67. https://doi.org/10.1016/j.clay.2015.09.003
16. He, H., Gan, Q., and Feng, C. (2017). Preparation and application of Ni( <scp>ii</scp> ) ion-imprinted silica gel polymer for selective separation of Ni( <scp>ii</scp> ) from aqueous solution. *RSC Advances*, *7*(25), 15102–15111. https://doi.org/10.1039/C7RA00101K
17. Hofmeister, A. M., and Bowey, J. E. (2006). Quantitative Infrared Spectra of Hydrosilicates and Related Minerals. *Monthly Notices of the Royal Astronomical Society*, *367*(2), 577–591. https://doi.org/10.1111/j.1365-2966.2006.09894.x
18. Hosseini, S. S. S., Khosravi, A., Tavakoli, H., Esmhosseini, M., and Khezri, S. (2015). Natural zeolite for nickel ions removal from aqueous solutions: optimization and modeling using response surface methodology based on central composite design. *Desalination and Water Treatment*, 1–9. https://doi.org/10.1080/19443994.2015.1082508
19. Hu, X., Liu, Y., Zeng, G., Wang, H., You, S., Hu, X., … Guo, F. (2015). Effects of inorganic electrolyte anions on enrichment of Cu(II) ions with aminated Fe3O4/graphene oxide: Cu(II) speciation

prediction and surface charge measurement. *Chemosphere*, *127*, 35–41. https://doi.org/10.1016/j.chemosphere.2015.01.013

20. Huang, R., Lin, Q., Zhong, Q., Zhang, X., Wen, X., and Luo, H. (2020). Removal of Cd(II) and Pb(II) from aqueous solution by modified attapulgite clay. *Arabian Journal of Chemistry*. https://doi.org/10.1016/j.arabjc.2020.01.022
21. Ismadji, S., Soetaredjo, F. E., and Ayucitra, A. (2015). *Clay Materials for Environmental Remediation*. https://doi.org/10.1007/978-3-319-16712-1
22. Kakaei, S., Khameneh, E. S., Hosseini, M. H., and Moharreri, M. M. (2020). A modified ionic liquid clay to remove heavy metals from water: investigating its catalytic activity. *International Journal of Environmental Science and Technology*. https://doi.org/10.1007/s13762-019-02527-9
23. Khan, M. ., Hegde, R. ., and Shabiimam, M. . (2017). Adsorption of Lead by Bentonite Clay. *International Journal of Scientific Research and Management*, *5*(7). https://doi.org/10.18535/ijsrm/v5i7.02
24. Khatoon, A., Uddin, M. K., and Rao, R. A. K. (2018). Adsorptive remediation of Pb(II) from aqueous media using Schleichera oleosa bark. *Environmental Technology and Innovation*, *11*, 1–14. https://doi.org/10.1016/j.eti.2018.04.004
25. Krupskaya, V., Novikova, L., Tyupina, E., Belousov, P., Dorzhieva, O., Zakusin, S., … Belchinskaya, L. (2019). The influence of acid modification on the structure of montmorillonites and surface properties of bentonites. *Applied Clay Science*, *172*, 1–10. https://doi.org/10.1016/j.clay.2019.02.001
26. Kyziol-Komosinska, J., Rosik-Dulewska, C., Franus, M., Antoszczyszyn-Szpicka, P., Czupiol, J., and Krzyzewska, I. (2015). Sorption Capacities of Natural and Synthetic Zeolites for Cu(II) Ions. *Polish Journal of Environmental Studies*, *24*, 1111–1123. https://doi.org/10.15244/pjoes/30923
27. Madejová, J., Gates, W. P., and Petit, S. (2017). *IR Spectra of Clay Minerals*. https://doi.org/10.1016/B978-0-08-100355-8.00005-9
28. Mahdi, Z., Yu, Q. J., and El Hanandeh, A. (2019). Competitive adsorption of heavy metal ions (Pb 2+ , Cu 2+ , and Ni 2+ ) onto date seed biochar: batch and fixed bed experiments. *Separation Science and Technology*, *54*(6), 888–901. https://doi.org/10.1080/01496395.2018.1523192
29. Malima, N., Lugwisha, E., and Mwakaboko, A. (2018). The efficacy of raw Malangali kaolin clay in the adsorptive removal of cadmium and cobalt ions from water. *Tanzania Journal of Science*, *44*(2), 30–64.
30. Manjaiah, K. M., Mukhopadhyay, R., Paul, R., Datta, S. C., Kumararaja, P., and Sarkar, B. (2019). Clay minerals and zeolites for environmentally sustainable agriculture. In *Modified Clay and Zeolite Nanocomposite Materials* (pp. 309–329). https://doi.org/10.1016/B978-0-12-814617-0.00008-6
31. Mejia Miranda, C., Laverde, D., Avella, V., and Peña Ballesteros, D. Y. (2015). Adsorción de iones Ni(II) sobre una arcilla bentonítica peletizada. *Revista ION*, *28*(2), 61–68. https://doi.org/10.18273/revion.v28n2-2015005
32. Melichová, Z., and Ľuptáková, A. (2016). Removing lead from aqueous solutions using different low-cost abundant adsorbents. *Desalination and Water Treatment*, *57*(11), 5025–5034. https://doi.org/10.1080/19443994.2014.999713
33. Meroufel, B., and Zenasni, M. A. (2018). Preparation, Characterization, and Heavy Metal Ion Adsorption Property of APTES-Modified Kaolin: Comparative Study with Original Clay. In *Handbook of Environmental Materials Management* (pp. 1–25). https://doi.org/10.1007/978-3-319-58538-3_132-1
34. Mnasri-Ghnimi, S., and Frini-Srasra, N. (2019). Removal of heavy metals from aqueous solutions by adsorption using single and mixed pillared clays. *Applied Clay Science*. https://doi.org/10.1016/j.clay.2019.105151
35. Mohd Zahri, N. A., Md Jamil, S. N. A., Abdullah, L. C., Jia Huey, S., Nourouzi Mobarekeh, M., Mohd Rapeia, N. S., and

Shean Yaw, T. C. (2020). Central composite design of heavy metal removal using polymer adsorbent. *Journal of Applied Water Engineering and Research*, 1–14. https://doi.org/10.1080/23249676.2020.1831978

36. Mu'azu, N. D., Bukhari, A., and Munef, K. (2020). Effect of montmorillonite content in natural Saudi Arabian clay on its adsorptive performance for single aqueous uptake of Cu(II) and Ni(II). *Journal of King Saud University - Science*, *32*(1), 412–422. https://doi.org/10.1016/j.jksus.2018.06.003

37. Nassef, E., Mahmoud, A., Salah, H., and El-Taweel, Y. (2017). Removal of Copper Ions from Liquid Wastes by Adsorption Technique. *International Journal of Research in Industrial Engineering*, *6*(3), 255.268. https://doi.org/10.22105/riej.2017.91532.1000

38. Padmavathy, K., and Murali, A. (2017). Adsorption of hexavalent chromium (Cr (VI)) from wastewater using novel chitosan/halloysite clay nanocomposite films. *Indian Journal of Chemical Technology*, *24*(6), 593–600.

39. Park, J.-H., Ok, Y. S., Kim, S.-H., Cho, J.-S., Heo, J.-S., Delaune, R. D., and Seo, D.-C. (2016). Competitive adsorption of heavy metals onto sesame straw biochar in aqueous solutions. *Chemosphere*, *142*, 77–83. https://doi.org/10.1016/j.chemosphere.2015.05.093

40. Rao, R. A. K., and Kashifuddin, M. (2012). Pottery glaze—An excellent adsorbent for the removal of Cu(II) from aqueous solution. *Chinese Journal of Geochemistry*, *31*(2), 136–146. https://doi.org/10.1007/s11631-012-0560-8

41. Rao, R. A. K., and Kashifuddin, M. (2016). Adsorption studies of Cd(II) on ball clay: Comparison with other natural clays. *Arabian Journal of Chemistry*, *9*, S1233–S1241. https://doi.org/10.1016/j.arabjc.2012.01.010

42. Ravikumar, K., and Udayakumar, J. (2020). Preparation and characterisation of green clay-polymer nanocomposite for heavy metals removal. *Chemistry and Ecology*. https://doi.org/10.1080/02757540.2020.1723559

43. Şahan, T. (2019). Application of RSM for Pb(II) and Cu(II) adsorption by bentonite enriched with SH groups and a binary system study. *Journal of Water Process Engineering*, *31*, 100867. https://doi.org/10.1016/j.jwpe.2019.100867

44. Salem, A., and Akbari Sene, R. (2012). Optimization of zeolite-based adsorbent composition for fabricating reliable Raschig ring shaped by extrusion using Weibull statistical theory. *Microporous and Mesoporous Materials*, *163*, 65–75. https://doi.org/10.1016/j.micromeso.2012.06.026

45. Shaban, M., and Abukhadra, M. R. (2017). Geochemical evaluation and environmental application of Yemeni natural zeolite as sorbent for Cd2+ from solution: kinetic modeling, equilibrium studies, and statistical optimization. *Environmental Earth Sciences*, *76*(8), 310. https://doi.org/10.1007/s12665-017-6636-3

46. Shehata, N., Geundi, M. S. El, Ashour, E. A., and Abobeah, R. M. A. (2016). Structural Characteristics of the Egyptian Clay as a Low-Cost Adsorbent. *International Journal of Chemical and Process Engineering Research*, *3*(2), 35–45. https://doi.org/10.18488/journal.65/2016.3.2/65.2.35.45

47. Sheydaei, M., Gasemsoltanlu, A. B., and Beiraghi, A. (2019). Optimization of ultrasonic-assisted copper ion removal from polluted water by a natural clinoptilolite nanostructure through a central composite design. *Clay Minerals*. https://doi.org/10.1180/clm.2019.46

48. Shi, J., Fang, Z., Zhao, Z., Sun, T., and Liang, Z. (2015). Comparative study on Pb(II), Cu(II), and Co(II) ions adsorption from aqueous solutions by arborvitae leaves. *Desalination and Water Treatment*, 1–8. https://doi.org/10.1080/19443994.2015.1089421

49. Uddin, M. K. (2017). A review on the adsorption of heavy metals by clay

minerals, with special focus on the past decade. *Chemical Engineering Journal*, *308*, 438–462. https://doi.org/10.1016/j.cej.2016.09.029

50. Uddin, M. K., Ahmed, S. S., and Naushad, M. (2019). A mini update on fluoride adsorption from aqueous medium using clay materials. *DESALINATION AND WATER TREATMENT*, *145*, 232–248. https://doi.org/10.5004/dwt.2019.23509
51. Uddin, M. K., and Fazul Rahaman, P. (2017). A study on the potential applications of rice husk derivatives as useful adsorptive material. In *Inorganic Pollutants in Wastewater* (pp. 149–186). https://doi.org/10.21741/9781945291357-4
52. Uddin, M. K., and Nasar, A. (2020). Walnut shell powder as a low-cost adsorbent for methylene blue dye: isotherm, kinetics, thermodynamic, desorption and response surface methodology examinations. *Scientific Reports*, *10*(1), 7983. https://doi.org/10.1038/s41598-020-64745-3
53. Uddin, M. K., Rao, R. A. K., and Chandra Mouli, K. V. V. (2018). The artificial neural network and Box-Behnken design for Cu2+ removal by the pottery sludge from water samples: Equilibrium, kinetic and thermodynamic studies. *Journal of Molecular Liquids*, *266*, 617–627. https://doi.org/10.1016/j.molliq.2018.06.098
54. Uddin, M. K., and Salah, M. M. (2018). Statistical analysis of Litchi chinensis's adsorption behavior toward Cr(VI). *Applied Water Science*, *8*(5), 140. https://doi.org/10.1007/s13201-018-0784-9
55. UNEP. (2016). *A Snapshot of the World's Water Quality: Towards a global assessment* (U. N. E. Programme, Ed.). Retrieved from https://www.unenvironment.org/es/node/719
56. Voulvoulis, N., and Georges, K. (2016). Industrial and Agricultural Sources and Pathways of Aquatic Pollution. In I. Global (Ed.), *Impact of water pollution on human health and environment sustainability* (pp. 29–54). https://doi.org/10.4018/978-1-4666-9559-7.ch002
57. Yang, X., Xu, G., Yu, H., and Zhang, Z. (2016). Preparation of ferric-activated sludge-based adsorbent from biological sludge for tetracycline removal. *Bioresource Technology*, *211*, 566–573. https://doi.org/10.1016/j.biortech.2016.03.140
58. Zhu, S., and Qin, Y. (2017). *Adsorption of Lead from Aqueous Solutions to Bentonite and Composite*. https://doi.org/10.1007/978-3-319-51382-9_11

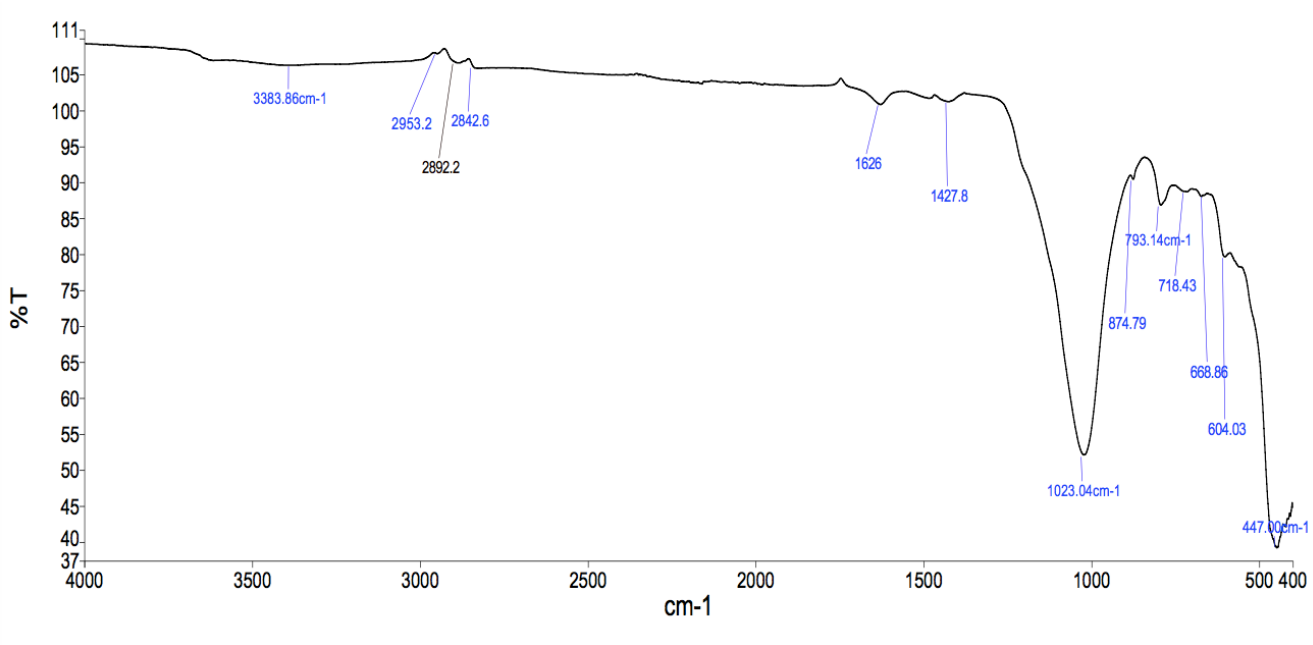


***Figure 1.*** *FTIR spectra of adsorbent pellets*

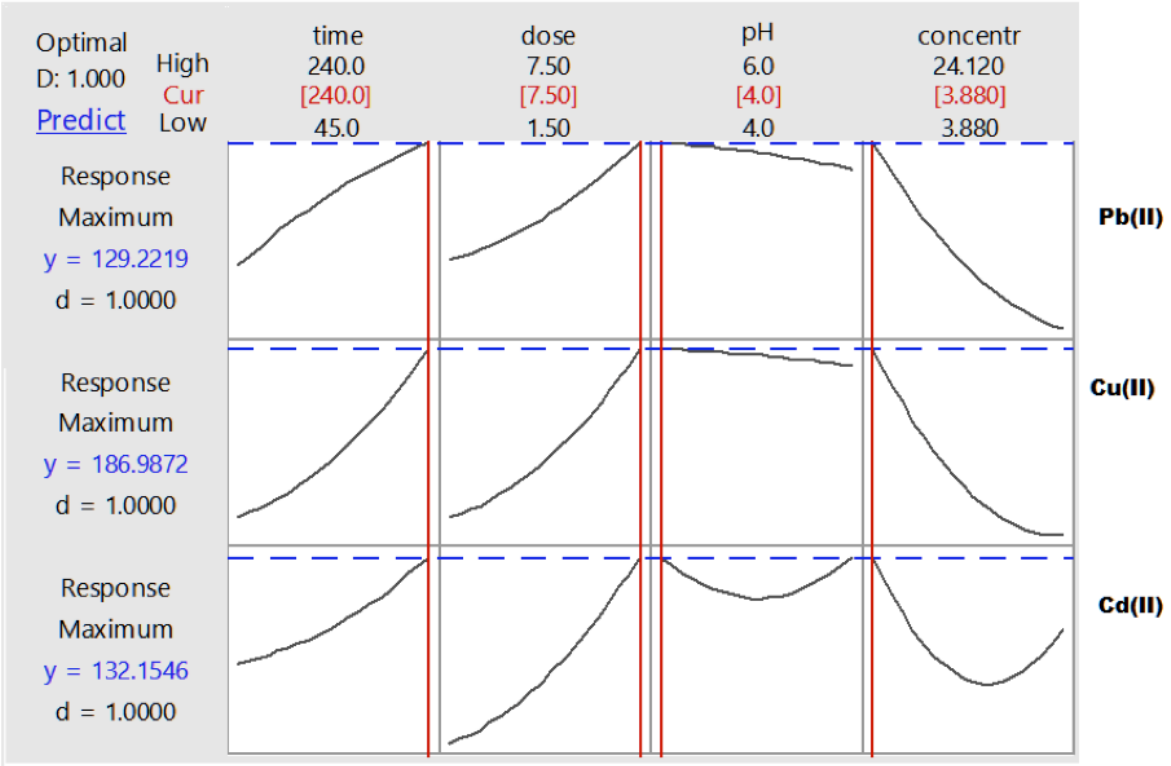


***Figure 2.*** *Response optimization plot*

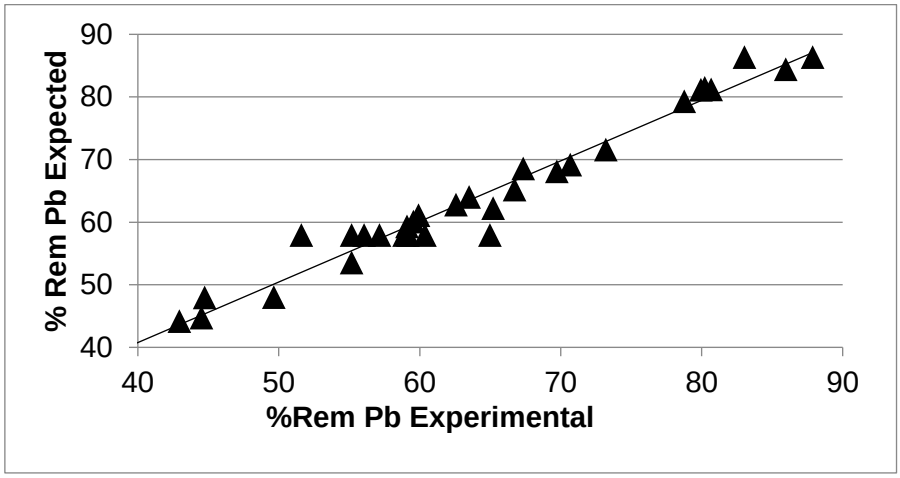


(a)

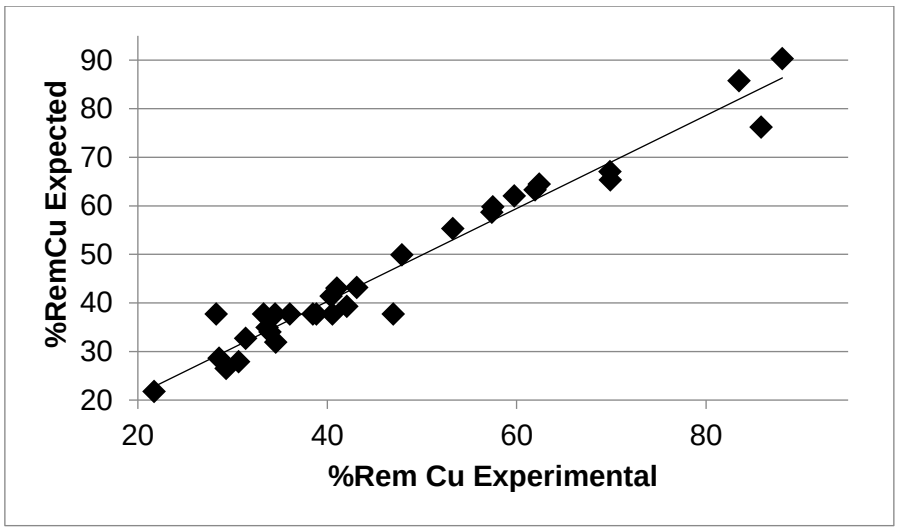


(b)

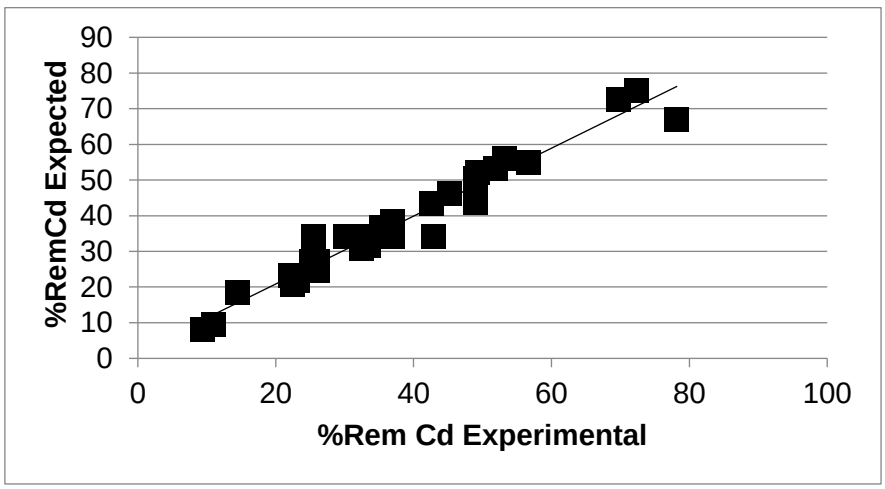


(c)

***Figure 3.*** *Experimental vs expected values for removal efficiency of lead (a), copper (b) and cadmium (c)*

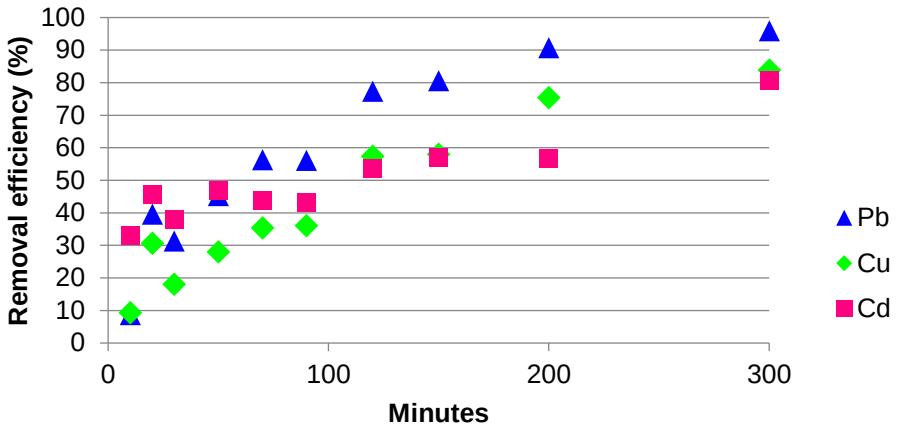


***Figure 4.*** *Kinetics of adsorption efficiency*

***Table 1.*** *Selected factors and levels for the CCRD*

| Factors | Levels | | | | |
|---|---|---|---|---|---|
| | **-2** | **-1** | **0** | **1** | **2** |
| A = Contact time (minutes) | 45 | 60 | 120 | 180 | 240 |
| B = Adsorbent dose (g/L) | 5 | 10 | 15 | 20 | 25 |
| C = pH | 4 | 4.5 | 5 | 5.5 | 6 |
| D = Initial concentration (mg/l) | | | | | |
| Pb | 3.88 | 11.14 | 15.89 | 17.4 | 24.12 |
| Cu | 4.2 | 10.6 | 23.8 | 26 | 50 |
| Cd | 1.57 | 3.02 | 7.38 | 9.94 | 13.73 |
| Response: Removal efficiency (% Rem) | | | | | |

***Table 2.*** *Chemical composition of the clays and zeolite*

| Element | Bentonite | Kaolin | Zeolite |
|---|---|---|---|
| $SiO_2$ | 62.63% | 44.60% | 65.91% |
| $Al_2O_3$ | 17.10% | 36.09% | 10.60% |
| $Fe_2O_3$ | 3.53% | 3.43% | 3.03% |
| CaO | 2.61% | 1.29% | 2.52% |
| MgO | 0.61% | 0.35% | 0.18% |
| $Na_2O$ | 0.99% | 0.30% | 3.77% |
| $K_2O$ | 0.07% | 0.19% | 0.14% |
| $TiO_2$ | 0.53% | 1.42% | 0.17% |
| $P_2O_5$ | 0.03% | 0.03% | 0.07% |
| Loss off ignition | 11.80% | 12.30% | 13.60% |

***Table 3.*** *Observed and predicted adsorption efficiencies for lead, copper and cadmium with a CCRD*

| Run | A | B | C | D | A (m) | B (g/L) | C | D (mg/L) | | | %Rem | | | | | |
|---|---|---|---|---|---|---|---|---|---|---|---|---|---|---|---|---|
| | | | | | | | | Pb | Cu | Cd | Pb | | Cu | | Cd | |
| | | | | | | | | | | | Obs | Pred | Obs | Pred | Obs | Pred |
| 1 | -1 | -1 | -1 | -1 | 60 | 3 | 4.5 | 11.14 | 10.6 | 3.02 | 55.2 | 53.5 | 47.9 | 49.9 | 35.3 | 36.7 |
| 2 | 1 | -1 | -1 | -1 | 180 | 3 | 4.5 | 11.14 | 10.6 | 3.02 | 70.7 | 69.2 | 59.8 | 62.0 | 53.3 | 56.0 |
| 3 | -1 | 1 | -1 | -1 | 60 | 6 | 4.5 | 11.14 | 10.6 | 3.02 | 73.2 | 71.6 | 62.4 | 64.4 | 49.0 | 50.4 |
| 4 | 1 | 1 | -1 | -1 | 180 | 6 | 4.5 | 11.14 | 10.6 | 3.02 | 87.9 | 86.3 | 88.1 | 90.3 | 72.4 | 75.2 |
| 5 | -1 | -1 | 1 | -1 | 60 | 3 | 5.5 | 11.14 | 10.6 | 3.02 | 49.6 | 48.0 | 41.0 | 43.1 | 36.9 | 38.2 |
| 6 | 1 | -1 | 1 | -1 | 180 | 3 | 5.5 | 11.14 | 10.6 | 3.02 | 66.7 | 65.2 | 57.5 | 59.7 | 49.3 | 52.0 |
| 7 | -1 | 1 | 1 | -1 | 60 | 6 | 5.5 | 11.14 | 10.6 | 3.02 | 69.7 | 68.1 | 53.2 | 55.3 | 52.0 | 53.3 |
| 8 | 1 | 1 | 1 | -1 | 180 | 6 | 5.5 | 11.14 | 10.6 | 3.02 | 86.0 | 84.4 | 83.5 | 85.7 | 69.8 | 72.5 |
| 9 | -1 | -1 | -1 | 1 | 60 | 3 | 4.5 | 17.4 | 26 | 9.94 | 44.5 | 44.7 | 28.6 | 28.6 | 9.5 | 8.0 |
| 10 | 1 | -1 | -1 | 1 | 180 | 3 | 4.5 | 17.4 | 26 | 9.94 | 63.5 | 64.0 | 33.7 | 34.9 | 26.1 | 27.1 |
| 11 | -1 | 1 | -1 | 1 | 60 | 6 | 4.5 | 17.4 | 26 | 9.94 | 62.6 | 62.8 | 43.1 | 43.1 | 23.2 | 21.7 |
| 12 | 1 | 1 | -1 | 1 | 180 | 6 | 4.5 | 17.4 | 26 | 9.94 | 80.7 | 81.2 | 62.0 | 63.2 | 45.3 | 46.2 |
| 13 | -1 | -1 | 1 | 1 | 60 | 3 | 5.5 | 17.4 | 26 | 9.94 | 39.0 | 39.2 | 21.7 | 21.8 | 11.0 | 9.6 |
| 14 | 1 | -1 | 1 | 1 | 180 | 3 | 5.5 | 17.4 | 26 | 9.94 | 59.5 | 60.1 | 31.4 | 32.7 | 22.1 | 23.1 |
| 15 | -1 | 1 | 1 | 1 | 60 | 6 | 5.5 | 17.4 | 26 | 9.94 | 59.1 | 59.3 | 33.9 | 34.0 | 26.1 | 24.7 |
| 16 | 1 | 1 | 1 | 1 | 180 | 6 | 5.5 | 17.4 | 26 | 9.94 | 78.8 | 79.3 | 57.4 | 58.7 | 42.6 | 43.6 |
| 17 | 0 | 0 | 0 | 0 | 120 | 4.5 | 5 | 15.89 | 23.8 | 7.38 | 56.0 | 57.9 | 34.5 | 37.7 | 31.3 | 34.2 |
| 18 | 0 | 0 | 0 | 0 | 120 | 4.5 | 5 | 15.89 | 23.8 | 7.38 | 55.2 | 57.9 | 33.3 | 37.7 | 30.2 | 34.2 |
| 19 | 0 | 0 | 0 | 0 | 120 | 4.5 | 5 | 15.89 | 23.8 | 7.38 | 60.4 | 57.9 | 40.5 | 37.7 | 36.9 | 34.2 |
| 20 | 0 | 0 | 0 | 0 | 120 | 4.5 | 5 | 15.89 | 23.8 | 7.38 | 51.6 | 57.9 | 28.3 | 37.7 | 25.6 | 34.2 |
| 21 | -2 | 0 | 0 | 0 | 45 | 4.5 | 5 | 15.89 | 23.8 | 7.38 | 44.8 | 47.9 | 34.6 | 31.9 | 14.5 | 18.5 |
| 22 | 2 | 0 | 0 | 0 | 240 | 4.5 | 5 | 15.89 | 23.8 | 7.38 | 79.9 | 81.1 | 69.9 | 65.3 | 49.0 | 43.8 |
| 23 | 0 | -2 | 0 | 0 | 120 | 1.5 | 5 | 15.89 | 23.8 | 7.38 | 43.0 | 44.2 | 29.3 | 26.5 | 22.5 | 20.7 |
| 24 | 0 | 2 | 0 | 0 | 120 | 7.5 | 5 | 15.89 | 23.8 | 7.38 | 80.2 | 81.4 | 69.8 | 67.0 | 56.7 | 54.9 |
| 25 | 0 | 0 | -2 | 0 | 120 | 4.5 | 4 | 15.89 | 23.8 | 7.38 | 67.3 | 68.5 | 42.1 | 39.3 | 33.5 | 31.7 |
| 26 | 0 | 0 | 2 | 0 | 120 | 4.5 | 6 | 15.89 | 23.8 | 7.38 | 59.9 | 61.1 | 30.7 | 27.9 | 32.5 | 30.7 |
| 27 | 0 | 0 | 0 | -2 | 120 | 4.5 | 5 | 3.88 | 4.2 | 1.57 | 83.0 | 86.3 | 85.8 | 76.2 | 78.2 | 67.1 |
| 28 | 0 | 0 | 0 | 2 | 120 | 4.5 | 5 | 24.12 | 50 | 13.73 | 65.2 | 62.2 | 40.4 | 41.4 | 25.2 | 27.1 |
| 29 | 0 | 0 | 0 | 0 | 120 | 4.5 | 5 | 15.89 | 23.8 | 7.38 | 58.9 | 57.9 | 38.5 | 37.7 | 35.0 | 34.2 |
| 30 | 0 | 0 | 0 | 0 | 120 | 4.5 | 5 | 15.89 | 23.8 | 7.38 | 59.2 | 57.9 | 38.8 | 37.7 | 35.4 | 34.2 |
| 31 | 0 | 0 | 0 | 0 | 120 | 4.5 | 5 | 15.89 | 23.8 | 7.38 | 65.0 | 57.9 | 47.0 | 37.7 | 42.9 | 34.2 |
| 32 | 0 | 0 | 0 | 0 | 120 | 4.5 | 5 | 15.89 | 23.8 | 7.38 | 57.2 | 57.9 | 36.0 | 37.7 | 32.8 | 34.2 |

***Table 4.*** *RSM regression coefficients for lead, copper and cadmium*

| | | ***Estimate*** | ***Standard error*** | ***T value*** | ***Pr(>\|t\|)*** | |
|---|---|---|---|---|---|---|
| Pb | Intercept | 2.95E+02 | 7.71E+01 | 3.83 | 0.001341 | ** |
| | A | -4.93E-02 | 1.57E-01 | -0.3147 | 0.756805 | |
| | B | -5.30E-01 | 1.90E+00 | -0.2793 | 0.783353 | |
| | C | -7.73E+01 | 2.52E+01 | -3.0631 | 0.00704 | ** |
| | D | -5.77E+00 | 2.66E+00 | -2.1727 | 0.044232 | * |
| | AB | -7.27E-04 | 2.62E-03 | -0.2773 | 0.784926 | |
| | AC | 1.30E-02 | 2.62E-02 | 0.4968 | 0.62572 | |
| | AD | 4.87E-03 | 4.08E-03 | 1.1932 | 0.249183 | |
| | BC | 2.04E-01 | 3.15E-01 | 0.6486 | 0.525271 | |
| | BD | 3.10E-16 | 4.82E-02 | 0 | 1 | |
| | CD | -1.29E-15 | 4.82E-01 | 0 | 1 | |
| | A^2 | 3.08E-04 | 2.09E-04 | 1.4729 | 0.159049 | |
| | B^2 | 4.87E-02 | 2.35E-02 | 2.071 | 0.053892 | . |
| | C^2 | 6.90E+00 | 2.35E+00 | 2.9348 | 0.009254 | ** |
| | D^2 | 1.43E-01 | 2.51E-02 | 5.6751 | 2.74E-05 | *** |
| Cu | Intercept | 1.65E+01 | 1.08E+02 | 0.153 | 0.88024 | |
| | A | -3.41E-01 | 2.33E-01 | -1.4614 | 0.16215 | |
| | B | -9.21E-01 | 2.81E+00 | -0.3275 | 0.74727 | |
| | C | 3.46E+01 | 3.81E+01 | 0.9061 | 0.37755 | |
| | D | -2.88E+00 | 1.60E+00 | -1.795 | 0.09045 | . |
| | AB | 1.15E-02 | 4.11E-03 | 2.7943 | 0.01245 | * |
| | AC | 3.82E-02 | 4.11E-02 | 0.9301 | 0.36533 | |
| | AD | -3.12E-03 | 2.54E-03 | -1.2269 | 0.23659 | |
| | BC | -2.31E-01 | 4.93E-01 | -0.4697 | 0.64456 | |
| | BD | -1.31E-15 | 2.96E-02 | 0 | 1 | |
| | CD | -1.42E-14 | 2.96E-01 | 0 | 1 | |
| | A^2 | 7.84E-04 | 3.28E-04 | 2.3883 | 0.0288 | * |
| | B^2 | 9.09E-02 | 3.66E-02 | 2.4871 | 0.02356 | * |
| | C^2 | -4.14E+00 | 3.66E+00 | -1.1319 | 0.27339 | |
| | D^2 | 4.60E-02 | 6.14E-03 | 7.4938 | 8.78E-07 | *** |
| Cd | Intercept | -4.72E+01 | 1.06E+02 | -0.4473 | 0.6603004 | |
| | A | 4.84E-01 | 2.34E-01 | 2.0664 | 0.0543697 | . |
| | B | -6.01E-01 | 2.80E+00 | -0.2146 | 0.8326278 | |
| | C | 3.27E+01 | 3.78E+01 | 0.8651 | 0.3990215 | |
| | D | -8.97E+00 | 3.97E+00 | -2.2611 | 0.0371558 | * |
| | AB | 4.52E-03 | 4.13E-03 | 1.0945 | 0.2890127 | |

| | | | | | |
|---|---|---|---|---|---|
| AC | -4.64E-02 | 4.13E-02 | -1.1239 | 0.2766802 | |
| AD | -3.65E-04 | 5.93E-03 | -0.0616 | 0.9516205 | |
| BC | 1.37E-01 | 4.96E-01 | 0.2758 | 0.7860121 | |
| BD | 4.59E-16 | 7.08E-02 | 0 | 1 | |
| CD | -6.73E-15 | 7.08E-01 | 0 | 1 | |
| A^2 | -6.56E-04 | 3.22E-04 | -2.036 | 0.0576376 | . |
| B^2 | 3.62E-02 | 3.64E-02 | 0.9958 | 0.3333122 | |
| C^2 | -2.97E+00 | 3.64E+00 | -0.8169 | 0.4253053 | |
| D^2 | 3.74E-01 | 8.88E-02 | 4.2088 | 0.0005903 | *** |

***Table 5.*** *Comparison of optimal operating conditions*

| | | ***Operating conditions*** | | | | | |
|---|---|---|---|---|---|---|---|
| ***Adsorbent*** | ***Metal*** | ***Time (minutes)*** | ***Dose (g/L)*** | ***pH*** | ***Initial concentration (mg/L)*** | ***%Rem*** | ***Reference*** |
| Ze/Bent/K | Pb | 150 | 25 | 4.3 | 4 | 99.84 | Present study |
| | Cu | 150 | 25 | 4.3 | 7 | 99.67 | |
| | Cd | 240 | 25 | 4.3 | 2 | 61.93 | |
| Ze | Cd | 116 | 5.4 | 7 | 25.07 | 80.77 | (Shaban and Abukhadra, 2017) |
| Bent-SH | Pb | 146 | 14.6 | 5.1 | 33 | 95.08 | (Şahan, 2019) |
| | Cu | 146 | 15.2 | 4.5 | 37.9 | 88.19 | |
| K | Cu | 24h | 20 | 5.5 | 20 | 65.0 | (Al-Makhadmeh and Batiha, 2016) |
| Ze | Cu | 24h | 20 | 5.5 | 70 | 99.6 | |
| K | Cd | 180 | 32 | 6 | 5 | 99.2 | (Malima *et al*., 2018) |
| K | Pb | 60 | 10 | 7 | 4.66 | 96.3 | (Aggour, Diab, Hegazy, and Elmekkawy Halawia, 2015) |
| | Cu | 60 | 10 | 8 | 4.66 | 79.5 | |
| | Cd | 60 | 10 | 7 | 0.62 | 91.9 | |

Bentonite (Bent), Kaolin (K), Zeolite (Ze), Bentonite enriched with SH groups (Be-SH)

***Table 6.*** *Parameters of lead, copper and cadmium adsorption isotherms*

| ***Model*** | ***Parameters*** | ***Pb*** | ***Cu*** | ***Cd*** |
|---|---|---|---|---|
| Langmuir | Qmax (mg/g) | 7.27 | 1.45 | 0.26 |
| | $K_L$ (L/mg) | 0.03 | 0.15 | 0.68 |
| | $R_L$ | 0.10 - 0.58 | 0.05 - 0.59 | 0.07 - 0.70 |
| | $R^2$ | 0.987 | 0.981 | 0.999 |
| Freundlich | $K_F$(mg/g).(L/mg)^(1/n) | 0.24 | 0.41 | 0.15 |
| | N | 1.09 | 3.30 | 6.09 |
| | $R^2$ | 0.986 | 0.968 | 0.987 |

***Table 7**. Parameters of kinetic models*

| Model | Parameters | Pb | Cu | Cd |
|---|---|---|---|---|
| PFO | Qe | 1.46 | 1.32 | 0.22 |
| | k1 | 0.01 | 0.01 | 3.45E-03 |
| | $R^2$ | 0.942 | 0.899 | 0.843 |
| PSO | Qe | 1.93 | 1.80 | 0.39 |
| | k2 | 5.60E-03 | 3.90E-03 | 0.06 |
| | $R^2$ | 0.950 | 0.918 | 0.625 |

PERIÓDICO TCHÊ QUÍMICA
ARTIGO ORIGINAL

# O EFEITO DA CANTARIDINA E DO ENDOTHALL NA EXPRESSÃO GENÉTICA DAS ENZIMAS REGULADORAS CHAVE EM *CICHORIUM INTYBUS* L.

# THE EFFECT OF CANTHARIDIN AND ENDOTHALL ON GENE EXPRESSION OF THE KEY REGULATING ENZYMES IN *CICHORIUM INTYBUS* L.

# تاثیر کانتاریدین و اندوتال روی بیان ژن آنزیم‌های کلیدی تنظیم کننده در *CICHORIUM INTYBUS* L.

GHOTBZADEH KERMANI, Yalda[1]; KHAVARI NEJAD, Ramazan Ali[1]; MAHMOODZADEH, Homa[2]*; SHAHROKH ABADI, Khadijeh[2];

[1]Islamic Azad University, College of Basic Science and Research Branch, Department of Botany, Tehran, Iran.

[2]Islamic Azad University, Mashhad branch, Department of Biology, Mashhad, Iran.

** Corresponding author*
*e-mail: homa_mahmoodzadeh@yahoo.com*

Received 20 November 2020; received in revised form 12 February 2021; accepted 28 February 2021

## RESUMO

**Introdução:** os mecanismos subjacentes que regulam a biossíntese e a própria existência de um sistema celular nas plantas ainda precisam ser esclarecidos a um ponto satisfatório. **Objetivo:** este experimento tentou revelar a influência da cantaridina e do endothall na expressão gênica de enzimas críticas, glutationa S-transferase, proteína fosfatase e aspartato fosfatase em *Cichorium intybus* L., uma importante planta medicinal. **Métodos:** duas concentrações de cantaridina e endothall, 2,5 e 10 $\mu gml^{-1}$, foram aplicadas em mudas de *C. intybus* e as alterações nos genes avaliadas na parte aérea e nas raízes. **Resultados e Discussão:** Mudas tratadas com cantaridina e endothall tiveram o menor nível de expressão de glutationa S-transferase em 2,5 $\mu gml^{-1}$ (0,92 ± 0,11 e 1,07 ± 0,61, respectivamente) enquanto em 10 $\mu gml^{-1}$, os níveis de expressão foram ligeiramente maiores. A expressão da glutationa S-transferase nas raízes seguiu uma tendência semelhante. O efeito da cantaridina nas proteínas fosfatases na parte aérea e nas raízes de *C. intybus* seguiu um padrão semelhante, onde o nível de expressão das proteínas fosfatases na parte aérea e nas raízes de Mudas tratadas com 2,5 $\mu gml^{-1}$ (0,51 ± 0,03 e 1,34 ± 0,12, respectivamente) foi reduzido. Com cantaridina 10 $\mu gml^{-1}$, a expressão das proteínas fosfatases aumentou acentuadamente na parte aérea e nas raízes (3,55 ± 0,21 e 3,96 ± 032, respectivamente). A expressão das proteínas fosfatases na parte aérea recebeu 2,5 $\mu gml^{-1}$ do endothall consideravelmente aumentado (43,21 ± 3,1), enquanto sua expressão foi próxima de zero nas raízes. A expressão das aspartato fosfatases nos brotos com cantaridina 2,5 $\mu gml^{-1}$ foi quase nula. Já em 10 $\mu gml^{-1}$, sua expressão foi radicalmente aumentada (3,76 ± 0,23). As raízes tratadas com cantaridina indicaram altos níveis de expressão, principalmente em 10 $\mu gml^{-1}$ (2,07 ± 0,11). A raiz tratada com 2,5 $\mu gml^{-1}$ de cantaridina não expressou aspartato fosfatases. Em mudas expostas ao endothall, o nível de expressão relativa de aspartato fosfatases em brotos com menos de 2,5 $\mu gml^{-1}$ foi de 17,49 ± 1,21, enquanto em raízes com 2,5 $\mu gml^{-1}$ foi de 0,45 ± 0,09. **Conclusões:** Pode ser expresso de forma confiável que a cantaridina e o endothal interrompem o crescimento da planta de uma maneira dependente da dosagem, regulando para baixo as enzimas críticas *C. intybus*.

**Palavras-chave**: *glutationa S-transferase, proteínas fosfatases e aspartato fosfatases, regulação negativa, expressão gênica, Cichorium intybus*

## ABSTRACT

**Background:** the underlying mechanisms regulating biosynthesis and the very existence of a cellular system in plants have yet to be clarified to a satisfying point. **Aim:** this experiment tried to reveal the influence of cantharidin and endothall on gene expression of critical enzymes, glutathione S-transferase, protein phosphatase and, aspartate phosphatase in *Cichorium intybus* L., an important medicinal plant. **Methods:** two concentrations of cantharidin and endothall, 2.5 and 10 $\mu gml^{-1}$, were applied on *C. intybus* seedlings, and the changes in genes evaluated in shoots and roots. **Results and Discussion:** Cantharidin and endothall-treated seedlings had the lowest expression level of glutathione S-transferase in 2.5 $\mu gml^{-1}$ (0.92±0.11 and 1.07±0.61, respectively) while in 10 $\mu gml^{-1}$, the expression levels were slightly higher. The glutathione S-transferase expression in roots followed a similar trend. The Cantharidin effect on protein phosphatases in shoots and roots of *C. intybus* followed a similar pattern where the expression level of protein phosphatases in shoots and roots of treated seedlings with 2.5 $\mu gml^{-1}$ (0.51±0.03 and 1.34±0.12, respectively) reduced. At 10 $\mu gml^{-1}$ cantharidin, protein phosphatases' expression

markedly increased in both shoots and roots (3.55±0.21 and 3.96±032, respectively). The expression of protein phosphatases in shoots received 2.5 µgml$^{-1}$ endothall considerably enhanced (43.21±3.1), whereas its expression was close to zero in roots. The expression of aspartate phosphatases in shoots with cantharidin 2.5 µgml$^{-1}$ was almost zero. Whereas in 10 µgml$^{-1,}$ its expression was radically increased (3.76±0.23). Roots treated with cantharidin indicated high levels of expression, particularly in 10 µgml$^{-1}$ (2.07±0.11). Root treated with 2.5 µgml$^{-1}$ cantharidin similarly did not express aspartate phosphatases. Seedlings exposed to endothall, the relative expression level of aspartate phosphatases in shoots under 2.5 µgml$^{-1}$ was 17.49±1.21 while in roots with 2.5 µgml$^{-1}$ was down to 0.45±0.09. **Conclusion:** It can be reliably expressed that cantharidin and endothall halt plant growth in a dosage-dependent manner by downregulating critical enzymes *C. intybus*.

**Keywords**: *glutathione S-transferase, protein phosphatases and aspartate phosphatases, downregulation, gene expression, Cichorium intybus*

**چکیده**

**پیشینه:** مکانیسم‌های بنیانی تنظیم بیوسنتز و وجود یک سیستم سلولی در گیاهان هنوز تا حد رضایت بخشی مشخص نشده است. **هدف:** آزمایشی برای آشکار کردن تأثیر کانتاریدین و اندوتال روی بیان ژن آنزیم‌های حیاتی گلوتاتیون S- ترانسفراز، پروتئین فسفاتاز و آسپارتات فسفاتاز در *Cichorium intybus* L.، یک گیاه دارویی مهم انجام گرفت. **روش‌ها:** دو غلظت کانتاریدین و اندوتال 2/5 و 10 µgml$^{-1}$ بر روی نهال *C. intybus* اعمال شده و تغییرات ژن‌ها در ساقه‌ها و ریشه‌ها ارزیابی شد. **نتایج و بحث:** نهال‌های تیمار شده با کانتاریدین و اندوتال کمترین میزان بیان گلوتاتیون S- ترانسفراز را در 2/5 µgml$^{-1}$ داشتند (0/11 ± 0/92 و 0/61 ± 1/07، به ترتیب) در حالی‌که در 10 µgml$^{-1}$ سطح بیان کمی بالاتر بود. بیان گلوتاتیون S- ترانسفراز در ریشه نیز روند مشابهی را دنبال نمود. اثر کانتاریدین بر پروتئین فسفاتاز در ساقه‌ها و ریشه‌های *C. intybus* از الگوی مشابهی پیروی کرد که در آن سطح بیان پروتئین فسفاتاز در ساقه‌ها و ریشه گیاهچه‌های تیمار شده با 2/5 µgml$^{-1}$ (0/03 ± 0/51 و 0/12 ± 1/34، به ترتیب) کاهش یافت. در 10 µgml$^{-1}$ کانتاریدین، بیان پروتئین فسفاتاز به طور قابل توجهی در هر دو ساقه و ریشه افزایش یافت (0/21 ± 3/55 و 0/32 ± 3/96، به ترتیب). بیان پروتئین فسفاتاز در ساقه‌های تحت 2/5 µgml$^{-1}$ اندوتال به میزان قابل توجهی افزایش یافته (3/1 ± 43/21) در حالی که بیان آن در ریشه نزدیک به صفر بود. بیان آسپارتات فسفاتاز در ساقه‌های موجود در 2/5 µgml$^{-1}$ کانتاریدین تقریباً صفر بود در حالی‌که در 10 µgml$^{-1}$ بیان آن به طور بنیادی افزایش یافت (0/23 ± 3/76). ریشه های تحت تیمار با کانتاریدین بیان سطح بالایی به ویژه در 10 µgml$^{-1}$ را نشان دادند (0/11± 2/07). ریشه تحت تیمار با 2/5 کانتاریدین به طور مشابهی اثری از بیان آسپارتات فسفاتاز را نشان نداد. دانهال‌های تحت اندوتال، میزان بیان نسبی آسپارتات فسفاتاز در ساقه‌های تحت تیمار 2/5 µgml$^{-1}$ افزایش یافت، 1/21 ± 17/49، در حالی‌که در ریشه‌ها با 2/5 µgml$^{-1}$ این مقدار به 0/9 ± 0/45 کاهش یافت. **نتیجه‌گیری:** با اطمینان می‌توان بیان کرد که کانتاریدین و اندوتال رشد گیاه را به روش وابسته به دوز و با کاهش بیان آنزیم‌های حیاتی *C. intybus* متوقف می‌کنند.

***کلمات کلیدی:*** *گلوتاتیون S-ترانسفراز، پروتئین فسفاتازها، آسپارتات فسفاتازها، تنظیم مقررات، بیان ژن، Cichorium intybus*

## 1. INTRODUCTION:

Endothall and cantharidin (Figure 1) are specific inhibitors of a protein phosphatase that are involved as markers for their function in defense against pathogens, response to cold treatment, and regulation of (Bajsa *et al.*, 2015; Dayan, 2019). The endothall's functional mechanism in the plant prohibits protein phosphatase (PP1) and (PP2A). Detailed investigation on the endothall controlling system on maize roots indicated abnormal cell division incidence, which consequently halted the root microtubule spindle structures leading to the cell cycle in the prometaphase (Bajsa *et al.*, 2012; Dayan, 2019). Further, Tresch *et al.* (2011) reported that endothall also blocks two checkpoints in the cell cycle. Another potent chemical compound with numerous biological activity from anti-cancer properties to pesticides is cantharidin, which has several analogs, including cantharidic acid and endothelium (Yan *et al.*, 2018).

These substances have an anti-tumor role and are used in pharmacological treatments as well as pesticides. Having such a large spectrum of cantharidin effects results from the biochemical blocking of the target protein cantharidin CBP (CA-binding protein), known as protein phosphatase 2A (PP2A). A regulatory enzyme that many controls cellular stages in eukaryotes (Durian *et al.*, 2016; Máthé *et al.*, 2019). Cantharidin is also a potent inhibitor of serine/threonine protein phosphatase, which is highly toxic and significantly affects Arabidopsis transcription. Serine/threonine-protein phosphatases are essential in conducting cellular signals (Dayan, 2019). In the plant, protein phosphatases are involved in various cellular stages, including cell cycle regulation, hormone signaling and transmission, flowering, photoperiod, cell

differentiation, cell proliferation, and plant defense (Prickett and Brautigan, 2006). Protein phosphatases are highly conserved and have homologous amino acid sequences among different species. Cantharidin binds to protein phosphatase binding sites. In the Arabidopsis genome, 19 phosphatase proteins belonging to 5 different classes (PP6, PP5, PP4, PP2A, PP1) have been identified that represent the target sites of cantharidin (Prickett and Brautigan, 2006; Shi *et al.*, 2006). Cantharidin is a toxin due to its effect on Arabidopsis protein phosphatases; And when plants are sprayed with 200 (Mm) cantharidin, the transcription of 1509 genes is very clearly affected within 2 hours, and all 19 arabidopsis phosphatase proteins are inhibited by cantharidin, indicating that the signal conduction pathways are affected ( Li and Casida, 1992; Bajsa *et al.*, 2015).

Endothelium was first discovered by Bruchhansen vom in 1929 and is a derivative of cantharidin; It is a natural product of a type of beetle called blister beetled and is reported to have herbicidal activity, which Niagra Chemical identified in 1948. The compound was registered as a plant growth regulator in 1950 by chemical Sharples. Endothall was first patented by pennsalt chemical in 1960 for controlling aquatic weeds (Hiltibran, 1963; Hiltibran, 1967; Hiltibran, 1972). The endothall's functional properties are white or colorless crystals that are stable to light and temperatures up to about 90 °C. Above this temperature, it slowly converts to anhydride. When endothall heats up to decompose, it emits intense smoke and steam. The technical endothall name is Aquathol, Hydrothal-47,191, also, endothelial amine salt is called Hydrothal, a dicarboxylic acid family's member. Endothelial amine and potassium salts are used as an aqueous herbicide to control a wide range of plants, including plankton, algae, and pondweed in irrigated lands and rice fields. It is also used to control annual weeds and broadleaf weeds in sugar beets and spinach. Rapid degradation of endothall depends on leaching and often disappears in soil within 7-21 days. It is 4-5 days in clay soils and nine days in soils with high organic content ( Hiltibran, 1972; Langel and Warner, 1986; Erdodi *et al.*, 1995; Skogerboe and Getsinger, 2001; Poovey *et al.*, 2002).

An important subclass of protein phosphatase is aspartate-based phosphatases (ASPT) that mediate metabolism at the cellular level. ASPT can be widely found in either prokaryotes or eukaryotes (Gantt *et al.*, 1992; Perego and Hoch, 1996; Liepman and Olsen, 2004; Dayan, 2019). It is responsible for catalyzing aspartate and ketoglutarate to generate oxaloacetate and glutamate. Due to its substrates' criticality, ASPT has been suggested to be involved in diverse metabolic processes. Some of these are: ASPT is considered a primary source of cellular aspartate, necessary for protein production. ASPT also plays a precursor role in producing the aspartate family of amino acids that covers the agronomically essential amino acids, particularly aspartate (Bryan, 1980; Uhrig *et al.*, 2013; Wadsworth, 1997). The biosynthesis of critical amino acids, asparagine, and ureides as leading nitrogen trans-port carriers also controlled by aspartate (Schubert, 1986).

*Cichorium intybus* L. (Chicory) is one of the most important medicinal plants of the Asteraceae family. As an annual herbaceous species, it has half to one meter long roots. The exterior color of the root is brown, and the inside is white. Chicory is a plant with blue flowers that grows mostly in spring and grows more in humid weather. These flowers open only in the sun and can not be seen in the sun's absence (Gemeinholzer *et al.*, 2005; Gianquinto, 1997). All parts of chicory, including roots and leaves, have medicinal values, and fresh leaves contain a lot of vitamin C, and its consumption improves gingivitis, which is caused by a deficiency of this vitamin ( Pushparaj *et al.*, 2007; Street *et al.*, 2013; Al-Snafi, 2016). Chicory grows in relatively moist roadsides, barren areas, and low slopes from Europe to Sweden, western and central Asia and North Africa, and semi-wild in North America ( Frese *et al.*, 1991; Das *et al.*, 2016). This plant is distributed in different regions of Iran, including the low slopes of Alborz, around Tehran, Lahijan, and Rasht, mountainous areas of Khorasan. Chemical compounds in chicory leaves, in addition to minerals, securic yen glucoside is also found. In chicory root, in addition to securic glucoside, two bitter substances called lactosine, interbin, and arsenic (in the range of 0.01 mg per 100 g of the root) are found (Heibatollah *et al.*, 2008; Nouri *et al.*, 2011; Amiri *et al.*, 2014).

These critical enzymes (glutathione S-transferase, aspartate phosphatases, and protein phosphatases) have a ubiquitous nature regulating the vital cellular mechanisms. Thus, this study aimed to clarify the impact of endothall and cantharidin on the expression of the critical genes associated with the crucial enzymes in the virtue of understanding how these herbicides are trampling the growth and development in *C. Intybus*.

## 2. MATERIALS AND METHODS:

### 2.1. Plant material and application of treatments

Chicory seeds (*Cichorium intybus* L.) were procured from a private company. Seeds were disinfected with sodium hypochlorite for 5 minutes with washed with distilled water. Then treated by different levels of cantharidin and endothall (Sigma-Aldrich, Germany 99%; 10, 50 and 100 $\mu gml^{-1}$) and were kept under 25 $^{o}C$ for a week to complete the germination. Only those treated with 10 $\mu gml^{-1}$ of cantharidin and endothall were germinated, placed in pots (4 seedlings per pot) filled with coco peat and perlite, and daily irrigated with 200 ml water for two weeks and kept under 16/8 day/night and 25°C.

Having the proper level of the two herbicides (10 $\mu gmL^{-1}$), first to calibrate the amount of solution required for each pot, using water a pot thoroughly sprayed which need 400 mL. The solution was prepared for each concentration in which 2.5 $\mu gmL^{-1}$(cantharidin or endothall), 1 mg solved in 400 ML water. In the case of the other treatment (10 $\mu g/mL^{-1}$), it was 4 mg (Table 1). The seedlings were sprayed to apply the treatments (Figure 2). To avoid the effect of the difference in the environment, pots were maintained under the controlled conditions of a greenhouse; day/night 16/8 and 25°C. Two months after applying treatments, samples of roots and leaves from treated seedlings of *C. intybus* were collected separately and used for the analysis. The samples were kept at -80 $^{o}C$ until RNA extraction.

### 2.2. RNA extraction

According to the instructions, RNA extraction was performed by a Sinaclone RNX-plus kit from frozen leaf and root samples of *C. intybus*. The quality of RNA extracted by gel electrophoresis was confirmed by 1.5%. The formation of two RNA bands indicated the quality of purified RNA. A spectrophotometer (UV-1280 Shimadzu, Japan) was used to evaluate the extraction quantitatively. In the next step, the extracted RNA was treated with DNase1 enzyme based on the method proposed by Fermentase Company.

### 2.3. cDNA library

The cDNA was prepared using the RevertAid M-MuLVReverse Transcriptase kit from Sinaclon. 0.1 to 5 µg of total RNA solution was mixed with 1 µl of Oligo-dT and 6 µl of deionized water. Then it was cold off by putting on ice for 5 minutes at + 65 °C and immediately on ice for 5 minutes. 2 µl of reaction buffer solution, 1 µl of deionized water, 2 µl of dNTP mixture, and 1 µl of RT enzyme were added to the reaction mixture. The tubes were placed at +45 °C for 60 minutes and then placed at + 70 °C to stop the reaction. Samples were stored at -20 °C until use.

### 2.4. Designing primers

Oligo Primer Analysis Software v. 7. was utilized for designing of the primers. The gene understudy has three coding regions (exons) and two non-coding regions (introns). For the quantitative RT-PCR reaction, pairs of specific primers were designed so that the return primer was in the range of the untranslated region 3´3´ (which is unique to each gene), and the forward primer was in the penultimate exon so that the product size PCR and RT-PCR are different and detectable (Table 2).

### 2.5. Study of the gene expression pattern

Gene expression pattern by quantitative RT-PCR using SuperScript One-Step RT-PCR (Light Cycler, Bio-Rad, USA) with Platinum Taq, Invitrogen, and Real-time PCR in three experimental replications glutathione S-transferase, protein phosphatase, and aspartate phosphatase were studied using BIO-RAD kit and quantitative RT-PCR which they considered as internal controls. Gene expression in Real-time PCR was calculated by 2-ΔΔCt (Livak et al., 2001). In this method, all data were normalized with s18 ribosomal acid ribonucleic acid gene as the internal control (normal). The amount of gene expression changes in different stresses was measured compared to the control (Kermani *et al.*, 2020).

### 2.6. Statistical Analysis

Minimum three independent replicates were used for each test. Using SPSS version 26 (SPSS Institute, Cary, NC, USA), ANOVA was conducted for the data. The Duncan test performed a comparison of the means at 1% and 5% probability. ChemDraw Ultra V12.0 (PerkinElmer) was used to design the chemical structure of cantharidin and endothall.

## 3. RESULTS AND DISCUSSION:

### 3.1. Effect of cantharidin and endothall on GST in shoot and root

Investigating the expression of glutathione S-transferase **(**GST) gene in a tissue-specific manner in *C. intybus* revealed its significant reduction in both shoots and roots exposed to cantharidin and endothall (Figure 3a and 3b). Cantharidin-treated seedlings experienced the

lowest expression level of GST in 2.5 µgml$^{-1}$ (0.92±0.11) while plants treated with ten µgml$^{-1}$ cantharidin comparably showed a higher expression quantity of GST gene in the shoot (2.94±0.61; Figure 3a). GST expression in shoot received 2.5 and 10 µgml$^{-1}$ cantharidin similarly declined (1.07±0.61 and 1.63± 0.23, respectively; Figure 3a). In endothall treated *C. intybus* seedlings (Figure 3b), the shoot of seedlings exposed to 2.5 and 10 µgml-1 endothall had a relative expression level of 1.03±0.08 and 1± 0.03, respectively; Figure 3b that were significantly lower compared to the control. The GST expression level in C. intybus roots applied with 2.5 and 10 µgml-1 of endothall was notably downregulated compared to control (0.71±0.06 and 1±0.08; Figure 3b). Generally, the two herbicides, cantharidin, and endothall generated a similar pattern affecting GST in both roots and shoots of *C. intybus*.

The GST family, as antioxidant factors, play an essential role in tolerating various stresses in plants. Bajsa *et al.* (2012) studied the effect of cantharidin on the Arabidopsis proteome reported that detoxifying enzymes, especially GST, were down-regulated by cantharidin. GST functions are closely associated with response to a wide variety of environmental stresses from abiotic to xenobiotic-types, to name a few, herbicides, low temperature, hypoxic stress, drought, physical damage, diseases, phytohormones (ethylene, auxin, trinitrotoluene, hydrogen peroxide (H2O2) (Chen et al., 1996; Seppanen *et al*., 2000; Brentner *et al*., 2008), its significant decrease in relative expression levels under cantharidin and endothall stress indicate the control mechanisms of these herbicides.

GST induction suggests that cantharidin induces pseudo-defense responses by inhibiting protein phosphatases through the primary role of GST in the detoxification processes of xenobiotic and endobiotic compounds regulating GST enzymes in addition to other metabolic pathways (Roxas et al., 1997). A prime example of the importance of GST in the plant is when the transgenic tobacco plants overexpressing GST exposed to salt and drought stress, which exhibited a higher level of resistance. In comparison to wild-type plants, these plants had a lower level of lipid peroxidation and showed a higher metabolic activity under salinity and drought stress (Roxas *et al*., 2000).

### 3.2. Effect of Cantharidin and endothall on PPO in shoot and root

The influence of Cantharidin on PPO in shoot and root of *C. intybus* followed a similar pattern (Figure 4a and 4b) where the expression level of PPO in shoots and roots of treated seedlings with 2.5 µgml$^{-1}$ (0.51±0.03 and 1.34±0.12, respectively) reduced in a statistically significant manner (5%) compared with control. On the contrary, at the highest level of Cantharidin (10 µgml$^{-1}$), the expression level of PPO markedly increased in both shoots and roots (3.55±0.21 and 3.96±032, respectively; Figure 4a). The expression of PPO in shoot received 2.5 µgml$^{-1}$ endothall strikingly enhanced (43.21±3.1, Figure 4a) whereas the expression of PPO in shoots treated with ten µg/ml$^{-1}$ declined to 0.19±0.02 (Figure 4b). Moreover, the roots of endothall treated *C*. *intybus* seedlings (Figure 4b) in general indicated an expression level of close to zero in which 2.5 and 10 µgml$^{-1}$ treatments showed 0.43±0.04 and 0.1±0.00 relative expression level with no significant difference at 5% level against control 0.55±0.03. Overall, cantharidin and endothall revealed an almost different pattern in PPO expression and in a dosage-dependent way.

Cantharidin and endothall are protein phosphatase inhibitors, especially PP2A and PP4 maintain the balance between dephosphorylated and phosphorylated forms of specific proteins. They play an essential role in transduction pathways regulating gene expression, cell proliferation and differentiation, and apoptosis. It was observed that both compounds inhibited the expression of protein phosphatase gene in the roots and shoots of chicory plants similar to Bajsa *et al.* (2015) that observed cantharidin significantly reduced transcription of light and auxin transduction genes by inhibiting protein phosphatases in Arabidopsis plants. Additionally, Bajsa *et al*. (2012) reported that endothelium and cantharidin altered the serine/threonine protein phosphatases gene expression in *Arabidopsis thaliana* Lemna paucicostata, which in turn affected the regulation of many biochemical processes in these plants. Li and Casida (1992) pointed to the inhibitory role of cantharidin and endothelium in PP2A phosphatase protein, consistent with the result of this study.

To give a perspective on the importance of PPOs in plants recently has been determined that a significant ratio of the sequenced *Arabidopsis* genome involved in encoding protein kinases and PPOs, which catalyzing reversible phosphorylation. An optimal regulation in plant cells requires a balance between kinases and phosphatases (Luan 2003). Thus, the influence of cantharidin and endothall on reducing PPO

expression was severe, particularly endothall. Application of catandirin on Arabidopsis plants revealed a notable reduction in PPOs while dramatically increased GST expression due to the role of GST in controlling the damage and maintaining the situation for the function of PPOs. However, in this study, the opposite where PPO did not downregulate while GST was reduced by increasing dosage (Bajsa *et al.*, 2015). The mechanism that has been proposed for the inhibitory effect of endothall at the cellular level involves distortion of the cell division orientation program and microtubule spindle formation, which initiates the prevention of the cell cycle in prometaphase. Although a lot has been revealed about the function of PPOs and the influence of herbicides on them, many territories of their cellular function still yet to be known (Tresch *et al*., 2011).

### 3.3. Effect of cantharidin and endothall on ASPT in shoot and root

The expression of ASPT in shoots under treatments, control, and 2.5 $\mu gml^{-1}$ cantharidin was almost zero (Figure 5a), while in 10 $\mu gml^{-1}$ treatment, its expression was radically increased (3.76±0.23). Differently, roots treated with cantharidin indicated high relative expression of ASPT, particularly in 10 $\mu gml^{-1}$ (2.07±0.11), which was lower than control (4.11±0.23) and made a statistically significant difference. Like shoots treated with 2.5 µgml-1 cantharidin, roots similarly did not express ASPT (Figure 5a). In *C. intybus* seedlings exposed to endothall, expression of ASPT followed a different behavior in which the relative expression level of ASPT in shoots under 2.5 $\mu gml^{-1}$ was 17.49±1.21 and made a significant difference with control (12.22±2.5) while in roots its expression level under 2.5 $\mu gml^{-1}$ was down to 0.45±0.09 (Figure 5b). Also, the expression of the root of ASPT in control (6.11±0.54) was considerably lower than control in shoots. Finally, similar to shoots under ten $\mu gml^{-1}$ endothall, the expression level of ASPT was downregulated markedly (Figure 5b).

ASPT is one of the main pathways for synthesizing and removing amino groups from a molecule, thereby facilitating internal conversion of carbohydrate and protein metabolism when plants are exposed to stress conditions to address the excessive energy demand (Gelfand and Steinberg, 1977; Liepman and Olsen, 2004). This enzyme exists at the cellular level in various isozyme forms. They are also differentially located in a minimum of four different subcellular compartments, namely the cytosol, plastids, mitochondria, and peroxisomes (Wadsworth, 1997). Aspartate-based protein phosphatases are one of the main classes of PPOs (Fuchs et al., 2013). Given the fundamental role of phosphatases, particularly ASPT, manipulating these enzymes can be a reliable approach for precise metabolic engineering to generate crop cultivars with improved stress tolerance.

Additionally, many phosphatases do not exist in animals, which may be suitable targets for herbicides (Givan, 1980; Nakamura and Tolbert, 1983; Reumann, 2000). Despite their primary role in plant metabolism and the fact that herbicides can be developed targeting these enzymes. So far, there is no published study exists addressing the effect of herbicides on ASPT in plants.

In all the eukaryote organisms, only 11 highly conserved metallo-dependent protein phosphatase exist which 9 of which are amino acids, that 4 of them are aspartate residues responsible for the coordination of metallic ions essential for catalytic processes. Unlike other protein families that have been the subject of many studies, ASPT has only been known for 10 years in animals and plants (Matsuda *et al*., 1997; Archambault *et al*., 1998; Moorhead *et al*., 2009).

Differences in responses to catalase and glutathione peroxidase enzymes in C. intybus and cantharidin and endothall have also been observed in a study conducted by this group (Kermani *et al*., 2020). By taking a comparative approach between the result of the previous study and this study, catalase and glutathione peroxidase enzymes, despite their critical role in plants under stress, were less responsive than PPO, GST ASPT in this study. The possible explanation could be that catalase and glutathione peroxidase enzymes are secondary defense mechanisms while PPO, GST, and ASPT regulate basically the whole plant organization. Further, the responses of PPO, GST, and ASPT to endothall were less remarkable in general compare to cantharidin.

## 4. CONCLUSIONS:

The influence of endothall and cantharidin herbicides on the gene expression changes of vital enzymes, including GST, PPO, and ASPT in *C. intybus* investigated in this study. These enzymes involved in the majority of biochemical processes in plant and herbicides used significantly reduced their expression. However, reduction in expression level often showed dose-dependency and tissue-specificity. Response to endothall and cantharidin concentrations in shoots and roots were different. Also, downregulation of the enzymes in the low level (2.5 $\mu gml^{-1}$) used in this

study in some cases did not follow the highest concentration (10 $\mu gml^{-1}$). Moreover, endothall is an analog of cantharidin but act differently in many instances. It can be speculated that the significant meddling of cantharidin and endothall in growth negatively affecting the critical enzymes in *C. intybus.* The effect of these herbicides at the physiological level on *C. intybus* is under study by this group and strongly recommends studying other essential enzymes along with a broader range of concentrations from these herbicides.

## 5. REFERENCES:


1. Al-Snafi, A. E. (2016). Medical importance of Cichorium intybus–A review. *Journal of Pharmacy,* 6, 41-56.
2. Amiri, M. S.; Joharchi, M. R., Taghavizadeh Yazdi, M. E. (2014). Ethno-medicinal plants used to cure jaundice by traditional healers of Mashhad, Iran. *Iranian Journal of Pharmcutical Research*, 13, 157.
3. Archambault, J.; Pan, G.; Dahmus, G. K.; Cartier, M.; Marshall, N.; Zhang, S.; Greenblatt, J. (1998). FCP1, the RAP74-interacting subunit of a human protein phosphatase that dephosphorylates the carboxyl-terminal domain of RNA polymerase IIO. *Journal of Biological Chemistry*, 273(42), 27593-27601.
4. Bajsa, J.; Pan, Z.; Dayan, F. E.; Owens, D. K.; Duke, S. (2012). Validation of serine/threonine protein phosphatase as the herbicide target site of endothall. *Pesticide biochemistry and physiology*,102, 38-44.
5. Bajsa, J.; Pan, Z.; Duke, S. (2015). Cantharidin, a protein phosphatase inhibitor, strongly upregulates detoxification enzymes in the Arabidopsis proteome. *Journal of plant physiology*, 173, 33-40.
6. Brentner, L.B.; Mukherji, S.T.; Merchie, K.M.; Yoon, J.M.; Schnoor, J.L.; Van Aken, B. (2008). Expression of glutathione S-transferases in poplar trees (Populus trichocarpa) exposed to 2,4,6-trinitrotoluene (TNT). *Chemosphere*, 73: 657-62.
7. Bryan, J. (1980). Synthesis of the aspartate family and branched-chain amino acids. In *Amino Acids and Derivatives* (pp. 403-452). Academic Press.
8. Chen, W.; Chao, G.; Singh, K.B. (1996). The promoter of an H2O2-inducible, Arabidopsis glutathione S-transferase gene contains closely linked OBF- and OBP1-binding sites. *Plant Journal* 1996, 10: 955-66.
9. Das, S.; Vasudeva, N.; Sharma, S. (2016). Cichorium intybus: A concise report on its ethnomedicinal, botanical, and phytopharmacological aspects. *Drug Development & Therapeutics,* 7, 1-12.
10. Dayan, F. (2019). Current status and future prospects in herbicide discovery. *Plants*, 8, 341.
11. Durian, G.; Rahikainen, M.; Alegre, S.; Brosché, M., Kangasjärvi, S. (2016). Protein Phosphatase 2A in the Regulatory Network Underlying Biotic Stress Resistance in Plants. *Frontiers in plant science,* 7, 812.
12. Erdodi, F.; Toth, B.; Hirano, K.; Hirano, M.; Hartshorne, D., Gergely, P. (1995). Endothall thioanhydride inhibits protein phosphatases-1 and-2A in vivo. *American Journal of Physiology-Cell Physiology*, 269, C1176-C1184.
13. Frese, L.; Dambroth, M., Bramm, A. (1991). Breeding potential of root chicory (Cichorium intybus L. var. sativum). *Plant Breeding,* 106, 107-113.
14. Fuchs, S.; Grill, E.; Meskiene, I.; Schweighofer, A. (2013). Type 2C protein phosphatases in plants. *The FEBS journa*l, 280(2), 681-693.
15. Gantt, J. S.; Larson, R. J.; Farnham, M. W.; Pathirana, S. M.; Miller, S. S., Vance, C. (1992). Aspartate aminotransferase in effective and ineffective alfalfa nodules: cloning of a cDNA and determination of enzyme activity, protein, and mRNA levels. *Plant physiology*, 98, 868-878.
16. Gelfand, D. H.; Steinberg, R. (1977). Escherichia coli mutants deficient in the aspartate and aromatic amino acid aminotransferases. *Journal of Bacteriology,*130, 429-440.
17. Gemeinholzer, B.; Bachmann, K. (2005). Examining morphological and molecular diagnostic character states of Cichorium intybus L.(Asteraceae) and C. spinosum L. *Plant Systematics and Evolution*, 253,105-123.

18. Gianquinto, G. (1997). Morphological and physiological aspects of phase transition in radicchio (Cichorium intybus L. var. silvestre Bisch.): influence of daylength and its interaction with low temperature. *Scientia horticulturae,* 71, 13-26.

19. Givan, C. V. (1980). Aminotransferases in higher plants. In *Amino acids and derivatives* (pp. 329-357). Academic press.

20. Heibatollah, S.; Reza, N. M.; Izadpanah, G.; Sohailla, S. (2008). Hepatoprotective effect of Cichorium intybus on CCl4-induced liver damage in rats. *African Journal of Biochemistry Research,* 2,141-144.

21. Hiltibran, R. (1963). Tests of herbicides for aquatic weed control in Illinois. Paper presented at the Proccedings of NCWCC, 20,112-114

22. Hiltibran, R. C. (1967). Effects of some herbicides on fertilized fish eggs and fry. *Transactions of the American Fisheries Society*, 96, 414-416.

23. Hiltibran, R. (1972). The Hydrolysis of Adeno sine Triphosphate by Bluegill Liver Mito chondria in the Presence of 2, 4, 5-T and Silvex Derivative. *Transactions of the Illinois State Academy of Science*, 65, 51.

24. Kermani, Y. G.; Nejad, R. A. K.; Mahmoodzadeh, H.; Abadi, K. S. (2020). Comparative effects of cantharidin and endothall on gene expression and activity of antioxidant enzymes in Cichorium intybus L. *Journal of Acta Slovinica,*116, 189-197.

25. Langeland, K.; Warner, J. (1986). Persistence of diquat, endothall, and fluridone in ponds. 24, 43-46.

26. Li, Y.-M.; Casida, J. (1992). Cantharidin-binding protein: identification as protein phosphatase 2A. *Proceedings of the National Academy of Sciences,* 89, 11867-11870.

27. Liepman, A. H.; Olsen, L. (2004). Genomic analysis of aminotransferases in Arabidopsis thaliana. *Critical Reviews in Plant Sciences,* 23, 73-89.

28. Livak, K. J.; Schmittgen, T. D. (2001). Analysis of relative gene expression data using real-time quantitative PCR and the 2− ΔΔCT method. *Methods*, 25(4), 402-408.

29. Luan, S. (2003). Protein phosphatases in plants. *Annual Review of Plant Biology*, 54(1), 63-92.

30. Máthé, C.; Garda, T.; Freytag, C. (2019). The Role of Serine-Threonine Protein Phosphatase PP2A in Plant Oxidative Stress Signaling—Facts and Hypotheses. *International journal of molecular sciences,* 20, 3028.

31. Matsuda, O.; Sakamoto, H.; Nakao, Y.; Oda, K..; Iba, K. (2009). CTD phosphatases in the attenuation of wound-induced transcription of jasmonic acid biosynthetic genes in Arabidopsis. *The Plant Journal*, 57(1), 96-108.

32. Moorhead, G. B.; De Wever, V.; Templeton, G.; Kerk, D. (2009). Evolution of protein phosphatases in plants and animals. *Biochemical Journal*, *417*(2), 401-409.

33. Nakamura, Y.; Tolbert, N. (1983). Serine: glyoxylate, alanine: glyoxylate, and glutamate: glyoxylate aminotransferase reactions in peroxisomes from spinach leaves. *Journal of Biological Chemistry,* 258, 7631-7638.

34. Nouri, J.; Lorestani, B.; Yousefi, N.; Khorasani, N.; Hasani, A.; Seif, F., Cheraghi, M. (2011). Phytoremediation potential of native plants grown in the vicinity of Ahangaran lead–zinc mine (Hamedan, Iran). *Environmental Earth Sciences,* 62, 639-644.

35. Perego, M.; Hoch, J. A. (1996). Protein aspartate phosphatases control the output of two-component signal transduction systems. *Trends in Genetics,* 12, 97-101.

36. Poovey, A. G.; Skogerboe, J.; Owens, C. (2002). Spring treatments of diquat and endothall for curlyleaf pondweed control. *Journal of Aquatic Plant Management,* 40, 63-67.

37. Prickett, T. D.; Brautigan, D. (2006). The α4 regulatory subunit exerts opposing allosteric effects on protein phosphatases PP6 and PP2A. *Journal of Biological Chemistry,* 281, 30503-30511.

38. Pushparaj, P.; Low, H.; Manikandan, J.; Tan, B.; Tan, C. (2007). Anti-diabetic effects of Cichorium intybus in streptozotocin-induced diabetic rats. *Journal of ethnopharmacology,* 111, 430-434.

39. Reumann, S. (2000). The structural properties of plant peroxisomes and their metabolic significance. *Biological chemistry*, 381, 639-648.

40. Roxas, V.P.; Smith, R.K.; Allen, E.R.; Allen, R.D. (1997). Overexpression of glutathione S-transferase/glutathione peroxidase enhances the growth of transgenic tobacco seedlings during stress. *Nature Biotechnology*, 15: 988-991.

41. Roxas, V. P.; Lodhi, S. A.; Garrett, D. K.; Mahan, J. R.; Allen, R. D. (2000). Stress tolerance in transgenic tobacco seedlings that overexpress glutathione S-transferase/glutathione peroxidase. *Plant and Cell Physiology*, 41(11), 1229-1234.

42. Seppanen, M.M.; Cardi T.; Hyokki, M.B.; Pehu, E. (2000). Characterisation and expression of cold-induced glutathione S-transferase in freezing tolerant Solanum commersonii, sensitive S. tuberosum and their interspecific somatic hybrids. *Plant Science*, 153: 125-33.

43. Shi, Y.; Reddy, B.; Manley, J. (2006). PP1/PP2A phosphatases are required for the second step of Pre-mRNA splicing and target specific snRNP proteins. *Molecular cell*, 23, 819-829.

44. Skogerboe, J. G.; Getsinger, K. (2001). Endothall species selectivity evaluations: southern latitude aquatic plant community. *Journal of Aquatic Plant Management*, 39,129-135.

45. Street, R. A.; Sidana, J.; Prinsloo, G.; Medicine, A. (2013). Cichorium intybus: Traditional uses, phytochemistry, pharmacology, and toxicology. *Evidence-Based Complementary and Alternative Medicine,* 2013

46. Tresch, S.; Schmotz, J.; Grossmann, K. (2011). Probing mode of action in plant cell cycle by the herbicide endothall, a protein phosphatase inhibitor. *Pesticide Biochemistry and Physiology*, 99, 86-95.

47. Ueda, A.; Li, P.; Feng, Y.; Vikram, M.; Kim, S.; Kang, C. H.; Kang, J. S.; Bahk, J.D.; Lee, S.Y.; Fukuhara, T.; Staswick, P.E.; Pepper, A.E.; Koiwa, H. (2008). The Arabidopsis thaliana carboxyl-terminal domain phosphatase-like 2 regulates plant growth, stress and auxin responses. *Plant Molecular Biology*, 67(6), 683.

48. Uhrig, R. G.; Labandera, A. M.; Moorhead, G. (2013). Arabidopsis PPP family of serine/threonine protein phosphatases: many targets but few engines. *Trends in plant science,* 18, 505-513.

49. Wadsworth, G. (1997). The plant aspartate aminotransferase gene family. *Physiologia Plantarum,* 100, 998-1006.

50. Yan, Y.; Liu, Q.; Zang, X.; Yuan, S.; Bat-Erdene, U.; Nguyen, C.; Gan, J.; Zhou, J.; Jacobsen, S. E., Tang, Y. (2018). Resistance-gene-directed discovery of a natural-product herbicide with a new mode of action. *Nature,* 559, 415-418.

***Table 1.*** *Concentrations of herbicides applied on C. intybus seedlings.*

| Treatments | Discription | Concentration (µg/mL$^{-1}$) |
|---|---|---|
| 1. | Control | Distilled water only |
| 2. | Cantharidin | 2.5 |
| | | 10 |
| 3. | Endothall | 2.5 |
| | | 10 |

***Table 2.*** *Sequences of primers used to evaluate endothall and cantharidin's influence on essential genes (protein phosphatases; PPO, glutathione S-transferase; GST, aspartate phosphatases; ASPT, in C. intybus).*

| Gene | Forward 5' → 3' | Reverse 5' → 3' |
|---|---|---|
| PPO | TCCGGTTCATATATGGACT | TCC CTC ACC TTG ACA CGAAC |
| GST | TCCTCC AGATGAACC CGGTA | TTTCTTCAT ATCCTCCT |
| ASPT | GAACAAGTACTA AAC CGTGTG | AATTTGCCTTCTTCATCCAC |

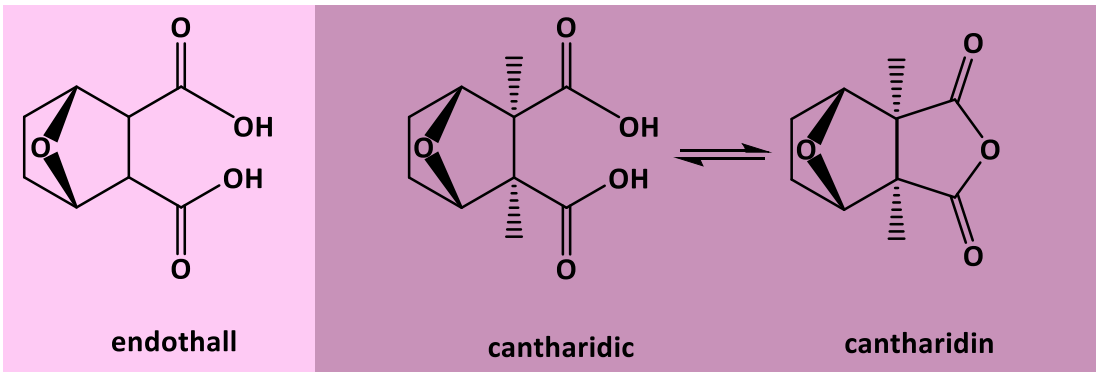


***Figure 1.*** *Structure of endothall, cantharidin, and its dicarboxylic acid analog.*

**Figure 2.** *C. intybus seedlings under treatments of various concentrations of endothall and cantharidin (mentioned in Table 1).*

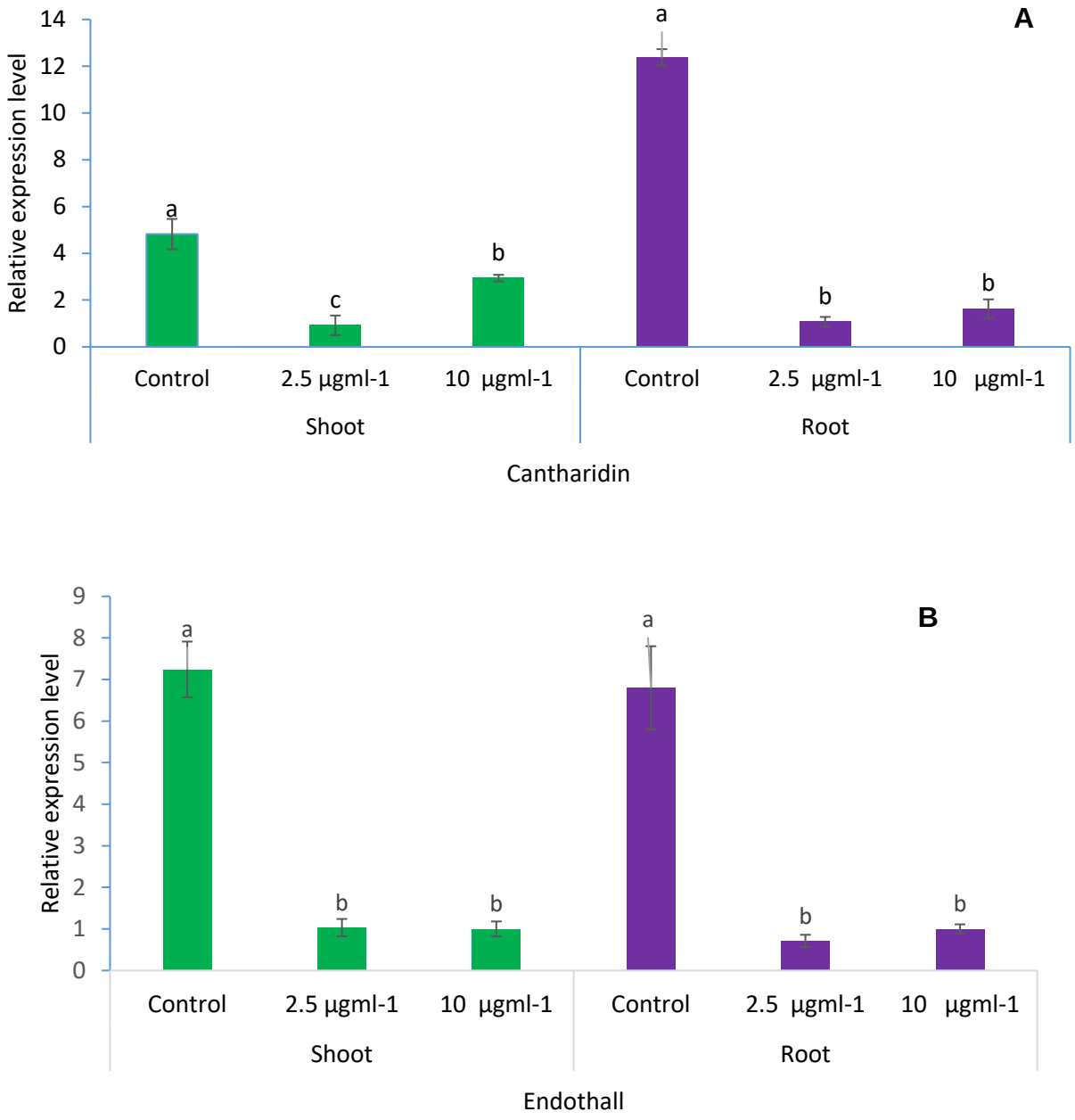


***Figure 3.*** *The expression level of GST in Chicorium intybus shoots and roots treated with cantharidin (a) and endothall (b).*

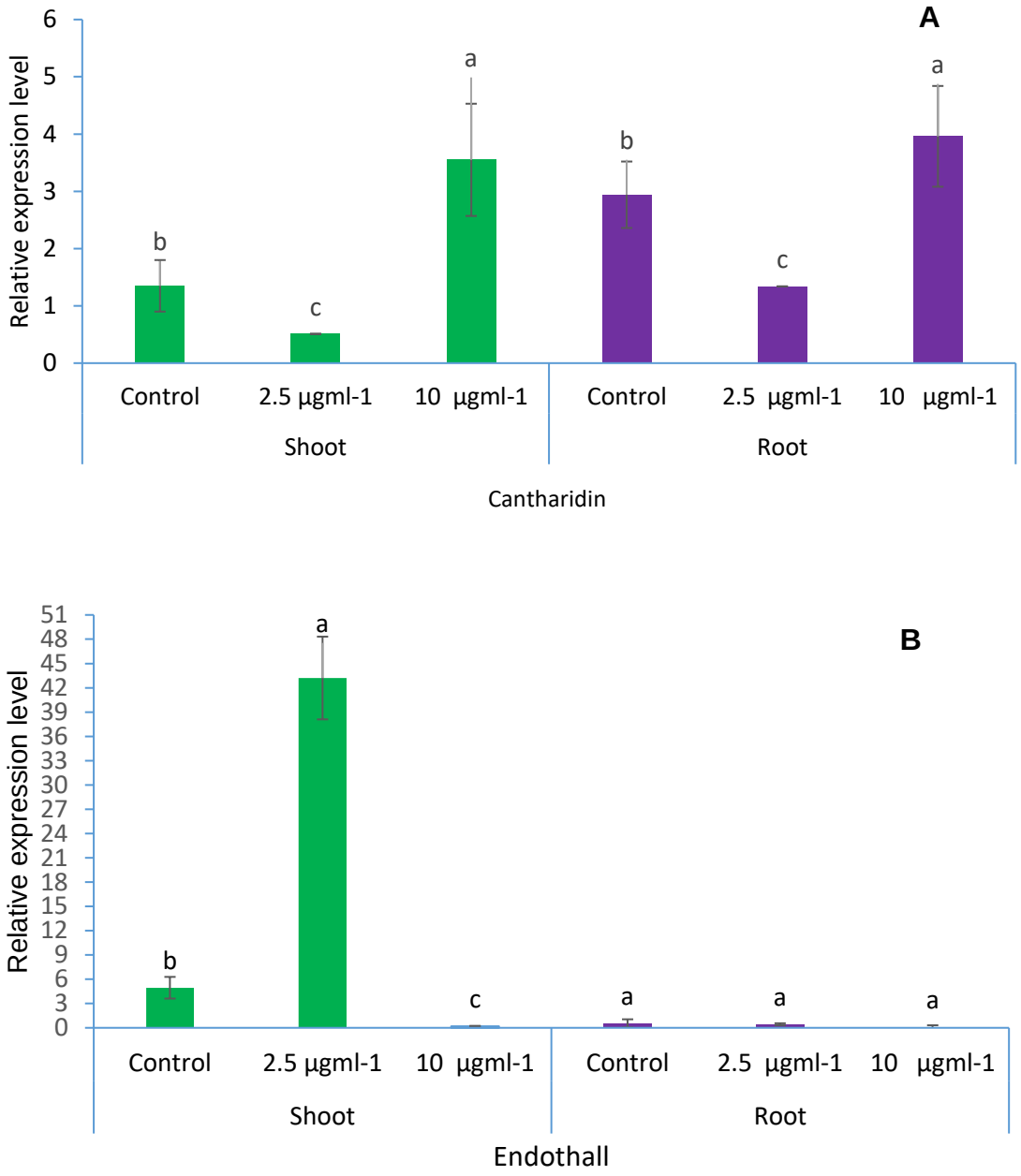


***Figure 4***. *The expression level of PPO in Chicorium intybus shoots and roots treated with cantharidin (a) and endothall (b).*

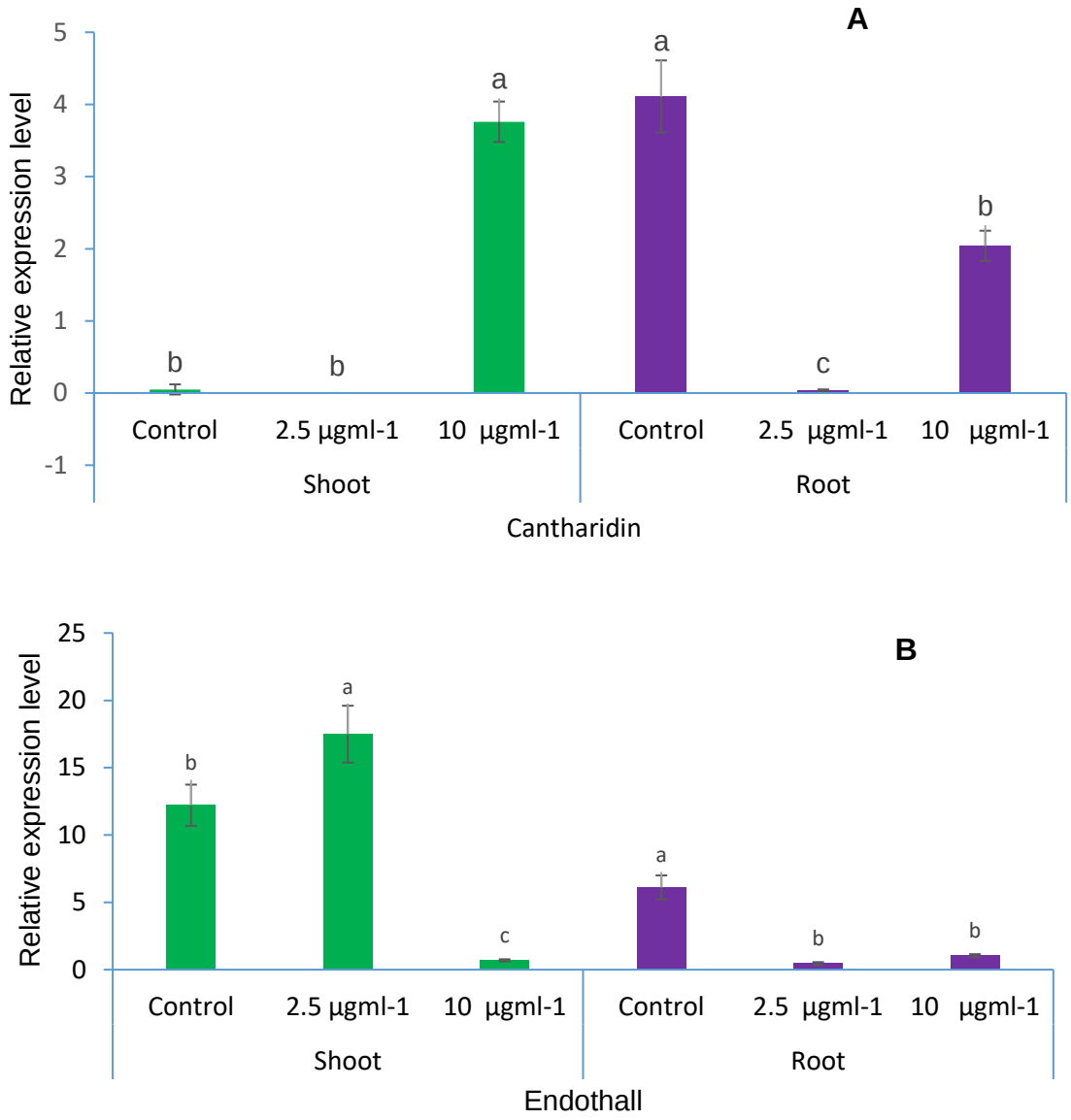


***Figure 5.*** *The expression level of ASPT in Chicorium intybus shoots and roots treated with cantharidin (a) and endothall (b).*

PERIÓDICO TCHÊ QUÍMICA
ARTIGO ORIGINAL

# ESTIMAÇÃO DE PARÂMETROS DE CÉLULAS / MÓDULOS FOTOVOLTAICOS USANDO UM ALGORITMO DE EVOLUÇÃO DIFERENCIAL ADAPTATIVO TRIANGULAR

# ESTIMATING OF PHOTOVOLTAIC CELLS/MODULES PARAMETERS USING A TRIANGULAR ADAPTIVE DIFFERENTIAL EVOLUTION ALGORITHM

# ESTIMASI PARAMETER SEL/MODUL FOTOVOLTAIK MENGGUNAKAN ALGORITMA EVOLUSI DIFERENSIAL ADAPTIF SEGITIGA

HIENDRO, Ayong[1*]; YUSUF, Ismail[2]; JUNAIDI[3]; ERWAN, Komala[4]

[1,2,3,4] Tanjungpura University, Faculty of Engineering, Department of Electrical Engineering. Indonesia.

** Corresponding author*
*e-mail: ayong.hiendro@ee.untan.ac.id*

Received 03 February 2021; received in revised form 17 February 2021; accepted 28 February 2021

## RESUMO

**Introdução:** Os sistemas fotovoltaicos (PV) se tornaram uma tecnologia de energia renovável promissora para fontes de eletricidade. A estimativa de parâmetro PV desempenha um papel vital na modelagem de sistemas PV. Embora muitos algoritmos de otimização tenham sido apresentados para obter parâmetros de PV, ainda é um desafio investigar algoritmos de alto desempenho. **Objetivo:** Este estudo teve como objetivo propor um algoritmo de evolução diferencial adaptativa triangular (TADE) para fornecer uma estimativa precisa dos parâmetros de PV. **Metodos:** Célula PV RTC-France, módulo PV Photowatt-PWP 201 e módulo PV KC200GT foram usados como estudos de caso usando modelos de circuito de diodo. O erro quadrático médio (RMSE) entre os dados medidos e estimados foi adotado para definir as funções objetivo dos parâmetros de PV. Um teste de Friedman foi usado para avaliar a confiabilidade dos algoritmos. Os resultados da estimativa dos parâmetros foram verificados para confirmar a precisão dos desempenhos do algoritmo TADE. O módulo PV operando em várias condições climáticas também foi realizado para avaliar o algoritmo TADE. **Resultados e Discussão**: Os resultados verificaram que na maioria dos casos o algoritmo TADE superou outros algoritmos de otimização de última geração. Para o modelo de diodo duplo, o algoritmo TADE obteve os parâmetros da célula PV RTC-France com o valor RMSE de 9,8243x10$^{-04}$, o mais preciso de todos os algoritmos. Os resultados experimentais também mostraram que o algoritmo TADE apresentou excelente capacidade e precisão na descoberta dos parâmetros PV e forneceu as melhores estimativas para dados experimentais I-V e P-V de células e módulos PV reais.. **Conclusões:** Os resultados comprovaram que o algoritmo TADE tem um ótimo desempenho em termos de precisão, confiabilidade e velocidade de convergência para estimativa de parâmetros PV, mesmo em diferentes condições climáticas.

**Palavras-chave**: *convergência; curva corrente-tensão; modelo de diodo duplo; raiz quadrada média do erro; modelo de diodo único.*

## ABSTRACT

**Background:** Photovoltaic (PV) systems have become a promising renewable energy technology for electricity sources. The PV parameter estimation plays a vital role in modeling PV systems. Even though many optimization algorithms have been presented to obtain PV parameters, it is still challenging to investigate high-performance algorithms. **Aim:** This study aimed to propose a triangular adaptive differential evolution (TADE) algorithm to give a precise estimate of PV parameters. **Methods:** RTC-France PV cell, Photowatt-PWP 201 PV module, and KC200GT PV module were used as the case studies by using diode circuit models. The root mean square error (RMSE) between measured and estimated data was adopted to define PV parameter objective functions. A Friedman test was used to assess the reliability of algorithms. The parameter estimation results were cross-checked to confirm the accuracy of TADE algorithm performances. The PV module operating under various weather conditions was also performed to evaluate the TADE algorithm. **Results and Discussion**: The results verified that in most of the cases, the TADE algorithm surpassed other state-of-the-art optimization algorithms. For the double-diode model, the TADE algorithm obtained the RTC-France PV cell parameters with the *RMSE* value of 9.8243x10$^{-04}$, the most accurate of all algorithms. Experimental results also showed that the TADE algorithm presented an excellent capability and accuracy in discovering the PV parameters and provided the best estimates for *I-V* and *P-V* experimental data of real PV cells and modules. **Conclusions:** The results have

proven that the TADE algorithm has a great performance in terms of accuracy, reliability, and convergence speed for estimating PV parameters, even in different weather conditions.

**Keywords**: *convergence; current-voltage curve; double-diode model; root mean square error; single-diode model*.

## ABSTRAK

**Latar Belakang:** Sistem fotovoltaik (PV) telah menjadi teknologi energi terbarukan yang menjanjikan sebagai sumber listrik. Estimasi parameter PV memainkan peran penting dalam pemodelan sistem PV. Meskipun telah banyak algoritma optimisasi telah dihadirkan untuk mendapatkan parameter PV, namun masih menantang untuk menemukan algoritma berkinerja tinggi. **Tujuan:** Penelitian ini bertujuan untuk mengusulkan algoritma evolusi diferensial adaptif segitiga (TADE) guna memberikan hasil estimasi yang teliti dari parameter PV. **Metode:** Sel PV RTC-France, modul PV Photowatt-PWP 201, dan modul PV KC200GT digunakan sebagai studi kasus dengan menggunakan model rangkaian dioda. Akar kuadrat rata-rata galat (RMSE) antara data yang diukur dan yang diperkirakan diadopsi untuk menentukan fungsi tujuan parameter PV. Tes Friedman digunakan untuk menilai reliabilitas algoritma. Hasil estimasi parameter diperiksa silang untuk memastikan keakuratan performa algoritma TADE. Modul PV yang beroperasi dalam berbagai kondisi cuaca juga dilakukan untuk mengevaluasi algoritma TADE. **Hasil dan Diskusi:** Hasil membuktikan bahwa di sebagian besar kasus, algoritma TADE melampaui algoritma optimisasi canggih lainnya. Untuk model dioda-ganda, algoritma TADE memperoleh parameter sel PV RTC-France dengan nilai *RMSE* = $9.8243 \times 10^{-04}$, hasil yang paling akurat dari semua algoritma. Hasil eksperimen juga menunjukkan bahwa algoritma TADE memberikan kemampuan dan akurasi yang sangat baik dalam menemukan parameter PV dan memberikan estimasi terbaik untuk data eksperimen *I-V* dan *P-V* sel dan modul PV. **Kesimpulan:** Hasil penelitian telah membuktikan bahwa algoritma TADE memiliki performa yang bagus dalam hal akurasi, reliabilitas, dan kecepatan konvergensi untuk mengestimasi parameter PV, bahkan dalam beragam kondisi cuaca.

**Kata kunci**: *konvergensi; kurva arus-tegangan; model dioda-ganda; galat akar rata-rata kuadrat; model dioda-tunggal.*

## 1. INTRODUCTION:

An accurate estimation of photovoltaic (PV) parameter values is very important to the design and performance assessment of PV systems. These parameters consist of photogenerated current, saturation current, diode ideality factor, and series and shunt resistances (Anani and Ibrahim, 2020).

The PV cells and modules are generally characterized by current (*I*)-voltage (*V*) and power (*P*)-voltage (*V*) curves. The PV parameters affect the *I-V* and *P-V* behavior of PV cells and modules, which change in electrical voltage, current, and power due to solar irradiance and temperature variations. As the output power of the PV cells and modules is dependent on solar irradiance and temperature, with knowing the PV parameters, engineers can design appropriate PV systems to operate under a variety of atmospheric conditions. It is also useful for the maintenance and monitoring operation of PV systems (Bosman *et al.*, 2020) and testing maximum power point tracking (MPPT) algorithms (Motahhir *et al.*, 2018) under various conditions and control of PV systems (Jordehi, 2016a).

The current-voltage curve of PV cells exhibits nonlinear and multivariable characteristics. The power delivered by PV cells and modules is the product of current and voltage. The *P-V* curve is obtained by multiplicating current and voltage, point for point, for all currents and voltages from open-circuit to short-circuit conditions. The estimation of the *I-V* and *P-V* curves can be conducted using online and offline measuring methods. The advantage of online measurement is its ability to measure real *I-V* and *P-V* characteristics based on site-specific conditions. However, the online measuring method is costly and requires long-term continuous monitoring (Zhu *et al.*, 2017).

On the other hand, the offline measurement for determining *I-V* and *P-V* curves is fast and accurate but cannot diagnose faults in PV systems. Therefore, PV cell models are necessary to extract the *I-V* and *P-V* characteristics offline. There are two PV cell models widely employed to represent the current-voltage relationship, such as the single-diode model (SDM) (Muhammadsharif *et al.*, 2019; Arabshahi *et al.*, 2020) and the double-diode model (DDM) (Khotbehsara and Shahhoseini, 2018). The SDM has five unknown parameters, while the DDM contained seven parameters to be estimated. The SDM is usually used in the estimation of PV parameters because of its simplicity. Yet, the DDM is considered to be more

accurate than the SDM, particularly in a low solar irradiance condition. The DDM also requires a longer running time than the SDM to perform the computational process (Abbassi *et al.*, 2019). However, both SDM and DDM need detailed information of all unknown parameters, which is generally not given by PV manufacturers. Besides, PV manufacturers still do not introduce any methods of extracting the PV parameters.

Many methods have been evolved to compute the PV parameters from the models. There are three techniques generally utilized to optimize the PV parameters, namely: analytical, numerical, and algorithmic through metaheuristics. The analytical approach is practically possible for solving the PV parameters problem. The analytical method has fast computation speed and gives relatively accurate results. However, the analytical method becomes very difficult and requires too much computational time to solve complex and large-sized problems. The analytical method has been used to compute PV parameters, such as Padé approximant (Lun *et al.*, 2013a), Taylor's Series Expansion (Lun *et al.*, 2013b), and Lambert W-function (Gao *et al.*, 2016; Chen *et al.*, 2018a). The numerical method is usually more accurate than the analytical process because it employed all the *I-V* curve points. The numerical method based on the Newton-Raphson iteration (Ghani *et al.*, 2014; Rodrigues *et al.*, 2018) or Gauss-Seidel (Et-torabi *et al.*, 2017) may converge to optimal values. The drawbacks of the numerical method that it needs extensive computational resources and will be susceptible to being nonconvergent if the search space is not convex. In order to overcome these inconveniences, metaheuristics algorithms have been developed to optimize the PV parameters. The metaheuristics algorithms have attracted more and more attention among the computational methods due to their effectiveness in solving complex problems. In the metaheuristic algorithms, the objective function and constraints do not rely on strict convexity, continuity, and differentiability. Moreover, the metaheuristic algorithms have better performance than numerical and analytical methods concerning accuracy, reliability, and convergence speed (Pillai and Rajasekar, 2018). Along with the development of the metaheuristic algorithms, they have been popular in determining the PV parameters for the last decade, for instance, Genetic Algorithm (GA) (Ismail *et al.*, 2013), Differential Evolution (DE) (Yang *et al.*, 2013), Particle Swarm Optimization (PSO) (Soon and Low, 2012), and Simulated Annealing (SA) (El-Naggar *et al.*, 2012). Other recent metaheuristic algorithms working on estimating the PV parameters are Supply-Demand-Based Optimization (SDO) (Xiong *et al.*, 2019), Chaotic Optimization Approach (COA) (Ćalasan *et al.*, 2019), Symbiotic Organisms Search (SOS) (Xiong *et al.*, 2018), and population classification evolution (PCE) (Zhang *et al.*, 2016).

Every algorithm has its own advantages and disadvantages. GA has the ability to avoid being trapped in the local optimum because it searches from parallel points. However, GA has a slow convergence process. DE is robust, but it requires the appropriate parameter settings to ensure the success of the algorithm. On the other hand, PSO is fast, but it is easy to fall into the local optimum in high-dimensional space. SA is known for its flexibility and ability to approach global optimum, but it needs much computational effort. For this reason, a single metaheuristic algorithm can be modified to improve its performance as in (Lin *et al.*, 2017; Yu *et al.*, 2017a; Chen *et al.*, 2018b; Kang *et al.*, 2018; Gao *et al.*, 2018; Li *et al.*, 2019a; Yu *et al.*, 2019; Chen *et al.*, 2019a; Pourmousa *et al.*, 2019; Liao *et al.*, 2020;). Another way to enhance the metaheuristic algorithm performance is hybridization with other algorithms as in (Jordehi, 2016b; Oliva *et al.*, 2017; Chen *et al.*, 2017; Yu *et al.*, 2017b; Beigi and Maroosi, 2018; Li *et al.*, 2019b; Chen *et al.*, 2019b; Chen *et al.*, 2019c; Long *et al.*, 2020). More often, two or more other metaheuristic algorithms are combined to create a single hybrid one. Hybridization is usually done to incorporate each of the desired features so that the overall algorithm becomes better than the single algorithm. It must be noted that a particular algorithm cannot very successfully deal with all problems. The algorithm may be very effective at solving one engineering problem, but it does not mean that the algorithm will also successfully deal with other engineering problems. For this reason, researchers utilize various kinds of algorithms to determine the most suitable one to solve a problem.

The objective function of the PV parameter optimization problem is conducted to minimize the difference between experimental and estimated data, which is stated as the root mean square error (*RMSE*). The *RMSE* has been commonly used as a standard statistical parameter to measure the performance of metaheuristic algorithms. However, the *RMSE* results reported by many metaheuristic algorithms presented in the literature do not fit with the objective function (Gnetchejo *et al.*, 2019). The *RMSE* values are not calculated correctly since the estimated PV output

current is incorrect (Ćalasan *et al.*, 2019). In order to be careful about the accuracy, the results should be cross-checked.

This study aimed to propose a triangular adaptive differential evolution (TADE) algorithm to estimate parameters from PV cells and modules and evaluate their *I–V* and *P-V* characteristics.

## 2. MATERIALS AND METHODS:

Four case studies were carried out to assess the performance of the TADE algorithm. In the first and second cases, SDM and DDM were implemented to estimate the RTC-France PV cell parameters under irradiance and temperature about 1000 W/m$^2$ and 33˚C, respectively. The experimental data consisted of 26 pairs of voltage and current values extracted from the experimental data in (Ma., 2014). In the third case, PMM was applied to estimate the Photowatt-PWP201 PV module parameters, which had 36 series-connected polycrystalline silicon cells under the irradiance and temperature of about 1000 W/m$^2$ and 45˚C, respectively. The experimental data contained 25 pairs of voltage-current values were obtained from (Ma., 2014). The last case referred to the KC200GT PV module, which consisted of 54 series connected polycrystalline silicon cells. The experimental data of the KC200GT PV module were obtained under varied environmental measurements.

### 2.1. Photovoltaic Model and Problem Formulation

In this section, the single-diode model (SDM), the double-diode model (DDM), the photovoltaic module model (PMM), and the problem formulation were represented. The PV cells and modules equivalent circuits can be described by using a current source with diodes connected in series or parallel, one resistor connected in series, and the other resistor connected in parallel.

#### *2.1.1 Single-Diode Model*

The electrical equivalent circuit of SDM for PV cells is illustrated in Figure 1. The SDM consists of a current source, diode, series resistance, and shunt resistance. The current source ($I_{PV}$) is a photogenerated current. The current flowing through the diode ($I_D$) is the diffusion current produced by the majority carrier (Hejri *et al.*, 2014). The series resistance ($R_S$) is the internal resistance that causes voltage drops and power losses when current is flowing, while the shunt resistance ($R_P$) is the resistance due to leakage current in the junction of p-n PV cells. The diffusion current can be calculated as follows:

$$I_D = I_O \left\{ \exp\left[ \frac{(V+IR_S)}{AV_{TH}} \right] - 1 \right\} \quad \text{(Eq. 1)}$$

According to the equivalent circuit in Figure 1, the output current and power of the PV cell in SDM are expressed as follows (Wolf *et al.*, 1977):

$$I = I_{PV} - I_O \left\{ \exp\left[ \frac{(V+IR_S)}{AV_{TH}} \right] - 1 \right\} - \frac{V+IR_S}{R_P} \quad \text{(Eq. 2)}$$

$$P = \left\{ I_{PV} - I_O \left\{ \exp\left[ \frac{(V+IR_S)}{AV_{TH}} \right] - 1 \right\} - \frac{V+IR_S}{R_P} \right\} V \quad \text{(Eq. 3)}$$

In Equations (2) and (3), $I_{PV}$ is the photogenerated current, $I_O$ is the reverse saturation current, A is the ideality factor, $V$ is the PV output voltage, $I$ is the PV output current, and $V_{TH}$ is the thermal voltage. The thermal voltage is depicted by

$$V_{TH} = N_S kT/q \quad \text{(Eq. 4)}$$

where $N_S$ is the number of PV cells connected in series, $k$ is the Boltzmann constant ($k$ = 1.38E-23 J/K), $q$ is the electron charge ($q$ = 1.6E-19 C), and $T$ is the absolute temperature of the PV cell measured in Kelvin.

In the SDM, the five parameters, i.e., $I_{PV}$, $I_O$, $R_S$, $R_P$, and $A$, are considered as unknown parameters to be estimated.

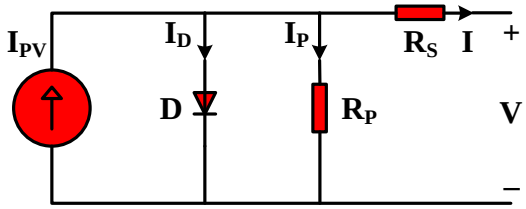


***Figure 1.*** *The equivalent circuit for the single-diode model*

#### *2.1.2 Double-Diode Model*

Unlike the SDM, the DDM has two diodes in the equivalent circuit, as shown in Figure 2. In the DDM, the recombination current is taken into account (Fuchs and Sigmund, 1986). The diffusion current due to majority carrier ($I_{D1}$) and the recombination current due to minority carrier ($I_{D2}$) can be calculated as follows:

$$I_{D1} = I_{O1} \left\{ \exp\left[ \frac{(V+IR_S)}{A_1 V_{TH}} \right] - 1 \right\} \quad \text{(Eq. 5)}$$

$$I_{D2} = I_{O2}\left\{\exp\left[\frac{(V+IR_S)}{A_2V_{TH}}\right] - 1\right\} \quad \text{(Eq. 6)}$$

In Equations (4) and (5), $I_{O1}$ and $I_{O2}$ are respectively reverse saturation currents due to the diffusion and the recombination phenomenon. The diffusion and recombination ideality factors are denoted by $A_1$ and $A_2$, respectively. Thus, the output current is as follows:

$$I = I_{PV} - I_{O1}\left\{\exp\left[\frac{(V+IR_S)}{A_1V_{TH}}\right] - 1\right\} - I_{O2}\left\{\exp\left[\frac{(V+IR_S)}{A_2V_{TH}}\right] - 1\right\} - \frac{V+IR_S}{R_P} \quad \text{(Eq. 7)}$$

The power generated by the PV cell is

$$P = \left\{I_{PV} - I_{O1}\left\{\exp\left[\frac{(V+IR_S)}{A_1V_{TH}}\right] - 1\right\} - I_{O2}\left\{\exp\left[\frac{(V+IR_S)}{A_2V_{TH}}\right] - 1\right\} - \frac{V+IR_S}{R_P}\right\}V \quad \text{(Eq. 8)}$$

Hence, for the DDM, seven unknown parameters must be estimated, i.e., $I_{PV}$, $I_{O1}$, $I_{O2}$, $R_S$, $R_P$, $A_1$, and $A_2$.

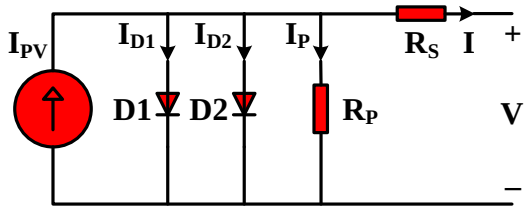


***Figure 2.*** *The equivalent circuit for the double-diode model*

#### *2.1.3 Photovoltaic Module Model*

A PV module is constructed by a sufficient number of PV cells, which are connected in series and parallel to increase the level of output power. Figure 3 presents the equivalent circuit of a PV module. The output current for the PMM is expressed as:

$$I = N_PI_{PV} - N_PI_O\left\{\exp\left[\frac{(V+IR_S(N_S/N_P))}{AV_{TH}N_S}\right] - 1\right\} - \frac{V+IR_S(N_S/N_P)}{R_P(N_S/N_P)} \quad \text{(Eq. 9)}$$

The power output of the PV module is

$$P = \left\{N_PI_{PV} - N_PI_O\left\{\exp\left[\frac{(V+IR_S(N_S/N_P))}{AV_{TH}N_S}\right] - 1\right\} - \frac{V+IR_S(N_S/N_P)}{R_P(N_S/N_P)}\right\}V \quad \text{(Eq. 10)}$$

where $N_P$ denotes the number of PV cells in parallel and $N_S$ is the number of PV cells in series.

For simplicity, Equations. (9) and (10) can be rewritten as

$$I = I_{PVM} - I_{OM}\left\{\exp\left[\frac{(V+IR_{SM})}{A_MV_{TH}}\right] - 1\right\} - \frac{V+IR_{SM}}{R_{PM}} \quad \text{(Eq. 11)}$$

$$P = \left\{I_{PVM} - I_{OM}\left\{\exp\left[\frac{(V+IR_{SM})}{A_MV_{TH}}\right] - 1\right\} - \frac{V+IR_{SM}}{R_{PM}}\right\}V \quad \text{(Eq. 12)}$$

where $I_{PVM} = N_PI_{PV}$, $I_{OM} = N_PI_O$, $R_{SM} = (N_S/N_P)R_S$, $R_{PM} = (N_S/N_P)R_P$, $A_M = N_SA$.

Considering the PMM, five unknown parameters, i.e., $I_{PVM}$, $I_{OM}$, $R_{SM}$, $R_{PM}$, and $A_M$, are estimated according to the *I-V* data of real PV modules.

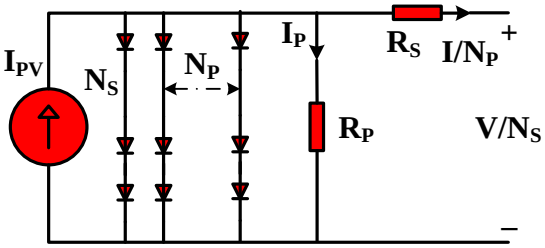


***Figure 3.*** *The equivalent circuit for the photovoltaic module model*

#### *2.1.4 Problem Formulation*

The parameters of PV cells and modules are unknown and variable with temperature and solar irradiance (Chaibi *et al.*, 2019). Thus, the estimation of PV parameters can be represented as an optimization problem, aiming to minimize the difference between the measured and the estimated I-V data. The problem here is defined as an objective function used for the optimization process.

In this study, the *RMSE* method is applied to describe objective functions. The *RMSE* method compares the difference between the measured and the estimated values. The *RMSE* for the photovoltaic problem is expressed as

$$RMSE = \sqrt{\frac{1}{N}\sum_{j=1}^{N}\left[f_j(V,I,\emptyset)\right]^2} \quad \text{(Eq. 13)}$$

$$f_j(V,I,\emptyset) = I_j - I_{estj} \quad \text{(Eq. 14)}$$

where $N$ is the number of measured *I-V* data points, $V$ and $I$ are the measured voltage and current, respectively, and $\emptyset$ is a vector containing the parameters to be calculated.

The difference between the measured

current ($I$) and the estimated current ($I_{est}$) at a point of the I-V curve is an individual error (IE), which is defined by the error function ($f$ ($V$, $I$, ∅)).

The estimated current of the SDM is then formulated as

$$I_{est} = I_{PV} - I_O \left\{ \exp\left[\frac{(V+IR_s)}{AV_{TH}}\right] - 1 \right\} - \frac{V+IR_s}{R_p} \quad \text{(Eq. 15)}$$

For the DDM, the estimated current is

$$I_{est} = I_{PV} - I_{O1} \left\{ \exp\left[\frac{(V+IR_s)}{A_1 V_{TH}}\right] - 1 \right\} - I_{O2} \left\{ \exp\left[\frac{(V+IR_s)}{A_2 V_{TH}}\right] - 1 \right\} - \frac{V+IR_s}{R_p} \quad \text{(Eq. 16)}$$

and the estimated current for the PMM is defined as

$$I_{est} = I_{PVM} - I_{\mathrm{OM}} \left\{ \exp\left[\frac{(V+IR_{SM})}{A_M V_{TH}}\right] - 1 \right\} - \frac{V+IR_{SM}}{R_{PM}} \quad \text{(Eq. 17)}$$

The error functions of the SDM, DDM, and PMM are summarized in Table 1.

### 2.2. Triangular Adaptive Differential Evolution Algorithm

Differential evolution (DE) is a population-based stochastic optimization algorithm. The advantages of the DE are (Ridha *et al.*, 2020): a) it can increase the search space capacity, b) it can find the optimal minimum from a multi-model search, and c) it has a robust mutation scheme. This evolution algorithm utilizes two control parameters, i.e., the mutation factor ($F$) and the crossover rate ($CR$). These two parameters control perturbance and enhance the convergence speed of the computation process. The triangular adaptive differential evolution (TADE) algorithm employs a triangular probability distribution and a population reduction strategy to improve the convergence speed during the evolution process

#### *2.2.1 Initialization and Evaluation*

The first step in the DE optimization process is initialized by randomly generating an initial population as the candidate solutions within defined boundaries. Such candidates must lie inside the feasible lower and upper bounds. If the population size is $NP$ and the dimension of the problem is $D$, the initialization is assigned by

$$x_{i,j}^{(G=1)} = x_{minj} + rand_j\left(x_{maxj} - x_{minj}\right) \quad \text{(Eq. 18)}$$

where $x_{i,j}^{(G=1)}$ is the initial population at generation-1, $x_{minj}$ and $x_{maxj}$ are the lower and upper bounds of the individuals, and $rand_j \in [0, 1]$, $j = 1, 2, \ldots, D$; $i = 1, 2, \ldots, NP$.

Evaluation of the population is employed to find which individuals of the current population will be the best candidates to satisfy the fitness value. The best individuals are selected by using

$$f_{bestj}^{(G)} = f\left(x_{bestj}^{(G)}\right), x_{bestj}^{(G)} \in x_{i,j}^{(G)} \quad \text{(Eq. 19)}$$

#### *2.2.2 Parameter Adaptation*

The control parameters at generation $G$, i.e., $F_i^{(G)}$ and $CR_i^{(G)}$, are adapted by applying triangular probability distribution as follows:

if $rand_j < \tau$

$$\alpha_i^{(G)} = \alpha_{min} + \left[rand_j(\alpha_{max} - \alpha_{min})(\alpha_{mod} - \alpha_{min})\right]^{0.5} \quad \text{(Eq. 20)}$$

otherwise,

$$\alpha_i^{(G)} = \alpha_{max} - \left[\left(1 - rand_j\right)(\alpha_{max} - \alpha_{min})(\alpha_{max} - \alpha_{mod})\right]^{0.5} \quad \text{(Eq. 21)}$$

where,

$$\tau = (\alpha_{mod} - \alpha_{min})/(\alpha_{max} - \alpha_{min}) \quad \text{(Eq. 22)}$$

The probability distribution within [0,1] is determined by using three values, i.e., the lower limit ($\alpha_{min}$), the mode ($\alpha_{mod}$), and the upper limit ($\alpha_{max}$). In this case, $\alpha_{min} \le \alpha_{mod} \le \alpha_{max}$.

#### *2.2.3 Mutation, Crossover, and Selection*

The mutation operation creates mutant individuals $v_{i,j}^{(G)}$ by perturbing randomly selected individuals with the difference between the two other randomly selected individuals. The TADE algorithm adopts the "DE/rand/2" mutation strategy, which is defined as:

$$v_{i,j}^{(G)} = x_{r1,j}^{(G)} + F_i^{(G)}\left(x_{r2,j}^{(G)} - x_{r3,j}^{(G)}\right) + F_i^{(G)}\left(x_{r4,j}^{(G)} - x_{r5,j}^{(G)}\right) \quad \text{(Eq. 23)}$$

In the mutation process, the indices $r1$, $r2$, $r3$, $r4$, and $r5$ are taken randomly from [1, $NP$]. The integers $i$, $r1$, $r2$, $r3$, $r4$, and $r5$, are randomly chosen mutually exclusive integers and must be different from each other and also different from

the base index *i*.

The crossover operation increases the diversity of the mutant individual by generating trial individuals $t_{i,j}^{(G)}$. TADE employs a binomial crossover strategy, which is expressed as:

$$t_{i,j}^{(G)} = \begin{cases} v_{i,j}^{(G)}, if\ \left(rand_j \le CR_i^{(G)}\right) or (j = j_{rand}) \\ x_{i,j}^{(G)}, otherwise \end{cases} \quad \text{(Eq. 24)}$$

where $i$ = 1,2,…,$NP$, $j$ = 1,2,…,$D$, and $j_{rand}$ is a randomly chosen number $\in$ {1,2,…,$D$} that guarantees $t_{i,j}^{(G)}$ to get at least one parameter from $v_{i,j}^{(G)}$.

Finally, the selection process compares the fitness values of the parents and trial individuals. The trial individuals are accepted for the next generation if and only if they have equal or lower fitness value than their parents. The selection operation is represented as:

$$x_{i,j}^{(G+1)} = \begin{cases} t_{i,j}^{(G)}, if\ f\left(t_{i,j}^{(G)}\right) \le f\left(x_{i,j}^{(G)}\right) \\ x_{i,j}^{(G)}, otherwise \end{cases} \quad \text{(Eq. 25)}$$

The best individuals are also selected here as

$$f_{bestj}^{(G+1)} = f\left(x_{bestj}^{(G+1)}\right), x_{bestj}^{(G+1)} \in x_{i,j}^{(G+1)} \quad \text{(Eq. 26)}$$

#### *2.2.4 Population Size Reduction Strategy*

In the DE algorithm, the population size *NP* is constant throughout the evolution process. In order to enhance the convergence rate of the TADE algorithm, a population size reduction strategy is applied to improve the exploitation and exploration processes. The population size reduction strategy is dynamically resizing the population during the evolution process [63]. After each generation *G*, the next-generation population size, $NP^{(G+1)}$, is computed according to the formula:

$$NP^{(G+1)} = round\left[\left(\frac{NP_{min} - NP^{(G)}}{MNFE}\right) NFE + NP^{(G)}\right] \quad \text{(Eq. 27)}$$

where $NP^{(G=1)}$ is the population size at generation 1 is, $NP_{min}$ is the population size at the end evolution process, *NFE* is the number of fitness evaluations, and *MNFE* is the maximum *NFE*. The value of $NP_{min}$ is set to the smallest possible value such that the evolutionary operator is usable. In the case of TADE, $NP_{min}$ is set to 5 due to the "DE/rand/2" mutation strategy in this study requires five individuals. Whenever $NP^{(G+1)} < NP^{(G)}$, the ($NP^{(G)} - NP^{(G+1)}$) individuals with worse fitness values are eliminated from the population. The steps involved in the TADE algorithm are tabulated in Algorithm 1.

## 3. RESULTS AND DISCUSSION:

### 3.1. Estimation of the Parameters of the RTC-France PV Cell

The SDM has five parameters to be determined. The typical design space of photogenerated current ($I_{PV}$), reverse saturation current ($I_O$), ideality factor ($A$), series resistance ($R_S$), and shunt resistance ($R_P$), are chosen to be within the range {0, 1} A, {0, 1} μA, {1, 2}, {0, 0.5} Ω, and {0, 100} Ω, respectively.

For the SDM, the performance results of TADE are compared with those of TLABC (Chen *et al.*, 2018a), IJAYA (Yu *et al.*, 2017a), GWOCS (Long *et al.*, 2020), SATLBO (Yu *et al.*, 2017b), DE, and TADE. The experimental results are obtained after 30 independent runs. Table 2 represents the estimated parameters of six distinct algorithms with their best, worst, mean, and standard deviation values of *RMSE*, respectively. Additionally, the *MNFE* of the convergence processes is also shown in the last row of Table 2. It should be noted that the lower the *RMSE* value, the more precise the estimation results of these PV parameters will be. Moreover, the low standard deviation indicates high reliability, while the mean value of *RMSE* quantifies the average accuracy of the algorithm.

From the results in Table 2, according to their best values of *RMSE*, all SATLBO, TLABC, DE, and TADE achieve the best result (i.e., $9.8602 \times 10^{-04}$), followed by GWOCS (i.e., $9.8607 \times 10^{-04}$) and IJAYA (i.e., $9.8603 \times 10^{-04}$). Both IJAYA and GWOCS obtain slightly higher best values of RMSE. Considering the standard deviation, mean, and worst of *RMSE*, TADE outperforms the other five algorithms. It is also observed that DE and TADE need less *MNFE* compared to different algorithms.

The convergence of the six compared algorithms for the SDM is presented in Figure 4. This figure clearly shows that TADE gives the fastest convergence performance, subsequently DE, GWOCS, IJAYA, TLABC, and SATBLO. The TADE and DE algorithms require less than 10000 and 20000 NFEs to reach their best *RMSE*, respectively. Figure 4 also shows that GWOCS,

TLABC, SATLBO, and IJAYA converge after 20000 number of function evaluations. Both GWOCS and IJAYA perform faster convergence than TLABC and SATLBO. But on the other hand, TLABC and SATLBO can find more accurate *RMSE* values than GWOCS and IJAYA.

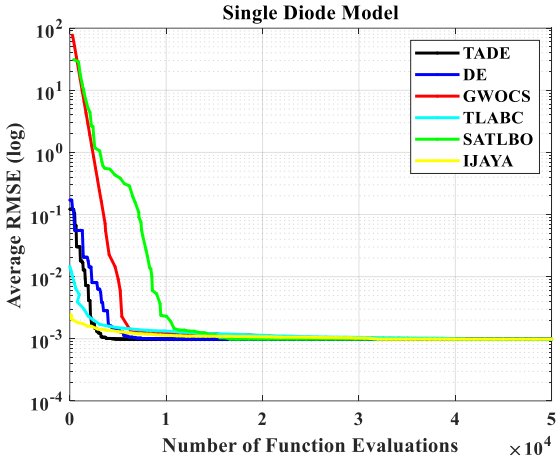


***Figure 4.*** *Convergence processes of the six algorithms for the RTC-France PV cell (SDM)*

Further investigations were carried out to assess the quality of estimated parameters and avoid inaccuracies in the TADE results. The estimated parameter values of the SDM, i.e., $I_{PV}$, $I_O$, $A$, $R_S$, and $R_P$, are entered into Equation (13). For TADE, the values of parameters found are $I_{PV}$ = 0.76077553 A, $I_O$ = 0.32302083x10$^{-06}$ A, $R_S$ = 0.03637709 Ω, $R_P$ = 53.71852506 Ω, and $A$ = 1.48118360. The *RMSE* result is 9.860219x10$^{-04}$, and this matches correctly.

Table 3 lists the *RMSE* value obtained by the TADE compared with other algorithms. It is seen that the *RMSE* value of the TADE algorithm is 9.860219x10$^{-04}$, and this value is as small as most of the algorithms, but in the different significant digits. However, the *RMSE* of the TADE algorithm is smaller than the *RMSE* values of SOS, MSSO, MABC, BLPSO, and GOTLBO. It is also seen that the BLPSO algorithm has the worst result, which the *RMSE* is 11.239x10$^{-04}$.

The individual abs(error) (*IAE*) and *I-V* and *P-V* curves between the measured and the estimated data over the entire voltage range are presented in Table 4 and Figure 5. Table 4 exhibits the measured and estimated currents and powers for the RTC-France PV cell at 26 different working conditions. The individual abs(error) values describe the error between the measured and the calculated data. The small *IAE* indicates the excellent estimated data. As seen in Table 4 and Figure 5(b), the values of individual abs(error) of current are less than 0.003 Ampere, while the values of individual abs(error) of power are less than 0.002 Watt. With these low errors, the measured data gained by TADE fits perfectly into the estimated data of the RTC-France PV cell, as shown in Figure 5(a). Table 4 and Figure 5 show that the PV parameters estimated by TADE have pretty good accuracy.

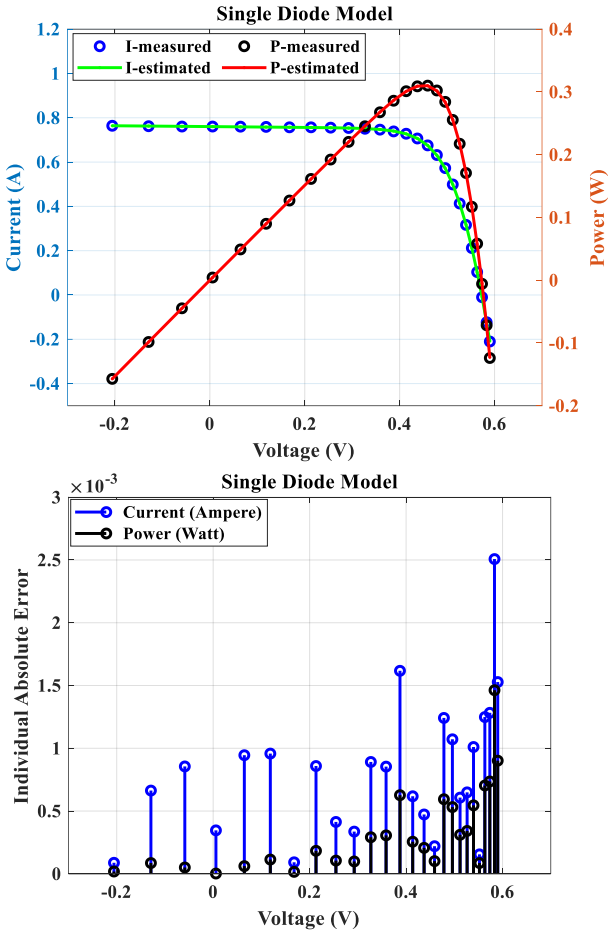


***Figure 5.*** E*stimated and measured data of SDM: (a) I-V/P-V curves, (b) Individual abs(error)*

In the second case, the parameter estimation of the RTC-France PV cell was carried out by using DDM. The DDM has seven parameters to optimize. Increasing the number of parameters will increase the difficulty level of the parameter estimating process. In this case, the typical design space of $I_{PV}$, $I_{o1}$, $I_{o2}$, $A_1$, $A_2$, $R_S$, and $R_P$, are specified within the range {0, 1} A, {0, 1} μA, {0, 1} μA, {1, 2}, {1, 2}, {0, 0.5} Ω, and {0, 100} Ω, respectively. Table 5 shows the estimated parameters and the *RMSE* values. The results acquired by TLABC, IJAYA, GWOCS, SATLBO, DE, and TADE are considered for comparison. Similar to the previous case, the results in Table 5 are obtained after 30 independent runs.

It is seen from Table 5 that the best value of *RMSE* obtained by TADE is as low as

9.8243x10$^{-04}$. The TADE algorithm also performs the best result in terms of the mean, standard deviation, and worst *RMSE*. It verifies that TADE is the most accurate among the algorithms being compared. It is also observed in Table 5 that both DE and TADE require less *MNFE* compared to other algorithms. Tables 2 and 5 show that TADE gives the best precision and reliability on both SDM and DDM on account it outperforms the five different algorithms regarding the best, worst, mean, and standard deviation of the *RMSE*. It is further observed that, as expected, the best *RMSE* values obtained in the DDM case are smaller than the value obtained for the SDM case. It is noted that DDM should estimate the unknown PV parameters more accurately than SDM.

To verify the convergence speed of the TADE algorithm, Figure 6 exhibits the convergence processes of six algorithms. The TADE performs the fastest convergence speed, and then subsequently DE, TLABC, IJAYA, GWOCS, and SATLBO. The TADE needs less than 20000 function evaluations to reach the best *RMSE*, which is the fastest convergence process of all the algorithms, as shown in Table 5 and Figure 6. Other algorithms converge after 20000 NFEs. Figure 6 also demonstrated that DE and TLABC converge much faster than GWOCS and SATLBO. Although it has the slowest convergence speed of all, SATLBO can achieve the best *RMSE* accuracy, which is better than other algorithms, except TADE.

The PV parameters found must fit the *RMSE*. In order to avoid inaccuracies occurred in the results, the estimated parameters can be cross-checked by using Equation (13). The parameters are $I_{PV}$ = 0.76077887 A, $I_{O1}$ = 0.57982851x10$^{-06}$ A, $I_{O2}$ = 0.26238944x10$^{-06}$ A, $R_S$ = 0.03661196 Ω, $R_P$ = 54.88852821 Ω, $A_1$ = 2.06856333, and $A_2$ = 1.46322217. The *RMSE* result is 9.824321x10$^{-04}$. This value matches the *RMSE* value found by the TADE algorithm very well.

A deeper investigation of the DDM of RTC-France PV cell found that the *RMSE* value can be as small as 9.727248x10$^{-04}$ if the search range of $A_1$ is within {1, 3}. It is observed that the corresponding parameters with the *RMSE* of 9.727248x10$^{-04}$ are: $I_{PV}$ = 0.760777759 A, $I_{O1}$ = 6.92409709x10$^{-06}$ A, $I_{O2}$ = 0.260629884x10$^{-06}$ A, $R_S$ = 0.036751455 Ω, $R_P$ = 57.63085158 Ω, $A_1$ = 2.931617412, and $A_2$ = 1.461203635. It is noted that for this *RMSE* value, $A_1$ = 2.931617412 is in the search range of {1, 3}. The estimated *RMSE* values of the DDM for TADE and other recent algorithms from literature are also summarized in Table 6. It is seen that TADE gives the *RMSE* value of 9.824321x10$^{-04}$, and this is the most accurate *RMSE* value among all compared algorithms. These results prove that TADE yields the highest accuracy in estimating the PV parameters of the DDM. By comparing Tables 3 and 6, as expected, it is also observed that TADE performance for DDM is better than for SDM.

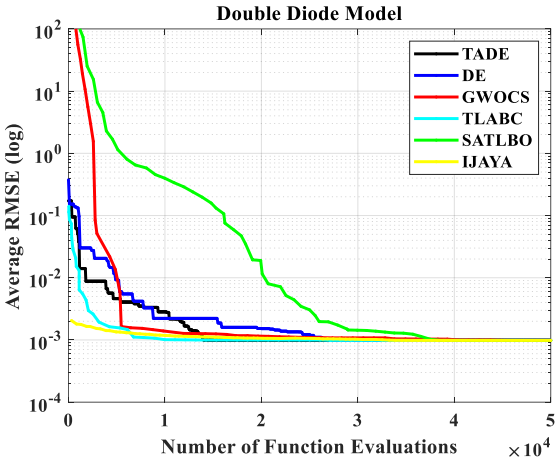


***Figure 6.*** *Convergence processes of the six algorithms for the RTC-France PV cell (DDM)*

Table 7 and Figure 7 show the individual abs(error) values and the *I-V* / *P-V* curves obtained by the TADE algorithm. Table 6 represents the measured and estimated currents and powers for the RTC-France PV cell at 26 different working conditions. As shown in Table 7 and Figure 7(b), the individual abs(error) values are less than 0.003 and 0.02 for current and power, respectively.

It indicates that the estimated data are reasonably very close to the measured data, meaning that TADE has an excellent capability in estimating parameters of DDM. The measured and calculated data are in perfect agreement, as shown in Figure 7(a). These confirm the high accuracy of the TADE algorithm for the PV parameter estimation of DDM.

### 3.2. Estimation of the Parameters of the Photowatt-PWP-201 PV Module

The PMM has five parameters to be determined. The typical range of $I_{PVM}$, $I_{OM}$, $A_M$, $R_{SM}$, and $R_{PM}$ for Photowatt-PWP 201 PV module are defined by {0, 2} A, {0, 50} μA, {1, 50}, {0, 2} Ω, and {0, 2000} Ω, respectively. Similar to the previous cases, estimating the Photowatt-PWP 201 PV module parameters is carried out by using six compared algorithms, i.e., TLABC, IJAYA, GWOCS, SATLBO, DE, and TADE. The results are obtained after 30 independent runs and tabulated in Table 8.

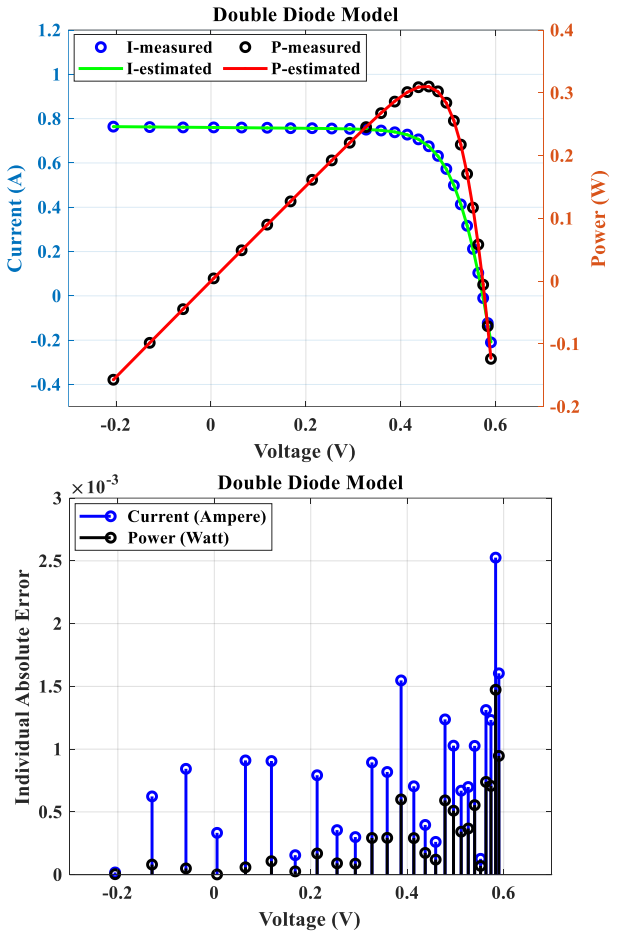


***Figure 7.*** *Estimated and measured data of DDM: (a) I-V/P-V curves, (b) Individual abs(error)*

It is seen from Table 8 that all six algorithms, including IJAYA, SATLBO, TLABC, GWOCS, DE, and TADE, obtain the smallest best value of *RMSE*, which is as low as 2.4251x10$^{-03}$. In terms of the standard deviation, TADE has the best result. Table 8 also shows that TADE obtains the smallest mean and worst values of *RMSE*. Moreover, TADE also requires less *MNFE* compared to IJAYA, SATBLO, TLABC, and GWOCS. Consequently, these prove that TADE can achieve highly accurate and reliable PV parameters on PMM because it outperforms the other five algorithms regarding the best, worst, mean, and *SD* values of *RMSE*. Furthermore, the *RMSE* value is plotted versus the number of function evaluations. In terms of the convergence speed, TADE yields the best performance for estimating the Photowatt-PWP 201 PV module parameters, as shown in Figure 8. All six algorithms achieve the same best *RMSE* values, but TADE performs the fastest convergence, subsequently DE, GWOCS, TLABC, IJAYA, and SATBLO. The simulations show that TADE requires less than 10000 NFEs to meet the best *RMSE* value. This result proves that the TADE algorithm has a speedy convergence performance.

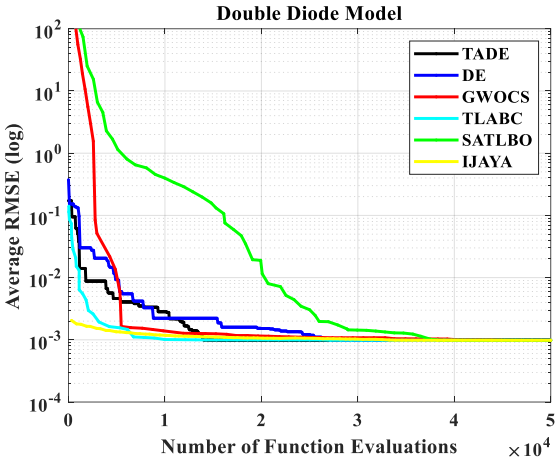


***Figure 8.*** *Convergence curves of the six algorithms for Photowatt PWP-201 PV module (PMM)*

To avoid inaccuracies in the results, the *RMSE* should be cross-checked using estimated values of $I_{PVM}$, $I_{OM}$, $A_M$, $R_{SM,}$ and $R_{PM}$, and measured current and voltage data. For TADE, the values of parameters found are $I_{PVM}$ = 1.03051430 A, $I_{OM}$ = 3.48226301x10$^{-06}$ A, $R_{SM}$ = 1.20127101 Ω, $R_{PM}$ = 981.98228397 Ω, and $A_M$ = 48.64283497. The *RMSE* result is 2.425075x10$^{-03}$ and this value matches correctly. Additionally, the estimated values of *RMSE* obtained by TADE and other recent algorithms from literature are listed in Table 9. Like the SDM case, Table 9 shows that TADE, together with most of the algorithms, acquire the same *RMSE* values in the different significant digits, except the TVACPSO algorithm, which yields the worst *RMSE* value.

Furthermore, Table 10 and Figure 9 are used to confirm the accuracy of TADE. Table 10 shows the measured and estimated currents and powers for the Photowatt PWP-201 PV module at 25 different working conditions. As seen in Table 10 and Figure 9, the individual abs(error), and the measured and estimated *I-V*/*P-V* curves show that they have a remarkable coincidence throughout the entire voltage range. Table 10 and Figure 9(b) show that the values of individual abs(error) of current are less than 0.005 Ampere, while the values of individual abs(error) of power are less than 0.08 Watt. These *IAE* values are small enough for a PV module and demonstrate the accuracy of estimated accuracy. Figure 9(a) shows a good matching between the measured and calculated data with these tiny errors. This observation, once more, verifies the accuracy of the TADE algorithm.

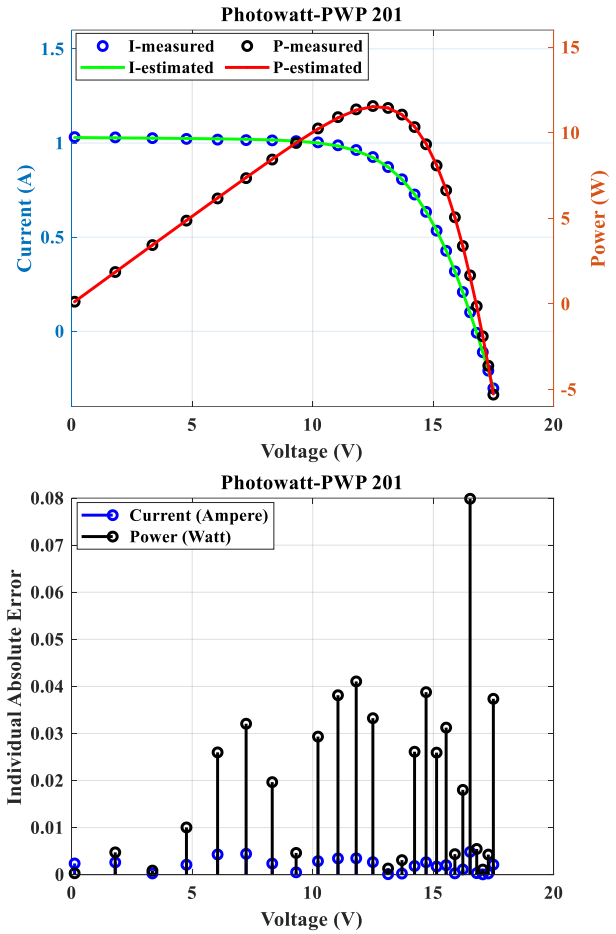


***Figure 9.*** *Estimated and measured data of the Photowatt-PWP-201 PV module: (a) I-V/P-V curves, (b) Individual abs(error)*

Additionally, the Friedman test (Alcalá-Fdez *et al.*, 2009) on SDM, DDM, and PMM PV parameter estimation problems is conducted to show the performance ranking of six algorithms. The results demonstrate that TADE achieves the best average ranking (1.40), followed by DE (2.67), GWOCS (4.63), IJAYA (5.76), TLABC (6.21), and SATLBO (7.93), as shown in Figure 10. According to the comparison results, it is evident that TADE has a high competitive achievement in the accuracy, reliability, and convergence speed of PV parameter estimation against the other algorithms.

### 3.3. Estimation of the Parameters of the KC200GT PV Module

In this section, the TADE algorithm is evaluated using a KC200GT PV module operating under various weather conditions. The KC200GT PV module experimental data at five solar irradiations and three different temperatures are used to investigate the influence of the irradiance and temperature on the performance of the TADE algorithm. These observations are important to estimate PV parameters under partial shading or different weather conditions (Chen *et al.*, 2019a). The typical design range of $I_{PVM}$, $I_{OM}$, $A_M$, $R_{SM}$, and $R_{PM}$ for KC200GT PV module are chosen to be {0, 10} A, {0, 3} μA, {1, 500}, {0, 100} Ω, and {0, 1} Ω, respectively.

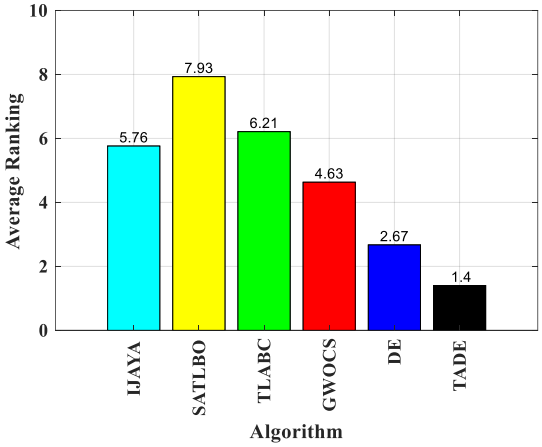


***Figure 10.*** *Friedman test results*

Table 11 presents the PV parameters estimation for the KC200GT PV module at various solar irradiation and temperature levels. Table 11 shows that under different solar irradiation levels and a constant temperature of 25℃, the TADE algorithm can estimate PV parameters with acceptable values of *RMSE*. Similarly, the TADE algorithm also works very well in acquiring the PV parameters under a constant irradiance of 1000 W/m$^2$ and various temperature conditions. From Table 11, it can also be seen that $I_{PVM}$ is increased while $I_{OM}$, $R_{SM}$, $R_{PM}$, and $A_M$ are decreased as the irradiance increasing. On the other hand, it can be found that $I_{PVM}$ is increased while $I_{OM}$, $R_{SM}$, $R_{PM}$, and $A_M$ are fluctuation as the temperature increases.

Again, to find out the accuracy of estimated parameters, the *I-V* and *P-V* curves of the KC200GT PV module at various irradiation and temperature conditions are plotted, as shown in Figures 11 and 12. It can be observed that under different irradiation and temperature conditions, the estimated and measured *I-V* and *P-V* curves are near enough. These results indicate that the TADE algorithm also performs well in estimating the PV module parameters under various irradiances and temperatures.

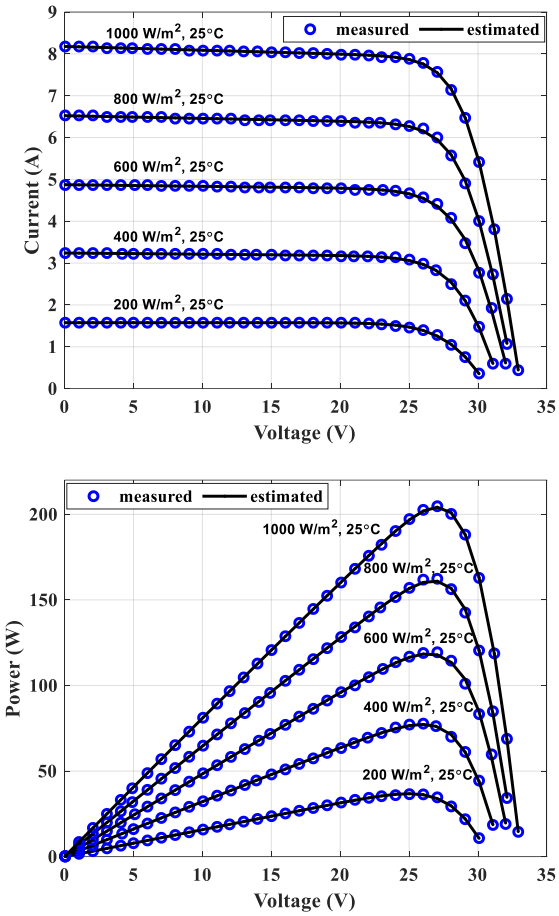


***Figure 11.*** *Estimated and measured data of TADE for the KC200GT PV module under various irradiances*

## 4. CONCLUSIONS:

TADE algorithm was successfully applied for optimally estimating the PV cell and module parameters. The experimental and statistical results showed that the TADE was outperformed most of the algorithms in accuracy, reliability, and convergence speed. Moreover, estimating PV parameters at different irradiance and temperature conditions also proved that the TADE algorithm could get outstanding results. Therefore, the proposed TADE algorithm could be recommended as an accurate and reliable technique for estimating PV cell and module parameters.

## 5. ACKNOWLEDGMENTS:

This study is conducted with financial support from DIPA Fakultas Teknik UNTAN 2021.

## 6. REFERENCES:

1. Abbassi, R; Abbassi, A; Heidari, A. A; Mirjalili, S. (2019). An efficient salp swarm-inspired algorithm for parameters identification of photovoltaic cell models. *Energy Conversion and Management*, 179, 362-372.

2. Alcalá-Fdez, J; Sánchez, L; Garcia, S; del Jesus, M. J; Ventura, S; Garrell, J. M; Otero, J; Romero, C; Bacardit, J; Rivas, V. M; Fernández, J. C; Herrera, F. (2009). KEEL: a software tool to assess evolutionary algorithms for data mining problems. *Soft Computing*, 13, 307-318.

3. Anani, N; Ibrahim, H. (2020). Adjusting the single-diode model parameters of a photovoltaic module with irradiance and temperature. *Energies*, 13(12), 3226.

4. Arabshahi, M. R; Torkaman, H; Keyhani, A. (2020). A method for hybrid extraction of single-diode model parameters of photovoltaics. *Renewable Energy*, 158, 236-252.

5. Beigi, A. M; Maroosi, A. (2018). Parameter identification for solar cells and module using a Hybrid Firefly and Pattern Search Algorithms. *Solar Energy*. 171, 435-446.

6. Bosman, L. B; Leon-Salas, W. D; Hutzel, W; Soto, E. A. (2020). PV system predictive maintenance: challenges, current approaches, and opportunities. *Energies*, 13(6), 1398.

7. Ćalasan, M; Jovanović, D; Rubežić, V; Mujović, S; Đukanović, S. (2019). Estimation of single-diode and two-diode solar cell parameters by using a chaotic optimization approach. *Energies*, 12(21), 4209.

8. Ćalasan, M; Aleem, S. H. E. A; Zobaa, A. F. (2020). On the root mean square error (RMSE) calculation for parameter estimation of photovoltaic models: A novel exact analytical solution based on Lambert W function. *Energy Conversion and Management*, 210, 112716.

9. Chaibi, Y; Allouhi, A; Malvoni, M; Salhi, M; Saadani, R. (2019). Solar irradiance and temperature influence on the photovoltaic cell equivalent-circuit models. *Solar Energy*, 188, 1102-1110.

10. Chen, X; Tianfield, H; Mei, C; Du, W; Liu,

G. (2017). Biogeography-based learning particle swarm optimization. *Soft Computing*, 21, 7519-7541.

11. Chen, Y; Sun, Y; Meng, Z. (2018a). An improved explicit double-diode model of solar cells: Fitness verification and parameter extraction. *Energy Conversion and Management*, 169, 345-358.

12. Chen, X; Xu, B; Mei, C; Ding, Y; Li, K. (2018b) Teaching learning-based artificial bee colony for solar photovoltaic parameter estimation. *Applied Energy*, 212, 1578-1588.

13. Chen, X; Yue, H; Yu, K. (2019a). Perturbed stochastic fractal search for solar PV parameter estimation. *Energy*, 189, 116247.

14. Chen, H; Jiao, S; Heidari, A. A; Wang, M; Chen, X; Zhao, X. (2019b). An opposition-based sine cosine approach with local search for parameter estimation of photovoltaic models. *Energy Conversion and Management*, 195, 927-942.

15. Chen, X; Yu, K. (2019c). Hybridizing cuckoo search algorithm with biogeography-based optimization for estimating photovoltaic model parameters. *Solar Energy*, 180, 192-206.

16. El-Naggar, K. M; AlRashidi, M. R; AlHajri, M. F; Al-Othman; A. K. (2012). Simulated Annealing algorithm for photovoltaic parameters identification. *Solar Energy Conversion and Management*, 86(1), 266-274.

17. Et-torabi, K; Nassar-eddine, I; Obbadi, A; Errami, Y; Rmaily, R; Sahnoun, S; El Fajri, A; Agunaou, M. (2017). Parameters estimation of the single and double diode photovoltaic models using a Gauss-Seidel algorithm and analytical method: A comparative study. *Energy Conversion Management*, 148, 1041-1054.

18. Fuchs; D; Sigmund, H. (1986). Analysis of the current-voltage characteristic of solar cells. *Solid-State Electronics*, 29(8), 791-795.

19. Gao, X; Cui, Y; Hu, J; Xu, G; Yu, Y. (2016). Lambert W-function based exact representation for double diode model of solar cells: Comparison on fitness and parameter extraction. *Energy Conversion and Management*, 127, 443-460.

20. Gao, X; Cui, Y; Hu, J; Xu, G; Wang, Z; Qu, J; Wang, H. (2018). Parameter extraction of solar cell models using improved shuffled complex evolution algorithm. *Energy Conversion and Management,* 157, 460-479.

21. Ghani, F; Rosengarten, G; Duke, M; Carson, J. K. (2014). The numerical calculation of single-diode solar-cell modelling parameters. *Renewable Energy*, 72, 105-112.

22. Gnetchejo, P. J; Essiane, S. N; Ele, P; Wamkeue, R; Wapet, D. M; Ngoffe, S. P. (2019). Important notes on parameter estimation of solar photovoltaic cell. *Energy Conversion and Management*, 197, 111870.

23. Hejri, M; Mokhtari, H; Azizian, M. R; Ghandhari, M; Soder, L. (2014). On the parameter extraction of a five-parameter double-diode model of photovoltaic cells and modules. *IEEE Journal of Photovoltaic*, 4(3), 915-923.

24. Ismail, M. S; Moghavvemi, M; Mahlia, T. M. I. (2013). Characterization of PV panel and global optimization of its model parameters using genetic algorithm. *Energy Conversion and Management*, 73, 10-25.

25. Jordehi, A. R. (2016a). Parameter estimation of solar photovoltaic (PV) cells: A review. *Journal of Renewable and Sustainable Energy*, 61, 354-371.

26. Jordehi, A. R. (2016b). Time varying acceleration coefficients particle swarm optimisation (TVACPSO): A new optimisation algorithm for estimating parameters of PV cells and modules. *Energy Conversion and Management*, 129, 262-274.

27. Kang, T; Yao, J; Jin, M; Yang, S; Duong, T. (2018). A novel improved cuckoo search algorithm for parameter estimation of photovoltaic (PV) models. *Energies*, 11(5), 1060.

28. Khotbehsara, A. Y; Shahhoseini, A. (2018). A fast modeling of the double-diode model for PV modules using combined analytical and numerical approach. *Solar Energy*, 162, 403-409.

29. Li, S; Gong, W; Yan, X; Hu, C; Bai, D; Wang, L; Gao, L. (2019a). Parameter extraction of photovoltaic models using an improved teaching learning-based optimization. *Energy Conversion Management*, 186, 293-305.

30. Li, S; Gong, W; Yan, X; Hu, C; Bai, D; Wang, L. (2019b). Parameter estimation of photovoltaic models with memetic adaptive differential evolution. *Solar Energy*, 190, 465-474.

31. Li, S; Gu, Q; Gong, W; Ning, B. (2020). An enhanced adaptive differential evolution algorithm for parameter extraction of photovoltaic models. *Energy Conversion Management*, 205, 112443.

32. Liao, Z; Chen, Z; Li, S. (2020). Parameters extraction of photovoltaic models using triple-phase teaching learning-based optimization. *IEEE Access*, 8, 69937-69952.

33. Lin, P; Cheng, S; Yeh, W; Chen, Z; Wu, L. (2017). Parameters extraction of solar cell models using a modified simplified swarm optimization algorithm. *Solar Energy*, 144, 594-603.

34. Long, W; Cai, S; Jiao, J; Xu, M; Wu, T. (2020). A new hybrid algorithm based on grey wolf optimizer and cuckoo search for parameter extraction of solar photovoltaic models. *Energy Conversion Management*, 203, 112243.

35. Lun, S; Du, C; Yang, G; Wang, S; Guo, T; Sang, J; Li, J. (2013a). An explicit approximate I-V characteristic model of a solar cell based on padé approximate. *Solar Energy*, 92, 147-159.

36. Lun, S; Du, C; Guo, T; Wang, S; Sang, J; Li, J. (2013b). A new explicit I-V model of a solar cell based on Taylor's series expansion. *Solar Energy*, 94, 221-232.

37. Ma, J. (2014). Optimization Approaches for Parameter Estimation and Maximum Power Point Tracking (MPPT) of Photovoltaic Systems. Ph.D. Thesis, University of Liverpool, Liverpool, UK.

38. Motahhir, S; El Hammoumi, A; El Ghzizal, A. (2018). Photovoltaic system with quantitative comparative between an improved MPPT and existing INC and P&O methods under fast varying of solar irradiation. *Energy Reports*, 4, 341-350.

39. Muhammadsharif, F. F; Hashim, S; Hameed, S. S; Ghoshal, S. K; Abdullah, I. K; Macdonald, J. E, Yahya, M. Y. (2019). Brent's algorithm based new computational approach for accurate determination of single-diode model parameters to simulate solar cells and modules. *Solar Energy*, 193, 782-798.

40. Oliva, D; Ewees, A. A; El Aziz, M. A; Hassanien, A. E; Cisneros, M. P. (2017b). A chaotic improved artificial bee colony for parameter estimation of photovoltaic cells. *Energies*, 10(7), 865.

41. Pillai, D. S; Rajasekar, N. (2018). Metaheuristic algorithms for PV parameter identification: A comprehensive review with an application to threshold setting for fault detection in PV systems. *Renewable and Sustainable Energy Reviews*, 82(Part 3), 3503-3525.

42. Pourmousa, N; Ebrahimi, S. M; Malekzadeh, M; Alizadeh, M. (2019). Parameter estimation of photovoltaic cells using improved Lozi map based chaotic optimization Algorithm. *Solar Energy*, 180, 180-191.

43. Ridha, H. M; Heidari, A. A; Wang, M; Chen, H. (2020). Boosted mutation-based Harris hawks optimizer for parameters identification of single-diode solar cell models. *Energy Conversion Management*, 209, 112660.

44. Rodrigues, E. M. G; Godina, R; Marzband, M; Pouresmaeil, E. (2018). Simulation and comparison of mathematical models of PV cells with growing levels of complexity. *Energies*, 11(11), 2902.

45. Soon, J. J; Low, K. S. (2012). Photovoltaic model identification using particle swarm

optimization with inverse barrier constraint. *IEEE Transactions on Power Electronics*, 27(9), 3975-3983.

46. Wolf, M; Noel, G. T; Stirn, R. J. (1977). Investigation of the double exponential in the current-voltage characteristics of silicon solar cells. *IEEE Transactions on Electron Devices*, 24(4), 419-428.

47. Xiong, G; Zhang, J; Yuan, X; Shi, D; He, Y. (2018). Application of symbiotic organisms search algorithm for parameter extraction of solar cell models. *Applied Sciences*, 8(11), 2155.

48. Xiong, G; Zhang, J; Shi, D; Yuan, X. (2019). Application of supply-demand-based optimization for parameter extraction of solar photovoltaic models. *Complexity*, 2019, 1-22.

49. Yang, X; Gong, W; Wang, L. (2019). Comparative study on parameter extraction of photovoltaic models via differential evolution. *Energy Conversion and Management*, 201, 112113.

50. Yu, K; Liang, J. J; Qu, B. Y; Chen, X; Wang, H. (2017a). Parameters identification of photovoltaic models using an improved JAYA optimization algorithm. *Energy Conversion and Management,* 150, 742-753.

51. Yu, K; Chen, X; Wang, X; Wang, Z. (2017b). Parameters identification of photovoltaic models using self-adaptive teaching-learning-based optimization. *Energy Conversion and Management*, 145, 233-246.

52. Yu, K; Qu, B; Yue, C; Ge, S; Chen, X; Liang, J. (2019). A performance-guided JAYA algorithm for parameters identification of photovoltaic cell and module. *Applied Energy*, 237, 241-257.

53. Zhang, Y; Lin, P; Chen, Z; Cheng, S. (2016). A population classification evolution algorithm for the parameter extraction of solar cell models. International Journal of Photoenergy, 2016, 2174573.

54. Zhu, Y; Lian, W; Lu, L; Kamunyu, P; Yu, C; Dai, S; Hu, Y. (2017). Online modelling and calculation for operating temperature of silicon-based PV bodules based on BP-ANN. *International Journal of Photoenergy*, 2017, 6759295.

***Table 1.*** *Error functions for SDM, DDM, and PMM*

| Model | $f(V, I, \emptyset)$ | $\emptyset$ |
|---|---|---|
| **SDM** | $I - \left(I_{PV} - I_O\left\{\exp\left[\frac{(V+IR_S)}{AV_{TH}}\right] - 1\right\} - \frac{V+IR_S}{R_P}\right)$ | $\{I_{PV}, I_O, R_S, R_P, A\}$ |
| **DDM** | $I - \left(I_{PV} - I_{O1}\left\{\exp\left[\frac{(V+IR_S)}{A_1V_{TH}}\right] - 1\right\} - I_{O2}\left\{\exp\left[\frac{(V+IR_S)}{A_2V_{TH}}\right] - 1\right\} - \frac{V+IR_S}{R_P}\right)$ | $\{I_{PV}, I_{O1}, I_{O2}, R_S, R_P, A_1, A_2\}$ |
| **PMM** | $I - \left(I_{PVM} - I_{\mathrm{OM}}\left\{\exp\left[\frac{(V+IR_{SM})}{A_MV_{TH}}\right] - 1\right\} - \frac{V+IR_{SM}}{R_{PM}}\right)$ | $\{I_{PVM}, I_{OM}, R_{SM}, R_{PM}, A_M\}$ |

***Algorithm 1.*** *Pseudocode of TADE*

1. Input values of *D* and *NP*
2. Define vector $x_{min}$ and $x_{max}$
3. Randomly generate a population of individuals by using Equation (18)
4. **while** termination criteria *NFE* < *MNFE* **do**
5. Evaluate the population to obtain the best candidates that satisfy the *RMSE*
6. Adapt control parameters $F_i^{(G)}$ and $CR_i^{(G)}$ as per Equations (20), (21), and (22)
7. Perform mutation to generate mutant individuals $v_{i,j}^{(G)}$ as per Equation (23)
8. Perform crossover to generate trial individuals $t_{i,j}^{(G)}$ as per Equation (24)
9. Select the best fitness values and individuals for next-generation $x_{i,j}^{(G+1)}$ using Equation (25).
10. Update the population for the next generation with Equation (27)
11. Increase the counter *G* = *G* +1
12. end **while** loop
13. Postprocess results and visualization

***Table 2.*** *Comparison of the RTC-France PV cell (SDM)*

| | IJAYA | SATLBO | TLABC | GWOCS | DE | TADE |
|---|---|---|---|---|---|---|
| $I_{PV}$ (A) | 0.7608 | 0.7608 | 0.7608 | 0.7608 | 0.7608 | 0.7608 |
| $I_O$ (μA) | 0.3228 | 0.3232 | 0.3230 | 0.3219 | 0.3230 | 0.3230 |
| $R_S$ (Ω) | 0.0364 | 0.0363 | 0.0364 | 0.0364 | 0.0364 | 0.0364 |
| $R_P$ (Ω) | 53.7595 | 53.7256 | 53.7164 | 53.6320 | 53.7185 | 53.7185 |
| *A* | 1.4811 | 1.4812 | 1.4812 | 1.4808 | 1.4812 | 1.4812 |
| Best | $9.8603\times10^{-04}$ | $9.8602\times10^{-04}$ | $9.8602\times10^{-04}$ | $9.8607\times10^{-04}$ | $9.8602\times10^{-04}$ | $9.8602\times10^{-04}$ |
| Worst | $1.0622\times10^{-03}$ | $9.9494\times10^{-03}$ | $1.0397\times10^{-03}$ | $9.9095\times10^{-04}$ | $1.5686\times10^{-03}$ | $9.8979\times10^{-04}$ |
| Mean | $9.9204\times10^{-03}$ | $9.8780\times10^{-04}$ | $9.9852\times10^{-04}$ | $9.8874\times10^{-04}$ | $1.1224\times10^{-03}$ | $9.8687\times10^{-04}$ |
| *SD* | $1.4000\times10^{-05}$ | $2.3000\times10^{-06}$ | $1.8602\times10^{-05}$ | $2.4696\times10^{-06}$ | $1.3800\times10^{-04}$ | $1.3448\times10^{-06}$ |
| *MNFE* | 50000 | 50000 | 50000 | 50000 | 20000 | 10000 |

***Table 3.*** *Estimated RMSE of the RTC-France PV cell (SDM) by different algorithms*

| Ref. | Algorithm | RMSE |
|---|---|---|
| Proposed | TADE | $9.860219 \times 10^{-04}$ |
| Liao *et al.*, 2020 | TPTLBO | $9.8602 \times 10^{-04}$ |
| Xiong *et al.*, 2019 | SDO | $9.8602 \times 10^{-04}$ |
| Yu *et al.*, 2019 | PGJAYA | $9.8602 \times 10^{-04}$ |
| Ćalasan *et al.*, 2019 | COA | $9.860221 \times 10^{-04}$ |
| Pourmousa *et al.*, 2019 | ILCOA | $9.86021 \times 10^{-04}$ |
| Li *et al.*, 2019a | ITLBO | $9.8602 \times 10^{-04}$ |
| Li, *et al.*, 2019b | MADE | $9.8602 \times 10^{-04}$ |
| Beigi and Maroosi, 2018 | HFAPS | $9.8602 \times 10^{-04}$ |
| Kang *et al.*, 2018 | ImCSA | $9.8602 \times 10^{-04}$ |
| Gao *et al.*, 2018 | ISCE | $9.860219 \times 10^{-04}$ |
| Xiong *et al.*, 2018 | SOS | $9.8609 \times 10^{-04}$ |
| Chen *et al.*, 2018a | pSFS | $9.8602 \times 10^{-04}$ |
| Lin *et al.*, 2017 | MSSO | $9.8607 \times 10^{-04}$ |
| Chen *et al.*, 2017 | BLPSO | $11.239 \times 10^{-04}$ |
| Oliva *et al.*, 2017 | CIABC | $9.8602 \times 10^{-04}$ |
| Zhang *et al.*, 2016 | PCE | $9.86022 \times 10^{-04}$ |

***Table 4.*** *Estimated results of the RTC-France PV cell (SDM) obtained using TADE*

| Item | Measured | | Estimated *I* | | Estimated *P* | |
|---|---|---|---|---|---|---|
| | ***V* (Volt)** | ***I* (Ampere)** | $I_{est}$ **(Ampere)** | ***IAE*** | $P_{est}$ **(Watt)** | ***IAE*** |
| 1 | -0.2057 | 0.7640 | 0.76408770 | 0.00008770 | -0.15717284 | 0.00001804 |
| 2 | -0.1291 | 0.7620 | 0.76266309 | 0.00066309 | -0.09845980 | 0.00008560 |
| 3 | -0.0588 | 0.7605 | 0.76135531 | 0.00085531 | -0.04476769 | 0.00005029 |
| 4 | 0.0057 | 0.7605 | 0.76015399 | 0.00034601 | 0.00433288 | 0.00000197 |
| 5 | 0.0646 | 0.7600 | 0.75905521 | 0.00094479 | 0.04903497 | 0.00006103 |
| 6 | 0.1185 | 0.7590 | 0.75804234 | 0.00095766 | 0.08982802 | 0.00011348 |
| 7 | 0.1678 | 0.7570 | 0.75709165 | 0.00009165 | 0.12703998 | 0.00001538 |
| 8 | 0.2132 | 0.7570 | 0.75614136 | 0.00085864 | 0.16120934 | 0.00018306 |
| 9 | 0.2545 | 0.7555 | 0.75508687 | 0.00041313 | 0.19216961 | 0.00010514 |
| 10 | 0.2924 | 0.7540 | 0.75366388 | 0.00033612 | 0.22037132 | 0.00009828 |
| 11 | 0.3269 | 0.7505 | 0.75139097 | 0.00089097 | 0.24562971 | 0.00029126 |
| 12 | 0.3585 | 0.7465 | 0.74735385 | 0.00085385 | 0.26792636 | 0.00030611 |
| 13 | 0.3873 | 0.7385 | 0.74011722 | 0.00161722 | 0.28664740 | 0.00062635 |
| 14 | 0.4137 | 0.7280 | 0.72738223 | 0.00061777 | 0.30091803 | 0.00025557 |
| 15 | 0.4373 | 0.7065 | 0.70697265 | 0.00047265 | 0.30915914 | 0.00020669 |
| 16 | 0.4590 | 0.6755 | 0.67528015 | 0.00021985 | 0.30995359 | 0.00010091 |
| 17 | 0.4784 | 0.6320 | 0.63075827 | 0.00124173 | 0.30175476 | 0.00059404 |

| | | | | | | |
|---|---|---|---|---|---|---|
| 18 | 0.4960 | 0.5730 | 0.57192836 | 0.00107164 | 0.28367647 | 0.00053153 |
| 19 | 0.5119 | 0.4990 | 0.49960702 | 0.00060702 | 0.25574883 | 0.00031073 |
| 20 | 0.5265 | 0.4130 | 0.41364879 | 0.00064879 | 0.21778609 | 0.00034159 |
| 21 | 0.5398 | 0.3165 | 0.31751011 | 0.00101011 | 0.17139196 | 0.00054526 |
| 22 | 0.5521 | 0.2120 | 0.21215494 | 0.00015494 | 0.11713074 | 0.00008554 |
| 23 | 0.5633 | 0.1035 | 0.10225131 | 0.00124869 | 0.05759816 | 0.00070339 |
| 24 | 0.5736 | -0.0100 | -0.00871754 | 0.00128246 | -0.00500038 | 0.00073562 |
| 25 | 0.5833 | -0.1230 | -0.12550741 | 0.00250741 | -0.07320847 | 0.00146257 |
| 26 | 0.5900 | -0.2100 | -0.20847233 | 0.00152767 | -0.12299867 | 0.00090133 |
| *RMSE* | | | | | | 0.00098602 |

***Table 5.*** *Comparison of the RTC-France PV cell (DDM)*

| | **IJAYA** | **SATLBO** | **TLABC** | **GWOCS** | **DE** | **TADE** |
|---|---|---|---|---|---|---|
| $I_{PV}$ (A) | 0.7601 | 0.7608 | 0.7608 | 0.76076 | 0.7608 | 0.7608 |
| $I_{O1}$ (μA) | 0.0050 | 0.2509 | 0.4239 | 0.53772 | 0.3756 | 0.5798 |
| $I_{O2}$ (μA) | 0.7509 | 0.5454 | 0.2401 | 0.24855 | 0.2715 | 0.2624 |
| $R_S$ (Ω) | 0.0376 | 0.0366 | 0.0367 | 0.03666 | 0.0366 | 0.0369 |
| $R_P$ (Ω) | 77.8519 | 55.1170 | 54.6680 | 54.7331 | 54.5704 | 54.8885 |
| $A_1$ | 1.2186 | 1.4598 | 1.9075 | 2.0000 | 1.9999 | 2.0685 |
| $A_2$ | 1.6247 | 1.9994 | 1.4567 | 1.4588 | 1.4664 | 1.4632 |
| Best | $9.8293x10^{-04}$ | $9.8280x10^{-04}$ | $9.8415x10^{-04}$ | $9.8334x10^{-04}$ | $9.8344x10^{-04}$ | $9.8243x10^{-04}$ |
| Worst | $1.4055x10^{-03}$ | $1.0470x10^{-03}$ | $1.5048x10^{-03}$ | $1.0017x10^{-03}$ | $1.4490x10^{-03}$ | $9.9664x10^{-04}$ |
| Mean | $1.0269x10^{-03}$ | $9.9811x10^{-04}$ | $1.0555x10^{-03}$ | $9.9411x10^{-04}$ | $1.0150x10^{-03}$ | $9.8730x10^{-04}$ |
| *SD* | $9.8300x10^{-05}$ | $1.9500x10^{-05}$ | $1.5503x10^{-04}$ | $9.5937x10^{-06}$ | $7.8100x10^{-05}$ | $2.4831x10^{-06}$ |
| *MNFE* | 50000 | 50000 | 50000 | 50000 | 30000 | 20000 |

***Table 6.*** *Estimated RMSE of the RTC-France PV cell (DDM) by different algorithms*

| **Ref.** | **Algorithm** | **RMSE** |
|---|---|---|
| Proposed | TADE | $9.824321x10^{-04}$ |
| Liao *et al.*, 2020 | TPTLBO | $9.8248x10^{-04}$ |
| Xiong *et al.*, 2019 | SDO | $9.8250x10^{-04}$ |
| Yu *et al.*, 2019 | PGJAYA | $9.8263x10^{-04}$ |
| Li *et al.*, 2019a | ITLBO | $9.8248x10^{-04}$ |
| Li, *et al.*, 2019b | MADE | $9.8261x10^{-04}$ |
| Beigi and Maroosi, 2018 | HFAPS | $9.8248x10^{-04}$ |
| Kang *et al.*, 2018 | ImCSA | $9.8249x10^{-04}$ |
| Gao *et al.*, 2018 | ISCE | $9.824849x10^{-04}$ |
| Xiong *et al.*, 2018 | SOS | $9.8518x10^{-04}$ |
| Chen *et al.*, 2018a | pSFS | $9.8255x10^{-04}$ |
| Lin *et al.*, 2017 | MSSO | $9.8281x10^{-04}$ |
| Chen *et al.*, 2017 | BLPSO | $11.042x10^{-04}$ |
| Oliva *et al.*, 2017 | CIABC | $9.8262x10^{-04}$ |

| | | |
|---|---|---|
| Zhang *et al.*, 2016 | PCE | $9.8248x10^{-04}$ |

***Table 7.*** *Estimated results of the RTC-France PV cell (DDM) obtained using TADE*

| Item | Measured | | Estimated *I* | | Estimated *P* | |
|---|---|---|---|---|---|---|
| | ***V* (Volt)** | ***I* (Ampere)** | **$I_{est}$ (Ampere)** | **IAE** | **$P_{est}$ (Watt)** | ***IAE*** |
| 1 | -0.2057 | 0.7640 | 0.76401767 | 0.00001767 | -0.15715844 | 0.00000364 |
| 2 | -0.1291 | 0.7620 | 0.76262337 | 0.00062337 | -0.09845468 | 0.00008048 |
| 3 | -0.0588 | 0.7605 | 0.76134325 | 0.00084325 | -0.04476698 | 0.00004958 |
| 4 | 0.0057 | 0.7605 | 0.76016689 | 0.00033311 | 0.00433295 | 0.00000190 |
| 5 | 0.0646 | 0.7600 | 0.75908981 | 0.00091019 | 0.04903720 | 0.00005880 |
| 6 | 0.1185 | 0.7590 | 0.75809445 | 0.00090555 | 0.08983419 | 0.00010731 |
| 7 | 0.1678 | 0.7570 | 0.75715526 | 0.00015526 | 0.12705065 | 0.00002605 |
| 8 | 0.2132 | 0.7570 | 0.75620793 | 0.00079207 | 0.16122353 | 0.00016887 |
| 9 | 0.2545 | 0.7555 | 0.75514501 | 0.00035499 | 0.19218440 | 0.00009035 |
| 10 | 0.2924 | 0.7540 | 0.75370046 | 0.00029954 | 0.22038201 | 0.00008759 |
| 11 | 0.3269 | 0.7505 | 0.75139440 | 0.00089440 | 0.24563083 | 0.00029238 |
| 12 | 0.3585 | 0.7465 | 0.74731819 | 0.00081819 | 0.26791357 | 0.00029332 |
| 13 | 0.3873 | 0.7385 | 0.74004752 | 0.00154752 | 0.28662040 | 0.00059935 |
| 14 | 0.4137 | 0.7280 | 0.72729568 | 0.00070432 | 0.30088222 | 0.00029138 |
| 15 | 0.4373 | 0.7065 | 0.70689623 | 0.00039623 | 0.30912572 | 0.00017327 |
| 16 | 0.4590 | 0.6755 | 0.67523883 | 0.00026117 | 0.30993462 | 0.00011988 |
| 17 | 0.4784 | 0.6320 | 0.63076307 | 0.00123693 | 0.30175705 | 0.00059175 |
| 18 | 0.4960 | 0.5730 | 0.57197238 | 0.00102762 | 0.28369830 | 0.00050970 |
| 19 | 0.5119 | 0.4990 | 0.49966913 | 0.00066913 | 0.25578063 | 0.00034253 |
| 20 | 0.5265 | 0.4130 | 0.41369849 | 0.00069849 | 0.21781226 | 0.00036776 |
| 21 | 0.5398 | 0.3165 | 0.31752601 | 0.00102601 | 0.17140054 | 0.00055384 |
| 22 | 0.5521 | 0.2120 | 0.21212636 | 0.00012636 | 0.11711496 | 0.00006976 |
| 23 | 0.5633 | 0.1035 | 0.10218829 | 0.00131171 | 0.05756266 | 0.00073889 |
| 24 | 0.5736 | -0.0100 | -0.00876745 | 0.00123255 | -0.00502901 | 0.00070699 |
| 25 | 0.5833 | -0.1230 | -0.12552567 | 0.00252567 | -0.07321912 | 0.00147322 |
| 26 | 0.5900 | -0.2100 | -0.20839585 | 0.00160415 | -0.12295355 | 0.00094645 |
| *RMSE* | | | | | | 0.00098243 |

***Table 8.*** *Comparison of the Photowatt-PWP 201 PV module*

| | IJAYA | SATLBO | TLABC | GWOCS | DE | TADE |
|---|---|---|---|---|---|---|
| $I_{PVM}$ (A) | 1.0305 | 1.0305 | 1.0306 | 1.03049 | 1.0305 | 1.0305 |
| $I_{OM}$ (μA) | 3.4703 | 3.4827 | 3.4715 | 3.465 | 3.4823 | 3.4823 |
| $R_{SM}$ (Ω) | 1.2016 | 1.2013 | 1.2017 | 1.2019 | 1.2013 | 1.2013 |
| $R_{PM}$ (Ω) | 977.3752 | 982.4038 | 972.9357 | 982.7566 | 981.9819 | 981.9823 |
| $A_M$ | 48.6298 | 48.6433 | 48.6313 | 48.62367 | 48.6428 | 48.6428 |

| | | | | | | |
|---|---|---|---|---|---|---|
| Best | $2.4251x10^{-03}$ | $2.4251x10^{-03}$ | $2.4251x10^{-03}$ | $2.4251x10^{-03}$ | $2.4251x10^{-03}$ | $2.4251x10^{-03}$ |
| Worst | $2.4393x10^{-03}$ | $2.4291x10^{-03}$ | $2.4458x10^{-03}$ | $2.4275x10^{-03}$ | $2.4384x10^{-03}$ | $2.4268x10^{-03}$ |
| Mean | $2.4251x10^{-03}$ | $2.4254x10^{-03}$ | $2.4265x10^{-03}$ | $2.4261x10^{-03}$ | $2.4259x10^{-03}$ | $2.4251x10^{-03}$ |
| *SD* | $3.7800x10^{-06}$ | $7.4100x10^{-07}$ | $3.9957x10^{-06}$ | $1.1967x10^{-06}$ | $2.7000x10^{-06}$ | $5.2004x10^{-07}$ |
| *MNFE* | 50000 | 50000 | 50000 | 50000 | 10000 | 10000 |

***Table 9.*** *Estimated RMSE of the Photowatt-PWP201 PV module by different algorithms*

| Ref. | Algorithm | RMSE |
|---|---|---|
| proposed | TADE | $2.425075x10^{-03}$ |
| Liao *et al.*, 2020 | TPTLBO | $2.4251x10^{-03}$ |
| Yu *et al.*, 2019 | PGJAYA | $2.425075x10^{-03}$ |
| Li *et al.*, 2019a | ITLBO | $2.4251x10^{-03}$ |
| Li, *et al.*, 2019b | MADE | $2.425x10^{-03}$ |
| Xiong *et al.*, 2018 | SOS | $2.4251x10^{-03}$ |
| Kang *et al.*, 2018 | ImCSA | $2.425x10^{-03}$ |
| Jordehi, 2016b | TVACPSO | $6.9665x10^{-03}$ |

***Table 10.*** *Estimated results of the Photowatt-PWP 201 PV module obtained using TADE*

| Item | Measured | | Estimated *I* | | Estimated *P* | |
|---|---|---|---|---|---|---|
| | ***V* (Volt)** | ***I* (Ampere)** | $I_{est}$ **(Ampere)** | ***IAE*** | $P_{est}$ **(Watt)** | ***IAE*** |
| 1 | 0.1248 | 1.0315 | 1.02911916 | 0.00238084 | 0.12843407 | 0.00029713 |
| 2 | 1.8093 | 1.0300 | 1.02738107 | 0.00261893 | 1.85884058 | 0.00473842 |
| 3 | 3.3511 | 1.0260 | 1.02574180 | 0.00025820 | 3.43736334 | 0.00086526 |
| 4 | 4.7622 | 1.0220 | 1.02410715 | 0.00210715 | 4.87700309 | 0.01003469 |
| 5 | 6.0538 | 1.0180 | 1.02229180 | 0.00429180 | 6.18875013 | 0.02598173 |
| 6 | 7.2364 | 1.0155 | 1.01993068 | 0.00443068 | 7.38062638 | 0.03206218 |
| 7 | 8.3189 | 1.0140 | 1.01636311 | 0.00236311 | 8.45502304 | 0.01965844 |
| 8 | 9.3097 | 1.0100 | 1.01049615 | 0.00049615 | 9.40741602 | 0.00461902 |
| 9 | 10.2163 | 1.0035 | 1.00062897 | 0.00287103 | 10.22272574 | 0.02933131 |
| 10 | 11.0449 | 0.9880 | 0.98454838 | 0.00345162 | 10.87423839 | 0.03812281 |
| 11 | 11.8018 | 0.9630 | 0.95952168 | 0.00347832 | 11.32408292 | 0.04105048 |
| 12 | 12.4929 | 0.9255 | 0.92283882 | 0.00266118 | 11.52893307 | 0.03324588 |
| 13 | 13.1231 | 0.8725 | 0.87259966 | 0.00009966 | 11.45121263 | 0.00130788 |
| 14 | 13.6983 | 0.8075 | 0.80727426 | 0.00022574 | 11.05828504 | 0.00309221 |
| 15 | 14.2221 | 0.7265 | 0.72833648 | 0.00183648 | 10.35847422 | 0.02611857 |
| 16 | 14.6995 | 0.6345 | 0.63713800 | 0.00263800 | 9.36561003 | 0.03877728 |
| 17 | 15.1346 | 0.5345 | 0.53621306 | 0.00171306 | 8.11537022 | 0.02592652 |
| 18 | 15.5311 | 0.4275 | 0.42951132 | 0.00201132 | 6.67078334 | 0.03123809 |
| 19 | 15.8929 | 0.3185 | 0.31877448 | 0.00027448 | 5.06625098 | 0.00436233 |
| 20 | 16.2229 | 0.2085 | 0.20738951 | 0.00111049 | 3.36445923 | 0.01801542 |

| | | | | | | |
|---|---|---|---|---|---|---|
| 21 | 16.5241 | 0.1010 | 0.09616717 | 0.00483283 | 1.58907597 | 0.07985813 |
| 22 | 16.7987 | -0.0080 | -0.00832539 | 0.00032539 | -0.13985566 | 0.00546606 |
| 23 | 17.0499 | -0.1110 | -0.11093648 | 0.00006352 | -1.89145593 | 0.00108297 |
| 24 | 17.2793 | -0.2090 | -0.20924727 | 0.00024727 | -3.61564628 | 0.00427258 |
| 25 | 17.4885 | -0.3030 | -0.30086359 | 0.00213641 | -5.26165284 | 0.03736266 |
| *RMSE* | | | | | | 0.00242507 |

***Table 11.*** *Estimated results for the KC200GT PV module at different irradiance and temperature obtained using TADE*

| | **Irradiance, Temperature** | | | | | | |
|---|---|---|---|---|---|---|---|
| | **200 W/m², 25℃** | **400 W/m², 25℃** | **600 W/m², 25℃** | **800 W/m², 25℃** | **1000 W/m², 25℃** | **1000 W/m², 50℃** | **1000 W/m², 75℃** |
| $I_{PVM}$ (A) | 1.57569399 | 3.24498143 | 4.88010408 | 6.53597163 | 8.19970756 | 8.23783237 | 8.35619048 |
| $I_{OM}$ (μA) | 0.01783577 | 0.00889579 | 0.00751949 | 0.00024648 | 0.00005773 | 2.36019426 | 0.10624394 |
| $R_{SM}$ (Ω) | 65.548458 | 62.590896 | 62.265731 | 53.080513 | 50.274351 | 71.148817 | 49.346298 |
| $R_{PM}$ (Ω) | 0.84520850 | 0.39610901 | 0.32958665 | 0.31117124 | 0.28686157 | 0.14227928 | 0.33271560 |
| $A_M$ | 124077.3595 | 349.256060 | 256.428075 | 153.274461 | 109.561569 | 224.722903 | 101.771266 |
| Best | $7.455108x10^{-03}$ | $1.293504x10^{-02}$ | $2.702622x10^{-02}$ | $2.275030x10^{-02}$ | $1.179859x10^{-02}$ | $6.527374x10^{-02}$ | $3.768100x10^{-02}$ |
| Worst | $7.498053x10^{-03}$ | $1.294912x10^{-02}$ | $2.739434x10^{-02}$ | $2.299584x10^{-02}$ | $1.199074x10^{-02}$ | $6.549381x10^{-02}$ | $3.788584x10^{-02}$ |
| Mean | $7.471488x10^{-03}$ | $1.293808x10^{-02}$ | $2.708569x10^{-02}$ | $2.288880x10^{-02}$ | $1.183797x10^{-02}$ | $6.537953x10^{-02}$ | $3.773224x10^{-02}$ |
| *SD* | $1.303167x10^{-05}$ | $4.587912x10^{-06}$ | $1.004395x10^{-04}$ | $7.942290x10^{-05}$ | $4.985857x10^{-05}$ | $7.861897x10^{-05}$ | $6.353135x10^{-05}$ |
| *MNFE* | 10000 | 10000 | 10000 | 10000 | 10000 | 10000 | 10000 |

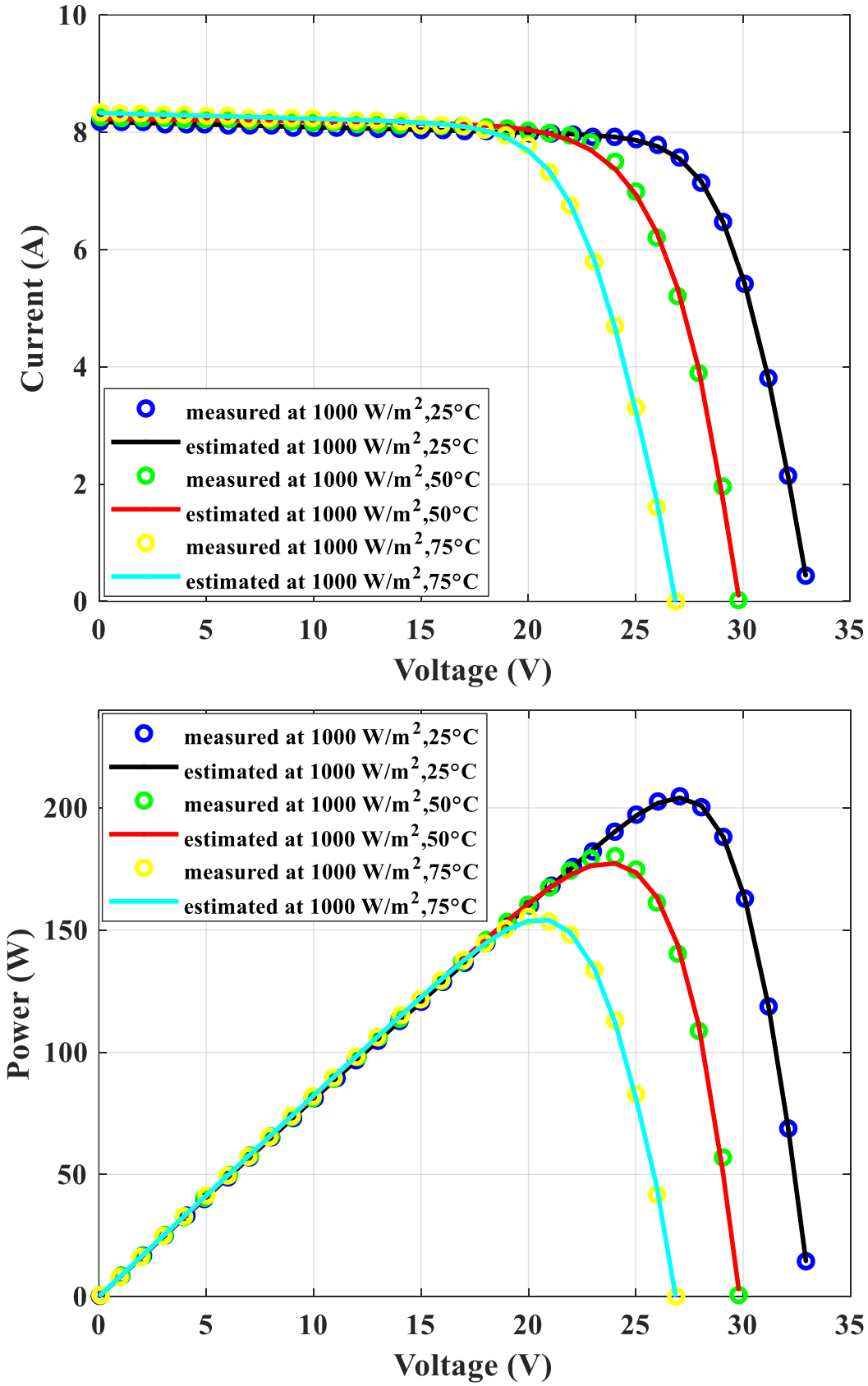


***Figure 12.*** *Estimated and measured data of the KC200GT PV module under various temperature levels*

PERIÓDICO TCHÊ QUÍMICA
ARTIGO ORIGINAL

# SOLUÇÃO ANALÍTICA DA EQUAÇÃO DE SCHRÖDINGER EM COORDENADA BISFÉRICA PARA POTENCIAL MOBIUS SQUARE PLUS MODIFIED YUKAWA USANDO O MÉTODO DE ANÁLISE FUNCIONAL NIKIFOROV UVAROV (NUFA) COM SUAS PROPRIEDADES DE TERMODINÂMICA PARA MOLECULAS DIATÔMICAS

# ANALYTICAL SOLUTION OF SCHRÖDINGER EQUATION IN BISPHERICAL COORDINATE FOR MOBIUS SQUARE PLUS MODIFIED YUKAWA POTENTIAL USING NIKIFOROV UVAROV FUNCTIONAL ANALYSIS (NUFA) METHOD WITH ITS THERMODYNAMICS PROPERTIES FOR DIATOMIC MOLECULES

# SOLUSI ANALITIS PERSAMAAN SCHRÖDINGER DALAM KOORDINAT BISPERICHAL UNTUK POTENSIAL MOBIUS SQUARE PLUS YUKAWA TERMODIFIKASI MENGGUNAKAN METODE NIKIFOROV UVAROV FUNCTIONAL ANALYSIS (NUFA) DENGAN SIFAT TERMODINAMIKANYA UNTUK MOLEKUL DIATOMIK

WIBAWA, Briant Sabathino Harya[1]; SUPARMI, A[2*]; CARI, C[3]

[1] Graduate student at Physics Department, Sebelas Maret University, Indonesia.

[2,3] Faculties member of Physics Department, Sebelas Maret University, Indonesia

** Corresponding author*
*e-mail: soeparmi@staff.uns.ac.id*

Received 24 November 2020; received in revised form 13 February 2021; accepted 23 February 2021

## RESUMO

**Introdução:** A solução analítica da equação de Schrödinger em coordenadas bisféricas tem atraído grande interesse para pesquisadores da física teórica no ramo da física quântica. A energia e a função de onda são soluções da equação de Schrödinger que são muito importantes porque contém todas as informações necessárias sobre o comportamento dos sistemas quânticos. **Objetivo.** Este estudo teve como objetivo obter energia, funções de onda radial e propriedades termodinâmicas para moléculas diatômicas da parte radial da equação de Schrödinger em coordenadas bisféricas para o quadrado de Mobius modificado mais potencial de Yukawa usando o método Nikiforov Uvarov Functional Analysis (NUFA). **Métodos:** O método de separação variável foi aplicado para reduzir a equação de Schrodinger em coordenadas bisféricas à parte radial e parte angular da equação de Schrodinger. A equação de Schrodinger da parte radial em coordenadas bisféricas foi resolvida usando o método Nikiforov Uvarov Functional Analysis (NUFA) para obter a equação de energia e a função de onda radial. Além disso, a função de partição vibracional *Z* foi obtida a partir da equação de energia. A energia vibracional média *U*, o calor vibracional específico *C*, a energia vibracional livre *F* e a entropia vibracional *S* foram obtidas a partir da função de partição vibracional *Z*. **Resultados e Discussão:** Os resultados mostraram que o aumento dos parâmetros de *n* e *α* causou a diminuição da energia, mas o aumento dos parâmetros de *L* e $m_0$ causou o aumento da energia. O número quântico radial n e a faixa de potencial α tiveram o maior efeito nas funções de onda. Os parâmetros $n_{max}$, *T* e *α* tiveram efeito na função de partição vibracional *Z*, energia média vibracional *U*, calor específico vibracional *C*, energia livre vibracional *F* e entropia vibracional *S*. **Conclusões:** A partir dos resultados deste estudo, pode-se concluir que a energia, função de onda radial e propriedades termodinâmicas para moléculas diatômicas foram obtidas usando o método Nikiforov Uvarov Functional Analysis (NUFA).

**Palavras-chave**: *Equação de Schrödinger, coordenada bisférica, quadrado Mobius mais potencial Yukawa modificado, método Nikiforov Uvarov Functional Analysis (NUFA), propriedades termodinâmicas.*

## ABSTRACT

**Background:** The analytical solution of the Schrödinger equation in bispherical coordinates has attracted a great deal of interest for theoretical physics researchers in the branch of quantum physics. The energy and wave function are solutions of the Schrödinger equation which are very important because it contains all necessary information regarding the behavior of quantum systems. **Aim:** This study aimed to obtain energy, radial wave functions and thermodynamic properties for diatomic molecules from the radial part of the Schrödinger equation

in bispherical coordinates for the modified Mobius square plus Yukawa potential using the Nikiforov Uvarov Functional Analysis (NUFA) method. **Methods:** The variable separation method was applied to reduce the Schrodinger equation in bispherical coordinates to the radial part and angular part Schrodinger equation. The Schrodinger equation of the radial part in bispherical coordinates was solved using the Nikiforov Uvarov Functional Analysis (NUFA) method to obtain the energy equation and radial wave function. Furthermore, the vibrational partition function $Z$ was obtained from the energy equation. The vibrational mean energy $U$, vibrational specific heat $C$, vibrational free energy $F$, and vibrational entropy $S$ were obtained from the vibrational partition function $Z$. **Results and Discussion**: The results showed that the increase of parameters of $n$ and $\alpha$ caused the decrease of energy, but the increase of parameters of $L$ and $m_0$ caused the increase of energy. The radial quantum number $n$ and the potential range $\alpha$ had the most effect to the wave functions. The parameters $n_{max}$, $T$, and $\alpha$ had effect to the vibrational partition function $Z$, vibrational mean energy $U$, vibrational specific heat $C$, vibrational free energy $F$, and vibrational entropy $S$. **Conclusions:** From the results of this study, it can be concluded that the energy, radial wave function, and thermodynamic properties for diatomic molecules have been obtained using the Nikiforov Uvarov Functional Analysis (NUFA) method.

**Keywords**: *Schrödinger equation, bispherical coordinate, Mobius square plus modified Yukawa potential, Nikiforov Uvarov Functional Analysis (NUFA) method, Thermodynamics properties*.

## ABSTRAK

**Latar Belakang:** Solusi analitis dari persamaan Schrödinger dalam koordinat bispherical telah menarik banyak minat bagi peneliti fisika teori dalam cabang fisika kuantum. Energi dan fungsi gelombang merupakan solusi dari persamaan Schrödinger yang sangat penting karena mengandung semua informasi yang diperlukan mengenai perilaku sistem kuantum. **Tujuan:** Penelitian ini bertujuan untuk mendapatkan energi, fungsi gelombang radial dan sifat termodinamika untuk molekul diatomik dari persamaan Schrödinger bagian radial dalam koordinat bispherical untuk potensial Mobius square plus Yukawa termodifikasi menggunakan metode Nikiforov Uvarov Functional Analysis (NUFA). **Metode:** Metode pemisahan variabel diterapkan untuk mereduksi persamaan Schrodinger dalam koordinat bispherical menjadi persamaan Schrodinger bagian radial dan bagian sudut. Persamaan Schrodinger bagian radial dalam koordinat bispherical diselesaikan menggunakan metode Nikiforov Uvarov Functional Analysis (NUFA) untuk mendapatkan persamaan energi dan fungsi gelombang radial. Selanjutnya fungsi partisi getaran diperoleh dari persamaan energi. Energi rata-rata getaran, kapasitas panas getaran, energi bebas getaran, dan entropi getaran diperoleh dari fungsi partisi getaran. **Hasil dan Diskusi:** Hasil penelitian menunjukkan bahwa peningkatan parameter $n$ dan $\alpha$ menyebabkan penurunan energi, sedangkan peningkatan parameter $L$ dan $m_0$ menyebabkan peningkatan energi. Bilangan kuantum radial n dan potensial range $\alpha$ memiliki pengaruh paling besar terhadap fungsi gelombang. Parameter $n_{max}$,, $T$, dan $\alpha$ berpengaruh terhadap fungsi partisi getaran $Z$, energi rata-rata getaran $U$, kapasitas panas getaran $C$, energi bebas getaran $F$, dan entropi getaran $S$. **Kesimpulan:** Dari hasil penelitian ini, dapat disimpulkan bahwa energi, fungsi gelombang dan sifat termodinamika untuk molekul diatomik telah diperoleh menggunakan metode Nikiforov Uvarov Functional Analysis (NUFA).

**Kata kunci**: *Persamaan Schrödinger, koordinat bispherical, Potensial Mobius square plus Yukawa termodifikasi, Metode Nikiforov Uvarov Functional Analysis (NUFA), Sifat termodinamika.*

## 1. INTRODUCTION:

There had been increasing interest in theoretical physics to obtain the exact solution of the Schrödinger equation in spacetimes with non-spherical topology. The primary purposes of this interest are to obtain the energy eigenvalue and the wave function in quantum systems. Various methods have been used to solve the Schrödinger equation, such as the factorization method (Dong, 2007), supersymmetry of quantum mechanics (SUSYQM) (Ahmadov *et al*., 2018), Nikiforov–Uvarov method (NU) (Ikot *et al*., 2013), Asymptotic Iteration Method (AIM) (Bayrak and Boztosun, 2007), and Hypergeometry (Hidayat *et al*., 2019).

Various methods used to solve the Schrödinger equation, such as the factorization method (Dong, 2007; Sadeghi, 2007; Mir-Kasimov, 2013), supersymmetry of quantum mechanics (SUSYQM) method (Ahmadov *et al*., 2018; Abu-Shady and Ikot, 2019; Hassanabadi *et al*., 2012), Nikiforov–Uvarov method (NU) (Ikot *et al*., 2013; Berkdemir, 2012; Deta *et al*., 2013), Asymptotic Iteration Method (AIM) (Bayrak and Boztosun, 2007; Rostami and Motavali, 2008; Falaye, 2012), and Hypergeometry method (Hidayat *et al*., 2019; Nurhidayati *et al*., 2018, Dianawati *et al*., 2019).

The factorization method is a type of basic technique that reduces the dynamic equations of a particular system to simple equations that are easier to solve. The basic idea is to consider a pair of first-order differential equations that can be

obtained from certain second-order differential equations with boundary conditions. This method is only applicable to the discrete energy spectrum because the continuous energy levels are not counted. This method can also write down the desired eigenvalues and normalized eigenvalues of a given Hamiltonian without using traditional quantum mechanical treatment methods such as the power series method or by solving second-order differential equations to get the correct solution of the studied quantum system (Dong, 2007).

The Supersymmetry of quantum mechanics (SUSYQM) method is a method for determining the eigenvalues and eigenstates of known analytical potentials that can be solved using the formalism of algebraic operators without having to solve the Schrödinger differential equation with the standard series method. However, operator methods have been applied only to one-dimensional problems and spherical symmetry. Supersymmetry (Dutt *et al*., 1988; Sohnius, 1985), by definition, is the symmetry between fermions and bosons. The supersymmetric field theoretical model consists of a set of quantum and lagrangian fields that show symmetry. Lagrangian is determined through the principle of action, equations of motion, and dynamic behavior of particles (Cari *et al*., 2016).

Nikiforov–Uvarov method (NU) is a method that reduces second-order linear differential equations to general equations in their hypergeometric form. This method has been used successfully to solve many differential equations of quantum mechanics, including the Schrödinger equation, the Dirac Relativistic equation, the Klein - Gordon equation, the Duffin - Kemmer - Petiau equation (DKP), and the spinless-Salpeter equation. The Nikiforov–Uvarov method (NU) is a simpler and more accurate direct method for determining the energy equation and the appropriate wave function (Onyenegecha *et al*., 2020).

The Asymptotic Iteration method (AIM) is a technique for solving analytically and approaching second-order linear differential equations, especially the problem of eigenvalues that often appears in theoretical physics and mathematics. This method can be solved using the asymptotic aspect of the iterative method (Ismail and Saad, 2020).

The Hypergeometric method is that any second-order ordinary differential equation with at most three ordinary singular points can be brought into the hypergeometric differential equation through the appropriate change of the variable. The solution of hypergeometric differential equations includes many of the most interesting mathematical physics special functions. Solutions for hypergeometric differential equations are constructed from hypergeometric series (Mubeen *et al*., 2014).

The method of separation of variables in various coordinate systems was a classic approach to find the exact solutions of the Schrödinger equation that had been widely studied. One such set of coordinates was the bispherical coordinate system.

The variable separation method is one of the most widely used techniques for solving partial differential equations. It is based on the assumption that the solutions of equations are separable; that is, the final solution can be represented as the product of several functions, each of which depends only on one independent variable. If this assumption is wrong, then a clear violation of mathematical principles will be evident from the analysis (Arfken *et al*., 2005). The method of separating variables in various coordinate systems is a classic approach to finding the correct solution of the Schrödinger equation in the form of a partial differential equation. The Schrödinger solution in the coordinate system with the variable separation method produces a partial differential equation that can be separated, namely the radial part equation and the angular part equation. One such set of coordinates is the bispherical system, but it would be said that some of the uses of this coordinate system have been hidden. Although the usual way of separating variables is suitable for some circumstances, there are other ways that are more suitable for certain classes of problems, particularly some of the problems attracting branches of macroscopic field theory, including electrostatics and magnetostatics (Stoy, 1989).

The bispherical coordinates are one of the non-spherical coordinates that have the spheres are designated by $\mu = const$, half-planes by $\phi = const$. The surfaces $\theta = const$ are spindles if $\eta < \frac{\pi}{2}$, a sphere at $\eta = \frac{\pi}{2}$, and apple-shaped surfaces if $\eta > \frac{\pi}{2}$ (Moon and Spencer, 1971). Bispherical coordinates use to solve other types of equations, such as Gegenbauer differential equations, to solve irrotational fluid motion (Deo and Tiwari, 2008). Other applications to solve the Poisson-Boltzmann theory numerically determine the force between spherical colloid particles (Carnie et al., 1994) and investigate heat transfer by conduction from the spheroidal and bispherical oblate surfaces into an infinite stationary medium (Jafari

*et al*., 2019).

On the other hand, the result of the energy equation from the solution of the radial part of the Schrödinger equation in bispherical coordinates can solve many problems, calculations of thermodynamic quantities (Irikura, 2014; Skouteri *et al*., 2016), investigating isotope effects (Lasaga *et al*., 2008), and calculating the equilibrium constant of gas-phase reaction (Buchowiecki, 2012). The route to these calculations is through partition functions. Acquiring a closed-form expression of the partition function is very useful and informative. The vibrational partition function can be calculated by direct summation over all possible vibrational energy levels. Many attempts have been made in the literature to obtain the analytical expression of the partition function for the potential energy function for diatomic and polyatomic molecules in various mathematical methods, such as the cumulant expansion approach (Strekalov, 2004), Poisson summation formula (Jia *et al*., 2017; Song *et al*., 2017), and Wigner-Kirkwood approach (Stratt and Miller, 1977; Korsch, 1979).

Therefore, this study aimed to find the energy spectrum equations and radial wave function equations, and also thermodynamic properties corresponding such as vibrational partition function, vibrational mean energy, vibrational specific heat, vibrational free energy, and vibrational entropy for diatomic molecules affected by the Mobius square plus modified Yukawa potential.

## 2. MATERIALS AND METHODS:

### 2.1 Review Before Bispherical Coordinates

Spherical coordinates are the most common and simple coordinates used to solve the Schrödinger equation to obtain the energy and wave function equations. Spherical coordinates also have symmetrical properties, so they are easier to solve using Schrödinger (Suparmi, 2011; Suparmi *et al*., 2020). Spherical coordinates, also called the polar coordinates of a sphere, are a system of curved coordinates to describe the position on a sphere. The definition $\theta$ is the azimuthal angle in the $xy$ plane of the $x$-axis with $0 \leq \theta < 2\pi$ (denoted $\lambda$ if it is called longitude), $\phi$ is the polar angle (also known as the zenithic angle and colatitude, with $\phi = 90^{\circ} - \delta$ where $\delta$ is the latitude) of the positive $z$-axis with $0 \leq \phi \leq \pi$, and $r$ being the distance (radius) from a point to the origin (Walton, 1967; Arfken, 1985). However, non-spherical coordinates such as bispherical coordinates can also be solved using the Schrödinger equation. The solution to the Schrödinger equation in bispherical coordinates is described in Section 2.3.

### 2.2. Bispherical Coordinate

Cartesian coordinates $(\mu, \eta, \phi)$ relate to bispherical $(\mu, \eta, \phi)$ which have four parameters namely $-\infty \leq \mu \leq +\infty$, $0 \leq \eta \leq \pi$, $0 \leq \phi < 2\pi$, and $0 < a < +\infty$. Cartesian coordinates are related to bispherical coordinates by (Stoy, 1989)

$$x = \frac{a \sin\eta \cos\phi}{\cosh\mu - \cos\eta} \quad \text{(Eq. 1)}$$

$$y = \frac{a \sin\eta \sin\phi}{\cosh\mu - \cos\eta} \quad \text{(Eq. 2)}$$

$$z = \frac{a \sinh\mu}{\cosh\mu - \cos\eta} \quad \text{(Eq. 3)}$$

$$\mu = \tanh^{-1}\left(\frac{2az}{\left(x^2 + y^2 + z^2 + a^2\right)}\right) \quad \text{(Eq. 4)}$$

$$\eta = \tan^{-1}\left(\frac{2a\left(x^2 + y^2\right)^{\frac{1}{2}}}{\left(x^2 + y^2 + z^2 - a^2\right)}\right) \quad \text{(Eq. 5)}$$

$$\phi = \tan^{-1}\left(\frac{y}{x}\right) \quad \text{(Eq. 6)}$$

The two poles $\mu \to \pm\infty$ are located on the $z$ axis at $z = \pm a$. The surface $\mu = \mu_o$ is a sphere of radius $a\ cosech|\mu_o|$ whose center is located on the $z$ axis at $z = a\ coth\mu_o$. The surface $\mu = 0$ is a sphere of infinite radius with center at $x = y = 0, z = \pm\infty$, which includes the central plane $z = 0$.

The surface $\eta = \eta_o$ is a fourth-order surface composed of arcs of circles rotated about the $z$ axis. For $\eta > \frac{1}{2}\pi$ there are sharp points at the poles, for $\eta = \frac{1}{2}\pi$ there is a sphere, and for $\eta < \frac{1}{2}\pi$ there are dimples at the poles. When $\eta = 0$ then $|z| > a$ for the $z$ axis, and when $\eta = \pi$ then $[z] < a$ for the $z$ axis. All surfaces of constant $\eta$ go through the two poles. Surfaces of constant $\phi$ are half-planes whose only boundaries are the $z$ axis (Stoy, 1989).

### 2.3. The solution of the Schrödinger equation in bispherical coordinate

The general time-independent Schrödinger equation with mass $(m)$ and vector potential $V(\mu)$ is given by (Taskin and Koçak, 2010)

$$\left[-\frac{\hbar^2}{2m}\nabla^2 + V(\mu)\right]\psi = E\psi \qquad \text{(Eq. 7)}$$

The square of the distance element in curvilinear coordinate space can be written as a quadratic form in the differentials $dqi$ (Arfken *et al*., 2005)

$$\begin{aligned} ds^2 &= dr\cdot dr = dr^2 = \sum_{ij}\frac{\partial r}{\partial q_i}\cdot\frac{\partial r}{\partial q_j}dq_i dq_j \\ &= g_{11}dq_1{}^2 + g_{12}dq_1dq_2 + g_{13}dq_1dq_3 \\ &+ g_{21}dq_2dq_1 + g_{22}dq_2{}^2 + g_{23}dq_2dq_3 \\ &+ g_{31}dq_3dq_1 + g_{32}dq_3dq_2 + g_{33}dq_3{}^2 = \sum_{ij} g_{ij}dq_i dq_j \end{aligned} \qquad \text{(Eq. 8)}$$

Eq. (8) was called metric or Riemannian. Eq. (8) can be written in a more explicitly form as follows

$$\begin{aligned} g_{ij}(q_1,q_2,q_3) &= \frac{\partial x}{\partial q_i}\frac{\partial x}{\partial q_j} + \frac{\partial y}{\partial q_i}\frac{\partial y}{\partial q_j} \\ &+ \frac{\partial z}{\partial q_i}\frac{\partial z}{\partial q_j} = \frac{\partial r}{\partial q_i}\cdot\frac{\partial r}{\partial q_j} \end{aligned} \qquad \text{(Eq. 9)}$$

By setting the orthogonal coordinate system, $g_{ij} = 0$ for $i \neq j$ and $g_{ii} = h_i^2$ in Eq. (9). Therefore, this will be gotten as follows

$$\begin{aligned} ds^2 &= \left(h_1dq_1\right)^2 + \left(h_2dq_2\right)^2 + \left(h_3dq_3\right)^2 \\ &= \sum_i \left(h_i dq_i\right)^2 \end{aligned} \qquad \text{(Eq. 10)}$$

The scale factor was obtained from Eq. (10) as follows

$$ds_i = h_i dq_i\,,\quad \frac{\partial r}{\partial q_i} = h_i\hat{q}_i \qquad \text{(Eq. 11)}$$

The area and volume elements can be developed from Eq. (11) as follows

$$\begin{aligned} d\sigma_{ij} &= ds_i ds_j = h_i h_j dq_i dq_j \\ ; d\tau &= ds_1 ds_2 ds_3 = h_1h_2h_3dq_1dq_2dq_3 \end{aligned} \qquad \text{(Eq. 12)}$$

By applying Eq. (11), the gradient in curvilinear coordinates can be obtained as follows

$$\begin{aligned} \nabla\psi(q_1,q_2,q_3) &= \hat{q}_1\frac{\partial\psi}{\partial s_1} + \hat{q}_2\frac{\partial\psi}{\partial s_2} + \hat{q}_3\frac{\partial\psi}{\partial s_3} \\ &= \hat{q}_1\frac{1}{h_1}\frac{\partial\psi}{\partial q_1} + \hat{q}_2\frac{1}{h_2}\frac{\partial\psi}{\partial q_2} + \hat{q}_3\frac{1}{h_3}\frac{\partial\psi}{\partial q_3} = \sum_i \hat{q}_i\frac{1}{h_i}\frac{\partial\psi}{\partial q_i} \end{aligned} \qquad \text{(Eq. 13)}$$

By applying Eq. (12), the divergence in curvilinear coordinates can be obtained as follows

$$\begin{aligned} \nabla\cdot V(q_1,q_2,q_3) &= \lim_{\int d\tau\to 0}\frac{\int V\cdot d\sigma}{\int d\tau} \\ &= \frac{1}{h_1h_2h_3}\left[\begin{aligned}&\frac{\partial}{\partial q_1}(V_1h_2h_3) + \frac{\partial}{\partial q_2}(V_2h_3h_1) \\ &+ \frac{\partial}{\partial q_3}(V_3h_1h_2)\end{aligned}\right] \end{aligned} \qquad \text{(Eq. 14)}$$

The laplacian equation was obtained by combining Eq. (13-14) and using $V = \nabla\psi(q_1, q_2, q_3)$ as follows

$$\begin{aligned} \nabla^2\psi = \nabla\cdot\nabla\psi &= \left[\frac{1}{h_1h_2h_3}\frac{\partial}{\partial q_1}\left(\frac{h_2h_3}{h_1}\frac{\partial\psi}{\partial q_1}\right)\right. \\ &\left. + \frac{\partial}{\partial q_2}\left(\frac{h_3h_1}{h_2}\frac{\partial\psi}{\partial q_2}\right) + \frac{\partial}{\partial q_3}\left(\frac{h_1h_2}{h_3}\frac{\partial\psi}{\partial q_3}\right)\right] \end{aligned} \qquad \text{(Eq. 15)}$$

Eq. (1-3) and Eq. (9) were used to obtain the scale factor of the bisperical coordinates with $g_{ii} = h_i^2$ as follows (Gongora and Koo, 1996; Gilbert and Giacomin, 2019)

$$\begin{aligned} h_\mu = h_\eta &= \frac{a}{\cosh\mu - \cos\eta}; \\ h_\phi &= \frac{a\sin\eta}{\cosh\mu - \cos\eta} \end{aligned} \qquad \text{(Eq. 16)}$$

Eq. (16) was inserted into Eq. (15), the operator Laplacian in bispherical coordinate can be obtained as follows

$$\begin{aligned} \nabla^2\psi &= \frac{1}{h_\mu{}^3}\left[\frac{\partial}{\partial\mu}\left(h_\mu\frac{\partial\psi}{\partial\mu}\right)\right. \\ &\left. + \frac{1}{\sin\eta}\frac{\partial}{\partial\eta}\left(h_\mu\sin\eta\frac{\partial\psi}{\partial\eta}\right) + \frac{h_\mu}{\sin^2\eta}\frac{\partial^2\psi}{\partial\phi^2}\right] \end{aligned} \qquad \text{(Eq. 17)}$$

Eq. (17) will be simplified by introducing a new wave function as $\psi = \sqrt{\cosh\mu - \cos\eta}F$ that it was reduced to

$$\begin{aligned} \nabla^2\psi &= \frac{(\cosh\mu - \cos\eta)^{5/2}}{a^2} \\ &\left[\frac{\partial^2F}{\partial\mu^2} + \frac{1}{\sin\eta}\frac{\partial}{\partial\eta}\left(\sin\eta\frac{\partial F}{\partial\eta}\right) + \frac{1}{\sin^2\eta}\frac{\partial^2F}{\partial\phi^2} - \frac{F}{4}\right] \end{aligned} \qquad \text{(Eq. 18)}$$

Eq. (18) and $\psi = \sqrt{\cosh\mu - \cos\eta}F$ were inserted into Eq. (7). Therefore, Eq. (7) can be written as

$$\frac{\left(\cosh\mu-\cos\eta\right)^2}{a^2}\left[-\frac{F}{4}+\frac{\partial^2 F}{\partial\mu^2}+\frac{1}{\sin\eta}\frac{\partial}{\partial\eta}\left(\sin\eta\frac{\partial F}{\partial\eta}\right)+\frac{1}{\sin^2\eta}\frac{\partial^2 F}{\partial\phi^2}\right]-\frac{2m}{\hbar^2}V(\mu)F=-\frac{2m}{\hbar^2}EF \quad \text{(Eq. 19)}$$

Eq. (19) is a Schrödinger equation in bispherical coordinate that can be solved analytically and exactly by introducing variable mass

$$m=\frac{m_0\left(\cosh\mu-\cos\eta\right)^2}{a^2} \quad \text{(Eq. 20)}$$

Where $m_0$ is reduced mass parameter, Eq. (20) was inserted into Eq. (19). Therefore, Eq. (19) can be written as

$$\frac{\partial^2 F}{\partial\mu^2}+\frac{1}{\sin\eta}\frac{\partial}{\partial\eta}\left(\sin\eta\frac{\partial F}{\partial\eta}\right)+\frac{1}{\sin^2\eta}\frac{\partial^2 F}{\partial\phi^2}-\frac{2m_0}{\hbar^2}V(\mu)F-\left(\frac{1}{4}-\frac{2m_0}{\hbar^2}E\right)F=0 \quad \text{(Eq. 21)}$$

Eq. (21) can be solved using the variable separation method and setting the new wave function $F=M(\mu)H(\eta)P(\phi)$ to obtain three parts with different direction as $\mu$, $\eta$, $\phi$ in Schrödinger equation in bispherical coordinates is given as

$$\frac{\partial^2 M}{\partial\mu^2}-\frac{2m_0}{\hbar^2}V(\mu)M-\left(\frac{1}{4}-\frac{2m_0}{\hbar^2}E\right)M=-\frac{1}{H\sin\eta}\frac{\partial}{\partial\eta}\left(\sin\eta\frac{\partial H}{\partial\eta}\right)-\frac{1}{P\sin^2\eta}\frac{\partial^2 P}{\partial\phi^2}=\lambda_1=L(L+1) \quad \text{(Eq. 22)}$$

$$-\frac{\sin\eta}{H}\frac{\partial}{\partial\eta}\left(\sin\eta\frac{\partial H}{\partial\eta}\right)+\frac{2m_0}{\hbar^2}V(\eta)\sin^2\eta-\lambda_1\sin^2\eta=\lambda_2 \quad \text{(Eq. 23)}$$

$$\frac{\partial^2 P}{\partial\phi^2}-\frac{2m_0}{\hbar^2}V(\phi)P=\lambda_2 P \quad \text{(Eq. 24)}$$

The radial part of the Schrödinger equation in bispherical coordinate in Eq. (22) was simplified to

$$\frac{\partial^2 M}{\partial\mu^2}-\frac{2m_0}{\hbar^2}V(\mu)M-E'M=0 \quad \text{(Eq. 25)}$$

With

$$E'=\frac{1+4L(L+1)}{4}-\frac{2m_0}{\hbar^2}E \quad \text{(Eq. 26)}$$

**2.4 Nikiforov Uvarov Functional Analysis (NUFA) Method**

The Schrödinger equation is transformed into a second-order differential equation of the form with an appropriate coordinate transformation of the form (Tezcan and Sever, 2008)

$$\frac{d^2\psi(s)}{ds^2}+\frac{\bar{\tau}(s)}{\sigma(s)}\frac{d\psi(s)}{ds}+\frac{\bar{\sigma}(s)}{\sigma^2(s)}\psi(s)=0 \quad \text{(Eq. 27)}$$

where $\sigma(s)$ and $\bar{\sigma}(s)$ are polynomials at most second degree and $\bar{\tau}(s)$ is a first-degree polynomial. In this method, one defines

$$\pi(s)=\frac{(\sigma'-\bar{\tau})}{2}\pm\sqrt{\left(\frac{\sigma'-\bar{\tau}}{2}\right)^2-\bar{\sigma}+k\sigma} \quad \text{(Eq. 28)}$$

and

$$\lambda=k+\pi'(s) \quad \text{(Eq. 29)}$$

Where $\lambda$ and $k$ are constants. Since the square root in the polynomial $\pi$ in Eq. (28) must be a square then this defines the constant $k$. By Replacing $k$ into Eq. (28), Eq. (28) can be defined as

$$\tau(s)=\bar{\tau}(s)+2\pi(s) \quad \text{(Eq. 30)}$$

Since $\rho(s)>0$ and $\sigma(s)>0$, hence the derivative of $\tau$ should be negative (Tezcan and Sever, 2008), this leads to the choice of the solution. If $\lambda$ in Eq. (29) is

$$\lambda=\lambda_n=-n\tau'-\frac{\left[n(n-1)\sigma''\right]}{2};\ n=0,1,2,.... \quad \text{(Eq. 31)}$$

The hypergeometric type equation has a particular solution with degree $n$. The solution of Eq. (27) can be obtained with the product of two independent parts

$$\psi(s)=\phi(s)y(s) \quad \text{(Eq. 32)}$$

where $y(s)$ can be written as

$$y_n(s) = \frac{B_n}{\rho(s)} \frac{d^n}{ds^n}\left[\sigma^n(s)\rho(s)\right] \quad \text{(Eq. 33)}$$

and $\rho(s)$ should satisfy the condition

$$\frac{d}{ds}\left[\sigma(s)\rho(s)\right] = \tau(s)\rho(s) \quad \text{(Eq. 34)}$$

The other factor is defined as

$$\frac{\phi'(s)}{\phi(s)} = \frac{\pi(s)}{\sigma(s)} \quad \text{(Eq. 35)}$$

The following equation is a general form of the Schrödinger equation written for any invariant shape potential reduces to the second-order differential equation is given as (Tezcan and Sever, 2008)

$$\frac{\partial^2\psi}{\partial s^2} + \frac{\alpha_1 - \alpha_2 s}{s(1-\alpha_3 s)}\frac{\partial\psi}{\partial s} + \frac{-\xi_1 s^2 + \xi_2 s - \xi_3}{s^2(1-\alpha_3 s)^2}\psi = 0 \quad \text{(Eq. 36)}$$

When Eq. (36) was compared with Eq. (27), Eq. (36) was obtained as follows

$$\bar{\tau} = \alpha_1 - \alpha_2 s; \sigma = s(1-\alpha_3 s) \\ ; \bar{\sigma} = -\xi_1 s^2 + \xi_2 s - \xi_3 \quad \text{Eq. 37)}$$

In this work, it had applied the Nikiforov Uvarov Functional Analysis **(**NUFA) method to obtain the energy equation and the wave function in the Schrödinger equation in bispherical coordinates for the Mobius square plus modified Yukawa potential. Then, it also had applied the energy equation results for the Mobius square plus modified Yukawa potential used to calculate the vibrational partition function $Z$, and investigated thermodynamic properties such as the vibrational mean energy $U$, vibrational specific heat $C$, vibrational free energy $F$, and vibrational entropy $S$ for the diatomic molecules CO, NO, $O_2$, and $I_2$.

The radial part of Schrödinger equation in bispherical coordinates for the Mobius square plus modified Yukawa potential was solved using the Nikiforov Uvarov Functional Analysis (NUFA) method to obtain the energy and wave function equations. Then, the vibrational partition function $Z$ was solved using the energy equation. The vibrational mean energy $U$, vibrational specific heat $C$, vibrational free energy $F$, and vibrational entropy $S$ were obtained from the vibrational partition function $Z$.

## 3. RESULTS AND DISCUSSION:

The Mobius square plus modified Yukawa potentials is defined as follows (Boonserm and Visser, 2011; Yukawa, 1935; Antia *et al*., 2015)

$$V = \frac{\left(a + be^{-\alpha r}\right)^2}{\left(c + de^{-\alpha r}\right)^2} + \frac{g + e^{-\alpha r}}{r} \quad \text{(Eq. 38)}$$

Where $a, b, c, d, g$ are the potential parameter and $\alpha$ is the potential range. By setting $r \to \mu$ for the special case in bispherical coordinate in Eq. (38), the form of Mobius square plus modified Yukawa potentials in bispherical coordinate can be obtained as follows

$$V(\mu) = \frac{\left(a + be^{-\alpha\mu}\right)^2}{\left(c + de^{-\alpha\mu}\right)^2} + \frac{g + e^{-\alpha\mu}}{\mu} \quad \text{(Eq. 39)}$$

By setting in Eq. (39)

$$\frac{1}{\mu} = \frac{\alpha c}{c\left(1 + \frac{d}{c}e^{-\alpha\mu}\right)} \quad \text{(Eq. 40)}$$

Where

$$1 + \frac{d}{c} = 0 \to -\frac{d}{c} = 1 \; ; \; z = -\frac{d}{c}e^{-\alpha\mu} \to z = e^{-\alpha\mu} \quad \text{(Eq. 41)}$$

By applying Eq. (40) in Eq. (39), Eq. (39) becomes

$$V(\mu) = \frac{\left(a + be^{-\alpha\mu}\right)^2}{c^2\left(1 + \frac{d}{c}e^{-\alpha\mu}\right)^2} + \frac{\left(g + e^{-\alpha\mu}\right)\alpha c}{c\left(1 + \frac{d}{c}e^{-\alpha\mu}\right)} \\ = \frac{a^2 + 2abe^{-\alpha\mu} + b^2\left(e^{-\alpha\mu}\right)^2}{c^2\left(1 + \frac{d}{c}e^{-\alpha\mu}\right)^2} + \frac{\alpha g + \alpha e^{-\alpha\mu}}{\left(1 + \frac{d}{c}e^{-\alpha\mu}\right)} \quad \text{(Eq. 42)}$$

Eq. (42) was inserted into Eq. (25). Therefore, Eq. (25) can be written as

$$\frac{\partial^2 M}{\partial \mu^2}-\frac{2m_0}{\hbar^2}\left(\frac{a^2+2abe^{-\alpha\mu}+b^2\left(e^{-\alpha\mu}\right)^2}{c^2\left(1+\frac{d}{c}e^{-\alpha\mu}\right)^2}+\frac{\alpha g+\alpha e^{-\alpha\mu}}{\left(1+\frac{d}{c}e^{-\alpha\mu}\right)}\right)M \quad \text{(Eq. 43)}$$

$$-E'M=0$$

by setting new variables as

$$\frac{\partial}{\partial \mu}=\frac{\partial}{\partial z}\frac{\partial z}{\partial \mu}=-\alpha z\frac{\partial}{\partial z};$$

$$\frac{\partial^2}{\partial \mu^2}=-\alpha z\frac{\partial}{\partial z}\left(-\alpha z\frac{\partial}{\partial z}\right)=\alpha^2 z^2\frac{\partial^2}{\partial z^2}+\alpha^2 z\frac{\partial}{\partial z} \quad \text{(Eq. 44)}$$

Eq. (41) and Eq. (44) were inserted into Eq. (43). Therefore, Eq. (43) can be written as

$$\alpha^2 z^2\frac{\partial^2 M}{\partial z^2}+\alpha^2 z\frac{\partial M}{\partial z}$$
$$-\frac{2m_0}{\hbar^2}\left\{\frac{a^2+2abz+b^2z^2}{c^2\left(1-z\right)^2}+\frac{\alpha\left(g+z\right)}{\left(1-z\right)}\right\}M-E'M=0 \quad \text{(Eq. 45)}$$

Eq. (45) was divided by $\alpha^2 z^2$. Therefore, Eq. (45) can be written as

$$\frac{\partial^2 M}{\partial z^2}+\frac{\left(1-z\right)}{z\left(1-z\right)}\frac{\partial M}{\partial z}-\frac{1}{z^2\left(1-z\right)^2}$$
$$\left(\frac{2m_0}{\hbar^2\alpha^2c^2}\begin{Bmatrix}a^2+\alpha c^2 g+\left(2ab+\alpha c^2\right)z\\-\alpha c^2 gz+\left(b^2-\alpha c^2\right)z^2\end{Bmatrix}\right)M \quad \text{(Eq. 46)}$$
$$-\frac{E'\left(1-z\right)^2}{\alpha^2z^2\left(1-z\right)^2}M=0$$

Eq. (46) can be written as

$$\frac{\partial^2 M}{\partial z^2}+\frac{\left(1-z\right)}{z\left(1-z\right)}\frac{\partial M}{\partial z}$$
$$+\frac{1}{z^2\left(1-z\right)^2}\begin{pmatrix}-\left(\frac{E'}{\alpha^2}+\frac{2m_0b^2}{\hbar^2\alpha^2c^2}-\frac{2m_0}{\hbar^2\alpha}\right)z^2\\+\left(\frac{2m_0g}{\hbar^2\alpha}-\frac{2m_0}{\hbar^2\alpha}\right.\\\left.-\frac{4m_0ab}{\hbar^2\alpha^2c^2}+\frac{2E'}{\alpha^2}\right)z\\-\left(\frac{2m_0a^2}{\hbar^2\alpha^2c^2}+\frac{2m_0g}{\hbar^2\alpha}+\frac{E'}{\alpha^2}\right)\end{pmatrix}M=0 \quad \text{(Eq. 47)}$$

By comparing Eq. (36)-(37) and (47). Therefore, Eq. (47) can be written as

$$\frac{\partial^2 M}{\partial z^2}+\frac{1-z}{z(1-z)}\frac{\partial M}{\partial z}+\frac{-\xi_1z^2+\xi_2z-\xi_3}{z^2\left(1-z\right)^2}M=0 \quad \text{(Eq. 48)}$$

With

$$\xi_1=\frac{E'}{\alpha^2}+\frac{2m_0b^2}{\hbar^2\alpha^2c^2}-\frac{2m_0}{\hbar^2\alpha} \quad \text{(Eq. 49a)}$$

$$\xi_2=\frac{2m_0g}{\hbar^2\alpha}-\frac{2m_0}{\hbar^2\alpha}-\frac{4m_0ab}{\hbar^2\alpha^2c^2}+\frac{2E'}{\alpha^2} \quad \text{(Eq. 49b)}$$

$$\xi_3=\frac{2m_0a^2}{\hbar^2\alpha^2c^2}+\frac{2m_0g}{\hbar^2\alpha}+\frac{E'}{\alpha^2} \quad \text{(Eq. 49c)}$$

$$\alpha_1=\alpha_2=\alpha_3=1 \quad \text{(Eq. 49d)}$$

Eq. (48) was multiplied by $z(1-z)$. Therefore, Eq. (48) can be written as

$$z(1-z)\frac{\partial^2 M}{\partial z^2}+(1-z)\frac{\partial M}{\partial z}$$
$$+\frac{-\xi_1z^2+\xi_2z-\xi_3}{z\left(1-z\right)}M=0 \quad \text{(Eq. 50)}$$

By setting a new wave function

$$M(\mathrm{z})=z^{\chi}(1-z)^{\gamma}\,f \quad \text{(Eq. 51)}$$

Substituting Eq. (51) in Eq. (50) gives the following equation

$$z(1-z)f''+\left\{\left(1+2\chi-\left(2\chi+2\gamma+1\right)z\right)f'\right\}$$
$$-\left\{\left((\chi+\gamma)^2-(\chi+\gamma)\right)+\left(\gamma-\xi_1+\chi\right)\right\}f$$
$$+\frac{\left\{\chi\left(\chi-1\right)+\chi-\xi_3\right\}}{z}f \quad \text{(Eq. 52)}$$
$$+\frac{\left\{\gamma\left(\gamma-1\right)+\xi_2-\xi_3-\xi_1\right\}}{(1-z)}f=0$$

To get gauss hypergeometric equation, Eq. (52) was set as follows

$$\xi_2-\xi_3-\xi_1+\gamma\left(\gamma-1\right)=0$$
$$\rightarrow\gamma=\frac{1}{2}\pm\frac{\sqrt{1-4\left(\xi_2-\xi_3-\xi_1\right)}}{2} \quad \text{(Eq. 53a)}$$

$$\chi\left(\chi-1\right)+\chi-\xi_3=0\rightarrow\chi=\pm\sqrt{\xi_3} \quad \text{(Eq. 53b)}$$

Eq. (53a)-(53b) was inserted into Eq. (52). The hypergeometry differential equation can be obtained as follows

$$z(1-z)f''+\left\{\left(1+2\chi-\left(2\chi+2\gamma+1\right)z\right)f'\right\} \\ -\left\{(\chi+\gamma)^2-(\chi+\gamma)+\left(\gamma-\xi_1+\chi\right)\right\}f=0 \quad \text{(Eq. 54)}$$

The energy equation is obtained from the last term in Eq. (54) that $a'=-n$ or $b'=-n$. Eq. (54) was obtained as

$$(\chi+\gamma)^2-(\chi+\gamma)+\left(\gamma-\xi_1+\chi\right)=0 \\ \rightarrow\left((\chi+\gamma)+\sqrt{\xi_1}\right)\left((\chi+\gamma)-\sqrt{\xi_1}\right)=0 \quad \text{(Eq. 55)}$$

With

$$a'=(\chi+\gamma)+\sqrt{\xi_1};b'=(\chi+\gamma)-\sqrt{\xi_1} \\ ;c'=1+2\chi \quad \text{(Eq. 56)}$$

Eq. (56) was chosen $a'=-n$. Therefore, Eq. (56) can be written as

$$-n=\chi+\gamma+\sqrt{\xi_1} \quad \text{(Eq. 57)}$$

Eq. (53a)-(53b) were inserted into Eq. (57). Therefore, Eq. (57) can be written as

$$-n=\sqrt{\xi_3}+\frac{1}{2}+\frac{1}{2}\sqrt{1-4\left(\xi_2-\xi_3-\xi_1\right)}+\sqrt{\xi_1} \quad \text{(Eq. 58)}$$

By substituting Eq. (49a)-(49c) in Eq. (58). Therefore, Eq. (58) can be written as

$$-n=\sqrt{\frac{2m_0a^2}{\hbar^2\alpha^2c^2}+\frac{2m_0g}{\hbar^2\alpha}+\frac{E'}{\alpha^2}} \\ +\frac{1}{2}+\frac{1}{2}\sqrt{1+\frac{16m_0ab}{\hbar^2\alpha^2c^2}+\frac{8m_0a^2}{\hbar^2\alpha^2c^2}+\frac{8m_0b^2}{\hbar^2\alpha^2c^2}} \quad \text{(Eq. 59)} \\ +\sqrt{\frac{E'}{\alpha^2}+\frac{2m_0b^2}{\hbar^2\alpha^2c^2}-\frac{2m_0}{\hbar^2\alpha}}$$

By setting in Eq. (59)

$$p=\frac{2m_0a^2}{\hbar^2\alpha^2c^2}+\frac{2m_0g}{\hbar^2\alpha} \quad \text{(Eq. 60a)}$$

$$o=1+\frac{16m_0ab}{\hbar^2\alpha^2c^2}+\frac{8m_0a^2}{\hbar^2\alpha^2c^2}+\frac{8m_0b^2}{\hbar^2\alpha^2c^2} \quad \text{(Eq. 60b)}$$

$$j=\frac{2m_0b^2}{\hbar^2\alpha^2c^2}-\frac{2m_0}{\hbar^2\alpha} \quad \text{(Eq. 60c)}$$

By substituting Eq. (60a)-(60c) in Eq. (59). Therefore, Eq. (59) can be written as

$$-n=\sqrt{p+\frac{E'}{\alpha^2}}+\frac{1}{2}+\frac{1}{2}\sqrt{o}+\sqrt{\frac{E'}{\alpha^2}+j} \\ \rightarrow\left(-n-\frac{1}{2}-\frac{1}{2}\sqrt{o}\right)-\sqrt{p+\frac{E'}{\alpha^2}}=\sqrt{\frac{E'}{\alpha^2}+j} \quad \text{(Eq. 61)}$$

By using simple mathematical manipulation, Eq. (61) becomes

$$4p+\frac{4}{\alpha^2}E'=\left(\frac{\left(j-p\right)}{\left(n+\frac{1}{2}+\frac{1}{2}\sqrt{o}\right)}-\left(n+\frac{1}{2}+\frac{1}{2}\sqrt{o}\right)\right)^2 \quad \text{(Eq. 62)}$$

By substituting Eq. (26) in Eq. (62). Therefore, Eq. (62) can be written as

$$E=-\frac{\hbar^2\alpha^2}{2m_0}\left(\frac{\left(j-p\right)}{2\left(n+\frac{1}{2}+\frac{1}{2}\sqrt{o}\right)}-\frac{\left(n+\frac{1}{2}+\frac{1}{2}\sqrt{o}\right)}{2}\right)^2 \quad \text{(Eq. 63)} \\ +\frac{\hbar^2\alpha^2}{2m_0}\left(p+\frac{1}{\alpha^2}\left(\frac{1}{4}+L\left(L+1\right)\right)\right)$$

Eq. (63) is the energy spectrum equation of the Mobius square plus modified Yukawa potential in bispherical coordinate. Table 1 showed the reduced mass of CO, NO, $O_2$, and $I_2$ diatomic molecules. The parameters in Table 1 are taken from reference (Bayrak *et al*., 2006). The numerical calculation of the energy spectra of some diatomic molecules, such as CO, NO, $O_2$, and $I_2$, that are influenced by Mobius square plus modified Yukawa potential, for various values of radial and angular quantum numbers, $n, L$, potential range $\alpha$, and mass of the molecules $m_0$ are shown in Figures 1-2.

The general solution of the wave function is

$$M(z)=z^{\chi}(1-z)^{\gamma}\,{}_2F_1\left(a',b',c',z\right) \quad \text{(Eq. 64)}$$

Where

$${}_2F_1\left(a',b',c',z\right)=1+\frac{a'b'}{c'}z \\ +\frac{a'\left(a'+1\right)b'\left(b'+1\right)}{c'\left(c'+1\right)}\frac{z^2}{2!}+.... \quad \text{(Eq. 65)}$$

By substituting Eq. (41), Eq. (56), and Eq. (65) in Eq. (64), the first three lowest un-normalized wave functions of the quantum system for Mobius

square plus modified Yukawa potentials can be obtained as follows

$$M_0 = \left(e^{-\alpha\mu}\right)^{\chi}(1-e^{-\alpha\mu})^{\gamma} \quad \text{(Eq. 66a)}$$

$$M_1 = \left(e^{-\alpha\mu}\right)^{\chi}(1-e^{-\alpha\mu})^{\gamma}\left(1-\frac{(\chi+\gamma)-\sqrt{\xi_1}}{1+2\chi}e^{-\alpha\mu}\right) \quad \text{(Eq. 66b)}$$

$$M_2 = \left(e^{-\alpha\mu}\right)^{\chi}(1-e^{-\alpha\mu})^{\gamma}\left(\begin{array}{l}1-\frac{2\left((\chi+\gamma)-\sqrt{\xi_1}\right)}{1+2\chi}e^{-\alpha\mu}\\ +\frac{\left((\chi+\gamma)-\sqrt{\xi_1}\right)\left((\chi+\gamma)-\sqrt{\xi_1}+1\right)}{(1+2\chi)(2+2\chi)}\left(e^{-\alpha\mu}\right)^2\end{array}\right) \quad \text{(Eq. 66c)}$$

The graphs of the wave function for various values of radial $n$, potential range $\alpha$, and mass of the molecules $m_0$ are shown in Figures 3-4 and un-normalized wave function equations expressed in Eq. 66a-66c.

The vibrational partition function can be calculated by the aid of direct summation over all possible vibrational energy levels,

$$Z = \sum_{n=0}^{n_{\max}} e^{-\beta E} \quad \text{(Eq. 67)}$$

Where $\beta = \frac{1}{kT}$, $k$ denotes the Boltzmann constant, $n_{max}$ is the upper bound vibration quantum number and $T$ is the temperature. By substituting Eq. (63) in Eq. (67), the following expression can be obtained as follows

$$Z = \sum_{n=0}^{n_{\max}} e^{-\beta\left[\begin{array}{l}-\frac{\hbar^2\alpha^2}{2m_0}\left(\frac{(j-p)}{2\left(n+\frac{1}{2}+\frac{1}{2}\sqrt{o}\right)}-\frac{\left(n+\frac{1}{2}+\frac{1}{2}\sqrt{o}\right)^2}{2}\right)\\ +\frac{\hbar^2\alpha^2}{2m_0}\left(p+\frac{1}{\alpha^2}\left(\frac{1}{4}+L(L+1)\right)\right)\end{array}\right]} \quad \text{(Eq. 68)}$$

For a finite summation with the maximum value $n_{max}$, the Poisson summation formula can be written as (Strekalov, 2007)

$$\sum_{n=0}^{n_{max}} f(n) = \frac{1}{2}\left[f(0) - f(n_{max}+1)\right] + \sum_{m=-\infty}^{\infty}\int_0^{n_{max}+1} f(x)e^{-i2\pi mx}dx \quad \text{(Eq. 69)}$$

Under the lowest-order approximation, neglecting the quantum corrections, which include the terms with $m \neq 0$, the summation formula in Eq. (69) can be written becomes

$$\sum_{n=0}^{n_{max}} f(n) = \frac{1}{2}\left[f(0) - f(n_{max}+1)\right] + \int_0^{n_{max}+1} f(x)dx \quad \text{(Eq. 70)}$$

In terms of expression of Eq. (70), Eq. (68) can be rewritten as follows

$$Z = \frac{1}{2}\left[e^{-\beta\left(\omega-\delta k_1^2\right)} - e^{-\beta\left(\omega-\delta k_2^2\right)}\right] + \int_0^{n_{\max}+1} e^{-\beta\left(\omega-\delta\left(\frac{t+x}{2}-\frac{s}{2(t+x)}\right)^2\right)}dx \quad \text{(Eq. 71)}$$

Where $\delta = \frac{\hbar^2\alpha^2}{2m_o}$, $s = j-p$, $t = \frac{1}{2}+\frac{1}{2}\sqrt{o}$, $\omega = \frac{\hbar^2\alpha^2}{2m_o}\left(p+\frac{1}{\alpha^2}\left(\frac{1}{4}+L(L+1)\right)\right)$, $k_1 = \frac{t}{2}-\frac{s}{2t}$, and $k_2 = \frac{t+1+n_{max}}{2}-\frac{s}{2(t+1+n_{max})}$. Introducing a new variable $\rho = \frac{t+x}{2}-\frac{s}{2(t+x)}$ and substituting it into Eq. (71), the integral part in the right-hand side of Eq. (71) can be rewritten as follows

$$\int_0^{n_{\max}+1} e^{-\beta\left(\omega-\delta\left(\frac{t+x}{2}-\frac{s}{2(t+x)}\right)^2\right)}dx = e^{-\beta\omega}\int_{k_1}^{k_2} e^{\beta\delta\rho^2}\left(1+\frac{\rho}{\sqrt{\rho^2+s}}\right)d\rho = \frac{e^{-\beta\omega}}{2}\sqrt{\frac{\pi}{\delta\beta}}\left[\begin{array}{l}-erfi\left(\sqrt{\beta\delta}k_1\right)+erfi\left(\sqrt{\beta\delta}k_2\right)\\ +e^{-\beta\delta s}erfi\left(\sqrt{\beta\delta\left(k_2^2+s\right)}\right)\\ -e^{-\beta\delta s}erfi\left(\sqrt{\beta\delta\left(k_1^2+s\right)}\right)\end{array}\right] \quad \text{(Eq. 72)}$$

The imaginary error function, denoted erfi, is defined as (Pearson, 1983)

$$erfi(z) = -ierf(iz) = \frac{2}{\sqrt{\pi}}\int_0^z e^{t^2}dt \quad \text{(Eq. 73)}$$

Where erf denotes the usual error function. The imaginary error function is implemented in mathematical software Matlab as $erfi\,(z)$.
By substituting Eq. (72) into Eq. (71), the following vibrational partition function $Z$ of the Mobius square plus modified Yukawa potential can be obtained as follows

$$Z=\frac{1}{2}e^{-\beta\omega}\left[e^{\beta\delta k_1^{\,2}}-e^{\beta\delta k_2^{\,2}}+\sqrt{\frac{\pi}{\delta\beta}}\left(-erfi\left(\sqrt{\beta\delta}k_1\right)\right.\right.$$
$$+erfi\left(\sqrt{\beta\delta}k_2\right)+e^{-\beta\delta s}erfi\left(\sqrt{\beta\delta\left(k_2^{\,2}+s\right)}\right) \qquad \text{(Eq. 74)}$$
$$\left.\left.-e^{-\beta\delta s}erfi\left(\sqrt{\beta\delta\left(k_1^{\,2}+s\right)}\right)\right)\right]$$

By using Eq. (74), the vibrational partition function $Z$ is visualized using Matlab as shown in Figures 5-6 for various $n_{max}$, $\alpha$, $T$, and mass of molecule $m_0$.

Having obtained the relevant classical vibrational partition function $Z$ in Eq. (74), The well-known thermodynamic formulas are used to calculate the thermodynamic functions for the diatomic molecules system are as follows :

**(1) Vibrational mean energy $U$**

$$U=-\frac{\partial\ln Z}{\partial\beta}=-\left[e^{\beta\delta k_1^{\,2}}-e^{\beta\delta k_2^{\,2}}+\sqrt{\frac{\pi}{\delta\beta}}\left(-erfi\left(\sqrt{\beta\delta}k_1\right)\right.\right.$$
$$+erfi\left(\sqrt{\beta\delta}k_2\right)+e^{-\beta\delta s}erfi\left(\sqrt{\beta\delta\left(k_2^{\,2}+s\right)}\right)$$
$$\left.\left.-e^{-\beta\delta s}erfi\left(\sqrt{\beta\delta\left(k_1^{\,2}+s\right)}\right)\right)\right]^{-1}\times\left[-\left(\omega-\delta k_1^{\,2}\right)e^{\beta\delta k_1^{\,2}}\right.$$
$$+\left(\omega-\delta k_2^{\,2}\right)e^{\beta\delta k_2^{\,2}}-\sqrt{\frac{\pi}{\delta}}\left(\frac{\omega}{\sqrt{\beta}}+\frac{1}{2\beta^{\frac{3}{2}}}\right)\left(-erfi\left(\sqrt{\beta\delta}k_1\right)\right.$$
$$+erfi\left(\sqrt{\beta\delta}k_2\right)+e^{-\beta\delta s}erfi\left(\sqrt{\beta\delta\left(k_2^{\,2}+s\right)}\right)$$
$$-e^{-\beta\delta s}erfi\left(\sqrt{\beta\delta\left(k_1^{\,2}+s\right)}\right)-\frac{k_1}{\beta}e^{\beta\delta k_1^{\,2}}+\frac{k_2}{\beta}e^{\beta\delta k_2^{\,2}}$$
$$+\frac{s\sqrt{\pi\delta}e^{-\beta\delta s}}{\sqrt{\beta}}erfi\left(\sqrt{\beta\delta\left(k_1^{\,2}+s\right)}\right)-e^{\beta\delta k_1^{\,2}}\left(\frac{\sqrt{k_1^{\,2}+s}}{\beta}\right)$$
$$\left.-\frac{s\sqrt{\pi\delta}e^{-\beta\delta s}}{\sqrt{\beta}}erfi\left(\sqrt{\beta\delta\left(k_2^{\,2}+s\right)}\right)+e^{\beta\delta k_2^{\,2}}\left(\frac{\sqrt{k_2^{\,2}+s}}{\beta}\right)\right] \qquad \text{(Eq. 75)}$$

By using Eq. (75), the vibrational mean energy $U$ is visualized using Matlab as shown in Figures 7-8 for various $n_{max}$, $\alpha$, $T$, and mass of molecule $m_0$.

**(2) Vibrational specific heat $C$**

$$C=\frac{\partial U}{\partial T}=-k\beta^2\frac{\partial U}{\partial\beta}=k\beta^2\left[e^{\beta\delta k_1^{\,2}}-e^{\beta\delta k_2^{\,2}}+\sqrt{\frac{\pi}{\delta\beta}}\right.$$
$$\left(-erfi\left(\sqrt{\beta\delta}k_1\right)+erfi\left(\sqrt{\beta\delta}k_2\right)-e^{-\beta\delta s}erfi\left(\sqrt{\beta\delta\left(k_1^{\,2}+s\right)}\right)\right.$$
$$\left.\left.+e^{-\beta\delta s}erfi\left(\sqrt{\beta\delta\left(k_2^{\,2}+s\right)}\right)\right)\right]^{-1}\times\left[\left(\omega-\delta k_1^{\,2}\right)e^{\beta\delta k_1^{\,2}}\right.$$
$$-\left(\omega-\delta k_2^{\,2}\right)e^{\beta\delta k_2^{\,2}}+\sqrt{\frac{\pi}{\delta}}\left(\frac{\omega^2}{\sqrt{\beta}}+\frac{\omega}{2\beta^{\frac{3}{2}}}+\frac{3}{4\beta^{\frac{5}{2}}}\right)$$
$$\times\left(-erfi\left(\sqrt{\beta\delta}k_1\right)+erfi\left(\sqrt{\beta\delta}k_2\right)-e^{-\beta\delta s}erfi\left(\sqrt{\beta\delta\left(k_1^{\,2}+s\right)}\right)\right.$$
$$\left.+e^{-\beta\delta s}erfi\left(\sqrt{\beta\delta\left(k_2^{\,2}+s\right)}\right)\right)-\sqrt{\frac{\pi}{\delta}}\left(\frac{\omega}{\sqrt{\beta}}+\frac{1}{2\beta^{\frac{3}{2}}}\right)$$
$$\times\left(-\sqrt{\frac{\delta}{\pi\beta}}k_1e^{\beta\delta k_1^{\,2}}+\sqrt{\frac{\delta}{\pi\beta}}k_2e^{\beta\delta k_2^{\,2}}+\delta se^{-\beta\delta s}erfi\left(\sqrt{\beta\delta\left(k_1^{\,2}+s\right)}\right)\right.$$
$$\left.-\sqrt{\frac{k_1^{\,2}+s}{\pi\beta}}e^{\beta\delta k_1^{\,2}}-\delta se^{-\beta\delta s}erfi\left(\sqrt{\beta\delta\left(k_2^{\,2}+s\right)}\right)+\sqrt{\frac{k_2^{\,2}+s}{\pi\beta}}e^{\beta\delta k_2^{\,2}}\right)$$
$$+\frac{k_1\left(\omega-\delta k_1^{\,2}\right)}{\beta}e^{\beta\delta k_1^{\,2}}+\frac{k_1}{\beta^2}e^{\beta\delta k_1^{\,2}}-\frac{k_2\left(\omega-\delta k_2^{\,2}\right)}{\beta}e^{\beta\delta k_2^{\,2}}$$
$$-\frac{k_2}{\beta^2}e^{\beta\delta k_2^{\,2}}-\frac{s\sqrt{\pi\delta}\left(\delta s+\omega\right)e^{-\beta\delta s}}{\sqrt{\beta}}erfi\left(\sqrt{\beta\delta\left(k_1^{\,2}+s\right)}\right)$$
$$-\frac{s\sqrt{\pi\delta}e^{-\beta\delta s}}{2\beta^{\frac{3}{2}}}erfi\left(\sqrt{\beta\delta\left(k_1^{\,2}+s\right)}\right)+\frac{s\delta\sqrt{k_1^{\,2}+s}}{\beta}e^{\beta\delta k_1^{\,2}}$$
$$+\frac{\sqrt{k_1^{\,2}+s}\left(\omega-\delta k_1^{\,2}\right)}{\beta}e^{\beta\delta k_1^{\,2}}+\frac{\sqrt{k_1^{\,2}+s}}{\beta^2}e^{\beta\delta k_1^{\,2}}$$
$$+\frac{s\sqrt{\pi\delta}\left(\delta s+\omega\right)e^{-\beta\delta s}}{\sqrt{\beta}}erfi\left(\sqrt{\beta\delta\left(k_2^{\,2}+s\right)}\right)$$
$$+\frac{s\sqrt{\pi\delta}e^{-\beta\delta s}}{2\beta^{\frac{3}{2}}}erfi\left(\sqrt{\beta\delta\left(k_2^{\,2}+s\right)}\right)-\frac{s\delta\sqrt{k_2^{\,2}+s}}{\beta}e^{\beta\delta k_2^{\,2}}$$
$$\left.-\frac{\sqrt{k_2^{\,2}+s}\left(\omega-\delta k_2^{\,2}\right)}{\beta}e^{\beta\delta k_1^{\,2}}-\frac{\sqrt{k_2^{\,2}+s}}{\beta^2}e^{\beta\delta k_2^{\,2}}\right]$$
$$-k\beta^2\left[e^{\beta\delta k_1^{\,2}}-e^{\beta\delta k_2^{\,2}}+\sqrt{\frac{\pi}{\delta\beta}}\left(-erfi\left(\sqrt{\beta\delta}k_1\right)\right.\right.$$
$$+erfi\left(\sqrt{\beta\delta}k_2\right)-e^{-\beta\delta s}erfi\left(\sqrt{\beta\delta\left(k_1^{\,2}+s\right)}\right)$$
$$\left.\left.+e^{-\beta\delta s}erfi\left(\sqrt{\beta\delta\left(k_2^{\,2}+s\right)}\right)\right)\right]^{-2}\times\left[-\left(\omega-\delta k_1^{\,2}\right)e^{\beta\delta k_1^{\,2}}\right.$$
$$+\left(\omega-\delta k_2^{\,2}\right)e^{\beta\delta k_2^{\,2}}-\sqrt{\frac{\pi}{\delta}}\left(\frac{\omega}{\sqrt{\beta}}+\frac{1}{2\beta^{\frac{3}{2}}}\right)\left(-erfi\left(\sqrt{\beta\delta}k_1\right)\right.$$
$$+erfi\left(\sqrt{\beta\delta}k_2\right)+e^{-\beta\delta s}erfi\left(\sqrt{\beta\delta\left(k_2^{\,2}+s\right)}\right)$$
$$-e^{-\beta\delta s}erfi\left(\sqrt{\beta\delta\left(k_1^{\,2}+s\right)}\right)-\frac{k_1}{\beta}e^{\beta\delta k_1^{\,2}}+\frac{k_2}{\beta}e^{\beta\delta k_2^{\,2}}$$
$$+\frac{s\sqrt{\pi\delta}e^{-\beta\delta s}}{\sqrt{\beta}}erfi\left(\sqrt{\beta\delta\left(k_1^{\,2}+s\right)}\right)-e^{\beta\delta k_1^{\,2}}\left(\frac{\sqrt{k_1^{\,2}+s}}{\beta}\right)$$
$$\left.\left.-\frac{s\sqrt{\pi\delta}e^{-\beta\delta s}}{\sqrt{\beta}}erfi\left(\sqrt{\beta\delta\left(k_2^{\,2}+s\right)}\right)+e^{\beta\delta k_2^{\,2}}\left(\frac{\sqrt{k_2^{\,2}+s}}{\beta}\right)\right]^2\right| \qquad \text{(Eq. 76)}$$

By using Eq. (76), the vibrational specific heat $C$ is visualized using Matlab as shown in Figures 9-10 for various $n_{max}$, $\alpha$, $T$, and mass of molecule $m_0$.

**(3) Vibrational free energy $F$**

$$
\begin{aligned}
F &= -kT\ln Z = -\frac{1}{\beta}\ln Z \\
&= -\frac{1}{\beta}\ln\left[\frac{1}{2}e^{-\beta\omega}\left(e^{\beta\delta k_1^{\,2}} - e^{\beta\delta k_2^{\,2}}\right.\right. \\
&+\sqrt{\frac{\pi}{\delta\beta}}\left(-erfi\left(\sqrt{\beta\delta}k_1\right) + erfi\left(\sqrt{\beta\delta}k_2\right)\right. \\
&+e^{-\beta\delta s}erfi\left(\sqrt{\beta\delta\left(k_2^{\,2}+s\right)}\right) \\
&\left.\left.\left.-e^{-\beta\delta s}erfi\left(\sqrt{\beta\delta\left(k_1^{\,2}+s\right)}\right)\right)\right]
\end{aligned}
\qquad \text{(Eq. 77)}
$$

By using Eq. (77), the vibrational free energy $F$ is visualized using Matlab as shown in Figures 11-12 for various $n_{max}$, $\alpha$, $T$, and mass of molecule $m_0$.

**(4) Vibrational entropy $S$**

$$
\begin{aligned}
S &= k\ln Z + kT\frac{\partial \ln Z}{\partial T} = k\ln Z - k\beta\frac{\partial \ln Z}{\partial \beta} \\
&= k\ln\left[\frac{1}{2}e^{-\beta\omega}\left(e^{\beta\delta k_1^{\,2}} - e^{\beta\delta k_2^{\,2}} + \sqrt{\frac{\pi}{\delta\beta}}\left(-erfi\left(\sqrt{\beta\delta}k_1\right)\right.\right.\right. \\
&+erfi\left(\sqrt{\beta\delta}k_2\right) + e^{-\beta\delta s}erfi\left(\sqrt{\beta\delta\left(k_2^{\,2}+s\right)}\right) \\
&\left.\left.\left.-e^{-\beta\delta s}erfi\left(\sqrt{\beta\delta\left(k_1^{\,2}+s\right)}\right)\right)\right] - k\beta\left[e^{\beta\delta k_1^{\,2}} - e^{\beta\delta k_2^{\,2}}\right. \\
&+\sqrt{\frac{\pi}{\delta\beta}}\left(-erfi\left(\sqrt{\beta\delta}k_1\right) + erfi\left(\sqrt{\beta\delta}k_2\right)\right. \\
&\left.\left.+e^{-\beta\delta s}erfi\left(\sqrt{\beta\delta\left(k_2^{\,2}+s\right)}\right) - e^{-\beta\delta s}erfi\left(\sqrt{\beta\delta\left(k_1^{\,2}+s\right)}\right)\right)\right]^{-1} \\
&\times\left[-\left(\omega-\delta k_1^{\,2}\right)e^{\beta\delta k_1^{\,2}} + \left(\omega-\delta k_2^{\,2}\right)e^{\beta\delta k_2^{\,2}}\right. \\
&-\sqrt{\frac{\pi}{\delta}}\left(\frac{\omega}{\sqrt{\beta}} + \frac{1}{2\beta^{\frac{3}{2}}}\right)\times\left(-erfi\left(\sqrt{\beta\delta}k_1\right) + erfi\left(\sqrt{\beta\delta}k_2\right)\right. \\
&+e^{-\beta\delta s}erfi\left(\sqrt{\beta\delta\left(k_2^{\,2}+s\right)}\right) - e^{-\beta\delta s}erfi\left(\sqrt{\beta\delta\left(k_1^{\,2}+s\right)}\right)\Big) \\
&-\frac{k_1}{\beta}e^{\beta\delta k_1^{\,2}} + \frac{k_2}{\beta}e^{\beta\delta k_2^{\,2}} + \frac{s\sqrt{\pi\delta}e^{-\beta\delta s}}{\sqrt{\beta}}erfi\left(\sqrt{\beta\delta\left(k_1^{\,2}+s\right)}\right) \\
&-e^{\beta\delta k_1^{\,2}}\left(\frac{\sqrt{k_1^{\,2}+s}}{\beta}\right) - \frac{s\sqrt{\pi\delta}e^{-\beta\delta s}}{\sqrt{\beta}}erfi\left(\sqrt{\beta\delta\left(k_2^{\,2}+s\right)}\right) \\
&\left.+e^{\beta\delta k_2^{\,2}}\left(\frac{\sqrt{k_2^{\,2}+s}}{\beta}\right)\right]
\end{aligned}
\qquad \text{(Eq. 78)}
$$

By using Eq. (78), the vibrational entropy $S$ is visualized using Matlab as shown in Figures 13-14 for various $n_{max}$, $\alpha$, $T$, and mass of molecule $m_0$.

**3.1. Numerical result**

Figures 1-2 showed that for four diatomic molecules, CO, NO, $O_2$, and $I_2$, for constant angular quantum number $L$ and potential range $\alpha$, the increase of the value of radial quantum number $n$ causes the decrease of the value of energy spectra, and for the constant values radial quantum number $n$, and potential range $\alpha$, the increase of angular quantum number $L$ causes the increase of the value of energy spectra. Figures 1 and 2 showed that the increase of the value of the potential range $\alpha$ causes the decrease of the energy spectra for constant radial and angular quantum number, $n$. Table 1 and Figures 1-2 showed that the larger of the reduced mass values $m_0$ corresponds to the higher values of the energy spectra. The spectra energy that is shown in Figures 1-2 were numerically calculated energy spectra by using Eq. (63) for the various values of $n$, $L$, $\alpha$, and molecules mass.

Figures 3-4 showed that the radial quantum number $n$ and the potential range $\alpha$ affect the wave functions. The increase of the radial quantum number, $n$, causes the increase of the amplitude of the wave functions. The wavelength of the wave function increases by the increase of the value of the potential range $\alpha$, shown in figures 3-4. Figures 3-4 showed that the CO molecule has a longer wavelength and higher amplitude than others, while $I_2$ molecule has a shorter wavelength and lower amplitude than others.

Figures 5-6 showed that the upper bound vibration quantum number $n_{max}$, temperature $T$, and the potential range $\alpha$ affect the vibrational partition function $Z$. Figures 5-6 showed that the increase of temperature $T$ causes the decrease of the values of vibrational partition function $Z$ for constant the upper bound vibration quantum number $n_{max}$ and potential range $\alpha$. Figures 5-6 showed that the increase of the upper bound vibration quantum number $n_{max}$ and potential range $\alpha$ causes the increase of the values of vibrational partition function $Z$ for constant temperature $T$.

Figures 7-8 showed that the upper bound vibration quantum number $n_{max}$, temperature $T$, and the potential range $\alpha$ affect the vibrational mean energy $U$. Figures 7-8 showed that the increase of temperature $T$ causes the increase of the values of vibrational mean energy $U$ for constant the upper bound vibration quantum

number $n_{max}$ and potential range $\alpha$. Figures 7-8 showed the increase of the upper bound vibration quantum number $n_{max}$ and potential range $\alpha$ causes the decrease of the values of vibrational mean energy $U$ for constant temperature $T$.

Figures 9-10 showed that the upper bound vibration quantum number $n_{max}$, temperature $T$, and the potential range $\alpha$ affect the vibrational specific heat $C$. Figures 9-10 showed that the increase of temperature $T$ causes the decrease of the values of vibrational specific heat $C$ for constant the upper bound vibration quantum number $n_{max}$ and potential range $\alpha$. Figures 9-10 showed the increase of the upper bound vibration quantum number $n_{max}$ and potential range $\alpha$ causes the increase of the values of vibrational specific heat $C$ for constant temperature $T$.

Figures 11-12 showed that the upper bound vibration quantum number $n_{max}$, temperature $T$, and the potential range $\alpha$ affect the vibrational free energy $F$. Figures 11-12 showed that the increase of temperature $T$ causes the increase of the values of vibrational free energy $F$ for constant the upper bound vibration quantum number $n_{max}$ and potential range $\alpha$. Figures 11-12 showed the increase of the upper bound vibration quantum number $n_{max}$ and potential range $\alpha$ causes the decrease of vibrational free energy $F$ for constant temperature $T$.

Figures 13-14 showed that the upper bound vibration quantum number $n_{max}$, temperature $T$, and the potential range $\alpha$ affect the vibrational entropy $S$. Figures 13-14 showed that the increase of temperature $T$ causes the increase of the values of vibrational entropy $S$ for constant the upper bound vibration quantum number $n_{max}$ and potential range $\alpha$. Figures 13-14 showed the increase of the upper bound vibration quantum number $n_{max}$ and potential range $\alpha$ causes the decrease of the values of vibrational entropy $S$ for constant temperature $T$.

When compared with the results of previous studies by Antia *et al*. (2015), there are differences in parameter variations, namely the potential parameter range $\alpha$. The energy results in this study are following the energy results in previous studies conducted by Antia *et al*. (2015) namely for constant angular quantum number $L$ and potential range $\alpha$, the increase of the value of radial quantum number $n$ causes the decrease of the value of energy spectra, and for the constant values radial quantum number $n$, and potential range $\alpha$, the increase of angular quantum number $L$ causes the increase of the value of energy spectra. The increase of the value of the potential range $\alpha$ causes the decrease of the energy spectra for constant radial and angular quantum number, $n$. Meanwhile, for the results of the wave function in a previous study by Antia *et al*. (2015) there is a difference, namely the equation of the wave function is different from this study, then the results of the wave function are not explained in detail such as the visualization image of the wave function. Meanwhile, the calculation results of thermodynamic properties such as vibrational partition function $Z$, vibrational mean energy $U$, vibrational specific heat $C$, vibrational free energy $F$, and vibrational entropy $S$ have not been explained in previous research conducted by Antia *et al*. (2015) so that the calculation of thermodynamic properties for the Mobius square plus modified Yukawa potential such as vibrational partition function $Z$, vibrational mean energy $U$, vibrational specific heat $C$, vibrational free energy $F$, and vibrational entropy $S$ are the latest ideas described in this paper.

The Schrödinger equation for Mobius square plus modified Yukawa potential in bispherical coordinate was solvable using Nikiforov Uvarov Functional Analysis (NUFA) method. Using new wave function and simple mathematical manipulation, the Schrödinger equation in bispherical coordinate reduced to the usual Schrödinger equation solvable using variable separation method. The energy spectra equation and radial wave function was obtained from the solution of the radial Schrödinger equation for Mobius square plus modified Yukawa potential solved using Nikiforov Uvarov Functional Analysis (NUFA) method. The calculated energy spectra, for radial and angular quantum numbers, $n, L$, potential range $\alpha$, and mass of the molecules $m_0$ showed that the increase of parameters of $n$ and $\alpha$ caused the decrease of the energy eigenvalues, but the increase of parameters of $L$ and $m_0$ caused the increase of the energy eigenvalues.

From the visualization of the ground state, first and second excited state wave functions, for various values of quantum numbers $n$, potential range $\alpha$, and mass of molecule $m_0$ were shown the radial quantum number $n$ and the potential range $\alpha$ had dominant effect to the wave functions.

It was also shown that the upper bound vibration quantum number $n_{max}$, temperature $T$, and the potential range $\alpha$ had effect to the vibrational partition function $Z$, vibrational mean energy $U$, vibrational specific heat $C$, vibrational free energy $F$ and vibrational entropy $S$.

## 4. CONCLUSIONS:

1. The energy spectra decrease with increasing parameters $n$ and $\alpha$. Meanwhile, the energy spectra increase with increasing $L$ and $m_0$.

2. The wave function is influenced by the dominant effect of the radial quantum number $n$ and the potential range $\alpha$.

3. Vibrational partition function $Z$, vibrational mean energy $U$, vibrational specific heat $C$, vibrational free energy $F$, and vibrational entropy $S$ are influenced by upper bound vibration quantum number $n_{max}$, temperature $T$, and potential range $\alpha$.

## 5. ACKNOWLEDGMENTS:

Sebelas Maret University supported this work under Mandatory Research Grant number 452/UN27.21/PN/2020.

## 6. REFERENCES:

1. Abu-Shady, M., and Ikot, A. N. (2019). Analytic solution of multi-dimensional Schrödinger equation in hot and dense QCD media using the SUSYQM method. *The European Physical Journal Plus*, 134(7). doi:10.1140/epjp/i2019-12685-y

2. Ahmadov, A. I., Naeem, M., Qocayeva, M. V., and Tarverdiyeva, V. A. (2018). Analytical Solutions of the Schrödinger Equation for the Manning-Rosen plus Hulthén Potential Within SUSY Quantum Mechanics. *Journal of Physics: Conference Series*, 965, 012001. doi:10.1088/1742-6596/965/1/012001

3. Antia, A. D., Essien, I. E., Umoren, E. B., and Eze, C. C. (2015). Approximate solutions of the non-relativistic Schrödinger equation with inversely quadratic Yukawa plus Mobius square potential via parametric Nikiforov–Uvarov method. *Advances in Physics Theories and Applications*, 44(1).

4. Arfken, G. (1985). *"Spherical Polar Coordinates". §2.5 in Mathematical Methods for Physicists*, 3rd ed. Orlando, FL: Academic Press, pp. 102-111.

5. Arfken, G. B., Weber, H. J., and Harris, F. E. (2005). *Mathematical Methods for Physicists* (Elsevier, Oxford).

6. Bayrak, O., Boztosun, I., and Ciftci, H. (2006). Exact analytical solutions to the Kratzer potential by the asymptotic iteration method. *International Journal of Quantum Chemistry*, 107(3), 540–544. doi:10.1002/qua.21141

7. Bayrak, O., and Boztosun, I. (2007). Analytical solutions to the Hulthén and the Morse potentials by using the asymptotic iteration method. *Journal of Molecular Structure: THEOCHEM*, 802(1-3), 17–21, 2007. doi:10.1016/j.theochem.2006.09.006

8. Berkdemir, C. (2012). Application of the Nikiforov-Uvarov Method in Quantum Mechanics. *Theoretical Concepts of Quantum Mechanics*. doi:10.5772/33510

9. Boonserm, P., and Visser, M. (2011). Quasi-normal frequencies: key analytic results. *Journal of High Energy Physics*, 2011(3). doi:10.1007/jhep03(2011)073

10. Buchowiecki, M. (2012). Quantum calculations of the temperature dependence of the rate constant and the equilibrium constant for the $NH_3 + H \rightleftharpoons NH_2 + H_2$ reaction. *Chemical Physics Letters*, 531 202–205. doi:10.1016/j.cplett.2012.01.075

11. Cari, C., Suparmi, A., and Saregar, A. (2016). Solution of The Schrödinger Equation for Trigonometric Scarf Plus Poschl-Teller Non-Central Potential Using Supersymmetry Quantum Mechanics. *Indonesian Journal of Applied Physics*, 4(01), 1. doi:10.13057/ijap.v4i01.1156

12. Carnie, S. L., Chan, D. Y. C., and Stankovich, J. (1994). Computation of Forces between Spherical Colloidal Particles: Nonlinear Poisson-Boltzmann Theory. *Journal of Colloid and Interface Science*, 165(1), 116–128. doi: 10.1006/jcis.1994.1212

13. Deo, S., and Tiwari, A. (2008). On the solution of a partial differential equation representing irrotational flow in bispherical polar coordinates. *Applied Mathematics*

*and Computation*, 205(1), 475–477. doi:10.1016/j.amc.2008.08.023

14. Deta, U. A., Suparmi, A., and Cari, C. (2013). Approximate solution of Schrödinger equation in D-dimensions for Scarf trigonometry potential using Nikiforov-Uvarov method. In *AIP Conference Proceeding*, Vol. 1554, 1, 190-193. doi:10.1063/1.4820317

15. Dianawati, D. A., Suparmi, A., and Cari, C. (2019). Study of Schrödinger Equation with Quantum Deformation for Three-Dimensional Harmonic Oscillator plus Inverse Quadratic Potential by Hypergeometric Method. *International Journal of Advanced Trends in Computer Science and Engineering*, 6, Vol 8, 2788-2793. doi: 10.30534/ijatcse/2019/17862019

16. Dong, S. H. (2007). *Factorization Method in Quantum Mechanics*. Springer.

17. Dutt, R., Khare, A., and Sukhatme, U. P. (1988). Supersymmetry, shape invariance, and exactly solvable potentials. *American Journal of Physics*, 56(2), 163–168. doi:10.1119/1.15697

18. Falaye, B. (2012). Any ℓ-state solutions of the Eckart potential via asymptotic iteration method. *Open Physics*, 10(4). doi:10.2478/s11534-012-0047-6

19. Gilbert, P. H., and Giacomin, A. J. (2019). Transport phenomena in bispherical coordinates. *Physics of Fluids*, 31(2), 021208. doi:10.1063/1.5054581

20. Gongora, A., and Koo, E. L. (1996). On the evaluation of the capacitance of bispherical capacitors, *Revista Mexicana de Física 42*, No. 4, 663-67.

21. Hassanabadi, H., Lu, L. L., Zarrinkamar, S., Liu, G. H., and Rahimov, H. (2012). Approximate Solutions of Schrödinger Equation under Manning-Rosen Potential in Arbitrary Dimension via SUSYQM. *Acta Physica Polonica A*, 122(4), 650–654. doi:10.12693/aphyspola.122.650

22. Hidayat, F., Suparmi, A., and Cari, C. (2019). Solution of Schrödinger equation in the presence of minimal length for cotangent hyperbolic potential using hypergeometric method. *IOP Conference Series: Materials Science and Engineering*, 578, 012095. doi:10.1088/1757-899x/578/1/012095

23. Ikot, A. N., Awoga, O. A., and Antia, A. D. (2013). Bound state solutions of d-dimensional Schrödinger equation with Eckart potential plus modified deformed Hylleraas potential. *Chinese Physics B*, 22(2), 020304. doi:10.1088/1674-1056/22/2/020304

*24.* Irikura, K. K. (2014). Anharmonic partition functions for polyatomic thermochemistry. *The Journal of Chemical Thermodynamics*, 73, 183–189. doi:10.1016/j.jct.2013.12.018

25. Ismail, M. E. H., and Saad, N. (2020). The asymptotic iteration method revisited. *Journal of Mathematical Physics*, 61(3), 033501. doi:10.1063/1.5117143

26. Jafari, K. S., Dehdashti, E., and Masoud, H. (2019). Conduction heat transfer from oblate spheroids and bispheres. *International Journal of Heat and Mass*, 139, 115–120. doi:10.1016/j.ijheatmasstransfer.2019.04.1

27. Jia, C. S., Zhang, L. H., and Wang, C. W. (2017). Thermodynamic properties for the lithium dimer. *Chemical Physics Letters*, 667, 211–215. doi:10.1016/j.cplett.2016.11.059

*28.* Korsch, H. J. (1979). A new semiclassical expansion of the thermodynamic partition function. *Journal of Physics A: Mathematical and General*, 12, 1521–1530. doi:10.1088/0305-4470/12/9/019

29. Lasaga, A. C., Otake, T., Watanabe, Y., and Ohmoto, H. (2008). Anomalous fractionation of sulfur isotopes during heterogeneous reactions. *Earth and Planetary Science Letters*, 268, 225–238. doi:10.1016/j.epsl.2008.01.016

30. Mir-Kasimov, R. M. (2013). Factorization method for Schrödinger equation in relativistic configuration space and q-deformations. *Physics of Particles and*

*Nuclei*, 44(3), 422–436. doi:10.1134/s1063779613030088
31. Moon, P., and Spencer, D. E. (1971). *Field Theory Handbook*. Second Edition. Springer-Verlag. Berlin.

32. Mubeen, S., Naz, M., Rehman, A., and Rahman, G. (2014). Solutions of k-hypergeometric differential equations. *Journal of Applied Mathematics*, 2014. doi:10.1155/2014/128787

33. Nurhidayati, I., Suparmi, A., and Cari, C. (2018). Analytical solution of Schrödinger equation in minimal length formalism for trigonometric potential using hypergeometry method. *Journal of Physics: Conference Series*, 997, 012016. doi:10.108 8/1742-6596/997/1/012016

34. Onyenegecha, C. P., Onate, C. A., Echendu, O. K., Ibe, A. A., and Hassanabadi, H. (2020). Solutions of Schrödinger equation for the modified Mobius square plus Kratzer potential. *The European Physical Journal Plus*, 135(3). doi:10.1140/epjp/s13360-020-00304-z

35. Pearson, C. E. (1983). *Handbook of Applied Mathematics*. Second Edition. Van Nostrand Reinhold. New York.

36. Rostami, A., and Motavali, H. (2008). Asymptotic iteration method: a powerful approach for analysis of inhomogeneous dielectric slab waveguides. *Progress In Electromagnetics Research B*, 4, 171–182. doi:10.2528/pierb08011701

37. Sadeghi, J. (2007). Factorization Method and Solution of the Non-Central Modified Kratzer Potential. *Acta Physica Polonica A*, 112(1), 23–28. doi:10.12693/aphyspola.112.23

*38.* Skouteri, D., Calderini, D., and Barone, V. (2016). Methods for calculating partition functions of molecules involving large amplitude and/or anharmonic motions. *Journal of Chemical Theory and Computation*, 12, 1011–1018. doi:10.1021/acs.jctc.5b01094

39. Sohnius, M. F. (1985). Introducing supersymmetry. *Physics Reports*, 128(2-3), 39–204. doi:10.1016/0370-1573(85)90023-7

40. Song, X. Q., Wang, C. W., and Jia, C. S. (2017). Thermodynamic properties for the sodium dimer. *Chemical Physics Letters*, 673, 50–55. doi:10.1016/j.cplett.2017.02.010

41. Stoy, R. D. (1989). Solution procedure for the Laplace equation in bispherical coordinates for two spheres in a uniform external field: Perpendicular orientation. *Journal of Applied Physics*, 66(10), 5093–5095. doi:10.1063/1.343737

*42.* Stratt, R. M., and Miller, W. H. (1977). A phase space sampling approach to equilibrium semiclassical statistical mechanics. *The Journal of Chemical Physics*, 67, 5894–5903. doi:10.1063/1.434796

43. Strekalov, M. L. (2004). On the partition function of Morse oscillators. *Chemical Physics Letters*, 393, 192–196. doi:10.1016/j.cplett.2004.06.028

44. Strekalov, M. L. (2007). An accurate closed-form expression for the partition function of Morse oscillators. *Chemical Physics Letters*, 439(1-3), 209–212. doi:10.1016/j.cplett.2007.03.052

45. Suparmi A. 2011. *Mekanika Kuantum II*. FMIPA UNS. Surakarta. ISBN 978-602-99344-2-7.

46. Suparmi, A., Dianawati, D. A., and Cari, C. (2020). Radial quantum deformation for Schrödinger equation on Coulomb potential by using Hypergeometric method. Journal of Physics: Conference Series, 1572, 012054. doi:10.1088/1742-6596/1572/1/012054

47. Taskin, F., and Koçak, G. (2010). Approximate solutions of Schrödinger equation for Eckart potential with centrifugal term. *Chinese Physics B*, 19(9), 090314. doi:10.1088/1674-1056/19/9/090314

48. Tezcan, C., and Sever, R. (2008). A General Approach for the Exact Solution of the Schrödinger Equation. *International Journal of Theoretical Physics*, 48(2), 337–350. doi:10.1007/s10773-008-9806-y

49. Walton, J. J. (1967). *Tensor Calculations on Computer: Appendix*. Comm. ACM 10, 183-186.

50. Yukawa, H. On the Interaction of Elementary Particles I. (1935). *Proceedings of the Physico-Mathematical Society of Japan*, 17, 48. doi: 10.1143/PTPS.1.1

***Table 1.*** *The characteristic of spectroscopic and reduces mass for diatomic molecules*.

| Parameter | CO | NO | $O_2$ | $I_2$ |
|---|---|---|---|---|
| $m_0(amu)$ | 6.860586000 | 7.468441000 | 7.997457504 | 63.45223502 |

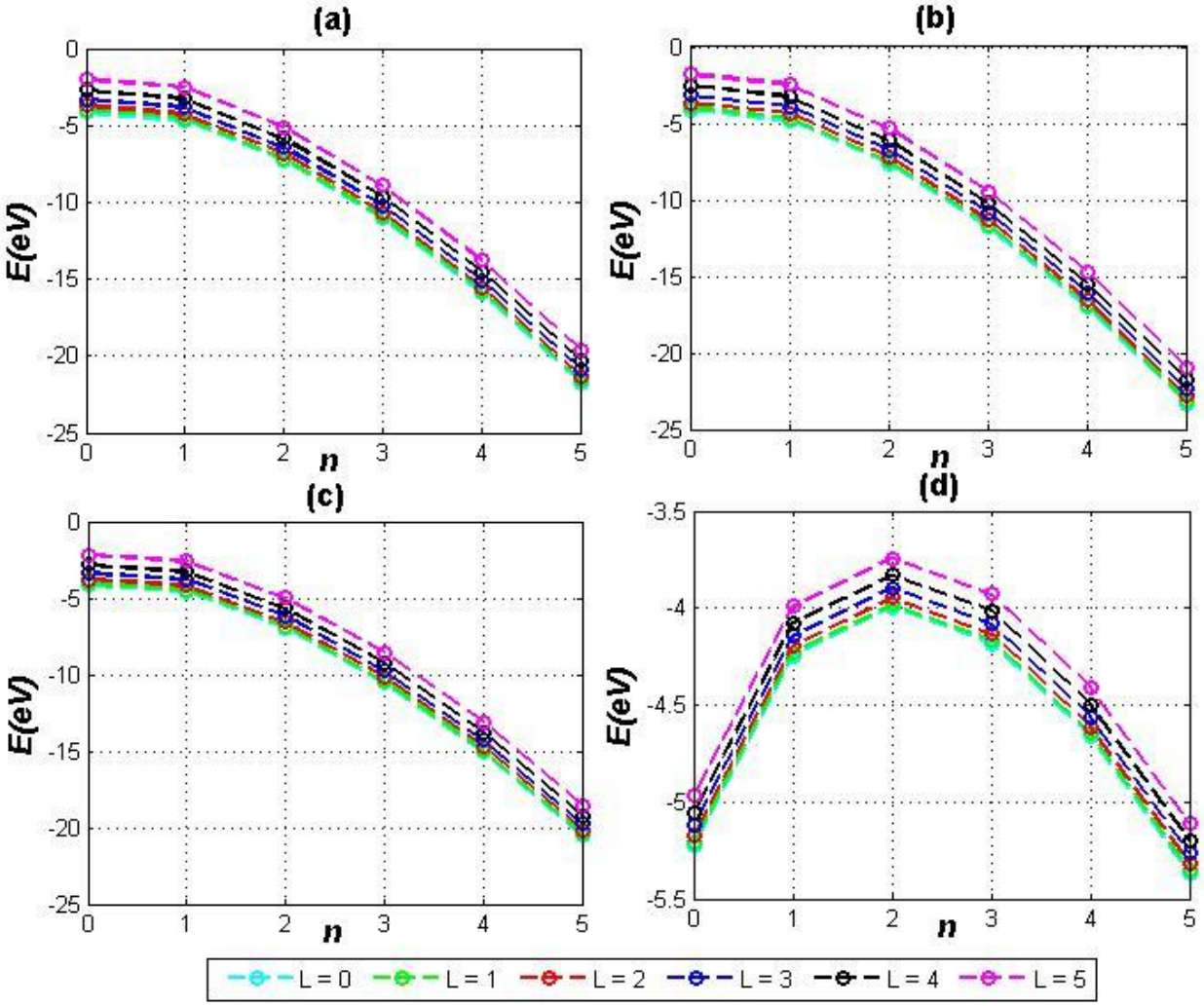


***Figure 1.*** *Spectrum Energy of Mobius square plus modified Yukawa potential* $(E)$ *for the various* $n$ *and* $L$ *quantum numbers,* $a = b = c = g = 1$*, and* $\alpha = 5$ *for (a) CO, (b) NO, (c)* $O_2$*, and (d)* $I_2$ *diatomic molecules*.

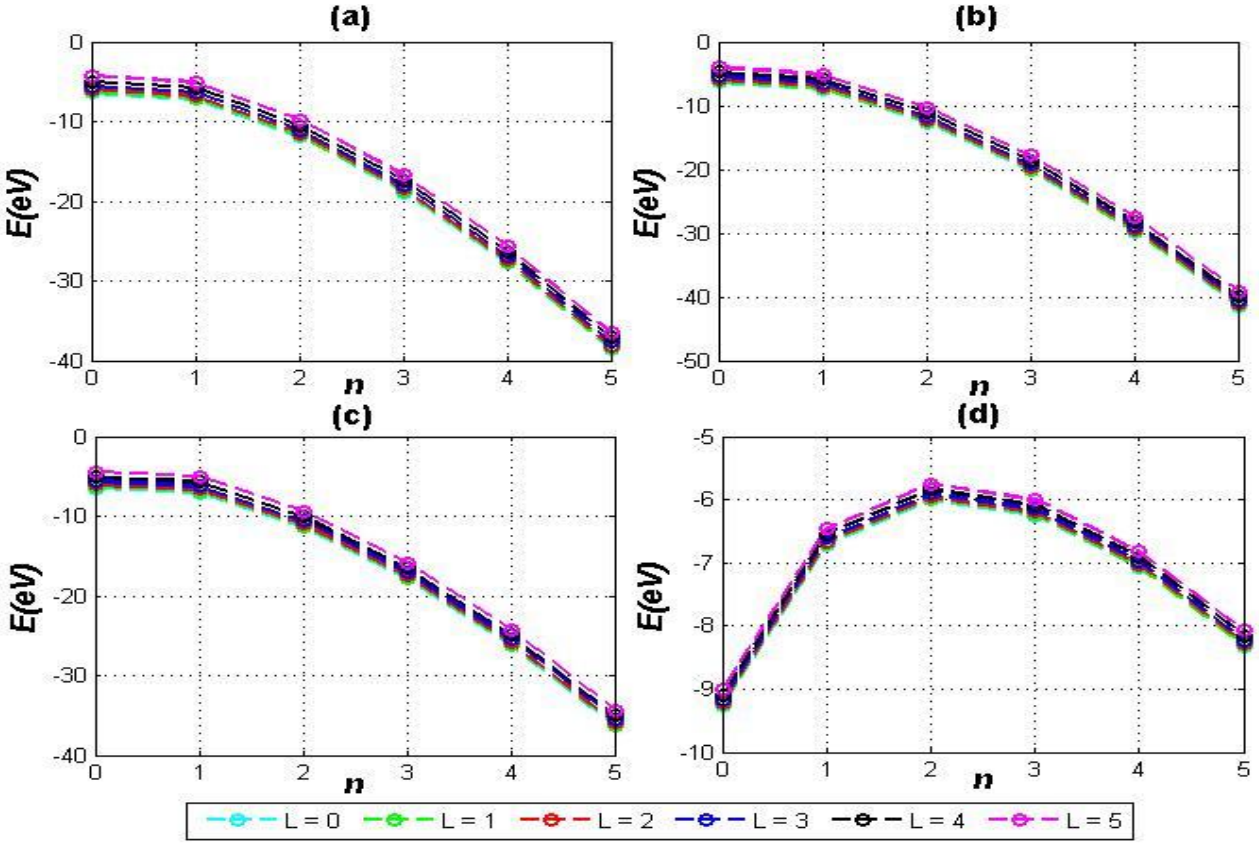


***Figure 2.*** *Spectrum Energy of Mobius square plus modified Yukawa potential* $(E)$ *for the various* $n$ *and* $L$ *quantum numbers,* $a = b = c = g = 1$*, and* $\alpha = 7$ *for (a) CO, (b) NO, (c)* $O_2$*, and (d)* $I_2$ *diatomic molecules*.

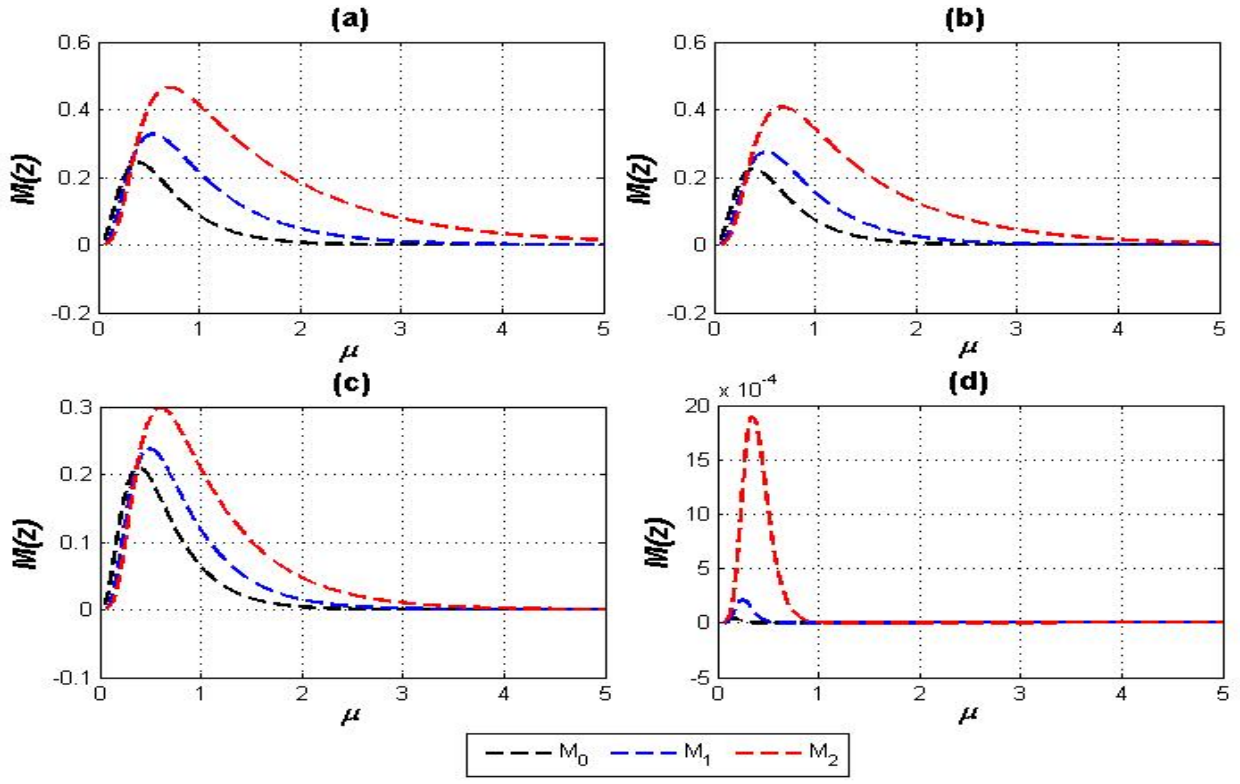


***Figure 3.*** *The graphs of the un-normalized wave function as a function of radial position, ground state (black line), the first excited (blue line) and second excited (red line) wave functions for* $a = b = c = g = 1$*,* $\alpha = 5$*, and* $L = 0$*, for (a) CO, (b) NO, (c)* $O_2$*, and (d)* $I_2$ *diatomic molecules*.

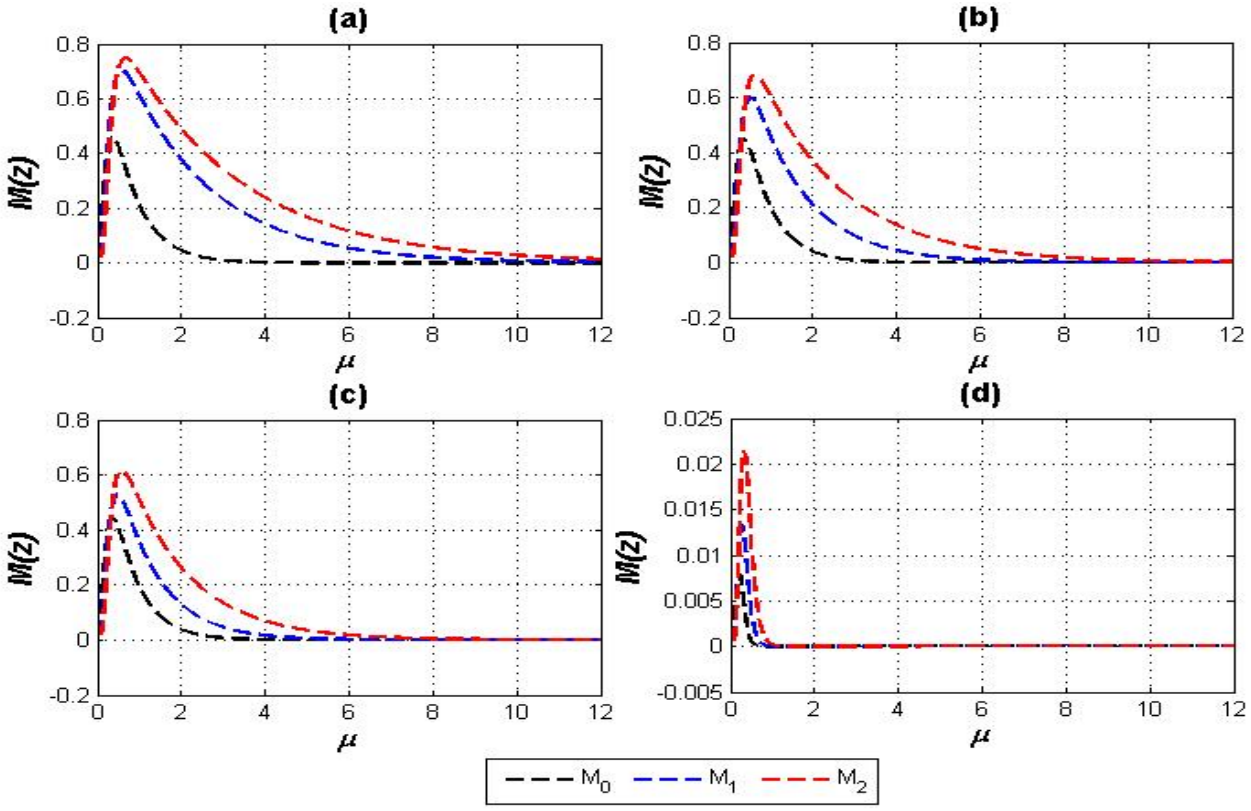


***Figure 4.*** *The graphs of the un-normalized wave function as a function of radial position, ground state (black line), the first excited (blue line) and second excited (red line) wave functions for* $a = b = c = g = 1$, $\alpha = 7$, *and* $L = 0$, *for (a) CO, (b) NO, (c)* $O_2$, *and (d)* $I_2$ *diatomic molecules.*

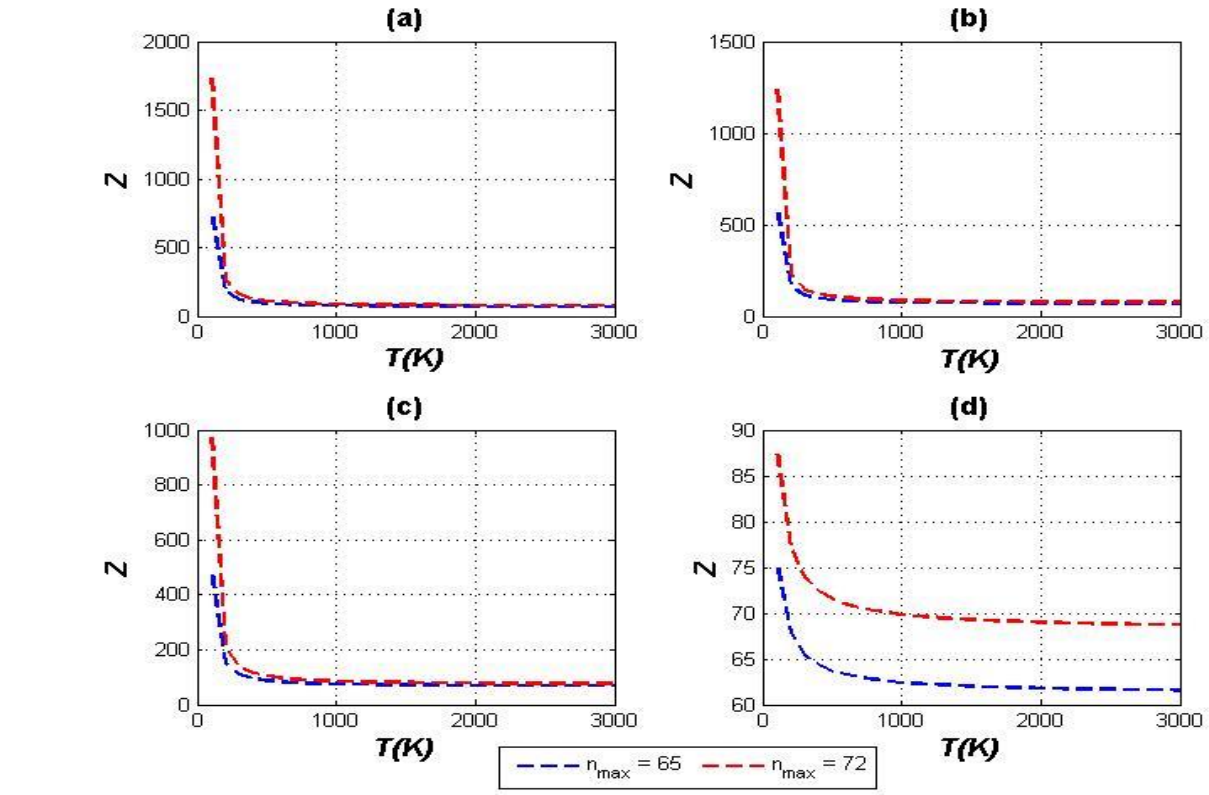


***Figure 5.*** *The graphs of the vibrational partition function* $Z$ *for the various* $n_{max}$ *and* $T$ *for* $a = b = c = g = 1$, $\alpha = 5$, *and* $L = 0$, *for (a) CO, (b) NO, (c)* $O_2$, *and (d)* $I_2$ *diatomic molecules.*

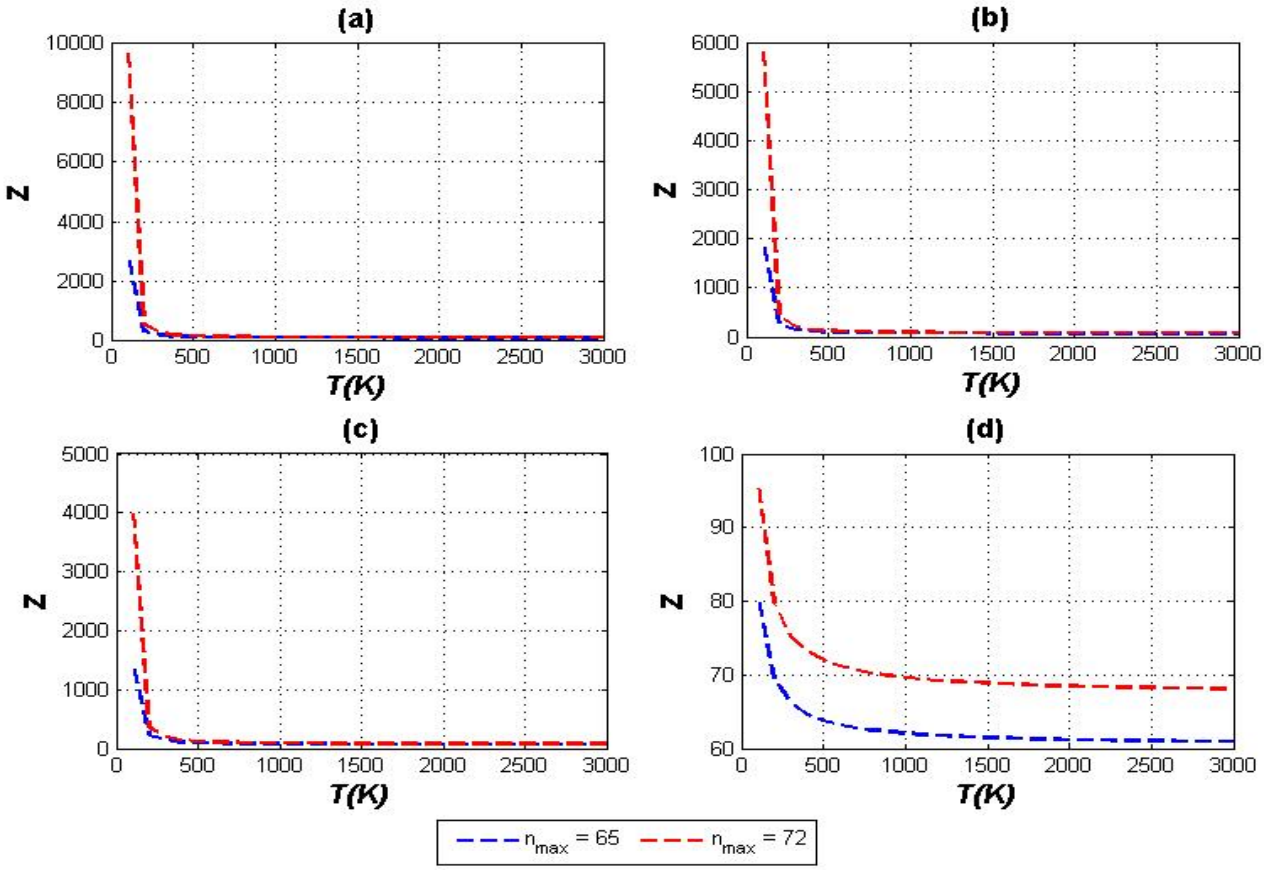


***Figure 6.*** *The graphs of the vibrational partition function $Z$ for the various $n_{max}$ and $T$ for $a = b = c = g = 1$, $\alpha = 7$, and $L = 0$, for (a) CO, (b) NO, (c) $O_2$, and (d) $I_2$ diatomic molecules.*

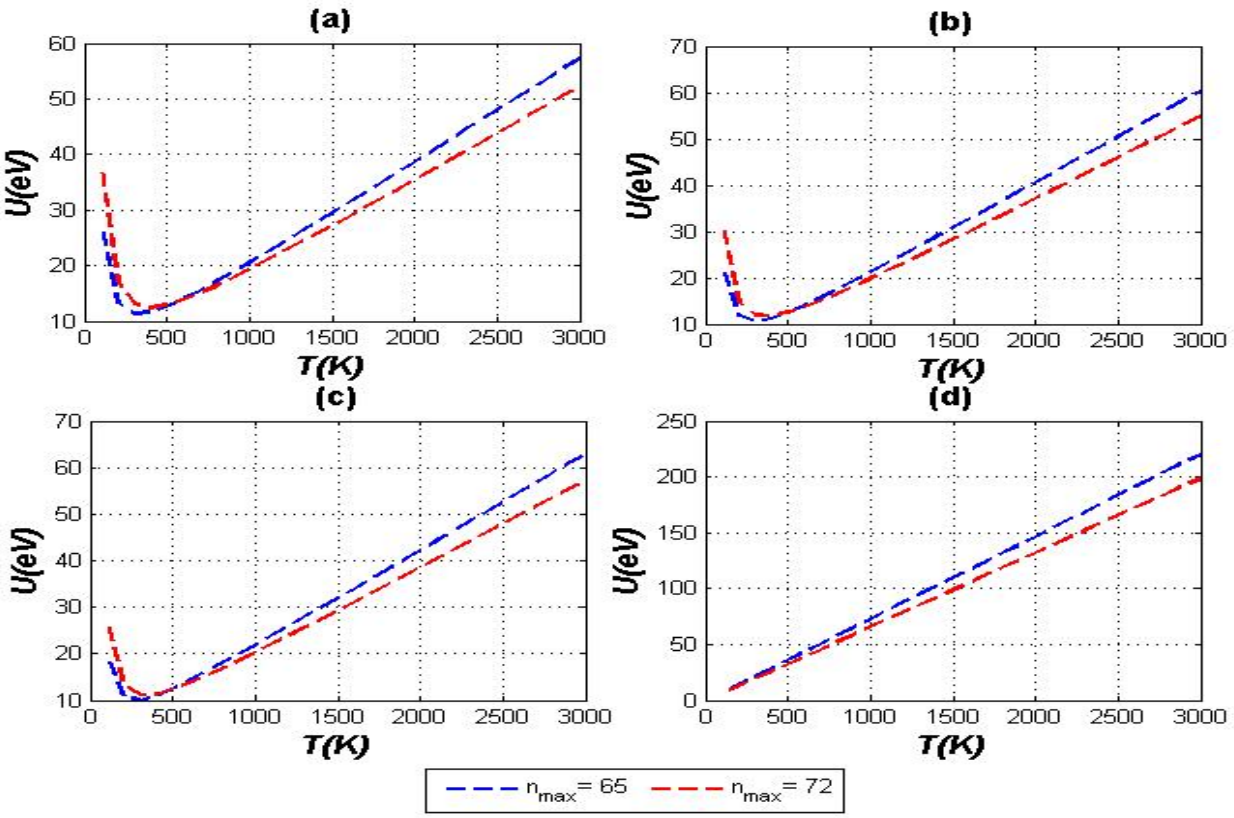


***Figure 7.*** *The graphs of the vibrational mean energy $U$ for the various $n_{max}$ and $T$ for $a = b = c = g = 1$, $\alpha = 5$, and $L = 0$, for (a) CO, (b) NO, (c) $O_2$, and (d) $I_2$ diatomic molecules.*

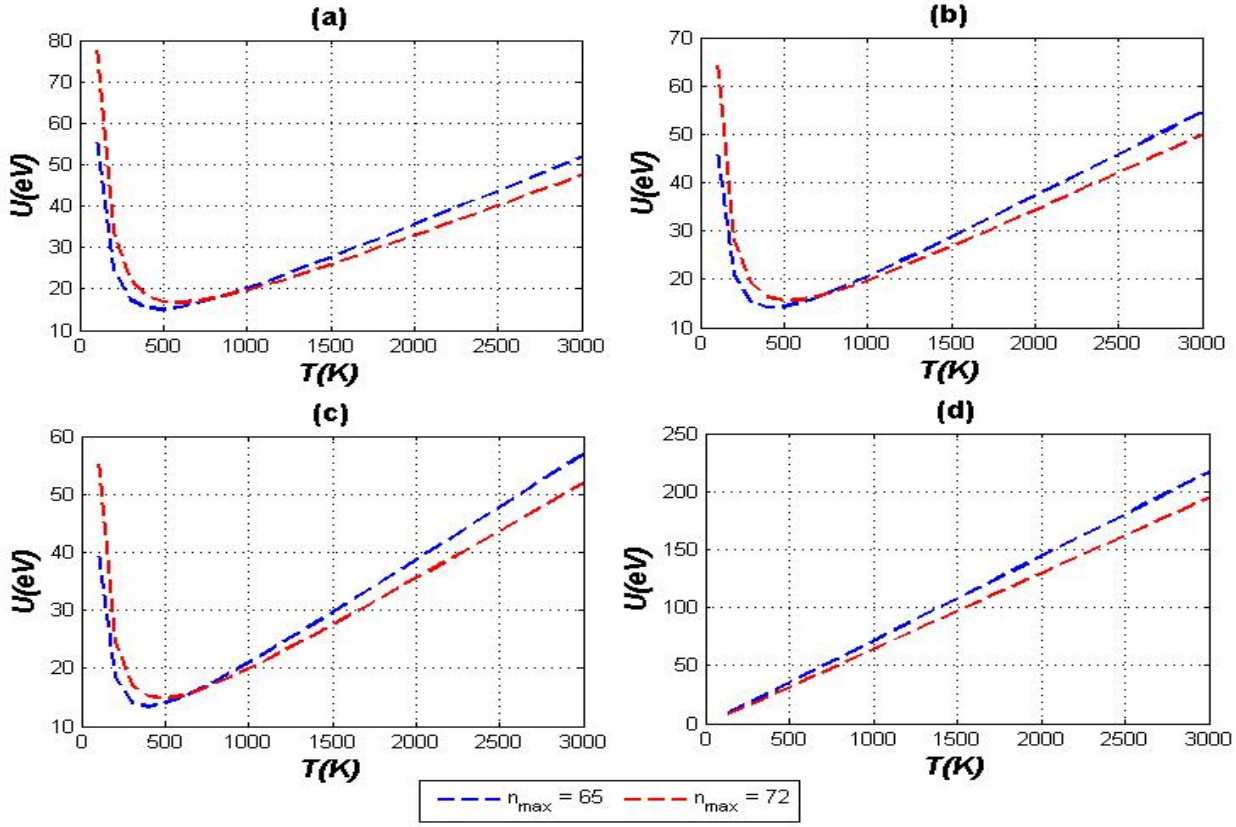


***Figure 8.*** *The graphs of the vibrational mean energy $U$ for the various $n_{max}$ and $T$ for $a = b = c = g = 1$, $\alpha = 7$, and $L = 0$, for (a) CO, (b) NO, (c) $O_2$, and (d) $I_2$ diatomic molecules.*

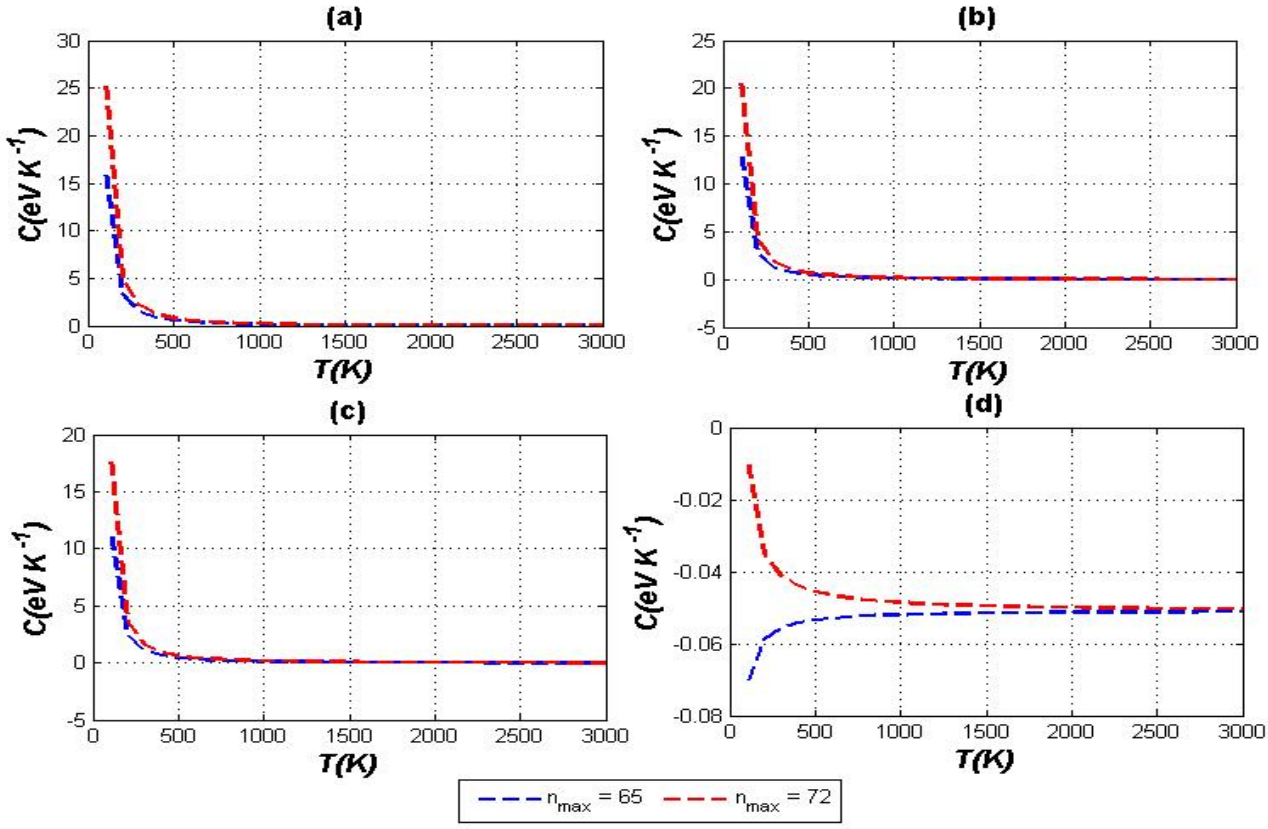


***Figure 9.*** *The graphs of the vibrational specific heat $C$ for the various $n_{max}$ and $T$ for $a = b = c = g = 1$, $\alpha = 5$, and $L = 0$, for (a) CO, (b) NO, (c) $O_2$, and (d) $I_2$ diatomic molecules.*

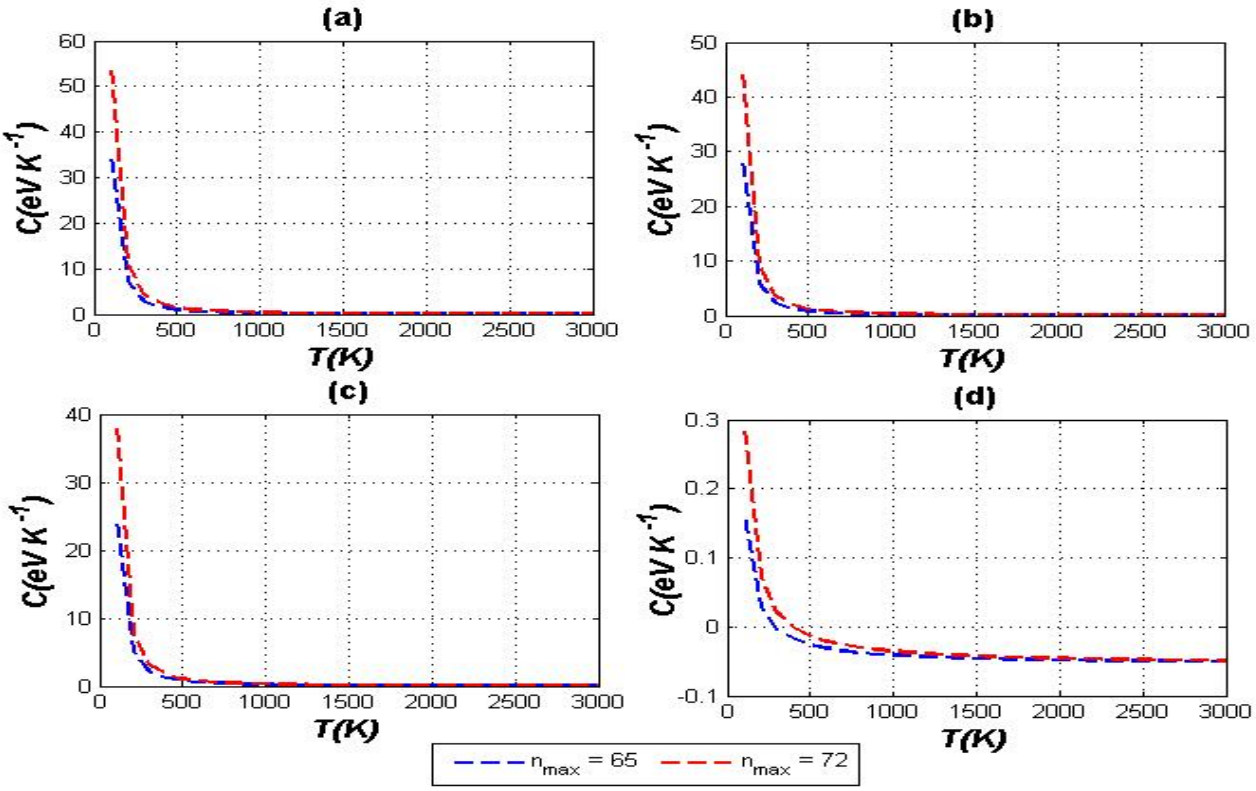


***Figure 10.*** *The graphs of the vibrational specific heat $C$ for the various $n_{max}$ and $T$ for $a = b = c = g = 1$, $\alpha = 7$, and $L = 0$, for (a) CO, (b) NO, (c) $O_2$, and (d) $I_2$ diatomic molecules.*

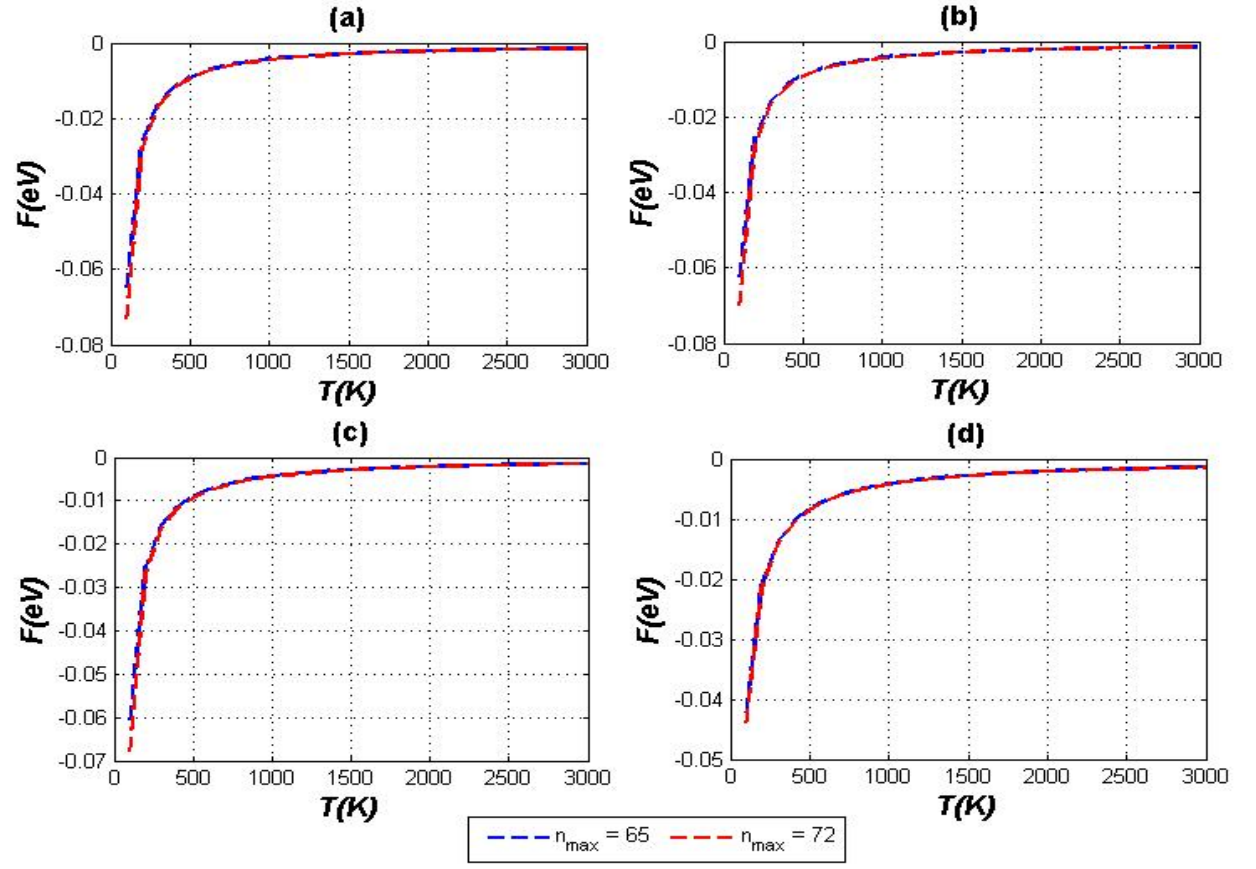


***Figure 11.*** *The graphs of the vibrational free energy $F$ for the various $n_{max}$ and $T$ for $a = b = c = g = 1$, $\alpha = 5$, and $L = 0$, for (a) CO, (b) NO, (c) $O_2$, and (d) $I_2$ diatomic molecules.*

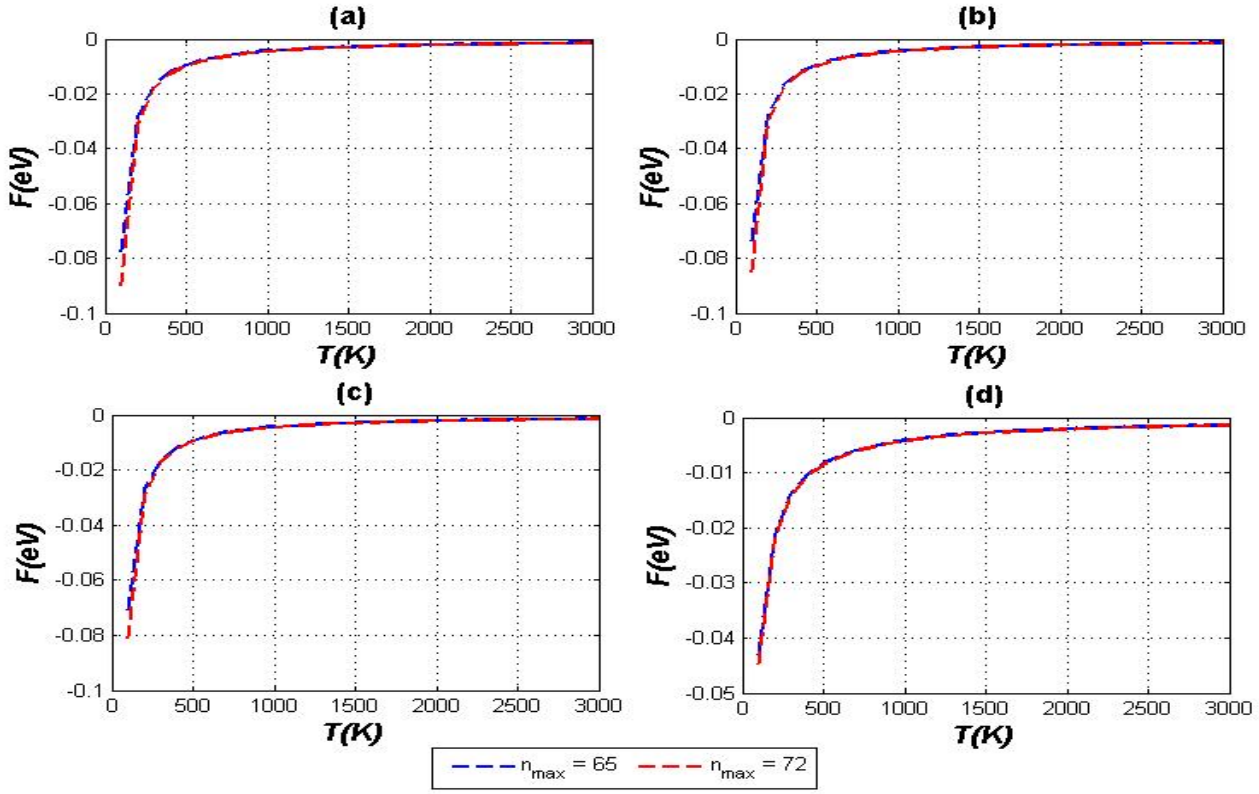


***Figure 12.*** *The graphs of the vibrational free energy $F$ for the various $n_{max}$ and $T$ for $a = b = c = g = 1$, $\alpha = 7$, and $L = 0$, for (a) CO, (b) NO, (c) $O_2$, and (d) $I_2$ diatomic molecules.*

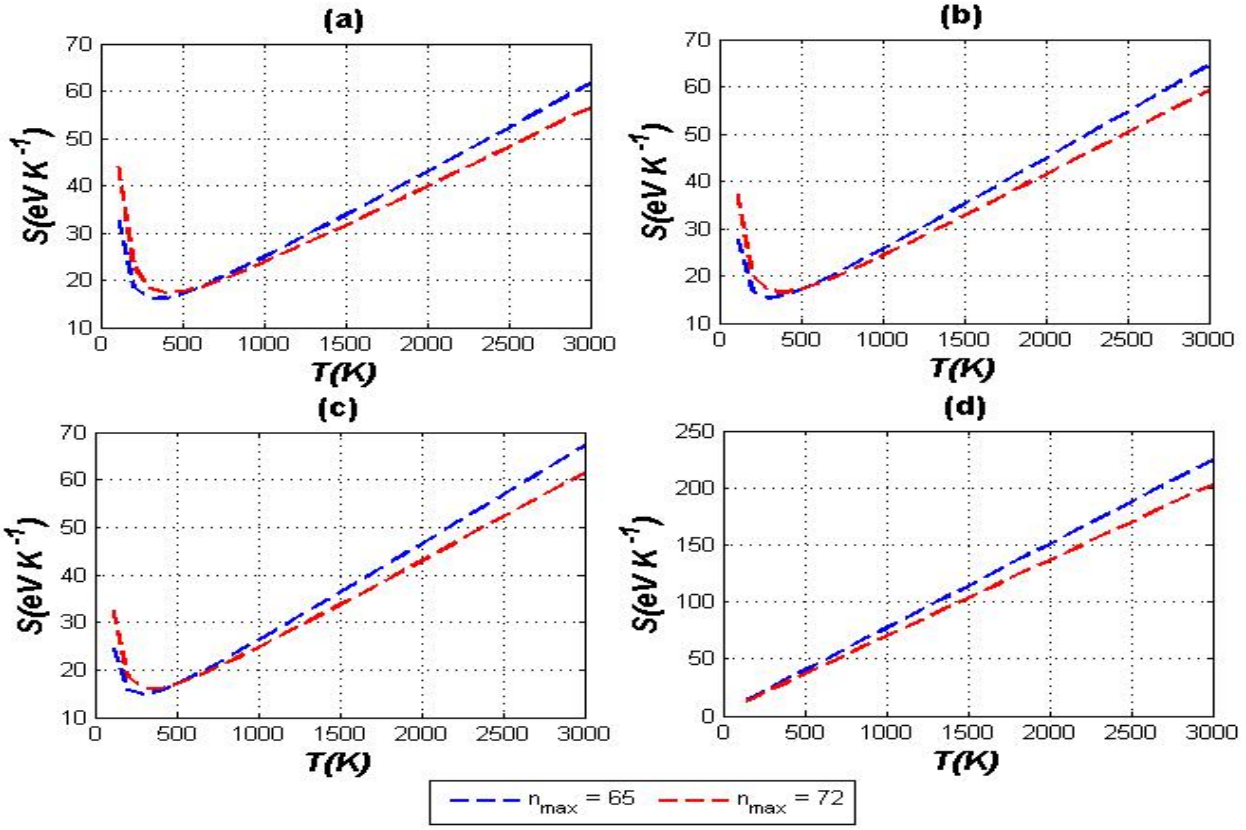


***Figure 13.*** *The graphs of the vibrational entropy $S$ for the various $n_{max}$ and $T$ for $a = b = c = g = 1$, $\alpha = 5$, and $L = 0$, for (a) CO, (b) NO, (c) $O_2$, and (d) $I_2$ diatomic molecules.*

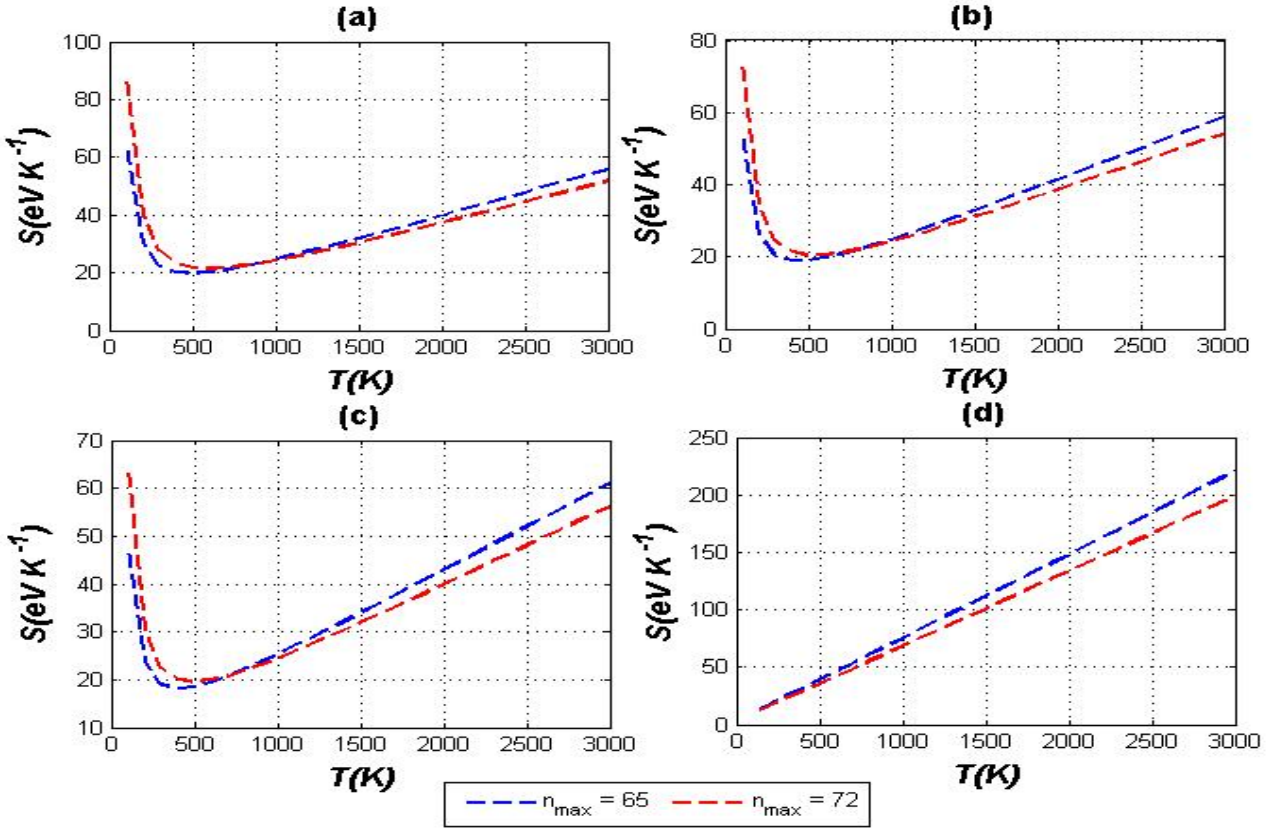


***Figure 14.*** *The graphs of the vibrational entropy $S$ for the various $n_{max}$ and $T$ for $a = b = c = g = 1$, $\alpha = 7$, and $L = 0$, for (a) CO, (b) NO, (c) $O_2$, and (d) $I_2$ diatomic molecules.*

PERIÓDICO TCHÊ QUÍMICA
ARTIGO ORIGINAL

# ERITROFERRONA COMO UM NOVO BIOMARCADOR ASSOCIADO À ANEMIA EM PACIENTES IRAQUIANOS COM DRC

# ERYTHROFERRONE AS A NEW BIOMARKER ASSOCIATED WITH ANEMIA IN IRAQI PATIENTS WITH CKD

# الإرثروفيرون كمؤشر حيوي جديد يرتبط بفقر الدم لدى المرضى العراقيين المصابين بأمراض الكلى المزمنة

**SHARBA, Intisar Razzaq [1]*; ALJABERY, Hasanat Abdulrazzaq [2]; AL-KHAKANI; Manal Farhan[3]**

[1]*Kufa University, Faculty of Science, Department of Biology. Iraq.*

[2]*Kufa University, College of Medicine, Department of Biochemistry, chemical pathology. Iraq.*

[3]*Kufa University, Faculty of Science, Department of Chemistry. Iraq.*

** Corresponding author*
*e-mail: intisar.sharba@uokufa.edu.iq*

Received 12 June 2020; received in revised form 14 October 2020; accepted 05 November 2020

## RESUMO

**Introdução**: A eritroferrona (ERFE) é uma glicoproteína de síntese e liberação de hormônio pelos eritroblastos. Recentemente identificado como um regulador eritropoiético e ativado em resposta ao estímulo da eritropoietina (Epo). Nas doenças renais crônicas (DRC), a anemia é um distúrbio característico devido a uma diminuição da hipossensibilidade eritropoiética à Epo; esses pacientes recomendaram o uso de agentes estimuladores de eritropoiese (AEEs). **Objetivos**: Este estudo teve como objetivo avaliar o nível sérico de ERFE em pacientes com DRC e investigar os efeitos contínuos do uso de AEE anêmico em longo prazo associado a marcadores de eritropoiese e metabolismo do ferro. **Métodos**: Sessenta e cinco pacientes com DRC foram divididos em dois grupos, incluindo 30 pacientes em hemodiálise (HD) e 35 pacientes com DRC sem hemodiálise (não-HD), foram comparados a 25 voluntários saudáveis pareados por sexo e idade inscritos no estudo. O nível sérico de ERFE foi medido através de um ensaio imunoenzimático (ELISA).. **Resultados**: Um aumento significativo nos níveis séricos de ERFE em pacientes em HD da mediana (IQR) de 17,25 (13,4) ng/mL, razão de possibilidades (OR = 10,161), (AUC 0,996) maior do que CKD 4 (6,1) ng/ml, (OR = 6,295), (AUC = 0,984) p <0,001; também, estes estão positivamente correlacionados com o uso de AEE em HD e CKD (r = 1,00 e r = 0,95), respectivamente, em comparação com o grupo saudável 2 (2,1) ng/ml. Os níveis séricos de ERFE foram significativamente negativos em pacientes com DRC e HD. (p <0,05) relacionado à TFG (r = -0,396, e r = -0,68), saturação de transferrina (TS%) (r = -0,842 e r = -0,877), níveis séricos de ferritina (r = -0,865 e r = -0,866), e Ferro (r = -0,860 e r = -0,851), RBC (r = -0,841 e r = -0,843), hemoglobina (Hb) (r = -0,758 e r = -0,796 ) **Conclusões**: O presente estudo demonstra que os níveis séricos elevados de ERFE associados à atividade eritropoiética e anemia são maiores em pacientes com DRC com HD e não-HD tratados com AEE do que em pacientes sem AEE. Este estudo sugeriu o uso de ERFE como uma ferramenta de sucesso para a inspeção da atividade eritropoiética na DRC, especialmente aqueles que tomam AEEs para tratar anemia.

**Palavras-chave**: *Eritroferrona, Anemia, Eritropoiese, Iron Status.*

## ABSTRACT

**Background**: Erythroferrone (ERFE) is a glycoprotein hormone synthesis and release by erythroblasts. Recently identified as an erythropoietic regulator and activated in response to stimulating erythropoietin (Epo). In chronic kidney diseases (CKD), anemia is a hallmark disorder due to a decrease in hyposensitive erythropoietic to the Epo; these patients recommended to use of Erythropoiesis-stimulating agents (ESAs). **The aim:** This study aimed to assess serum ERFE level in patients with CKD and investigate the continuing effects of long-term anemic ESA use associated with markers of erythropoiesis and iron metabolism. **Methods**: Sixty-five CKD patients divided in two groups, included 30 hemodialyses (HD) and 35 without hemodialysis (non-HD) CKD patients, were compared to 25 healthy voluntaries matched by gender and age enrolled in the current study. Serum ERFE level was measured by an enzyme-linked immunosorbent assay (ELISA). **Results:** Serum ERFE level was significantly elevated in HD patients median (IQR) about 17.25 (13.4) ng/mL, odds ratio (OR = 10.161), (AUC 0.996) greater than CKD 4(6.1) ng/ml, (OR = 6.295), (AUC = 0.984) p<0.001; also, these are positively correlated with the use of ESA in HD, and CKD (r = 1.00 and r = 0.95) respectively as compared to healthy group 2(2.1) ng/ml. Serum

ERFE levels were significantly negative (p<0.05) in both CKD and HD patients related to GFR (r = -0.396, and r = -0.68), transferrin saturation (TS%) (r = -0.842, and r = -0.877), serum levels of Ferritin (r = -0.865 and r = -0.866), and Iron (r = -0.860, and r = -0.851), RBC (r = -0.841, and r = -0.843), hemoglobin (Hb) (r = -0.758, and r = -0.796). **Conclusion:** The present study demonstrated that elevated serum ERFE levels associated with erythropoietic activity and anemia are higher in CKD with HD and non -HD patients treated with ESA than in non-ESA patients. This study suggested using ERFE as a successful tool for erythropoietic activity inspection in CKD, especially those taking ESAs to treat anemia.

**Keywords**: *Erythroferrone, Anemia, Erythropoiesis, Erythropoiesis-stimulating agents, hemodialysis, and CKD*

**الملخص:**

**معلومات اساسية**: الإرثروفيرون (ERFE) هرمون بروتيني سكري يتم تصنيعه وإفرازه من مولدات خلايا الدم الحمراءerythroblasts تم تحديده مؤخرا كمنظم لتكوين كريات الدم الحمر ويتم تنشيطه استجابة لتحفيز هرمون الأريثروبويتين (Epo) في أمراض الكلى المزمنة CKD يعد فقر الدم اضطرابًا مميزًا بسبب نقص الشديد في حساسية الكريات الحمر لهرمون الأريثروبويتين. لذلك كان هؤلاء المرضى يوصون باستخدام عوامل تحفيز تكوين الكريات الحمر (ESAs). **الهدف**: هدفت هذه الدراسة إلى تقييم مستوى الإرثروفيرون ERFE في مصل المصابين بأمراض الكلى المزمنة والتحقق من تأثير الاستخدام المستمر ل ESA كعلاج لفقر الدم على المدى الطويل وعلاقته بمؤشرات الدم وايض الحديد. **طرائق العمل**: شملت الدراسة الحالية 65 مريضا مقسَّمين إلى مجموعتين تضمنت 30 حالة غسيل كلى (الديلزة الدموية (HD و35 حالة أمراض الكلى مزمنة دون ديلزة مقارنة مع 25 من المتطوعين الاصحاء مع تطابق الجنس والعمر في الدراسة الحالية. تم تقييم مستوى الإرثروفيرون في المصل بالمقايسة الامتصاصية المناعية للإنزيم المرتبط (ELISA). **النتائج**: اظهرت ارتفاعا معنويا (P<0.05) في مستوى الدليل الحيوي الإرثروفيرون ERFE في مرضى الغسيل الكلوي HD بوسيط median ومجال ربيعي (IQR) مقداره 17.25 (13.4) نانوغرام/مل، ونسبة ارجحية (OR=10.161) ومساحة تحت المنحني (AUC= 0.996)، أكبر من مجموعة المرضى بدون غسيل كلوي بوسيط median ومجال ربيعي (IQR) مقداره 4 (6.1) نانوغرام/مل، ونسبة ارجحية (OR=6.295) ومساحة تحت المنحني (AUC=0.984)، p<0.001. كما أظهرERFE وجود علاقة ارتباطية معنوية ايجابية (P<0.05) مع استخدام علاج (ESAs) في كلا المجموعتين CKD وHD وبمعامل ارتباط ( r=1.00, r=0.95) على التوالي. ان مستويات ERFE في مصل مرضى HD وCKD ترتبط ارتباطا معنويا عكسيا مع كل من معدل الترشيح الكلوي GFR (r=- 0.396, r=-0.68) نسبة تشبع الترانسفيرين TS% (r=-0.842, r=-0.877)، مستوى الفيريتين في المصل r=-0.865 r=-0.866) مستوى الحديد (r=- 0.860, r=-0.851)، اعداد كريات الدم الحمراء RBC (r=-0.841, r=-0.843) ومستوى الهيموغلوبين (Hb). (r=-0.758, and r=-0.796) على التوالي. **الاستنتاج**: الخلاصة: توضح الدراسة الحالية أن ارتفاع مستويات ERFE في المصل ترتبط بنشاط تكوين خلايا الدم الحمراء وفقر الدم وتكون أعلى في مرضى CKD الذين عولجوا بـ ESAs مقارنةً بالمرضى الذين لا يستخدمون ESAs. اقترحت هذه الدراسة الى امكانية استخدام الدليل الحيوي ERFE كأداة ناجحة للكشف عن نشاط خلايا الدم الحمراء في مرضى الكلى المزمنة، خاصة الذين يتعاطون محفزات تكوين الحمر ESAs كعلاج لفقر الدم.

**الكلمات المفتاحية**: الإريثروفيرون (ERFE)، فقر الدم ، تكوين كريات الدم الحمراء، عوامل المحفزة لتكوين كريات الحمر ESAs، الغسيل الدموي. وامراض الكلى المزمنة

## 1. INTRODUCTION:

Chronic kidney disease (CKD) is categorized by a frequent complication of anemia, especially in the end phases (5 stages) of the disease (Fishbane and Spinowitz, 2018). Anemia is a common feature of many patients with CKD and is associated with reduced quality of life, the mechanisms of anemia pathogenetic in CKD by decreased synthesis of erythropoietin and reticuloendothelial iron invasion caused by chronic renal inflammation, and recently that GDF-15 is a possible mediator of anemia through hepcidin in adult renal transplant recipients and stratification factor for achieving the end stage of diabetic kidney disease (Abass and Sharba, 2020; Mikhali *et al.*, 2017).

In CKD, deficiency of erythropoietin (EPO) synthesis and shorting of erythrocytes lifespan were played an important role in anemia pathogenesis (Kautz *et al.*, 2014; Sharba and Al-Zahid, 2016). Besides, patients of hemodialysis (HD) suffer from an iron deficiency for erythropoiesis. EPO exogenic or known by erythropoiesis-stimulating agents (ESAs), and iron supplementation are essential components of anemia administration in CKD patients (Atkinson and Warady, 2018).

Many studies have indicated the association between ESA and iron metabolism biomarkers in HD patients, such as hepcidin 25 a key regulator of stored iron release and the primary mediators of iron deficiency (Honda *et al.,* 2019; Webster *et al.*, 2017). ESA significantly suppresses levels of hepcidin 25 and ferritin, and the long treatment with acting ESA results in effective erythropoiesis and stored iron release (Honda *et al.,* 2019).

Erythroferrone (ERFE) is an erythropoietic-driven encoded by the FAM132B gene. It was a new regulator of iron homeostasis ( Kautz *et al.,* 2014).

ERFE was expressed and released from erythroblasts in response to endogenous or exogenous erythropoietin (EPO) hormone (Kautz *et al.*, 2015). It regulated iron metabolism by inhibiting hepcidin and excess absorption with iron mobilization, making available a compensated supply during stress erythropoiesis such as rapid growth or hemostasis (Ganz, 2019). ERFE a newly identified cause of increasing anemia severity associated with a high iron and ferritin level in human patients with the major and intermediate beta-thalassemia, especially with splenectomized (Almousawi and Sharba, 2019).

This study aimed to assess serum ERFE levels in patients with CKD and investigate the continuing effects of long-term anemic ESA use associated with erythropoiesis and iron metabolism markers. Also, determine their potential in early erythropoietic activity prediction and anemia.

## 2. MATERIALS AND METHODS:

### 2.1. Subject of Patients

The study protocol was approved by the Ethics Committee of the faculty science, university of Kufa N0. 6097 on 26/11/2019. Moreover, it was conducted following the Declaration of Helsinki Principles and related ethical guidelines. All participants or their guardians involved in this research received verbal consent. A cross-sectional study was performed of Ninety participants in the present study; they have included sixty-five patients with CKD aged range (25-63) years, about 23 were males, and 12 females, 15 with Diabetic Mellitus, and 20 without Diabetic Mellitus who attended two Units for kidney disease at Al-Sadder Teaching Hospital and Al-Hakeem General Hospital in Al-Najaf, Iraq. This study was carried out from December 2019 via January 2020. CKD patients with different stages would include two independent groups: a group of 30 patients with end-stage (4-5) CKD eGFR <45 mL/min/1.73 m2, under hemodialysis (HD) for a time of median (IQR) 42 (17-85) months, about twice a week with standard bicarbonate dialysis in different types of non-cellulosic membrane filters. All patients were treated with intravenous iron and the individual dose of using 4000 units ESA. Our current study excluded patients with transplanted, cancer, chronic inflammatory diseases, and any end-stage complicated diseases. CKD Patients with diabetic mellitus were defined as type 1 (TDM1) or type 2 (TDM2).

Additionally, there are 35 stable clinical patients of CKD (1-3 stage) eGFR ≥45 mL/min/1.73 m2 with no acute or rapidly developing kidney disorders, intercurrent infections, or acute inflammatory processes. Such patients were not transplanted, not pregnant, and non-cancer. When These Patients did have laboratory evidence of iron deficiency were treated with oral iron supplements. All patients with renal transplant recipients are excluded from the study.

### 2.2. Healthy group

Twenty-five volunteers of both sexes (13 men and 12 women) as a control group were recruited from working in these hospitals and science faculty institution, which had no diseases such as diabetes, cardiovascular disorders, anemia, and kidney diseases.

### 2.3. Demographic Information and Laboratory Measurements

BMI (Body Mass Index) is performed by electronic balance and height device, for calculating the weight and height, and applied the Equation (Eq. 1).

$$BMI = \text{Weight (kg)} / \text{Height (m}^2\text{)} \quad \text{(Eq. 1).}$$

GFR can be calculated mathematically from the Modification of Diet in Renal Disease (MDRD) by Equation 2 (Levey *et al.*, 2009).

$$GFR\ (\text{ml/min/1.73 m}^2) = 186 \times (\text{creatinine concentration})^{-1.154} \times (\text{Age})^{-0.203} \times (0.742 \text{ if female}) \times (1.210 \text{ if black}) \quad \text{( Eq. 2).}$$

Five ml of blood was collected from all participants in the early morning and before one-hour of dialysis session for the HD patients, then divided into 2.5 ml put in EDTA-containing tubes for CBC, and 2.5 ml in gel tube and centrifuged for separated serum supernatants were stored at −deep freeze until batch analyses of ERFE and biomarkers of iron status.

### 2.4. Measurement of Hematologic Parameters

Complete blood counts were performed at the laboratory by an automatic blood analyzer device (Mythic 18, RINGELSAN CO., Turkey) using three reagents: a diluent, a lysis reagent, and a cleaning solution. A cyanide-free spectrophotometry method was used to measure hemoglobin by the formation of oxyhemoglobin at 555 nm (Van *et al.,* 1961). Serum phosphate, and calcium, depended on the standard laboratory procedure, were performed by the automatic biochemical analyzer (bt 35i) using the Direct

Method kit, which supplies from manufactures (Monobind Inc., USA). (Wassmuth *et al.,* 2011).

### 2.5. Measurement of TS%, Iron, and Ferritin

Serum ferritin levels quantification through the immunoenzymatic technique Enzyme-Linked Immunosorbent Assay (ELISA) using automated Elisa (Italy), testing of according to the manufacturing company, the Human Accu Bind Ferritin ELISA Kit was achieved (Monobind Inc., USA). Serum iron, transferrin, and total iron-binding capacity (TIBC) were measured by iron kit (using the chromogen ferrozine method and reagent Ferrozine 16.7 mM in Hydroxylamine hydrochloride). This processing with the advice of bt 35i (Turkey).TS % was measured from serum iron and total iron-binding capacity (TBIC). The Equation 3, (Horak and Sunderman, 1974).

Serum iron × 100/ TBIC. (Eq. 3)

### 2.6. Measurement of ERFE Biomarker

Serum ERFE level was estimated based on sandwich enzyme-linked immune-sorbent assay technology, by Automated Elisa (Italy) with using the human kit of (ELISA) was provided from (MyBioSource, San Diego, CA, USA) Depended on (Ganz et al., 2017).

### 2.7. Statistical Analysis

All data were analyzed by the SPSS software (V.24 Inc., Chicago, Illinois, USA) and GraphPad Prism (La Jolla, CA, USA, v.8.2.1). Kolmogorov-Smirnov test for variables distribution. Normally distributed Numerical Variables were compared between two groups by Independent t-test, and among two groups with ANOVA, all data expressed as (mean ± SD) standard deviation. The non-parametric Mann-Whitney U test was used to compare qualitative and quantitative values that were not normal, data expressed as median with inter-quartile range (IQR), and Kruskal-Wallis, respectively. Nominal variables were presented as frequency and percentage (%) were compared between studied groups using the Chi-square test. Correlation coefficient analysis was completed with Pearson's or Spearman rank. Whereas the point-biserial correlation coefficient is used in correlation analysis between continuous and binary variables. The receiver operating characteristic curve (ROC) analytical curve has been used to estimate the diagnostic efficiency of ERFE and TS% clinically viable by assay the ratio of area under the curve (AUC). ERFE has been recognized as an independent indicator of anemia in groups of patients through nominal regression data were expressed as odds ratios (OR), 95% confidence intervals (CI), and p values; Significance of differences was detected at $p<0.05$.

## 3. RESULTS AND DISCUSSION:

### 3.1. Demographic and clinical Characteristic of study populations

Demographic and laboratory clinical data characteristics of the CKD and HD patients are compared with Healthy subjects demonstrated in table 1. Sixty-five of CKD patients of different stages (1-5), and ranged in age (25-66) year were subdivided into thirty-five patients without hemodialysis, they are from (1-3) stages as CKD, and thirty patients with hemodialysis in (4-5) stage. These two populations of patients were compared with twenty-five healthy participation with matched age and gender.

The patients with CKD were a (mean ±SD) age of (50 ±10), range (25-63) years, about 23 (65.7%) were males, and 12 (34.3%) females, 4 (11.4%), and 11 (31.4) patients had TDM1 and TDM2, while 20 (57.1%) without Diabetic Mellitus respectively. The mean BMI (27.34±4.72) (kg/$m^2$), and the period of disease was (35.49±11.57) months. Only 12(34.3%) patients received ESA drugs, and 23 (65.7%) null ESA. The mean eGFR was (64.37±15.11) mg/mL/1.73 $m^2$, and the median (IQR) of Phosphate was 3.01(1.5) mg/dl, and calcium 8.9 (0.7) mg/dl.

In the HD patients had (mean±SD) age of (51.53±8.55), range (34-66) years, about 14 (46.7%) were male and 16 (53.3%) females, out of 30 HD patients, 5(16.7%) had TDM, 21(70.0%) TDM2, and 4(13.3%) without Diabetic Mellitus respectively. The mean BMI (27.88±3.64) kg/ $m^2$, and the disease period was (47.97±12.31) months. All patients of HD 30(100%) were treated with ESA. The mean eGFR was (12.21±6.16) mg/mL/1.73 $m^2$, and the median (IQR) of Phosphate and calcium were 4.65 (1.2) mg/dl and 7.3 (1.5) mg/dl, respectively.

Such patient outcomes were not significantly different $p>0.05$ in age (46.44±10.45), 13 (52%) males and 12 (48%) females compared to the healthy group. The Means of BMI (29.24±2.74) kg/$m^2$, but these were significant ($p<0.001$) decreased in variables eGFR (99.68±4.62) mg/mL/1.73$m^2$, and calcium were 9.1 (0.4) mg/dl, while a significant ($p<0.001$) increased of Phosphate 2.5 (1.0) mg/dl.

### 3.2. Relationship between Serum Erythroferrone Level and erythropoiesis status

In all study populations, after Tests of Normality (Kolmogorov-Smirnov), a skewed distribution of serum ERFE levels and the results represented as a median (IQR) value in Table 1 showed significantly ($p<0.001$) higher levels of ERFE 4, 6.1 ng/ml and a range of 2.2-10.5 ng/ml; mean 5.43 ng/ml for patients with CKD, and HD patients median (IQR) of 17.25 (13.4) ng/mL and a range (6.3-28.4) ng/ml; mean of 16.14 ng/ml when compared with a healthy group a median (IQR) of 2 (2.1) ng/ml and a rang (1.3-3.7) ng/ml; mean of 2.22 (ng/ml). Serum TS% levels showed a significantly increased in CKD (mean±SD) of (28.89±3.98) and (35.08±4.58) in HD patients as compared with the healthy group (mean±SD) of (24.4±3.56) ($p<0.001$).

Serum Ferritin levels indicated a significant increase in HD, a median (IQR) of 489 (118) ng/ml when compared with CKD, a median (IQR) of 121 (77) ng/ml; and a median (IQR) of 89 (25) ng/ml ($p<0.001$) for a healthy population. No significant difference in serum Iron levels between CKD and HD patients, but compared to healthy groups, rendered a highly significant difference ($p=0.02$). The results showed a significant decrease in mean of $RBC_S$ (4.34±0.56) ($10^6$/ml), and Hb levels (11.97±1.53) g/dl in patients with CKD and (4.06±0.43) ($10^6$/ml), and (11.24±1.56) g/dl; compared with healthy group $RBC_S$ of (4.68±0.42) ($X10^6$/ml), and Hb of (12.67±0.98) g/dl; ($p<0.001$, and $p=0.019$) respectively.

Person correlation coefficient or Spearman were estimated of ERFE with other Independent in both patients with CKD and HD (table 2). Serum ERFE level was a positively significant ($p < 0.001$) with the age ($r = 0.477$, and $r=0.6361$), treated with ESA ($r = 0.951$, and $r=1$), and DM ($r = 0.650$, and $r = 0/.41$) respectively. but it was inversely related with GFR ($r =-0.396$, and $r=-0.68$), TS% ($r =-0.842$, and $r=-0.877$), Ferritin ($r =-0.865$, and $r=-0.866$), Iron ($r =-0.860$, and $r=-0.851$), RBC ($r=-0.841$, and $r=-0.843$), hemoglobin ($r =-0.758$, and $-0.796$) respectively.

Despite the management of the fundamental disorders with anemia of chronic disease, and this was impracticable, persistent anemia accompanied symptoms and inaccurate diagnosis in many conditions; New therapeutic strategies to understand the pathophysiology of chronic disease anemia must be facilitated for this purpose. Recently, Dr. Kautz and colleagues in 2014 were discovered an important hormone in hematology (Kautz *et al.,* 2014). ERFE was the major role of iron supply as an erythropoietic regulator. It acts straight on liver cells to inhibit hepcidin expression (Kautz and Nemeth, 2014). Recent research has shown that ERFE plays a significant role in the increased severity of anemia in beta-thalassemia (Almousawi and Sharba, 2019; El-Gamal *et al.*, 2020). In the current study, ERFE has consistently been associated with mortality and progressive anemia in CKD and HD patients; However, publications that deal with these subjects in patients were very few studies in all world (Hanudel *et al.*, 2018; Honda *et al*., 2016; Spoto *et al*., 2019). This study was represented the modern study suggested in Iraq.

In The current study of CKD and patients under hemodialysis (HD) compared with the healthy group, I observed high levels of serum ERFE in both groups of patients CKD and HD as the comparison with healthy; this finding agreement with a recent study by author Ganz et al., ERFE level was measured in 97 HD patients (15.7 (7.9–32.5) ng/mL) but twice higher than in 51 patients with CKD 6.1 (2.6–15.0) ng/mL when compared with 161 healthy subjects 7.8 (4.7–13.2) ng/ml, (Ganz *et al.*, 2017). Moreover, another recent study in 2019 by Spoto *et al*. they have indicated a highly significant increase in serum levels of ERFE in both cohorts CKD, and HD with the mean value of (3.4–7.5, and 7.8 –10.5 ng/mL), respectively, with do not become significant in male and female patients. Who has advocated that ERFE was consistent with these patients and related to mortality and various severity with Cardiovascular events because these cohorts using ESA drugs lead to elevated serum ERFE level (Spoto *et al*., 2019). It has been extensively synthesized in the bone marrow and the spleen responsible for the erythropoietin hormone responsible for the erythroblasts to stimulate the survival and differentiation of the erythroid (Coffey *et al.*, 2018) or after exposures to blood loss and EPO injection (Kautz *et al.*, 2015; Rainville *et al.,* 2016). Because HD patients were persistent uptake of exogenous EPO hormone, it was stimulation and decreased renal clearance, thus elevated ERFE levels (Hanudel *et al.*, 2018). This was confirmed by the outcomes of the current study (Figure 2) showed a high level of serum ERFE in groups that deal with ESA more than a non-ESA group.

Additionally, the current study found correlations between ERFE levels and RBC, Hb, Ferritin, Iron, TS% inversely (Table 2). Agreement with recent studies of El Gendy *et al*. (El Gendy *et al.*, 2018). Who reported to that serum ERFE levels negatively correlated with serum iron (r=-

0.63; p=0.001), ferritin (r=-0.46; p=0.004), TS% levels (r=-0.66; p=0.001), and Hb (r =-0.39; p=0.01). Other studies (Honda *et al*., 2016; Sulovska *et al.*, 2016) also suggested that ERFE levels were negatively correlated with ferritin and hepcidin and positively correlated with sTfR in HD patients and that there was a positive correlation between hepcidin / ERFE ratio and hepcidin with those of ferritin.

These authors were attributed to the patients with IDA, ERFE as a physiological hepcidin suppressor, and elevated ERFE was an important role and injurious effects in clinical conditions with ineffective erythropoiesis such as β- thalassemia (Russo *et al.*, 2016). A study by (Kautz *et al*., 2015) indicated that significantly increased erythroblasts in ineffective erythropoiesis generate significant amounts of ERFE. On the other hence, patients with HD suffering from elevated iron accumulation as resultant, a major constituent of ineffective erythropoiesis, in which erythroblast count is greatly expanded, but the erythroblasts undergo intramedullary apoptosis before completing differentiation (Honda *et al.*, 2016; Mirciov *et al.*, 2017; Sulovska *et al*., 2016). Dysfunction of kidneys in patients with CKD and HD, inflammations, hypoxia, hemolysis, and iron status were affected by serum levels of hepcidin hormone (Wang *et al.*, 2017). This hormone regulates the iron absorption from the digestive canal. That iron stored out of the reticuloendothelial system is released. When it uses a recombinant Epo (rhEpo), this stimulated ERFE production suppresses hepcidin synthesized by inhibiting BMP/SMAD signaling in hepatocytes (Robach *et al.,* 2020).

On determining the critical point or threshold levels for serum TS% and ERFE levels to predict the development of anemia in CKD and HD patients, the results indicated that candidate TS% cutoff (>29.5) might not represent anemia. However, this result agrees with previous studies that describing that transferrin saturation (TS%) levels were assayed from fasting serum iron and transferrin concentrations, iron decreased in deficiency anemia highly changeable, accordingly, inappropriate for the iron depletion, and deficiency anemia; increased transferrin is synthesized associated with the iron store. As the TS% < 15%, the supply of iron for hemoglobin production in the bone marrow do not adequate; In that case, it is considered sensitive enough as screening tools of deficiency anemia (Clénin, 2017; Mikhali *et al.*, 2017). In other hence, we believed serum levels of TS%, if it is more than 15%, it is unsuitable tools for anemia; for example, most hereditary anemia such as thalassemia, have higher increased cutoff levels of TS% ≥75% and used to predict the iron overload, but these patients still suffering from severe anemia (Eissa and El-Gamal, 2014)

**3.3. ROC curve analysis for ERFE, and TS%**

By estimating the cutoff thresholds for parameters of erythropoiesis to identify patients with thresholds for serum ERFE and TS% levels to predict progressive anemia and emerging active erythropoiesis in patients. According the results which founded in Table 3, and Figure 1. In patients with HD the results of ROC curve analysis showed, (Figure.1A) Serum ERFE (ng/ml) was a highly positive cutoff ratio of > 3,650 (AUC= 0,996; sensitivity = 0,967; and specificity = 0,960) compared to the cutoff TS% of > 29,50 (AUC= 0,965; sensitivity = 0,867; and specificity = 0,96). But in patients with serum ERFE (ng/ml) was acknowledged as the superlative predictor of progressive anemia at a cutoff value of > 2.600 (AUC =0.894; sensitivity = 0.886 and a specificity = 0.760) in comparison with TS% levels at the cutoff > 29.50 (AUC =0.789; sensitivity =0.486; specificity = 0.960), (Figure.1B). Furthermore, ROC curve analysis of ERFE (ng/ml) was elevated of positive ratio in HD patients vs. CKD patients for a cutoff value of > 6.50 (AUC =0.919; sensitivity = 0.90, and a specificity = 0.68). (Figure.1C).

The results of Table 5 referred to Nominal Regression models to Estimates the predictors of ERFR in CKD and HD patients. The reference category is Healthy, in CKD patients, ERFE level of (OR=6.295, B=1.840, and Intercept=-5.159, p-value 0.001), as comparison high positive in HD patients of (OR=10.161, B=2.319, and Intercept=-9.569, p-value <0.001).

**3.3. Comparison between with and without Erythropoiesis Stimulating Agents (ESA) in measurements of erythropoiesis indicator**.

The results of the Box plot showed that ERFE and TS% high significantly (p<0.001) increased in HD patients with ESA treated (right green box) as a comparison with CKD patients with and without ESA (left green and blue box) (Figure 2A and B) respectively. The results indicated that both groups of HD and CKD patients with (ESA) a significant decrease (p<0.05) in the values of Hb and RBCs (green box plot) when compared to patients non -ESA treated (blue box plot). (Figure. 2C and D) respectively.

Th findings in the current study of Nominal Regression models and ROC analysis showed higher serum ERFE level (OR 10.161,95% CI

(3.281 to 31.467, and (AUC =0.991) in HD, more than (OR 6.295,95% CI (2.113 to 18.759), and (AUC=0.894) in CKD vs. healthy respectively. A recently study by Honda *et al.* (2019) that mentioned ERFE as an important biomarker in patients with CKD and the improvements following ESA management for this, the anemia in CKD patients requires a comprehensive assessment of ERFE levels with the attention of their best and physiological levels during erythropoiesis, as considering identifying variant ERFE as a specific biomarker of clonal erythropoiesis. (Bondu *et al.*, 2019). Despite these patients treated with ESA, significant numbers remain anemic (Atkinson and Warady, 2018). The current study supposed that associated with the prevalence of anemia in HD more than CKD because HD patients were persisted in ESA treatment lead to high expression of ERFE as a regulator of the erythroid mediator from erythroblast. It is a new sensitive biomarker in humans to estimate the relationship between iron metabolism and erythropoiesis and noticed that ESA might have a detrimental effect in the antidoping field (Kautz and Nemeth, 2014; Ramirez Cuevas *et al.*, 2020). As a result, hyperactivation of erythropoiesis and accelerated synthesis of the erythroid progenitor, but this undergo intramedullary apoptosis before the differentiation process is completed, therefore can cause anemia.

## 4. CONCLUSION:

Overall, the high levels of ERFE and the relationship with the hematological parameters of RBCs, HB, IRON, ferritin, and TS%, in HD patients WITH ESA treated more than CKD patients, has confirmed the suggested that regulatory role of ERFE in these parameters, and it possible that ERFE used as a successful tool for erythropoietic activity inspection in CKD and potential value in the identification of anemia risk, especially with ESAs treated. Future deep studies are needed to understand the role of ERFE as a biomarker of erythropoietic activity and exogenic erythropoietin (ESA) sensitivity at all levels of CKD-related anemia.

## 5. ACKNOWLEDGMENTS:

The author grateful for all the patients, physicians, and staff workers in the kidney disease unit laboratory at both Al-Sadder Teaching and Al-Hakeem General Hospitals; Who contributed to the accomplishment of the current study.

## 6. REFERENCES:

1. Almousawi, A. S., Sharba, I. R. (2019). Erythroferrone Hormone a Novel Biomarker is associated with Anemia and Iron Overload in Beta-Thalassemia Patients. Journal of Physics: Conference Series, 1294, 062045.
2. Abass RJ and Sharba IR. (2020). GDF-15 A potential Biomarker of Diabetic Nephropathy in Iraq Patients with Chronic Kidney Disease. Trop J Nat Prod Res, 4(12):1081-1087.
3. Atkinson, M. A., Warady, B. A. (2018). Anemia in chronic kidney disease. In *Pediatric Nephrology*.
4. Bondu, S., Alary, A.-S., Lefèvre, C., Houy, A., Jung, G., Lefebvre, T., Rombaut, D., Boussaid, I., Bousta, A., Guillonneau, F., Perrier, P., Alsafadi, S., Wassef, M., Margueron, R., Rousseau, A., Droin, N., Cagnard, N., Kaltenbach, S., Winter, S., Fontenay, M. (2019). A variant erythroferrone disrupts iron homeostasis in SF3B1 -mutated myelodysplastic syndrome . *Science Translational Medicine*, *11*(500), eaav5467.
5. Clénin, G. E. (2017). The treatment of iron deficiency without anaemia (in otherwise healthy persons). *Swiss Medical Weekly*, *147*(2324), 1–17.
6. Coffey, R., Sardo, U., Kautz, L., Gabayan, V., Nemeth, E., Ganz, T. (2018). Erythroferrone is not required for the glucoregulatory and hematologic effects of chronic erythropoietin treatment in mice. *Physiological Reports*, *6(19)*, e13890.
7. Eissa, D., El-Gamal, R. (2014). Iron overload in transfusion-dependent β-thalassemia patients: defining parameters of comorbidities. *The Egyptian Journal of Haematology*, *39(3)*, 164.
8. El-Gamal, R. A. E. R., Abdel-Messih, I. Y., Habashy, D. M., Zaiema, S. E. G., Pessar, S. A. (2020). Erythroferrone, the new iron regulator: evaluation of its levels in Egyptian patients with beta-thalassemia. *Annals of Hematology*, *99(1)*, 31–39.
9. El Gendy, F. M., El-Hawy, M. A., Shehata, A. M. F., Osheba, H. E. (2018). Erythroferrone and iron status parameters levels in pediatric patients with iron deficiency anemia. *European Journal of Haematology*, *100(4)*, 356–360.
10. Fishbane, S., Spinowitz, B. (2018). Update on Anemia in ESRD and Earlier Stages of CKD: Core Curriculum 2018. *American Journal of Kidney Diseases*. 2017.09.026
11. Ganz, T. (2019). Erythropoietic regulators of iron metabolism. *Free Radical Biology*

*and Medicine*, *133*, 69–74.
12. Ganz, T., Jung, G., Naeim, A., Ginzburg, Y., Pakbaz, Z., Walter, P. B., Kautz, L., Nemeth, E. (2017). Immunoassay for human serum erythroferrone. *Blood*, *130(10)*, 1243–1246.
13. Hanudel, M. R., Rappaport, M., Chua, K., Gabayan, V., Qiao, B., Jung, G., Salusky, I. B., Ganz, T., Nemeth, E. (2018). Levels of the erythropoietin-responsive hormone erythroferrone in mice and humans with chronic kidney disease. *Haematologica*, *103(4)*, e141–e142.
14. Honda, H., Hosaka, N., Ganz, T., Shibata, T. (2019). Iron Metabolism in Chronic Kidney Disease Patients. in CKD-Associated Complications: Progress in the Last Half Century. *Karger Publishers*, *198*, 103–111.
15. Honda, H., Kobayashi, Y., Onuma, S., Shibagaki, K., Yuza, T., Hirao, K., Yamamoto, T., Tomosugi, N., Shibata, T. (2016). Associations among erythroferrone and biomarkers of erythropoiesis and iron metabolism, and treatment with long-term erythropoiesis-stimulating agents in patients on hemodialysis. *PLoS ONE*, *11(3)*, 1–10.
16. Horak, E., Sunderman, W. (1974). An accurate spectrophotometric method for serum iron and iron-binding capacity without deproteinization or centrifugation. *Annals of Clinical and Laboratory Science*.
17. Kautz, Léon, Jung, G., Du, X., Gabayan, V., Chapman, J., Nasoff, M., Nemeth, E., Ganz, T. (2015). Erythroferrone contributes to hepcidin suppression and iron overload in a mouse model of β-thalassemia. *Blood*, *126(17)*, 2031–2037.
18. Kautz, Léon, Jung, G., Nemeth, E., Ganz, T. (2014). Erythroferrone contributes to recovery from anemia of inflammation. *Blood*, *124(16)*, 2569–2574.
19. Kautz, Leon, and Nemeth, E. (2014). Molecular liaisons between erythropoiesis and iron metabolism. *Blood, The Journal of the American Society of Hematology*, *124(4)*, 479–482.
20. Levey, A. S., Stevens, L. A., Schmid, C. H., Zhang, Y. L., Castro, A. F. Feldman, H. I., Kusek, J. W., Eggers, P., Van Lente, F., Greene, T., Coresh, J. (2009). A new equation to estimate glomerular filtration rate. *Annals of Internal Medicine*, *150*(9), 604–612.
21. Mikhali, A., Brown, C., Williams, J. A., Mathrani, V., Shrivastava, R., Evans, J., Issc, H., Bhandari, S. (2017). Clinical Practice Guideline Anaemia of Chronic Kidney Disease. *Anaemia of Chronic Kidney Disease*, *2017*(June), 7–49.
22. Mirciov, C. S. G., Wilkins, S. J., Dunn, L. A., Anderson, G. J., Frazer, D. M. (2017). Characterization of putative erythroid regulators of hepcidin in mouse models of anemia. *PLoS ONE*, *12*, 1.
23. Rainville, N., Jachimowicz, E., Wojchowski, D. M. (2016). Targeting EPO and EPO receptor pathways in anemia and dysregulated erythropoiesis. *Expert Opinion on Therapeutic Targets*, *20(3)*, 287–301.
24. Ramirez Cuevas, K., Schobinger, C., Gottardo, E., Voss, S. C., Kuuranne, T., Tissot, J. D., Favrat, B., Townsend, N., Leuenberger, N. (2020). Erythroferrone as a sensitive biomarker to detect stimulation of erythropoiesis. *Drug Testing and Analysis*, *12(2)*, 261–267.
25. Robach, P., Gammella, E., Recalcati, S., Girelli, D., Castagna, A., Roustit, M., Lundby, C., Lundby, A.-K., Bouzat, P., Vergès, S., Séchaud, G., Banco, P., Uhr, M., Cornu, C., Sallet, P., Cairo, G. (2020). Induction of erythroferrone in healthy humans by micro-dose recombinant erythropoietin or high-altitude exposure. *Haematologica*.
26. Russo, R., Andolfo, I., Manna, F., De Rosa, G., De Falco, L., Gambale, A., Bruno, M., Matte, A., Ricchi, P., Girelli, D., De Franceschi, L., Iolascon, A. (2016). Increased levels of ERFE-encoding FAM132B in patients with congenital dyserythropoietic anemia type II. *Blood*, *128(14)*(14), 1899–1902.
27. Sharba, I. R., Al-Zahid, J. M. (2016). Relationship of Sclerostin with PTH and Erythropoietin in-patient with CKD on dialysis in AL-Najaf Province. *International Journal of Advanced Research*, *4(2)*, 601–610.
28. Spoto, Kakkar, Lo, Devalaraja, Pizzini, Torino, Leonardis, Cutrupi, Tripepi, Mallamaci, Zoccali. (2019). Serum Erythroferrone Levels Associate with Mortality and Cardiovascular Events in Hemodialysis and in CKD Patients: A Two Cohorts Study. *Journal of Clinical Medicine*, *8(4)*, 523.
29. Sulovska, L., Holub, D., Zidova, Z., Divoka, M., Hajduch, M., Mihal, V., Vrbkova, J., Horvathova, M., and Pospisilova, D. (2016). Characterization of iron

metabolism and erythropoiesis in erythrocyte membrane defects and thalassemia traits. *Biomedical Papers*, *160(2)*, 231-237.
30. Van Kampen EJ, Zijlstra WJ. (1961). Standardization of hemoglobinometry II The hemiglobincyanide method. Clin Chim Acta 1961; 6: 538-44
31. Wang, C., Fang, Z., Zhu, Z., Liu, J., Chen, H. (2017). Reciprocal regulation between hepcidin and erythropoiesis and its therapeutic application in erythroid disorders. *Experimental Hematology*, *52*, 24–31.
32. Wassmuth, A. K., Riond, B., Hofmann-Lehmann, R., Lutz, H. (2011). Evaluation of the mythic 18 hematology analyzer for use with canine, feline, and equine samples. *Journal of Veterinary Diagnostic Investigation*, *23*(3), 436–454.
33. Webster, A. C., Nagler, E. V., Morton, R. L., Masson, P. (2017). Chronic Kidney Disease. In *The Lancet*. 6736(16)32064-5.

***Table 1.*** *Clinical demographic and laboratory data characteristics of CKD and HD patients with healthy subjects*

| VARIABLES | CKD n=35 | | HD n=30 | | Healthy n=25 | | p-value |
|---|---|---|---|---|---|---|---|
| | Statistics value | 95% CI | Statistics value | 95% CI | Statistics value | 95% CI | |
| Age (year) mean (SD) | 50.86 (10.0) | 47.42-54.29 | 51.53 (8.55) | 48.34-54.73 | 46.44(10.45) | 42.13-50.75 | 0.117 |
| Male Female n (%) | 23(65.7%) 12(34.3%) | - | 14(46.7%) 16(53.3%) | - | 13(52%) 12(48%) | - | 0.279 |
| No-DM n (%) | 20(57.1%) | | 4(13.3%) | | 25(100%) | | |
| TDM1 n (%) | 4(11.4%) | - | 5(16.7%) | - | 0 0.0% | - | <0.001 |
| TDM2 n (%) | 11(31.4%) | | 21(70.0%) | | 0 0.0% | | |
| Non-ESA n (%) | 23(65.7%) ab | - | 0 (0.0%) ab | - | 25(100%) | - | <0.001 |
| ESA n (%) | 12(34.3%) ab | | 30(100%) ab | | 0(0.0%) | | |
| BMI (kg/m2) Mean (SD) | 27.34 (4.72) | 25.72-28.96 | 27.88 (3.64) | 26.53-29.24 | 29.24 (2.74) | 28.11-30.37 | 0.245 |
| Period diseases (mo.) mean (SD) | 35.49 (11.57) a | 31.51-39.46 | 47.97 (12.31) ab | 43.37-52.56 | 0.00 | 0.00 | <0.001 |
| GFR (mL/min/1.73m2) Mean (SD) | 64.37 (15.11) ab | 59.18-69.56 | 12.21 (6.16) ab | 9.91-14.51 | 99.68 (4.62) | 97.77-101.59 | <0.001 |
| Phosphate (mg/dl) Median (IQR) | 3.01 (1.5) ab | 2.82-3.46 | 4.65 (1.2) ab | 4.20-4.95 | 2.5 (1.0) | 2.26-2.76 | <0.001 |
| Calcium (mg/dl) Median (IQR) | 8.9 (0.7) b | 8.48-8.86 | 7.3 (1.5) ab | 7.12-7.76 | 9.1 (0.4) | 8.87-9.17 | <0.001 |
| TS% mean (SD) | 28.89 (3.98) ab | 27.52-30.26 | 35.08 (4.58) ab | 33.37-36.79 | 24.40 (3.56) | 22.93-25.87 | <0.001 |
| Ferritin (ng/ml) Median (IQR) | 121 (77) b | 108.04-136.24 | 489 (118) ab | 449.6-529.48 | 89 (25) | 80.11-95.73 | <0.001 |
| IRON (mg/ml) mean (SD) | 64.77 (21.56) a | 57.36-72.18 | 61.18 (22.23) a | 52.88-69.48 | 49.92 (15.33) | 43.59-56.25 | 0.020 |
| ERFE (ng/mL) Median (IQR) | 4.0 (6.1) ab | 4.41-6.46 ab | 17.25 (13.4) ab | 13.35-18.93 | 2.0 (1.2) | 1.91-2.52 | <0.001 |
| RBC (X106/ml) Mean (SD) | 4.34 (0.56) ab | 4.15-4.53 | 4.06 (0.43) ab | 3.99-4.32 | 4.68 (0.42) | 4.50-4.85 | <0.001 |
| Hb (g/dl) Mean (SD) | 11.97 (1.53) ab | 11.45-12.50 | 11.24 (1.65) ab | 11.03-12.62 | 12.67 (0.98) | 12.26-13.07 | 0.019 |

*a: Significant difference between groups of patients CKD, and HD with the healthy group at p-value <0.05. b: Significant differences between the groups of patients CKD, and HD at p-value <0.05. SD: Standard deviation, IQR: Inter Quartile range, CI: Confidence interval, TDM: Type Diabetic Mellites, ESA: Erythropoiesis-stimulating agents, BMI: Body Max Index, GFR: Glomerular Filtration Rate, TS: Transferrin saturate.*

***Table 2:*** *Correlation coefficient of ERFE with other variables in both CKD and HD patients.*

| VARIABLES | CKD n=53 | | | HD n=30 | | |
|---|---|---|---|---|---|---|
| | r | R squared | P-value (two-tailed) | r | R squared | P-value (two-tailed) |
| Age (year) | 0.477 | 0.228 | 0.006 [ab] | 0.636 | 0.405 | 0.001 [ab] |
| ESA | 0.951 | 0.904 | 0.001 [ab] | 1 | 1 | 0.001 [ab] |
| DM | 0.650 | 0.422 | 0.001 [ab] | 0.41 | 0.168 | 0.02 [a] |
| GFR (mL/min/1.73 m2) | -0.396 | 0.157 | 0.02 [a] | -0.68 | 0. 462 | 0.001 [ab] |
| TS% | -0.842 | 0.709 | 0.001 [ab] | -0.877 | 0.769 | 0.001 [ab] |
| Iron (mg/ml) | -0.865 | 0.7478 | 0.001 [ab] | -0.866 | 0.748 | 0.001 [ab] |
| Ferritin (ng/ml) | -0.860 | 0.740 | 0.001 [ab] | -0.851 | 0.724 | 0.001 [ab] |
| RBC ($X10^6$/ml) | -0.841 | 0.706 | 0.001 [ab] | -0.843 | 0.710 | 0.001 [ab] |
| Hb (g/dl) | -0.758 | 0.575 | 0.001 [ab] | -0.796 | 0.63 | 0.001 [ab] |

*[a] significant difference at p-value <0.05. [ab] significant differences at p-value <0.01*

***Table 3.*** *ROC curve analysis for the viability of ERFE (ng/ml), and TS% to use a clinically diagnostic of anemia between both patients' groups CKD and HD and with healthy subject*

| CATEGORIES | CKD n=35 vs. Healthy n=25 | | HD n=30 vs. Healthy n=25 | | HD n=30 vs. CKD n=35 | |
|---|---|---|---|---|---|---|
| | ERFE | TS% | ERFE | TS% | ERFE | TS% |
| AUC | 0.894 | 0.789 | 0.996 | 0.965 | 0.920 | 0.8410 |
| Std. Error | 0703.040 | 0.059 | 0.005 | 0.022 | 0.036 | 0.047 |
| 95% CI | 0.816-0.972 | 0.673-0.904 | 0.986-0.00 | 0.921-0.000 | 0.828 - 0.97 | 0.747-0.934 |
| Youden index | 0.647 | 0.446 | 0.927 | 0.827 | 0.676 | 0.490 |
| Optimum Cutoff | > 2.600 | > 29.50 | > 3.650 | > 29.50 | > 7.80 | > 33.1 |
| Sensitivity | 0.886 | 0.486 | 0.967 | 0.867 | 0.933 | 0.633 |
| 95% CI | 0.740- 0.954 | 0.329-0.644 | 0.833-0.99 | 0. -0.947 | 0.786-0.99 | 0.455-0.781 |
| Specificity | 0.760 | 0.960 | 0.960 | 0.960 | 0.743 | 0.857 |
| 95% CI | 0.5650.885 | 0.804-0.997 | 0.805-0.998 | 0.805-0.998 | 0.5790-0.858 | 0.706-0.937 |
| Likelihood ratio | 3.690 | 12.140 | 24.170 | 21.670 | 3.630 | 4.433 |
| P- value | <0.001a | <0.001 a | <0.001 a | <0.001 a | <0.001 a | <0.001 a |

*AUC: Aera Under Curve. CI: Confidence interval a significant difference at p-value <0.05.*

***Table 4.*** *Nominal Regression models to Parameter Estimates ERFR as independent predictors in CKD and HD patients*

| PATIENTS GROUPS [a] | | B | Std. Error | Wald | df | Sig. | OR | 95% CI for OR | |
|---|---|---|---|---|---|---|---|---|---|
| | | | | | | | | Lower | Upper |
| CKD | Intercept | -5.159 | 1.544 | 11.173 | 1 | 0.001 | | | |
| | ERFE (ng/mL) | 1.840 | 0.557 | 10.907 | 1 | 0.001 | 6.295 | 2.113 | 18.759 |
| | TS% | 0.685 | 0.234 | 8.550 | 1 | 0.003 | 1.984 | 1.254 | 3.141 |
| | RBC (X106/ml) | -2.085 | 1.450 | 2.068 | 1 | 0.150 | 0.124 | 0.007 | 2.131 |
| | Hb (g/dl) | -.510 | 0.472 | 1.169 | 1 | 0.280 | 0.601 | 0.238 | 1.513 |
| HD | Intercept | -9.569 | 1.957 | 23.909 | 1 | 0.001 | | | |
| | ERFE ng/mL) | 2.319 | 0.577 | 16.163 | 1 | <0.001 | 10.161 | 3.281 | 31.467 |
| | TS% | 1.961 | 0.581 | 11.412 | 1 | 0.001 | 7.109 | 2.278 | 22.185 |
| | RBC (X106/ml) | -6.500 | 2.635 | 6.086 | 1 | 0.014 | 0.002 | 8.603E-6 | 0.263 |
| | Hb (g/dl) | -2.443 | 1.315 | 3.449 | 1 | 0.063 | 0.087 | 0.007 | 1.145 |

*a. The reference category is Healthy. CI: Confidence interval. OR: Odds Ratio. df: degree freedom.*

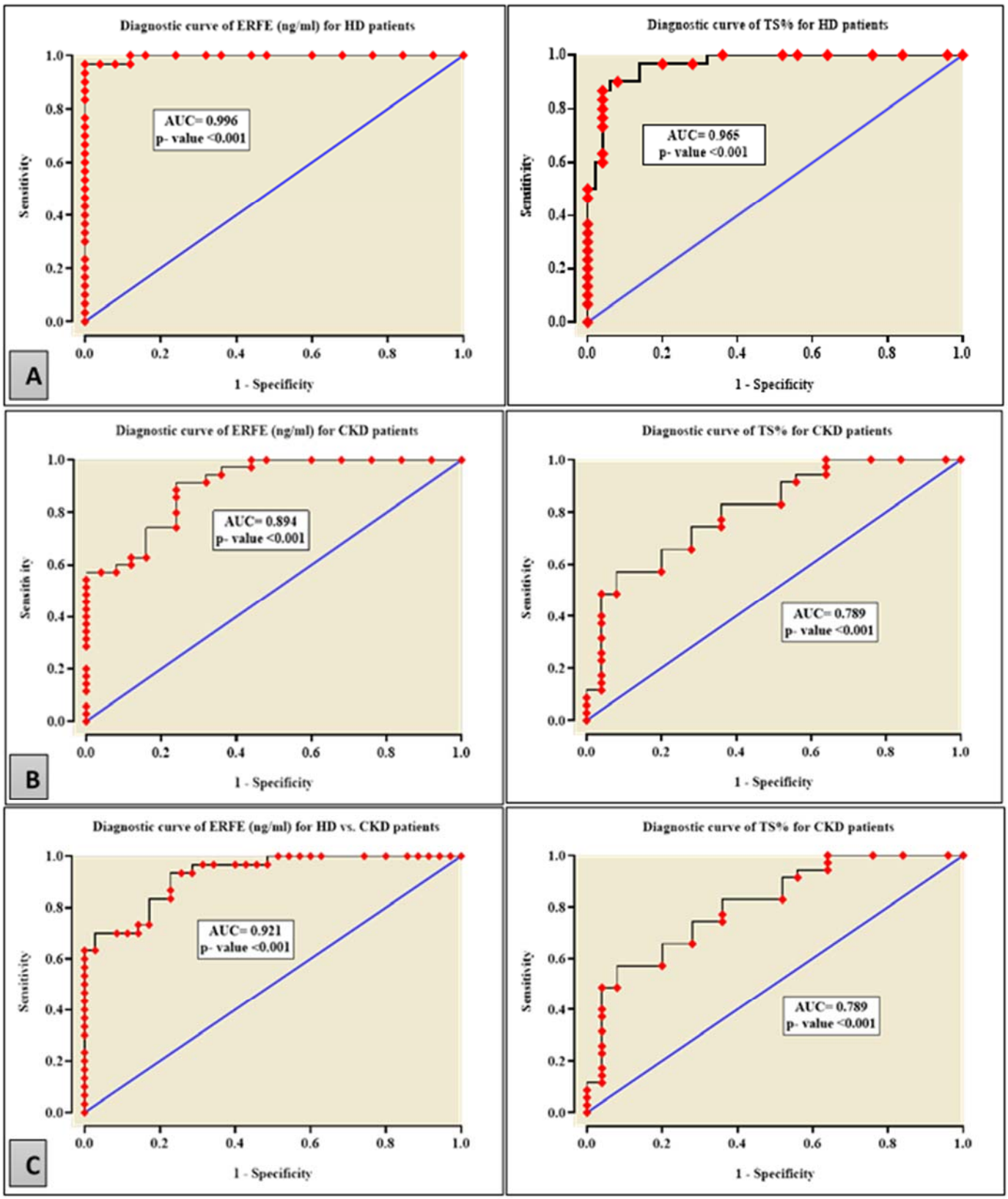


***Figure 1****: Receiver operating characteristic curve (ROC) analysis of ERFE, and TS% for a viability diagnostic of (A) HD patients vs. healthy subjects by ERFE (upper), and TS% (lower). (B) CKD patients vs. healthy subjects by ERFE (upper), and TS% (lower). (C) HD vs. CKD subject by ERFE (upper), and TS% (lower).*

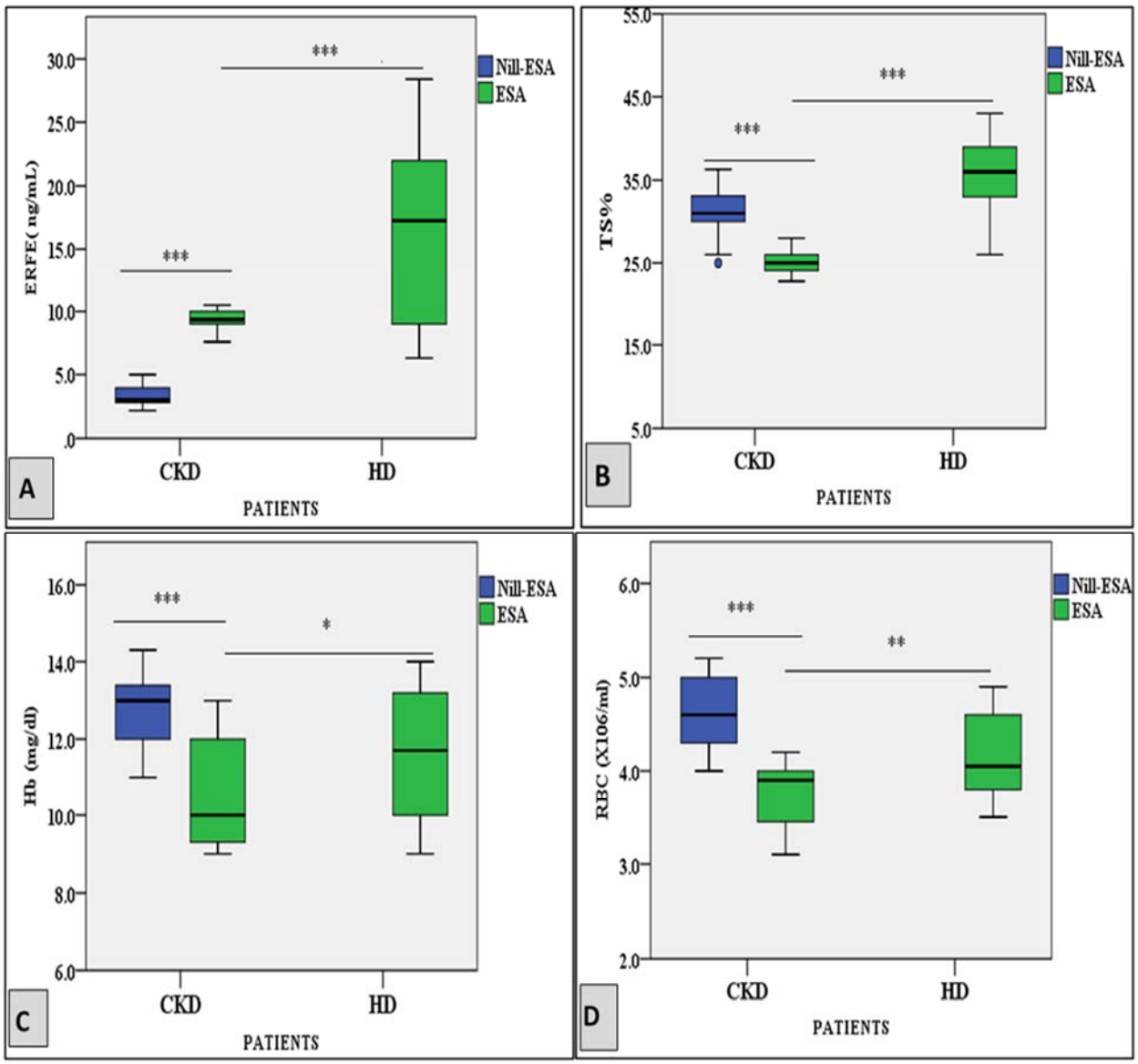


***Figure.2****. Box plot showing a change of serum ERFE, TS%, HB, and RBC in CKD and HD patients with and without erythropoiesis-stimulating agents (ESA). A= Serum ERFE levels. B=TS%, C=HB, and D=RBC. Significant differences at three levels: * p-value <0.05, ** p-value<0.01, and *** p-value<0.001.*

PERIÓDICO TCHÊ QUÍMICA
ARTIGO ORIGINAL

# O EFEITO DA IMPLEMENTAÇÃO DA AUTOAVALIAÇÃO NOS PROCESSOS CIENTÍFICOS NAS ATITUDES CIENTÍFICAS E OS RESULTADOS DA APRENDIZAGEM DE FÍSICA, CONTROLANDO O CONHECIMENTO INICIAL

# THE EFFECT OF THE IMPLEMENTATION OF SELF ASSESSMENT WITH SCIENCE PROCESSES ON SCIENTIFIC ATTITUDES AND PHYSICS LEARNING OUTCOMES BY CONTROLLING INITIAL KNOWLEDGE

# PENGARUH IMPLEMENTASI ASESMEN DIRI BERMUATAN PROSES SAINS TERHADAP SIKAP ILMIAH DAN HASIL BELAJAR FISIKA DENGAN MENGONTROL PENGETAHUAN AWAL

WILANTARA, I Putu Eka[1*]; SUMA[2], Ketut; SUARNI[3], Ni Ketut; CANDIASA[4], I Made

[1] Ganesha University of Education, Faculty of Math and Science, Science Education Department. Indonesia.

[2] Ganesha University of Education, Faculty of Math and Science, Physics Department. Indonesia.

[3] Ganesha University of Education, Faculty of Science Education, Guidance and Counselling Department. Indonesia.

[4] Ganesha University of Education, Faculty of Math and Science, Mathematics Department. Indonesia.

** Corresponding author*
*e-mail: ewilantara@yahoo.com*

Received 19 December 2020; received in revised form 02 February 2021; accepted 20 February 2021

## RESUMO

**Introdução:** Diversos estudos demonstram que a autoavaliação contendo processos científicos aplicados na aprendizagem de física afetará a atitude científica e os resultados de aprendizagem de física dos alunos. Verificou-se também que o conhecimento inicial também contribui para determinar o nível de atitudes científicas e os resultados de aprendizagem de física dos alunos. No entanto, o conhecimento inicial precisa ser controlado para que o efeito puro da autoavaliação no aprendizado da física nas atitudes científicas e nos resultados do aprendizado da física seja conhecido. **Objetivos:** Este estudo examinou o efeito da implementação da autoavaliação com processos científicos sobre as atitudes científicas e os resultados da aprendizagem de física, controlando o conhecimento inicial. **Metodos:** Esta pesquisa foi conduzida com uma abordagem quase experimental para 143 alunos do primeiro ano do ensino médio com especialização em ciências na cidade de Singaraja (Indonésia) utilizando um projeto de grupo independente de fator único com o uso de covariável. A amostra da pesquisa foi escolhida por meio da técnica de amostragem aleatória em múltiplos estágios. Os instrumentos utilizados foram um questionário de atitude científica, o teste de conhecimento inicial e o teste de resultado do aprendizado de física. Os dados foram processados por meio de análise de covariância multivariada. **Resultados e Discussões:** Os resultados mostraram que houveram diferenças nas atitudes científicas e nos resultados de aprendizagem dos alunos que realizaram o aprendizado de física com a autoavaliação contendo o processo de ciências e dos alunos que realizaram o aprendizado da física com a avaliação convencional após controlar seus conhecimentos iniciais, de forma independente ou simultaneamente. O conhecimento prévio dos alunos contribuiu para as atitudes científicas em 22,8% e para os resultados do aprendizado de física em 19,4%. **Conclusões:** concluíu-se que a autoavaliação contendo processos científicos na aprendizagem de física afetou as atitudes científicas e os resultados da aprendizagem ao controlar o conhecimento inicial.

**Palavras-chave**: *autoavaliação, processo científico, atitude científica, resultados de aprendizagem de física, conhecimento inicial.*

## ABSTRACT

**Background:** Various studies show that self-assessment containing scientific processes applied in physics learning will affect the scientific attitude and the physics learning outcomes of the students. It is also found that Initial knowledge also contributes to determining the level of scientific attitudes and the physics learning outcomes of physics. However, initial knowledge needs to be controlled so that the pure effect of self-assessment in learning physics on scientific attitudes and learning outcomes of physics is known. **Aim:** This study examines the effect of the implementation of self-assessment with science processes on scientific attitudes and physics learning outcomes by controlling initial knowledge. **Methods:** This research was conducted with a quasi-experimental approach to 143 1st grade high school students majoring in science in Singaraja City using a single factor independent group design with the use of covariate. The sample of the research was chosen by using a multistage random sampling technique. The instruments used were the scientific attitude questionnaire, the initial knowledge test, and the physics learning outcome test. The data were processed using multivariate covariance analysis. **Results and Discussion:** The results showed that there were differences in scientific attitudes and learning outcomes of students who took physics learning with self-assessment containing the science process and students who took physics learning with the conventional assessment after controlling their initial knowledge, either independently or simultaneously. The prior knowledge of the students contributed to scientific attitudes by 22.8%, and to physics learning outcomes by 19.4%. **Conclusions:** it can be concluded that self-assessment containing scientific processes in physics learning affected scientific attitudes and learning outcomes by controlling initial knowledge.

**Keywords:** *self-assessment, science process, scientific attitude, learning outcomes of physics, initial knowledge*

## ABSTRAK

**Latar Belakang:** Berbagai penelitian menunjukkan bahwa penilaian diri yang mengandung proses ilmiah yang diterapkan dalam pembelajaran fisika akan mempengaruhi sikap ilmiah dan hasil belajar fisika siswa. Ditemukan juga bahwa pengetahuan awal juga berkontribusi untuk menentukan tingkat sikap ilmiah dan hasil belajar fisika siswa. Namun, pengetahuan awal perlu dikontrol sehingga efek murni penilaian diri dalam belajar fisika pada sikap ilmiah dan hasil belajar fisika dapat diketahui. **Tujuan:** Penelitian ini meneliti efek dari pelaksanaan penilaian diri dengan proses sains pada sikap ilmiah dan hasil pembelajaran fisika dengan mengendalikan pengetahuan awal. **Metode:** Penelitian ini dilakukan dengan pendekatan kuasi-eksperimental kepada 143 siswa SMA kelas 1 jurusan SAINS di Kota Singaraja dengan menggunakan satu faktor desain kelompok mandiri dengan penggunaan kovaat. Sampel penelitian dipilih dengan menggunakan teknik multistage random sampling. Instrumen yang digunakan adalah kuesioner sikap ilmiah, tes pengetahuan awal, dan tes hasil belajar fisika. Data diproses menggunakan analisis kovarians multivariat. **Hasil dan Diskusi:** Hasil penelitian menunjukkan bahwa ada perbedaan sikap ilmiah dan hasil belajar siswa yang mengambil pembelajaran fisika dengan penilaian diri yang berisi proses sains dan siswa yang mengambil pembelajaran fisika dengan penilaian konvensional setelah mengendalikan pengetahuan awal mereka, baik secara mandiri atau bersamaan. Pengetahuan siswa sebelumnya berkontribusi pada sikap ilmiah sebesar 22,8%, dan hasil pembelajaran fisika sebesar 19,4%. **Kesimpulan:** Dapat disimpulkan bahwa penilaian diri yang mengandung proses ilmiah dalam pembelajaran fisika mempengaruhi sikap ilmiah dan hasil belajar dengan mengendalikan pengetahuan awal.

**Kata kunci**: *asesmen diri, proses sains, sikap ilmiah, hasil belajar fisika, pengetahuan awal*

## 1. INTRODUCTION:

### 1.1 Background

The biggest challenge in the era of industrial revolution 4.0 is accelerating technological changes that affect every life aspect. In the 21st century, the industrial revolution with massive changes in various fields eliminates the boundaries between the physical, digital, and biological worlds (Gandasari *et al*., 2020).

It takes strategic maturity as well as mental strength to be able to compete in global competition. In this case, education needs to make breakthroughs in various innovations to create a smart, qualified, and competitive generation (Wan et al., 2020). The national education system faces very complex challenges in preparing human resources to compete in the era of globalization (Malik, 2019).

To prepare human resources who can compete in globalization, a quality education system is needed. Quality education functions to develop capabilities and shape the character and

civilization of a nation with dignity in order to educate the people's life, develop the potential of students to become human beings who believe and fear the Almighty God, have a noble character, are healthy, knowledgeable, capable, creative, independent and become a democratic and responsible citizen.

The low quality of Indonesia's human resources in global competition is a challenge in education. Students must be able to achieve various competencies with the application of Higher Order Thinking Skills or HOTS (Pratama and Retnawati, 2018).

These competencies include critical thinking, creative and innovative thinking, communication skills, collaboration skills, and confidence. These five factors are the character targets attached to the evaluation system and are part of the skills of the 21st century (Suarni, 2019).

The results of the Trends in International Mathematics and Science Study (TIMSS), the Program for International Student Assessment (PISA), the results of the National Physics Examination of Buleleng Regency High School students for the 2018/2019 academic year, findings of the low level of student science process skills and findings related to research on the scientific attitudes of the students show that there are problems with science process skills, physics learning outcomes and student scientific attitudes. The factors that determine learning outcomes, process skills, and scientific attitudes include teachers, learning, assessment, students, and the environment. (Jain and Prasad, 2018). These factors must always be considered in achieving learning objectives. The most dominant factors affecting learning outcomes and scientific attitudes are learning and assessment factors.

The concerns of education experts, supported by the results of the two international studies above, should be used as a basis for reorienting the learning process (Gürses *et al*., 2015). Many factors cause the low ability of our students. One of the contributing factors is that students are generally less trained to work on real life problems. This situation is not in line with the characteristics of TIMSS and PISA questions, whose substance is contextual, which demands reasoning, argumentation, and creativity in solving them (Muszyński, 2020).

In the learning process, students are also required to have direct experience to develop their skills. By using process skills in learning, there will be interactions between the concepts/principles/theories that have been found (Kurniawati, 2019). With these interactions, the attitudes and values required for scientific discovery will emerge. These values include: conscientious, creative, diligent, tolerant, responsible, critical, objective, diligent, honest, open, and disciplined (Mulyeni et al., 2019).

Direct experiences as learning experiences can be used to develop science process skills (Zeitoun and Hajo, 2015). Through direct experience, one can become more deeply involved in the process. One of the other dominant factors considered to influence scientific attitudes and physics learning outcomes is the assessment used by the teacher in assessing the process and learning outcomes of physics learning. In the learning cycle, assessment is one of the stages whose role is very important and cannot be ignored.

The assessment model that is suitable for learning with a scientific approach is an authentic assessment. It is strongly relevant to scientific approach as this type of assessment can depict an increase in the learning outcomes of the students, either in the context of observing, reasoning, experimenting, building networks, or others (Sabri *et al*., 2019).

Authentic assessments tend to focus on complex or contextual tasks, enabling students to demonstrate their competencies, including attitudes, knowledge, and skills. Educators can use the authentic assessment results to plan programs for improvement, enrichment, or counseling services (Taufina and Chandra, 2018). Also, authentic assessment results can be used as materials to improve the learning process that meets educational assessment standards.

One of the authentic assessments that fit the constructivism paradigm is self-assessment (Ratminingsih et al., 2018). Self-assessment is an assessment technique in which students are asked to assess themselves concerning the process and level of achievement of their learning (Kunandar, 2015). Self-assessment is an assessment carried out by students in assessing activities or work carried out by themselves. The role of assessment in learning is basically to identify the gaps between the achievements achieved and the expected achievements and provide opportunities for students to overcome these gaps (Wride, 2017).

The use of assessment is not just knowing the achievement of learning outcomes, what is

more, important is how the assessment can improve the ability of students in the learning process. Assessment is carried out through three approaches, (1) assessment of learning, (2) assessment for learning, and (3) assessment as learning (Hidayati, 2017).

Self-assessment as an assessment as learning functions as a formative assessment during the learning process (Sadeghi and Rahmati, 2017). In its implementation, self-assessment involves students actively in these assessment activities. Assessment as learning is an assessment process carried out by educators that allow students to see their learning achievements and progress to determine learning targets (Earl and Katz, 2006).

Self-assessment containing scientific processes is very urgent to be applied. This is in order to transform the assessment in the measurement of the scientific process. PISA has identified three major dimensions of scientific literacy, namely the science process, science content, and the context of science application. The scientific process refers to the mental processes involved when answering a question or solving a problem, such as identifying and interpreting evidence and explaining conclusions (Bahar and Aksüt, 2020).

The scientific process is the application of the scientific method in understanding, developing, and discovering science (Darling-Hammond et al., 2020). The scientific process is very important for every student to use the scientific method in developing science, and it is hoped that they will acquire new knowledge/develop the knowledge they already have (Mehtap *et al*., 2020).

Self-assessment containing the scientific process provides opportunities for students to carry out their learning activities according to their needs, abilities, and interests and opportunities for self-reflection and the application of the scientific process itself. These opportunities provide a very broad space for students to improve learning outcomes and scientific attitudes. Thus, self-assessment containing scientific processes in physics learning can affect scientific attitudes and learning outcomes of physics.

Luque's finding was that self-assessment improved the skills of their students during the learning process. Students will have good classroom abilities and in the family environment (Luque and Mendoza, 2019). The research results from Pantiwati also state that self-assessment in learning can increase metacognitive awareness, which will have implications for the competence of the students (Pantiwati and Husamah, 2017).

The study of a literature review of 37 empirical studies in the last decade (2008-2018), which aims to investigate the contribution of the self-assessment of the students to increased learning motivation, increased academic achievement, development of independent learning, and increased self-esteem, found that most of the studies that concluded that the self-assessment of the students contributes positively in improving the quality of learning (Papanthymou and Darra, 2018).

Apart from assessment as an external factor, the learning process is also influenced by internal factors such as interest, motivation, intelligence, self-concept, cognitive style, initial knowledge, and others. Internal factors related to scientific attitudes and physics learning outcomes are initial knowledge. Initial knowledge is the knowledge that students have before the learning process in the classroom, obtained through informal learning or daily experiences and formal learning at school at a previous level. Initial knowledge is an asset for students in learning activities because learning activities are a vehicle for negotiating meaning between teachers and students regarding learning materials (Juhji and Nuangchalerm, 2020).

Based on the above description, it can be assumed that self-assessment containing scientific processes applied in physics learning will affect the scientific attitude and the physics learning outcomes of the students. Initial knowledge also contributes to determining the level of scientific attitudes and the physics learning outcomes of the students. Initial knowledge is an internal factor that influences the scientific attitudes and physics learning outcomes of the students. Initial knowledge needs to be controlled so that the pure effect of self-assessment in learning physics on scientific attitudes and learning outcomes of physics is known.

To prove this assumption, a study was conducted to examine the effect of self-assessment with scientific processes in learning physics on scientific attitudes and learning outcomes by controlling initial knowledge.

### 1.2 Research Problems

Following the background of the problem, the

formulation of the research problems is as follows. 1) Are there differences in scientific attitudes and physics learning outcomes between students who take physics learning with self-assessment with scientific processes and students who take physics learning with conventional assessment individually? 2) Are there differences in scientific attitudes and physics learning outcomes between students who take physics learning with self-assessment with scientific processes and students who take physics learning with the conventional assessment after controlling their initial knowledge either individually or simultaneously? 3) How big is the contribution of the initial knowledge of the students to the scientific attitudes and physics learning outcomes of students?

### 1.3 Research Significance

Theoretically, the results of this study are expected to provide empirical support for the effectiveness of self-assessment with scientific processes in improving the scientific attitudes and learning outcomes of the students. This empirical evidence will strengthen the theory, concepts, and practices of self-assessment as a learning assessment.

Its theoretical value for education is that the results of this study can be used as a theoretical reference, which can be further developed in further studies, thereby increasing insight into the field of assessment.

The results of this study are expected to contribute ideas in order to develop the repertoire of science in education and improve the quality of natural science education, especially physics. The practical value of this research can be used by educational experts and practitioners, especially concerning the use of assessment models to improve physics education quality.

For education experts, the practical value is that the results of this research can be used as an empirical reference that can be developed in the form of further studies and research to gain insight into the field of learning and evaluation in physics. For practitioners, the practical value is that the results of this study can be applied in the learning process to improve the quality of physics learning in high schools.

## 2. MATERIALS AND METHODS:

The hypotheses of this study are as follows. 1) There are differences in scientific attitudes and physics learning outcomes between students who take physics learning with self-assessment with scientific processes and students who take physics learning with conventional assessment either individually or simultaneously, 2) There are differences in scientific attitudes and physics learning outcomes between students who take physics learning with self-assessment containing scientific processes and students who take physics learning with the conventional assessment after controlling initial knowledge either individually or simultaneously, 3) Initial knowledge contributes to the scientific attitudes and physics learning outcomes of the students.

This research was conducted at public high schools in Singaraja City, Buleleng Regency, Bali. The schools that implemented the 2013 curriculum include Public High Schools no 1,2,3, and 4 Singaraja. The selection of the schools was based on affordability and feasibility considerations. Affordability is easy to access so that the smooth running of research can be guaranteed. Feasibility is an opportunity to realize experimental learning. Also, no similar research has been conducted at the research site.

This research was conducted with a quasi-experimental approach in high school students in Singaraja City using a single factor independent group design using covariate. The experimental design matrix is shown in Table 1.

**Table 1**. Experimental Design Matrix

| **Assessment (A)** | | | | | |
|---|---|---|---|---|---|
| ($A_1$) | | | ($A_2$) | | |
| X | $Y_1$ | $Y_2$ | X | $Y_1$ | $Y_2$ |
| . | . | . | . | . | . |
| . | . | . | . | . | . |

Explanation:

$A_1$ : Self-assessment containing a scientific
$A_2$ : process
X : Conventional
$Y_1$ : Assessment

$Y_2$ Initial Knowledge
Scientific Attitude
Physics Learning
Outcomes

The research procedure was carried out in three stages: the initial stage, the experimental stage, and data collection, and the final stage. This study involved 143 1st grade high school students majoring in science as the research sample, drawn by a multistage random sampling technique. Data collection using instruments: 1) scientific attitude questionnaire with a reliability coefficient of 0.887; 2) physics learning outcomes test with a reliability coefficient of 0.618, and 3) the initial knowledge test with a reliability coefficient of 0.837.

The treatment variable in this study was self-assessment containing the scientific process. The class designated as the experimental group followed the physics learning with self-assessment containing the scientific process. The class designated as the control group took the physics lesson with a conventional assessment.

Hypothesis testing used multivariate covariance analysis with the help of the SPSS 23.0 program. Hypothesis testing used a significance level $\alpha$ = 0.05. The prerequisite testing for data analysis conducted before testing the hypothesis includes testing for normality of data distribution, multivariate normality, homogeneity of group variance, regression linearity, the meaning of regression lines, the similarity in the slope of regression direction, and multicollinearity.

## 3. RESULTS AND DISCUSSION:

### 3.1 Description of Research Data

The data described in this study are scientific attitudes and physics learning outcomes resulting from the treatment between the application of self-assessment containing scientific processes and conventional assessment in learning physics by controlling initial knowledge.

The recapitulation of research data is presented in Table 2.

Based on the data in Table 2, the results of the analysis are as follows. 1) The average initial knowledge of students who took physics learning with process-loaded self-assessment was M = 20.85 and Sd = 2.73 were in the high category, 2) The average initial knowledge of students who took physics learning with conventional assessment was M = 19.75 and Sd = 2.66 were in the high category, 3) The average scientific attitude of students who took physics learning with self-assessment containing scientific processes was M = 169.56 and Sd = 9.98 were in the high category , 4) The average scientific attitude of students who took physics learning with conventional assessment was M = 153.89 and Sd = 11.55 were in the high category, 5) The average physics learning outcomes of students who took physics learning with self-assessment the science process was M = 65.17 and Sd = 11.78 were in the high category, 6) The average physics learning outcomes of students who took physics learning with conventional assessment were M = 56.07 and Sd = 10.03 were in the category enough.

### 3.2 Data Analysis Requirements Testing Results

#### *3.2.1 Data Normality*

The data normality test was carried out to determine whether the frequency distribution of the scores on each variable was normally distributed or not (Candiasa, 2011). This study tested the normality of data distribution using the Kolmogorov-Smirnov technique through the SPSS 23.0 program. The results are presented in Table 3.

**Table 3.** Data Normality Test Results

| Data Groups | Sig. | α | Conclusion |
|---|---|---|---|
| $X_1$ | 0.072 | 0.05 | Normal |
| $X_2$ | 0.088 | 0.05 | Normal |
| $Y_{11}$ | 0.200 | 0.05 | Normal |
| $Y_{21}$ | 0.200 | 0.05 | Normal |
| $Y_{12}$ | 0.087 | 0.05 | Normal |
| $Y_{22}$ | 0.200 | 0.05 | Normal |

#### *3.2.2 Multivariate Normality Test*

The multivariate normal distribution test is used to determine whether the data is multivariate normally distributed or not. The

multivariate normality test is carried out by calculating the Mahalanobis distance for each observation point with its average (Leys et al., 2018).

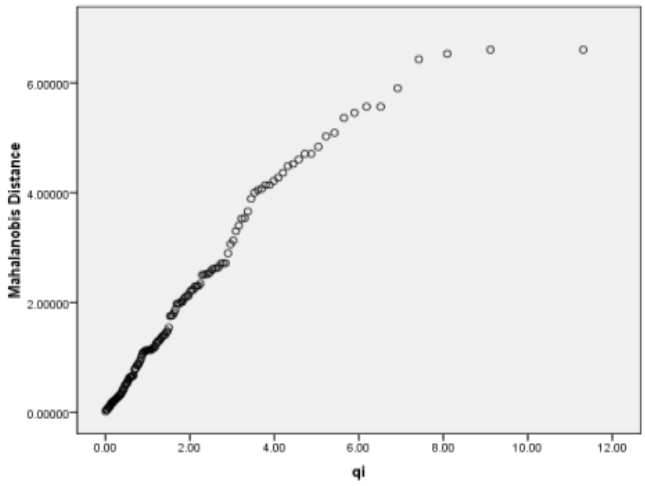


**Figure 1**. Scatter Plot of Normality Multivariate

The correlation coefficient obtained from the calculation was 0.972 with a sig value <0.05. It means that there was a significant correlation. The scatter-plot means that the data comes from a multivariate normally distributed sample.

### *3.2.3 Homogeneity of Group Variance*

The homogeneity test of the group variance was carried out to ensure that the differences in the dependent variable were not caused by differences within groups but differences between groups. The homogeneity test of variance was carried out on the data group of the prior knowledge scores of the students in learning physics, the scientific attitudes scores of the students, and the physics learning outcomes of the students.

In this study, the variance homogeneity test was carried out in two stages, namely: 1) testing the homogeneity of group variance with the Levene test to test the variance homogeneity of the two data groups, namely: between the experimental group and the control group individually, and 2) homogeneity testing. The covariance variance matrices were carried out using Box's test of equality of covariance matrices, aiming to test the homogeneity of group variance simultaneously, namely the group of data on scientific attitudes and student learning outcomes of physics. These data sets must satisfy the assumption that each group has the same variance. All tests use the help of the SPSS 23.0 program.

The statistical hypotheses tested were $H_0 : \sigma_1^2 = \sigma_2^2$ dan $H_1 : \sigma_1^2 \neq \sigma_2^2$. Criteria for acceptance or rejection of Ho: if the resulting significance value was more than the specified significance number, namely 0.05, then Ho was accepted, and in other conditions, Ho was rejected. Accepting Ho means that the variance between groups was homogeneous, and rejecting Ho means that the group variance was not homogeneous. Based on the analysis of group variance homogeneity with the Levene's and Box's M Test, the following summary results were obtained.

***Table 4***. Homogeneity Test Results

| No | Data Groups | F | Sig. |
|---|---|---|---|
| 1 | X | 0.034 | 0.854 |
| 2 | $Y_1$ | 0.397 | 0.530 |
| 3 | $Y_2$ | 3.238 | 0.074 |
| 4 | $\binom{Y_1}{Y_2}$ | 1.144 | 0.330 |

Referring to the analysis results in Table 4, the significance figures generated for each data group were all more than 0.05. It means that the data group of the prior knowledge scores of the students in learning physics, the data group of scientific attitudes scores of the students, the data group of the physics learning outcomes scores of the students, and the data group of the scientific attitudes and physics learning outcomes of the students had homogeneous variances.

### *3.2.4 Regression Linearity Testing*

One of the prerequisites for multivariate covariance analysis is the linear influence of covariates on dependent variables. For this reason, it was testing the linearity of covariate regression on dependent variables. Regression linearity testing was carried out to ensure a linear relationship between the variables tested so that it is appropriate to be used as the variables in the study. The regression linearity test was carried out on the covariables of the prior knowledge in learning physics of the students against the variables of scientific attitudes and the covariables of the prior knowledge of the students in learning physics to the variables of physics learning outcomes.

The statistical hypothesis tested was Ho : $\beta = 0$ and H1 : $H_1 : \beta \neq 0$. The test criterion accepts Ho, which states that the regression is linear at the significance level ($\alpha$) = 0.05 if the test results show that the F value was on the deviation from

linearity that had a significance number of more than 0.05. It means that the covariable of the prior knowledge of the students in learning physics and the variable of the scientific attitudes of the students, the covariable of the initial knowledge of the students in learning physics, and the physics learning outcomes of the students was a form of linear regression relationship.

The significance value was obtained from the calculation results at the value of F deviation from linearity more than 0.05, so that Ho was accepted. It means that the regression between the covariables of the prior knowledge of the students in learning physics and the variables of the scientific attitudes of the students, the regression between the covariables of the prior knowledge of the students in learning physics, and student variables learning outcomes in physics had a linear relationship.

#### *3.2.5 Testing the Meaning of Regression Directions*

Testing the meaning of the regression direction was carried out to test whether the X covariate had a significant effect on the Y variable. The test for the meaning of the regression direction was carried out by testing the regression coefficient $Y = \beta_2 X + \beta_1 + \varepsilon$, using the F test. The statistical hypothesis tested is $H_0 : \beta_2 = 0$ dan $H_1 : \beta_2 \neq 0$.

From the analysis, it can be concluded that the significance number at the F linearity value was less than 0.05 so, that Ho was rejected. Thus, it can be concluded that the covariate of the prior knowledge of the students in learning physics had a significant linear effect on scientific attitudes, and the covariate of the prior knowledge of the students in learning physics had a significant linear effect on physics learning outcomes.

#### *3.2.6 Testing Alignment of Regression Lines*

Testing the alignment of the regression lines was carried out to determine whether the coefficient of the regression line direction of the covariate effect on the dependent variable of each sample group was parallel. From the calculation results, the F-count value for the alignment of the regression lines of the prior knowledge of the students in learning physics and the scientific attitudes of the students was 0.527, and a significance value was 0.881. Because the significance value obtained was more than 0.05, Ho was accepted. There was no difference in the slope of the regression line of the prior knowledge of the students in learning physics and the scientific attitudes of students from the self-assessment group containing the scientific process and the conventional assessment group.

Similarly, the alignment of the regression lines of the prior knowledge of the students in learning physics and the physics learning outcomes of the students showed the F-count value of 1.800 with a significance value of 0.062. The significance figure obtained was more than the significance figure set at 0.05. It means that Ho was accepted or there was no difference in the slope of the regression line of the initial knowledge of the students in learning physics and the physics learning outcomes of the students from the group formed by the assessment. Thus, the regression line of the initial knowledge in physics learning and the physics learning outcomes of the students from all groups in this study were parallel.

#### *3.2.7 Multicollinearity*

Multivariate covariance analysis requires that two or more dependent variables do not have a high correlation. For this reason, multicollinearity testing was carried out. The multicollinearity test of data was carried out to ensure that the two dependent variables could be used as different criteria. Multicollinearity testing in this study was carried out on the variables of the scientific attitudes of the students and the physics learning outcomes of the students with the help of the SPSS 23.0 linear regression program by looking at the collinearity value of variance inflation factor (VIF). The dependent variables have multicollinearity if the VIF value is more than 10.

Based on the linear regression analysis results, the VIF value= 1.00 or the tolerance value= 1.00, with a significance less than 0.001. Because the VIF value was less than 10, the dependent variable was the scientific attitude of the students. The physics learning outcomes of the students did not experience multicollinearity, so it could be used as a criterion individually and simultaneously.

All the requirements related to the multivariate covariance analysis as above had been fulfilled, so that inferential analysis in the context of testing the research hypothesis using the Manakova statistical technique could be continued.

### 3.3 Hypotheses Testing

To test the effect of self-assessment with scientific processes in physics learning both individually and simultaneously on scientific attitudes and physics learning outcomes by controlling initial knowledge using multivariate covariance analysis. The recapitulation of the analysis results is presented in Tables 5 and 6.

Based on the recapitulation of the results of data analysis, the results of testing the research hypothesis can be described as follows: (1) there was a significant difference in scientific attitudes and learning outcomes between students who took physics learning with self-assessment with scientific processes and students who took physics learning with conventional assessment (2) there were significant differences in scientific attitudes and learning outcomes of physics between students who took physics learning with self-assessment with scientific processes and students who took physics learning with the conventional assessment after controlling initial knowledge both individually and simultaneously (3) initial knowledge students in learning physics contributed significantly to 22.8% of the scientific attitudes of the students and 19.4% to the physics learning outcomes of the students.

### 3.4 Discussion of Research Results

This study proved that physics learning with self-assessment containing scientific processes positively affected the scientific attitudes and learning outcomes of the students.

Theoretically, these findings indicate that physics learning with self-assessment with scientific processes positively affected the scientific attitudes and learning outcomes of the students. The scientific attitude and physics learning outcomes of the students were influenced by the type of physics learning assessment. The learning process tended to follow the type of assessment applied. If the assessment used required an understanding of the concept, the learning process was also based on understanding it. The interactions of the students in learning were also adjusted to the demands of the assessment. Their interactions in the learning process largely determined the learning outcomes of the students.

Learning physics with self-assessment containing scientific processes would improve the scientific attitudes of the students. With an improved scientific attitude, learning outcomes would also increase. In contrast to physics learning with conventional assessment, it was less demanding to develop the scientific attitudes of the students.

In conventional assessment, the opportunity for students to carry out their learning activities according to their needs, abilities, and interests, as well as opportunities for self-reflection from self-evaluation and feedback, were not available in conventional assessments. Even though these opportunities provided a very broad space for the students to spur their achievement to excel, these assessments were commonly used worldwide for time and cost-efficiency. The assignments and performance of the students tended to be ignored and were not considered a more meaningful alternative assessment model. Pure multiple-choice tests contributed less to learning and were therefore not appropriate for all assessments conducted in schools. The conventional assessment model could not measure the actual ability of students because it only focused on a few aspects, so it did not provide opportunities for students to demonstrate their respective abilities and strengths.

Empirically, the results of this study are supported by Zi Yan's research, which concluded that the physics learning outcomes of students assessed by self-assessment were higher than those of the physics learning outcomes of the students assessed by conventional assessment (Yan, 2020). The results of this study are also in line with Juhji's findings that components in science learning such as respect for evidence and facts, desire to change paradigms, critical thinking, diligent, optimistic, creative, honest, responsible, open-minded, objective, tolerance, careful at work, and positive thinking so that it is always developed in learning activities. A good scientific attitude will significantly affect the knowledge of the students, as indicated by a correlation coefficient of 0.842 (Juhji and Nuangchalerm, 2020). The findings of this study are also in line with Stavros A. Nikou that there has been a significant increase in the learning achievement of low achieving students. Who participated in the mobile and computer-based self-assessments. The positive effect of using computers and mobile devices in learning also increased the motivation of the students. It can be used as a promising alternative to complement paper and pencil-based assessments (Nikou and Economides, 2016).

The finding that learning physics with self-assessment containing a scientific process had a positive effect on scientific attitudes and learning

outcomes after the prior knowledge of the students in learning physics was controlled, meaning that differences in scientific attitudes and learning outcomes between experimental and control classes were solely due to the treatment given, namely self-assessment containing a scientific process. Learning physics with a combination of scientific approaches and self-assessment, students could build their knowledge, plan and monitor their development as expected. Through self-assessment, learners could see their strengths and weaknesses, and then this deficiency became the goal of improvement. Thus, students were more responsible for the learning process and the achievement of learning goals. Self-assessment had a positive impact on students, including (1) it could foster the self-confidence of the students, (2) students were aware of their strengths and weaknesses because in the assessment process, they had to reflect on their abilities, and (3) could encourage, accustom and train students to act objectively and honestly. It was what contributed to strengthening the scientific attitudes of the students.

Self-assessment containing scientific processes was meaningful because students could feel their learning progress, feel that they had greater autonomy, feel that they were doing useful activities for themselves, and not just do the teacher's assignment. Thus, self-assessment is an element of metacognition that plays a very important role in the learning process because through self-assessment, students can find out what is known and know what is not yet known. This self-assessment containing a scientific process reinforces the efforts to achieve increased the learning outcomes of the students.

The controlled variable in this study is initial knowledge. This initial knowledge variable needed to be controlled because this variable was suspected of affecting scientific attitudes and learning outcomes of physics in the treatment process. Therefore, the scientific attitude and physics learning outcomes obtained in this study were purely due to the treatment process by controlling the initial knowledge variable.

The prior knowledge of the students is an important consideration to be netted before starting learning. Regarding the initial knowledge of the students, when the negotiation of meaning took place, the received information changed slowly from the general context into the specific context of science. It was linked to various activities that would spur students to continue to seek and find. Therefore, the success of the teacher in learning would be determined by the identification of the initial knowledge of the students. The physics initial knowledge of the students could be in the form of knowledge about the discovery process and physics products consisting of the concepts, principles, and laws of physics.

The initial knowledge about discovering physics products of the students would be very influential when in the learning process there were process activities to find physics products. The process of finding a physical product was carried out by a scientific process or scientific method. The scientific process to find physical products required a scientific attitude that included curiosity, respect for facts or evidence, a willingness to change views, and critical thinking. In finding physics products based on the initial knowledge of these findings, students would be able to develop scientific attitudes. The initial knowledge of physics products of the students would be very influential when there are activities to describe and apply physics products in the learning process. The activity of describing and applying physics products based on prior knowledge about these products could improve learning outcomes in physics, especially in the cognitive domain.

Thus, this initial knowledge is a good predictor of the interest and achievement in physics lessons of the students. It indicates that initial knowledge is a variable that deserves to be controlled to determine the effect of purer self-assessment with scientific processes on the scientific attitudes and physics learning outcomes of the students.

Empirically, the results of this study reinforce the results of research conducted by Liang Yi Li that students who had high initial knowledge had a more positive scientific attitude and showed higher learning outcomes than students with low initial knowledge (Li, 2019).

### 3.5 Implications of Research Results

The results of this study provide the following implications. (1) Implications of the results of this study on the curriculum in physics learning. Implementing the 2013 Curriculum in physics learning in schools should be understood not only as adjustments to the material substance and curriculum format with the demands of development, but a paradigm shift towards a physics learning approach oriented towards self-assessment as a reference for students'

graduation. This change in orientation had implications for the expansion of assessment methods and techniques. Physics teachers must be able to choose the right type of assessment in physics learning with the material being taught because one of the determinants of scientific attitudes and students' learning outcomes is the assessment applied by the teacher during the learning process. Suppose a teacher can apply learning strategies well, master the material proficiently, and select and use learning assessments appropriately and carefully. In that case, student success in learning will be achieved as well. Self-assessment containing scientific processes has an important role in improving students' learning outcomes. Assessment is an integral part of the learning process. Selection of self-assessment containing appropriate scientific processes can improve students' scientific attitudes to learning so that it will lead to improving the quality and learning outcomes of students. (2) The implication of the results of this study for learning strategies is that teachers should design learning strategies that can facilitate students to construct their knowledge through authentic and meaningful experiences. With self-assessment containing scientific processes, students will monitor their level of knowledge, learning, abilities, thoughts, actions, and strategies based on scientific procedures. Learning strategies are designed to provide opportunities for students to actively participate in learning. In learning, students build their knowledge through students' interaction with the environment. The learning strategy developed also considers students' initial knowledge to improve scientific attitudes and students' learning outcomes. (3) Implications of the results of this study on learning assessment. Self-assessment containing scientific processes should be developed and implemented, in line with the findings of this study, and in order to improve the quality of physics learning, as well as to improve scientific attitudes and physics learning outcomes, one alternative that teachers can do is to multiply and expand the use of process-loaded self-assessment science in physics learning, both in the learning process and in assessing students' physics learning outcomes. Through self-assessment, students can see the strengths and weaknesses, and then this deficiency becomes the goal of improvement. Thus, learners are more responsible for the learning process and the achievement of learning goals. Self-assessment is meaningful because students can feel their learning progress, feel they have greater autonomy, feel that they are doing something useful for themselves, not just doing the assignment of the teacher. Conventional assessments should only be carried out for certain things so that physics learning is more meaningful. Self-assessment containing scientific processes has advantages in revealing students' potential in problem-solving, reasoning, and communication in written and oral form. Self-assessment containing a scientific process must be based on the assessment of the rater's observations of himself. Therefore, self-assessment containing scientific processes is very well used to assess students' abilities and reflect student learning success. The habit of using self-assessment with a scientific process will stimulate students to create scientific attitudes, which in turn will improve the quality of learning and student learning outcomes. Self-assessment containing scientific processes should be developed and improved for physics learning, especially physics learning at the high school level. It has been proven to be able to improve scientific attitudes and students' physics learning outcomes. In contrast to the learning process with the conventional assessment. The learning process with conventional assessment tends to place students as objects filled with problems. It impacts decreasing the ability of students to solve the problems faced so that scientific attitudes and learning outcomes are not good.

(4) Implications of research results on the prior knowledge of the students. The prior knowledge of the students in learning physics contributes to the scientific attitudes and to physics learning outcomes of the students. It shows that initial knowledge will affect the academic abilities of the students. The amount of initial knowledge will determine the amount of effort made to achieve success. Students' initial knowledge of physics can be in the form of knowledge about the discovery process and physical products, consisting of the concepts, principles, and laws of physics. Early knowledge is very important to be extracted and used to direct learning activities. It means that the initial knowledge, which is an internal factor of students, should be considered because it influences the learning outcomes of the students.

## 4. CONCLUSIONS:

Based on the hypothesis testing results, it can be concluded that self-assessment containing scientific processes in physics learning affected scientific attitudes and learning outcomes by controlling initial knowledge. In

more details, it can be concluded as follows: (1) there were significant differences in scientific attitudes and learning outcomes of physics between students who took physics learning with self-assessment with scientific processes and students who took physics learning with conventional assessment, either individually or independently. Simultaneously, (2) there was a significant difference in scientific attitudes and simultaneous physics learning outcomes between students who took physics learning with self-assessment with scientific processes and students who took physics learning with conventional assessment by considering the effect of initial knowledge, both individually and simultaneously, (3) students 'prior knowledge in learning physics contributed significantly to the scientific attitudes and the physics learning outcomes of the students.

## 5. ACKNOWLEDGMENTS:

To my beloved wife and children, thank you for your endless support. I would like to thank my parents and my parents-in-law for the countless prayers. To all the participants of this research, thank you, I would not make it if it were not because of your participation. Finally, I would like to extend my highest gratitude to all the people who have shown their support and contributed to the completion of this dissertation.

## 6. REFERENCES:

1. Bahar, M., and Aksüt, P. (2020). Investigation on the effects of activity-based science teaching practices in the acquisition of problem solving skills for 5-6 year old pre-school children. *Journal of Turkish Science Education*. https://doi.org/10.36681/tused.2020.11

2. Candiasa, I. M. (2011). *Statistik Multivariat Disertai Aplikasi SPSS*. Undiksha Press.

3. Darling-Hammond, L., Flook, L., Cook-Harvey, C., Barron, B., and Osher, D. (2020). Implications for educational practice of the science of learning and development. *Applied Developmental Science*. https://doi.org/10.1080/10888691.2018.1537791

4. Earl, L., and Katz, S. (2006). Rethinking Classroom Assessment with Purpose in Mind. In *Learning*.

5. Gandasari, D., Dwidienawati, D., and Sarwoprasodjo, S. (2020). Discourse analysis: The impact of industrial revolution 4.0 and society 5.0 in Indonesia. *International Journal of Advanced Science and Technology*.

6. Gürses, A., Çetinkaya, S., Doğar, Ç., and Şahin, E. (2015). Determination of Levels of Use of Basic Process Skills of High School Students. *Procedia - Social and Behavioral Sciences*. https://doi.org/10.1016/j.sbspro.2015.04.243

7. Hidayati, D. W. (2017). Penerapan Problem Based Learning Berbasis Self-Directed Learning Oriented Assessment. *Journal of Medives : Journal of Mathematics Education IKIP Veteran Semarang*, *1*(1), 17–24.

8. Jain, C., and Prasad, N. (2018). *Understanding Factors Affecting Student Outcomes and Learning Behaviour*. Springer.

9. Juhji, J., and Nuangchalerm, P. (2020). Interaction between scientific attitudes and science process skills toward technological pedagogical content knowledge. *Journal for the Education of Gifted Young Scientists*. https://doi.org/10.17478/jegys.600979.XX

10. Kunandar. (2015). Penilaian Autentik (Penilaian Hasil Belajar Pesrta Didik Berdasarkan Kurikulum 2013. In *Jurnal Evaluasi Pendidikan*.

11. Kurniawati, I. D. (2019). Development of Problem-Based Kinematics Teaching Material to Improve Students' Critical Thinking Skills. *JIPF (Jurnal Ilmu Pendidikan Fisika)*, *4*(1), 21. https://doi.org/10.26737/jipf.v4i1.910

12. Leys, C., Klein, O., Dominicy, Y., and Ley, C. (2018). Detecting multivariate outliers: Use a robust variant of the Mahalanobis distance. *Journal of Experimental Social Psychology*. https://doi.org/10.1016/j.jesp.2017.09.011

13. Li, L. Y. (2019). Effect of Prior Knowledge on Attitudes, Behavior, and Learning Performance in Video Lecture Viewing. *International Journal of Human-Computer Interaction*. https://doi.org/10.1080/10447318.2018.1543086

14. Luque, P. A., and Mendoza, M. L. R. (2019). Application of Self-assessment and Co-Evaluation on Learning Processes. *International Journal of Physics and*

*Mathematics*.

15. Malik, A. (2019). Creating Competitive Advantage through Source Basic Capital Strategic Humanity in the Industrial Age 4 . 0. *International Research Journal of Advanced Engineering and Science*.
16. Mehtap, Y., Dilek, S. A., and Melek, Y. K. (2020). Investigation of in-Service and Pre-Service Science Teachers' Perceptions of Scientific Process Skills. *Asian Journal of University Education (AJUE)*, *16*(2), 105–106.
17. Mulyeni, T., Jamaris, M., and Suprjyati, Y. (2019). Improving Basic Science Process Skills Through Inquiry-Based Approach in Learning Science for Early Elementary Students. *Journal of Turkish Science Education*. https://doi.org/10.12973/tused.10274a
18. Muszyński, M. (2020). *Validity of the Overclaiming Technique As a Method To Account for Response Bias in Self-Assessment Questions .*
19. Nikou, S. A., and Economides, A. A. (2016). The impact of paper-based, computer-based and mobile-based self-assessment on students' science motivation and achievement. *Computers in Human Behavior*. https://doi.org/10.1016/j.chb.2015.09.025
20. Pantiwati, Y., and Husamah. (2017). Self and Peer Assessments in Active Learning Model to Increase Metacognitive Awareness and Cognitive Abilities. *International Journal of Instruction*, 186–202.
21. Papanthymou, A., and Darra, M. (2018). The Contribution of Learner Self-Assessment for Improvement of Learning and Teaching Process: A Review. *Journal of Education and Learning*. https://doi.org/10.5539/jel.v8n1p48
22. Pratama, G. S., and Retnawati, H. (2018). Urgency of Higher Order Thinking Skills (HOTS) Content Analysis in Mathematics Textbook. *Journal of Physics: Conference Series*. https://doi.org/10.1088/1742-6596/1097/1/012147
23. Ratminingsih, N. M., Marhaeni, A. A. I. N., and Vigayanti, L. P. D. (2018). Self-Assessment: The effect on students' independence and writing competence. *International Journal of Instruction*. https://doi.org/10.12973/iji.2018.11320a
24. Sabri, M., Retnawati, H., and Fitriatunisyah. (2019). The implementation of authentic assessment in mathematics learning. *Journal of Physics: Conference Series*. https://doi.org/10.1088/1742-6596/1200/1/012006
25. Sadeghi, K., and Rahmati, T. (2017). Integrating assessment as, for, and of learning in a large-scale exam preparation course. *Assessing Writing*. https://doi.org/10.1016/j.asw.2017.09.003
26. Suarni, N. K. (2019). Psychological Data Information Specialization Services in Increasing Student's Self Understanding. *The 5th International Conference on Education and Technology*.
27. Taufina, T., and Chandra, C. (2018). *The Implication of Authentic Assessment in Thematic Integrated Learning Process at Lower Level Elementary School Early Childhood Development*. https://doi.org/10.2991/icece-17.2018.36
28. Wan, Q., Liu, M., Gao, B., Chang, T., and Huang, T. (2020). The Relationship between Self-regulation and Flow Experience in Online Learning: A Case Study of Global Competition on Design for Future Education. *IEEE 20th International Conference on Advanced Learning Technologies (ICALT)*, 365–367. https://doi.org/10.1109/ICALT49669.2020.00116.
29. Wride, M. (2017). Guide to peer-assessment. *Academic Practice and ELearning (CAPSL) Resources*.
30. Yan, Z. (2020). Self-assessment in the process of self-regulated learning and its relationship with academic achievement. *Assessment and Evaluation in Higher Education*. https://doi.org/10.1080/02602938.2019.1629390
31. Zeitoun, S., and Hajo, Z. (2015). Investigating the Science Process Skills in Cycle 3 National Science Textbooks in Lebanon. *American Journal of Educational Research*. https://doi.org/10.12691/education-3-3-3

***Table 2.*** *Recapitulation of Research Data*

| Statistics | $A_1$ | | | $A_2$ | | |
|---|---|---|---|---|---|---|
| | **X** | **$Y_1$** | **$Y_2$** | **X** | **$Y_1$** | **$Y_2$** |
| Lots of Data | 71 | 71 | 71 | 72 | 72 | 72 |
| Amount of Data | 1480 | 12039 | 4627 | 1422 | 11080 | 4037 |
| Max Score (ideal) | 28 | 210 | 100 | 28 | 210 | 100 |
| Min Score (ideal) | 0 | 42 | 0 | 0 | 42 | 0 |
| Maximum Score | 27 | 191 | 85 | 26 | 190 | 77 |
| Minimum Score | 15 | 145 | 36 | 14 | 128 | 35 |
| Interval | 12 | 46 | 49 | 12 | 62 | 42 |
| Average | 20.85 | 169.56 | 65.17 | 19.75 | 153.89 | 56.07 |
| Median | 21 | 170 | 65 | 20 | 155 | 57 |
| Mode | 20 | 175 | 72 | 19 | 162 | 64 |
| Standard Deviation | 2.73 | 9.98 | 11.78 | 2.66 | 11.55 | 10.03 |
| Variance | 7.45 | 99.68 | 138.74 | 7.09 | 133.51 | 100.57 |

Explanation:

$A_1$ : Learning physics with self-assessment containing scientific processes

$A_2$ : Physics learning with conventional assessment

X : Students' initial knowledge in learning physics

$Y_1$ : Students' scientific attitude

$Y_2$ : Students' physics learning outcomes

**Table 5.** Recapitulation of Manova and Manakova Analysis Results

| Difference Test | | | | |
|---|---|---|---|---|
| Effects | | F-*Wilk's Lambda* | | Sig. |
| Assessment | | 7.724 | | 0.001 |
| Assessment | Scientific Attitude | 75.479 | | 0.000 |
| | Learning Outcomes | 24.766 | | 0.000 |
| Assessment + Initial Knowledge Control | | 43.292* | | < 0.001 |
| Assessment + Initial Knowledge Control | Scientific Attitude | 69.084* | | 0.000 |
| | Learning Outcomes | 18.189* | | 0.000 |
| Test of Significance of Differences | | | | |
| Effects | | Mean Difference | F Value | Significance |
| Assessment | | - | 7.724 | 0.001 |
| Assessment | Scientific Attitude | 13.708 | 75.479 | 0.000 |
| | Learning Outcomes | 7.314 | 24.766 | 0.000 |
| Assessment + Initial Knowledge Control | | - | 43.292 | < 0.001 |
| Assessment + Kontrol Pengetahuan awal | Scientific Attitude | 15.703** | 69.084 | 0.000 |
| | Learning Outcomes | 9.100** | 18.189 | 0.000 |

* Residual F Value

** Corrected Mean Value

**Table 6**. Recapitulation of Analysis of the Contribution of Covariates to Bound Variables

| Regression | R | $R^2$ | $R^2$ Adjustments | F | Sig. |
|---|---|---|---|---|---|
| $X - Y_1$ | 0.460 | 0.211 | 0.206 | 40.161 | < 0.001 |
| $X - Y_2$ | 0.427 | 0.183 | 0.177 | 33.498 | < 0.001 |

PERIÓDICO TCHÊ QUÍMICA
ARTIGO ORIGINAL

# UMA ABORDAGEM PARA ESTIMAR A TAXA DE FORMAÇÃO DE DEPÓSITO ORGÂNICO EM UMA HASTE E SELEÇÃO DE MÉTODOS PARA PREVENÇÃO DE DEPÓSITO

# AN APPROACH TO ESTIMATING THE RATE OF ORGANIC DEPOSIT FORMATION IN A HOLLOW ROD STRING AND SELECTION OF METHODS FOR DEPOSIT PREVENTION

# СПОСОБ ОЦЕНКИ ИНТЕНСИВНОСТИ ОБРАЗОВАНИЯ ОРГАНИЧЕСКИХ ОТЛОЖЕНИЙ В КОЛОННЕ ПОЛЫХ ШТАНГ И ПОДБОР МЕТОДОВ БОРЬБЫ С НИМИ

KRIVOSHCHEKOV, Sergey Nikolaevich[1*]; VYATKIN, Kirill Andreevich[2]; KOCHNEV, Aleksandr Aleksandrovich[3,4]; KOZLOV, Anton Vadimovich[5]

[1,2,3,5] Perm National Research Polytechnic University, Mining and Oil Faculty, Perm, Russian Federation

[4] LUKOIL-Engineering PermNIPIneft LLC, Department of Geological and Hydrodynamic Modeling, Perm, Russian Federation

** Corresponding author*
*e-mail: krivoshchekov@gmail.com*

Received 05 November 2020; received in revised form 28 December 2020; accepted 20 February 2021

## RESUMO

**Introdução**. Atualmente, falta uma metodologia que possa permitir determinações altamente precisas das taxas de formações de depósito de asfalteno (AD) em caso de operação dupla de dois reservatórios de petróleo por meio de um único poço multi-zona produtor de petróleo usando hastes ocas de pequeno diâmetro parte do equipamento de bombeamento de fundo de poço. Essa metodologia visa minimizar os custos das empresas de petróleo e gás com a manutenção de tais poços de petróleo e prevenir o seu fracasso. **Objetivos**. Criação de uma metodologia voltada para estimativas quantitativas precisas das taxas de formação de depósitos orgânicos na parte interna das colunas de hastes ocas. **Métodos**. Cálculos de distribuições de temperatura ao longo da superfície interna da coluna de haste oca; apresentações gráficas dos dados calculados; testes de laboratório usando uma unidade Cold Finger para as seções selecionadas das cordas da haste oca e as apresentações gráficas dos resultados. **Resultados e discussão**. O algoritmo sugerido foi testado em campo em um poço produtor de petróleo multi-zona alvo do campo de petróleo Pavlovka em Perm Krai da Federação Russa. Usando o algoritmo sugerido, uma variação nas taxas de formação de depósito orgânico ao longo do comprimento da coluna de haste oca foi avaliada e a profundidade da taxa máxima de formação de depósito foi determinada. Para evitar os depósitos em questão ao longo da coluna de haste oca em um poço produtor de petróleo alvo do campo de petróleo de Pavlovka, testes de laboratório foram conduzidos para determinar a eficiência do emprego da tecnologia química, ou seja, o uso de inibidores de AD, bem como uma tecnologia para a remoção dos depósitos formados usando solventes AD. **Conclusões**. O algoritmo proposto é mais preciso e requer menos tempo e dinheiro em comparação com os algoritmos existentes. Permite uma avaliação mais eficaz da profundidade de formação dos depósitos orgânicos e da intensidade nestas marcas. Ao avaliar os resultados dos estudos laboratoriais, pode-se notar que o uso das tecnologias consideradas para eliminar depósitos orgânicos é altamente eficaz e pode ser utilizado para este fim.

**Palavras-chave**: *depósito de asfalteno, operação dupla, poços com várias zonas, temperatura, inibidor.*

## ABSTRACT

**Background**. There is currently a lack of a methodology that can enable highly-precise determinations of rates of asphaltene deposit (AD) formations in case of dual operation of two oil reservoirs via a single multi-zone oil-producing well using small-bore hollow rods as part of downhole pumping equipment. This methodology aims to minimize the costs of oil and gas companies for servicing such oil wells and preventing their failure. **Aims.** Creating a methodology aimed at accurate quantitative estimations of the organic deposit formation rates at the inner part of the hollow rod strings. **Methods.** Calculations of temperature distributions along the hollow rod

string inner surface; graphic presentations of the calculated data; laboratory tests using a Cold Finger unit for the selected sections of the hollow rod strings and the graphic presentations of the results. **Results and Discussion.** The suggested algorithm was field-tested at a target multi-zone oil-producing well of Pavlovka oil field in Perm Krai of the Russian Federation. Using the suggested algorithm, a variation in organic deposit formation rates along the hollow rod string length was evaluated, and the depth of the maximum deposit formation rate was determined. To prevent the deposits in question along the hollow rod string at a target oil-producing well of Pavlovka oil field, laboratory tests were conducted to determine the efficiency of employing the chemical technology, i.e., the use of AD inhibitors, as well as a technology for the removal of the formed deposits using AD solvents. **Conclusions.** The proposed algorithm is more accurate and requires less time and money compared to existing algorithms. It enables the most effective evaluation of the formation depth of the organic deposits and the intensity at these marks. When evaluating the laboratory studies results, it can be noted that the use of the considered technologies to eliminate organic deposits is highly effective and can be used for this purpose.

**Keywords**: *asphaltene deposit, dual operation, multi-zone wells, temperature, inhibitor*.

## ABSTRACT

**Актуальность:** Актуальность исследования обусловлена отсутствием методики позволяющей с высокой точностью определить характер и степень изменения интенсивности образования асфальтосмолопарафиновых отложений при одновременно – раздельной эксплуатации двух нефтяных пластов единой транзитной нефтедобывающей скважиной с применением в составе глубинно-насосного оборудования полых штанг с малым внутренним диаметром. Применение данной методики направлено на минимизацию затрат нефтегазовых компаний на обслуживание данных нефтедобывающих скважин и предотвращение их отказа. **Цель:** создать методику, позволяющую осуществлять точно количественное определение интенсивности образования органических отложений на внутренней поверхности полых штанг. **Методы:** расчет распределения температуры внутренней поверхности колонны полых штанг; графическое представление расчетных данных; проведения лабораторных исследований на установке «Холодного стержня» в выбранных, по итогу анализа графических данных сечениях колонны полых штанг, и графическое представление результатов. **Результаты и Обсуждение**: Предложенный алгоритм апробирован на целевой транзитной нефтедобывающей скважине Павловского нефтяного месторождения Пермского края Российской Федерации. В результате применения предложенного алгоритма получено изменение интенсивности образования органических отложений по длине колонны полых штанг, определена глубина наибольшей интенсивности образования отложений. С целью борьбы с рассматриваемыми отложениями в колонне полых штанг целевой нефтедобывающей скважины Павловского нефтяного месторождения проведены лабораторные исследования по определению эффективности применения технологии химизации–применение ингибиторов асфальтосмолопарафиновых отложений, а также технологии удаления сформировавшихся отложений растворителями асфальтосмолопарафиновых отложений. **Заключение:** Предложенный алгоритм обладает большей точностью и требует меньших временных и денежных затрат в сравнении с существующими алгоритмами. Используя данный алгоритм становится возможным наиболее эффективно оценивать глубины образования органических отложений и интенсивность на данных отметках. Оценивая результаты лабораторных исследований можно отметить что применение рассматриваемых технологий борьбы с органическими отложениями высокоэффективно и может использоваться для данной цели.

**Keywords**: *асфальтеносмолопарафиновые отложения, одновременно-раздельная эксплуатация, транзитные скважины, температура, ингибитор*.

## 1. INTRODUCTION:

At present, a crucial task for oil production enterprises is to improve the profitability of oil-producing wells operation in the context of decreasing hydrocarbon production rates and increased proportion of difficult oil fields with production zones featuring low permeability, low net oil pay values, and complicated pore volume structure, which raise the question of employing the technologies for increasing the technical and economic efficiency of the development of oil fields (Bahgizin *et al*., 2019; Shaislamov *et al*., 2007; Putilov, I. *et al*., 2020).

Among such technologies is dual operation (DO) of multi-zone wells. This technology is used for the following purposes:

- Operation of multi-zone formations where productive reservoirs may be separated into numerous interlayers.
- Reduction of capital investment and

operating costs related to oil field drilling and operation.

• Enabling of accounting of recovered products from each reservoir along with a working agent injected into it.

• Operating the formations featuring multiple productive reservoirs exhibiting stark difference regarding their geological and geophysical parameters as well as the chemical composition of recovered products (Ivanov *et al*., 2013; Garifov *et al*., 2013)

Field experience with operating two and more production facilities of a single multi-zone oil-producing well demonstrates the high efficiency of this technology. On average, capital investment and operating costs are reduced by 30 % as compared with the costs related to oil field drilling and operation utilizing individual networks at each oil reservoir (Nurgaliev and Habibullin, 2016). The use of dual operation technology enables increasing the density of well networks without increasing the drilling depth. The increased operational efficiency results in the increased capacity of oil-producing wells. Therefore, the DO technology enables a significant reduction in oil production costs (Ivanovskij, 2010; Josset *et al*., 2015; Nurgaliev and Habibullin, 2015).

At present, multiple design solutions are available for dual operation equipment. Examples of existing DO units are detailed in papers (Shrajbman *et al*., 2008; Pepeljaev and Krivonosov 2008, 2009; Volodin *et al*., 2008). Upon analyzing the specified papers, it can be concluded that hollow pumping rods are often used as part of equipment employed for the dual operation of two oil reservoirs. Among the practical advantages of employing hollow rods are the following (Latypov, 2012; Hisamov *et al*., 2009; Krjakushin *et al*., 2009).

• Capability of monitoring bottom-hole pressure across the upper development facility by marking the dynamical level value.

• Capability of taking separate oil flow rate measurements and separate samples at each development facility.

• Capability of process washing of downhole pumping equipment operating both in the upper and lower productive intervals.

• Increasing the rate of fluid lifting along the wellbore.

Among disadvantages of employing hollow rods, an increased withdrawal of sand from the bottom hole can be considered along with the fact that selection and calculation of hollow rods can be difficult due to design complexity and presence of concentric pressure as well as reservoir fluid impact upon both the inner and outer rod walls (Dubinov, and Ivanovskij, 2016)

The use of hollow rods enables separate operation of two oil reservoirs; however, in this scenario, lifting of products recovered from one of them is performed along a string with a small hydraulically equivalent diameter. Hollow rods with an inner diameter of 9.52 to 18.0 mm are employed at Russian oil fields. Lifting of fluid along a small-bore string is often hindered by organic deposits, which results in the built-up of additional hydraulic resistance. Engineers implementing the DO technology employing hollow rods must anticipate the possibility of organic deposit formation in a hollow rod string and select appropriate technologies for taking care of possible hindrances to prevent premature failure of downhole pumping equipment.

At present, various methods are available to forecast the possibility of organic deposit formation in an oil-producing well. These methods can be divided into three groups.

The first group of methods presented in the works of Turbakov *et al*. (2009), Kishhenko *et al*. (2018), Erofeev *et al*. (2010), and Osipov *et al*. (2016) involves solving two mathematical equations in sequence.

Examples of these equations are presented in Equations 1 and 2. The first expression describes the change in the temperature of the inner surface of the tubing. The second expression is an empirical formula aimed at determining the paraffin saturation temperature of degassed oil.

$$t_{\text{ст}} = t_{\text{пл}} - (H_{\text{скв}} - \text{H}) \cdot \frac{0{,}034 + 0{,}725 \cdot \omega}{10^{Q/(1728 \cdot \rho_{\text{f}} \cdot d^{2.67})}} \qquad \text{(Eq.1)}$$

$$t_{\text{нас}} = 70{,}5 \cdot e^{-\frac{3.686}{\Pi}} \qquad \text{(Eq.2)}$$

where $\text{t}_{\text{ст}}$ is the hollow rod inner surface temperature, ℃; $\text{t}_{\text{пл}}$ is formation temperature (fluid temperature in the downhole) ℃; $\omega$ is geothermic gradient, $℃/\text{m}$; $H_{\text{скв}}$ is the well depth , m; H is the depth from the well mouth , m; $Q$ is the well mass discharge with flow rate, $t/day$; $\rho_{\text{f}}$ is the fluid density, $\text{kg/m}^3$; d is inner diameter of the liquid transporting pipe, m; $\Pi$ is the mass fraction of asphaltenes in oil, %.

The first equation is a function of temperature distribution along the inner surface of a rod through which lifting of fluid is performed inside the well. The second equation is a function of the temperature of oil saturation with paraffin dependent on various physical parameters; this function can be evaluated based on various empirical dependencies. In these dependencies, the following factors affect the temperature of oil saturation with paraffin: pressure and gas content distribution along the wellbore, the mass fraction of asphaltenes, resins, and paraffin in the produced fluid, as well as oil saturation temperature under surface conditions. Among the disadvantages of this group of methods is that it is only possible to evaluate the depth at which organic deposit formation begins and the introduction of significant errors related to the determination of the temperature of oil saturation with paraffin. This error is composed of three constituents: continuous change of physical and chemical properties of the recovered fluid in the production process, variation in pressure distribution along the wellbore as well as consequent variation in gas content, and availability of various methods for estimating the temperature of degassed oil saturation with paraffin. Among them are visual, refractometric, rheological, volumetric, gravimetric, photometric methods, nuclear magnetic resonance methods, and differential scanning calorimetry.

The second group of methods is presented in the works of Misnik and Galikeev (2011) and (Korobov and Rogachev, 2015). This method is based on the study of asphaltene (A), and resinous (R) compounds impact on the paraffin formation process and, in particular, on paraffin crystallization temperature. This method describes a linear statistical relationship between A/R ratio and field data representing depths of well clean-up and organic deposits. Among disadvantages of this method is a continuous variation of the A/R ratio in recovered products, the presence of numerous deviations from the suggested linear law, as well as the need to conduct multiple laboratory tests and obtain statistical data to determine the linear law of interest for each of the surveyed oil fields.

The third group of methods features Robinson and Peng equations of state (Robinson and Peng, 1976) and is presented in the work of Falovskij *et al*. (2011), Farayola *et al*. (2010), and Dalirsefat and Feyzi (2007). This method is based on laboratory tests used to determine critical parameters of each component in a hydrocarbon mixture. Upon discovering the critical parameters, it is possible to determine Pressure Volume Temperature (PVT) ratios for the hydrocarbon mixture in question. This method has some disadvantages, i.e., the need to employ expensive equipment, reliance on sophisticated mathematical techniques, and excessive time-consuming laboratory researches and subsequent mathematical calculations.

In light of all of the above, it becomes evident that the problem of lacking a precise method for determining the depth at which organic deposit formation begins in oil-producing well and in particular in hollow rod strings needs to be addressed with the vital task of discovering ways to assess the rate of organic deposit formation. High-accuracy forecasting of organic deposit formation rate is crucial when operating small-bore downhole pumping equipment.

## 2. MATERIALS AND METHODS

The target facility for determining the pattern of the hollow rod inner surface temperature variation along its length, a multi-zone oil-producing well of Pavlovka oil field in Perm Krai of the Russian Federation, was selected. To estimate the hollow rod inner surface temperature under the method described in the Methods chapter, the values presented in Table 1 were required. These values included both the physical and chemical properties of the recovered product and the geothermic properties of the well. All considered values were determined by the technological documents or the previous laboratory surveys of the studied target facility. However, the geothermal gradient (ω) was calculated under Equation 3.

$$\omega = \frac{t_{\text{пл}} - t_{\text{н.с.}}}{D_{\text{пл}} - D_{\text{н.с.}}} \cdot 100\% \qquad \text{(Eq.3)}$$

where $t_{\text{н.с.}}$ is reference datum temperature °C; $D_{\text{пл}}$ was base formation top depth, m; $D_{\text{н.с.}}$ was reference datum depth, m.

The given well operates two oil reservoirs. The upper productive interval was Tl-Bb interval. The fluids recovered from the reservoir were pumped inside the pumping and compressor pipes (PCP). The lower productive interval was T interval. The fluids recovered from this reservoir

were pumped through the hollow rod string. The downhole pumping equipment installed in the given well was used to separate product from two oil reservoirs.

***Table 1.*** *Input data for the hollow rod inner surface temperature distribution calculation*

| Value | Size | Reservoir | |
|---|---|---|---|
| | | T | Tl-Bb |
| $t_{пл}$ | ℃ | 25 | 24 |
| $D_{пл}$ | m | 1479 | 1470 |
| $D_{насос}$ | m | 1509 | 1400 |
| $\beta_в$ | % | 8.4 | 7.1 |
| $D_{dyn}$ | m | - | 694 |
| $\rho_f$ | $kg/m^3$ | 870 | 834 |
| $q$ | $m^3/day$ | 4.9 | 13.9 |
| $t_{н.с.}$ | ℃ | 7 | |
| $\omega$ | ℃/m | 0.013 | |
| $d_{эк1}$ | mm | 146 | |
| $d_{эк2}$ | mm | 132 | |
| $d_{ш1}$ | mm | 38 | |
| $d_{ш2}$ | mm | 19 | |
| $d_{нкт1}$ | mm | 73 | |
| $d_{нкт2}$ | mm | 62 | |
| $d_{скв}$ | mm | 216 | |
| $\lambda_{нкт}$ | W/ (m · ℃) | 64 | |
| $\lambda_{цемента}$ | W/ (m · ℃) | 1.51 | |
| $\lambda_н$ | W/ (m · ℃) | 0.1325 | |
| $\lambda_в$ | W/ (m · ℃) | 0.593 | |
| $R_{гр}$ | m · ℃/W | 120 | |
| $c_в$ | J/kg · ℃ | 4182 | |
| $c_н$ | J/kg · ℃ | 2100 | |

where $D_{насос}$ was pump suspension depth, m; $\beta_в$ was fluid water cut, %; $D_{dyn}$ was dynamical level depth, m; $d_{скв}$ was the well diameter, mm; $d_{эк1}$ was the outer diameter of the production string, mm; $d_{ш1}$ was the outer diameter of the hollow rod, mm; $d_{нкт1}$ was the outer diameter of the pumping and compressor pipe, mm; $d_{эк2}$ was the inner diameter of the production string, mm; $d_{ш2}$ was the inner diameter of the hollow rod, mm; $d_{нкт2}$ was the inner diameter of the pumping and compressor pipe, mm; $\lambda_{нкт}$ was the heat conductivity coefficient of the pump-compressor pipe, W/ (m · ℃); $\lambda_{цемента}$ was cement stone heat conductivity coefficient, W/ (m · ℃); $\lambda_в$ was water heat conductivity coefficient, W/ (m · ℃); $\lambda_н$ was oil heat conductivity coefficient, W/ (m · ℃); $R_{гр}$ was the thermal resistance of the rock surrounding the well, m · ℃/W; $c_в$ was water heat capacity, J/kg · ℃; $c_н$ was oil heat capacity, J/kg · ℃.

Forecasting asphalt deposits (AD) formation in hollow rods of a target facility required plotting a chart representing surface temperature distribution along the length of hollow rod inner wall. The following initial data were required for this calculation:

- Geometric characteristics and thermal conductivity of the material of cement stone (CS), production string (PS), pumping and compressor pipes (PCP), and hollow rods.
- Well production rate.
- Depth and temperature of the reference datum in the given region.
- Top and bottom temperature and elevations of the operated oil reservoirs.
- Pump-setting depth.
- Thermal conductivity of geological material around the well.
- Dynamical level value of the given well.
- Physical and chemical properties of liquid fluids (density, dynamic viscosity, water cut of recovered products, and thermal conductivity).
- Associated petroleum gas composition.

The pattern of inner wall surface temperature variation along hollow rod length was determined based on expressions presented in (Korobov and Mordvinov, 2013; Gorshkov, 2014; Krajnov *et al*., 2010; Malashkina, 2015). First, it was required to calculate the total thermal resistance as per Equation 4 for fluids recovered from both productive reservoirs:

$$K = \frac{1}{\frac{1}{\alpha} + R} \qquad \text{(Eq.4)}$$

where $\alpha$ was the internal pipe fluid heat transfer coefficient, W/ ($m^2$ · ℃); R was the thermal resistance of the media surrounding the well, $m^2$ · ℃/W; $K_T$ was the coefficient of heat condition from the fluid to the environment, W/ ($m^2$ · ℃).

Coefficient α was calculated based on the criteria dependent function for laminar flow presented in Equation 5:

$$\alpha = 4 \cdot \frac{\lambda_t}{d} \qquad \text{(Eq.5)}$$

where $\lambda_t$ was pipe material heat conductivity coefficient, W/ (m · ℃).

Coefficient R could be calculated based on Equation 6:

$$\mathrm{R} = \sum \frac{h_i}{\lambda_i} \quad \text{(Eq.6)}$$

where $\lambda_\mathrm{i}$ was insulating material heat conductivity coefficient, $\mathrm{W}/(\mathrm{m} \cdot ℃)$; $\mathrm{h_i}$ was insulation layer thickness, m

However, coefficient R could not be applied to the entire well depth because different components determine it. For this reason, calculations were made for three different thermal resistance modes and their corresponding sections: from bottom-hole to pump-setting depth ($R_1$), from pump-setting depth to dynamical level ($R_2$), from dynamical level to well-head ($R_3$). Under all three modes, thermal resistance was an aggregate of various combinations of resistance values corresponding to hollow rod body, the fluid moving inside pumping and compressor pipes (PCP) string, casing string PCP wall, cement stone, and geological material around the well.

By applying Equations 5 and 6 to expression Eq. 7, the following was obtained:

$$K_\mathrm{T} = \frac{1}{\frac{d}{4 \cdot \lambda_t} + \sum \frac{h_i}{\lambda_i}} \quad \text{(Eq.7)}$$

Coefficient K was calculated based on the assumption of complete alignment of all well components. Because coefficient R varied along with the well depth, coefficient K varied within a similar range.

To determine the pattern of temperature variation along the wellbore, Equation 8 was written down. Its left-hand member was representing the quantity of heat given up by liquid in the elementary area $\mathrm{d}L$ upon lifting the recovered products by PCP or hollow rod with the lateral area amounting to $\pi \cdot D \cdot \mathrm{d}L$. The right-hand member of this expression represented the decrease of fluid temperature upon its lifting.

$$K_\mathrm{T} \cdot [t_\mathrm{ст} - (t_\mathrm{пл} - \omega \cdot L)] \cdot \pi \cdot d \cdot \mathrm{d}L = c_\mathrm{f} \cdot \omega \cdot \rho_\mathrm{f} \cdot u \cdot F_\mathrm{тр} \cdot \mathrm{d}t_\mathrm{f} \quad \text{(Eq.8)}$$

where L was the vertical distance from the bottom-hole to the studied elementary pipe section, m; dL was elementary pipe section, m; $c_f$ was water-in-oil emulsion heat capacity $\mathrm{J}/\mathrm{kg} \cdot ℃$; u was the average fluid flow rate, m/sec; wass a clear opening area, $\mathrm{m}^2$; $\mathrm{dt_f}$ was a fluid temperature change in the elementary section, ℃.

To perform the integration of Equation 8, it was required to use the equation of integration constant ($C_1$), which was determined based on initial conditions with $h = 0$ и $t_\mathrm{ст} = t_\mathrm{пл}$ obtained from Equation 9:

$$C_1 = \frac{c_\mathrm{f} \cdot \omega \cdot \rho_\mathrm{f} \cdot q}{K_\mathrm{T} \cdot \pi \cdot d} \quad \text{(Eq.9)}$$

where q was volumetric fluid flow, $\mathrm{m}^3/\mathrm{day}$.

In Eq. 8, the product of the average fluid flow rate ($u$) and clear pipe area ($F_\mathrm{тр}$) corresponded to the volumetric flow rate value presented in Equation 10:

$$u \cdot F_\mathrm{тр} = q \quad \text{(Eq.10)}$$

A solution to Eq. 8, taking into account Eq. 10, was found via Eqs. 11 or 12:

$$t_\mathrm{ст} = t_\mathrm{пл} - \omega \cdot L + \frac{c_\mathrm{f} \cdot \omega \cdot \rho_\mathrm{f} \cdot q}{K_\mathrm{T} \cdot \pi \cdot d} - C_1 \cdot e^{\frac{K_\mathrm{T} \cdot \pi \cdot d \cdot L}{c_f \cdot \rho_f \cdot q}} \quad \text{(Eq.11)}$$

$$t_\mathrm{ст} = t_\mathrm{пл} - \omega \cdot L + \frac{c_f \cdot \omega \cdot \rho_f \cdot q}{K_T \cdot \pi \cdot d} \cdot \left(1 - e^{\frac{K_T \cdot \pi \cdot d \cdot L}{c_f \cdot \rho_f \cdot q}}\right) \quad \text{(Eq.12)}$$

Upon calculating inner temperature distribution across hollow rod surface along the well length, a chart was plotted based on Eq. 11. The created chart was required to select several sections with characteristic temperatures (maximum, minimum, closest to the initial paraffin crystallization temperature (IPCT)) and intermediate temperature values. The obtained temperature values would be subsequently used in laboratory tests for determining the rate of AD formation on the Cold Finger unit. To improve the accuracy of tests conducted on this unit, 4 unconnected Cold Fingers were used simultaneously. Because the Cold Finger unit was a "reverse pipeline", the temperature of the refrigerant fluid used for cooling the inner surface of Cold Fingers was taken as equal to the temperature of the hollow rod inner surface, which was calculated based on Equation 11. The assessed oil sample mixing speed was taken based on the calculated recovered products flow rate along the internal surface of hollow rods. Based on the obtained laboratory test results, the rate of AD formation was assessed using Equation 13:

$$I = \frac{m_\mathrm{AD}}{m_{oil}} \cdot 100 \quad \text{(Eq.13)}$$

where $\mathrm{I}$ was AD formation intensiveness, %; $\mathrm{m_{AD}}$ was the mass of adhered AD equal to the difference of the Cold Finger masses before and after survey, g; $\mathrm{m_{oil}}$ was AD mass of the studied oil sample, g.

The effectiveness estimation of applying inhibitor reagents was made according to Equation 14:

$$\mathrm{K_{ing}} = \frac{\mathrm{I_2} - \mathrm{I_1}}{\mathrm{I_2}} \cdot 100\% \qquad \text{(Eq.14)}$$

where $\mathrm{K_{ing}}$ is specific inhibition capacity, %; $\mathrm{I_1}$ is AD formation intensiveness after AD inhibitor application, %; $\mathrm{I_2}$ is AD formation intensiveness before AD inhibitor application, %.

The effectiveness estimation of the hydrocarbon solvents was made based on Equation 15.

$$K_\mathrm{s} = \frac{m_{\mathrm{AD2}} - m_{\mathrm{AD1}}}{m_{\mathrm{AD2}}} \cdot 100\% \qquad \text{(Eq.15)}$$

## 3. RESULTS AND DISCUSSION

### 3.1. Calculation of the technological parameters of the target multi-zone oil-producing well operating two oil reservoirs

The temperature distribution along the well depth was carried out with the algorithm presented in the Methods chapter. The preparatory stage of the calculation is the determination of such parameters as thermal resistance of the media surrounding the well ($R$), coefficient of heat conductivity from the fluid to the environment ($K_\mathrm{T}$), water-in-oil emulsion heat conductivity coefficient ($\lambda_\mathrm{f}$), water-in-oil emulsion heat capacity ($c_\mathrm{f}$)and inner pipe surface fluid heat transfer coefficient, ($\alpha$). Calculation $R, K_\mathrm{T}, \alpha$ is carried out under Eqs. 3,1,2 respectively. The water-in-oil emulsion heat capacity values ($c_\mathrm{f}$) are used by Eq. 16. The water-in-oil emulsion heat conductivity values are found in Eq. 17.

$$c_f = c_\mathrm{н} \cdot (1 - \beta_\mathrm{в}) + c_\mathrm{в} \cdot \beta_\mathrm{в} \qquad \text{(Eq.16)}$$

$$\lambda_\mathrm{f} = \lambda_\mathrm{н} \cdot \left[\frac{2 \cdot \lambda_\mathrm{н} + \lambda_\mathrm{в} - 2 \cdot \beta_\mathrm{в} \cdot (\lambda_\mathrm{н} - \lambda_\mathrm{в})}{2 \cdot \lambda_\mathrm{н} + \lambda_\mathrm{в} + 2 \cdot \beta_\mathrm{в} \cdot (\lambda_\mathrm{н} - \lambda_\mathrm{в})}\right] \qquad \text{(Eq.17)}$$

These parameters need to be determined for the three intervals the producing well was conventionally divided into. The first interval is the distance from the depth of reservoir T to the pump suspension depth ($\boldsymbol{R_1, K_{T1}}$), the second is the distance from the pump suspension depth to the dynamical level mark ($\boldsymbol{R_2, K_{T2}}$), and third is the distance from the dynamical level mark to the oil-producing well mouth ($\boldsymbol{R_3, K_{T3}}$). The parameters calculated for the given producing well are presented in Table 2.

Based on Equation 11, the temperature graph of the inner surface of the pumping and compressor pipes used for pumping product from Tl-Bb reservoir and the temperature graph of the inner surface of the hollow rod body string transporting the product from T reservoir have been formed and presented in Figure 1.

Analysing Figure 1, we may conclude that the temperature of the inner surface of the hollow rods changes more intensively compared to the inner surface of the pumping and compressor pipes (PCP). This is explained by the fact that the fluid recovered from reservoir T features two additional thermal resistance values (resistance of the liquid layer and resistance of the hollow rod body). For this reason, the fluid loses temperature faster as it approaches the well mouth. The reason for changing the temperature distribution pattern above the dynamic level ($D_\mathrm{dyn}$) is the change of the fluid contained in the annulus (thermal resistance of the gas mix increases the same oil parameter several-fold).

### 3.2. The result of determining possibilities of the organic deposit formations according to the methods described in paragraph 1

The solution of the equations describing the temperature of the string and the temperature of oil saturation with paraffin, which are the first group of methodologies, is shown in Figure 2. The second group of methodologies does not have a graphical solution, since it is based on the analysis of the existing graphs of the dependence of the formation depth of the organic deposits on the ratio of asphaltene and resinous phase. According to the results of this analysis, for the fluid under consideration, the ratio of the mass content of asphaltenes to resins (A/R) is 0.21, and the depth of the onset of sediment formation is 600 m. Application of the third group of methodologies is not possible due to the need for

high-precision and expensive equipment, which is its main disadvantage.

After analyzing this graph and the results given for the second group of methods, we can say that these methods are inaccurate, do not take into account many factors and are based on empirical dependencies, not on laboratory studies, so we cannot recommend them for use.

### 3.3. Determination of the intensiveness of AD formation in laboratory conditions

The laboratory studies of AD formation intensiveness were carried out with the CF-4 cold finger unit presented in Figure 3.

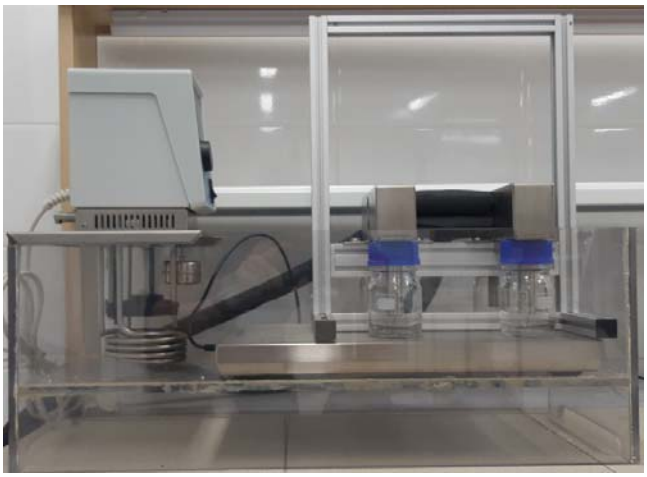

***Figure 3.*** The Cold Finger laboratory unit CF-4

Based on the analysis of Fig. 1 for the laboratory studies of the AD formation intensiveness, 5 temperatures were selected to match the estimated temperatures of the inner surface of the hollow rod within the given intervals of the well depth. In each of the intervals, the studies were carried out at the sample mixing rate of 300 rpm for 25 minutes, which equals the time of fluid elevation through the studied intervals. The study was carried out on 4 samples simultaneously and under the same conditions to minimize the possible error of the survey results. The AD formation intensiveness was assessed based on Equation 13. Figure 4 presents the examples of Cold Fingers before the survey and after its completion.

a) b)

***Figure 4.*** Cold Finger picture example: a) before the survey; b) after the survey

Table 3 shows the results of the survey of the AD formation intensiveness within the studied intervals.

***Table 3.*** *AD formation intensiveness in the studied intervals*

| $t_{ш}$, ℃ | $I$, % |
|---|---|
| 24.29 | 0 |
| 22.21 | 0.33 |
| 16.47 | 0.30 |
| 11.35 | 0.27 |
| 7.36 | 0.31 |

where $t_{ш}$ is Hollow rod inner surface temperature, ℃.

Analyzing these data, we may conclude that the intensiveness of AD formation on the inner surface of the hollow rod changes throughout the rod length. The most intensive AD formation process was found at the temperature of 22.21 degrees, which corresponds to the depth of 1079 meters from the well mouth. This peak of AD formation intensiveness is associated with the drop of recovered fluid temperature below the paraffin appearance temperature (IPCT), and then below the mass paraffin phase appearance temperature (MPAT). As the temperature further drops to 16.47 ℃, and then to 11.35 ℃ at a depth of 779 m and 379 m, respectively, the AD formation intensiveness correspondingly reduces. This fact may be explained by the active precipitation of AD previously, at a depth of 1079 m, and the absence of sufficient temperature gradient between the fluid and the hollow rod inner surface. At the temperature of 7.36 ℃, the second peak of AD formation intensiveness is observed in the well mouth. This peak may be

associated with the intensive growth of the temperature gradient between the hollow rod inner surface and the recovered fluid.

The collected results of the laboratory survey of the changes in the intensiveness of the AD formation in the hollow rod string are depicted in the temperature graph of the inner surface of the hollow rod string and the inner surface of the PCP string and presented in Figure 4.

In Figure 4, it can be seen two epicenters of AD formation within the studied oil-producing well. During operation, the greatest share of the organic deposits forms at a depth of 800-1100 meters, thereby facilitating the emergence of additional hydraulic resistances. Generally, as a result of the simulation of oil elevation through the hollow rod string, 0.76 g of asphaltene deposits for the studied 63.677 g of oil was found.

### 3.4. Determination of technological efficiency of the counter-AD technologies used in the hollow rod strings

At the present moment, there are many methods of AD appearance prevention. The most economically feasible and efficient individual counter-AD technology shall be selected in the diversity of recovered fluids and recovery conditions at every target facility (Caeiro *et al*. 2015). There is a known classification of counter-AD formation methods that divides all methods into two groups: AD formation prevention methods and methods of combating the developed deposits. Different deposit combat measures shall be applied depending on the physical, chemical, and rheological properties of the recovered fluids, their composition, temperature, and recovery conditions. These methods may be classified into thermal, chemical, physical, and mechanical. The thermal methods are based on heating the oil above the IPCT temperature followed by the dissolution of the wax component of the fluid, preventing its recovery from the fluid volume (Putilov, *et al*., 2020; Revel'-Muroz *et al*., 2017 Reza and Farzaneh, 2007) The chemical methods assume the application of the reagents preventing the AD formation (inhibitor reagents) or the substances that eliminate the existing deposits (hydrocarbon solvents, detergents) (Robinson and Peng, 1976; Shaislamov, *et al*., 2007; Shrajbman, *et al*., 2008). The physical meth-ods require various physical fields (magnetic, acoustic, ultrasound, electric) and mechanic deposit removal methods (Turbakov, et al., 2009; Volodin, et al., 2008). Due to the specificity of a configuration of the downhole pumping equipment used for dual operation (DO), there are certain restrictions for the applicability of the counter-AD measures.

This way, it was considered two AD removal technologies applicable for this type of oil operation, which are the application of chemicals (inhibitor reagent application) and AD removal using hydrocarbon solvents.

The research of technological efficiency of applying the inhibitor reagents to prevent deposit formation on the inner surface of the hollow rods was carried out with the Cold Finger unit. The research covered three different reagents: FLEK-IP-106, EFRIL-IPO417M grade DP and SNPH-7909. The studies were carried on two concentrations for each of the studied reagents: 200 g/tonne and 400 g/tonne. The intensiveness of AD formation under the use of inhibitor reagents was calculated with Eq. 10. The results of these studies are presented in Fig. 5. Upon the results of the laboratory researches, the specific inhibition capacity of the studied reagents was calculated. This property was determined using Eq. 14. These value calculation results are shown in Table 4. Based on the results shown in Figure 5, and in Table 4, it may be concluded that for the oil recovered from the target oil-producing well of Pavlovka oil field, the most efficient AD inhibitor is EFRIL-IPO417M grade DP. The specific efficiency is 48.1% at the chemical reagent dose of 200 g/tonne.

***Table 4.*** *Calculated specific efficiency of the studied reagent application*

| Considered inhibitor | C (g/tonne) | $K_{ing}$ (%) |
|---|---|---|
| FLEK-IP-106 | 200 | 7.9 |
| | 400 | -4.0 |
| EFTIL-IPO417M grade DP | 200 | 48.1 |
| | 400 | 12.1 |
| SNPH-7909 | 200 | 36.8 |
| | 400 | 29.5 |

The technological efficiency of AD solvent washes for removing the formed deposits was also determined with the Cold Finger unit. In the current survey, three different AD solvents were used: EFRIL-270, FLEK R-016, RTS-1. The survey was carried out in the AD samples collected from the reservoir fluid collected from the target oil-producing well by sinking the Cold Finger into the free volume of solvent for 60, 120, and 150 seconds. The solvent efficiency was assessed with Eq. 15. The results of the completed laboratory are shown in Table 5.

***Table 4.*** *Results of the solvent capacity studies of the considered AD solvents.*

| Considered solvent | $T_{иссл}$ (°C) | $K_s$ (%) |
|---|---|---|
| EFRIL-270 | 60 | 66.4 |
| | 120 | 71.1 |
| | 150 | 74.1 |
| FLEK R-016 | 60 | 76.3 |
| | 120 | 86.2 |
| | 150 | 92.4 |
| RTS-1 | 60 | 79.5 |
| | 120 | 85.2 |
| | 150 | 88.5 |

Analyzing these data, it may be noticed that the most efficient AD solvent for the product recovered from the target oil-producing well is FLEK R-016. The solvent capacity coefficient for the treatment time of 150 s was 92.4%.

## 4. CONCLUSIONS:

1. A method is proposed for assessing the formation rate of the organic deposits on the inner surfaces of the string and hollow rods in case of a dual operation of two oil reservoirs. This method is based on assessing the temperature distribution of the oil-producing well and conducting laboratory studies.

2. The hollow rod inner surface temperature distribution has been calculated. The laboratory survey was carried out to assess the nature and the AD formation intensiveness change degree on the studied surface based on the calculations.

3. The nature and the degree of AD formation intensiveness change on the studied surface have been analyzed. The analysis of the changes may discover the reason for the AD formation intensiveness changes along the depth length. It requires further studies due to the lack of theoretical materials to describe the phenomenon. Based on the AD formation intensiveness change analysis, it became possible to forecast the AD deposit formation in hollow rods and, particularly, to determine the depth of the most intensive organic deposit formation.

4. A comparison of the proposed method for assessing the formation depth of the organic deposits with existing analogs is given. Based on this comparison, we can conclude that the proposed method has high accuracy and efficiency; and we recommend it for use at existing oil production facilities to explore limitations of its applicability.

5. The technological applicability of the chemical technology (AD solvent and inhibitor application) has been assessed. According to the laboratory survey results, the application of both deposit removal technologies is technologically efficient with the correctly selected reagent.

## 5. ACKNOWLEDGMENTS:

This research was funded by the state assignment of the Ministry of Science and Higher Education of the Russian Federation as part of a government assignment, grant number FSNM-2020-0027.

## 6. REFERENCES:

1. Bahgizin, R. N.; Urazakov, K. R.; Usmanov, R. V.; Tugunov, P. M. (2019). Investigation of the thermal regime of a productive reservoir during simultaneous and separate operation of rod and electric center-run pump installations. *Oil Industry,* 4: 80-83. DOI: 10.24887/0028-2448-2019-4-80-83.
2. Caeiro, M.H.; Demyanov, V.; Soares, A. (2015). Optimized History Matching with Direct Sequential Image Transforming for Non-Stationary Reservoir, *Mathematical Geosciences,* 47(8): 975-994. DOI: 10.1007/s11004-015-9591-0
3. Demyanov, V.; Soltani, S.; Kanevski, M.; Canu, S.; Maignan, M.; Savelieva, E.; Timonin, V.; Pisarenko, V. (2001). Wavelet analysis residual kriging vs. neural network residual kriging, *Stochastic Environmental Research and Risk Assessment*, 15(1): 18-32. DOI: 10.1007/s004770000056
4. Dubinov, Ju. S.; Ivanovskij, V. N. (2016). Optimization of the hollow pump rod head design. *Oil and Gas Territory* 3: 66-69.
5. Erofeev, A. A.; Turbakov, M. S.; Mordvinov, V. A. (2010). To calculate the temperature distribution of oil saturation with paraffin in the production wells of the Siberian oil field. *Perm Journal of Petroleum and Mining Engineering,* 5: 57-60.
6. Falovskij, V. I.; Horoshev, A. S.; Shahov, V. G. (2011). Modern approach to modeling phase transformations of hydrocarbon systems using the Peng-

Robinson equation of state. *Izvestija Samarskogo nauchnogo centra Rossijskoj akademii nauk*, 13(4-1): 120-125.

7. Farayola, K. K.; Adeboye, Y. B.; Adekomaya, O. A.; Olatunde, A. O. (2010). Thermodynamics prediction of wax precipitation using the Patel-Teja equation of state. Paper presented at the Nigeria Annual International Conference and Exhibition, Tinapa - Calabar, Nigeria, 31 July – 7 August. SPE 136966 DOI: 10.2118/136966-MS
8. Garifov, K. M.; Kadyrov, A. H.; Ibragimov, N. G., Fadeev, V. G.; Zabbarov, R. G. (2013). Development of technology for simultaneous and separate reservoir exploitation in JSC Tatneft. *Oil Industry*, 7, 44-47.
9. Gawas, K.; Krishnamurthy, P.; Wei, F; Acosta, E.; Jiang, Y. (2015). Study on Inhibition of High-Molecular-Weight Paraffins for South Eagle Ford Condensate. Paper presented at the SPE Annual Technical Conference and Exhibition, Houston, TX, USA, 28-30 September. Paper SPE 174817. https://doi.org/10.2118/174817-MS SPE-174817-MS
10. Glushchenko, V.N.; Shipiguzov, L.M.; Yurpalov, I.A. (2007). Evaluation of the effectiveness of asphaltene-resin-paraffin deposits inhibitors. *Oil Industry*, 5: 84-87.
11. Gorshkov, A. S. (2014). Modeling of non-stationary heat transfer processes in wall structures made of aerated concrete blocks. *Magazine of Civil Engineering*, 8 (52): 38-48.DOI: 10.5862/MCE.52.5
12. Hisamov, P. C.; Evdokimov, A. M.; Sultanov, A. S. (2009). . Improvement of the oil Field development system using equipment for simultaneous separate well operation. OILFIELD ENGINEERING, 5: 33-39.
13. Struchkov, I. A.; Rogachev, M. K. (2017). Risk of Wax Precipitation in Oil Well. *Natural Resources Research*, 26 (1): 67-73. DOI: 10.1007/s11053-016-9302-7
14. Ivanov, D. V.; Chizhov, A. P. (2013). Simultaneous exploitation of small deposits in the conditions of the Melekessky depression deposits. *Problems of collecting, preparing, and transporting oil and petroleum products*, 4 (94): 5-11.
15. Ivanovskij, V. N. (2010). SSO and intellectualization of wells: yesterday, today, tomorrow. *Oil and Gas Territory*, 3: 28-39.
16. Jalalnezhad, M. J.; Kamali, V. (2016). Development of an intelligent model for wax deposition in oil pipeline. *Journal of Petroleum Exploration and Production Technology,* 6(1): 129–133. DOI 10.1007/s13202-015-0160-3
17. Josset, L.; Demyanov, V.; Elsheikh, A.H.; Lunati, I.. (2015). Accelerating Monte Carlo Markov chains with proxy and error models. *Computers and Geosciences,* 85: 38-48. DOI: 10.1016/j.cageo.2015.07.003
18. Kishhenko, M. A.; Aleksandrov, A. N.; Rogachev, M. K.; Kibirev, E. A. (2018). Modeling of the formation of organic deposits of paraffin type during the operation of wells with electric centrifugal pumps. *Exposition Oil & Gas*, 5 (65): 29-34.
19. Korobov, G. Ju.; Mordvinov, V. A. (2013). Temperature distribution in the production well bore. *Oil Industry*, 4: 57-59.
20. Korobov, G. Ju.; Rogachev, M. K. (2015). Investigation of the influence of asphalt-resinous components in oil on the formation of asphalt-resin-paraffin deposits. *Oil and Gas Business*, 3: 162-173.
21. Krajnov, D. V.; Safin, I. Sh.; Ljubimcev, A. S. (2010). Calculation of additional heat losses through heat-conducting inclusions of enclosing structures (on the example of a window slope node). *Magazine of Civil Engineering*, 6: 17-22.
22. Krjakushin, A. I.; Shljapnikov, Ju. V.; Agafonov, A. A.; Nikishov, V. I. (2009). Results and prospects of implementation of simultaneous-separate operation of reservoirs in one well. *Oil and Gas Territory*, 12: 50-53.
23. Latypov, B. M. (2012). Installation of a rod screw pump for oil production in com-plicated conditions. *Oil and Gas Business*, 10(1): 13-15.
24. Ljapin, A. Ju.; Astahov, A. V.; Mihaljov, Ju. P. (2017). study of the crystallization temperature of paraffins in oil in order to reduce the formation of asphalt-resin-paraffin de-posits. *Science and technologies: oil and oil products pipeline transportation*, 7(6): 28-35. DOI: 10.28999/2541-9595-2017-7-6-28-35

*25.* Loskutova, Ju. V.; Judina, N. V. (2006). Evaluation of the effectiveness of asphaltene-resin-paraffin deposits inhibitors. *Bulletin of the Tomsk Polytechnic University. Geo Assets Engineering*, 309 (4): 104-108.

*26.* Malashkina, V. A. (2015). Features of thermodynamic processes in underground degas-sing pipelines made of composite materials in coal mines. *Mining informational and analytical bulletin (scientific and technical journal)*, (9): 198-204.

27. Misnik, V. V.; Galikeev, R. M. (2011). Method of forecasting the depth of formation of asphalt-resin-paraffin deposits in wells. *Oil and Gas Business*, (6):345-349.

28. Nurgaliev, A. A.; Habibullin, L. T. (2015). Analysis of the efficiency of SSO in small deposits in the South-East of the Republic of Tatarstan. *Interexpo GEO-Siberia*, 2(3): 169-172.

29. Nurgaliev, A. A.; Habibullin, L. T. (2016). Analysis of the efficiency of simultaneous and separate operation of wells in the fields of the South-East of the Republic of Tatarstan. *Interexpo GEO-Siberia*, 2(3): 230-233.

30. Osipov, A. V.; Galiullin, A. A.; Piskarev, M. A.; Gribennikov, O. A.; (2016). Determination of the depth of the beginning of paraffin crystallization. *Scientific research: from theory to practice*, (3), 205-208. DOI: 10.21661/r-112093

31. Pepeljaev V.V.; Krivonosov Ju.A. (2009). Hollow pump rod. *Patent of the Russian Federation № 2371565.*

32. Pepeljaev V.V.; Krivonosov Ju.A. (2008). Hollow pump rod. *Patent of the Russian Federation № 2398091.*

33. Putilov, I.; Krivoshchekov, S.; Vyatkin, K.; Kochnev A.; Ravelev K. (2020). Methods of predicting the effectiveness of hydrochloric acid treatment using hydrodynamic simulation, *Applied Sciences (Switzerland),* 10 (14). DOI: 10.3390/app10144828

34. Revel'-Muroz, P. A.; Bahtizin, R. N.; Karimov, R. M.; Mastobaev, B. N. (2017). Joint use of thermal and chemical methods of influence during transportation of high-viscosity and solidifying oils. *SOCAR Proceedings*, 2(2): 49-55.

35. Reza, D.; Farzaneh, F. (2007). A thermodynamic model for wax deposition phenomena. *Fuel*, 86 (10-11): 1402-1408. DOI: 10.1016/j.fuel.2006.11.034

36. Robinson, D.B.; Peng, D.Y. (1976). A New Two-Constant Equation of State Industrial and Engineering Chemistry: Fundamentals. *Industrial & Engineering Chemistry Fundamentals*, 15: 59-64. http://dx.doi.org/10.1021/i160057a011

37. Shaislamov, Sh. G.; Antonin, R. A.; Antonin, A. S.; Laptev, V. V. (2007). About simultaneous operation of several layers (interlayers) by one well. *Drilling and Oil*, (10): 21-23.

38. Shrajbman, V. M.; Kolupaev, A. M.; Dolmatov, V. P.; Ponurovsky, A. G. (2008) Method of making a pump rod. *Patent of the Russian Federation № 2342216*.

39. Turbakov, M. S.; Erofeev, A. A.; Lekomcev, A. V. (2009). For determining the depth of the early formation of asphal-tenes-operating with sediments in the operation of oil wells. *Geology, geophysics and development of oil and gas fields*, (10): 62-65.

40. Volodin, A. M.; Artes, A. E.; Sorokin, V. A.; Sosenushkin, E. N.; Petrov, N. P.; Tretyukhin, V. V.; Sharapov, K. M. (2008) Method for manufacturing a hollow pump rod for gas and oil wells. *Patent of the Russian Federation № 2384384*.

***Table 2.*** *Interim results of the calculation of temperature distribution along with the target oil-producing Pavlovka oil field well. Source: the author*

| Value | Size | Reservoir | | | | | |
|---|---|---|---|---|---|---|---|
| | | T | | | Tl-Bb | | |
| | | Interval | | | | | |
| | | 1 | 2 | 3 | 1 | 2 | 3 |
| $R$ | $\mathrm{m^2 \cdot ℃/W}$ | 0.41 | 0.33 | 1.36 | - | 0.28 | 1.31 |
| $K_\mathrm{T}$ | $\mathrm{W/(m^2 \cdot ℃)}$ | 2.24 | 2.72 | 0.71 | - | 3.21 | 0.74 |
| $c_f$ | $\mathrm{J/kg \cdot ℃}$ | 2238.6 | | | 2217.15 | | |
| $\lambda_\mathrm{f}$ | $\mathrm{W/(m \cdot ℃)}$ | 0.151 | | | 0.148 | | |
| $\alpha$ | $\mathrm{W/(m^2 \cdot ℃)}$ | 36.04 | | | 27.53 | | |

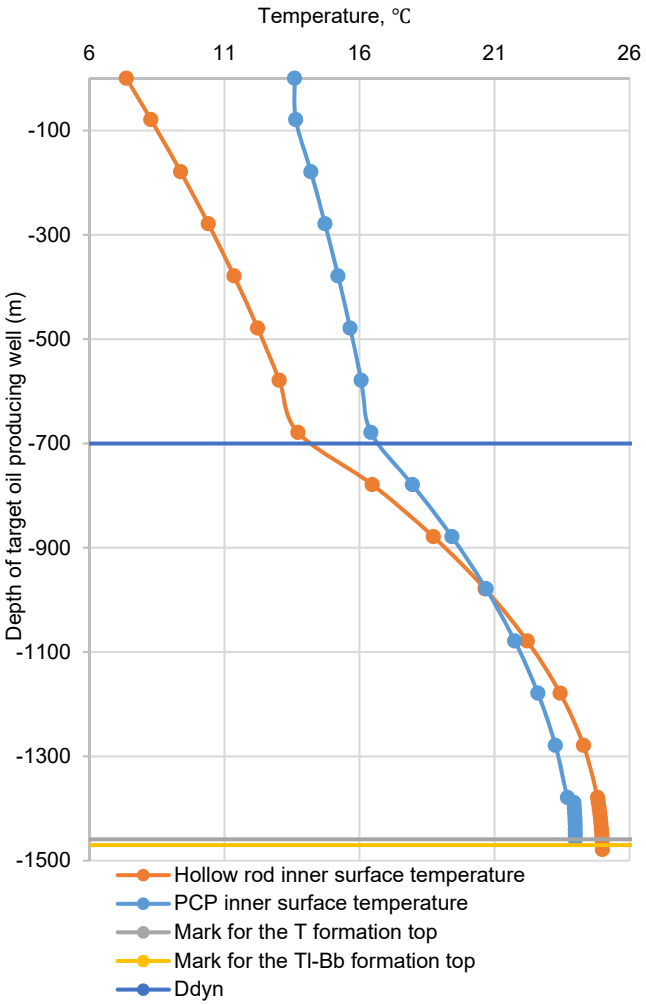


**Figure 1.** PCP string inner surface temperature graph and the hollow rod string inner surface temperature graph

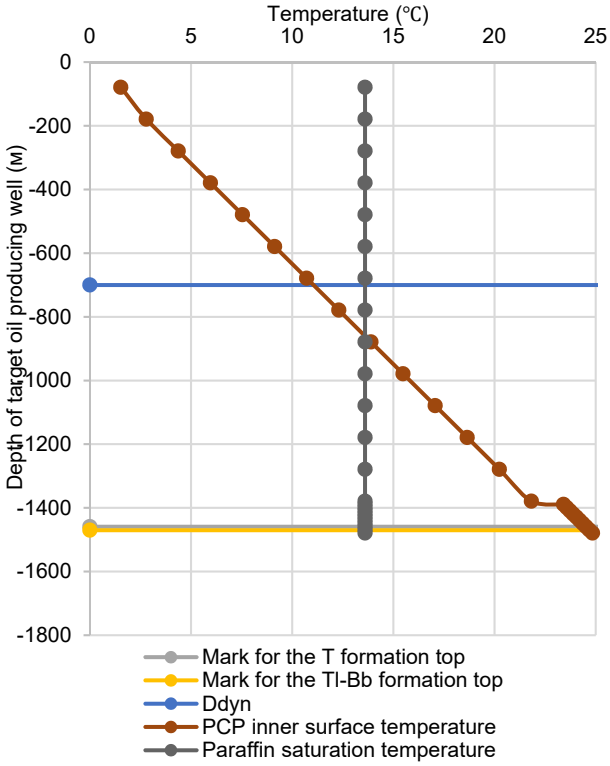


**Figure 2.** The results of calculating the depth of the starting formation of the organic deposits according to the first group of methods

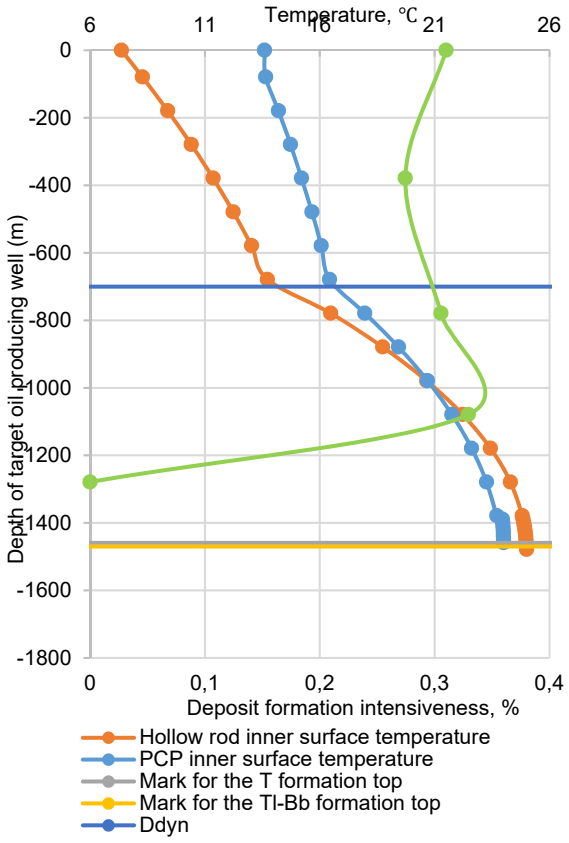


***Figure 4.*** The dependency of the AD formation intensiveness along the hollow rod string

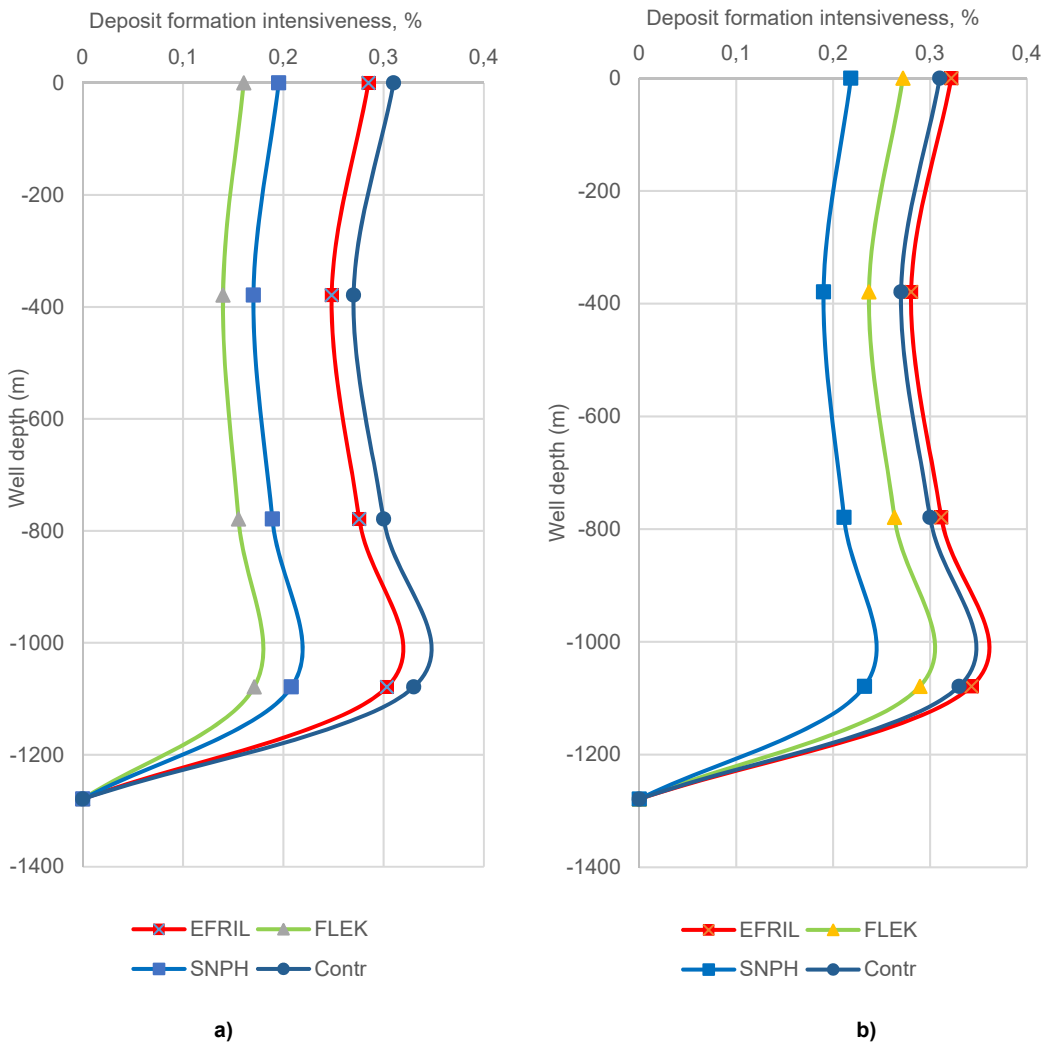


***Figure 5.*** Changes of the AD formation intensiveness in the selected sections: a) upon application of the given inhibitor dose of 200 g/tonne; b) upon application of the given inhibitor dose of 400 g/tonne

PERIÓDICO TCHÊ QUÍMICA
ARTIGO ORIGINAL

# IDENTIFICAÇÃO DE DIVERSIDADE DE SEMENTES DE BETERRABA HÍBRIDAS E DECENDENTES

# IDENTIFICATION OF SEEDS DIVERSITY IN SUGAR BEET HYBRIDS AND LINES

# ОПРЕДЕЛЕНИЕ РАЗНОКАЧЕСТВЕНОСТИ СЕМЯН ГИБРИДОВ И ЛИНИЙ САХАРНОЙ СВЕКЛЫ

VOSTRIKOVA, Tatiana V.[1]*; SKACHKOV Sergey I.[1]

[1] Federal State Budgetary Scientific Institution “A.L. Mazlumov All-Russian Research Institute of Sugar Beet and Sugar”, Voronezh, Russian Federation.

** Correspondence author*
*e-mail: tanyavostric@rambler.ru*

Received 10 September 2020; received in revised form 02 February 2021; accepted 23 February 2021

## RESUMO

**Introdução**: A diversidade das sementes manifesta-se na sua heterogeneidade de acordo com as características morfológicas e qualidades de semeadura, que dependem do genótipo e das condições de cultivo. Um dos principais indicadores das diferentes qualidades das sementes de beterraba é a energia germinativa e a capacidade de germinação, que dependem do genótipo. A influência de fatores agrotécnicos na diversidade de sementes supera a genética. **Objetivos**: o objetivo do estudo é identificar os efeitos do tratamento de pré-semeadura do composto químico inorgânico na diversidade de sementes de beterraba sacarina (*Beta vulgaris* L.) para linhagens e híbridos. **Métodos**: Como os sinais da diversidade de sementes são compreendidos, energia germinativa, comprimento da muda, massa da muda. Foi apresentado um método para identificação da diversidade genética de sementes de híbridos e linhagens de *Beta vulgaris*, incluindo o tratamento de sementes com solução aquosa da substância química inorgânica na concentração de 10% com exposição de 15 s, cálculo de critérios para a diversidade de sementes: energia germinativa, comprimento da muda, massa da muda. **Resultados e Discussão**: Foram utilizadas altas concentrações do composto químico inorgânico para revelar a diversidade genética das sementes. As reações dos genótipos da beterraba sacarina no fator provocativo (a substância química inorgânica) foram diferentes umas das outras. O composto químico inorgânico foi utilizado como fator provocativo e o método agrotécnico, e as características de comprimento da muda e massa da muda foram levadas em consideração como indicadores da heterogeneidade de híbridos e linhagens nos estágios iniciais de desenvolvimento da planta. **Conclusões**: O estudo permitiu revelar a diversidade genética de sementes de beterraba sacarina segundo os critérios energia de germinação e avaliar a heterogeneidade de híbridos e linhagens em estágios iniciais de desenvolvimento vegetal de acordo com as características de comprimento da muda e massa da muda.

**Palavras-chave**: *diversidade de sementes, energia germinativa, comprimento da muda, massa da muda.*

## ABSTRACT

**Background:** Seeds diversity manifests in their heterogeneity according to morphological characteristics and sowing qualities, depending on the genotype and growing conditions. One of the main indicators of the different qualities of beet seeds is the germinative energy and germination capacity, which depend on the genotype. The influence of agrotechnical factors on the diversity of seeds exceeds genetic. **Aim:** The purpose of the study is to identify the effects of the pre-sowing treatment of the inorganic chemical compound on the diversity of sugar beet (*Beta vulgaris* L.) seeds for lines and hybrids. **Methods:** As the signs of the seeds diversity is understood, germinative energy, seedling length, seedling mass. It is presented a method for identifying the genetic diversity of seeds of hybrids and lines of *Beta vulgaris*, including the treatment of seeds with an aqueous solution of the inorganic chemical substance at a concentration of 10 % with an exposure of 15 s, calculation of criteria for the diversity of seeds: germinative energy, seedling length, seedling mass. **Results and Discussion:** It was used high concentrations of the inorganic chemical compound for revealing the genetic diversity of seeds. Reactions of genotypes of sugar beet on the provocative factor (the inorganic chemical substance) were different from

each other. The inorganic chemical compound is used as a provocative factor and agrotechnical method, and the characteristics of seedling length and seedling mass are taken into account as indicators of the heterogeneity of hybrids and lines in the early stages of plant development. **Conclusions:** The study allows to reveal the genetic diversity of sugar beet seeds according to the criteria "germination energy" and to assess the heterogeneity of hybrids and lines at early stages of plant development according to the characteristics of seedling length, and seedling mass.

**Keywords**: *seeds diversity, germinative energy, seedling length, seedling mass*.

## АННОТАЦИЯ

**Предпосылки:** Разнокачественность семян проявляется в их неоднородности по морфологическим признакам и посевным качествам, которые зависят от генотипа и условий выращивания. Одним из главных показателей разнокачественности семян свеклы является энергия прорастания и всхожесть, зависящие от генотипа. Влияние агротехнических факторов на разнокачественность семян превышает генетические. **Цель:** Целью исследования являлось выявить действие предпосевной обработки неорганическим химическим соединением на разнокачественность семян гибридов и линий сахарной свеклы (*Beta vulgaris* L.). **Методы:** Под показателями разнокачественности семян понимались энергия прорастания, длина проростка, масса проростка. Представлен способ выявления генетической разнокачественности семян гибридов и линий *Beta vulgaris*, включающий обработку семян водным раствором неорганического химического вещества в концентрации 10 % с экспозицией 15 с, подсчет критериев разнокачественности семян: энергии прорастания, длины проростка, массы проростка. **Результаты и Обсуждение:** Для выявления генетического разнообразия семян используются высокие концентрации неорганического химического соединения. Реакции генотипов сахарной свеклы на провокационный фактор (неорганическое химическое вещество) отличались друг от друга. Неорганическое химическое соединение используется в качестве провоцирующего фактора и агротехнического приема, а признаки «длина проростка», «масса проростка» учитываются как индикаторы разнородности гибридов и линий на ранних стадиях развития растения. **Выводы:** Исследование позволяет выявить генетическую разнокачественность семян сахарной свеклы по критерию «энергия прорастания» и произвести оценку разнородности гибридов и линий на ранних стадиях развития растения по признакам «длина проростка», «масса проростка».

**Ключевые слова**: *разнокачественность семян, энергия прорастания, длина проростка, масса проростка*

## 1. INTRODUCTION

In connection with climate changes and environmental conditions, the introduction into production of a new generation of hybrids, soil cultivation methods, and fertilization systems, the emergence of preparative forms of chemical and bacteriological agents for the fight against the pathogenic microflora, researches in this direction is an urgent task. Every year, scientific achievements that promote a significant increase in yield of agricultural crops and reduce their cultivation technology expenses are more and more introduced into agricultural production practice. When cultivating sugar beet, many disease agents can affect plants even at initial growth, and development stages accumulate in soil of crop rotations. Long-term practice of sugar beet cultivation has shown that control of pathogenic microflora is one of the major tasks of the crop yield and technological qualities' increase.

It is known that the use of various chemicals, growth regulators, natural stimulants significantly accelerates the flowering of plants, and some agents also facilitate their adaptation to fluctuations in weather conditions, protect against various diseases (Bashmakov *et al*., 2012; Denisov *et al*., 2014 b). The use of some biological growth regulators makes it possible to obtain a crop with a lower content of lead and cadmium ions (Titov *et al*., 2011). Attempts are being made to apply the effect of "pre-adaptation" to increase plant resistance based on species-specific and non-specific reactions (Oudalova and Geras'kin, 2012; Pozolotina *et al*., 2010a, b). One example of species-specific reactions to external environmental factors (and internal factors of the organism) is the diversity of seeds.

The diversity of seeds manifests in their heterogeneity according to morphological characteristics and sowing qualities (Vostrikova, 2011), depending on the genotype and growing

conditions. The influence of agrotechnical factors on the diversity of seeds exceeds genetic (Balagura and Levshakov, 2013). Seeds diversity can be tested by cytogenetic (Kalaev *et al*., 2006; Yakymchuk, 2015; Baranova and Kalaev, 2017; Burmenko *et al*., 2018a,b) molecular-genetic (Popov *et al*., 2011; Baranova *et al*., 2018; Fachi *et al*., 2019) and functional: physiological (Welbaum, 1998; Ivanov, 2011; Lyanguzova, 2011; Opalko and Opalko, 2015; Kuzemko, 2016; Bome *et al*., 2015), biochemical (Neverova, 2004; Vetchinnikova, 2004; Bukharina, 2011; Gar'kova *et al*., 2011; Lapshina, 2016) characteristics.

A direct relationship was found between the yield of root crops and the size of seeds, only when comparing the extreme fractions (2.5-3.0 and 4.5-5.5 mm). However, when sowing with seeds of fractions of 3.25-3.5 mm, the productivity of male-sterile hybrids was practically the same as when sowing with seeds of fractions 3.5-4.5 mm (Balagura, Levshakov, 2013). A similar pattern was obtained for sugar content (Balan, 2000). One of the leading indicators of the different quality of beet seeds is the germinative energy and the germinating capacity, which depend on the genotype (Balagura, Levshakov, 2013).

The effect of different planting schemes for the male-sterile maternal component and the pollinator in the production of hybrid sugar beet seeds on the seed yield, as well as the germinating capacity, the germinative energy, and the yield properties of the obtained seeds, has been established (Tsareva, 2010, 2013).

The results of studying the effect of low temperatures on the germinative energy and the germinating capacity of seeds of O-type sugar beet lines, which are directly dependent on temperature, are presented (Polishchuk, 2013). However, it is noted that in breeding work, when creating hybrids that are adapted to growing conditions using intensive technologies, an important feature of the initial breeding material is the provision of the high germinative energy and the seed germinating capacity at low temperatures, which makes it possible to sow heterotic sugar beet hybrids in earlier terms (Polishchuk, 2013).

Thus, the main criteria for determining the different quality of beet seeds are the size of seeds, germinative energy, germinating capacity, and indicators of the growth activity of early stages of the development (seedling) are not taken into account. Also, as provocative backgrounds for the study of the reaction of the sugar beet as a field crop to external influences, meteorological conditions, and agrotechnical methods, other than the use of chemical compounds, are often used. Preparations based on the colloidal silver, surface modified with various biologically active surfactants and polymers, are created and studied by specialists of Chemistry and Biology Faculties of Moscow State University named after M. V. Lomonosov, with the support of AgroKhimProm Group of Companies. They are suitable for use in agriculture as plant growth stimulators, effective contact fungicides and bactericides for leaf treatments, dressing agents for grain and tubers both before planting and before storage. The preparation "Zerox" is based on chemically modified highly dispersed silver as an element of the effective fight against bacterial and fungal epiphytoties of agriculturally significant plants (Zherebin *et al.*, 2014). Colloidal silver has an eliciting effect that belongs to immunizing fungicides. It affects metabolism, increases the concentration of reactive oxygen forms in plant tissues (Zherebin *et al.*, 2014, 2015).

A promising active ingredient for such preparations is the colloidal silver, which combines the high bactericidal and fungicidal activity against a wide range of phytopathogenic microorganisms with low toxicity in relation to humans, animals, and higher plants (Jo *et al*., 2009; Kim *et al*., 2012).

Pure silver is slightly soluble in water. The toxicity of soluble silver compounds is a well-known fact. At the same time, all types of silver nanoparticles are characterized by low or zero toxicity. Silver nanoparticles have a large specific surface area that increases the area of contact of the element with pathogenic organisms and improves its bactericidal effect (Krutyakov *et al*., 2008; Zherebin *et al.*, 2014, 2015). Silver nanoparticles of 2-4 nm in the high-colloidal solution contain 6%, 4-6 nm – 15 %, 6-8 nm – 19 %, 8-10 nm – 18 %, 10-12 nm – 7 %, 12-14 nm– 4 %, 14-16 nm – 2 %, 16-18 nm – 1 % (Denisov *et al*., 2014 b; Elansky *et al*., 2014). Silver nanoparticles contained in the preparation are fixed and retained on the cell walls of phytopathogenic microorganisms. Silver nanoparticles oxidize and release silver ions, which disrupt the function of membrane proteins, especially transport proteins, that lead to the death of the pathogen. The gradual oxidation of silver nanoparticles provides a prolonged action of the preparation (Krutyakov *et al*., 2008; Elansky *et al.*, 2014). Synthesis, biosynthesis, and properties of silver nanoparticles are

described previously in other studies (Krutyakov *et al*., 2008). An effective agent against bacterial burns of fruit and vegetable crops, Zerox® is in the registration process (Lisichkin, 2019). The silver surface in the preparation was modified by amphoteric surfactant – ampholac – natrium amphopolycarboxyglycinate (Lisichkin, 2019). In order to produce the preparation, an aqueous solution of a silver salt (silver nitrate, acetate, citrate, chloride, bromide, iodide and sulfate) was mixed under rapid agitation with a solution of amphoteric surfactant and a solution of a reducing agent (sodium borohydride $NaBH_4$) (Denisov *et al*., 2014 a).

It is known the fungicidal and bactericidal preparation with a wide spectrum of action against phytopathogenic fungi, oomycetes, and bacteria, the active substance of which are nanosized particles of silver, the surface-modified with the ecologically safe biodegradable amphoteric surfactant. In vitro studies have shown the high efficiency of the preparation "Zerox®" (high-colloidal solution) in concentrations from 3 to 30 mg/l for silver against a wide range of fungal pathogens of potatoes (Zherebin *et al*., 2015). This is the inorganic chemical compound.

The purpose of the study is to identify the effects of the pre-sowing treatment of the inorganic chemical compound on the diversity of sugar beet (*Beta vulgaris* L.) seeds for lines and hybrids. As the signs of the seeds, diversity is understood germinative energy, seedling length, seedling mass.

## 2. MATERIALS AND METHODS

The object of the studies were non-pelleted seeds of 8 sugar beet hybrids and lines from the collection of the A. L. Mazlumov All-Russian Research Institute of Sugar Beet and Sugar: O-type 709, MS 709, Karioka, Mitika, Michelle, Granate, Zephyr, Murray, Portland, Tinker, and Veitura. They were soaked in 10 %, 20 %, and 30 % aqueous solution of the silver preparation (high-colloidal solution) for 15 seconds.

To obtain a silver solution, tap water was used. In order to obtain a 10% aqueous solution of the preparation, 10 ml of it was diluted with 90 ml of water. In a 20% aqueous solution, the proportion of components was 20 ml of it and 80 ml of water, in 30 % aqueous solution – 30 ml and 70 ml accordingly.

Seeds sprouted on a filter paper in plastic containers in four replications with 100 seeds per replication. The containers were kept under laboratory conditions at a constant temperature range of 22-25 °C. As a control, seeds of the same hybrid were used. They were soaked in tap water. Analysis of the solution influence on sugar beet seed sowing qualities – germinative energy, seedling length, seedling mass – were carried out. To study the emergence rate of seeds, seedlings were counted four days after the beginning of seed sprouting according to Russian Standards of seed germination (GOST 22617.2-94). The germinative energy of seeds is the germination speed expressed as the percent of emerged seeds (the ones that have formed roots that length is half of the seed length and seedlings) within the period determined by preliminary seed sprouting experiments. For field crops, it varies in the range from 3 to 15 days (Geister, 1934). A seedling is a plant at one of the initial ontogenesis stages, in the period from the moment of seed germination (that is, the moment when the developing embryo breaks through seed coat) till the moment when the leaf of the main shoot (the shoot developed from embryo bud) appears (Korovkin, 2007). The seedling length was measured with the help of a ruler four days after the experiment starts. The seedling mass was determined at four days using an electronic balance.

Statistical processing of the results was conducted using the Stadia software package. The procedure of data grouping and processing is stated in A. P. Kulaichev (2006) work. Average values of seedling lengths and seedling mass were compared using Student's *t*-test. The emergence rate of seeds in control and experimental variants were compared using Z-test for equality of frequencies. An increase in sugar beet emergence rate, length of seedlings, and mass of seedlings in the experiment as compared to the control (%) were calculated. The influence of the factor "treatment with the chemical compound" in different concentrations upon the listed traits was determined using a one-way analysis of variance. Power of influence was calculated according to Snedecor (%).

## 3. RESULTS AND DISCUSSION:

The influence of the preparation on the germinative energy, seedling length, and seedling mass is presented in Tables 1 and 2. Analyzing Table 1, it was noted an increase in the germinative energy after the treatment of sugar beet seeds with a 10% aqueous solution of the chemical compound in the studied hybrids

compared to the control (P<0.05). The exceptions were Karioka, Mitika, Michelle, Veitura, characterized by high (93-100%) germinative energy in the control variant and lower in the experiment, Portland (81%), and Tinker (92 %). 20 and 30 % concentration of the solution in some variants inhibited seed germination (Table 2). In general, the increase of the germinative energy in the experimental variant of 10 % concentration was 4-12% concerning the control.

Table 1 shows an increase of the seedling length in hybrids, including Carioca and Portland, compared to the control (P<0.05, P<0.01), after seed treatment with a 10% nanosilver solution, except such as Mitika, Michelle, Veitura. The increase in the average length of the seedling in the O-type 709 hybrid was 37.8%; for MS 709 – 67.5%; Karioka – 38.1%; from Granate and Zephyr – 22.2%; Portland – 22.4% and Tinker – 16.1% concerning the control.

However, a decrease in the seedling length was revealed in comparison with the control variant (P<0.05) in the Murray hybrid, which showed an increase in germinative energy. This indicates a different reaction of the embryo of hybrids to the treatment factor with the preparation: positive in seeds with lower germinative energy and, conversely, negative – in seeds with high sowing qualities, which is evidence of the genetic diversity of seeds.

Seedling mass was not in all cases associated with length. For example, an increase of the seedling length in the experimental variant (P<0.05) did not cause a corresponding increase of the mass in hybrids Pomegranate, Zephyr, Tinker (Tables 1 and 2). This indicates the heterogeneity of the hybrids in their properties. The seedling mass change corresponded to the length in the remaining hybrids after seed treatment with a 10% solution, which is not typical in cases of 20 and 30% concentration for the same variants (Table 2). The increase of the average seedling mass in the experimental variant of 10% concentration in the O-type 709 hybrid was 23.1%; for MS 709 - 60%; Karioka – 28.6% concerning the control. The seed treatment with 20 and 30% solution of the preparation more often had a depressing effect on the seedling length and the seedling mass.

Power of influence of the factor “sugar beet seed treatment with an aqueous solution of the chemical compound” on the germinative energy, the seedling length, and weight were evaluated according to the results of one-way analysis of variance (Tables 3, 4, 5). The power of influence of the factor “sugar beet seed treatment with an aqueous solution of the chemical compound” on emergence rate was lower than on seedling length and mass.

Thus, the different reaction of the embryo to the factor of seed treatment with the chemical substance of the same solution concentration to different hybrids indicates the genetic diversity of seeds. This is manifested in unequal changes of the studied traits: germinative energy, seedling length, seedling mass. Treatment of seeds of sugar beet hybrids with germinative energy below 92% by an aqueous solution of the preparation in 10% concentration allows to reveal their variability and improve sowing qualities.

Previously conducted experiments have shown suppression of radial growth of colonies of all the fungi species investigated when adding the modified colloidal silver in concentration (active substance) more than 10 ppm (1 ppm = 1 mkg/ml = 1 mg/l) (Mitsa *et al.*, 2014). Fungicidal properties have been evaluated on agar pea medium with the addition of Zerox in the concentrations of 0.1, 1, 10, and 100 mg/l (active substance). The fungicide effectiveness evaluation on the nutrient medium under laboratory conditions has shown that the stabilized colloidal silver is effective against strains of all the investigated species of fungi and oomycetes ($EC_{50}$ <19 ppm) (Elansky *et al.*, 2014).

The colloidal silver fungicidal effect evaluation results were similar to the data obtained during the evaluation of fungicidal effectiveness of silver nanoparticles in other laboratories of the world (Elansky *et al.*, 2014; Mitsa *et al.*, 2014). In works of other authors, similar $EC_{50}$ values for unmodified silver nanoparticles were presented: *Alternaria alternata* ($EC_{50}$=38 mg/l), *A. solani* (about 10 mg/l), *Fusarium* (from 9 to 55 mg/l in different species), *Pithium* (about 2 mg/l), *Colletotrichum* (from 8 to 100 mg/l in different species) (Lamsal *et al.*, 2011; Kim *et al.*, 2012). Effective concentrations ($EC_{50}$) for silver nanoparticles concerning sclerotium-forming species (6-7 mg/l) (Min *et al.*, 2009) exceed the $EC_{50}$ for the preparation regarding the same species (0.4-3.9 mg/l, accordingly) (Elansky *et al.*, 2014; Lamsal *et al.*, 2011; Kim *et al.*, 2012; Min *et al.*, 2009). Synergism of antibiotics and the silver preparation effect concerning the strains resistant to antibiotics has been revealed, though, with the addition of the silver preparation, no intensification of effective antibiotics’ influence has been registered (Khodykina *et al.*, 2014). There are used more concentrations: 300-900

mg/l (active substance) for revealing the genetic diversity of seeds in our experiments. Reactions of genotypes of sugar beet on the provocative factor (chemical compound) were different from each other.

A method of pre-sowing treatment for seeds of agricultural plants by spraying the seeds with a solution of the biologically-active substance in which a source of silver ions was the colloidal solution of silver nanoparticles AgBion-2 before sowing is known; the concentration of the substance in the working solution is 0.0047 %, and the rate of its application is 10 l/ton of seeds (Usanova *et al.*, 2012). However, the method of treatment by spraying seeds with a solution of the biologically-active substance has a disadvantage: an uneven distribution of the compound over the seed surface is possible. To avoid it, an additional device (generator) for even distribution of the compound is necessary (Pshechenkov *et al.*, 2016). Soaking of seeds in an aqueous solution of the silver preparation promotes even distribution of the compound over seed surface and allows the entire use of its potentialities with minimal material inputs.

## 4. CONCLUSIONS:

Thus, the direction of the research on the effect of the pre-sowing seed treatment with a silver solution is to study the response of genotypes of different lines and hybrids of sugar beet seeds and the systemic formation of a biologically active nutrient and fungicidal environment on the seed surface with a complex effect on growth processes in the embryo, suppression of pathogenic principles on the surface of seeds that enter the soil. All of the above leads to an increase in the field germination, the activation of seedlings in the early stages of growth and the development, as a result, to an increase in yield. In this regard, it is relevant to study compounds that can be used as pesticides and growth regulators and provoking factors to identify genetic heterogeneity at the early stages of plant development.

## 5. REFERENCES:


1. Balagura, O. V., Levshakov, L. V. (2013). Diversity of sugar beet seeds and its significance. *Bulletin of the Kursk State Agricultural Academy*, 9, 52-54.
2. Balan, V. N. (2000). Diversity of seeds. *Sugar beet*, 1, 15-17.
3. Baranova, T. V., Kalaev, V. N. (2017). Comparative Cytogenetic Analysis of Indigenous and Introduced Species of Woody Plants in Conditions of Anthropogenic Pollution. In: Nourani, C. F., Zaikov, G. E., Weisfeld, L. I., Lisitsyn, E. M., Bekuzarova, S. A. (Eds.); Heavy Metals and Other Pollutants in the Environment: Biological Aspects. Oakville: Apple Academic Press Inc., 241-254.
4. Baranova, T. V., Kalendar, R. N., Kalaev, V. N., Sorokopudov, V. N., Burmenko, Yu. V. (2018). Relationship between cytogenetic characteristics and molecular-genetic differences in species of the genus Rhododendron L. when introduced. *Agricultural Biology*, *53(3)*, 511-520. DOI: 10.15389/agrobiology
5. Bashmakov, D. I., Pynenkova, N. A., Sazanova, K. A., Lukatkin, A. S. (2012). Effect of the synthetic growth regulator Cytodef and heavy metals on oxidative status in cucumber plants. *Russian Journal of Plant Physiology*, 59(1), 59-64.
6. Bome, N. A., Weisfeld, L. I., Bekuzarova, S. A, Bome, A. Y. (2015). Optimization of the Structurally Functional Changes in the Cultured Phytocoenoses in the Areas with Extreme Edaphic-Climatic Conditions. In: Weisfeld, L. I., Opalko, A. I., Bome, N. A., Bekuzarova, S. A. (Eds.); Biological Systems, Biodiversity, and Stability of Plant Communities, Oakville: Apple Academic Press Inc., 19-32.
7. Bukharina, I. L. (2011). Features of the dynamics of the content of ascorbic acid and tannins in the shoots of woody plants under the conditions of the city of Izhevsk. *Plant Resources*, *47(2)*, 109–117.
8. Burmenko, Yu. V., Baranova, T. V., Kalaev, V. N. (2018 a). Comparative Study of Cytogenetic Response of Silver Birch and *Rhododendron Ledebourii* Seeds to Urban Pollution in Voronezh. *Russian Journal of Forest Science*, *1*, 65-73. DOI: 10.7868/S0024114818010060
9. Burmenko, Yu. V., Baranova, T. V., Kalaev, V. N., Sorokopudov, V. N. (2018 b). Cytogenetic polymorphism of seed progeny of introduced plants on the example of Rhododendron ledebourii Pojark. *Turczaninowia*, 21 (1), *164–173.*

DOI: *10.14258/turczaninowia.21.1.16*

10. Denisov, A.N., Krutyakov, Yu.A., Kudrinsky, A.A., Zherebin, P.M., Elansky, S.N., Pobedinskaya, M.A., Klimov, A.I. (2014 a). Antiseptic preparation and methods for producing and using same: Patent WO2014200380 Russian Federation. International Application PCT/RU2013/000477, declared 10.06.13, published 18. 12.14.
11. Denisov, A.N., Krutyakov, Yu.A., Kudrinsky, A.A., Zherebin, P.M., Elansky, S.N., Pobedinskaya, M.A., Klimov, A.I. (2014 b). Fungicide and method of its use: Patent WO2014200379 Russian Federation. International Application PCT/RU2013/000476, declared 10.06.13, published 18. 12.14.
12. Elansky, S. N., Pobedinskaya, M. A., Kokaeva, L. Yu., Kutuzova, I. A., Pronicheva, I. S., Mytsa, E. D., Klimov, A. I., Kuznetsova, M. A., Kozlovsky, B. E., Zherebin, P. M., Denisov, A. N., Krutyakov, Yu. A. (2014). New preparate Zerox based on colloidal silver: laboratory test results. *Potato protection*, 1, 41–43.
13. Fachi, L. R., Krause, W., Duarte, H., Viana, A. P. (2019). Digital image analysis to quantify genetic divergence in passion fruit (*Passiflora edulis*) seeds. *Genetics and Molecular Research*, *18(3)*. DOI: 10.4238 / gmr18331
14. Gar'kova, A. N., Rusyaeva, M. M., Nushtaeva, O. V., Aroslankina, Y. N., Lukatkin, A. S. (2011). Treatment with the herbicide granstar induces oxidative stress in cereal leaves. *Russian Journal of Plant hysiology*, *58(6)*, 1074-1081.
15. Geister, A. I. (1934). Agricultural Dictionary. Moscow–Leningrad: Selkhozgiz**.**
16. GOST 22617.2-94. (1994). Sugar beet seeds. Methods for determining germination, single sprout and good quality. Interstate Council for Standardization, Metrology and Certification. Minsk.
17. Ivanov, V. B. (2011). Using the roots as test objects for the assessment of biological action of chemical substances. *Russian Journal of Plant Physiology, 58(6)*, 1082-1089.
18. Jo, Y. K., Kim, B. H., Jung, G. (2009). Antifungal activity of silver ions and nanoparticles on phytopathogenic fungi. *Plant. Dis.*, 93, 1037–1043.
19. Kalaev, V. N., Butorina, A. K., Sheluchina, O. Yu. (2006). Assessment of anthropogenic pollution in the districts of Stary Oskol based on cytogenetic indicators of seed seedlings of weeping birch. *Ecological genetics*, 4(2), 9–23.
20. Khodykina, M.V., Politiko, V.A., Kyrova, E.I., Krutyakov, Yu.A., Zherebin, P.M., Ignatov, A.N. (2014). Antibacterial activity of antibiotics in combined with Zerox® silver preparation against pathogens of a number bacterioses of plants. *Potato protection*, 2, 83–86.
21. Kim, S. W., Jung, J. H., Lamsal, K., Kim, Y. S., Min, J. S., Lee, Y. S. (2012). Antifungal effect of silver nanoparticles (AgNPs) against various plant pathogenic fungi. *Micobiology*, 40(1), 53–58.
22. Korovkin, O. A. (2007). Anatomy and morphology of higher plants: glossary. Moscow: Drofa**.**
23. Krutyakov, Yu. A., Kudrinskiy, A. A., Olenin, A. Yu., Lisichkin, G. V. (2008). Synthesis and properties of silver nanoparticles: advances and prospects. *Russ. Chem. Rev.*, 77 (3), 233–
257 DOI: https://doi.org/10.1070/RC2008v077n03ABEH003751
24. Kulaichev, A. P. (2006). Methods, and tools for integrated data analysis. Moscow: FORUM: INFA-M.
25. Kuzemko, A. A. (2016). Influence of Anthropogenic Pressure on Environmental Characteristics of Meadow Habitats in the Forest and Forest-Zones. In: Bekuzarova, S. A., Bome, N. A., Opalko, A. I. (Eds.); Temperate Crop Science and Breeding: Ecological and Genetic Studies, Oakville: Apple Academic Press Inc., 385-404.
26. Lamsal, K., Kim, S. W., Jung, J. H., Kim, Y. S., Kim, K. S., Lee, Y. S. (2011). Application of silver nanoparticles for the control of Colletotrichum species in vitro and pepper anthracnose disease in field. *Mycobiology*, 39(3), 94–199.
27. Lapshina, L. A., Reunov, A. V., Nagorskaya, V. P. (2016). Effects of exogenous $H_2O_2$ on the content of

endogenous $H_2O_2$, activities of catalase and hydrolases, and cell ultrastructure in tobacco leaves. *Biology Bulletin*, *43(5)*, 419-425.

28. Lisichkin, G. V. (2019). Surface Compound Chemistry, and its applications. http://www.chemnet.ru/rus/SummerSchool2019/presentations/lisichkin.pdf
29. Lyanguzova, I. V. (2011). Effect of industrial air pollution on wild plant seed germination and seedling growth. *Russian Journal of Plant Physiology,* 58(60), 991-998.
30. Min, J. S., Kim, K. S., Kim, S. W., Jung, J. H., Lamsal, K., Kim, S. B., Jung, M., Lee, Y.S. (2009). Effect of colloidal silver nanoparticles on sclerotium-forming phytopathogenic fungi. *Plant Pathology Journal*, 25, 376–380.
31. Mita, E. D., Elansky, S. N., Kokaeva, L. Yu., Pobedinskaya, M. A., Ignatov, A. N., Kuznetsova, M. A., Kozlovsky, B. E., Denisov, A. N., Zherebin, P. M., Krutyakov, Yu. A. (2014). New pesticide Zerox – assessment of fungicidal and bactericidal properties in vitro. *Achievements of science and technology of the agro-industrial complex*, 28(12), 16–19.
32. Neverova, O. A. (2004). Ecological assessment of the state of woody plants and environmental pollution of an industrial city (by the example of Kemerovo): Thesis for the degree of Doctor of Biology: Moscow**.**
33. Opalko, A. I., Opalko, O. A. (2915). Anthropo-Adaptability of Plants as a Basis Component of a New Wave of the “Green Revolution”. In: Weisfeld, L. I., Opalko, A. I., Bome, N. A., Bekuzarova, S. A. (Eds.); Biological Systems, Biodiversity, and Stability of Plant Communities, Oakville: Apple Academic Press Inc., 3-18.
34. Oudalova, A. A., Geras’kin, S. A. (2012). The Time Dynamics and Ecological Genetic Variation of Cytogenetic Effects in the Scots Pine Populations Experiencing Anthropogenic Impact. *Biology Bulletin Reviews*, 2(3), 254–267.
35. Polishchuk, V. V. (2013). Seed quality, and productivity of sugar beet O-type lines at low temperatures. *Plant Varieties Studying and Protection*, 2, 20-22.
36. Popov, V. N., Eprintsev, A. T., Maltseva, E. V. (2011). Activation of genes encoding mitochondrial proteins involved in alternative and uncoupled respiration of tomato plants treated with low temperature and reactive oxygen species. *Russian Journal of Plant Physiology*, *58(5)*, 914-920.
37. Pozolotina, V. N., Antonova, E. V., Bezel, V. S. (2010 a). Long-Term Effects in Plant Populations from Zones of Radiation and Chemical Pollution. *Radiological Biology. Radioecology,* 4, 414–422.
38. Pozolotina, V. N., Antonova, E. V., Karimullina, E. M. (2010 b). Assessment of Radiation Impact on Stellaria graminea coenopopulations in the Zone of the Eastern Ural Radioactive Trace. *Russian Journal of Ecology*, 41(6), 459–468.
39. Pshechenkov, K. A., Zeyruk, V. N., Elansky, S. N., Maltsev, S. V., Pryamov, S. B. (2016). Potato storage. Moscow: Agrospas**.**
40. Titov, V. N., Smyslov, D. G., Dmitrieva, G. A., Bolotova, O. I. (2011). Plant growth regulators as a biological factor in reducing the level of heavy metals in a plant. *Vestnik OrelGAU*, *31(4),* 4–6.
41. Tsareva, L. E. (2010). Influence of seed planting schemes on the yield and properties of sugar beet seeds. *Bulletin of Altai State Agrarian University*, 3(65), 21-24.
42. Tsareva, L. E. (2013). Technique of improving yielding features of seeds in reproduction of sugar beet hybrids. *Bulletin of Altai State Agrarian University*, 1 (99), 17–19.
43. Usanova, Z. I., Shalnov, I. V., Ivanyutina, N. N., Sutyagina, T. I., Babich, N. V. (2012). Method of presowing treatment of seeds of agricultural plants. Patent 2463757, Russian Federation, FSEI HPE "TGSA" (RU), 29.
44. Vetchinnikova, L. V. (2004). Birch: questions of variability (morphophysiological and biochemical aspects) (Ed.); Titov, A. F., M.: Science.
45. Vostrikova, T. V. (2011). Ecological and biological features of rhododendrons during introduction in the conditions of the Central Chernozem region. *Bulletin of*

*Krasnoyarsk State Agrarian University*, *4*, 27–30.

46. Welbaum, G. E., Bradford, K. J., Yim, K.-O. Booth, D. T. (1998). Biophysical, physiological and biochemical processes seed germination. *Seed Science Research*, *8(02),* 161–172.
47. Yakymchuk, R. A. (2015). Cytogenetic After-Effects of Mutagen Soil Contamination with Emissions of Burshtynska Thermal Power Station. In: Opalko, A. I., Weisfeld, L. I., Bekuzarova, S. A., Bome, N. A., Zaikov, G. E. (Eds.); Ecological Consequences of Increasing Crop Productivity: Plant Breeding and Biotic Diversity: New Jersey: Apple Academic Press Inc., 217-227.
48. Zherebin, P. M., Ignatov, A. N., Elansky, S. N., Pobedinskaya, M. A., Lisichkin, G. V., Denisov, A. N., Krutyakov, Yu. A. (2014). “Zerox”-silver-based preparate for an effective control of bacterial and fungal epidemic diseases of agricultural plants. *Potato protection*, 2, 43–45.
49. Zherebin, P. M., Krutyakov, Yu. A., Kudrinsky, A. A., Klimov, A. I., Elansky, S. N., Pobedinskaya, M. A., Ignatov, A. N. (2015). "Zerox": a new bactericide and fungicide of wide spectrum of action based on colloidal silver. *Young scientist*, 9.2, 25-26.

***Table 1.*** *Qualities of seeds and seedlings from sugar beet treated with 10 % aqueous solution of the inorganic chemical compound*

| No | Line/ hybrid | Control (tap water) | | | 10 % solution | | |
|---|---|---|---|---|---|---|---|
| | | GE, % | length, cm | mass, g | GE, % | length, cm | mass, g |
| 1 | O-type 709 | 83 | 3,7±0,1 | 1,3±0,02 | 95* | 5,1±0,1** | 1,6±0,02* |
| 2 | MS 709 | 81 | 4,0±0,1 | 1,0±0,01 | 85* | 6,7±0,2** | 1,6±0,02** |
| 3 | Karioka | 93 | 4,2±0,1 | 1,4±0,02 | 87* | 5,8±0,2** | 1,8±0,02* |
| 4 | Mitika | 98 | 5,4±0,2 | 2,0±0,03 | 96 | 3,8±0,1** | 1,4±0,02** |
| 5 | Michelle | 100 | 7,1±0,3 | 2,4±0,03 | 96 | 6,8±0,3 | 1,8±0,03* |
| 6 | Granate | 81 | 5,4±0,1 | 1,9±0,02 | 92* | 6,6±0,2* | 1,5±0,02* |
| 7 | Zephyr | 92 | 5,4±0,2 | 1,6±0,02 | 97* | 6,6±0,3* | 1,5±0,02 |
| 8 | Murray | 90 | 6,8±0,3 | 2,0±0,03 | 98* | 6,0±0,2* | 1,9±0,03 |
| 9 | Portland | 81 | 4,9±0,1 | 1,8±0,02 | 81 | 6,0±0,3* | 2,0±0,03 |
| 10 | Tinker | 92 | 5,6±0,2 | 2,4±0,03 | 93 | 6,5±0,3* | 2,3±0,03 |
| 11 | Veitura | 97 | 6,3±0,3 | 2,0±0,02 | 87* | 3,5±0,2** | 1,4±0,02** |

*Note: GE – seed germinative energy; length – seedling length; mass – seedling mass; * –differences with the control are reliable (P<0.05); ** – differences with the control are reliable (P<0.01).*

***Table 2.*** *Qualities of seeds and seedlings from sugar beet treated with 20 and 30 % aqueous solution of the inorganic chemical compound*

| No | Line/ hybrid | Control (tap water) | | | 20 % solution | | | 30 % solution | | |
|---|---|---|---|---|---|---|---|---|---|---|
| | | GE, % | length, cm | mass, g | GE, % | length, cm | mass, g | GE, % | length, cm | mass, g |
| 1 | O-type 709 | 83 | 3,7±0,1 | 1,3±0,02 | 79 | 4,7±0,1* | 1,2±0,01 | 84 | 3,6±0,1 | 1,4±0,02 |
| 2 | MS 709 | 81 | 4,0±0,1 | 1,0±0,01 | 72* | 4,7±0,1* | 1,0±0,01 | 85* | 4,1±0,1 | 1,2±0,01 |
| 3 | Karioka | 93 | 4,2±0,1 | 1,4±0,02 | 95 | 4,9±0,1* | 1,5±0,02 | 90 | 4,4±0,2 | 1,2±0,01 |
| 4 | Mitika | 98 | 5,4±0,2 | 2,0±0,03 | 90* | 4,1±0,1* | 1,4±0,02** | 96 | 3,6±0,1** | 1,5±0,02* |
| 5 | Michelle | 100 | 7,1±0,3 | 2,4±0,03 | 92* | 6,0±0,3* | 1,8±0,03* | 86* | 5,1±0,2** | 1,4±0,02** |
| 6 | Granate | 81 | 5,4±0,1 | 1,9±0,02 | 91* | 4,2±0,1* | 1,5±0,02* | 84 | 4,2±0,2* | 1,2±0,02** |
| 7 | Zephyr | 92 | 5,4±0,2 | 1,6±0,02 | 96* | 5,6±0,2 | 1,4±0,02 | 95 | 4,0±0,1* | 1,2±0,02* |
| 8 | Murray | 90 | 6,8±0,3 | 2,0±0,03 | 90 | 5,0±0,2* | 1,4±0,02** | 80* | 4,7±0,2* | 1,2±0,01** |
| 9 | Portland | 81 | 4,9±0,1 | 1,8±0,02 | 81 | 4,8±0,2 | 1,3±0,02* | 82 | 5,8±0,3* | 1,3±0,02* |
| 10 | Tinker | 92 | 5,6±0,2 | 2,4±0,03 | 92 | 3,3±0,1** | 1,3±0,01** | 76* | 4,1±0,1* | 1,1±0,01** |
| 11 | Veitura | 97 | 6,3±0,3 | 2,0±0,02 | 90* | 4,2±0,2** | 1,3±0,02** | 68* | 3,0±0,1** | 1,0±0,01** |

*Note: GE – seed germinative energy; length – seedling length; mass – seedling mass; * –differences with the control are reliable (P<0.05); ** – differences with the control are reliable (P<0.01).*

***Table 3.*** *Power of influence of the factor "sugar beet seed treatment with an aqueous solution of the chemical compound" on germinative energy (%)*

| No. | Line / hybrid | With control | Without control |
|---|---|---|---|
| 1 | O-type 709 | 4.0** | 4.5** |
| 2 | MS 709 | 3.0** | 3.7** |
| 3 | Karioka | 2.9** | 3.2** |
| 4 | Mitika | 3.4** | 3.1** |
| 5 | Michelle | 3.8** | 3.3** |
| 6 | Granate | 3.6** | 3.4** |
| 7 | Zephyr | 2.7** | - |
| 8 | Murray | 3.1** | 3.5** |
| 9 | Portland | - | - |
| 10 | Tinker | 3.0** | 3.3** |
| 11 | Veitura | 4.7** | 4.4** |

*Note: ** – the influence of factor is reliable (P<0.01).*

***Table 4.*** *Power of influence of the factor "sugar beet seed treatment with an aqueous solution of the chemical compound" on seedling length (%)*

| No. | Line / hybrid | With control | Without control |
|---|---|---|---|
| 1 | O-type 709 | 6.0** | 6.5** |
| 2 | MS 709 | 7.3** | 7.1** |
| 3 | Karioka | 6.5** | 6.3** |
| 4 | Mitika | 6.7** | 6.1** |
| 5 | Michelle | 5.8** | 4.3** |
| 6 | Granate | 6.5** | 6.8** |
| 7 | Zephyr | 6.4** | 6.9** |
| 8 | Murray | 5.7** | 5.2** |
| 9 | Portland | 6.1** | 6.3** |
| 10 | Tinker | 5.0** | 6.3** |
| 11 | Veitura | 6.8** | 4.4** |

*Note: ** – influence of factor is reliable (P<0.01).*

***Table 5.*** *Power of influence of the factor "sugar beet seed treatment with an aqueous solution of the chemical compound" on seedling mass (%)*

| No. | Line / hybrid | With control | Without control |
|---|---|---|---|
| 1 | O-type 709 | 4.0** | 4.5** |
| 2 | MS 709 | 6.3** | 6.0** |
| 3 | Karioka | 5.5** | 5.2** |
| 4 | Mitika | 5.7** | 5.1** |
| 5 | Michelle | 6.8** | 5.3** |
| 6 | Granate | 5.5** | 5.8** |
| 7 | Zephyr | 5.4** | 5.9** |
| 8 | Murray | 4.7** | 3.2** |
| 9 | Portland | 4.5* | 4.8** |
| 10 | Tinker | 6.0** | 7.3** |
| 11 | Veitura | 7.8** | 5.4** |

*Note: ** – influence of factor is reliable (P<0.01).*

PERIÓDICO TCHÊ QUÍMICA
ARTIGO ORIGINAL

# ESTUDO DE REVESTIMENTOS ISOLANTES TÉRMICOS LÍQUIDOS PARA ECONOMIZAR ENERGIA COM BASE EM SISTEMAS LOCAIS FINAMENTE DISPERSOS

# STUDY OF ENERGY-SAVING LIQUID THERMAL INSULATING COATINGS BASED ON LOCAL FINELY DISPERSED SYSTEMS

# ИССЛЕДОВАНИЕ ЭНЕРГОСБЕРЕГАЮЩИХ ЖИДКИХ ТЕПЛОИЗОЛЯЦИОННЫХ ПОКРЫТИЙ НА ОСНОВЕ МЕСТНЫХ ТОНКОДИСПЕРСНЫХ ЗЕРНИСТЫХ СИСТЕМ

ZHUMADILOVA, Zhanar O.[1]; SELYAEV, Vladimir P.[2]; NURLYBAEV, Ruslan E.[3]; ORYNBEKOV, Yelzhan S.[4], SANGULOVA, Indira B.[5]

[1,5] Satbayev University, Institute of Architecture and Civil Engineering, Department of Construction and Building Materials, Department of Engineering Physics, 22 Satpayev Str., zip code 050013, Almaty – Republic of Kazakhstan

[2] Ogarev Mordovia State University, 68 Bolshevistskaya Str., zip code 430005, Saransk – Republic of Mordovia, Russia

[3, 4] LLP SAVENERGY, Industrial zone, zip code A03A2C6, Almaty – Republic of Kazakhstan

** Corresponding author*
*e-mail: zhanar_85@mail.ru*

Received 16 December 2020; received in revised form 12 February 2021; accepted 25 February 2021

## RESUMO

**Introdução**: Nos últimos anos, na ciência dos materiais de construção, tem havido uma tendência para a introdução ativa de microesferas ocas de vários tipos para modificar as propriedades dos materiais de construção. As microesferas ocas são mais amplamente utilizadas na produção de revestimentos isolantes térmicos líquidos, que reduzem a perda de calor, protegem as estruturas da corrosão e superaquecimento, evitam a formação de condensação, reduzem os custos operacionais e aumentam o tempo entre reparos. **Objetivo**: Avaliar a influência das características estruturais de sistemas granulares nas propriedades de materiais isolantes térmicos. **Métodos**: Propõe-se determinar e avaliar as características estruturais de pós de carga pelo método de espalhamento de raios-X a baixo ângulo. A característica mais importante deste método é analisar a estrutura interna de sistemas desordenados - partículas, espaço de poros, interfaces entre heterogeneidades de substâncias heterogêneas. Ao avaliar a condutividade térmica e a resistência térmica, o método de fluxo de calor estacionário foi usado de acordo com GOST 30290-94. A essência do método é criar um fluxo de calor estacionário que passa por uma amostra plana de uma certa espessura e dirigido perpendicularmente às faces frontais (maiores) da amostra, medindo a densidade desse fluxo de calor, a temperatura das faces frontais opostas e a espessura da amostra. **Resultados e discussões**: O artigo discute os resultados de estudos experimentais que possibilitaram a criação de revestimentos isolantes térmicos líquidos (LTIC) à base de ligantes poliméricos, pós minerais finos e um complexo de aditivos modificadores. Estudos experimentais da estrutura e propriedades de revestimentos de isolamento térmico com base em ligantes de polímero preenchidos confirmam sua superioridade sobre análogos estrangeiros. **Conclusões**: Foi estabelecido que durante a produção de LTIC, suas propriedades de blindagem térmica podem ser reguladas alterando: a pressão, a viscosidade do peso molecular do gás; a porosidade da macroestrutura e aglomerados; a condutividade térmica da fase sólida e gasosa do sistema; o coeficiente de acomodação; número de coordenação; tamanho de partícula primária; dimensão fractal que caracteriza as características topológicas da estrutura das partículas, agregados, glóbulos, aglomerados e sua tendência para dissipar a energia das moléculas de gás.

**Palavras-chave**: *microssílica, condutividade térmica, diatomita, pós minerais, fuligem branca.*

## ABSTRACT

**Introduction:** In recent years, in building materials science, there has been a tendency for the active

introduction of hollow microspheres of various types for modifying the properties of building materials. Hollow microspheres are most widely used in the production of liquid thermal insulating coatings, which reduce heat loss, protect structures from corrosion and overheating, prevent condensation formation, reduce operating costs and increase the time between repairs. **Aim:** Assessment of the influence of the structural characteristics of granular systems on the properties of thermal insulating materials. **Methods:** It is proposed to determine and evaluate the structural characteristics of filler powders by the method of small-angle X-ray scattering. The most important feature of this method is analyzing the internal structure of disordered systems - particles, pore space, interfaces between heterogeneities of heterogeneous substances. When assessing thermal conductivity and thermal resistance, the stationary heat flux method was used following GOST 30290–94. The essence of the method is to create a stationary heat flux passing through a flat sample of a certain thickness and directed perpendicular to the front (largest) faces of the sample, measuring the density of this heat flux, the temperature of the opposite front faces and the thickness of the sample. **Results and Discussion**: The paper discusses the results of experimental studies that make it possible to create liquid thermal insulation coatings (LTIC) based on polymer binders, fine mineral powders, and a complex of modifying additives. Experimental studies of the structure and properties of heat-insulating coatings based on filled polymer binders confirm their superiority over foreign analogs. **Conclusions:** It has been established that during the production of LTIC, their heat-shielding properties can be regulated by changing: pressure, the viscosity of the molecular weight of the gas; porosity of macrostructure and clusters; the thermal conductivity of the solid and gas phase of the system; the coefficient of accommodation; coordination number; primary particle size; fractal dimension characterizing the topological features of the structure of particles, aggregates, globules, clusters and their tendency to dissipate the energy of gas molecules.

**Keywords:** *microsilica, thermal conductivity, diatomite, mineral powders, white soot.*

## АБСТРАКТ

**Введение.** В последние годы в области строительного материаловедения намечается тенденция активного внедрения полых микросфер различного вида для модификации свойств строительных материалов. Наиболее широкое применение полые микросферы находят при производстве жидких теплоизоляционных покрытий, которые снижают теплопотери, защищают конструкции от коррозии и перегревов, препятствуют образованию конденсата, позволяют снизить эксплуатационные затраты и увеличить срок межремонтной службы. **Цель.** Оценка влияния структурных характеристик зернистых систем на свойства теплоизоляционных материалов. **Методы.** Определение и оценку структурных характеристик порошков наполнителей предлагается выполнять методом малоуглового рентгеновского рассеяния. Важнейшей особенностью данного метода является возможность анализа внутренней структуры разупорядоченных систем – частиц, порового пространства, поверхностей раздела между неоднородностями гетерогенных веществ. При оценке теплопроводности и теплового сопротивления применяли метод стационарного теплового потока в соответствии с ГОСТам. Сущность метода заключается в создании стационарного теплового потока, проходящего через плоский образец определенной толщины и направленного перпендикулярно к лицевым (наибольшим) граням образца, измерении плотности этого теплового потока, температуры противоположных лицевых граней и толщины образца. **Результаты и обсуждение.** В статье рассмотрены результаты экспериментальных исследований, которые позволяют создавать жидких теплоизоляционных покрытий (ЖТП) на основе полимерных связующих, тонкодисперсных минеральных порошков и комплекса модифицирующих добавок. Проведенные экспериментальные исследования структуры и свойств теплоизоляционных покрытий, на основе наполненных полимерных связующих, подтверждают их превосходство над зарубежными аналогами. **Заключение.** Установлено, что при производстве ЖТП их теплозащитные свойства можно регулировать путем изменения: давления, вязкости молекулярного веса газа; пористости макроструктуры и кластеров; теплопроводности твердой и газовой фазы системы; коэффициента аккомодации; координационного числа; размера первичных частиц; фрактальной размерности, характеризующей топологические особенности строения частиц, агрегатов, глобул, кластеров и их склонность к диссипации энергии молекул газа.

**Ключевые слова:** *микрокремнезем, коэффициент теплопроводности, диатомит, минеральные порошки, белая сажа.*

## 1. INTRODUCTION:

There is a wide selection of various thermal insulation materials on the construction market. To the already existing and well-proven polystyrene foam, mineral wool heaters, more and more new materials are added, which manufacturers offer to use to consumers in

various climatic and building conditions (Danilov V. I., 2014; Selyaev V. P., 2012; Golovanova L. A., 2014).

Relatively recently, some companies began to offer modern ultra-thin liquid composite heat-insulating coatings for insulating house facades, as well as engineering communications. According to the manufacturers themselves, the use of such heat-insulating materials can lead to significant energy savings (Komkov V. A., 2010; Beregovoy A. M., 2008). However, the thermal and physical properties of the presented heat-insulating coatings have not yet been fully studied. Available studies by various authors (Shirinyan V. T., 2007; Golovach Yu. Yu., 2008; Maneshev I. O., 2013; Loginova N. A., 2010) on the determination of the thermal conductivity coefficient of the same types of liquid thermal insulation coatings (LTIC) often show a significant difference.

One of the most important parameters determining the thermal insulation properties of materials based on microstructured mineral powders (silica, diatomite) is thermal conductivity. Knowing some characteristics of dispersed systems, such as the size, thermal conductivity of the material of primary particles, the filling method, and some others, it is possible to theoretically calculate the thermal conductivity of granular systems based on the polystructural theory of Solomatov V.I. (Solomatov V. I., 1991) and the model of. Dulnev G. N. (Dulnev G. N., Zarichnyak Yu. P., 1974).

In this regard, it was decided to conduct experimental studies of the thermal conductivity of liquid heat-insulating coatings to identify their true values and dependence on the composition and properties of the main components.

## 2. MATERIALS AND METHODS:

### 2.1.1. Materials and methods for determining the thermal conductivity of LTIC

To study the properties (distribution of inhomogeneities in size, particle size, topography, and shape of nanoobjects) of microdispersed materials were used the small-angle X-ray diffractometer Hecus S3 MICRO.

In the analysis of the internal structure of disordered systems - particles, pore space, interfaces between inhomogeneities of heterogeneous substances, small-angle X-ray scattering was used based on the diffraction method, which is widely used to study highly dispersed powders.

As the scattering coordinate, were used the magnitude of the scattering vector modulus $s = 4\pi \sin\theta/\lambda$, where $2\theta$ was the scattering angle, $\lambda = 1.5418$ Å is the wavelength of the radiation used. The scattering intensities were recorded in the range of s values from 0.0094 to 0.40 Å-1, which made it possible to study inhomogeneities with linear dimensions $L \sim (2\pi)/S$, in the range of 2 to 60 nm.

The methods for determining the coefficient of thermal conductivity of thin-layer heat-insulating coatings given in (Anisimov M. V., 2015; Selyaev V. P. *et al.*, 2018; Khabibullin Yu. Kh., 2015; Pavlov M. V., 2014) in accordance with the following methods based on the following GOSTs for determining the thermal conductivity coefficient. Undoubtedly, when conducting research, it is advisable to use GOST test tools (test tools with methods for each GOST are given below) (GOST 30290–94, 1996; GOST 7076-99, 2000; GOST 28574-90, 1991; GOST 52487-2005 (ISO 3251:2003), 2007) which allows obtaining a reliable, reproducible assessment of the studied characteristics. When assessing thermal conductivity and thermal resistance, the method of stationary heat flux was used accordingly to (GOST 30290–94, 1996; GOST 7076-99, 2000; GOST 28574-90, 1991; GOST 52487-2005 (ISO 3251:2003); 2007).

According to the composition (formulation) of liquid thermal insulation coatings, the following methods were used:

- Determination of thermal conductivity and thermal resistance in the stationary thermal regime of the LTIC following GOST 7076-99.

The essence of the method is to create a stationary heat flux passing through a flat sample of a certain thickness and directed perpendicularly to the front (largest) faces of the LTIC, measuring the density of this heat flux, the temperature of opposite front faces, and the thickness of the sample.

Thermal conductivity was determined on an ITS-1 device after preparing a sample of a rectangular parallelepiped.

The following devices are used to test LTIC:

- for measuring effective thermal conductivity and thermal resistance - ITS-1;
- device for determining the thickness - vernier caliper;
- drying electrical cabinet, - ShS-80-01-SPU up to 200 °C;

- laboratory scales for general purpose - maximum load no more than 1 g, actual scale division from 1 to 0.01 mkg.

Determination of thermal conductivity:

- preliminarily prepared liquid composite heat-insulating coatings were applied to glass with a size of 150×150 and a thickness of 3 mm. The thickness of the applied layers was from 1 to 2-6 mm, ± 0.02-0.03 mm, and drying was carried out within 24 hours to constant weight. On each sample, presetting the thickness from 1 to 6 mm, the heat flux density, thermal resistance, and thermal conductivity coefficient were determined for the ITS-1 devices. According to the ITS-1 device, the surface of the heater and refrigerator plates are made of metal. The deviation from the flatness of the working surfaces should be no more than 0.025% of their maximum linear size.

- Thermal conductivity of LTIC in accordance with GOST 30290–94.

This method applies to building materials and products with thermal conductivity from 0.02 to 1 W/m·K and establishes a method for non-destructive accelerated determination of thermal conductivity in the temperature range 278-313 K (5-40 °C).

The method consists of creating a one-sided short-term heat pulse on the surface of the product and recording the temperature change on this surface.

The tests were carried out with a steady thermal equilibrium between the investigated LTIC, the body of the primary transducer, and the environment, for which the primary transducer was installed on the surface of the LTIC prepared for testing following this GOST 30290–94, and held until steady readings appeared on the display of the second measuring device.

The following devices are used to test LTIC:

- thermocouple;
- voltmeter;
- device for determining the thickness - vernier caliper;
- drying electrical cabinet, - ShS-80-01-SPU up to 200 ° C;
- laboratory scales for general purpose - maximum load no more than 1 g, actual scale division from 1 to 0.01 mkg.

Determination of thermal conductivity:

- preliminarily prepared liquid composite heat-insulating coatings, as in GOST 7076-99, were applied to glass with a size of 150 × 150 and a thickness of 3 mm (samples must have a flat surface to accommodate the primary converter and ensure thermal contact between them). The thickness of the applied layers was from 1 to 2-6 mm, ± 0.02-0.03 mm, and drying was carried out within 24 hours to constant weight.

For testing thermal conductivity, a measuring complex is used: a primary transducer designed to convert a pulse of electrical energy into thermal energy and create an electrical signal characterizing the change in the surface temperature of LTIC product under the influence of a thermal pulse and a secondary meter for recording an electrical signal.

The used GOST 30290–94 is not the main one, but rather auxiliary and comparative.

- Adhesion of protective coatings for LTIC following GOST 28574-90.

When testing the adhesion of coatings in laboratory conditions, on each type of element of the protected structure, five places were selected at a distance of at least 300 mm from one another, and metal disks were glued to the coating in accordance with GOST.

The essence of the method consists in measuring the force required to detach the coating from the protected concrete surface in the direction perpendicular to the plane of the coating using a glued metal disk and a dynamometer.

The following devices and apparatuses are used to test LTIC:

- press for testing materials in tension with a maximum force of 10000 N;
- a device for cutting paint and varnish coatings near glued metal discs;
- organic solvents according to the materials for the test coatings;
- drying electrical cabinet, - ShS-80-01-SPU up to 200 °C;
- laboratory scales for general use - maximum load no more than 1 g, actual scale division from 1 to 0.01 mkg;
- metal spatula;
- metal (wire) and hairbrush;
- sandpaper for dry sanding.

Determination of adhesion of LTIC:

Preliminarily prepared metal discs 25 mm high and 20 or 50.6 mm in diameter with a hinge for transferring tensile forces and plates with dimensions of 100x100 mm and a thickness of at least 40 mm, made of cement-sand mortar composition. On the surface of the slabs, a layer of LTIC from 1 to 2-6 mm, ± 0.02-0.03 mm is applied and dried within 24 hours to constant

weight. At the end of the holding (drying) period, metal disks are glued to the LTIC coating of the samples. Determination of the adhesion of coatings to the surface of the structure is carried out at the end of the period of complete curing of the adhesive by tearing the metal discs from the plate.

- Mass fraction of non-volatile substances according to GOST 52487-2005.

The essence of the method consists in drying a cup with LTIC in an oven at a temperature of 80 °C, a heating time of 60 minutes, and determination of the mass of the dry residue on the cup according to GOST.

The following devices and apparatuses are used to test the LTIC:

- a flat-bottomed cup made of metal or glass with a diameter of (75 ± 5) mm and a side height of at least 5 mm;
- drying electrical cabinet ShS-80-01-SPU up to 200 °C;
- analytical balance with weighing accuracy up to 0.1 mg;
- a desiccator with a suitable desiccant such as dry silica gel.

Determination of the mass fraction of non-volatile substances of LTIC:

According to GOST 52487-2005, the dish was degreased and cleaned; the mass of a clean, dry dish ($m_0$) was determined with an accuracy of 1 mg. Then, the LTIC for testing was weighed to an accuracy of 1 mg in a dish ($m_1$) and evenly distributed over the bottom using a tared metal wire. After weighing, the cup ($m_1$) was placed in an oven preheated to a predetermined temperature, and the cup was kept in the cupboard for a predetermined heating time. At the end of the heating time, the dish was transferred to a desiccator and cooled to room temperature, and the ($m_2$) dish with the residue was determined to the nearest 1 mg. The mass fraction of non-volatile substances *NV*, %, was determined using the following Equation 1:

$$NV = \frac{(m_2 - m_0)}{(m_1 - m_0)} 100 \qquad \text{(Eq.1)}$$

***2.1.2. Prediction of thermal conductivity and assessment of the influence of the structural characteristics of granular systems on the properties of thermal insulation materials***

The features of structural heterogeneities of microsilica (Maneshev I. O., 2013; Dombrovsky L. A., 2005; Selyaev V. P., 2012) and natural diatomite of the Utesai deposit, as well as a powder-filler of a vacuum insulating panel, were investigated using the method of small-angle X-ray scattering.

The experimental material was obtained in the form of small-angle X-ray scattering indicatrices for all investigated dispersed powders. As the scattering coordinate, we used the magnitude of the scattering vector $s = 4\pi \sin\theta/\lambda$, where $2\theta$ is the scattering angle, $\lambda$=1.5418 Å is the wavelength of the radiation used. Scattering intensities were recorded in the range of s values from 0,0094 till 0,40 $Å^{-1}$, which made it possible to study inhomogeneities with linear dimensions $L \sim \frac{2\pi}{s}$, within 2 ... 60 nm. In Figure 1 shows the experimental small-angle X-ray scattering curves of the natural diatomite of the Utesay field and the filler powder of the insulating panel. The scattering indicatrices of the other three microsilica are similar to the small-angle X-ray scattering curve.

It was used the China city method (Selyaev V. P., 2012), the small-angle X-ray scattering curves were rearranged into the coordinates $\ln I(s) - s^2$ of the dependences shown in Figure 2. Pore size distribution curves for dispersed microsilica have pronounced maxima; a similar natural diatomite function is bimodal. Table 1 shows the results of the analysis of distribution curves - the maxima of the distribution functions $d_в$; average values of linear dimensions of scattering inhomogeneities <d>; variances of distribution functions Δd.

The fractal characteristics of all studied materials are shown in Table 2.

Dispersed microsilica obtained from natural diatomite, and natural diatomite, has three types of scattering inhomogeneities, two of which are mass fractals with dimensions D = 2.32 and D = 2.13. The scale of such objects is d = 4 ÷ 8 nm. Small-scale pores d = 8-40 nm have rather heavily indented interfaces with fractal dimensions ($D_S$ = 6-$\alpha$ = 2.64). Condensed silica fume (production waste) does not have X-ray scattering inhomogeneities attributed to mass fractals. The surfaces of $SiO_2$ particles - pores have a fractal dimension $D_S$ = 2.40. White soot contains fractal clusters of pore space with linear dimensions of 4 - 25 nm. The interface surfaces of larger scattering formations (25-40 nm) are strongly indented - their fractal dimension is $D_S$ = 2.83. The scattering curve $\lg I(s)$ $\lg s$ of the

filler powder has two crossover points: branched porous aggregates with dimensions of 20-40 nm have a fractal dimension D = 2.59, and irregularities on a scale of 12-20 nm have a highly irregular surface c $D_S$ = 2.70. Also, the data of small-angle X-ray scattering allow us to suggest that on the surface of the smallest elements of the structure of the filler powder (4-12 nm), layers of scattering inhomogeneities with a lower electron density than that of silicon dioxide (parameter α=4.10) are possible.

### *2.1.3 A fractal model of heat transfer and the main parameters of a granular system affecting the thermal conductivity of a liquid thermal insulating coating (LTIC) product*

The heat transfer mechanism in granular, porous systems is rather complicated since heat transfer occurs in a multiphase material.

Heat transfer in LTIC can be carried out from one solid particle to another (inductive component $-\lambda_1$). In this case, thermal conductivity will depend on: the chemical and elemental composition of the material; particle size distribution; surface topology - the presence of inhomogeneities, defects on the surface; the number of touches, and the area of contact between the particles.

It has been experimentally established that in the process of condensation in a colloidal solution from particles of silicon oxide, which have a size of 1/3 nm and are nuclei, particles with a size of 5/7 nm grow.

After that, the aggregation of particles begins, and the formation of globules with a size of 20-40 nm, from which clusters of a globular type with a size of 300/400 nm are formed. Depending on the conditions of synthesis and the process of cluster formation, the size of globules can reach sizes up to 1200 nm (Boldyrev, P.P., 1989). Then these globules form a macrostructure with a cubic or other type of packing.

The change in the particle size distribution of microsilica during the synthesis was recorded using a Shimadzu SALD 3101 particle size analyzer and an OLYMUSGX – 71 inverted microscope.

The obtained micrographs and granulometric histograms are shown in Figure 3 and Figure 4.

In the synthesis process, an opal microsilica structure is formed, which can be represented as a fractal model (Figure 5), which is represented as a fractal cluster with a coordination number *K* = 2.2 with a sticking probability *P* = 1 and if *P* = 0.2, then *K* = 2.514.

Equation 2 relates the cluster radius R and the number of particles in it n (Selyaev V.P., 2012):

$$n = \left(\frac{R}{r_0}\right)^D \qquad \text{(Eq.2)}$$

where $r_0$ - is the radius of an individual particle; *D* - fractal dimension of the cluster.

The mass of the formed cluster *m* is related to the radius R by Equation 3:

$$m = m_0\left(\frac{R}{r_0}\right)^D \qquad \text{(Eq.3)}$$

To determine the parameters of the fractal model using a diffractometer, we obtained the experimental dependences of the scattering intensity $I(S)$ on the scattering vector modulus *S* for amorphous silica synthesized from diatomite (Figure 6).

The character of the obtained experimental small-angle scattering curves $I(S)$ indicates two systems of relatively homogeneous scattering clusters in the synthesized microsilica. Clusters with a size d = 40.6 nm represent the first; the second – d = 7.5 ÷ 14.9 nm ≈ 10.1 nm. The size distribution of the scattering particles of the synthesized silica is shown in Figure 7. From the analysis of the graph, it follows that small-scale fractal formations make the main contribution to the scattering of radiation with a size d = 4/8 nm.

Consequently, the dispersed powder of amorphous silica of silicon dioxide contains three types of scattering objects of the nanoscale level with different fractal dimensions.

Fractal properties of porous systems made of amorphous silica are shown in Table 2.

The results obtained make it possible to calculate the maximum pore size $R_{max}$ using Equation 4, which has the form:

$$R_{\max} = r_0\left(\frac{\rho_0}{\bar{\rho}}\right)^{\frac{1}{(3-D)}} \qquad \text{(Eq.4)}$$

where $r_0$- the size of the primary particle of silicon dioxide; $\rho_0$- true density $SiO_2$; $\bar{\rho}$ - density of matter in a cluster of size *r*; *D* - fractal dimension.

The density of the matter in a cluster of size *r* (Equation 5):

$$\bar{\rho}(r) = \rho_0 (\frac{r_0}{r})^{3-D} \qquad \text{(Eq. 5)}$$

From Equation 5, one can obtain the relationship between the average density $\bar{\rho}(r)$ and the cluster size $r$.

The results of calculating the average density of clusters are shown in Table 3. Two cases were considered: 1 - primary particle size $r_0$=1; 2 - $r_0 = 2$. Particle density $\rho_0$=2.2 g/m$^3$, fractal dimension D = 2.5.

The ratio between the density $\rho$ and the porosity *P*, the porosity of the granular system was determined by Equation 6:

$$P = 1 - \rho_i/\rho_0 \qquad \text{(Eq.6)}$$

The calculated values of density and porosity are shown in Table 3.

The last row of Table 3 shows the values of the maximum pore sizes of clusters in the process of their growth, which are calculated by Equation 7:

$$R_{max} = r_0 (\rho_0/\rho_i)^{1/(3-D)} \qquad \text{(Eq.7)}$$

According to the literature data, the free path of a molecule in the air is $\ell = 1.1 \cdot 10^{-6}\text{cm} - 11\text{nm}$. Then the Knudsen criterion $K_n = \ell/d$ equal to the ratio of the mean free path of gas molecules $\ell_K$ to the distance *d* between the walls limiting the volume, in almost all cases will be less than 1, $K_n = \ell/2R < 1$. Consequently, a convective heat transfer mechanism is realized in the pores of the system.

At low pressures, *P* and temperatures *T*, heat transfer by gas molecules in the pores will occur when they collide with the pore walls.

Consequently, the thermal conductivity of granular fillers LTIC will depend on the accommodation coefficient, which characterizes the degree of completeness of energy exchange when a gas molecule collides with a surface. It is always less than one.

The value of the coefficient $\alpha$ depends on the surface topography. The more irregularities, defects on the surface, the greater the values $\alpha$. This conclusion has been established experimentally.

The topography of the solid phase surface of the pore structure is estimated by fractal dimension *D*.

#### *2.1.4 Experimental studies of the structure and properties of LTIC*

In the course of the experimental study, the following were evaluated: density in the liquid and dry state, thermal conductivity (GOST 7076-99, 2000; GOST 30290–94, 1996. GOST – Government standard), adhesive strength to concrete bases (GOST 28574-90; 1991) and the mass fraction of non-volatile substances (GOST 52487-2005; 2007). The thermal conductivity of LTIC was determined using an ITS-1 device based on the method of stationary flows. The equipment and methods of the experiment are described in the above section “Materials and methods” for determining the thermal conductivity of LTIC for each GOST.

The search for optimal solutions was carried out based on scalarization methods and experimental-statistical modeling based on the concept of material property fields. The optimization of the compositions was carried out to achieve 4 minimum characteristics in terms of thermal conductivity and density in dry and liquid states while ensuring sufficient adhesion characteristics.

## 3. RESULTS AND DISCUSSION:

1. Based on the data obtained, it has been experimentally proved (Figure 8) that the optimization of the compositions of LTIC makes it possible to reduce the thermal conductivity of the coatings to 0.05V/m·K, which is comparable to those for the Korund LTIC (0.0546 V/m·K) and lower than for the Isollat LTIC (0.0713 V/m·K). The study of the adhesion characteristics of LTIC showed that the highest adhesive strength is possessed by compositions containing: 24% acrylic dispersion, 5% diatomite, and 2÷6% white soot.

2. Based on the experimental study, the compositions of LTIC have been developed that have high-performance characteristics that are not inferior, and sometimes even surpass the compositions adopted in comparative tests as standards (Gladkov S. O., 2008; Inin A. E. *et al.*, 2013; Druzhinina T. Ya., 2013; Vasilyeva I. L., 2018; Abramyan S. G. *et al.*, 2018). The technological scheme of the production process has been developed.

3. Sequentially applied 6 layers of thermal insulation coating with a thickness of about each layer 1 mm with intermediate drying for 24 hours. The number of layers and the thickness of the coating by the coefficient of thermal conductivity on glass with dimensions of 150 × 150 mm and a thickness of 3 mm. Using the ITS-1 device at each stage, equivalent indicators were determined: heat flux density, thermal resistance, and thermal conductivity coefficient of three-layer samples. The results obtained are presented in Table 4.

4. It has been experimentally established that the effective thermal conductivity of LTIC based on heterogeneous finely dispersed granular systems even at atmospheric pressure may be lower than the thermal conductivity of the gas filling the pores (Table 4).

5. From the analysis of the data obtained, it was established that the equivalent heat flux density of three-layer flat samples, depending on the thickness of the heat-insulating layer, is described by a logarithmic dependence by Equation 8:

$$q_{eq.} = 141.94 - 21.36 \cdot l_n(\delta_{LTIC}) \quad \text{(Eq. 8)}$$

Equivalent indicators of thermal resistance and thermal conductivity coefficient - linear Equations 9 and 10 of the form (Maneshev I. O., 2013):

$$R_{eq.} = 0.0292 + 0.0109 \cdot (\delta_{LTIC}) \quad \text{(Eq. 9)}$$

$$\lambda_{eq.} = 0.1747 - 0.0085 \cdot (\delta_{LTIC}) \quad \text{(Eq. 10)}$$

The calculated data (Equations 9 and 10) on the change in the coefficient of thermal conductivity of LTIC from the number of coating layers are presented in Table 4 and Figure 9.

It has been established that with an increase in the thickness of the coating in the range from 1 to 6 mm, an increase in $\lambda_{LTIC}$ from 0.0358 till 0.0739 W/m·K is observed. The largest change in $\delta_{LTIC}$ with an increase in the coating thickness was recorded in the interval 1÷2 mm with the stabilization of the indicator for coatings with a thickness of 4÷6 mm. The coefficient of variation of this indicator over the entire investigated interval is 22.9%; narrowing of the investigated range of coating thicknesses leads to its significant decrease: 9.43% - for 2÷6 mm; 5.363% - for 3÷6 mm; 2.01% - for 4÷6 mm; 2.37% - for 5÷6 mm.

The results obtained indicate that this technique is promising, based on using the ITS-1 thermal conductivity meter for evaluating the thermal-physical indicators of thin thermal insulating coatings. For stable performance, it is advisable to research thermal insulating coatings with a thickness of 3/6 mm.

6. To predict the thermal conductivity of LTIC, topological models can be used that take into account the fractality of the structure of granular fillers and coating material.

7. It has been found that dispersed microsilica obtained from natural diatomite has three types of scattering inhomogeneities mass fractals with dimensions 2.32 and 2.13. The scale of such objects is 8-40 nm. Small-scale pores 4-8 nm have rather heavily indented interfaces ($D_S$ = 2.64).

The results obtained confirm the presence of developed pore space of particles and agglomerates of dispersed silicon dioxide of nanometer sizes, which can be used to reduce the effective thermal conductivity of heterogeneous systems, for example, mineral silica powders of various origins. The investigated dispersed materials have similar parameters of the pore system at the nanometer level.

Analysis based on obtained gives grounds to believe that dispersed microsilica obtained from diatomite is most suitable: for creating a new generation of thermal insulation materials; as fillers for LTIC, VIP (VIP-vacuum insulation panel).

## 4. CONCLUSIONS:

1. As a result of the analysis of the influence of the structural parameters of the granular system formed from the synthesized particles of silicon dioxide, it was found that during the production of iron and steel products, their heat-shielding properties can be controlled by changing: pressure, viscosity, the molecular weight of gas; porosity of macrostructure and clusters; the thermal conductivity of the solid and gas phase of the system; the coefficient of accommodation; coordination number; primary particle size; fractal dimension characterizing the topological features of the structure of particles, aggregates, globules, clusters and their tendency to dissipate the energy of gas molecules.

2. Based on the research work carried out, it has been established that an additional decrease in thermal conductivity is possible due

to the optimization of the compositions of binders and the use of mineral fillers with low density. The performed analysis showed that the most promising fillers from this point of view are white soot and powders with an opal structure synthesized from diatomite's.

## 5. ACKNOWLEDGMENTS:

This research is funded by the Science Committee of the Ministry of Education and Science of the Republic of Kazakhstan and was done as part of the project AP08855714 "Thermal insulation coatings based on finely dispersed mineral granular systems" in the framework of "Grant funding for scientific and (or) scientific and technical projects for 2020-2022 with an implementation period of 27 months". The authors are grateful to the leadership of the Satbayev University and Science Committee of the ME&S RK for creating the conditions for carrying out this work.

## 6. REFERENCES:

1. Danilov V. I., Danilova M. E., Stanevich V. T. Modern thermal insulation materials for energy-efficient construction/ Tutorial. Pavlodar: Ed. Kereku, 2014. 73 p.
2. Selyaev V. P., Kupriyashkina L. I., Osipov A. K., Sedova A. A., Suponina L. A. Mineral-based thermal insulation materials. Bulletin BPO RAASN issue 15, Nizhny Novgorod, 2012, p. 166-171.
3. Golovanova L. A., Blum E. D. Energy-efficient building structures and technologies. "Scientific Notes of PNU" 2014, Volume 5, No. 4, pp. 71 – 77.
4. Komkov V. A., Timakhova N. S. Energy saving in housing and communal services. - M .: Infra-M, 2010 .- 320 p.
5. Beregovoy A. M., Viktorova O. L., Beregovoy V. A. Energy saving in residential buildings with alternative energy sources. Building materials. - 2008. - No. 5. - P. 34–38.
6. Shirinyan V. T. Hike of liquid-ceramic "super heat-insulating" coating along the heating networks of Russia // News of heat supply. - 2007. - No. 9. - P. 46–51.
7. Golovach Yu. Yu., Shvetsov A. V., Kolkhir Yu. F. The method of setting up the experiment and calculating the thermal conductivity coefficient for ultra-thin thermal insulation materials. - Kazan, 2008. URL: http://innt.com/teploprovodnost/index.html (date accessed: 30.05.2014).
8. Maneshev I. O., Pravnik Yu. I., Sadykov. I. A. Safin R. A., Eremin S. A. Experimental determination of the coefficients of thermal conductivity and efficiency of ultrathin heat-insulating coatings. News of KazGASU. - 2013. - No. 1 (23). P. 135-42.
9. Loginova N. A. Determination of the effectiveness of thin-film heat-insulating coatings as applied to heat supply systems. Author's abstract. - M., 2010 .-- 133 p.
10. Solomatov V. I., Virova V. N., Selyaev V. P. Polystructural theory of composite building materials. - Tashkent: FAN, 1991. 345 p.
11. Dulnev G. N., Zarichnyak Yu. P. Thermal conductivity of mixtures and composite materials. Reference book. - L.: Energy, 1974. 264 p.
12. Anisimov M. V., Rekunov V. S. Experimental determination of the thermal conductivity coefficient of ultra-thin liquid composite heat-insulating coatings. Bulletin of the Tomsk Polytechnic University. Engineering of georesources. 2015. No. 9. P. 15–22.
13. Selyaev V. P., Nurlybaev, R. E., Neverov, V. A., Aidarova. S. B., Zhuginisov. M. T., Murzagulova A. A. Nanostructured irregularity study by X-ray small-angle scattering (Article) International Journal of Chemical Sciences Volume 13, Issue 3, 2015, Pages 1421-1429.
14. Nizina T. A, Selyaev V. P, Nizin D. R., Balykov A. S., Korovkin D. I and Kanaeva N. S. Application of fractal analysis methods in the study of deformation mechanisms and composite building materials fracture (Article) IOP Conference Series: Materials Science and Engineering, 2018, 456 (1). Paper number 012058.
15. Khabibullin Yu. Kh., Barysheva O. B. Development of heat-insulating coatings and methods for determining their thermal-physical properties. News of KGASU. 2015. No. 3. P. 245–249.

16. Pavlov M. V., Karpov D. F., Sinitsyn A. A., Mnushkin N. V. Determination of the thermal conductivity coefficient of liquid thermal insulation in laboratory conditions. Bulletin of Volgograd State Architectural University. 2014. No. 37. P. 79–86.

17. GOST 30290–94. Building materials and products. Method for determining thermal conductivity by a surface transducer. - 01.01.1996. - M.: Gosstroy of Russia, 1996. 12 p.

18. GOST 7076-99. Building materials and products. Method for determination of thermal conductivity and thermal resistance under stationary thermal conditions. 04.01.2000. - M.: Gosstroy of Russia, 2000. 20 p.

19. GOST 28574-90. Corrosion protection in construction. Concrete and reinforced concrete structures. Methods for testing the adhesion of protective coatings - Introduction. 01.01.1991 - M .: Gosstroy of Russia, 1991. - 9 p.

20. GOST 52487-2005 (ISO 3251: 2003). Paints and varnishes. Determination of the mass fraction of non-volatile substances - Introduction. 01.01.2007 – M.: Gosstroy of Russia, 2007. - 12 p.

21. Dombrovsky L. A. Modeling of thermal radiation of a polymer coating containing hollow microspheres // Thermophysics of high temperatures. - 2005. - V. 43. - No. 1. - P. 1–11.

22. Selyaev V. P., Osipov A. K., Neverov V. A., Mashtaev O. G., Sidorov V. V. Polystructural model of heat-insulating material based on dispersed microsilica. Regional architecture and construction. - 2012. - No. 2 (13). - P. 5 - 11.

23. Boldyrev P. P. Zolotov A. N. Luisov A. S. Building materials: Handbook. M.: Stroyizdat. 1989.- 567p.

24. Gladkov S. O. Gas-kinetic model of thermal conductivity of heterogeneous substances // JTF. - 2008. - V.78, No. 7. - S. 12 - 15.

25. Inin A. E., Nizina T. A., Neverov V. A. Development of liquid thermal insulation coatings using local mineral raw materials // Actual problems of construction and construction industry: materials of the XIV Intern. scientific and technical conf. - Tula, 2013. - P. 40–41.

26. Druzhinina T. Ya., Kopylova A. A. The relevance of the use of liquid ultra-thin thermal insulation in the construction and operation of industrial and civil facilities // Vestnik IGTU. Irkutsk. Issue: 2 (73), 2013 - P. 101-105

27. Vasilyeva I. L., Nemova D. V. Energy-efficient materials of a new generation in construction // Ecology and construction. 2018. No. 4. P. 18-24.

28. Abramyan S. G., Mikhailova N. A., Kotlyarevsky A. A., Semochkin V. O. Thermal insulation materials providing energy efficiency of facade systems // Network scientific journal "Engineering Bulletin of the Don". No. 4. 2018.

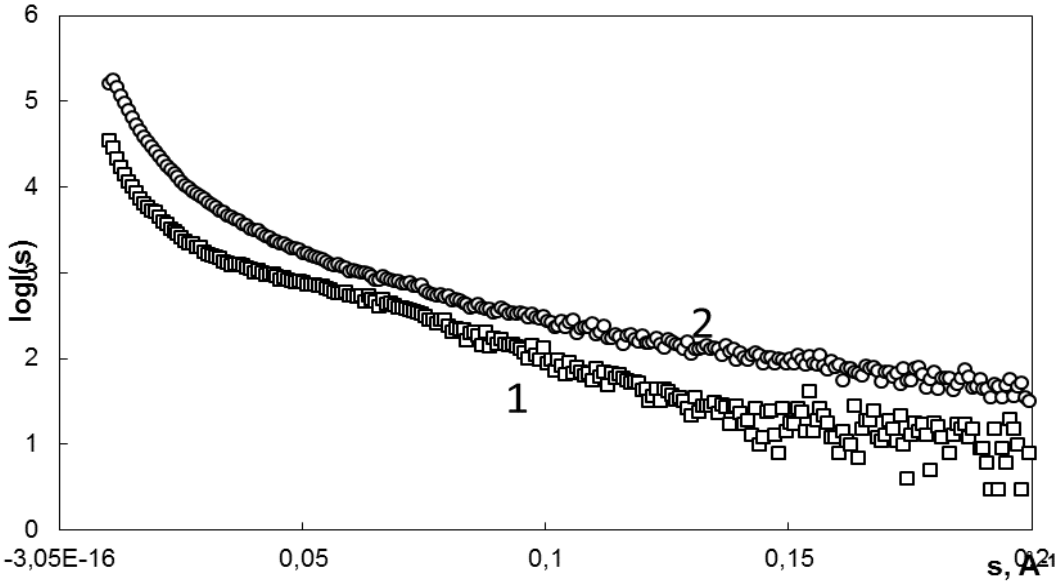


***Figure 1.*** *Small-angle X-ray scattering curves of dispersed powders: 1 - natural diatomite; 2 - filler powder.*

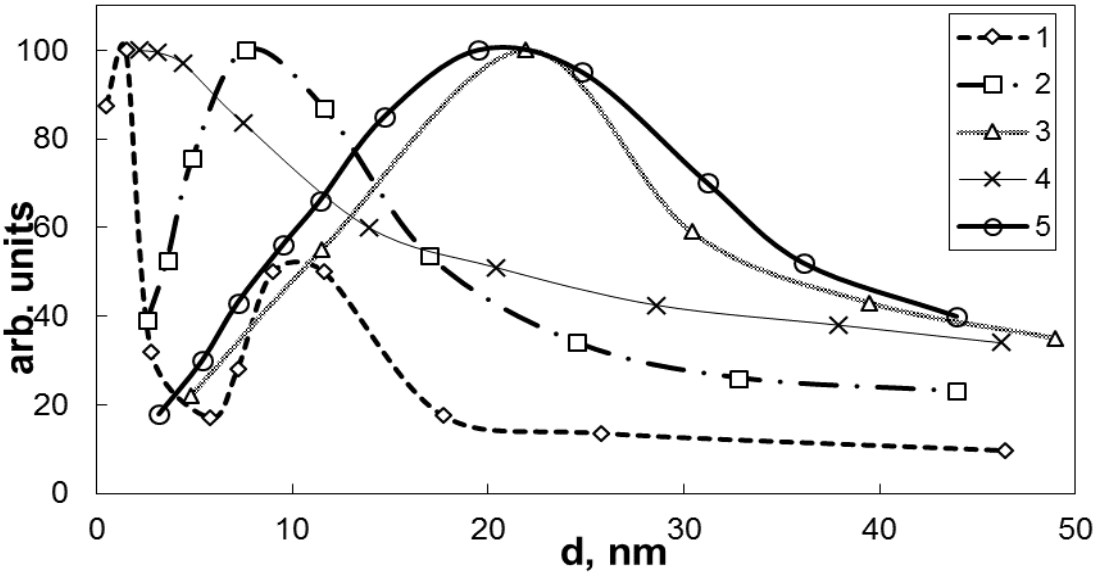


***Figure 2.*** *Size distribution of scattering inhomogeneities: 1 - natural diatomite; 2 - dispersed microsilica obtained from diatomite; 3 - condensed microsilica; 4 - white soot; 5 - filler powder.*

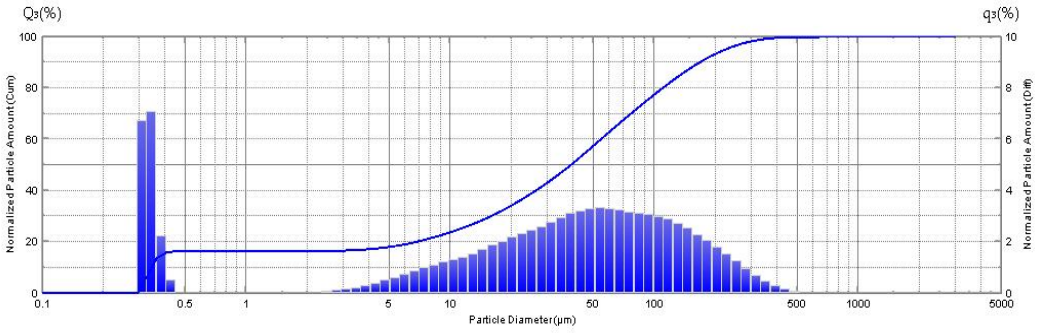


***Figure 3.*** *Particle size distribution of synthesized silicon dioxide determined experimentally using a Shimadzu SALD 3101 analyzer*

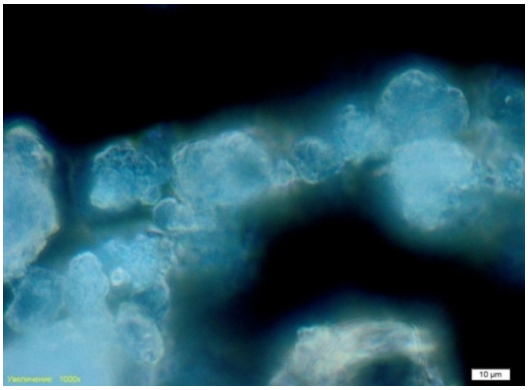

***Figure 4.*** *Image of particles of amorphous silicon dioxide synthesized from diatomite, obtained using an OLYMUSGX - 71 invented microscope*

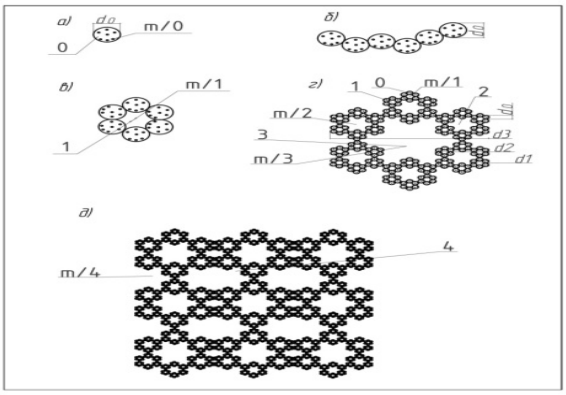


***Figure 5.*** *Fractal model of the structure of dispersed microsilica: a) primary particle; b) fibrillar (chain) cluster; c) globular (spherical) cluster; d) associated cluster (CCA); e) the spatial framework of the macrostructure made of CCA clusters.*

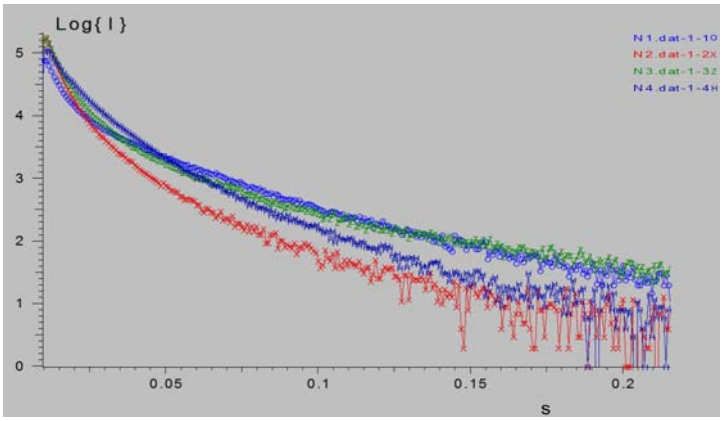


***Figure 6.*** *Scattering intensity $I(S)$ versus the scattering vector modulus S for amorphous silica synthesized from diatomite*

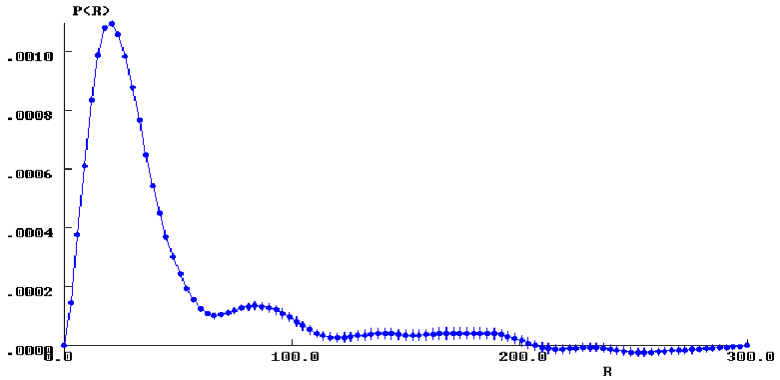


***Figure 7.*** *Size distribution R (in angstroms A) of synthesized silica scattering particles*

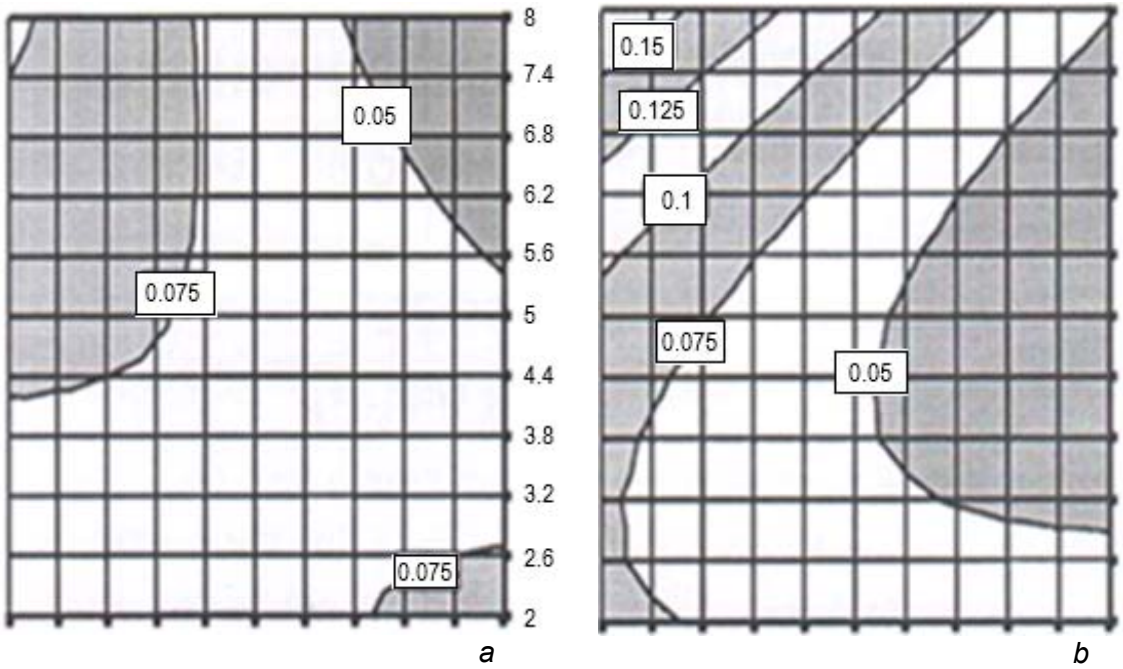


*a* *b*

***Figure 8.*** *Isolines of changes in the thermal conductivity of LTIC depending on the content of diatomite, silica, and acrylic dispersion: a - 16%; b - 20% (White soot content in% of binder mass)*

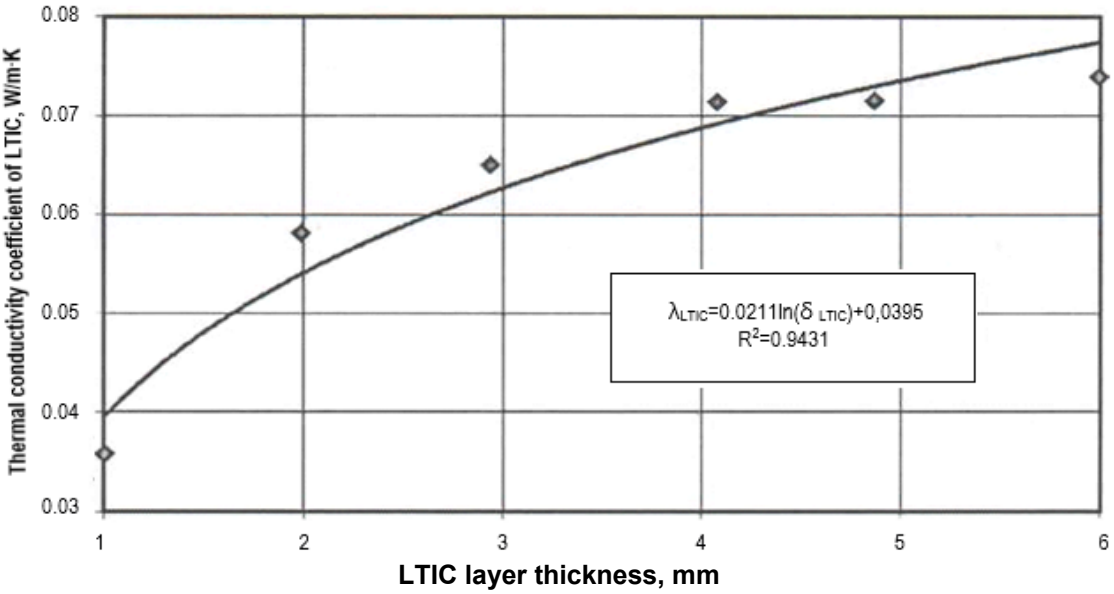


***Figure 9.*** *Change in the coefficient of thermal conductivity of liquid thermal insulation* depending on the thickness of the coating

***Table 1**. Pore size distribution of dispersed microsilica*

| Powder type | $d_B$, nm | < d >, nm | Δd, nm |
|---|---|---|---|
| Natural diatomite | 2 10 | 2 7 | 7 - 15 |
| Dispersed microsilica obtained from diatomite | 8 | 12 | 3 – 18 |
| Condensed silica fume | 22 | 26 | 10 – 34 |
| White soot | 2 | 13 | 2 - 21 |
| Powder - filler | 20 | 20 | 8 - 37 |

***Table 2.** Fractal characteristics of the investigated materials*

| No. | Material | Δs, $Å^{-1}$ | α | D | $D_S$ | d, nm |
|---|---|---|---|---|---|---|
| 1 | Natural diatomite | 0.013 – 0.026<br>0.031 – 0.061<br>0.067 – 0.095 | 2.59<br>1.56<br>3.73 | 2.59<br>1.56 | <br><br>2.27 | 24 – 48<br>10 – 20<br>7 – 9 |
| 2 | Dispersed microsilica obtained from diatomite | 0.016 – 0.025<br>0.025 – 0.080<br>0.080 – 0.160 | 2.32<br>2.13<br>3.36 | 2.32<br>2.13 | <br><br>2.64 | 25 – 40<br>8 – 25<br>4 – 8 |
| 3 | Condensed silica fume | 0.016 – 0.160 | 3.60 | | 2.40 | 4 – 40 |
| 4 | White soot | 0.016 – 0.025<br>0.025 – 0.160 | 3.17<br>2.66 | <br>2.66 | 2.83 | 25 – 40<br>4 – 25 |
| 5 | Powder - filler | 0.016 – 0.032<br>0.032 – 0.056<br>0.056 – 0.160 | 2.59<br>3.30<br>4.10 | 2.59 | <br>2.70 | 20 – 40<br>12 – 20<br>4 – 12 |

***Table 3.** Density and porosity of silica clusters synthesized from diatomite*

| *i* | 0 | 1 | 2 | 3 | 4 | 5 | 6 |
|---|---|---|---|---|---|---|---|
| $r_i$, nm | 1.0 | 5.0 | 10.0 | 40.0 | 100.0 | 300.0 | 1200.0 |
| $r_0(1)/r_i$ | 1.0 | 0.2 | 0.1 | 0.025 | 0.01 | 0.003 | 0.00083 |
| $\rho_1(r_i)$, g/ | 2.2 | 0.97 | 0.7 | 0.35 | 0.22 | 0.132 | 0.066 |
| $P_1(r_i)$, % | 0 | 56 | 68 | 84 | 90 | 94 | 97 |
| $r_0(2)/r_i$ | 1 | 0.4 | 0.2 | 0.05 | 0.02 | 0.006 | 0.00166 |
| $\rho_2(r_i)$, g/ | 2.2 | 1.39 | 0.98 | 0.49 | 0.311 | 0.18 | 0.089 |
| $P_2(r_i)$, % | 0 | 37 | 56 | 78 | 86 | 92 | 96 |
| $R_{max}$, nm | 4 | 9.98 | 20.2 | 80.6 | 201 | 595 | 2440 |

***Table 4.*** *Measurement of thermal-physical parameters of three-layer samples depending on the number of layers and the thickness of the liquid thermal insulating coating*

| Layer number | Thickness of applied layers, mm | Equivalent heat flux density $q_{eq.}$, W/m$^2$ | Equivalent thermal resistance $R_{eq.}$, m$^2$K/W | Equivalent thermal conductivity coefficient, $\lambda_{eq.}$, W/m·K | Thermal conductivity coefficient $\lambda_{LTIC}$, W/m·K |
|---|---|---|---|---|---|
| 1 | 1.01 | 0.043 | 142.4 | 0.163 | 0.0358 |
| 2 | 1.99 | 0.049 | 125.9 | 0.163 | 0.0581 |
| 3 | 2.94 | 0.060 | 118.7 | 0.149 | 0.0651 |
| 4 | 4.08 | 0.072 | 114.0 | 0.140 | 0.0713 |
| 5 | 4.87 | 0.083 | 106.6 | 0.131 | 0.0714 |
| 6 | 5.98 | 0.096 | 104.0 | 0.125 | 0.0739 |

PERIÓDICO TCHÊ QUÍMICA
ARTIGO ORIGINAL

# AVALIAÇÃO DAS CARACTERÍSTICAS DE FORÇA DE COROA ENDODÔNTICA ADESIVA DE CERÂMICA HÍBRIDA

# EVALUATION OF STRENGTH CHARACTERISTICS OF ENDOCROWNS FROM HYBRID CERAMICS

# ОЦЕНКА ПРОЧНОСТНЫХ ХАРАКТЕРИСТИК ЭНДОКОРОНОК ИЗ ГИБРИДНОЙ КЕРАМИКИ

DOROFEEV Aleksei*; KUZNETSOV Ivan

I. M. Sechenov First Moscow State Medical University (Sechenov University), E.V. Borovsky Institute of dentistry, Department of propaedeutic of dental diseases. Russia.

** Corresponding author*
*e-mail: aedorofeev@mail.ru*

Received 19 December 2020; received in revised form 20 February 2021; accepted 27 February 2021

## RESUMO

**Introdução:** A restauração dos dentes após o tratamento endodôntico é um problema urgente. Existe uma grande seleção de materiais e estruturas para restauração dentária após o tratamento endodôntico. **Objetivo:** O objetivo deste trabalho foi determinar as características de resistência de coroa endodôntica adesiva (endocrowns) feitas de cerâmica híbrida, dependendo de várias condições. **Métodos:** O estudo envolveu 40 amostras de dentes removidos (molares inferiores). O tratamento mecânico e médico dos canais radiculares era realizado previamente nos dentes, após o qual os canais radiculares eram selados com cimento e guta-percha. O defeito na parte da coroa do dente foi reparado com endocrown de cerâmica híbrida. Endocrowns foram feitos por moagem. Os endorocrowns foram cimentados de acordo com o protocolo de cimentação padrão para restaurações de cerâmica. Todas as amostras de dentes foram divididas em 2 grupos de 20 dentes cada grupo. O grupo 1 foi colocado no termostato por 24 horas a uma temperatura de + 37 ± 1 °C, o grupo 2 foi submetido à ciclagem térmica. Em seguida, as amostras dos grupos estudados foram submetidas à compressão uniaxial até o momento da destruição. Foram realizadas as medições de carga máxima (kN), tensão máxima (MPa) e% de deformação no momento da ruptura. Todos os resultados obtidos foram processados estatisticamente. **Resultados e Discussão:** De acordo com os resultados do estudo, as amostras do grupo 1 apresentaram maiores valores de resistência e elasticidade do que as amostras do grupo 2. **Conclusões:** Fornecer apenas conclusões diretamente suportadas pelos resultados; evitar especulação e generalização excessiva. Indique se estudo adicional é necessário; Dê igual ênfase a descobertas positivas e negativas de igual mérito científico; aponta coisas que podem ter sido esquecidas e sugere áreas para pesquisas futuras; resumo de sua pesquisa. Alguns pesquisadores também incluem: contribuição de conhecimento, limitação de pesquisa e recomendação de pesquisa futura na seção de conclusões.

**Palavras-chave**: *cerâmica híbrida, ciclagem térmica, restauração indireta, endocrown, odontologia*

## ABSTRACT

**Background:** Restoration of teeth after endodontic treatment is an urgent problem. There is a large selection of materials and structures for dental restoration after endodontic treatment. **Aim:** This work aimed to determine the strength characteristics of endocrowns made of hybrid ceramics, depending on various conditions. **Methods:** The study involved 40 samples of removed teeth (mandibular molars). Mechanical and medical treatment of root canals was previously carried out in the teeth, after which the root canals were sealed with a sealer and gutta-percha. The defect in the crown part of the tooth was repaired with a hybrid ceramic endocrown. Endocrowns were made by milling. The endorocrowns were cemented according to the standard cementation protocol for ceramic restorations. All tooth samples were divided into 2 groups of 20 teeth each group. Group 1 was placed in the thermostat for 24 hours at a temperature of +37±1°C, and group 2 was subjected to thermal cycling. After that, the samples of the studied groups were subjected to uniaxial compression until the moment of destruction. The measurements of the maximum load (kN), maximum stress (MPa), and % of deformation at the moment of failure were carried out. All the results obtained were statistically processed. **Results and Discussion**: According to the results of the study, the samples of group 1 showed higher values of strength and elasticity than samples

of group 2. **Conclusions:** Thus thermocycling, which simulates the natural oral environment negatively affects the durability of the hybrid ceramic. However, the obtained values make it possible to use it for the restoration of teeth after endodontic treatment.

**Keywords**: *hybrid ceramics, thermal cycling, indirect restoration, endocrown, dentistry*.

## АННОТАЦИЯ

**Актуальность:** Восстановление зубов после эндодонтического лечения является актуальной проблемой. Существует большой выбор материалов и конструкций для реставрации зубов после эндодонтического лечения. **Цель:** Целью данной работы явилось определить прочностные характеристики эндокоронок изготовленных из гибридной керамики в зависимости от различных условий. **Материалы и методы:** В исследовании было зайдействовано 40 образцов удаленных зубов (моляров нижней челюсти). В зубах предварительно была проведена механическая и медикаментозная обработка корневых каналов, после чего корневые каналы были запломбированы силлером и гуттперчей. Дефект коронковой части зуба выл восстановлен эндокоронкой из гибридной керамики. Эндокоронки изготавливались методом фрезерования. Фиксация эндорокоронк проводилась по стандартному протоколу фиксации керамическийх реставраций. Все образцы зубов были разделены на 2 группы о 20 зубов в каждой. Группа 1 помещалась в термостат на 24 часа при температуре +37±1°C, группа 2 подвергалась термоциклированию. После этого образцы исследуемых групп подвергались одноосному сжатию до момента разрушения. Проводилось измерения максимума нагрузки (кН), максимума напряжения (МПа) и % деформации в момент разрушения. Все полученные результаты были статистически обработаны. **Результаты и обсуждение**: По результатам исследования образцы группы 1 показали более высокие значения прочности и эластичности чем образцы группы 2. **Заключение:** Таким образом термоциклирование, которое имитирует естественную среду полости рта негативно сказывается на прочности гибридной керамики. Однако полученные значения позволяют применять ее для реставрации зубов после эндодонтического лечения.

**Ключевые слов**а: гибридная керамика, термоциклирование, непрямая реставрация, эндокоронка, стоматология.

## 1. INTRODUCTION:

Restoration of a destroyed tooth crown after endodontic treatment is an urgent problem in modern dentistry. Untimely access to the dentist for the treatment of caries leads to various complications. The most common complications of caries are pulpitis and periodontitis. As a result, the patient needs to remove the inflamed or damaged dental pulp (Frankenberger *et al.*, 2015, Utyuzh *et al*., 2019, Yumashev *et al*., 2020). This leads to the loss of a significant amount of hard tooth tissues and, consequently, to the weakening of the entire tooth. In this regard, the question arises about the method and material for the restoration of lost tissues (Coldea *et al*., 2013, Venturini *et al*., 2019, Sevbitov *et al*., 2020). The most accessible and simple method is the restoration of the tooth with a direct restoration from a dental composite. However, the dental composite is not without its drawbacks (Della Bona *et al*., 2014, Arora *et al.,* 2016, Yildirim *et al*., 2017). According to some authors, the service life of a composite restoration is 5 years on average. During the operation of such a restoration, staining of the tooth-restoration border, discoloration of the restoration, chipping of the filling material or the tooth itself, loss of the restoration may occur (Belleflamme *et al.,* 2017, Spitznagel *et al*., 2018, Hampe *et al*., 2019).

An alternative option for restoring teeth after endodontic treatment is to restore them with artificial crowns. There are many materials for making them (Awada and Nathanson, 2015, Albero *et al*., 2015, Choi *et al*., 2017). Previously, the most commonly used combined artificial crowns made of metal and ceramic. Currently, the most popular are artificial crowns made of ceramic, zirconium oxide, or a combination of both (Belli *et al.,* 2016; Alarwali *et al*., 2018; Amesti-Garaizabal *et al*., 2019). However, in all cases, a large amount of intact tooth tissues must be excised, which contradicts the principle of minimally invasive treatment to preserve as much healthy tissue as possible (Yu *et a*l., 2017, Alshouibi and Alaqil, 2019; Brandt *et al*., 2019).

According to a number of authors, the most

optimal option for restoring teeth after endodontic treatment is the manufacture of endocrowns (Carlos *et al.,* 2013, Argyrou *et al.,* 2016, Sevbitov *et al*., 2020). This design allows the preservation of a greater volume of healthy tissue but does not reduce the strength and durability of the restoration. The principle of preparation of tooth tissues under the endocrowns is similar to the technique of preparation of teeth under the onlay (El Zhwai *et al*., 2016, Xu *et al*., 2017, Eldafrawy *et al*., 2018).

However, there is a problem with the choice of material for the manufacture of this type of restoration. There are various materials currently on the market that are suitable for the manufacture of endocrowns (Chu *et al*., 2018, Facenda *et al*., 2018). However, all materials have their own positive and negative properties. The dental composite for the manufacture of endocrowns is not strong enough (Grenade *et al*., 2016, Goujat *et al*., 2018, Sevbitov *et al.*, 2018). On the contrary, metal and zirconium oxide are too hard material, due to which tooth decay can occur. The abrasion of the teeth - antagonists also occurs during the tooth restoration with zirconium oxide (Sieper *et al*., 2017, Nishioka *et al*., 2018). One of the most popular materials for making endocrowns is ceramics. There are several types of it. The most popular types of ceramics are feldspar ceramics and lithium disilicate ceramics (Ahrberg *et al.,* 2016; Mainjot *et a*l., 2016, Nouh *et al.*, 2019).

In this study, it was considered another material that combines the properties of composite materials and ceramics. Hybrid ceramics (polymer-infiltrated ceramic-network material, PICN) structure a sintered ceramic matrix impregnated with a polymer matrix (Campos *et al.,* 2016; Steinbrenne *et al.,* 2018). Due to its hybrid ceramic and polymer structure, this material is highly reliable. Manufacturers noted that after fixation, hybrid ceramics are resistant to stress and optimally distribute chewing force (Min et al., 2016, Alp *et a*l., 2018, Furtado de Mendonca *et al.*, 2019).

This work aimed to determine the strength characteristics of endocrowns made of hybrid ceramics, depending on various conditions.

## 2. MATERIALS AND METHODS:

The study was conducted on 40 samples of extracted teeth. For the study, removed mandibular molars with preserved crown part of the tooth, on which endodontic treatment had not previously been performed, were selected. After extraction, all teeth were disinfected and placed in distilled water for storage. Samples of teeth with a shelf life of 1 to 6 months after extraction were included in the experiment. All tooth samples were endodontically treated with rotating nickel-titanium instruments using the Crown-Down technique, creating a root canal taper of 6%. The root canal was sealed with a sealer based on AH-plus epoxy resin (Densply, USA) and gutta-percha using the vertical compaction technique.

After endodontic preparation of the teeth, all specimens were reconstructed using Vita Enamic (Germany) hybrid ceramic endocrowns. The mouths of the root canals were closed with a packable dental composite. The tooth preparation design was the same for all samples. On all teeth, the masticatory tubercles were reduced to the equator level (Figure 1).

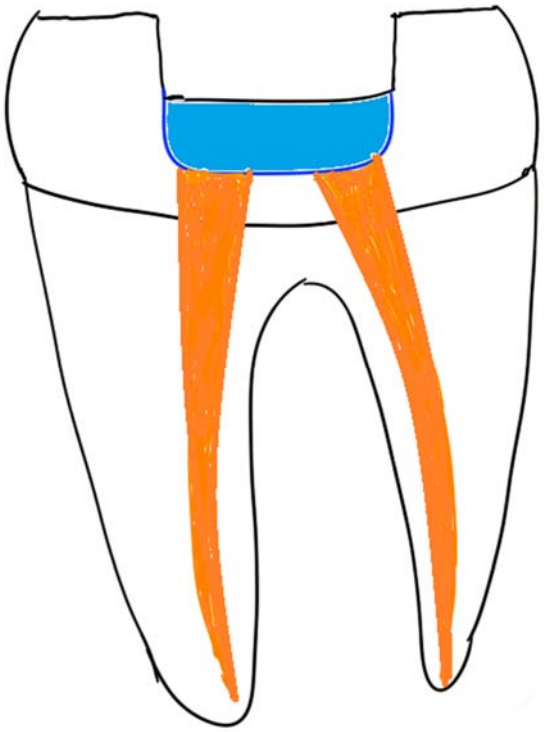

***Figure 1.*** Tooth preparation design

The teeth after preparation were scanned using a Cerec AC Bluecam intraoral camera (Sirona, Germany). The restoration was modeled using the Cerec 4.2 software (Sirona, Germany). Then the restoration was milled from a Vita Enamic hybrid ceramic block (Germany). The next step was fitting and fixing the endocrown. The fixation included the following actions:

1. Treatment of the inner surface of the

endocrown using a sandblasting apparatus RondoFlex plus 360 (KaVo, Germany) with aluminum oxide particles 27 μm at a pressure of 2 bar.

2. Application of 4% hydrofluoric acid (Bisco's Porcelain Etchants, USA) for 40 seconds.

3. Removal of the etching agent within 40 seconds with a stream of water from the pustar

4. Placing the ceramic restoration in a container with 95% alcohol solution and placing this container in an ultrasonic bath (AG Sonic TB-30, China)

5. Removing moisture

6. Coating the fixed surface with a silanizing agent (Bis-Silane, USA)

7. Application to the fixed surface with a bonding system (Bisco All-Bond Universal, USA) and storage without access to light until introduced into the tooth cavity.

8. Treatment of the tooth cavity with 50 μm aluminum oxide particles under a pressure of 2 bar with a sandblasting machine RondoFlex plus 360 (KaVo, Germany)

9. Adding an etching gel 37.5% phosphoric acid (Kerr Gel Etchant, USA) on the enamel for 30 seconds and on the dentin for 20 seconds.

10. Removal of the etching agent within 60 seconds with a stream of water from the pustar

11. Removing excess moisture

12. Application of the 5th generation adhesive system on the etched surface (Kerr OptiBond Solo Plus, USA)

13. Applying the luting composite to the restoration (Kerr NX3, USA)

14. Using the applicator, spread the luting material over the surface of the restoration to evenly distribute the luting layer

15. Introduction and fixation of the restoration into the tooth cavity

16. Removal of the curetted excess fixation material

17. Applying glycerin gel to the border of the restoration to remove the oxygen-inhibited layer

18. Final polymerization of the restoration within 60 seconds (Ivoclar Vivadent Bluephase N, Liechtenstein)

19. Removal of glycerin gel

20. Polishing the border of the restoration and hard tissues of the tooth using polyurethane heads of various abrasiveness (Densply Enhance, USA).

After the restoration of the teeth, they were randomly assigned to 2 groups of 20 teeth each. Samples of group 1 were placed in a container with distilled water and kept in a thermostat at a temperature of + 37 ± 1 °C for 24 hours, after which the test was carried out. Samples of group 2 were subjected to thermal cycling before testing. For thermal cycling, the samples of group 2 were placed in a container, which was immersed in a water thermostat with a water temperature of + 5 ± 1 °C for 30 seconds, after which the cuvette was removed and kept at room temperature for 20 seconds. Then the cuvette with the samples was immersed in a water thermostat with a temperature of + 60 ± 1 °C for 30 seconds, after which it was removed and kept at room temperature for 20 seconds. The performed complex of manipulations was taken as one cycle. In total, 1500 cycles were performed within 2 weeks, which corresponded to the one-year life of the restoration in the oral cavity.

The next step was testing the compressive strength of the endocrown samples. To accommodate the teeth in the apparatus, metal sleeves were used, in which samples of teeth were placed and recorded with self-hardening plastic. Specimens of both groups were subjected to vertical axial compressive load in an Instron-5982 apparatus (USA) at a speed of 0.70 mm/min until fracture began. During the test, the following parameters were measured: maximum load, maximum stress, deformation at failure. The obtained results were processed in the IBMSPSS program, version 21.0.

## 3. RESULTS AND DISCUSSION:

During tests under uniaxial compression, the following results were obtained (Table 1).

All samples of the extracted teeth differed slightly in diameter. However, according to the results of the study, it was noted that the diameter of the samples did not affect the strength parameters of the endocrown.

The maximum load up to the moment of destruction in group 1 was more than in group 2 by 0.79 kN ($p < 0.05$). Thus, the samples in group 2 showed lower strength than the samples in group 1. When comparing the maximum stress at the moment of failure, the samples of group 1 by 5.23 ($p < 0.05$) MPa showed a higher value than the samples of group 2. Deformation at fracture in

the samples of group 1 was more than in the samples of group 2 by 1.13% ($p < 0.05$). Thus, it can be argued that thermal cycling, which mimics the natural environment of the oral cavity, negatively affects the strength and elasticity of hybrid ceramic endocrowns.

When comparing the results of this study with the studies of other authors, it can be noted that hybrid ceramics turned out to be less strong than lithium-disilicate ceramics and stronger than feldspar ceramics. However, the elasticity of the hybrid ceramic is comparable to that of the hard tissues of the tooth, which allows it to more evenly distribute the load during chewing.

## 4. CONCLUSIONS:

According to the study results, it can be noted that thermal cycling, which imitates the natural environment of the oral cavity, has a negative effect on the strength characteristics of hybrid ceramic specimens. However, the robust characteristics of hybrid ceramic endocrowns make it possible to use it in the chewing group of teeth without negative consequences. This type of material has good elasticity, which allows it to more evenly distribute the occlusal load.

## 5. ACKNOWLEDGMENTS:

This work was done at Sechenov University with supported by the "Russian Academic Excellence Project 5-100".

## 6. REFERENCES:

1. Ahrberg, D; Lauer, H. C; Ahrberg, M; Weigl, P. (2016). Evaluation of fit and efficiency of CAD/CAM fabricated all-ceramic restorations based on direct and indirect digitalization: a double-blinded, randomized clinical trial. *Clin Oral Investig*, 20(2), 291-300.
2. Alarwali, A. M; Kutty, M. G; Al-Haddad, A. Y; Gonzalez, M. A. G. (2018). Fracture resistance of three different all-ceramic crowns: In vitro study. *Am. J. Dent.*, 31(1), 39-44.
3. Albero, A., Pascual, A., Camps, I., and Grau-Benitez, M. (2015). Comparative characterization of a novel CAD-CAM polymer-infiltrated-ceramic-network. *Journal of Clinical and Experimental Dentistry*, 7(4), 495-500.
4. Alp, G., Subaşı, M. G., Johnston, W. M., and Yilmaz, B. (2018). Effect of different resin cements and surface treatments on the shear bond strength of ceramic-glass polymer materials. *Journal of Prosthetic Dentistry*, 120(3), 454-461.
5. Alshouibi, E; Alaqil, F. (2019). Masking a Metal Cast Post and Core Using High Opacity e.max Ceramic Coping: A Case Report. *J Int Soc Prev Community Dent*, 9(6), 646-651.
6. Amesti-Garaizabal, A; Agustín-Panadero, R; Verdejo-Solá, B; Fons-Font, A; Fernández-Estevan, L; Montiel-Company, J; Solá-Ruíz, M. F. (2019). Fracture Resistance of Partial Indirect Restorations Made With CAD/CAM Technology. A Systematic Review and Meta-analysis. *J Clin Med*, 8(11), 1932.
7. Argyrou, R., Thompson, G. A., Cho, S. -., and Berzins, D. W. (2016). Edge chipping resistance and flexural strength of polymer infiltrated ceramic network and resin nanoceramic restorative materials. *Journal of Prosthetic Dentistry*, 116(3), 397-403.
8. Arora, R; Raiyani, C. M; Singh, V; Katageri, A. A. (2016). Postendodontic restoration of severely decayed primary tooth using modified omega loop as a post. *J Nat Sci Biol Med*, 7(1), 107-109.
9. Awada, A; Nathanson, D. (2015). Mechanical properties of resin-ceramic CAD/CAM restorative materials. *J Prosthet Dent,* 114(4), 587-593.
10. Belleflamme, M. M., Geerts, S. O., Louwette, M. M., Grenade, C. F., Vanheusden, A. J., and Mainjot, A. K. (2017). No post-no core approach to restore severely damaged posterior teeth: An up to 10-year retrospective study of documented endocrown cases. *Journal of Dentistry*, 63, 1-7.
11. Belli, R; Petschelt, A; Hofner, B; Hajtó, J; Scherrer, S. S; Lohbauer, U. (2016). Fracture Rates and Lifetime Estimations of CAD/CAM All-ceramic Restorations. *J Dent Res*, 95(1), 67-73.
12. Brandt, S; Winter, A; Lauer, H. C; Kollmar, F; Portscher-Kim, S. J; Romanos, G. E. (2019). IPS e.max for All-Ceramic Restorations: Clinical Survival and Success Rates of Full-Coverage Crowns and Fixed Partial Dentures. *Materials (Basel),* 12(3), 462.
13. Campos, F; Almeida, C. S; Rippe, M. P; de Melo, R. M; Valandro, L. F; Bottino, M. A. (2016). Resin Bonding to a Hybrid Ceramic: Effects of Surface Treatments

and Aging. *Oper Dent*, 41(2), 171-178.
14. Carlos, R. B; Thomas Nainan, M; Pradhan, S; Roshni Sharma; Benjamin, S; Rose, R. (2013). Restoration of endodontically treated molars using all ceramic endocrowns. *Case Rep Dent*, 210763.
15. Choi, S., Yoon, H. -., and Park, E. -. (2017). Load-bearing capacity of various CAD/CAM monolithic molar crowns under recommended occlusal thickness and reduced occlusal thickness conditions. *Journal of Advanced Prosthodontics*, 9(6), 423-431.
16. Chu, J; Bennani, V; Aarts, J. M; Chandler, N; Lowe, B. (2018). The effect of different geometric shapes and angles on the fracture strength of IPS e.max computer-aided designed ceramic onlays: An in vitro study. *J Conserv Dent*, 21(2), 210-215.
17. Coldea, A., Swain, M. V., and Thiel, N. (2013). In-vitro strength degradation of dental ceramics and novel PICN material by sharp indentation. *Journal of the Mechanical Behavior of Biomedical Materials*, 26, 34-42.
18. Coldea, A., Swain, M. V., and Thiel, N. (2013). Mechanical properties of polymer-infiltrated-ceramic-network materials. *Dental Materials*, 29(4), 419-426.
19. Coldea, A., Swain, M. V., and Thiel, N. (2014). Hertzian contact response and damage tolerance of dental ceramics. *Journal of the Mechanical Behavior of Biomedical Materials*, 34, 124-133.
20. Della Bona, A., Corazza, P. H., and Zhang, Y. (2014). Characterization of a polymer-infiltrated ceramic-network material. *Dental Materials*, 30(5), 564-569.
21. El Zhawi, H., Kaizer, M. R., Chughtai, A., Moraes, R. R., and Zhang, Y. (2016). Polymer infiltrated ceramic network structures for resistance to fatigue fracture and wear. *Dental Materials*, 32(11), 1352-1361.
22. Eldafrawy, M., Ebroin, M. G., Gailly, P. A., Nguyen, J. -., Sadoun, M. J., and Mainjot, A. K. (2018). Bonding to CAD-CAM composites: An interfacial fracture toughness approach. *Journal of Dental Researc*h, 97(1), 60-67.
23. Facenda, J. C., Borba, M., and Corazza, P. H. (2018). A literature review on the new polymer-infiltrated ceramic-network material (PICN). *Journal of Esthetic and Restorative Dentistry*, 30(4), 281-286.
24. Frankenberger, R; Zeilinger, I; Krech, M; Mörig, G; Naumann, M; Braun, A; Krämer, N; Roggendorf, M. J. (2015). Stability of endodontically treated teeth with differently invasive restorations: Adhesive vs. non-adhesive cusp stabilization. *Dent Mater,* 31(11), 1312-1320.
25. Furtado de Mendonca, A; Shahmoradi, M; Gouvêa, C. V. D; De Souza, G. M; Ellakwa, A. (2019). Microstructural and Mechanical Characterization of CAD/CAM Materials for Monolithic Dental Restorations. *J Prosthodont*, 28(2), 587-594.
26. Goujat, A., Abouelleil, H., Colon, P., Jeannin, C., Pradelle, N., Seux, D., and Grosgogeat, B. (2018). Mechanical properties and internal fit of 4 CAD-CAM block materials. *Journal of Prosthetic Dentistry*, 119(3), 384-389.
27. Grenade, C., De Pauw-Gillet, M. -., Gailly, P., Vanheusden, A., and Mainjot, A. (2016). Biocompatibility of polymer-infiltrated-ceramic-network (PICN) materials with human gingival fibroblasts (HGFs). *Dental Materials*, 32(9), 1152-1164.
28. Grenade, C., De Pauw-Gillet, M. -., Pirard, C., Bertrand, V., Charlier, C., Vanheusden, A., and Mainjot, A. (2017). Biocompatibility of polymer-infiltrated-ceramic-network (PICN) materials with human gingival keratinocytes (HGKs). *Dental Materials*, 33(3), 333-343.
29. Hampe, R; Theelke, B; Lümkemann, N; Eichberger, M; Stawarczyk, B. (2019). Fracture Toughness Analysis of Ceramic and Resin Composite CAD/CAM *Material. Oper Dent,* 44(4), 190-201.
30. Mainjot, A. K., Dupont, N. M., Oudkerk, J. C., Dewael, T. Y., and Sadoun, M. J. (2016). From artisanal to CAD-CAM blocks: State of the art of indirect composites. *Journal of Dental Research*, 95(5), 487-495.
31. Mamedov A., Morozova N., Yumashev A., Dybov A., Nikolenko D. (2019) Criteria for provisional restorations used in preparation for comprehensive orthodontic and orthopedic rehabilitation. Periodico Tche Quimica, 16(32): 647-655.
32. Min, J., Arola, D. D., Yu, D., Yu, P., Zhang, Q., Yu, H., and Gao, S. (2016). Comparison of human enamel and polymer-infiltrated-ceramic-network material "eNAMIC" through micro- and nano-mechanical testing. *Ceramics International*, 42(9), 10631-10637.
33. Nishioka, G., Prochnow, C., Firmino, A., Amaral, M., Bottino, M. A., Valandro, L. F.,

and Renata Marques de, M. (2018). Fatigue strength of several dental ceramics indicated for CAD-CAM monolithic restorations. *Brazilian Oral Research*, 32, 53.
34. Nouh, I; Kern, M; Sabet, A. E; Aboelfadl, A. K; Hamdy, A. M; Chaar, M. S. (2019). Mechanical behavior of posterior all-ceramic hybrid-abutment-crowns versus hybrid-abutments with separate crowns-A laboratory study. *Clinical Oral Implants Research*, 30(1), 90-98.
35. Sevbitov A., Pogosyan D., Enina Yu., Dorofeev A., Kalinovskiy S., Pustokhina I., Timoshina M. Study of the Border Adjustment of Indirect and Direct Restorations by Thermo cycling Method with Following Staying. Journal of Global Pharma Technology. 2020. 12(09): 231-235.
36. Sevbitov, A. V; Brago, A. S; Enina, Y. I; Dorofeev, A. E; Mironov, S. N. (2018). Experience in the application of hybrid ceramic restorations in the cervical region. *Asian Journal of Pharmaceutics*, 12(3), 1106-1109.
37. Sevbitov, A., Mitin, N., Kuznetsova, M., Dorofeev, A., and Ershov, K. (2020). A new modification of the dental prosthesis in the postoperative restoration of chewing function. *Opcion*, 36(Special Edition 26), 864-875.
38. Sieper, K., Wille, S., and Kern, M. (2017). Fracture strength of lithium disilicate crowns compared to polymer-infiltrated ceramic-network and zirconia reinforced lithium silicate crowns. *Journal of the Mechanical Behavior of Biomedical Material*s, 74, 342-348.
39. Spitznagel, F. A., Boldt, J., and Gierthmuehlen, P. C. (2018). CAD/CAM ceramic restorative materials for natural teeth. *Journal of Dental Research*, 97(10), 1082-1091.
40. Spitznagel, F. A., Scholz, K. J., Strub, J. R., Vach, K., and Gierthmuehlen, P. C. (2018). Polymer-infiltrated ceramic CAD/CAM inlays and partial coverage restorations: 3-year results of a prospective clinical study over 5 years. *Clinical Oral Investigations*, 22(5), 1973-1983.
41. Steinbrenner, H. (2018). Multichromatic and highly translucent hybrid ceramic Vita Enamic. *International Journal of Computerized Dentistry*, 21(3), 239-250.
42. Utyuzh, A., Nikolenko, D., Yumashev, A., Volchkova, I., and Samusenkov, V. (2019). Adhesion of periodontal pathogens to materials used for long-term temporary crowns. *Periodico Tche Quimica*, 16(33), 60-69.
43. Venturini, A. B., Prochnow, C., Pereira, G. K. R., Segala, R. D., Kleverlaan, C. J., and Valandro, L. F. (2019). Fatigue performance of adhesively cemented glass-, hybrid- and resin-ceramic materials for CAD/CAM monolithic restorations. *Dental Materials*, 35(4), 534-542.
44. Xu, Z., Yu, P., Arola, D. D., Min, J., and Gao, S. (2017). A comparative study on the wear behavior of a polymer infiltrated ceramic network (PICN) material and tooth enamel. *Dental Materials*, 33(12), 1351-1361.
45. Yildirim, G., Uzun, I. H., and Keles, A. (2017). Evaluation of marginal and internal adaptation of hybrid and nanoceramic systems with microcomputed tomography: An in vitro study. *Journal of Prosthetic Dentistry*, 118(2), 200-207.
46. Yu, P., Xu, Z., Arola, D. D., Min, J., Zhao, P., and Gao, S. (2017). Effect of acidic agents on the wear behavior of a polymer infiltrated ceramic network (PICN) material. *Journal of the Mechanical Behavior of Biomedical Materials*, 74, 154-163.
47. Yumashev A, Berestova A, Karapetyan A (2020) Cervical Caries: Modern Methods of Diagnosis and Treatment. Journal of Global Pharma Technology, 12(1): 89-96.
48. Yumashev, A. V., Utyuzh, A. S., Mikhailova, M. V., Samusenkov, V. O., and Volchkova, I. R. (2018). Selecting clinical and laboratory methods of manufacture of orthopaedic titanium alloy structures using a biopotentiometer. *Current Scienc*e, 114(4), 891-896.
49. Yumashev, A., and Mikhaylov, A. (2020). Development of polymer film coatings with high adhesion to steel alloys and high wear resistance. *Polymer Composites*, 41(7), 2875-2880.

***Table 1.*** *Strength characteristics of endocrowns made of hybrid ceramics*

| Index | Group 1 X±δ | Group 2 X±δ |
|---|---|---|
| Sample diameter (mm) | 12,12±0,58 | 12,09±0,32 |
| Maximum load (kN) | 2,26±0,14* | 1,47±0,16* |
| Maximum stress (MPa) | 12,41±0,58* | 7,18±0,49* |
| Breaking strain (%) | 4,17±0,17* | 3,04±0,21* |

X – average value
δ – standard deviation
Note: * – $p<0,05$

PERIÓDICO TCHÊ QUÍMICA
ARTIGO ORIGINAL

# ESTUDO CITOLÓGICO DA DINÂMICA DO PROCESSO DE FERIDAS EM LESÕES PURULENTES DA SÍNDROME DO PÉ DIABÉTICO COM O USO DE TECNOLOGIAS DE REABILITAÇÃO PROGRAMÁVEL

# CYTOLOGICAL STUDY OF THE DYNAMICS OF THE WOUND PROCESS IN PURULENT LESIONS OF THE DIABETIC FOOT SYNDROME WITH THE USE OF PROGRAMMABLE REHABILITATION TECHNOLOGIES

# ЦИТОЛОГИЧЕСКОЕ ИССЛЕДОВАНИЕ ДИНАМИКИ РАНЕВОГО ПРОЦЕССА ПРИ ГНОЙНЫХ ПОРАЖЕНИЯХ СИНДРОМА ДИАБЕТИЧЕСКОЙ СТОПЫ С ПРИМЕНЕНИЕМ ПРОГРАММИРУЕМЫХ САНАЦИОННЫХ ТЕХНОЛОГИЙ

SERGEEV, Vladimir Anatolievich[1*]; GLUKHOV, Alexander Anatolyevich[2]; SOROKIN, Alexander Sergeevich[3];

[1] Oryol State University named after I.S.Turgenev, Department of Specialized Surgical Disciplines, Medical Institute, Russia.

[2] Voronezh State Medical University named after N.N. Burdenko, Institute of Surgical Infection, Russia.

[3] Plekhanov Russian University of Economics, Department of Mathematical Methods in Economics,Russia.

** Corresponding author*
*e-mail: sergeevdoc60@yandex.ru*

Received 10 September 2020; received in revised form 18 February 2021; accepted 28 February 2021

## RESUMO

**Introdução:** Lesões purulentas dos pés no diabetes mellitus trazem sofrimento excruciante ao paciente, reduzem a qualidade de vida e muitas vezes levam à amputação do membro e possível morte. Os resultados decepcionantes do tratamento de complicações purulentas do diabetes encorajam a busca por novas abordagens de tratamento e métodos para avaliar o potencial reparador de defeitos de feridas. **Objetivo:** O estudo teve como objetivo melhorar os resultados do tratamento das complicações purulento-necróticas do pé diabético, estudar a avaliação morfológica dos processos de cicatrização ao usar métodos de tratamento promissores, como tecnologias de higinização programáveis. **Metodos:** Nos últimos 10 anos, foram analisados os resultados do tratamento de 106 pacientes com complicações necróticas purulentas da síndrome do pé diabético (SLD) sem isquemia crítica. Os pacientes foram randomizados em dois grupos. No grupo experimental (n = 55), após o tratamento cirúrgico, a ferida foi suturada firmemente e, no pós-operatório, foi realizado o desbridamento programado com o aparelho AMP-01 original. No grupo controle de pacientes (n = 51), a ferida purulenta não foi suturada no pós-operatório, o tratamento local foi realizado com soluções de iodóforos, pomadas a base de polietilenoglicol. Para avaliar a dinâmica dos processos reparadores em feridas purulentas, foi utilizado um método citológico, que permite avaliar de forma rápida e confiável o estágio do processo da ferida e a eficácia do tratamento. A simplicidade e disponibilidade do método permitem que seja recomendado a todos os especialistas praticantes. **Resultados e Discussões:** No grupo experimental, no dia 9 após a cirurgia, o número de formas degenerativas de neutrófilos em esfregaços citológicos foi 2,9 vezes menor do que no grupo controle - 12,3 ± 0,3% versus 36,4 ± 0,4% (p <0,001), o indicador RDI no grupo experimental foi 3,4 vezes maior em comparação com o grupo controle - 2,6 ± 0,1 e 0,9 ± 0,1, respectivamente (p <0,001). Isso indicava fagocitose mais ativa, limpeza mais rápida da cavidade purulenta. Um aparecimento mais precoce de células de tecido conjuntivo jovem foi observado no grupo experimental, o número de fibroblastos no dia 9 após a cirurgia foi 4,6 vezes maior (6,4 ± 0,4%) do que no grupo controle - 1,4 ± 0,1% (p <0,001), que confirmou a presença de processos regenerativos ativos na ferida. **Conclusões:** O uso de tecnologias de higienização programáveis no tratamento de complicações purulentas do pé diabético leva a uma redução mais significativa na duração da fase de inflamação e aceleração dos processos reparadores.

**Palavras-chave:** *síndrome do pé diabético, complicações necróticas purulentas, tecnologias de sanação programáveis, processo de reparo citológico.*

## ABSTRACT

**Background:** Purulent lesions of the feet in diabetes mellitus bring excruciating suffering to the patient, reduce the quality of life and often lead to limb amputation and possible death. The disappointing results of the treatment of purulent complications of diabetes encourage the search for both new approaches to treatment and methods for assessing the reparative potential of wound defects. **Aim:** This study aimed to improve the treatment of purulent-necrotic complications of the diabetic foot by studying the morphological assessment of healing processes when using promising treatment methods such as then programmed debridement. **Methods:** Over the past 10 years, the results of treatment of 106 patients with purulent-necrotic complications of diabetic foot syndrome (DFS) without critical ischemia have been analyzed. The patients were randomized into two groups. In the experimental group (n = 55), after surgical treatment, the wound was sutured tightly, and in the postoperative period, programmed debridement was carried out using the original AMP-01 device. In the control group of patients (n = 51), the purulent wound was not sutured after the operation, and local treatment was carried out with solutions of iodophors, ointments based on polyethylene glycol. To assess the dynamics of reparative processes in purulent wounds, a cytological method was used, which makes it possible to quickly and reliably assess the stage of the wound process and the effectiveness of the treatment. The simplicity and availability of the method allows it to be recommended to all practicing specialists. **Results and Discussion:** In the experimental group, by day 9 after surgery, the number of degenerative forms of neutrophils in cytological smears was 2.9 times lower than in the control group - 12.3 ± 0.3% versus 36.4 ± 0.4% ($p < 0.001$) - and the RDI indicator in experimental group was 3.4 times higher compared with the control group - 2.6 ± 0.1 and 0.9 ± 0.1, respectively ($p < 0.001$). This indicated more active phagocytosis, more rapid cleansing of the purulent cavity. An earlier appearance of cells of young connective tissue was observed in the experimental group. The number of fibroblasts by day 9 after surgery was 4.6 times higher (6.4 ± 0.4%) than in the control group - 1.4 ± 0.1% ($p < 0.001$), which confirmed the presence of active regenerative processes in the wound. **Conclusions:** The use of programmable sanitation technologies in treating purulent complications of a diabetic foot leads to a more significant reduction in the duration of the inflammation phase and acceleration of reparative processes.

**Keywords:** *Diabetic foot syndrome, purulent-necrotic complications, Programmable sanitation technologies, cytological reparative process.*

## АННОТАЦИЯ

**Актуальность:** Гнойные поражения стоп при сахарном диабете – это источник мучительных страданий пациента, снижающих качество жизни и нередко приводящих к ампутации конечности и возможному летальному исходу. Неутешительные результаты лечения гнойных осложнений диабета побуждают заниматься поиском как новых подходов к лечению, так и методов оценки репаративного потенциала раневых дефектов. **Цель:** Исследование было направлено на улучшение результатов лечения гнойно-некротических осложнений диабетической стопы, на изучение морфологической оценки процессов заживления при применении перспективных методов лечения -программируемых санационных технологий. **Методы:** За последние 10 лет проанализированы результаты лечения 106 пациентов с гнойно-некротическими осложнениями синдрома диабетической стопы (СДС) без явлений критической ишемии. Пациенты рандомизированы на две группы. В группе 1(n=55) после хирургической обработки рана ушивалась наглухо, а в послеоперационном периоде осуществлялись программируемые санации с использованием оригинального устройства АМП-01. В группе 2 (n=51) после операции пациенты получали традиционное местное лечение. Для оценки динамики репаративных процессов в гнойных ранах использовали цитологический метод, позволяющий быстро и достоверно оценить стадию течения раневого процесса и эффективность проводимого лечения. Простота и доступность метода позволяет его рекомендовать всем практикующим специалистам. **Результаты и обсуждение:** В группе 1 к 9 суткам количество дегенеративных форм нейтрофилов в цитологических мазках было в 2.9 раза ниже, чем в группе 2 -12.3±0.3% против 36.4±0.4% ($p<0,001$), показатель РДИ в группе 1 был в 3.4 раза больше по сравнению с группой 2 - 2.6±0.1 и 0,9±0,1соответственно ($p<0,001$). Это свидетельствовало о более активном фагоцитозе, более быстром очищении гнойной полости. В группе 1 наблюдалось более раннее появление клеток молодой соединительной ткани, количество фибробластов к 9 суткам было в 4.6 раза больше (6.4±0.4%), чем в группе 2 - 1.4±0.1% ($p<0,001$), что подтверждало наличие активных регенераторных процессов в ране. **Выводы:** Применение программируемых санационных технологий при лечении гнойных осложнений диабетической стопы приводит к более значимому сокращению сроков фазы воспаления и ускорению репаративных процессов.

**Ключевые слова:** *Синдром диабетической стопы, гнойно-некротические осложнения, Программируемые санационные технологии, цитологическое репаративный процесс.*

## 1. INTRODUCTION:

At the present stage, the problem of diabetes mellitus (DM) is acquiring medical and social significance, which is explained by the high progressive prevalence, significant disability, and increased mortality in patients with diabetes (Galstyan, Vikulova, *et al.*., 2018; Dedov, Shestakova, *et al.*., 2017; Mitish, Paskhalova, *et al.*., 2014; Bakker, Apelqvist, *et al.*., 2016).

According to the World Health Organization (WHO), diabetes currently affects approximately 285 million people, and experts predict an increase in the number of patients with diabetes to 600 million by 2035 (Galstyan, Vikulova, *et al.*., 2018; Dedov, Shestakova, *et al.*, 2017; Stupin, Silina, *et al.*, 2019). In Russia, the mortality rate from type 2 diabetes is 60.3 per 100 thousand population (Galstyan, Vikulova, *et al.*, 2018). In the United States, diabetes affects approximately 9.4% of the population over 18 (Guariguata, Whiting, *et al.*, 2011). In 2013, diabetes-related health care costs cost US$ 548 billion, or 11% of total adult health spending, and are projected to exceed US$ 627 billion by 2035 (Bordianu, Bobircă, *et al.*, 2018).

Every year in the world, complications of diabetes become the cause of death in 1.6 million people, and, according to scientists, this figure will double in 10 years (Ray, Valentine, *et al.*, 2005). Approximately 25% of diabetics are at risk of developing diabetic foot ulcer (DFU), which is the main reason for their hospitalization, which costs US $ 40,000 per event (Armstrong, Boulton, *et al.*, 2017; Jang, Hong, *et al.*, 2015; Nickerson, 2018).

It is possible to achieve healing of diabetic ulcers by conservative measures only in 63–81% of cases; amputation of various limb levels is required in 14–24% of patients, while mortality rates reach 13%. These figures emphasize the need to search for innovative approaches to the problem of treating purulent-necrotic complications of diabetes mellitus (Ivanov, Serebryakova, *et al.*, 2018; Yusupova, Nabiev, *et al.*, 2017). Most experts consider the conservative approach to their treatment to be the main and decisive one; however, the duration of such therapy is many months. At the same time, invasive methods of treatment are expensive, and standard schemes of local drug therapy for wound and ulcerative defects are ineffective (Mitish, Paskhalova, *et al.*, 2014; Ray, Valentine, *et al.*, 2005); Ivanov, Serebryakova, *et al.*, 2018; Yusupova, Nabiev, *et al.*, 2017).

Slowing down of the healing process in purulent lesions of diabetes is due to polyneuropathy, angiopathy, osteoarthropathy, which are interrelated factors and lead to the development of formidable complications. These complications often lead to the loss of a limb, and sometimes pose a real threat to the patient's life (Braun, L.R., Fisk, W.A. *et al.*, 2014; Zaytseva, E.L., Doronina, L.P. *et al.*, 2014).

Over the past decade, fundamental research in molecular cell biology has made possible a better understanding of the underlying mechanisms of wound healing in diabetes. In this case, a violation of the synthesis of growth factors is observed due to a decrease in the activity of macrophages. The role of inflammatory cytokines and matrix metalloproteases in reducing the rate of extracellular matrix remodeling and the rate of collagen accumulation has been proven (Baltzis, Eleftheriadou, *et al.*, 2014; Liu, Min, *et al.*, 2009); Li, Z., Guo, *et al.*, 2013; Dinh, Tecilazich, *et al.*, 2012; Brancato, Albina, 2011; Mingyuan, Yiwen, *et al.*, 2012). These and other pathophysiological mechanisms lead to a chronic protracted course of wound defects in diabetes with a delay in their healing.

Today, it is becoming more and more urgent to solve the problems of predicting the course of reparative processes that underlie the structural and functional restoration of altered tissues. In this regard, there is an urgent interest in the development of both new approaches to treatment and methods for assessing the dynamics of healing of wound defects in DFS (Zemskov, Chorochilov, *et al.*, 2011; Lacci, Dardik, 2010; Han, Wang, *et al.*, 2012; Larichev, Shishlo, *et al.*, 2011; Kuzin, Kostyuchenok, 1990).

This research aimed to study the results of a cytological study of healing processes in purulent lesions of diabetic foot syndrome (DFS) using programmable sanitation technologies.

## 2. MATERIALS AND METHODS:

### 2.1. Sample

A total of 106 patients with purulent-necrotic complications (PNC) of Diabetic Foot Syndrome (DFS) without critical ischemia were treated at the Oryol Regional Clinical Hospital for the period 2008-2018.

### 2.2 Ethics

This study was carried out under the requirements of the Declaration of Helsinki on

World Medical Practice (revised in 2013). The study was approved by the Ethics Committee of the Oryol State University named after I. S. Turgenev, Protocol No. 16 of 20.11.2020

### 2.3. Inclusion and Exclusion criteria

Inclusion criteria: patients with type 1 and type 2 diabetes, no critical ischemia with TcPO2 values not lower than 27 mm Hg, degree of foot tissue damage according to F.W. Wagner (1979) Grade II-IV, signed informed consent. The study did not include patients under 18 years of age, with Wagner grade I and V of DFS, with TcPO2 in the foot skin below 27 mm Hg, with extensive skin defects in the surgical treatment area. The presence of malignant tumors, concomitant diseases in the stage of decompensation, circulatory and respiratory insufficiency of the III degree, endocrine-metabolic and cerebral obesity, drug addiction, pregnancy and lactation were also exclusion criteria.

### 2.4. Groups of study

The patients included in the study were randomized into two groups depending on the methods of rehabilitation of purulent foci in the postoperative period. The experimental group consisted of 55 (51.9 %) patients (25 men and 30 women), after surgical treatment of the purulent focus, tubular drains were installed in the wound cavity, removed out through separate incisions, and the wound was sutured tightly. Drains were connected to the original AMP-01 device (patent for invention No. 2539165 dated 27.11.2014), which was used for programmed sanitation in the postoperative period. The control unit of the device was equipped with an individually selected program of cyclic irrigation processes, antiseptic aspiration and constant vacuuming, carried out in an Autonomous mode. The set vacuum level in the purulent cavity was maintained using a built-in pressure sensor.

The control group included 51 (48.1 %) patients (23 men and 28 women); after surgical treatment of a purulent focus, they received traditional local treatment using solutions of iodophores, ointments based on polyethylene glycol, and after the inflammation was stopped, plastic foot reconstruction (PRS) was performed or the wound was healed by secondary tension

Table 1 presents a comparative description of the clinical parameters of the study groups. The groups of patients were comparable in age, gender, type of DM, clinical form of SDS and indicators of transcutaneous oximetry in the skin of the foot.

The volume of PNC of the diabetic foot in patients of the study groups was diverse. In 75.5% of cases, the bone and joint apparatus of the foot was involved in the purulent-destructive process. In 27 (25.5%) cases, there were purulent-necrotic and purulent-granulating wounds after finger amputations or foot resection performed in other medical institutions. Tissue damage in the form of dry gangrene was found in 21 (19.8%) patients, and in the form of phlegmon, wet gangrene – in 15 (14.2%) patients. There was no correlation between the distribution of patients according to the nosological form of PNC of DFS and the lesion volume in the study groups ($\chi^2$- Pearson criterion $p$=0,989). The distribution of patients in the study groups depending on the nosological form of PNC of DFS and the volume of lesion in accordance with the classification of F.W. Wagner (1979) is shown in table 2.

In the experimental group of patients with neuropathic form, radical surgical treatment and plastic reconstruction of the foot (PRS) were performed in one stage. Stage-by-stage sanation of the purulent focus was performed in the neuroishemic form, and after the inflammation was stopped, PRS was performed. Programmable sanation was used in all cases in the postoperative period after wound suturing.

Patients of the study groups received complex therapy, which included complete foot relief, insulin therapy with fractional administration of adequate doses of the drug under the control of glycemia, etiotropic antibiotic therapy, and anticoagulants and immunomodulators were prescribed according to indications. Patients with neuro-ischemic DFS were prescribed perfusion vascular therapy. Primary surgical operations in patients in the study groups are presented in table 3. According to Pearson's $\chi^2$-test, there are no differences between the groups (p=0.72).

### 2.5. Research methods

Patients underwent the following research methods: a collection of complaints, anamnesis of the disease, assessment of comorbital conditions, clinical examination of organs and systems. All patients underwent laboratory tests, radiography of the feet in two projections, assessment of macro - and microhemodynamics using ultrasound duplex scanning of the arteries, Doppler examination of the lower extremity arteries, transcutaneous oximetry on the TSM 400 device of Radiometer medical (Denmark), and

bacteriological examination of the wound discharge in dynamics.

### 2.6. Cytological examination

To access the healing of purulent foci of the diabetic foot, a cytological research method was used which makes it possible to quickly and reliably assess the stage of the wound process and the effectiveness of the treatment (Ivanusa, S.Y., Risman, B.V. *et al.*, 2016; Kamaev, M.F., 1954).

In the experimental group, material was taken from the depth of the sutured wound using the "puncture biopsy" method (Kaem and Karlov, 1977; Sergel and Goncharova, 1990). According to this technique, the wound exudate and cellular tissue elements were aspirated from the depth of the wound and its walls with a syringe through a sterile injection needle, which was attached to it and inserted into the depth of the wound. The resulting material was applied to a glass slide, evenly spreading and drying at room temperature. In the control group, the method of surface biopsy was used according to M.P. Pokrovskaya and M.S. Makarov (1942) modified by M.F.Kamaev (1954) (Kamaev M.F., 1954). With this material sampling technique, the surface layer of the wound is scraped with a special spatula or the handle of a surgical scalpel. The resulting material was applied to a glass slide, evenly distributed in a thin layer, and dried at room temperature. The smears thus obtained were immersed in methanol for 5 minutes for fixation and then stained according to the Romanovsky-Giemsa method using a solution (1 ml of standard liquid paint + 2 ml of basic buffer solution at pH 6.4-6.5 + 47 ml distilled water). Staining was carried out for 40–120 min, and the duration of staining was selected empirically. The swabs were then rinsed in distilled water, dried, and examined by immersion.

Cytological examination of smears from the surface of wounds was carried out in dynamics: on the first day at the time of randomization, and then on the 3rd, 5th, 7th, and 9th days. Smears were studied by microscopy with a magnification of 630 times with the calculation of shaped elements and the output of the average for 10 fields of view. The resulting value was expressed as a percentage per 100 counted cells. Used an Axio A1 light microscope (Zeiss, Germany) with a set of accessories. Photographs were taken using the AxioCam 105 color camera (Zeiss, Germany) using the ZEN 2 blue edition software (Zeiss, Germany), which was calibrated using an object micrometer of transmitted light with a division price of 0.005 mm.

The study followed the characteristics of cytograms with the definition of one of the 6 types of cytological picture according to V. F. Kamaev (1954), corresponding to different stages of the wound process: degenerative-necrotic type, degenerative-inflammatory type, inflammatory type, inflammatory-regenerative type, regenerative-inflammatory type, regenerative type (Davydov, Larichev, Abramov, 1990).

To fully assess the wound healing picture, the regenerative-degenerative index (RDI) was calculated, which was determined by the formula RDI = (STAB+SEGS)/DN, where STAB is the number of rod – shaped neutrophils in the field of vision; SEGS is the number of segmented neutrophils; DFN is the number of degenerative forms of neutrophils (Davydov *et al.*., 1990; (Davydov, Larichev, Abramov, 1990). If the RDI was less than one, it indicated a pronounced inflammatory process in the wound, if the value of this indicator became more than one, it meant the transition of the wound process to the regeneration phase.

### 2.7. Statistics

The work was performed in the design of a simple randomized comparative controlled study in parallel groups. The SPSS Statistics 25 (IBM) program was used for statistical processing of the obtained data. To study the relationship between qualitative features, conjugacy tables and calculated Pearson's $\chi^2$-criterion or the Fisher's exact criterion were made. If there is a relationship between qualitative features, the shares of features were compared using the z-criterion of equal shares. The significance of differences between groups by quantitative characteristics was evaluated using the student's parametric t-test and the nonparametric Mann-Whitney test for unrelated groups. For related groups, the parametric t-test for dependent samples and the nonparametric Wilcoxon sign test were used. To assess changes in the dynamics of quantitative indicators, an analysis of variance with repeated measurements with the setting of a time factor and a group was used. As a result of the analysis of variance with repeated measurements, hypotheses were tested: whether the change in indicators over time is significant, whether there is a difference between groups, and if there is a statistically significant interaction between the time factor and the group. The latter hypothesis allowed us to prove the difference in the change of controlled indicators over time depending on the

group. Differences were considered statistically significant when the probability value was less than 0.05 for a two-way critical region.

## 3. RESULTS AND DISCUSSION:

In cytological smears at the time of randomization in both groups of the study, patients with PNC of DFS had a pronounced predominance of degenerative neutrophils (DN) (82.6±3.2%), and there were very few preserved forms of white blood cells. The regenerative-degenerative index (RDI) was significantly lower than one (0.2±0.1). A degenerative-necrotic type of cell reaction characterized the cytological picture. Microflora was present in large numbers, mainly extracellularly, but sometimes it could be found intracellularly in a state of incomplete or perverted phagocytosis. The preparations contained accumulations of necrotic masses and amorphous gelatinous interstitial substance. The cellular composition of cytological smears in patients with purulent complications of DFS in the study groups at the time of randomization is presented in table 4.

All parameters of the statistical assessment of the cellular composition of cytological smears on the first day of observation in both study groups are close in values ($p > 0.05$), which made it possible to judge the homogeneity of the groups.

On the 5th day after randomization in the experimental group, the cytological picture corresponded to the inflammatory or inflammatory-regenerative cellular reaction type. There was a statistically significant decrease in the number of degenerative neutrophils (DN) (37.34 ± 2.33%), an increase in the number of preserved forms of neutrophils: segmented neutrophils amounted to 38.69 ± 1.33%, stab - 5.55 ± 0.39% ($p < 0.001$).

There was a statistically significant increase in the regenerative-degenerative index (RDI) - 1.19 ± 0.09 ($p < 0.001$). Plasma cells, histiocytes appeared. There was a statistically significant increase in the number of active macrophages - 3.59 ± 0.25%, lymphocytes - 4.79 ± 0.24%, fibroblasts - 3.21 ± 0.31% ($p < 0.001$). Groups of cells of young connective tissue in the form of fibrocytes, fibroblasts, fibrous fibers were found. Microflora was determined in small amounts at the stage of complete phagocytosis.

In the control group, on the 5th day of treatment, the cytological picture in smears changed little, the number of DNs significantly decreased - 72.5 ± 1.37% ($p < 0.05$), the number of segmented and stab neutrophils slightly increased, the degree of their preservation slightly increased. The RDI value decreased statistically significantly - 0.49 ± 0.04 ($p < 0.05$). Microflora was found in moderate quantities; cases of completed phagocytosis were more often observed. The appearance of low-differentiated mononuclear cells was noted. There were single actively phagocytic leukocytes, lymphocytes, single elements of granulation tissue (table 5). The cytological picture corresponded to the degenerative-inflammatory type of cell reaction, reflecting the weak course of inflammatory reactions in the wound. Figures 1 and 2 show fragments of cytological smears from the wound surface on the 5th day in the study groups.

When assessing the dynamics of the cellular composition of cytological smears on the 5th day of the postoperative period, a significant difference was obtained between the study groups. According to the results of analysis of variance with repeated measurements, it was proved that there are statistically significant changes in the cellular composition of cytograms in both groups on the 5th day after surgery ($p < 0.001$). There was a statistically significant presence of interaction between the time factor and the group ($p < 0.001$).

On the 9th day of the postoperative period, a statistically significant decrease in degenerative neutrophils (12.28 ± 0.29%) was observed in the experimental group, preserved forms of neutrophils prevailed - segmented - 28.21 ± 0.94%, stab - 3.63 ± 0,18% ($p < 0.001$). There was a statistically significant increase in RDI values - 2.61 ± 0.09, the number of macrophages - 12.17 ± 0.68%, fibroblasts - 6.44 ± 0.38% ($p < 0.001$). Young elements of connective tissue, polyblasts prevailed over neutrophils and were located among the fibrous structures of the intermediate substance. The epithelium was presented in smears in the form of sheets of cells. Microflora was absent. The cytological picture corresponded to the regenerative-inflammatory or regenerative type of cellular reactions.

By the 9-10th day, the cytological picture began to acquire features characteristic of regenerative processes in the control group. The number of degenerative neutrophils decreased statistically significantly - 36.42 ± 0.36%, there were more preserved forms: HF - 24.31 ± 0.88%, PN - 8.09 ± 0.84% ($p < 0.05$). There was a statistically significant increase in the RDI value, which approached one - 0.90 ± 0.03. Microbes in the wound were detected in small numbers and

were intracellularly in the phase of complete phagocytosis. The number of mononuclear cells significantly decreased, and the detection of their derivative forms in the process of differentiation became natural: the number of polyblasts increased, fibroblasts appeared - 1.39 ± 0.13%, the number of macrophages increased (2.21 ± 0.19%). Along with cellular elements, delicate fibers of the intermediate substance were observed. The cytological picture in smears corresponded to the inflammatory regenerative type of cellular reactions (Table 5). Figures 3 and 4 show fragments of cytological smears from the wound surface on the 9th day in the study groups.

For both groups, statistically significant changes in the cellular composition in cytograms on the 1st and 9th days of the postoperative period were proved: a decrease in the number of degenerative neutrophils in the experimental group (M ± σ) from 82.5 ± 1.9% to 12.3 ± 0.3%, in the control group from 84.6 ± 3.7% to 36.4 ± 0.4% ($p < 0.001$); an increase in the preserved forms of neutrophils (segmented neutrophils) - in the experimental group (M ± σ) from 14.2 ± 0.2% to 28.2 ± 0.9%, in the control group from 16.2 ± 0.3% to 24 .3 ± 0.9% ($p < 0.001$); increase in RDI value - in the experimental group (M ± σ) from 0.2 ± 0.1% to 2.6 ± 0.1%, in the control group from 0.2 ± 0.1% to 0.9 ± 0, 03% ($p < 0.001$).

In the experimental group, where programmable sanitation technologies were used, there was a faster decrease in the number of degenerative neutrophils, an increase in their preserved forms, a faster increase in RDI, and the differences between the groups were statistically significant in general over the entire observation period ($p < 0.001$). The presence of a significant interaction between the time factor and the group ($p < 0.001$) was also found, in the experimental group by the 9th day the number of degenerative forms was significantly lower - 12.28 ± 0.29%, in contrast to the control group (36.42 ± 0.36 %), the number of intact forms of neutrophils was higher - 28.21 ± 0.94% and 24.31 ± 0.88%, respectively. There was a more rapid increase in RDI in the experimental group on day 9 (2.61 ± 0.09) compared with the control group (0.90 ± 0.03). This indicated a more active phagocytosis, rapid cleansing of the purulent cavity. The dynamics of the average values of degenerative neutrophils and RDI in the study groups is shown in Figures 5 and 6.

To assess the reparative potential of purulent wounds, a cytological assessment of the quantitative composition of lymphocytes, macrophages and fibroblasts in the study groups on the 1st and 9th days of the postoperative period was carried out. For both groups, a statistically significant increase in the number of lymphocytes was proved - in the experimental group (M ± σ) from 0.4 ± 0.1% to 7.5 ± 0.6%, in the control group from 0.2 ± 0.1% up to 2.5 ± 0.6% ($p < 0.001$); statistically significant increase in the number of active macrophages - in the experimental group (M ± σ) to 12.2 ± 0.7%, in the control group to 2.2 ± 0.2% ($p < 0.001$). Also, on day 9, a statistically significant increase in fibroblasts was observed - in the experimental group (M ± σ) up to 6.4 ± 0.4%, in the control group up to 1.4 ± 0.1% ($p < 0.001$).

In the experimental group, where programmable sanitation technologies were used, there was a faster increase in the number of lymphocytes, earlier appearance of macrophages and cells of young connective tissue in the form of fibrocytes, fibroblasts, and the differences between the groups were statistically significant in general over the entire observation period ($p < 0.001$).

The presence of a significant interaction between the time factor and the group ($p < 0.001$) was also found, in the experimental group by the 9th day the number of lymphocytes was significantly higher - 7.5 ± 0.6%, in contrast to the control group (2.5 ± 0.6%), the number of macrophages was higher - 12.17 ± 0.68% and 2.21 ± 0.19%, respectively. In the experimental group, there was an earlier appearance of young connective tissue cells in the form of fibrocytes, fibroblasts, and their increase by day 9 to 6.44 ± 0.38%, in contrast to the control group - 1.39 ± 0.13%. This indicated active regenerative processes in the wound in the experimental group of patients. A regenerative type characterized the structure of cytograms. The dynamics of the average values of macrophages and fibroblasts in the cytograms of both study groups is shown in Figures 7 and 8.

Thus, analyzing the dynamics of the cytological picture in patients with purulent-necrotic complications of DFS in the study groups, it was noted that traditional treatment revealed a low intensity of cellular reactions in the wound, an elongation of the inflammatory phase, and the inflammatory type of cytograms was noted only by the 9th day after surgery. Also, the control group observed sluggishness of reparative processes in the wound, causing a significant duration of the regeneration phase, and later onset of the scar reorganization phase. This led to a lengthening of the timing healing.

The use of programmable sanitation

technologies allowed to create conditions for better sanitation of the purulent focus, led to a reduction in all phases of the wound process. Surgical treatment of the purulent focus, long-term washing of the wound cavity in the postoperative period, and software for the drainage process made it possible to clear the wound of non-viable tissues, toxins, and proteolytic enzymes in a short time, reducing microbial contamination in the wound. As a result, the stage of rejection of necrotic tissues was extremely reduced. Early closure of the wound with sutures using active drainage under conditions of minimal inflammatory reaction in the wound significantly accelerated the reparative processes, creating conditions for developing and completing the regeneration phase. Already on the 3rd day after the operation in the experimental group, the smears showed the appearance of a large number of mononuclear cells, the rapid maturation of which later led to the appearance of fibroblasts and the predominance of non-cellular elements of connective tissue. The regeneration phase and the rumen reorganization phase were reduced.

## 4. CONCLUSIONS:

Cytological examination of smears in patients with purulent lesions of diabetic foot syndrome using programmed sanitation technologies revealed a higher rate of cellular reactions in the wound. There was a statistically significant faster decrease in degenerative forms of neutrophils, a positive redistribution of rod and segmentonuclear neutrophils in combination with an increase in the regenerative-degenerative index, indicating an acceleration of the relief of the inflammatory process. The appearance of macrophages and young connective tissue cells in the form of fibrocytes, fibroblasts, and fibrous fibers was also reliably observed at an earlier time, which indicated active regenerative processes in the wound.

## 5. REFERENCES:


1. Galstyan, G.R., Vikulova, O.K., Isakov, M.A., Zheleznyakova, A.V., Serkov, A.A., Egorova D.N. (2018). Epidemiology of diabetic foot syndrome and lower limb amputations in the Russian Federation according to the Federal register of diabetes patients (2013–2016). Diabetes mellitus, 21(3), 170–177. doi: 10.14341/DM9688
2. Dedov, I.I., Shestakova, M.V., Vikulova, O.K. (2017). Epidemiology of diabetes mellitus in the Russian Federation: clinical and statistical analysis according to the Federal register of Diabetes Mellitus. Diabetes mellitus, 20(1), 13–41. doi: 10.14341/DM8664
3. Mitish, V.A., Paskhalova, Y.S., Eroshkin, I.A., Galstyan, G.R., Doronina, L.P. (2014). Purulent necrotic lesions in the neuroischemic form of diabetic foot syndrome. Surgery. Magazine them. N.I. Pirogov, 1, 48–53. doi: 10.18499/2070-478X-2017-10-2-165-172
4. Bakker, K., Apelqvist, J., Lipsky, B.A., Van Netten, J.J. (2016). International Working Group on the Diabetic Foot. The 2015 IWGDF guidance documents on prevention and management of foot problems in diabetes: development of an evidence-based global consensus. *Diabetes Metab. Res. Rev*., 32, 2–6. doi: 10.1002/dmrr.2694
5. Stupin, V.A., Silina, E.V., Koreyba, K.A., Goryunov, S.V. (2019). Diabetic foot syndrome (epidemiology, pathophysiology, diagnosis and treatment). Moscow: Litterra. doi: 10.1088 / 1755-1315 / 125/1/012161
6. Centers for Disease Control and Prevention (2014) National Diabetes Statistics Report: Estimates of Diabetes and Its Burden in the United States, 2014. US Department of Health and Human Services, Atlanta. doi: 10.2337 / dc14-2973. [PubMed: 25908153].
7. Guariguata, L., Whiting, D., Weil, C., Unwin, N. (2011). The International Diabetes Federation diabetes atlas methodology for estimating global and national prevalence of diabetes in adults. Diabetes Res Clin Pract, 94(3):322–32. doi: 10.1016/j.diabres.2011.10.040. [PubMed: 22079683].
8. Bordianu, A., Bobircă, F., Patrascu, T. (2018). Grafting in the Treatment of Diabetic Foot Soft Tissue Defects. Surgery (Happy), 113(5), 644–650. doi: 10.21614 / chirurgia.113.5.644. [PubMed: 30383991].
9. Ray, J.A., Valentine, W.J., Secnik, K., Oglesby, A.K., Cordony, A., Gordois, A. (2005). Review of the cost of diabetes complications in Australia, Canada, France, Germany, Italy and Spain. Curr Med Res Opin, 21(10), 1617–29. doi:

10.1185 / 030079905X65349. [PubMed: 16238902].

10. Armstrong, D.G., Boulton, A.J.M., Bus, S.A. (2017). Diabetic foot ulcers and their recurrence. N Engl J Med, 376(24), 2367–75. doi: 10.1056/NEJMra1615439
11. Jang, M.Y., Hong, J.P., Bordianu, A., Suhet, H.S. (2015). Using a contradictory approach to treat a wound induced by hematoma in a patient with antiphospholipid antibody syndrome using negative pressure wound therapy. Low Extrem. Wounds, 14(3), 303–306. doi: 10.1177 / 1534734615598421. [PubMed: 26248826].
12. Nickerson, D.S. (2018). Improving outcomes in recurrent and other new foot ulcers after healed plantar forefoot diabetic ulcer. Wound Repair and Regeneration, 26(1), 108–109. doi: 10.1111 / wrr.12611
13. Ivanov, D.P., Serebryakova, O.V., Ivanov, P.A. (2018). Diabetic foot syndrome: classification and diagnosis of ischemic form, current state of the issue. Trans-Baikal Medical Bulletin, 4, 111–122. doi: 10.1055 / s-0034-1366455. [PubMed: 25014093].
14. Yusupova, S., Nabiev, M.K., Saykhunov, K.D. (2017). Comparative analysis of the results of a comprehensive operative-medical treatment of patients with complicated forms of diabetic foot syndrome. Bulletin of Avicenna, 19(2), 203–208. doi: 10.1016 / S0140-6736 (20) 30566-3. [PubMed: 32171076].
15. Armstrong, D.G., Boulton, A.J.M., Bus S.A. (2017). Diabetic foot ulcers and their recurrence. N Engl J Med, 376(24), 2367–75. doi: 10.1056/NEJMra1615439. doi: 10.5124 / jkma.2015.58.9.795
16. Braun, L.R., Fisk, W.A., Lev-Tov, H., Kirsner, R.S., Isseroff, R.R. (2014). Diabetic foot ulcer: an evidence-based treatment update. Am J Clin Dermatol, 15(3), 267–81. doi: 10.1007/s40257-014-0081-9.
17. Zaytseva, E.L., Doronina, L.P., Molchkov, R.V., Voronkova, I.A., Mitish, V.A., Tokmakova, A.Y. (2014). Effect of negative pressure therapy on repair of soft tissues of the lower extremities in patients with neuropathic and neuroischaemic forms of diabetic foot syndrome. Diabetes, 3, 113–121. doi: 10.14341/DM20143113-121
18. Baltzis, D., Eleftheriadou, I., Veves, A. (2014). Pathogenesis and Treatment of Impaired Wound Healing in Diabetes Mellitus: New Insights. Adv. Ther, 31, 817–836. doi: 10.1007 / s12325-014-0140-x. [PubMed: 25069580].
19. Liu, Y., Min, D., Bolton, T., Nubé, V., Twigg, S.M., Yue, D.K., McLennan, S.V. (2009). Increased matrix metalloproteinase–9 predicts poor wound healing in diabetic foot ulcers. Diabetes Care, 32(1), 117–119. doi: 10.2337 / dc08-0763. [PubMed: 18835949].
20. Li, Z., Guo, S., Yao, F., Zhang, Y., Li, T. (2013). Increased ratio of serum matrix metalloproteinase–9 against TIMP–1 predicts poor wound healing in diabetic foot ulcers. J Diabetes Complications, 27, 380–382. doi: 10.1016 / j.jdiacomp.2012.12.007. [PubMed: 23357650].
21. Dinh, T., Tecilazich, F., Kafanas, A., Doupis, J., Gnardellis, C., Leal, E. (2012). Mechanisms Involved in the Development and Healing of Diabetic Foot Ulceration. Diabetes, 61, 2937–2947. doi.org/10.2337/db12-0227. [PubMed: 22688339].
22. Brancato, S., Albina, J. (2011). Wound macrophages as key regulators of repair origin, phenotype, and function. Am J Pathol, 178, 19–27. doi: 10.1016 / j.ajpath.2010.08.003. [PubMed: 21224038].
23. Mingyuan, M., Yiwen, N., Ting, X., Bo, Y., Chun, Q., Shuliang, L. (2012). Diabetes-impaired wound healing and altered macrophage activation: A possible pathophysiologic correlation. Wound Rep. Reg, 20, 203–213. doi: 10.1111/j.1524-475X.2012.00772.x. [PubMed: 22380690].
24. Bjarnsholt, T, Cooper, R, Fletcher, J. (2016). Management of biofilms. World Union of Wound Healing Societies. doi: 10.12968/jowc.2014.23.11.570 [PubMed: 25375405].
25. Eskes, A.M., Gerbens, L.A., van der Horst, C.M., Vermeulen, H., Ubbink, D.T. (2011). Is the red-^ellow-black scheme suitable to classify site wounds? An inter-observer

analysis. Burns, 37(5), 822-826. doi: 10.1016/j.burns.2010.12.019. [PubMed: 21345594].

26. Zemskov, M.A., Chorochilov, A.A., Iljina, E.M., Domnich, O.A. (2011). Peculiarities of changes of immune status in chronic inflammatory diseases. Journal of experimental. and clinical surgery, 4(3), 468-72. doi: 10.18499/2070-478X-2011-4-3-468-472
27. Lacci, K., Dardik, A. (2010). Platelet-rich plasma: support for its use in wound healing. Yale J Biol Med, 83(1), 1-9. [PubMed: 20351977].
28. Han, T, Wang, H, Zang, Y.Q. (2012). Combining platelet-rich plasma and extracellular matrix-derived peptides promote impaired cutaneus wound healing in vivo. *J Craniofac Surg*, 23(2), 439-47. doi: 10.1371 / journal.pone.0032146. [PubMed: 22384158].
29. Larichev, A.B., Shishlo, V.K., Lisovsky, A.V., Chistyakov, A.L., Vasiliev, A.A.(2011). Wound infection prevention and morphological aspects of aseptic wound healing. *J of Exp and Clin Surg*, 4(4), 728-33. doi.org/10.18499/2070-478X-2011-4-4-728-733.
30. Kuzin, M.I., Kostyuchenok, B.M. (1990). Wounds and wound infections: A guide for physicians. Moscow: Medicine, 592. Available at: http://med-books.by/hirurgiya/2948-rany-i-ranevaya-infekciya-kuzin-mikostyuchenok-bm-1990-god-592-s.html.
31. Ivanusa, S.Y., Risman, B.V., Ivanov, G.G. (2016). Modern ideas about methods of assessment the course of the wound process in patients with purulo-necrotic complications of the diabetic foot syndrome. *Herald of the Russian Military Medical Academy*, 54(2), 190–194. Internet address: http://elibrary.ru/item.asp?id=26280216
32. Kamaev, M.F. (1954). Types of cytograms in a superficial biopsy of the wound. *Collection of works of the Odessa medical Institute named after N. I. Pirogov*. Kiev, 267-276.
33. Davydov, I.A., Larichev, A.B., Abramov, A.I. (1990). Substantiation of Using Forced Early Secondary Suture in the Treatment of Suppurative Wounds by the Method of Vacuum Therapy. Vestn Khir Im I I Grek, 44(3):126-8. [PubMed: 2169094].

***Table 1.*** *Comparative characteristics of the clinical parameters of the studied groups. Source: the author*

| **Parameter** | | **Experimental group (*n*=55)** | **Control group (*n*=51)** | **p-value of significance of differences between groups** |
|---|---|---|---|---|
| Average age *Me* (M±σ)*** | | 56(59±8) | 59(60±9) | 0,26* |
| Gender | male (*n*, %) | 25 (45,5%) | 23 (45,1%) | 1,00** |
| | female (*n*, %) | 30 (54,5%) | 28 (54,9%) | |
| Diabetes mellitus type | Type 1 | 5 (9,1%) | 4 (7,8%) | 1,00** |
| | Type 2 | 50 (90,9%) | 47 (92,2%) | |
| DFS form | neuropathic | 32 (58,2%) | 31 (60,8%) | 0,66** |
| | neuroischemic | 23 (41,8%) | 20 (39,2%) | |
| TcPO2 (*Me* [Q1;Q3])*** mm Hg | neuropathic | 32,8 [32,3; 34,8] | 33,2 [32,2; 34,8] | 0,462* |
| | neuroischemic | 28,8 [27,8; 29,4] | 28,6 [27,8; 29,4] | 0,536* |

Notes: * t-test for independent samples; ** Fisher's exact test *** *Me*-median, M±σ - mean and standard deviation, Q1-lower quartile, Q3-upper quartile

***Table 2.*** *Distribution of patients in the study groups depending on the nosological form of purulent-necrotic complications of DFS and the extent of the lesion in accordance with the classification of F.W. Wagner (1979). Source: the author*

| **Nosological form of purulent-necrotic process on the foot** | **The volume of the lesion under the classification of F.W. Wagner (1979)** | **Experimental group (*n*=55)** | | **Control group (*n*=51)** | | **Total** |
|---|---|---|---|---|---|---|
| | | ***n*** | **%** | ***n*** | **%** | |
| Deep ulcer | 2 | 5 | 9,1 | 4 | 7,8 | 9 |
| Deep ulcer + Chronic osteomyelitis of the finger | 3 | 3 | 5,5 | 3 | 5,9 | 6 |
| Phlegmon of the toe + phlegmon of the foot | 2 | 5 | 9,1 | 6 | 11,8 | 11 |
| Osteomyelitis of the toe + phlegmon of the foot | 3 | 8 | 14,5 | 9 | 17,6 | 17 |
| Purulent wound after amputation of toes or resection of the foot, previously performed in other medical institutions | 3 | 14 | 25,5 | 13 | 25,5 | 27 |
| Dry gangrene of one or more fingers | 4 | 12 | 21,8 | 9 | 17,6 | 21 |
| Wet gangrene of the toe + phlegmon of the foot | 4 | 8 | 14,5 | 7 | 13,7 | 15 |
| Total: | | 55 | 100 | 51 | 100 | 106 |

***Table 3.*** *Primary operations in patients of the study groups*

| Primary operations | Experimental group (*n*=55) | | Control group (*n*=51) | | Total |
|---|---|---|---|---|---|
| | ***n*** | **%** | ***n*** | **%** | |
| Surgical treatment | 9 | 16,4 | 9 | 17,6 | 18 |
| Opening phlegmon | 13 | 23,6 | 18 | 35,3 | 31 |
| Finger amputation | 9 | 16,4 | 6 | 11,8 | 15 |
| Amputation of the distal foot | 12 | 21,8 | 8 | 15,7 | 20 |
| Transmetatarsal amputation of the foot | 12 | 21,8 | 10 | 19,6 | 22 |
| Total: | 55 | 100 | 51 | 100 | 106 |

***Table 4.*** *Cell composition of cytological smears in patients with purulent complications of DFS in the study groups at the time of randomization, in% per 100 cells*

| Cell types | Experimental group | | Control group | | p-value of t-test | p-value of the Mann-Whitney test |
|---|---|---|---|---|---|---|
| | M±σ*, in% per 100 cells | Me[Q1;Q3]* | M±σ*, in% per 100 cells | Me[Q1;Q3]* | | |
| STAB | 1,8±0,2 | 1.8 [1.7;1.9] | 1,8±0,2 | 1,7 [1,6;1,8] | 0,706 | 528,500 |
| SEGS | 14,2±0,4 | 14,2 [14,0;14,4] | 16,2±0,4 | 16,2 [16,0;16,2] | 0,647 | 502,500 |
| DN | 82,6±3,2 | 64,5 [64,5;72,4] | 84,2±6,2 | 68,2 [68,2;72,4] | 0,005 | 317,500 |
| RDI | 0,2±0,1 | 0,2 [0,1;0,2] | 0,2±0,1 | 0,2 [0,1;0,2] | 0,976 | 558,000 |
| L | 0,4±0,2 | 0,4 [0,3;0,5] | 0,2±0,1 | 0,2 [0,1;0,2] | 0,000 | 69,000 |

Notes: stab - stab neutrophils, segs - segmented neutrophils, DN - degenerative neutrophils, RDI - regenerative-degenerative index, L – lymphocytes**Me*-median, M±σ - mean and standard deviation, Q1-lower quartile, Q3-upper quartile

***Table 5.*** *Cell composition of cytological smears in patients with purulent complications of DFS in the study groups (M ± σ), % per 100 cells*

| Cell types | Experimental group | | Control group | |
|---|---|---|---|---|
| | 5 days after surgery | 9 days after surgery | 5 days after surgery | 9 days after surgery |
| DN | 37,34±2,33 | 12,28±0,29 | 72,5±1,37 | 36,42±0,36 |
| STAB | 5,55±0,39 | 3,63±0,18 | 6,2±0,24 | 8,09±0,84 |
| SEGS | 38,69±1,33 | 28,21±0,94 | 28,96±2,25 | 24,31±0,88 |
| RDI | 1,19±0,09 | 2,61±0,09 | 0,49±0,04 | 0,90±0,03 |
| L | 4,79±0,24 | 6,81±0,48 | 0,77±0,23 | 1,84±0,43 |
| M | 3,59±0,25 | 12,17±0,68 | 0,17±0,06 | 2,21±0,19 |
| F | 3,21±0,31 | 6,44±0,38 | 0,12±0,02 | 1,39±0,13 |

Notes: DN - degenerative neutrophils, STAB - stab neutrophils, SEGS- segmented neutrophils, RDI - regenerative-degenerative index, L - lymphocytes, M - macrophages, F - fibroblasts

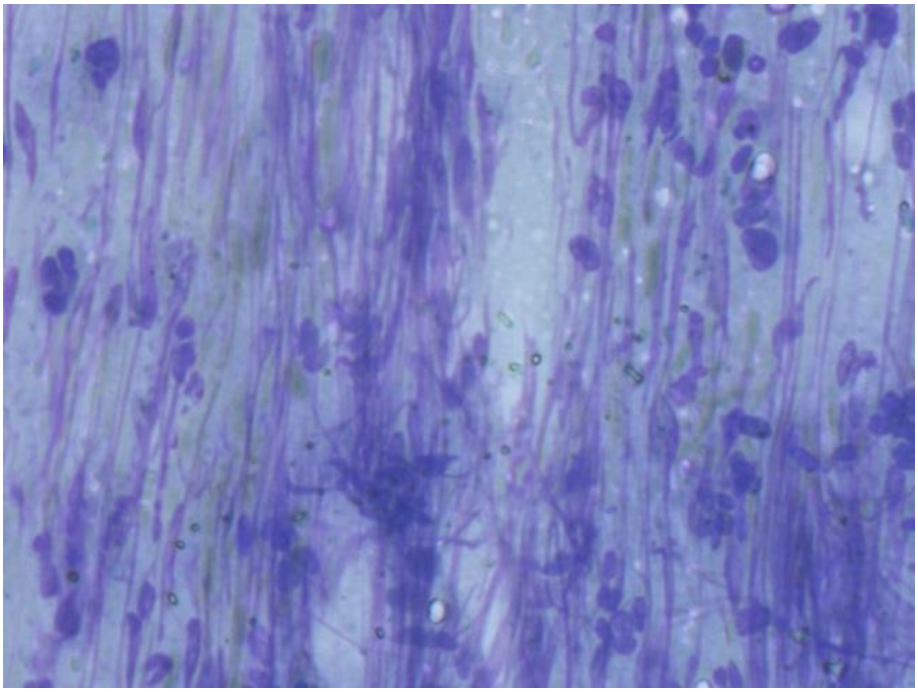

***Figure 1.*** *Fragment of a cytogram of a smear from the wound surface on the 5th day, the in the experimental group. Among neutrophils and polyblasts, fibrocytes, fibroblasts, fibrous fibers were found. Romanovsky-Giemsa staining. Magnification × 63*

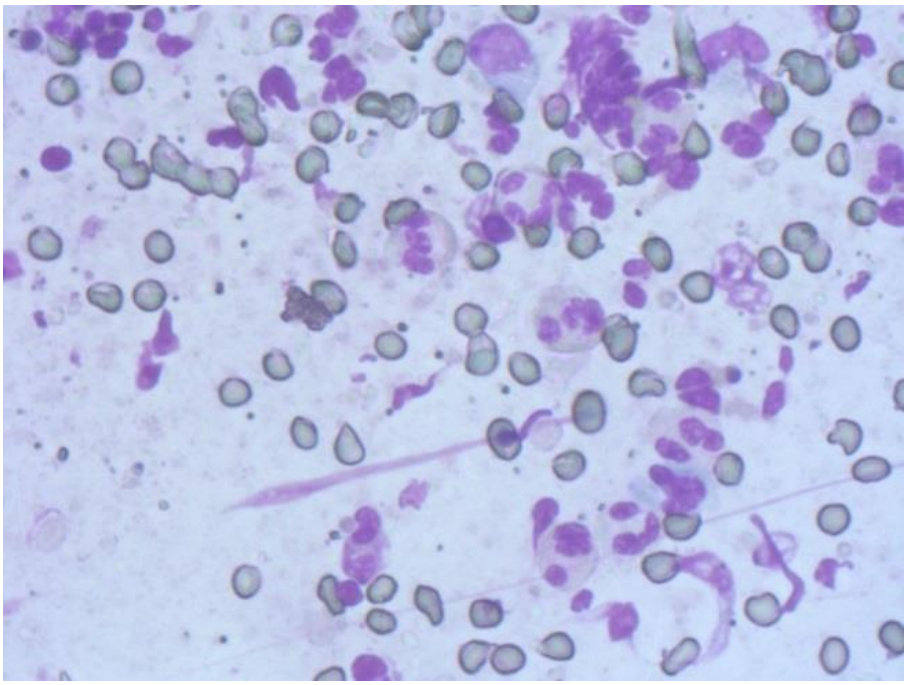

***Figure 2.*** *Fragment of the cytogram of a smear from the wound surface on the 5th day, the control group. There are single actively phagocytic leukocytes, macrophages, lymphocytes. Elements of granulation tissue are rare. Romanovsky-Giemsa staining. Magnification × 63*

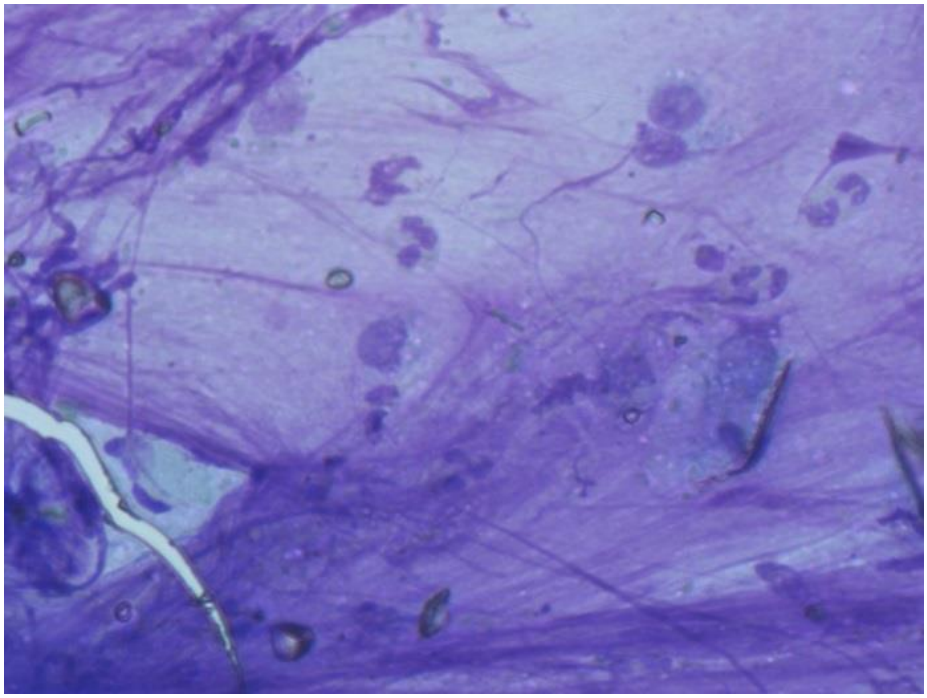

***Figure 3.*** *A cytogram fragment for a smear from the wound surface, Day 9, Intervention group. New elements of connective tissue, fibroblasts, polyblasts, macrophages are located among the fibrous structures of the intercellular substance. The epithelium is presented in the form of layers of cells. Romanovsky-Giemsa staining. × 63 lens*

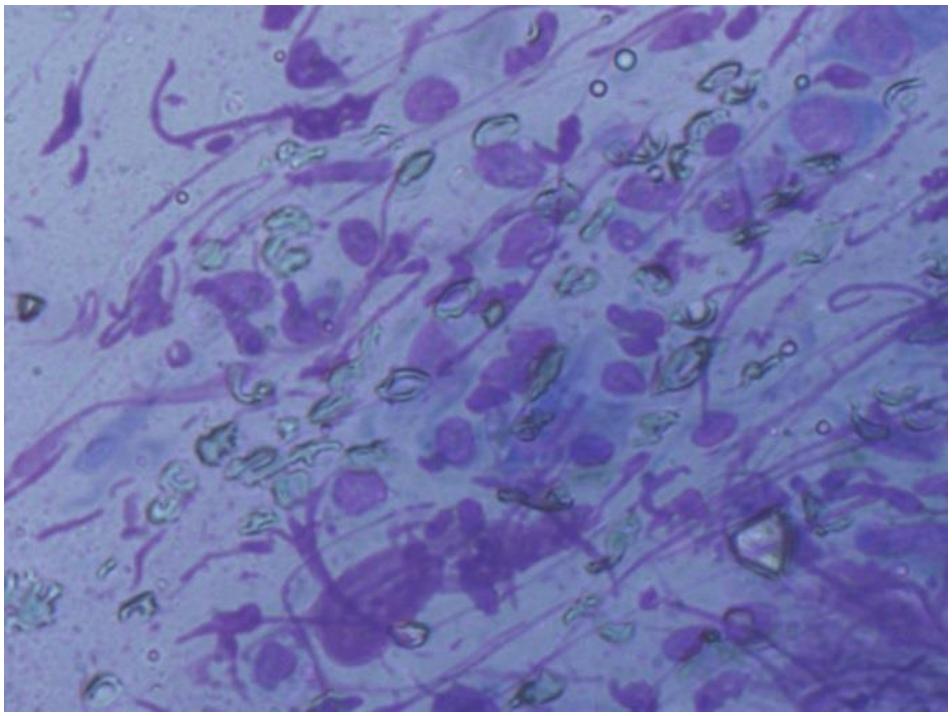

***Figure 4.*** *Fragment of the cytogram of a smear from the wound surface on the 9th day, the control group. The number of mononuclear cells has decreased, the number of polyblasts, fibroblasts, and macrophages has increased. Delicate fibrous structures of the intermediate were observed. Romanovsky-Giemsa staining. Magnification × 63*

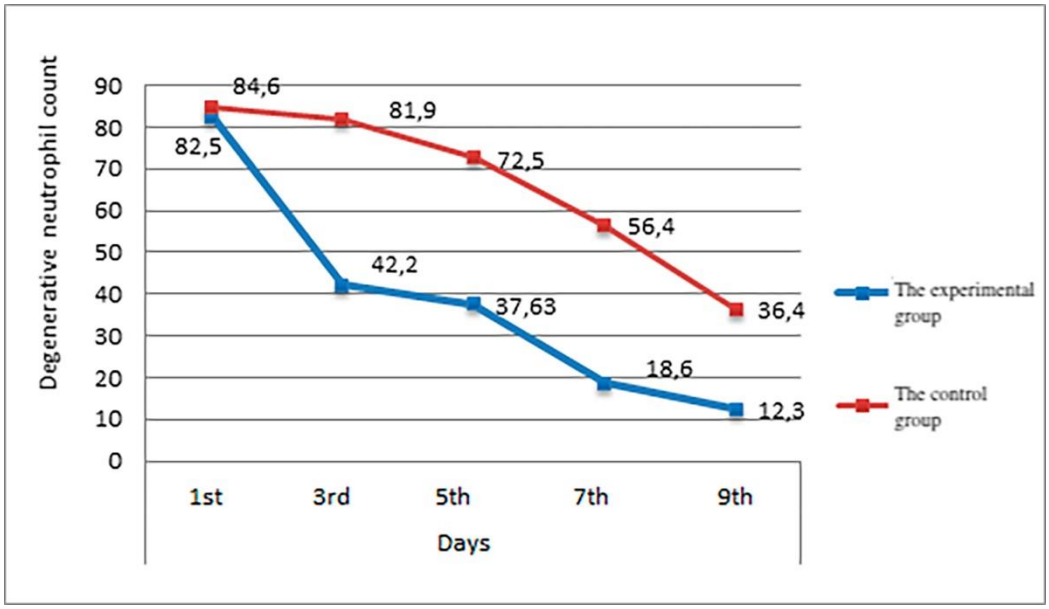


***Figure 5.*** *Dynamics of mean values of degenerative neutrophils in cytograms of both study groups. Source: the author*

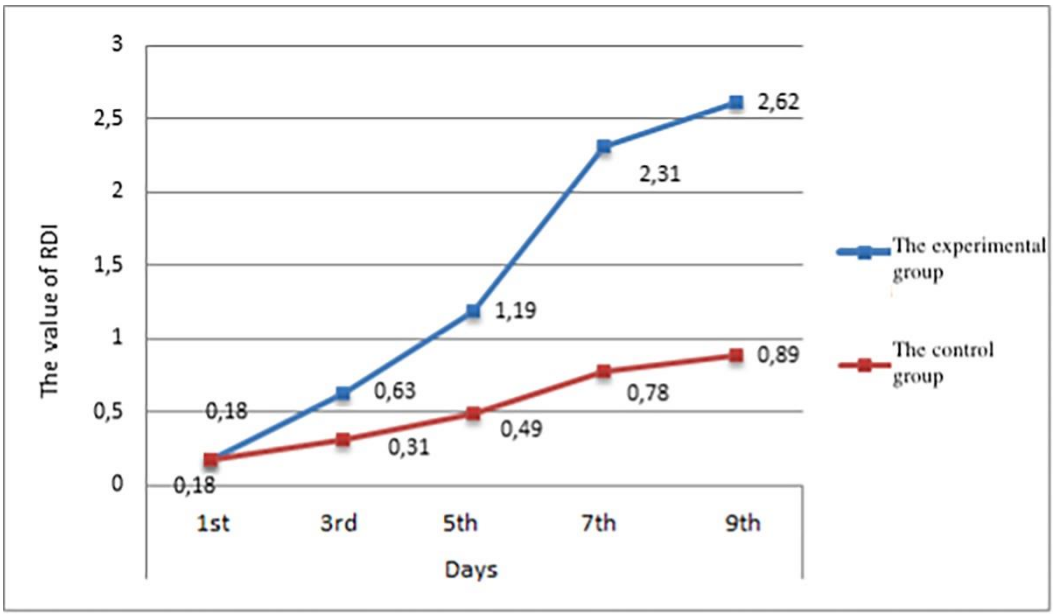


***Figure 6.*** *Dynamics of average RDI values in cytograms of both study groups. Source: the author*

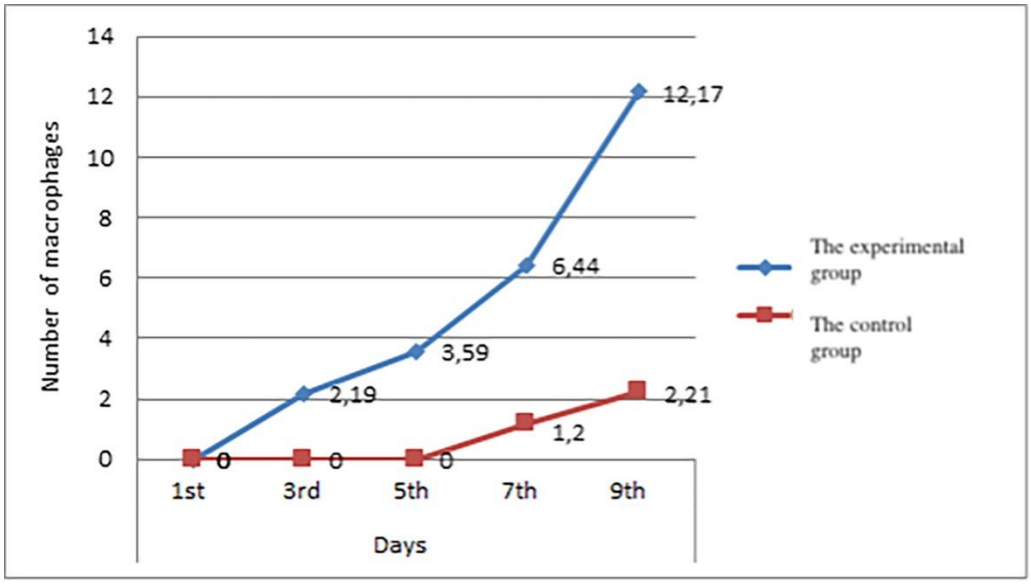


***Figure 7.*** *Dynamics of mean values of macrophages in cytograms of both study groups. Source: the author*

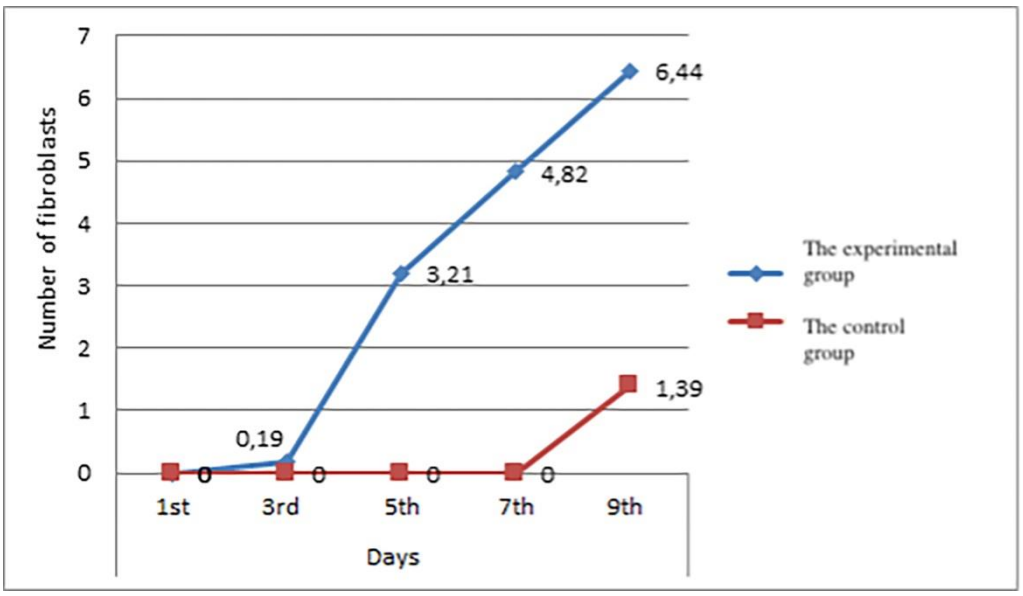


***Figure 8.*** *Dynamics of average fibroblast values in cytograms of both study groups. Source: the author*

PERIÓDICO TCHÊ QUÍMICA
ARTIGO ORIGINAL

# ESTUDO DE ROCHAS DE TUFO VULCÂNICO E DESENVOLVIMENTO DE CONCRETO ESTRUTURAL LEVE USANDO O TUFO COMO BASE

# STUDY OF OVERBURDEN TUFF ROCKS AND DEVELOPMENT ON ITS BASIS OF LIGHTWEIGHT STRUCTURAL CONCRETE

# ИСЛЛЕДОВАНИЕ ВСКРЫШНОЙ ТУФОВОЙ ПОРОДЫ И РАЗРАБОТКА НА ЕЕ ОСНОВЕ ЛЕГКОГО КОНСТРУКЦИОННОГО БЕТОНА

ZHUMADILOVA, Zhanar O.[1]; ZHUGINISSOV, Maratbek T.[1]; KHAMZA, Yerlan Y.[1]

[1] Satbayev University, Institute of Architecture and Civil Engineering, Department of Construction and Building Materials, 22 Satpayev Str., zip code 050013, Almaty – Republic of Kazakhstan

** Corresponding author*
*e-mail: zhanar_85@mail.ru*

Received 12 December 2020; received in revised form 10 February 2021; accepted 02 March 2021

## RESUMO

**Introdução**. O trabalho apresenta os resultados da pesquisa no desenvolvimento de tecnologia para concreto estrutural leve a partir de rochas tufas recobertas. Para desenvolver a tecnologia de concreto estrutural leve, é usada rocha de tufo de cobertura (região de Almaty, na República do Cazaquistão), que é formada durante a extração de tufo vulcânico para a fabricação de telhas de revestimento. **Objetivos**: Estudar as propriedades físicas, mecânicas e químicas básicas do tufo, desenvolvimento de composições estruturais de concreto leve. **Métodos**. A rocha de tufo sobrecarregada foi esmagada em um britador de mandíbula e peneirada por meio de um conjunto de telas padrão. Como resultado, foram obtidos agregados do tufo das frações: 0,16-5 mm, 5-10 mm e 10-20 mm. A composição do concreto tufado foi selecionada por cálculo de acordo com o procedimento padrão. Após o cálculo da composição do concreto tufo, todas as matérias-primas: cimento, agregados, aditivos e água são dosadas e misturadas. A mistura de concreto foi colocada em um molde e compactada por vibrocompressão em uma mesa vibratória. O endurecimento de amostras de concreto é realizado em condições úmidas por 7, 14 e 28 dias, e vaporização em uma câmara de vaporização por 12-16 horas. **Resultados e discussões**. Após o endurecimento, foram determinadas as propriedades: resistência à compressão, densidade média e coeficiente de transferência de calor das amostras de concreto de acordo com métodos padrão. O grau de concreto de tufo está na faixa de 15,0-20,0 MPa. A densidade média do concreto tufado é 1822-1910 kg/m$^3$. O coeficiente de condutividade térmica (λ) está na faixa de 0,66-0,75 W/m·K. Foi estabelecida a possibilidade de fabricar ladrilhos de acabamento a partir de concreto tufo por meio de lixamento e polimento de sua superfície. A partir de areia tufada, com granulometria de 3-5 mm, foram realizadas por prensagem vibratória pedras de concreto com dimensões de 390x190x188 mm com 2 vazios tecnológicos. O vazio da pedra é de 51% do seu volume total, o grau de resistência à compressão é 2,5-3,5 MPa. **Conclusões**. Como resultados da pesquisa, foram estudadas as principais propriedades físicas, mecânicas e químicas das rochas tufas recobertas como enchimento de concreto estrutural leve. As possibilidades de fabricação de blocos de parede e lajes de revestimento foram estabelecidas.

**Palavras-chave**: *construção, agregados energeticamente eficientes, shungite, condutividade térmica, porosidade.*

## ABSTRACT

**Introduction.** The work presents the research results on the development of technology for lightweight structural concrete based on overburden tuff rocks. To develop the technology of lightweight structural concrete, overburden tuff rock (Almaty region of the Republic of Kazakhstan) is used, which is formed during the extraction of volcanic tuff for the manufacture of facing tiles. **Aim.** Study of the basic physical, mechanical and chemical properties of tuff, development of lightweight structural concrete compositions. **Methods**. The overburden tuff rock is crushed in a jaw crusher and screened through a set of standard screens. As a result, aggregates from tuff of fractions were obtained: 0.16-5 mm, 5-10 mm, and 10-20 mm. The composition of tuff concrete was selected by calculation according to the standard procedure. After calculating the composition of tuff concrete, all raw materials: cement, aggregates, additives, and water are dosed and mixed. The concrete

mixture is placed in a mold and compacted by vibro-compression on a vibrating table. Hardening of concrete samples is carried out in humid conditions for 7, 14, and 28 days and steaming in a steaming chamber for 12-16 hours. **Results and Discussion.** After hardening, the properties were determined: compressive strength, average density, and heat transfer coefficient of concrete samples according to standard methods. The tuff concrete grade is in the range of 15.0-20.0 MPa. The average density of tuff concrete is 1822-1910 kg/m$^3$. The thermal conductivity coefficient (λ) is in the range of 0.66-0.75 W/m·K. The possibility of manufacturing finishing tiles from tuff concrete by grinding and polishing its surface has been established. Based on tuff sand, with a grain size of 3-5 mm, concrete stones with dimensions of 390x190x188 mm with 2 technological voids were made by vibration pressing. The hollowness of the stone is 51% of its total volume, and the compressive strength grade is 2.5-3.5 MPa. **Conclusions.** As a research result, the main physical, mechanical and chemical properties of overburden tuff rocks as a filler for lightweight structural concrete were studied. The possibilities of manufacturing wall blocks and facing slabs have been established.

**Keywords:** *construction, energy-efficient aggregates, shungite, thermal conductivity, porosity.*

## АБСТРАКТ

**Введение.** В статье приведены результаты исследований по разработке технологии легкого конструкционного бетона на основе вскрышных туфовых пород. Для разработки технологии легкого конструкционного бетона используется вскрышная туфовая порода (Алматинская область РК), которая образуются при добыче вулканического туфа для изготовления облицовочной плитки. **Цель.** Изучение основных физико-механических и химических качеств туфа, разработка составов легкого конструкционного бетона. **Методы.** Вскрышная туфовая порода подвергается дроблению в щековой дробилке и просеиванию через набор стандартных сит. В результате получены заполнители из туфа фракций: 0,16-5 мм, 5-10 мм и 10-20 мм. Состав туфобетона подбирался расчетным путем согласно стандартной методике. После расчета состава туфобетона все сырьевые компоненты: цемент, заполнители, добавки и вода дозируются и смешиваются. Бетонная смесь укладывается в форму и уплотняется вибропрессованием на вибростоле. Твердение бетонных образцов осуществляется во влажностных условиях в течении 7, 14 и 28 суток, а также пропариванием в пропарочной камере в течении 12-16 часов. **Результаты и обсуждение.** После твердения были определены свойства: прочность при сжатии, средняя плотность и коэффициент теплороводности бетонных образцов по стандартным методикам. Марка туфобетона находится в пределах 15,0-20,0 МПа. Средняя плотность туфобетона составляет 1822–1910 кг/м$^3$. Коэффициент теплопроводности (λ) находится в пределах 0,66-0,75 Вт/м·К. Установлена возможность изготовления отделочной плитки из туфобетона, путем шлифования и полирования ее поверхности. На основе туфового песка, с размерами зерен 3-5 мм, методом вибропрессования были изготовлены бетонные камни с размерами 390 х190х188 мм с 2-мя технологическими пустотами. Пустотность камня составляет 51% от общего его объема, марка по прочности на сжатие 2,5-3,5 МПа. **Заключение.** В результате исследований изучены основные физико-механические и химические качества вскрышных туфовых пород в качестве заполнителя для легкого конструкционного бетона. Установлены возможности изготовления стеновых блоков и облицовочных плит.

**Ключевые слова:** *строительство, энергоэффективные заполнители, шунгит, теплопроводность, пористость.*

## 1. INTRODUCTION:

The construction of energy-efficient, energy-saving houses involves using new design solutions, technologies, and thermal protection materials. The basis of construction is precast concrete, and in recent years it has undergone qualitative changes in the direction of weight reduction, thermal conductivity, and sound insulation. This is realized by introducing lightweight concrete based on porous natural and artificial aggregates. Modified structural lightweight concretes are produced in the same way as heavy concretes of similar structures, but the weight saving is 20-50%. Also, the heat transfers of buildings decrease, their level of thermal protection and vapor permeability increases, which leads to an increase in the comfort of living. One effective, lightweight aggregates for lightweight concrete is natural porous aggregates - volcanic tuffs, pumice, and others. In volcanic tuffs, porosity is in the range of 21.3-46.6%, their density ranges from 1400 to 1800 kg/m$^3$.

Moreover, the strength of volcanic tuffs is not inferior to, for example, marble. The bulk density of tuff sand is on average 1000 kg/m$^3$,

crushed stone with a fraction of 5-10 mm - 970 kg/m$^3$, and crushed stone with a fraction of 10-20 - 950 kg/m$^3$. These indicators are much lower than that of construction sand and crushed stone based on granite, limestone, and other dense rocks. Therefore, based on tuff, it is possible to obtain lightweight structural concrete suitable for the manufacture of enclosing structures and piece wall products for the construction of energy-efficient housing.

To expand the raw material base and improve technical indicators, research is being carried out on the use of natural lightweight aggregates, particularly tuffs, to produce lightweight concrete based on them.

The authors (Silber A., 1994; Rube´nLo´pez-Doncel, 2012; Reference book on geology, 2017; Wedekind W., 2011; Stueck H., 2006; Siegesmund S., 2011; Trunov P. V., 2014) investigated the chemical and mineralogical compositions, as well as the structure of various tuffs.

According to (Silber A., 1994), volcanic tuff contains more than 90% volcanic material, from 50 to 90% is tuff-containing. If volcanic material content is less than half, the name is given for the predominant material of a different origin. Volcanic tuffs, depending on their composition, are liparite, trachytic, basaltic, and andesite. The chemical composition of tuffs varies widely: $SiO_2$ 49-72%, $Al_2O_3$ 10-24%, $Fe_2O_3$ 2-6%, MgO 1-2,5% and others.

According to researchers from the Krakow Polytechnic Institute named after Tadeusz Kosciuszko (Silber A., 1994, tuff has a density of 0.8–1.5 g/cm$^3$ and a total porosity of 60–80%, depending on its origin and the screening (grinding) process. Tuff has a buffering capacity and can adsorb or release substances, especially during growth. They developed an artificial volcanic tuff stone that is solidified ash. They mixed tuff with other components - alkaline solutions and water glass. The resulting material (geopolymer) turned out to be as hard as granite.

Unlike other geopolymers, the new material can withstand high temperatures. When the temperature rises to 800-900 °C, it becomes even more robust and more reliable. These unique characteristics will make inorganic geopolymer an ideal building material; it will entirely replace expanded polystyrene in the usual thermal insulation of houses. Due to its unusual porous structure, the geopolymer breathes perfectly: it absorbs water, regulates the level of humidity in the room, and can even absorb unpleasant odors.

According to (Rube´nLo´pez-Doncel, 2012), tuff is a grayish-red to red volcanic rock with a characteristic porphyry tissue. Loseros (Mexico) tuff is a volcaniclastic rock with a rhyolite composition, consisting of very well-graded sand-sized crystals of fine to medium size and clastic rocks, enclosed in the ash-rich durable altered groundmass. Loseros (Mexico) tuff can have different color shades such as greenish, reddish, purple, and grayish, but the greenish variety is characteristic and most commonly used in construction (Rube´nLo´pez-Doncel, 2012).

In (Novi Asniar, 2019), it is shown that tuff has such geotechnical properties as 18-25 kN/m$^3$ specific gravity, 1.5-2.4 g/cm$^3$ bulk density, 2.29-2.64 g/cm$^3$ density particles, the compressive strength varies greatly depending on the degree of weathering, 0 - 1.45 MPa adhesion, friction angle = 24 ° - 45 ° and 4% - 42% porosity. The properties of tuff soil depend on the environment at the location of the deposit and the particle size.

The authors of (Wedekind W., 2011) studied the Habichtswald tuff and found that it contains a wide range of fragment grain sizes from a few millimeters to 5 cm. Its characteristic dark grayish, glassy or microcrystalline groundmass contains large amounts of montmorillonite. This tuff has a hypocrystalline structure with idiomorphic olivine-pyroxene crystals, and plagioclase, amphibole, and biotite can also be distinguished. Fragments of pre-existing basic rocks are also present in the form of glassy fragments.

In the study (Stueck H., 2006), most of the tuff structure grains are quartz, plagioclase, and fragments of volcanic rocks. Crystals are in the form of plagioclase from angular to subidiomorphic, angular quartz, and strongly altered biotite flakes. In thin sections, microlamination (plates) can be recognized due to variations in the frequency of fragments the size of sand. The difference is related to grain size and lime content. Inside the matrix can be found from 5% to over 20% calcite. The Eger-Damien tuff is grayish to light brown rock with fragments of various sizes. Fragments ranging in size from 1 to 30 mm are mainly elongated flattened fragments of pumice, in addition to which large plagioclase phenocrysts can be distinguished. Microcrystalline porphyry tissue with eutaxite or vitreous texture with flattened well-welded vitroclast can also be observed. The main constituents are idiomorphic to

subiomorphic plagioclase crystals, which exhibit a very impressive zonal structure, together with plagioclase, subidiomorphic quartz, corroded hornblende, and altered biotite. Smectite occurs in relatively large quantities, about 10% by weight.

According to Siegesmund S. (2011), the studied tuff rocks have a low (up to 50%) or many micropores. According to Klopfer, microporosity is defined as pores from 0 to 0.01 mcm, capillary-active pores are from 0.01 to 10 mcm. For microprobes with pore diameters <0.1 mcm, water will condense below 99% relative humidity. Capillary absorption occurs in pores from 1 mcm to 1 mm. The microporosity of the studied rocks ranges from 13 to 97%.

According to Trunov P. V. (2014), the quality factor of volcanic tuff as a binder component compared to other sands of technogenic origin shows the quality factor K equal to 0.96. The microporosity of the studied rocks ranges from 13 to 97%. Volcanic tuff is characterized by a polydisperse distribution of particles with varying sizes from about 1 to 350 mcm (Trunov P.V., 2014).

The authors (Movsisyan M.S., 1993) proposed composition for obtaining a firing material, including 60-77% natural tuff, 20-30% glass powder, and 3-10% alkaline silicate solution. The mixture is stirred until a homogeneous mass is obtained, then it is poured into a metal mold, covered with a lid, and fired in a muffle furnace at a temperature of 800-890 °C for 10-15 minutes. After cooling, the product is removed and shaped, resulting in a lightweight, porous and durable material. The average density of the product is 700-900 kg/m$^3$, and the compressive strength is 50-100 kg/cm$^2$. The resulting material can produce facing and partition plates, blocks for industrial, civil, individual buildings, and housing construction.

To Gonchikov Z. M. (1998), the natural tuff of the Kamensk deposit of the Kabardino-Balkarian Autonomous Soviet Socialist Republic (KBASSR) was used to obtain a mixed binder as a pozzolanic additive together with SP S-3 (superplasticizer, grade S-3). Finely ground tuff is added in an amount of 40-60% to portland cement PC-D20 and PC-D0 (PC - portland cement). The tuff addition made it possible to reduce the thermal conductivity of dry cement stone from 0.537 to 0.4 W/m·°C. The optimal addition to PC-D0 cement is 40% tuff and 1% S-3 by weight of cement, which provides the grade of mixed binder M 400. Compositions of tuff concrete on aggregates and tuff using PC and MB (mixed binder) as binders have been developed. The resulting tuff concrete at the PC has an average density of 1340 kg/m$^3$ and compressive strength of 4.9 MPa, tuff concrete with a mixed binder (MB) has an average density of 1330 kg/m$^3$ and a compressive strength of 4 MPa. Porous tuff concretes were obtained at PC and MB with an average density of 1220 and 1250 kg/m$^3$ and compressive strength of 8.2 and 8.2 MPa.

Babayan G. G. (1992) has developed a concrete composition based on which a stone for masonry walls is made. The concrete composition contains, weight, %: portland cement 4-7; cement dust 9-18; tuff crushed stone 0.5-12; tuff sand 60-67.5 and water 10-12. The technology of manufacturing products is as follows: dosed components: cement, crushed tuff stone, and tuff sand are mixed at the beginning dry (1 min), and then water is added, and mixing is continued for 1.5 - 2 minutes, mixing time is 3-3.5 minutes. Then, samples are molded from the resulting mass at a pressure of 30-50 MPa and subjected to steaming according to the regime: raising the temperature for 2 hours, holding at a temperature of 90 °C for 6 hours, lowering the temperature for 2 hours (10 hours in total). Samples of products have an average density of 1655-1890 kg/m$^3$, compressive strength 15.6-23 MPa, softening coefficient after 25 cycles 0.8-0.92.

The same authors (Babayan G. G., Mikhaelyan V. G., 1992) proposed concrete using tuff. The composition includes weight, %: cement dust 38-42, tuff crushed stone 0.5-1.2, tuff sand 33-44, lime 0.5-2.0, gypsum 1-3, water 3-9, wastewater of asbestos-cement production 3-9. Concrete is used for the manufacture of autoclave-free building products. Building products is carried out in several production operations: preparation of a binder from furnace dust, lime, and gypsum. Dosage of dry binder, tuff sand, crushed stone, dry mixing of components, the dosage of asbestos-cement production wastewater and water, wet mixing of components, and molding of products at a pressure of 25-50 MPa. Steaming products according to the regime: raising the temperature to 90 °C for 2 hours, holding at a temperature of 90 °C for 6 hours, lowering the temperature for 2 hours (10 hours in total). Samples of products have an average density of 1600-1950 kg/m$^3$, compressive strength 18-25 MPa, water absorption 8.5-9.5%.

The authors Babayan G. G., and

Dashtoyan S. A. (1992) proposed a composition including cement dust 35.5-38.0%, tuff crushed stone 1-2.5%, tuff sand 33-40%, lime 0.5-2%, gypsum 0.5 -3%, water 9-10%, carbonate sludge, formed when cutting carbonate rocks 10-15%. The composition is used for the manufacture of partition plates, blocks, bricks, and others. The manufacturing technology of products is similar to that described above. Samples of products have an average density of 1645-2020 kg/m$^3$, compressive strength 16-23 MPa, water absorption 7.0-7.9%.

In the study (Gukosyan S. Zh., 1997) to obtain highly filled composites, wastes from the production of tuff stone and emulsion polyvinyl chloride, as well as polyvinyl butyral, were used. Wastes from the tuff stone production were sieved through sieves before use, and fractions <100mcm<200 mcm<300 mcm were selected for research. In the composition of the composites, the content of tuff powder varied within 70–90%. Mixing and ingredients (filler and polymer powders) were carried out in a mixer with a horizontal rotating chamber. Studies have shown that the optimal mixing time is 1.5-2 hours; the structure of the pressed samples judged the homogeneity of the composition. Samples for testing composites were prepared by compression pressing. The obtained samples were tested for strength in compression and bending, for water absorption for 24 hours at 20 °C. Testing composite samples showed that the most optimal additive is the tuff powder of fraction <200 mcm in an amount of 80%. The flexural strength of the composite is 27.8 MPa, and water absorption is 12.1%. Composites can be used for the production of PVC and linoleum boards.

In the study of Zagoyruko T. V. (2011), the composition of heat-resistant concrete was developed using expanded shungite as a filler. Expanded shungite possesses high heat resistance, strength, non-toxic, does not rot, prevents the spread of mold, has high-temperature resistance, fire resistance, and reflectivity. Based on optimization, the compositions of heat-resistant concrete with the addition of shungite with the specified properties were selected: strength 10 MPa, density 1500 kg/m$^3$. Tests were carried out on samples of heat-resistant concrete with the addition of shungite and without shungite (reference concrete). Comparative tests of the samples showed that the composition of heat-resistant concrete with the addition of shungite makes it possible to increase the heat resistance of concrete at 900 °C by 12 times and at 1100 °C by six times.

The authors of (Jehad Al-Zou'by, 2014) found that the use of zeolite filler in the manufacture of concrete, in the amount of 5, 10, and 15%, leads to an increase in its compressive strength. Simultaneously, with an increase in the amount of zeolite, the strength of concrete increases accordingly. The authors also investigated the strength of concrete on a volcanic tuff filler. It has been established that concrete containing 30% of a volcanic tuff aggregate has a strength of 28% lower than that of ordinary concrete on a limestone aggregate ($R_c$ = 300 kg/cm$^2$) after 28 days of hardening. In concrete manufacture, aggregates with a maximum particle size of 10, 20, and 40 mm were used, which have a noticeable effect on concrete strength. The dependence of concrete strength on the size of aggregate fractions has been established. Tests have shown that with an increase in the aggregate fraction, the strength of concrete on a limestone aggregate by 0.2; 5 and 14%, respectively, higher than on volcanic tuff. The same pattern is shown in the study of high-strength concrete ($R_c$ = 800 kg/cm$^2$) on limestone and volcanic tuff aggregate. Concrete made with limestone aggregate has a compressive strength of 4, 6, and 7% higher than concrete with a volcanic tuff aggregate of the same fractions.

Al Dwairi (2007), volcanic tuff in Jordan is present in the northeastern, central, and southern parts of the country. Volcanic tuffs in Jordan are studied for mineralogy, petrology, and their ecological, industrial, and agricultural applications. Volcanic tuff (detrital) differs depending on location and depending on the rate of weathering and zeolitization processes, reflecting the mineral content and the amount of secondary minerals associated with volcanic tuff zeolites being the most important.

Gradstein, F. M. (2012), the volcanic tuff from Al-Khala-1, Jordan is strongly changed in zeolite from brown to gray. The thickness of the colored cut is more than 50 m. The volcanic tuff from Al-Khala-2 is a fresh black slag. Tuff in both places is of Paleocene and Neogene age.

The authors Reyad A. Al Dwairi (2018) investigated the possibility of using volcanic tuff as lightweight structural concrete, for this two samples were subjected to the following laboratory tests: determination of specific gravity and water absorption, average density and porosity, which was determined following ASTM C29/C29M - 17a., and the abrasion of the tuff in the abrasion machine. The analyses were carried out in the Civil Engineering Department of the Tafil Technical University laboratories in Southern

Jordan.

Thus, natural tuff and waste from the production of tuff stone are widely used to manufacture building materials for various purposes. In Kazakhstan, there is practically no research and development on the use of natural tuff and waste from the production of tuff stone in the technology of concretes, binders, and other materials.

Research on the use of tuff and its waste in technology is carried out in Armenia, Russia, and Poland. In Poland, based on tuff, a fire-resistant geopolymer was obtained that replaces expanded polystyrene and absorbs unpleasant odors. In Armenia, based on natural tuff and waste from the production of tuff stone, compositions and raw mixtures have been developed to manufacture of wall stones, partition plates, blocks, and bricks. Also obtained are polymer composite materials, where finely ground tuff powders are used as fillers. A mixed binder and porous tuff concrete products were obtained in KBASSR using tuff and Portland cement.

## 2. MATERIALS AND METHODS:

### *2.*1 Materials.

As the main raw material, overburden volcanic rocks are used, formed during volcanic tuff extraction (Chundzha village, Uygur district of Almaty region, Kazakhstan) represent volcanic tuff of a lower quality, not suitable for the manufacture of piece goods. For research, we used pieces of overburden volcanic rocks with dimensions of 50-150 mm. The overburden was crushed in a jaw crusher and screened through a set of standard sieves to make aggregates. As a result, aggregates were obtained from tuff fractions: 0.16-5 mm, 5-10 mm, and 10-20 mm. The first fraction corresponds to the fine aggregate - sand, the second and third fractions - to the coarse aggregate - crushed stone. Figure 1 shows photographs of crushed tuff stone. For the manufacture of lightweight structural concrete, Portland cement CEM I 32.5 N (GOST 31108-2003) was used as a binder.

### 2.2 Methods

The crushing capacity of crushed stone was determined by the degree of destruction of the grains during compression (crushing) in the cylinder with the size 150 mm (GOST 8269.0-97, 2018).

The calculation of the composition of tuff concrete was carried out according to the method described in the DBC (Departmental building codes) (Departmental building codes, 1992).

#### *2.2.1 Determination of the bulk density of aggregates.*

According to GOST 9758-86 (GOST – Governmental standard), the bulk density of aggregates obtained from tuff was determined. Porous inorganic aggregates for construction work. It was used: a set of graduated cylindrical vessels, an electric drying cabinet, a metal ruler. The aggregate dried to constant weight was poured into a pre-weighed measuring vessel from a height of 100 mm above its upper edge until a cone formed above the top of the vessel, which was removed with a metal ruler flush with the edges of the vessel (without compaction) and weighed. The porous sand was poured through a funnel. The size of the measuring vessel and the volume of the test sample depends on the aggregate size.

#### *2.2.2 Determination of the average density of tuff concrete.*

According to GOST 27005-2014, the average density of lightweight concrete was determined. Lightweight and cellular concrete. Average density control rules. It was used laboratory scales and a drying cabinet. For a unit value of concrete density, the average density of a series of samples made from one sample of a concrete mixture or the average density of a series of selected samples is taken. Concrete samples hardened under normal conditions for 28 days were weighed on an electronic laboratory balance. The average density of the three samples was determined by arithmetic.

#### *2.2.3 Determination of the strength of aggregates when pressed in a cylinder.*

The strength of the tuff aggregate under compression in the cylinder was determined by the load corresponding to the immersion of the punch by 20 mm into the layer of the aggregate test sample. Were used: hydraulic press, steel composite cylinder with a diameter of 150 mm, drying cabinet. The punch was pressed in without skewing at a speed of 0.5-1.0 mm/s. The sample dried to constant weight was placed in a cylinder and installed in a hydraulic press. Strength is determined according to GOST 9758-2012 Porous inorganic fillers for construction work. Test methods. The strength of the aggregate of an individual fraction under compression in the cylinder was calculated for each aggregate fraction as the arithmetic means of the results of two parallel tests of this fraction.

### *2.2.4 Determination of the strength of tuff concrete.*

The compressive strength of tuff concrete samples was determined according to GOST 10180-2012 Concrete. Methods for determining the strength of control samples. It was used: testing machine, metal ruler. The concrete samples were installed in a testing machine (Hydraulic Press). The samples were loaded continuously at a constant rate of increase in the load until its destruction. The maximum force achieved during the test is taken as the breaking load.

### *2.2.5 Determination of thermal conductivity.*

The thermal conductivity of tuff concrete was determined using an ITP-MG4 (250) thermal conductivity meter based on GOST 7076-99 (GOST 7076-99). Samples were made of tuff concrete with a size of 250x250x100 mm for the test equipment dimensions. The samples hardened under normal conditions for 28 days. During the test, the temperature difference between the face faces of the sample was set in the range of 10-30 K. The average temperature of the sample during testing must be specified in the regulatory document for a specific type of material or product. After reaching a stationary thermal regime, the thickness of the sample placed in the device is measured with a caliper with no more than 0.5% error. After the end of the test, determine the mass of the sample. The average arithmetic mean values of thermal resistance and effective thermal conductivity of all tested samples were taken as the test result.

X-ray diffractometric analysis was carried out on a DRON-3.0 diffractometer with $Cu_{K\alpha}$ - radiation, $\beta$ - filter. Conditions for recording diffraction patterns: $U$ = 35 kV; $I$ = 20 mA; shooting θ-2θ; detector 2 deg/min. Semi-quantitative X-ray phase analysis was carried out based on the diffraction patterns of powder samples using equal portions and artificial mixtures. The quantitative ratios of the crystalline phases were determined. The interpretation of the diffractograms was carried out using ICDD card index data: the database of powder diffractometric data PDF2 (Powder Diffraction File) and diffractograms of minerals free of impurities.

## 3. RESULTS AND DISCUSSION:

The research results on the development of compositions and technological parameters of lightweight structural concrete based on overburden formed during volcanic tuff extraction. They are of particular interest for the production of lightweight structural concrete and facing tiles on its basis.

The chemical composition of the tuff was determined by X-ray spectral local analysis (RLA) using a JCTXA-733 electron probe microanalyzer. Table 1 shows the results of the chemical analysis of volcanic tuff.

Overburden tuff rock from the village Chundzha, Uygur District, Almaty Region, is yellowish to orange-brownish (hypercrystalline to aphanite texture) with various debris sizes.

Figure 2 shows a diffractogram of overburden volcanic tuff. All the given diffraction peaks belong only to the phases indicated above. The results of semi-quantitative X-ray phase analysis showed that the content of minerals in the tuff composition is: sanidine $(K_{0.831}Na_{0.169})(AlSi_3O_8)$ – 29,2 %; kaolinite $Al_2Si_2O_5(OH)_4$ – 24,4 %; zeolite (heulandite) $Na_{5.68}Ca_{1.52}(Al_{8.6}Si_{27.4}O_{72})(H_2O)_{21.4}$ – 23,3 %; kyanite $Al_2O(SiO_4)$ – 14,2 %; calcite $Ca(CO_3)$ – 7,3 %; micas $KAl_2(AlSi_3O_{10})(OH)_2$ – 1,5 %.

Fragments are mainly light brown to brownish-reddish poorly flattened pumice and other lithoclasts (basalts and other volcanic fragments), which can range in diameter from a few mm (the size of sand grains) to 5 cm, and sometimes more (Figure 3).

One of the main requirements for the suitability of the crushed stone for the manufacture of concrete is the value of the indicator of its crushing capacity. Depending on the index of crushing (Cr), crushed stone (gravel) is divided into the following grades: Cr8 (with a weight loss of up to 8%), Cr12 (with a weight loss of 8 to 12%), Cr16 (with a weight loss of 13 to 16%) and Cr24 (with a weight loss of 16 to 24%).

The crushing capacity of tuff crushed stone was determined in 2 fractions: 5-10 and 10-20 mm. The crushed tuff stone obtained by us corresponds to the Cr24 brand.

To calculate the composition of lightweight concrete on porous aggregates, it is necessary to determine the bulk density of the aggregates ($\rho_{bulk}$). The best ratio was established between fine and coarse aggregates on schedule. A binder was added to the resulting mixture of aggregates per 1 $m^3$ of the total volume of small and large aggregates. For each of the three compositions mentioned above, the optimal water consumption was determined. The output of concrete at given compaction would be the

smallest, and therefore, the concrete would be the most workable and durable. Bulk densities were determined for aggregates obtained from two batches. Bulk densities of aggregates from the first batch of tuff (GOST 9758-2012):

- $\rho_{bulk}$, tuff sand – 970 kg/m$^3$;
- $\rho_{bulk}$, tuff crushed stone fractions 5-10 mm – 988 kg/m$^3$;
- $\rho_{bulk,}$ tuff crushed stone fractions 10-20 mm – 999,7 kg/m$^3$;
- $\rho_{bulk,}$ (average value of the sum of 2 fractions) – 995 kg/m$^3$.

Bulk densities of aggregates from the second batch of tuff:

- $\rho_{bulk}$, tuff sand – 1040 kg/m$^3$;
- $\rho_{bulk}$, tuff crushed stone fractions 5-10 mm – 950,7 kg/m$^3$;
- $\rho_{bulk}$, tuff crushed stone fractions 10-20 mm – 961kg/m$^3$;
- $\rho_{bulk,}$ (average value of the sum of 2 fractions) – 956,4 kg/m$^3$.

The bulk densities of crushed stone and sand of the first and second batches differ markedly from each other, indicating an unstable (uneven) volcanic tuff density. This factor is associated with the different porosity of the volcanic rock, which depends on the cooling conditions of the volcanic lava.

After calculating the composition of tuff concrete, all raw materials: cement, aggregates, additives, and water are dosed and mixed. The concrete mix is placed in a mold and compacted by Vibro-compression on a vibrating table. To determine the properties of tuff concrete, sample cubes with dimensions of 100x100x100 mm were made. The hardening of concrete samples is carried out in moisture conditions for 7, 14, and 28 days and steaming in a steaming chamber for 12-16 hours. After hardening, the properties (strength, average density, thermal conductivity coefficient) of concrete samples were determined according to the above standard procedures. Table 2 shows the compositions and properties of concrete samples based on volcanic tuff.

Tuff concrete samples No. 6 and No. 7 were made from aggregates obtained from 2 batches of overburden tuff rocks.

As can be seen from the data in the table, the compressive strength of tuff concrete samples of compositions No. 6 and No.7 is lower than that of concretes obtained based on tuff from the first batch. Therefore, in the manufacture of tuff concrete products, each time after crushing tuff into the sand and crushed stone from a new batch, it is necessary to check their bulk density, crushing capacity, and strength of crushed stone.

The average density of tuff concrete is 1822-1910 kg/m$^3$, the grade of tuff concrete is in the range of 15.0-20.0 MPa. The thermal conductivity coefficient (λ) is within the range of 0.611-0.757 W/m·K, which is lower than the thermal conductivity of heavy cement concrete with a density of 2100-2500 kg/m$^3$ (0.9-1.3 W/m·K), (GOST 25820-2014).

The possibility of manufacturing finishing tiles from tuff concrete by grinding and polishing its surface has been established. Simultaneously, the structure of aggregates of various shades is exposed, giving it a decorative effect (Figure 4).

Based on tuff sand, with a grain size of less than 3 mm, a concrete stone with dimensions of 390x190x188mm with two technological voids was made by Vibro-compression (GOST 6133-99). The emptiness of stone is 51% of its total volume. The ratio of cement: tuff sand = 1:5. The concrete stone hardened at room temperature (18-20 °C) for 18 days after forming. Compressive strength tests of concrete stone were carried out. It was found that the compressive strength is 30.8 kg/cm$^2$ or 3.1 MPa, which corresponds to the M25 grade.

When transporting a wall block (stone) made of lightweight concrete of a low grade and laying walls, vertical cracks, chips, crumbling corners, and other types of defects are formed (Figure 5). Such a wall block can be used for individual construction of a one-story house in non-seismic areas. According to (GOST 6133-99), lightweight concrete wall stones are grades 100, 75, 50, 35, 25. By agreement with the consumer, the grade of the block on tuff sand can be increased to M50-M100.

## 4. CONCLUSIONS:

1. One of the main requirements of lightweight concrete manufacturing technology is the use of porous aggregates. Such aggregates were obtained by crushing porous volcanic tuff rocks. The porosity was in the range of 21.3-46.6% in volcanic tuffs; its density ranges from 1400 to 1800 kg/m$^3$.

2. In this work, overburden volcanic rock was used as the main raw material, which was formed during the extraction of volcanic tuff (Chundzha village, Uygur district of Almaty

region, Kazakhstan) and is a volcanic tuff of lower quality, not suitable for the manufacture of piece products.

3. The chemical composition of the overburden volcanic tuff was determined. The X-ray diffractometric and X-ray phase analyses were carried out on a semi-quantitative basis based on the diffractograms of powder samples. The main crystalline phases of overburden volcanic tuff were represented by kaolinite $Al_2Si_2O_5(OH)_4$, zeolite (heulandite) $Na_{5.68}Ca_{1.52}(Al_{8.6}Si_{27.4}O_{72})(H_2O)_{21.4}$, kyanite $Al_2O(SiO_4)$, calcite $CaCO_3$, and mica $KAl_2(AlSi_3O_{10})(OH)_2$.

4.Tuff sand with bulk density was obtained by crushing and sieving 970-1040 kg/m$^3$; tuff crushed stone 5-10 mm - 950.7-988 kg/m$^3$; tuff crushed stone fraction 10-20 mm - 961- 999.7 kg/m$^3$. The compositions were calculated, mixtures were compiled, and samples of tuff concrete were made. Moreover, the tuff content in the concrete was 80%.

5. It was established that the bulk densities of aggregates obtained from different volcanic tuff batches differ from each other; therefore, the compressive strength of tuff concrete specimens of compositions No. 6 and No.7 was lower than that of concretes obtained based on tuff from the first batch. Therefore, each time after crushing the tuff into the sand and crushed stone, it is necessary to check their bulk density, crushing capacity, and strength of the crushed stone from a new batch.

6. The obtained samples of tuff concrete have an average density of 1822-1910 kg/m$^3$, in terms of compressive strength, they correspond to B12.5-15 classes (GOST 25820-2014). The thermal conductivity of tuff concrete samples is in the range of 0.611-0.757 W/m·K. These indicators satisfy the requirements for lightweight structural concrete.

7. The possibility of making finishing tiles from tuff concrete by grinding and polishing its surface was established. Simultaneously, the structure of aggregates of various shades is exposed, giving it a decorative effect.

8. The possibility of manufacturing wall concrete blocks of the M 25-35 brand with dimensions of 390x190x188mm with two technological voids (GOST 6133-99) was established. The weight of the block is 17-18 kg, which is lighter than similar blocks on conventional aggregates, and, accordingly, it has lower thermal conductivity and higher thermal insulation properties.

## 5. ACKNOWLEDGMENTS:

This work was done as part of the project AP08855714 “Thermal insulation coatings based on finely dispersed mineral granular systems” in the framework of "Grant funding for scientific and (or) scientific and technical projects for 2020-2022 with an implementation period of 27 months” of the Science Committee of the Ministry of Education and Science of the Republic of Kazakhstan. The authors are grateful to the leadership of the Satbayev University and Science Committee of the ME&S RK for creating the conditions for carrying out this work.

## 6. REFERENCES:

1. Silber A., Bar-Yosef B., Singer A., Chen Y. Mineralogical and chemical composition of three tufts from northern Israel. Geoderma 63. –1994. – P. 123-144.
2. Rube´nLo´pez-Doncel, Wanja Wedekind, Reiner Dohrmann, Siegfried Siegesmund. Moisture expansion associated to secondary porosity: an example of the Loseros Tuff on Guanajuato, Mexico. 1189-1201. 2012.
3. Novi Asniar, Yusep Muslih Purwana, Niken Silmi Surjandari. Tuff as rock and soil: Review of the literature on tuff geotechnical, chemical, and mineralogical properties around the world and in Indonesia. AIP Conference Proceedings. Volume 2114, 26 June 2019. Number of conference paper 050022.
4. Wedekind W, Ruedrich J, Siegesmund S Natural building stones of Mexico–Tenochtitlán: their use, weathering, and rock properties at the Templo Mayor, Palace Heras Soto, and the Metropolitan Cathedral. Environ Earth Sci. 63(7/8). – 2011. – P. 1787-1798.
5. Stueck H. Materialeigenschaften und Verwitterungsprozesse bruchfrischer und konsolidierter Vulkanite. Diploma-thesis, University of Goettingen. – 2006. – P.158-164.
6. Siegesmund S, Duerrast H. Physical and mechanical properties of rocks. In: Siegesmund S, Snethlage R (eds) Stone

in architecture: properties, durability, 4th Ed. Springer, Berlin. – 2011. – P. 97-225.

7. Trunov P. V. Prospects for the use of volcanic tuff of Kamchatka as a siliceous component of composite binders. Journal of Basic Research. - 2014. - No. 3 (part 3) - P. 490-494..
8. Movsisyan M. S., Sargsyan N. Z. Patent No. 1790564. A method of manufacturing lightweight building materials. 23.01.1993. Bul. No. 3.
9. Gonchikov Z. M. Expanded clay and tuff concretes of low thermal conductivity with the complex use of tuff. Author's abstract. Ulan Ude, 1998.22 p.
10. Babayan G. G., Dashtoyan S. A., Mikhaelyan V. G. Patent No. 1766867 A1. Composition for the manufacture of building material. Bul. fig. No. 37. 07.10.1992.
11. Babayan G. G., Mikhaelyan V. G., Dashtoyan S. A. Ed. wit. USSR No. 1765137 A1. Composition for the manufacture of building materials. Bul. No.36. 30.09.1992.
12. Babayan G. G., Dashtoyan S. A., Mikhaelyan V. G. Patent No. 1765135 A1. Composition for the manufacture of building products. Bul. No.36. 30.09.1992.
13. Gukosyan S. Zh. Building finishing highly filled composite materials based on waste from the production of tuff stone. Author's abstract. Yerevan, 1997. 23 p.
14. Zagoyruko T. V., Pertsev V. T. The use of heat-resistant materials based on lightweight aggregates to improve the fire resistance of building structures / Bulletin of the Voronezh Institute of the State Fire Service of the Ministry of Emergency Situations of Russia, 2011, No. 1. P. 29 - 31.
15. Jehad Al-Zou'by; Kamel K. Al-Zboon. Effect of volcanic tuff on the characteristics of cement mortar. Al-Huson University College, Al-Balqa' Applied University. 2014.
16. Al Dwairi, R. Characterization of the Jordanian zeolitic tuff and its potential use in Khirbet Samra wastewater treatment plant. Author's abstract. University of Jordan, Jordan, P. 204. 2007.
17. Gradstein, F. M, Ogg, J. G., Schmitz, M. D. (2012). The Geologic Time Scale 2012: Boston, USA, Elsevier, DOI: 10.1016/B978-0-444-59425-9.00004-4.
18. Reyad A. Al Dwairi, Bety Al Saqarat, Fathi Shaqour, Mohmd Sarireh. Characterization of Jordanian Volcanic Tuff and its Potential Use as Lightweight Aggregate. P. 127 – 133. 2018
19. GOST 8269.0-97 “Crushed stone and gravel from dense rocks and industrial waste and waste for construction work. Physical and mechanical test methods. Published by: GUP CPP (CPP GUP 1998) Standartinform (2018).
20. Departmental building codes (DBC). The use of concretes on natural porous aggregates for the construction of transport tunnels. DBC 212-91. Moscow 1992.
21. GOST 7076-99 "Method for determining thermal conductivity and thermal resistance in a stationary thermal regime".
22. GOST 9758-2012 Porous inorganic fillers for construction work. Test methods.
23. GOST 25820-2014 Light concretes. Technical conditions.
24. GOST 6133-99 Concrete wall stones. Technical conditions.
25. ASTM C29 / C29M - 17a. Standard Test Method for Bulk Density (“Unit Weight”) and Voids in Aggregate. DOI: 10.1520/C0029_C0029M-17A.

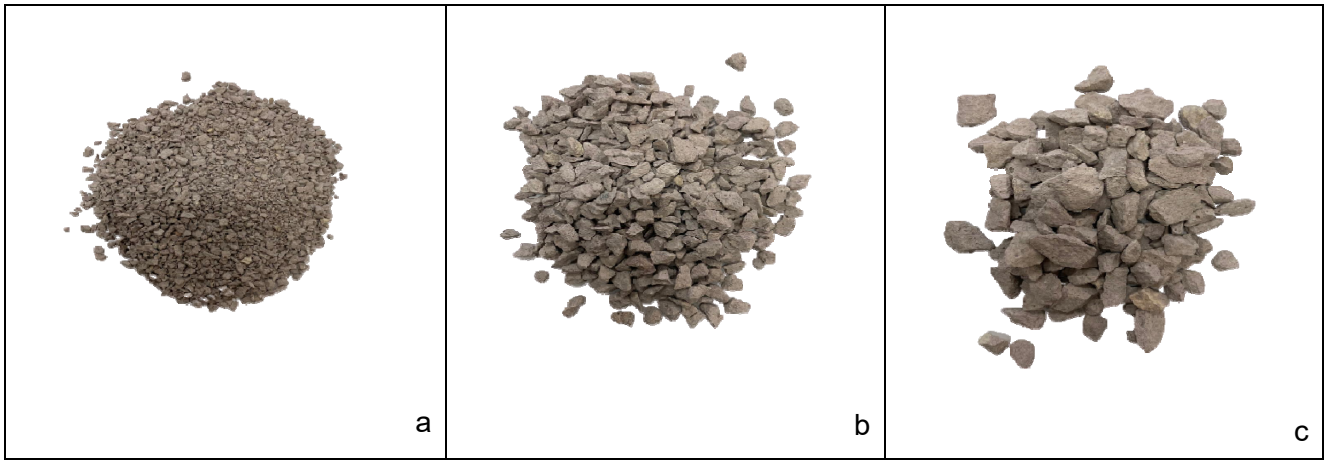


***Figure 1.*** *Tuff rubble. Fraction 0.16-5 mm (a); fraction 5-10 mm (b); fraction 10-20 mm (c).*

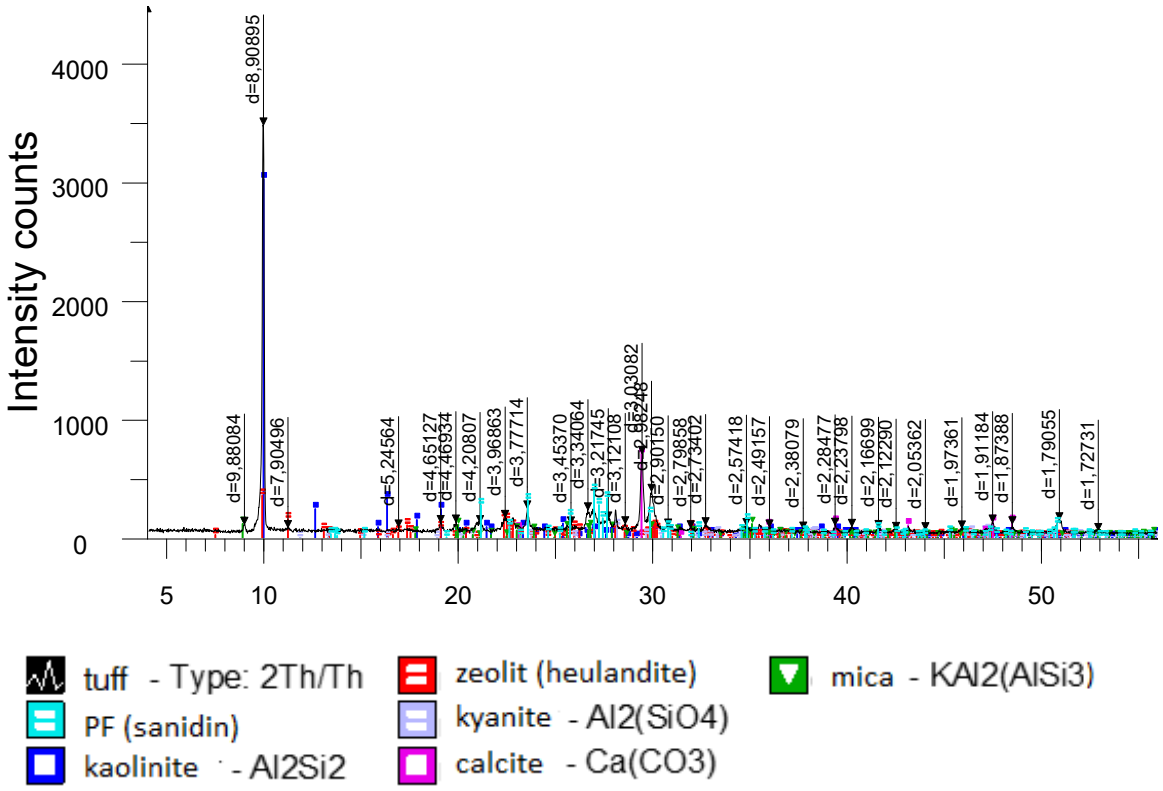


***Figure 2.*** *Diffractogram of volcanic tuff*

***Figure 3.*** *Overburden volcanic tuff structure*

***Figure 4.*** *Decorative facing tiles made of tuff concrete*

***Figure 5.*** *Tuff concrete wall block*

***Table 1**. The chemical compound of volcanic tuff*

| Compound, % by mass | | | | | | | | |
|---|---|---|---|---|---|---|---|---|
| $SiO_2$ | $Al_2O_3$ | $K_2O$ | $Na_2O$ | CaO | FeO | MgO | $TiO_2$ | MnO |
| 72.36 | 14.04 | 5.14 | 3.54 | 2.36 | 1.47 | 0.67 | 0.16 | 0.26 |

***Table 2.** The Cement content and properties of tuff concrete samples*

| No. | Cement content in 1m$^3$ of concrete | Average density ($\rho_{av}$) of concrete, kg/m$^3$ | | Compressive strength, MPa | | Concrete class | Thermal conductivity, λ, W/m·K |
|---|---|---|---|---|---|---|---|
| | | Estimated | Factual | After heat treatment humidity (HTH) | After 28 days | | |
| 1 | 380 | 1800 | 1910 | 14.3 | 20.0 | B15 | 0.7545 |
| 2 | 350 | 1800 | 1900 | 12.3 | 17.5 | B12.5 | 0.7490 |
| 3 | 350 | 1800 | 1880 | 11.5 | 16.4 | B12.5 | 0.7230 |
| 4 | 350 | 1800 | 1822 | 13.1 | 20.0 | B15 | 0.6651 |
| 5 | 350 | 1800 | 1843 | 13.7 | 21.08 | B15 | 0.6742 |
| 6 | 350 | 1800 | 1918 | 10.2 | 14.6 | B12.5 | 0.7557 |
| 7 | 350 | 1700 | 1879 | 12.4 | 17.7 | B12.5 | 0.7430 |

PERIÓDICO TCHÊ QUÍMICA
ARTIGO ORIGINAL

# ANÁLISE DE HABILIDADES COGNITIVAS PARA APRENDIZAGEM DE CIÊNCIA, TECNOLOGIA, ENGENHARIA E MATEMÁTICA: DOIS PONTOS DE VISTA, DUAS OPINIÕES

# ANALYSIS OF COGNITIVE ABILITIES FOR STEM LEARNING: TWO VIEWPOINTS, TWO OPINION

# АНАЛИЗ КОГНИТИВНЫХ НАВЫКОВ ПРИ ОБУЧЕНИИ STEM: ДВЕ ПОЗИЦИИ, ДВА ВЗГЛЯДА

NIKULOVA Galina[1*]; BOBROVA Lubov[2]

[1 2] Lipetsk State Pedagogical University, Lipetsk, Russia

[1] Department of Informatics, Information Technology, and Information Security

[2] Department of Mathematics and Physics

** Corresponding author*
*e-mail: niklipp@mail.ru*

Received 12 December 2020; received in revised form 20 February 2021; accepted 07 March 2021

## RESUMO

**Introdução:** A abordagem da educação com foco na cognição é um dos fatores fundamentais para preparar a geração mais jovem para dominar ainda mais o espaço educacional e informativo. **Objetivo:** o objetivo é determinar os tipos de dificuldades cognitivas em alunos de disciplinas *STEM* (ciências, tecnologia, engenharia e matemática) na escola, para determinar uma conexão entre as habilidades e habilidades cognitivas e determinar sua importância para ambos os lados do processo educacional - os professores e os alunos. **Métodos:** O método básico do estudo é pesquisar os respondentes, usando o questionário criado pelo autor do estudo, em seguida, analisar e processar estatisticamente os resultados. O estudo incluiu três etapas: identificação de dificuldades significativas dos alunos em realizar atividades educacionais dentro de uma disciplina específica, identificação das habilidades e habilidades cognitivas mais exigidas, busca de conexões e determinação da correspondência de habilidades e habilidades cognitivas. **Resultados e Discussão:** Foram identificados os tipos de estudos que mais apresentaram dificuldades aos alunos e a interligação entre as competências cognitivas. Diferenças foram reveladas ao comparar as respostas dos dois grupos de respondentes sobre a complexidade e a importância das ações educativas no estudo da física e da matemática e o tipo de atitude dos alunos em relação ao nível reprodutivo da educação ou aos algoritmos de ações mais claros e memoráveis. As competências mais significativas para o sucesso do processo educacional foram extrapoladas. A análise de correlação em pares de capacidade cognitiva / habilidade cognitiva possibilitou corrigir as ideias iniciais sobre a relação. **Conclusões:** Os dados coletados permitiram estabelecer a complexidade das atividades educacionais e as habilidades e habilidades cognitivas aplicadas à disciplina. A sistematização dos resultados do estudo das opiniões subjetivas de alunos e professores sobre a importância das competências cognitivas para o *STEM* possibilita transformar propositalmente o processo educacional, levando em consideração as necessidades de seus participantes e da sociedade..

**Palavras-chave** *habilidade cognitiva, dificuldades de aprendizagem, processo de aprendizagem, escola, cognição STEM*

## ABSTRACT

**Background:** Cognition-focused approach to education is one of the foundational factors for preparing the younger generation to further mastering the educational and informational space. **Aim:** The purpose is to determine the types of cognitive difficulties in students of STEM disciplines (science, technology, engineering, and mathematics) in school, to determine a connection between cognitive abilities and skills, and to determine their significance for both sides of the educational process – the teachers, and the students. **Methods:** The basic method of the study is polling the respondents, using the questionnaire created by the study's author, then

analyzing and statistically processing the results. The study included three stages: identifying significant difficulties of students in performing educational activities within a specific discipline, identifying the most demanded cognitive abilities and skills, searching for connections, and determining the correspondence of cognitive abilities and skills. **Results and Discussion:** Types of studies that presented the most difficulties to students were identified and the interconnection between the cognitive competencies. Differences were revealed when comparing the answers of both groups of respondents about the complexity and importance of educational actions in the study of physics and mathematics and the attitude type of schoolchildren to the reproductive level of education or the clearest and memorable algorithms of actions. Competencies most significant to the success of the educational process were extrapolated. Correlation analysis in pairs of cognitive ability/cognitive skill made it possible to correct the initial ideas about their relationship. **Conclusions:** The data collected allowed establishing the complexity of the educational activities and significant cognitive subject-applied abilities and skills. Systematizing the results of studying the subjective opinions of students and teachers about the importance of cognitive competencies for STEM makes it possible to purposefully transform the educational process, taking into account the needs of its participants and society.

**Keywords**: *cognitive ability, learning difficulties, learning process, school, STEM cognition*

## ABSTRACT

**Предпосылки:** Подход к образованию, ориентированный на познание, является одним из основополагающих факторов, позволяющих добиться успеха в подготовке подрастающего поколения к дальнейшему освоению образовательного и информационного пространства. **Цель:** определить типы когнитивных трудностей у обучающихся STEM дисциплинам (наука, технология, инженерия и математика) в школе, определить связь между когнитивными способностями и навыками и определить их значимость для обеих сторон образовательного процесса – учителей и учеников. **Методы.** Основной метод исследования – это опрос респондентов с использованием анкеты, созданной автором исследования, с последующим анализом и статистической обработкой результатов. Исследование включало 3 этапа: выявление существенных трудностей студентов при выполнении учебной деятельности в рамках конкретной дисциплины, выявление наиболее востребованных когнитивных способностей и навыков, поиск связей и определение соответствия когнитивных способностей и навыков. **Результаты и обсуждение:** Были определены типы исследований, которые представляли наибольшие трудности для студентов, а также взаимосвязь между когнитивными компетенциями. Различия выявлены при сравнении ответов обеих групп респондентов о сложности и важности учебных действий при изучении физико-математических наук и о типе отношения школьников к репродуктивному уровню образования или к наиболее четким и запоминающимся алгоритмам действий. Были экстраполированы компетенции, наиболее важные для успеха учебного процесса. Корреляционный анализ в парах когнитивные способности / когнитивные навыки позволил скорректировать первоначальные представления об их отношениях. **Выводы:** собранные данные позволили установить сложность учебной деятельности и значимые познавательные предметно-прикладные способности. Систематизация результатов изучения субъективных мнений студентов и преподавателей о важности когнитивных компетенций для STEM позволяет целенаправленно трансформировать образовательный процесс с учетом потребностей его участников и общества.

**Ключевые слова**: *когнитивные способности, трудности обучения, учебный процесс, школа, STEM познание*

## 1. INTRODUCTION:

All our lives are intertwined with cognition and education, and the individual success of each person, by far, is ensured by the presence and possession of cognitive abilities and skills. Thinking skills, aptitude for learning, ability to understand and comprehensively resolve issues are the basic, foundational skills of the 21st Century (Jang, 2016; UNESCO, 2017). The refined diagnostics of problems ensures the chances for educational success as part of the specific environment of the educational process implementation. This study focuses on the determination of opinions of both sides of the educational process, challenges for students, and the importance of procedures, activities, and individual qualities of students to the success of the educational process.

The cognition-focused approach to planning and implementation of the educational process implies the formation and development of cognitive skills and abilities of the students for each discipline or set of disciplines being studied

(Booth *et al.*, 2017; Coyle, 2019; Santoso *et al.*, 2017; DTEUH, 2015). The authors of cognition-focused methodologies in educational environment development for physics and algebra, such as R. Teodorescu and other scientists (Teodorescu *et al.*, 2014; Gierl *et al.*, 2005; Yilmaz, 2011), assert that new educational qualities are oriented at the necessity for the student to actively participate in cognitive processing of the educational information. Yet, they do not solve the arising problems of the cognitive organization of work. Marzano's cognitive system (National Training and Education Office, NTEO) complements Bloom's taxonomy and integrates knowledge recovery, comprehension – information synthesis and representation; analysis – similarities, differentiation, systematization, specification, generalization, error analysis; knowledge utilization – decision making, problem-solving, heuristic activities and research (Marzano and Kendall, 2007; Wilson, 2016).

In this study, there was an attempt to determine the type of cognitive difficulties in mastering physics and mathematics at school, identifying the significance of cognitive abilities and skills, and affiliated educational activities – for both participating sides of the educational process – the students and the teachers. The pool of disciplines for which the basic analysis of cognitive skills' evaluations and significance is conducted was not randomly selected:

- It is the natural science, such as mathematics and informatics, that allows adapting – and it is not only applicable to an individual but to humanity in general, is constantly changing world's conditions;
- STEM (science, technology, engineering, and mathematics) is the testing ground for the trials of innovative pedagogical theories and technologies;
- STEM set of disciplines as an instrument for other sciences is the fertilizing ground for forming and developing cognitive abilities (Teodorescu *et al*., 2014; Villafañe and Lewis, 2016). Often, physics, combined with problem-solving, is considered the discipline most suited for developing critical thinking skills, well beyond the specifics of only the context of physics (Ertmer and Newby, 2013; Yuliati *et al*., 2018).

The main purpose of the study is to determine cognitive components that assist with a successful implementation of the educational process for physics and mathematics. It is believed that the study results will allow clarifying the extent of the concurrence of points of view for two generations to collaborate in the search and implementation of methods and forms of education.

## 2. MATERIALS AND METHODS:

In analyzing numerous publications, a reasonable question arose: what did the authors mean by cognitive skills? Often this term was used arbitrarily, and the cognitive skills were confused with cognitive abilities and processes. Despite the similarities and overlaps, it was important to understand that these definitions were different (Figure 1).

Cognitive abilities provided opportunities for collection, selection, accumulation, preservation, and processing of the incoming information and creating new information – therefore, for learning about the world and adapting to the changing conditions in general and the educational process specifically. This happened through cognitive processes. And cognitive abilities were the basis for developing cognitive skills, which, to an extent, could compensate for the minimal abilities in a specific vocation. Skills represented the content of critical thinking and focused on theorists and practitioners of education (Etkina and Planinšič, 2015; Vilia *et al.*, 2017; Yuliati *et al.*, 2018; Santoso *et al.*, 2017). Skills were formed within a certain context by the repetition of actions to make them automatic. For achieving success, subjective cognitive skills (SCS) were very important. Those had been previously formed, stable methods, predispositions, and experience of perceptive and mental activity for studying a specific discipline. Cognitive processes differed by structure and composition and dominance of particular mental activities (Wilson, 2016; Booth *et al.*, 2017; Parameswar, 2018; Ardura and Pérez-Bitrián, 2019; Coyle, 2019).

Studies (Teodorescu *et al.*, 2014; UNESCO, 2014, 2017) demonstrated that most methods and approaches to achieving objectives in physics were grounded in mathematics and logic. There were main stages of solutions – understanding the nature of the process or event (i.e., analysis of conditions), information collection, planning and implementing the solution, evaluating the result achieved and learning from mistakes. Cognitive actions and affiliated skills correlated with the steps of problem-solving in NTEO: problem evaluation →

categorization (what part or segment did the assignment belong to), data visualization → symbolization, conceptualization (the algorithms of information collection and identification) → integration (selection of critical informational components); solution execution → execution; results' analysis → analysis of mistakes and presumptions; understanding and analysis of application → creation; summarizing the results of education → metacognition.

Based on the fundamental determinations of Marzano's new taxonomy and the description of the abovementioned abilities and skills, which were part of the cognitive approach to learning the STEM set of disciplines, and as part of the requirements for questionnaire development, a questionnaire was created for determination of critical (from the standpoint of both teachers and students) actions and skills of the students' cognitive activity. The poll was also designed to identify the main challenges in achieving educational goals by comparing the views of two participating sides of the educational process.

The publicly accessible on the internet "Cognitive Skills" questionnaire included the following participants: 168 students (grades 8 through 11, of which 61% study STEM disciplines, and 39% study humanities), and 105 teachers (51% of physics and mathematics, and 49% of informatics and computer technologies) (CSQ, 2020). Teachers of informatics were included in this sample for the following reasons: a) much older generation teachers of physics and mathematics transitioned to being teachers of informatics; b) integrating digital technologies into the educational process increased the importance of their opinions about SCS in the inter-discipline context.

The following main attributes of respondents were accounted for: their role in the educational process, the disciplines they taught (for teachers), class, and discipline (for students). Questions and answers were represented in multiple formats: yes or no, multiple choices, and grading the list entries. The questionnaire included questions about the cognitive aspects of education in two basic disciplines of the STEM set – mathematics and physics (Figure 2).

The study was conducted in 3 stages: identification of significant challenges for the students in the execution of the educational activities within each discipline, determination of the cognitive skills and abilities that were most in-demand, identification of connections, and determination of matching cognitive abilities and skills.

Integration of digital technologies into the educational process did not soften but rather immensely intensified the issues related to the optimal selection of its tactics and strategy, as well as forms and details of its organization following the challenges of the modern social environment, specific traits of the disciplines, and demands of the process participants (Gierl *et al*., 2005). Cognition and education played a vital role in the entire life. The individual success of each person was based on, to a large extent, possession of cognitive abilities and skills (UNESCO, 2014). The skills of thinking, aptitude for learning, and problem-solving based on comprehension were listed as fundamental skills of the 21st century (Etkina and Planinšič, 2015; UNESCO, 2017). This was why the search for the optimal types and structure of the educational process was ongoing, and in the process, they were formed, developed, and improved.

P. A. Ertmer and T. J. Newby (2013) pointed out that, despite the multitude of verified and justified educational theories and affiliated verified educational strategies, methods, and instructions for making education easier, designers of the educational process and teachers themselves worked in the conditions of limited theoretical background. This affected the determination of educational goals and near term developments. It was in serious doubt that the teachers were consciously oriented at teaching only. A significant role belonged to the development of skills related to the management of the students' learning activities, feeling pleased with it, and achieving specific individual results. The opportunities for educational success were grounded in the verification of the diagnosed problems in specific conditions of implementation. It was important to assess the attitude towards the complexity of the educational activities and the nature of challenges – for both sides of the educational process – the students, who were the consumers of the main acts of learning, and teachers – as the bearers, transmitters, and moderators of the educational means and materials.

Cognition-focused approach to planning and implementation of the educational process at all levels became a commonly used trend (Gierl *et al*., 2005; Jang, 2016; Vilia *et al*., 2017; Lunsford *et al*., 2018), reflected in national and international educational standards (UNESCO, 2014, 2017). It dictated the necessity of simultaneous forming and development of

comprehensive cognitive abilities of the students of either specific discipline or set of disciplines (Booth *et al.*, 2017). However, the authors of innovative cognition-focused approaches to the creation of the educational environment for physics and mathematics, such as R. Teodorescu, C. Bennhold, G. Feldman, and L. Medskerb from George Washington University (Teodorescu *et al*., 2014) noted, that new educational materials and means were oriented at the necessity of student's active participation in cognitive processing of educational information, but they di not solve the problems arising with the cognitive organization of work. In the works of these authors, descriptions were found and evaluations of the success of the problem-focused learning in physics while taking into account cognitive processes necessary for the successful completion of assignments.

The forms of knowledge monitoring that existed in most countries did not include reproductive actions during all types of tests, including questionnaires, in person and online testing, but rather entail the use of all cognitive abilities (for example, SAT (SATM) (Gierl *et al*., 2005; Lunsford *et al*., 2018). Additionally, the new forms of education described in the study (Nikulova and Bobrova, 2016) involved a significant cognitive burden on students, already at the stage of planning their educational trajectory, collecting and selecting necessary and sufficient information, virtual and real-life project creation.

The absolute priority was the ability to think independently and apply SCS in practice (DTEUH, 2015; Yilmaz, 2011; Vilia *et al.*, 2017). This was a fact that reflected the imperative demands of the society for thinkers, able to pose questions and find answers based on experience and information available in the digital environment (Coyle, 2019). Moving further with the study, the older respondents' opinions began to differ from those of the younger. Teachers attributed success in education to cognitive abilities and skills, which comprised the gist of critical thinking (Booth *et al.*, 2017, Tolstenko *et al.*, 2019). The students were geared towards instant results and assign a second place to the skills of quickly switching between the types of cognitive activity. These abilities were customary for one of the education styles – "activist", where the users of this style preferred action, often at the expense of consideration. However, subsequently, the order of succession of cognitive abilities and skills in descending order of importance exactly corresponded to that established by teachers with a shift of one position. (Lunsford *et al.*, 2018). "Tendency to test ideas through experience" and "ability to act and arrive at conclusions quickly and decisively" was the lowest in the ranking order, where the general range of every cognitive component was calculated. This was possibly the result of partial virtualization of the service industry, including educational services (Teodorescu *et al*., 2014; Mutmainah *et al*., 2019).

Based on the collective opinion of all participants of the study, completing assignments was ranked as the most difficult among the disciplines considered. In the study, it was determined that the most popular among both the teachers and the students were the resources, oriented at the description of approaches to solving problems of an advanced level of complexity. This indirectly confirmed that both sides of the educational process were interested in possession of specific skills (74% – teacher's evaluation, 61% – students of humanities, 53% – Math students). One of the main obstacles to solving problems in physics was the inability to analyze the set condition and, therefore, the "Where Did I Begin" type of challenges that followed. The reason was that the students underestimated the importance of analysis and synthesis of knowledge obtained and the skills required to apply that knowledge in new conditions. Surprising was also the underestimation of operations used by students to generalize and systematize knowledge. This testified to the low level of metacognitive skills for intellectual self-evaluation. Students were more often fixated on memorizing the facts, laws, and rules at the expense of thinking about their manifestations, limitations, and essence. Teachers saw cause-and-effect connections between successfully mastering the subject and a higher level of SCS, including components of critical thinking (see Figure 1). They considered lab work and oral answers the easiest. However, it was difficult for the students to formulate conclusions based on the results of lab work. Significant differences were also observed in both groups of respondents when comparing complex action choices while studying math. Analytical activities proved most problematic: 57% of teachers considered the analysis of graphic assignments and their results most difficult, and 53% assigned the highest level of difficulty to work with equations. Opinions differed mostly on evaluating the level of difficulty in expressing one of the approaches: 49% of teachers against 9–14% of students. However, this is a critical skill for STEM. Teachers considered oral answers and

building graphs the least difficult in math. The common trend was clear – it was the orientation of students towards reproductive education and simple actions.

## 3. RESULTS AND DISCUSSION:

### 3.1. Stage I. Determination of significant challenges in execution of educational activities

As shown in Figure 2, the types of educational activities for STEM disciplines connected to SCS of students are different for physics as compared to mathematics.

Respondents had to choose 1-3 positions out of the list offered and answer which of the educational activities are most difficult for students. Results for physics are shown in Figures 3 and 4. Letters represent activities shown in Figure 2.

According to teachers, the most difficult in physics is problem-solving (74%), knowledge generalization and systematization (65%), and control/diagnostics (59%).

Light color columns in Figure 4 – represent the answers of humanities students (HS), dark – those of students of math (EM). Students in both groups consider solving physics problems most difficult (53% math students and 61% – humanities students). Second in difficulty are diagnostics when connected to problem-solving.

The least difficult in physics, according to students, is generalization and systematization of knowledge, and according to teachers – oral answers and lab work. The assessment results of difficulties in the study of mathematics are given in Figures 5 and 6.

More than half (57%) of teachers opine that the most difficult is graphs analysis, while 53% think it is equations. 49% noted significant difficulties with an expression of one quantity. According to teachers, the least difficult are oral answers and building graphs.

Math students did not demonstrate that they have a domineering difficulty: each activity received 22-30% of the votes. Humanities students chose F, which corresponds to graphs analysis (41%). Most of the teachers (57%) concurred. Next in the level of difficulty, according to teachers, are equations (53%) and diagnostics (41%). Students consider the expression of one of the quantities the easiest (D): 14% of Math students and 9% Humanities students. However, 49% of teachers consider this task difficult because it often leads to errors in problem-solving. According to teachers, graph building is the least difficult.

These differences are most likely due to students expressing opinions on how they feel in the process of various educational activities and the teachers describing impressions derived from the results of educational activities.

### 3.2. Stage II. Determination of the most significant cognitive abilities and skills used in the execution of educational tasks

The success of the educational process is closely connected with cognitive abilities and cognitive skills (cognitive competencies). Respondents were offered to rank the cognitive competencies in demand for the STEM set of disciplines (Figure 2).

According to the hypothesis, there is a connection between cognitive abilities and corresponding applicable cognitive skills (Figure 7).

In part II of the questionnaire, it is asked the respondents to rank abilities and skills necessary for one type of educational activity by dragging each position up or down, according to its subjective significance. The information was particularly interested in the following two aspects:

- Which SCS are important for teachers, vs. for students
- What is the connection between cognitive abilities and skills?

Four types of activities significant for the STEM set of disciplines were selected for ranking:

1. Lab work completion;
2. Tasks solving in physics and mathematics;
3. Graphical tasks solving;
4. Preparation for control and diagnostics measures.

Results of ranking cognitive abilities and skills necessary for successful completion of lab work are shown in Tables 1 and 2.

Figures in the top horizontal row of the table signify rank (place by significance) of the ability or skill; letters listed vertically in the far left column correspond to cognitive abilities and skills from the original list. Poll results are presented as percentage points of the total number of teachers.

To determine the significance of cognitive abilities and skills based on the aggregate data, the generalized rank is calculated (GR) by Equation 1:

$$GR = \sum_{i}^{N} \frac{x_i}{k_i}, \quad \text{(Eq. 1)}$$

Where $x_i$ – frequency of selection of this position during ranking of the specific cognitive component (A-H) in percentage points; $k_i$ – the meaning of the rank; $N$ changes from 0 to 8 by the number of positions in the list.

Teachers consider most important for lab work the ability to think independently and apply skills and abilities to solve the problems that arise (in grey) (B) and tendency to test ideas through personal experience (F).

The meaning of EMR – the result of GR for Math students; HumR's component – GR for Humanities students. According to students, the most important is the ability to think independently and apply skills and abilities to solve problems that arise (B).

Similar calculations were conducted for other types of activities. Tables 3 and 4 demonstrate *GR* by type of educational activity.

***Table 3.*** *GR of cognitive abilities and skills (teachers). (Source: the author)*

| | 1 | 2 | 3 | 4 |
|---|---|---|---|---|
| **A** | 26.046 | 24.824 | 26.991 | 26.329 |
| **B** | 57.669 | 60.867 | 51.333 | 45.067 |
| **C** | 29.056 | 33.25 | 35.807 | 30.955 |
| **D** | 27.706 | 23.136 | 22.412 | 28.491 |
| **E** | 28.527 | 64.552 | 57.067 | 44.236 |
| **F** | 29.824 | 24.757 | 43.519 | 59.712 |
| **G** | 21.18 | 17.586 | 15.471 | 19.393 |
| **H** | 50.095 | 17.723 | 16.592 | 14.82 |

The experts (teachers) designated the ability to think independently and apply skills and abilities as the absolute leader among all types of activities considered (B); for laboratory work, it is important to have a tendency to test ideas empirically (H); for types 2-4 also important is the ability to think rationally and logically (D); and for diagnostics preparation most important is systematization (F).

Schoolchildren opinions differ from expert ones. Globally important for them is thinking independently and applying skills and abilities for solving the problems that arise (B); to successfully solve physics and mathematics problems. Math students selected the ability to think rationally and logically (E); for solving graphic problems and preparing for control, the skills that allow switching fast are significant (A).

### 3.3. Stage III. Determination of correlation of cognitive abilities and skills

To verify the original hypothesis that cognitive abilities and skills correlate, the Pearson linear correlation coefficient was calculated for the teachers' answers, paired, at the expert selection. Critical value of Pearson coefficient for $n$ = 105, degree of freedom $df = N - 2 = 102$, $r_{кр}$ = 0.194 for the probability of significance value $p$ = 0.05 of one criterion (sample of more than 30 participants).

Most prominent are inverse correlations ($p < 0$) between most abilities and skills. However, for GA, in all cases, there is a pronounced direct correlation. Less pronounced are the correlations in other pairs of "ability-skill". It can conclude that the most pronounced ability to think independently and apply skills and abilities (B) is most correlated with the skills of anticipation of possible problems and taking others' experience into account (D). Ability to think logically and rationally (E) – with systematizing the data and arriving at conclusions. (F). Additionally, there is a definite correlation between abilities E and B and between ability H and skill D.

Inverse correlations appear rather interesting, and among the most pronounced are BH (- 0.550), AE (-0.500), DE (-0.537), FG (-0.508). Therefore, it can state with certainty that cognitive components in pairs "Ability to think rationally and logically", "Skills of quick switching between types of cognitive activity", "Ability to think independently and apply skills and abilities to problem-solving", "Tendency to test ideas through experience", "Ability to act and draw conclusions quickly and decisively", and "Skills to systematize data and draw conclusions" are in anti-phase. It is possibly not the abilities that influence the development of these skills, but rather the personality type of the students, which predetermines the genetic contradiction between "speed" and "systematic approach" in students, where the educational process is concerned.

The analysis of the generalized range of cognitive competencies, based on the questionnaire's results, allowed ranking them in

the order of decreasing significance to the success of educational activities (Figure 8).

Deviation in students' answers can be due to metacognitive aspects of educational activities (14), an emotional reaction (1), for example, for humanities students, who evaluate activities in subject matters that are not most important to them. The results derived correlate with the process and skills analysis, in general, by the novices (in this case – students) and experts (teachers). Novices immediately move to the process of obtaining a solution (cognitive skills of lower level), using the already known algorithms and procedures, and they do not always understand the results they receive. Experts begin with the analysis – of the conditions and specifics of the situation. They finish with analysis, too – to verify that the result or answer is justifiable and valid. Experts are aware of their own approaches to problem solving and skills, identifying strengths and weaknesses. Novices suffer cognitive overload (selective insufficiency of separating what is essential) and spend their intellectual resources on procedures. R. Teodorescu points out the necessity to help students form "advanced habits" (sustainable skills) for categorization, classification, and schematization of problems (Teodorescu *et al*., 2014).

Undertaking the correlation analysis in pairs of cognitive ability-cognitive skills allowed to correct the initial assumptions about their interconnection. The changes mostly pertain to the central part of the chart, where a strong connection was discovered between the ability to think rationally and logically and skills of data systematization and the ability to think independently and apply skills and abilities. The anti-phase of abilities to rational and logical thinking (E) and skills to anticipate possible problems and consider others' mistakes and experience (D), most likely, is due to these components being part of different types of activities – thinking and procedural. Therefore, as a result of the correlation analysis between cognitive components, the pattern of interconnections of skills and abilities have changed, new connections were identified, and it can presume they are related to the change in conditions of the educational process implementation (Gierl *et al*., 2005; Villafañe and Lewis, 2016; Vilia *et al.*, 2017; Lunsford *et al*., 2018; Mutmainah *et al*., 2019) (Figure 9).

Based on the number of connections, the leader of the chart is the ability to think rationally and logically – the gist of critical thinking.

## 4. CONCLUSIONS:

Thus, the types of studies that presented the most difficulties to students were identified and the interconnection between the cognitive competencies. Differences were revealed when comparing the answers of both groups of respondents about the complexity and importance of educational actions in the study of physics and mathematics and the attitude type of schoolchildren to the reproductive level of education or the clearest and memorable algorithms of actions. Competencies most significant to the success of the educational process were extrapolated. Correlation analysis in pairs of cognitive ability/cognitive skill made it possible to correct the initial ideas about their relationship. The data derived from this study allow to correct and design the educational process in the digital environment more consciously and to take into account the points of view of both students and teachers about the demands in developing their cognitive skills. The data collected allowed establishing the complexity of the educational activities and significant cognitive subject-applied abilities and skills. Systematizing the results of studying the subjective opinions of students and teachers about the importance of cognitive competencies for STEM makes it possible to purposefully transform the educational process, taking into account the needs of its participants and society. Therefore, modern education aims to overcome the disconnection between thinking skills and the ability to act. It is to keep the educational process for students to create stimuli and motivation to act while thinking and think while keeping the next action in mind.

## 5. ACKNOWLEDGMENT:

In closing, the authors wish to express sincere gratitude to the Expert Committee responsible for grading the Unified State Exam in physics in the Lipetsk region. Their professional contributions to the questionnaire increased the quality of results and provided with certainty about the necessity and importance of this study's subject matter.

## 6. REFERENCES:


1. Ardura, D., and Pérez-Bitrián, A. (2019). Motivational pathways towards academic achievement in physics and chemistry: A comparison between students who opt out and those who persist. *Chemistry Education Research and Practice*, *20*, 618–632.
2. Booth, J. L., McGinn, K. M., Barbieri, C., Begolli, K. N., Chang, B., Miller-Cotto, D., Young, L. K. and Davenport, J. L. (2017). Evidence for cognitive science principles that impact learning in mathematics. In D. C. Geary, D. B. Berch, R. Ochsendorf and K. M. Koepke (Eds.). *Acquisition of complex arithmetic skills and higher-order mathematics* (pp: 297–325). London: Elsevier.
3. Cognitive Skills questionnaire (CSQ). (2020). https://testograf.ru/ru/oprosi/aktualnie/0170d0e97fd349eee.html
4. Coyle, T. R. (2019) Tech tilt predicts jobs, college majors, and specific abilities: Support for investment theories. *Intelligence*, *75*, 33–40.
5. Department of Teacher Education University of Helsinki (DTEUH). (2015). Innovative schools: Teaching and learning in the digital era. Brussels: European Parliament. https://www.europarl.europa.eu/RegData/etudes/STUD/2015/563389/IPOL_STU(2015)563389_EN.pdf
6. Ertmer, P. A., and Newby T. J. (2013). Behaviorism, cognitivism, constructivism: comparing critical features from an instructional design perspective. *Performance Improvement Quarterly*, *26*(2), 43–71.
7. Etkina, E., and Planinšič, G. (2015). Defining and developing 'critical thinking' through devising and testing multiple explanations of the same phenomenon. *Physics Teacher*, *53*(7), 432–437.
8. Gierl, M. J., Tan, X., and Wang, C. (2005). Identifying content and cognitive dimensions on the SAT (Ser.: College Board Research Report, No. 11). New York: The College Board. https://files.eric.ed.gov/fulltext/ED562685.pdf
9. Jang, H. (2016). Identifying 21st century STEM competencies using workplace data. *Journal of Science Education and Technology*, *25*, 284–301.
10. Lunsford, M. L., Poplin, P. L., and Pederson, J. G. (2018). From research to practice: Using assessment and early intervention to improve student success in introductory statistics. *Journal of Statistics Education*, *26*(2), 125–134.
11. Marzano, R. J., and Kendall, J. S. (2007). The new taxonomy of educational objectives. Thousands Oaks, USA: Corwin Press.
12. Mutmainah, M., Taruh, E., Abbas, N., and Umar, M. K. (2019). The influence of blended learning-based guided inquiry learning model and self-efficacy on students' scientific literacy. *European Journal of Education Studies*, *6*(6), 137–150.
13. Nikulova, G. A., and Bobrova, L. N. (2016). Online education resources and student needs: Stylistic aspects. *Indian Journal of Science and Technology*, *9*(42), 1–10.
14. Parameswar, H. (2018). Developing problem solving and critical thinking skills in physics and engineering physics courses. https://www.researchgate.net/publication/237638083_Developing_Problem_Solving_and_Critical_Thinking_Skills_in_Physics_and_Engineering_Physics_Courses
15. Santoso, T., Yuanita, L., and Erman, E. (2017). The role of student's critical asking question in developing student's critical thinking skills. *Journal of Physics: Conference Series*, *953*, 012042.
16. ,Teodorescu, R. E., Bennholda, C., Feldman, G., and Medskerb, L. (2014). Curricular reforms that improve students' attitudes and problem-solving performance. *European Journal of Physics Education*, *5*(1), 15–44.
17. Tolstenko, A., Baltovskij, L., and Radikov, I. (2019). Chance of civic education in Russia. *Sage Open, 9(3),* 1–16.
18. UNESCO. (2014). Unesco education strategy 2014-2021. Paris: Unesco. https://unesdoc.unesco.org/ark:/48223/pf0000231288http://www.unesco.org/new/fileadmin/MULTIMEDIA/FIELD/Santiago/pdf/

Habilidades-SXXI-Buenos-Aires-Eng.pdf

19. UNESCO. (2017). E2030: Education and skills for the 21st century January 31, 2017. Paris: Unesco. http://www.unesco.org/new/fileadmin/MULTIMEDIA/FIELD/Santiago/pdf/Habilidades-SXXI-Buenos-Aires-Eng.pdf
20. Vilia, P. N., Candeias, A. A., Neto, A. S., Franco, G. S., and Melo, M. (2017), Academic achievement in physics-chemistry: The predictive effect of attitudes and reasoning abilities. *Frontiers in Psychology*, *8*, Article 1064.
21. Villafañe, S. M., and Lewis, J. E. (2016). Exploring a measure of science attitude for different groups of students enrolled in introductory college chemistry. *Chemistry Education Research and Practice*, *17*(4), 731–742.
22. Wilson, L. O. (2016). Anderson and Krathwohl Bloom's taxonomy revised: Understanding the new version of Bloom's taxonomy. – https://quincycollege.edu/content/uploads/Anderson-and-Krathwohl_Revised-Blooms-Taxonomy.pdf
23. Yilmaz, K. (2011). The cognitive perspective on learning: its theoretical underpinnings and implications for classroom practices. *The Clearing House*, *84*, 204–212.
24. Yuliati, L., Fauziah, R., and Hidayat, A. (2018) Student's critical thinking skills in authentic problem based learning. *IOP Conf. Series: Journal of Physics*, *1013*(1), Article 012025.

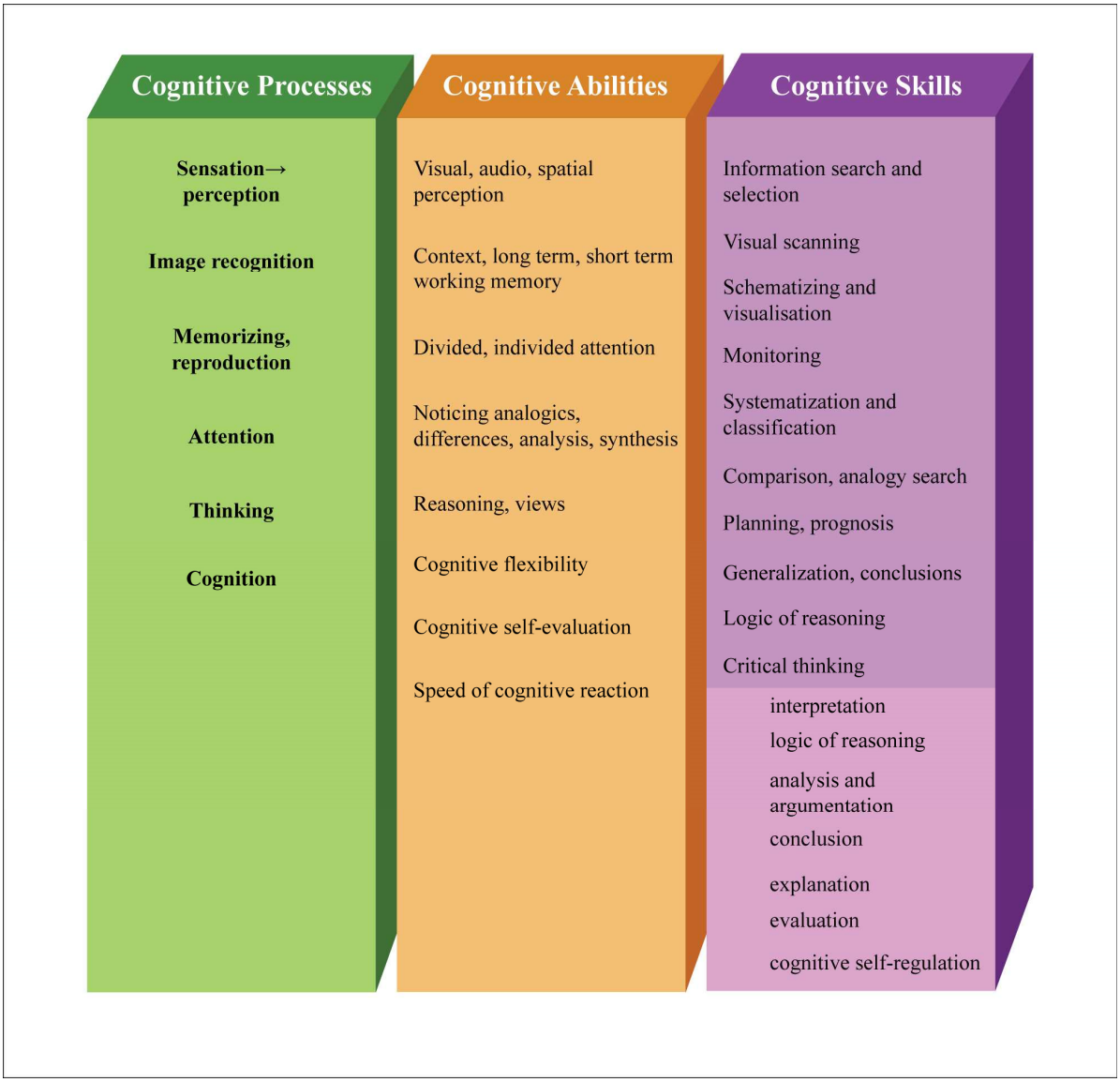


***Figure 1.*** *Differentiation of general cognitive processes, abilities, skills. Source: the author*

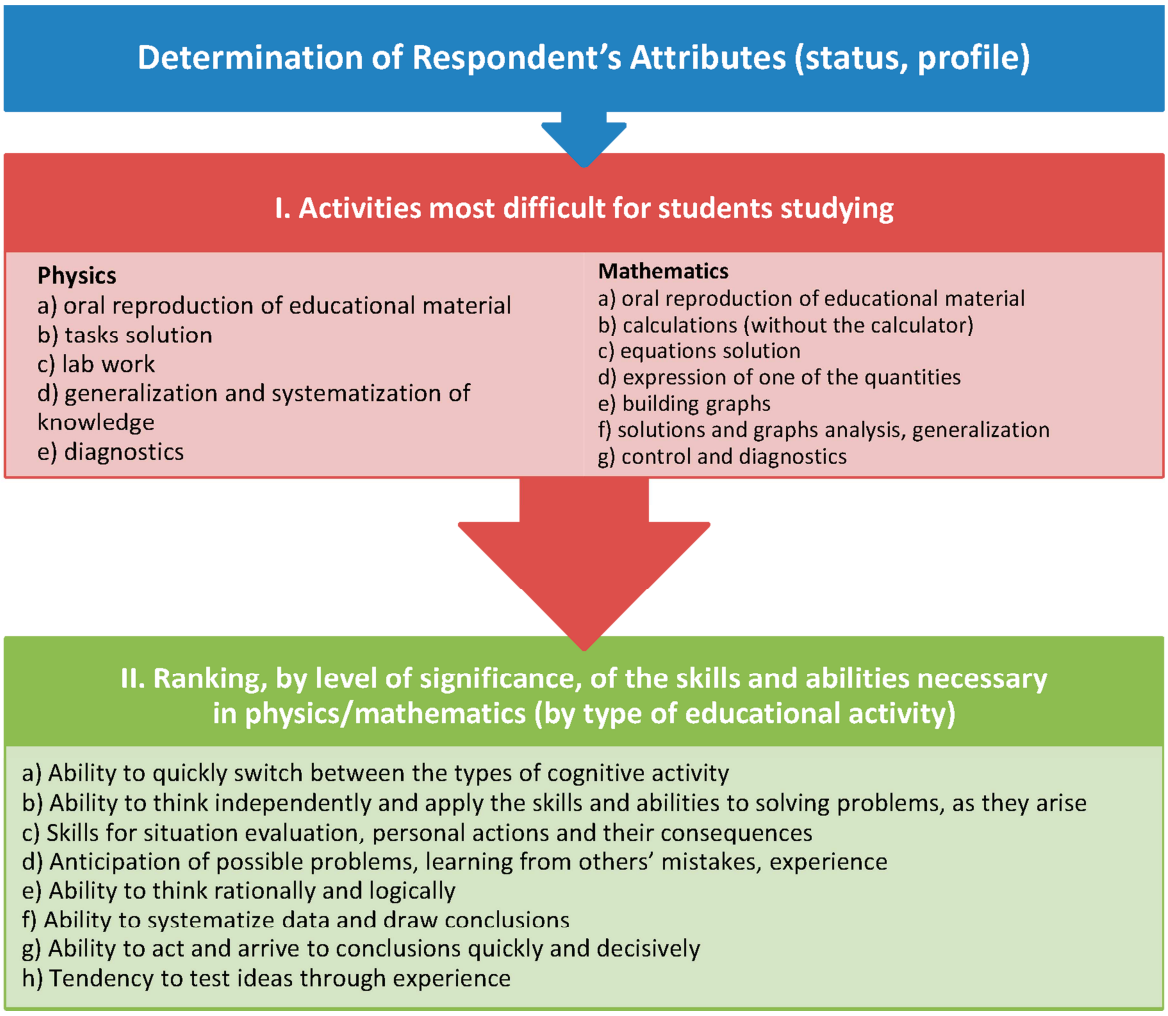


***Figure 2.*** *Cognitive skills questionnaire. Source: the author*

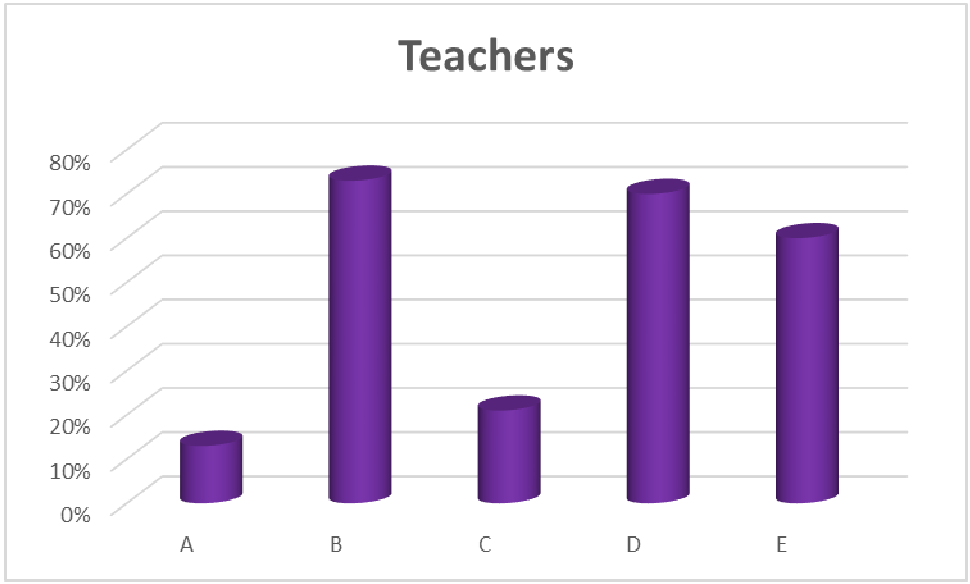


***Figure 3.*** *Ranking of the main challenges that students of physics face (teachers' opinions). Source: the author*

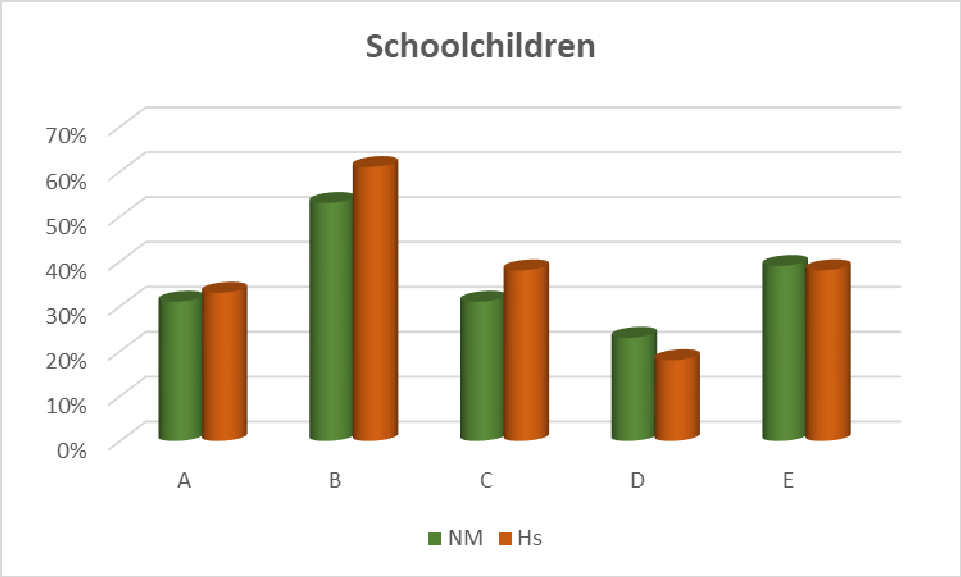


***Figure 4.*** *Ranking of the difficulties in studying physics (students' opinion). Source: the author*

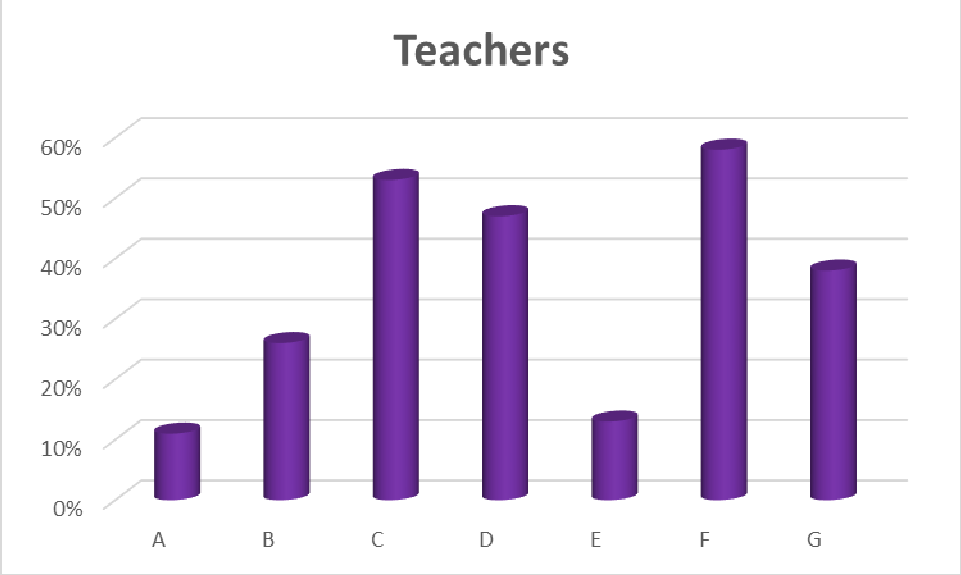


***Figure 5.*** *Ranking of the difficulties in studying math (teachers' opinion). Source: the author*

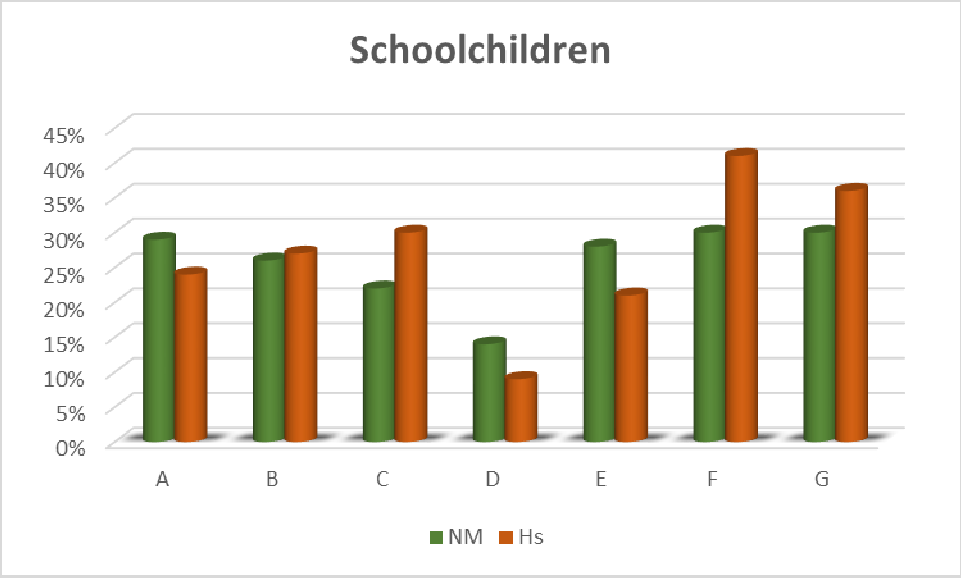


***Figure 6.*** *Ranking of the difficulties while studying math (students' opinion). Source: the author*

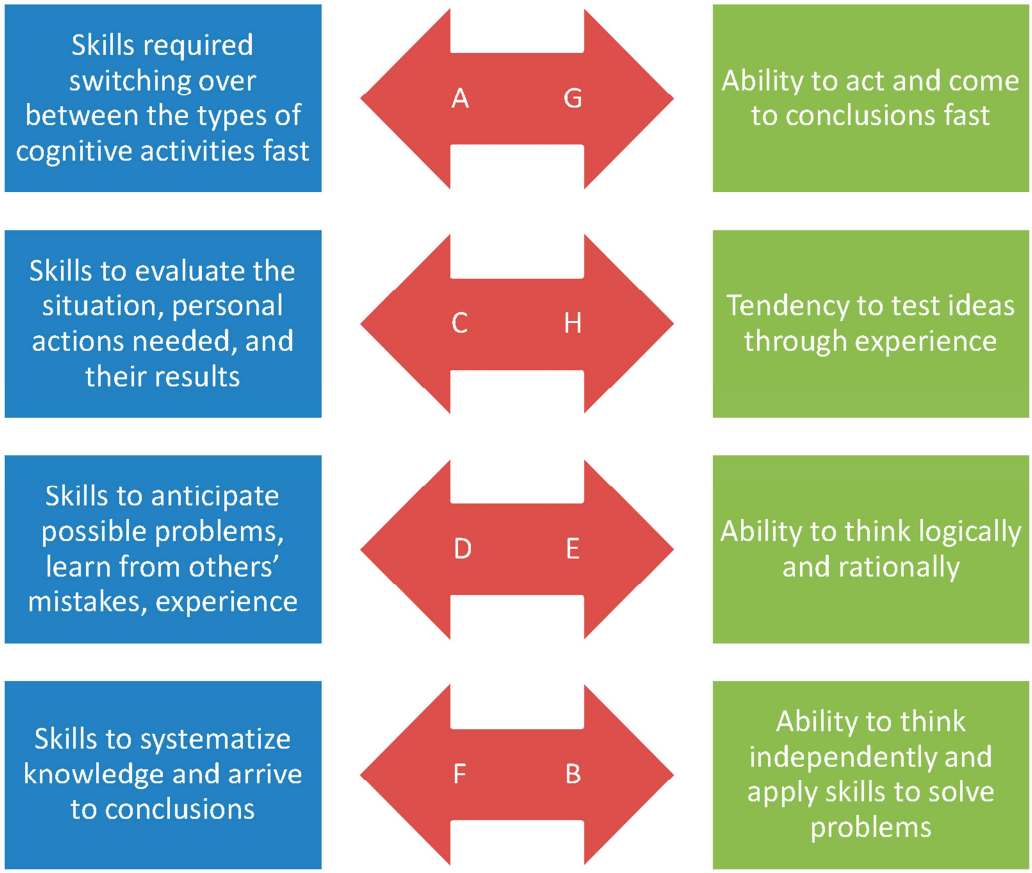


***Figure 7.*** *Correlation between cognitive abilities and SCS. Source: the author*

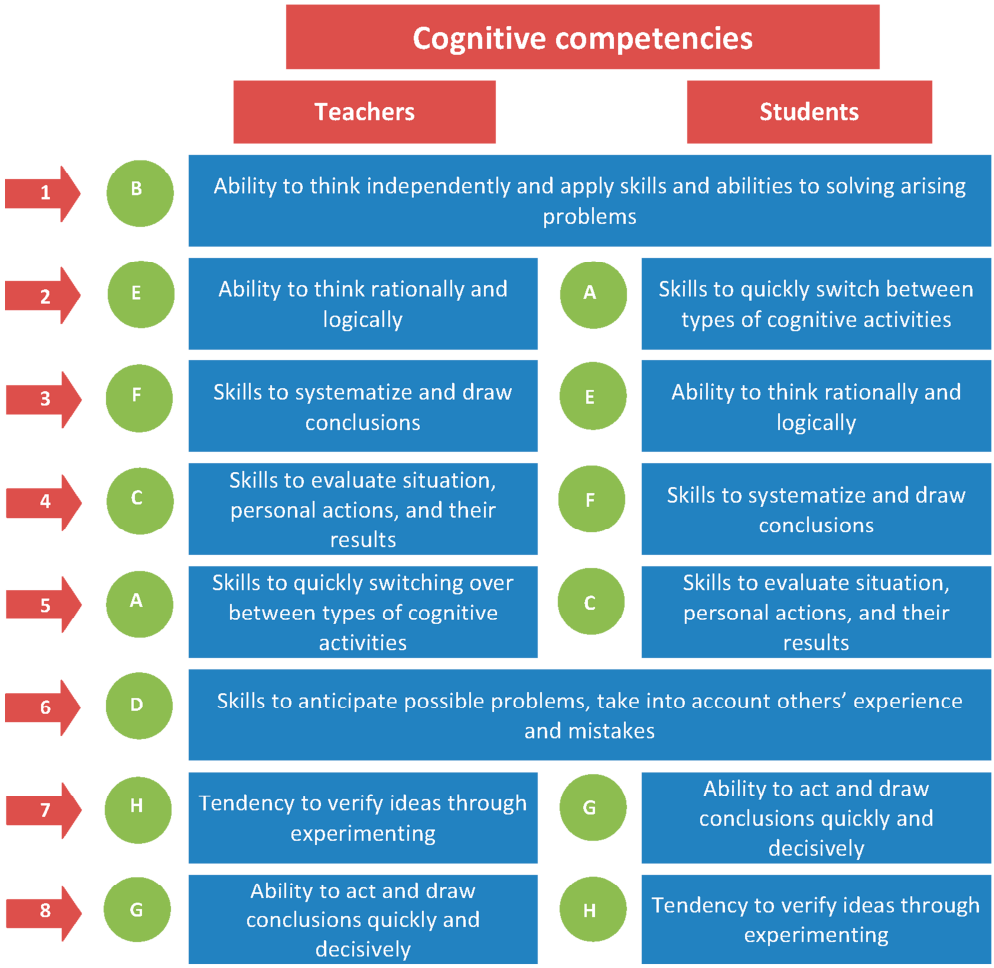


***Figure 8.*** *Ranking of cognitive competencies by their significance to the educational process. Source: the author*

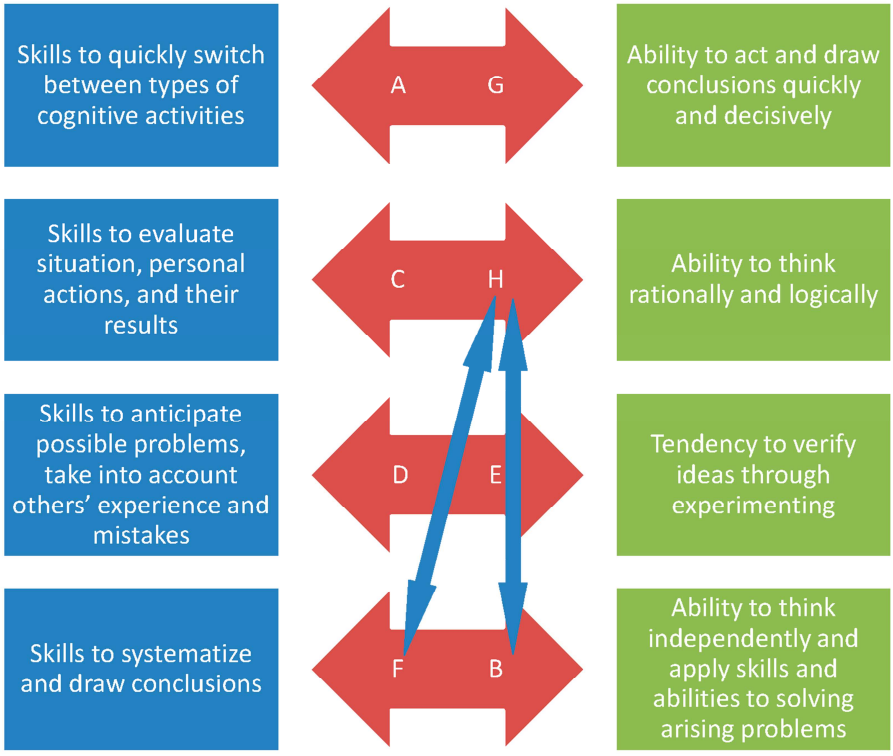


***Figure 9.*** *Correlations between cognitive abilities and cognitive skills after verification of correlation parameters. Source: the author*

***Table 1.*** *Results of ranking SCS and cognitive abilities by teachers (for lab work), %. Source: the author*

| Types of activity/cognitive components | 1 | 2 | 3 | 4 | 5 | 6 | 7 | 8 | GR |
|---|---|---|---|---|---|---|---|---|---|
| **A** | 6 | 7 | 13 | 13 | 8 | 10 | 18 | 25 | 26.04643 |
| **B** | 37 | 19 | 17 | 7 | 14 | 4 | 2 | 0 | 57.66905 |
| **C** | 3 | 18 | 16 | 14 | 19 | 11 | 12 | 7 | 29.05595 |
| **D** | 3 | 18 | 7 | 18 | 16 | 17 | 12 | 9 | 27.70595 |
| **E** | 4 | 15 | 12 | 17 | 16 | 22 | 9 | 5 | 28.52738 |
| **F** | 6 | 13 | 17 | 13 | 14 | 21 | 6 | 10 | 29.82381 |
| **G** | 3 | 3 | 11 | 9 | 7 | 10 | 32 | 25 | 21.17976 |
| **H** | 36 | 7 | 7 | 10 | 5 | 5 | 10 | 20 | 50.09524 |

***Table 2.*** *Results of ranking SCS and cognitive abilities by students (for lab work), %. Source: the author*

| | 1 | | 2 | | 3 | | 4 | | 5 | | 6 | | 7 | | 8 | | MathR | HumR |
|---|---|---|---|---|---|---|---|---|---|---|---|---|---|---|---|---|---|---|
| | Math | Hum | Math | Hum | Math | Hum | Math | Hum | Math | Hum | Math | Hum | Math | Hum | Math | Hum | | |
| A | 15 | 12 | 11 | 5 | 9 | 9 | 7 | 16 | 10 | 14 | 8 | 10 | 11 | 17 | 29 | 17 | 33.78 | 30.52 |
| B | 34 | 29 | 23 | 21 | 16 | 27 | 7 | 7 | 11 | 9 | 5 | 2 | 2 | 3 | 2 | 2 | 56.15 | 53.06 |
| C | 3 | 9 | 10 | 19 | 13 | 22 | 27 | 14 | 17 | 9 | 15 | 18 | 8 | 7 | 7 | 2 | 27.00 | 35.38 |
| D | 7 | 7 | 7 | 9 | 1 | 12 | 19 | 16 | 21 | 16 | 14 | 17 | 14 | 9 | 7 | 14 | 28.33 | 28.57 |
| E | 14 | 18 | 22 | 21 | 7 | 12 | 14 | 13 | 12 | 16 | 17 | 6 | 9 | 8 | 5 | 6 | 37.98 | 41.84 |
| F | 11 | 12 | 12 | 10 | 24 | 5 | 6 | 16 | 9 | 5 | 17 | 22 | 11 | 21 | 10 | 9 | 33.95 | 31.46 |
| G | 5 | 7 | 7 | 9 | 8 | 9 | 13 | 12 | 10 | 21 | 13 | 10 | 31 | 18 | 13 | 14 | 24.0 | 27.69 |
| H | 9 | 5 | 9 | 5 | 12 | 3 | 8 | 7 | 9 | 16 | 12 | 12 | 14 | 16 | 27 | 36 | 28.68 | 22.24 |

***Table 4.*** *GR of cognitive abilities and skills (schoolchildren). Source: the author*

| | 1 | | 2 | | 3 | | 4 | |
|---|---|---|---|---|---|---|---|---|
| | Math | Hum | Math | Hum | Math | Hum | Math | Hum |
| **A** | 33.78 | 30.52 | 43.87 | 37.75 | 46.94 | 51.34 | 52.05 | 44.42 |
| **B** | 56.15 | 53.06 | 52.57 | 56.79 | 46.98 | 47.49 | 43.71 | 50.35 |
| **C** | 27 | 35.38 | 31.73 | 34.72 | 31.2 | 32 | 32.57 | 35.5 |
| **D** | 28.33 | 28.57 | 23.4 | 24.01 | 23.63 | 23.87 | 35.49 | 26.75 |
| **E** | 37.98 | 41.84 | 49.75 | 45.45 | 40.35 | 39.67 | 27.51 | 32.56 |
| **F** | 33.95 | 31.46 | 31.73 | 27.29 | 39.71 | 34.19 | 33.57 | 36.89 |
| **G** | 24.64 | 27.69 | 20.26 | 27.68 | 20.29 | 25.29 | 25.23 | 28.51 |
| **H** | 28.68 | 22.24 | 22.24 | 18.37 | 22.7 | 20.15 | 21.29 | 16.33 |

## Appendix. The questionnaire

### Cognitive skills in learning activities

**Welcome to our survey page!**
**It will not take much time, but it can significantly help teachers and organizers to correctly and effectively build the educational process itself.**
**Thank you very much for your participation!**

**- Your status (in relation to training)**
• student
• teacher
• schoolboy
• parent
• administrator
- **What class do you study in?**
**- Indicate the form of training**
**- What is the profile of the direction of your study/teaching**
**- What types of educational activities cause the greatest difficulties in the study of physics?** *you can choose several answers, but no more than 3*
• oral reproduction of educational material
• solving problems
•laboratory works
• generalization and systematization of knowledge
• control and diagnostic measures
**- What types of learning activities are the most difficult when studying mathematics?** *You can choose several answers, but no more than 3*
• verbal response
• performing calculations (without a calculator)
• solving equations
• expression of one of the quantities
• plotting
• graph analysis
• control and diagnostic measures
**- Rank the skills, abilities, and abilities required to successfully complete laboratory work (for example, physics, chemistry, etc.)**
*You should grab the desired item with the mouse and drag it to the appropriate place. The most important points should be higher*
 Skills to quickly switch between types of cognitive activities during academic work
 Ability to think independently and apply skills and abilities to solve emerging problems
 Skills in assessing the learning situation, their actions, and their results
 Skills of anticipating possible problems and taking into account other people's experience, mistakes
 Ability for rational and logical thinking
 Skills to organize data and draw conclusions
 Ability for quick and decisive action and conclusions
 A tendency to test ideas empirically
**- Rank the skills, abilities, and abilities required to successfully solve physics and math problems in order of importance** *You should grab the desired item with the mouse and drag it to the appropriate place. The most important points should be higher*
 Skills to quickly switch between types of cognitive activities during academic work
 Ability to think independently and apply skills and abilities to solve emerging problems
 Skills in assessing the learning situation, their actions, and their results
 Skills of anticipating possible problems and taking into account other people's experience, mistakes
 Ability for rational and logical thinking
 Skills to organize data and draw conclusions
 Ability for quick and decisive action and conclusions
 A tendency to test ideas empirically
**- Rank the skills, abilities, and abilities needed to successfully solve graphics problems (physics, mathematics)** *You should grab the desired item with the mouse and drag it to the appropriate place. The most important points should be higher*
 Skills to quickly switch between types of cognitive activities during academic work
 Ability to think independently and apply skills and abilities to solve emerging problems
 Skills in assessing the learning situation, their actions, and their results
 Skills of anticipating possible problems and taking into account other people's experience, mistakes
 Ability for rational and logical thinking

 Skills to organize data and draw conclusions
 Ability for quick and decisive action and conclusions
 A tendency to test ideas empirically

**- Rank the skills, abilities, and abilities necessary for successful preparation for control and diagnostic activities (systematization, generalization of training materials, creation of reference notes)** *You should grab the desired item with the mouse and drag it to the appropriate place. The most important points should be higher*

 Skills to quickly switch between types of cognitive activities during academic work
 Ability to think independently and apply skills and abilities to solve emerging problems
 Skills in assessing the learning situation, their actions, and their results
 Skills of anticipating possible problems and taking into account other people's experience, mistakes
 Ability for rational and logical thinking
 Skills to organize data and draw conclusions
 Ability for quick and decisive action and conclusions
 A tendency to test ideas empirically

**- What difficulties are significant when performing laboratory work**? *You can choose no more than 3 answers.*

• assembly of the installation and search for an error if it does not work
• work with equipment (selection of the desired device, setting)
• conducting experiment or measurements
• processing of results (calculations, graphing)
• analysis of experiment results
• formulation of conclusions

**- Name the main difficulties in solving problems and assignments in physics, mathematics, chemistry.** *You can choose several answers, but no more than 3.*

• analysis of the condition of the problem and consideration of where to start solving
• a short record of the condition (given) and the conversion of units into the required system
• building a schedule or diagram according to the condition of the problem
• defining data from a picture or graph
• carrying out mathematical transformations
• analysis of the solution result (for likelihood)

**- Indicate the main difficulties in verbal response** *You can choose several answers, but no more than 3.*

• remember what to tell
• build the logic of the response (sequence)
• highlight the main idea or definition
• explain and prove your point of view with additional questions
• perform a generalization and systematization of the material (classification, conclusions)
• give examples on the topic

The survey was available at the link https://www.testograf.ru/ru/oprosi/aktualnie/0170d0e97fd349eee.html
04/16/2018 (08:47) - 04/16/2019 (12:00)

PERIÓDICO TCHÊ QUÍMICA
ARTIGO ORIGINAL

# UM ESTUDO COMPARATIVO DOS EFEITOS DA OPINIÃO DOS PARES NA ANÁLISE DE SISTEMAS DINÂMICOS EM ESTUDANTES DE TECNOLOGIA DA ELETRICIDADE

# A COMPARATIVE STUDY OF THE EFFECTS OF PEER FEEDBACK IN THE ANALYSIS OF DYNAMIC SYSTEMS ON STUDENTS OF ELECTRICAL TECHNOLOGY

# UN ESTUDIO COMPARATIVO DE LOS EFECTOS DE LA RETROALIMENTACIÓN ENTRE PARES EN EL ANÁLISIS DE SISTEMAS DINÁMICOS DE ESTUDIANTES DE TECNOLOGÍA EN ELECTRICIDAD

MARTINEZ, Fredy[1*]; MARTINEZ, Fernando[1]; MONTIEL, Holman[1]

[1] Universidad Distrital Francisco José de Caldas, Facultad Tecnológica, Bogotá DC. Colombia.

** Corresponding author*
*e-mail: fhmartinezs@udistrital.edu.co*

Received 02 December 2020; received in revised form 26 February 2021; accepted 07 March 2020

## RESUMO

**Introdução**: O COVID-19 chegou de surpresa e, em pouco tempo, mudou os hábitos sociais. O ambiente educacional não ficou imune a essas mudanças e em pouco tempo teve que modificar sua estratégia de treinamento. Uma estratégia generalizada tem sido o treinamento a distância pela Internet. No entanto, em muitos casos, a sala de aula foi transferida para uma plataforma digital sem considerar sua eficácia. Um dos elos do treinamento é a avaliação. Um esquema de avaliação formativa em consonância com a educação a distância é a co-avaliação por pares. Esses esquemas permitem retroalimentar os processos a partir dos resultados, ao mesmo tempo que se modificam hábitos e se estimula a motivação. **Objetivos**: Este estudo tem como objetivo avaliar os efeitos da avaliação por pares como estratégia ativa no modelo transitório de educação a distância de alunos de graduação da Universidade Distrital Francisco José de Caldas. O objetivo é determinar sua utilidade e efeitos na formação dos alunos em dois espaços acadêmicos. **Métodos**: Estes cursos são ministrados nos últimos semestres do programa Tecnologia em Energia Elétrica. O estudo aborda um esquema quase experimental em que duas populações equivalentes são tomadas. A primeira turma é composta por 31 alunos do primeiro semestre de 2020, que atuaram como grupo controle, e a segunda turma é composta por 34 alunos do segundo semestre de 2020 que formaram o grupo de feedback de pares. Como instrumento, o estudo utilizou testes escritos clássicos. **Resultados e Discussão**: Os dados foram coletados por meio de inquéritos e analisados quantitativa e qualitativamente. As conclusões do estudo estabelecem que a técnica de avaliação pelos pares é útil para o reforço de alguns aspectos do processo de formação, nomeadamente para a consolidação de conceitos e motivação para o estudo autónomo. **Conclusões**: Os resultados comparativos indicam que a estratégia tem um impacto positivo ao nível do desempenho escolar, mas também apresenta algum nível de sobrecarga nos alunos, tema não explorado e que suscita necessidade de estudos mais aprofundados.

**Palavras-chave**: *Autonomia, avaliação pelos pares, desempenho acadêmico, avaliação formativa.*

## ABSTRACT

**Background**: The COVID-19 arrived by surprise, and in a very short time, it has changed social habits. The educational environment has not been immune to these changes, and in a short time, it has had to modify its training strategy. A generalized strategy has been distance training through the Internet. However, in many cases, the classroom was moved to a digital platform without considering its effectiveness. One of the links of the training is the assessment. A scheme of formative evaluation in line with distance education is the co-evaluation by peers. These schemes allow feedbacking the processes from results, at the same time that habits are modified, and the motivation is stimulated. **Aims**: This study has the purpose of evaluating the effects of the evaluation by peers as an active strategy in the transitory model of distance education of undergraduate students in the Universidad Distrital Francisco José de Caldas. The objective is to determine its utility and effects in forming the students in two academic spaces. **Methods**: These courses are taught in the last semesters of the Technology in Electricity program. The study addresses a quasi-experimental scheme under which two equivalent populations are taken. The first group comprises 31 students from the first semester of 2020, who operated as a control group, and a second group is made up of 34 students from the second semester of 2020 who formed the peer feedback group.

As an instrument, the study used classic written tests. **Results and Discussion**: The data was collected through surveys and were analyzed both quantitatively and qualitatively. The conclusions of the study establish that the technique of peer evaluation is useful for strengthening some aspects of the training process, particularly for consolidation of concepts and motivation towards autonomous study. **Conclusions**: The comparative results indicate that the strategy has a positive impact in terms of academic performance, but also shows some level of overload in students, a topic not explored, and that raises the need for further study.

**Keywords**: *Autonomy, peer assessment, academic performance, formative assessment.*

## RESUMEN

**Antecedentes**: El COVID-19 llegó por sorpresa, y en muy poco tiempo, ha modificado las costumbres sociales. El entorno educativo no ha sido ajeno a estos cambios, y en poco tiempo ha tenido que modificar su estrategia de formación. Una estrategia generalizada ha sido la formación a distancia a través de internet. Sin embargo, en muchos casos, se trasladó la clase presencial a una plataforma digital sin considerar su eficacia. Uno de los eslabones de la formación es la evaluación. Un esquema de evaluación formativa acorde con la educación a distancia es la co-evaluación por pares. Estos esquemas permiten realimentar los procesos a partir de resultados, al tiempo que se modifican hábitos y se estimula la motivación. **Objetivos**: Este estudio tiene el propósito de evaluar los efectos de la evaluación por pares como estrategia activa en el modelo transitorio de educación a distancia de estudiantes de pregrado en la Universidad Distrital Francisco José de Caldas. El objetivo es determinar su utilidad y efectos en el proceso de formación de los estudiantes en dos espacios académicos. **Métodos**: Estos cursos se imparten en los últimos semestres del programa de Tecnología en Electricidad. El estudio aborda un esquema cuasi-experimental bajo el cual se toman dos poblaciones equivalentes. Un primer grupo está conformado por 31 estudiantes del primer semestre de 2020, los cuales operaron como grupo de control, y un segundo grupo conformado por 34 estudiantes del segundo semestre de 2020 los cuales conformaron el grupo de retroalimentación entre pares. Como instrumento, el estudio utilizó pruebas escritas clásicas. **Resultados y Discusión**: Los datos se recogieron mediante encuestas, y se analizaron cuantitativa y cualitativamente. Las conclusiones del estudio establecen que la técnica de evaluación por pares es útil para fortalecer algunos aspectos del proceso de formación, en particular con respecto a consolidación de conceptos y motivación hacia el estudio autónomo. **Conclusiones**: Los resultados comparativos indican que la estrategia tiene una incidencia positiva en cuanto a desempeño académico, pero evidencia también algún nivel de sobrecarga en los estudiantes, tópico no explorado y que platea la necesidad de un estudio más profundo.

**Palabras clave**: *Autonomía, co-evaluación por pares, desempeño académico, evaluación formativa.*

## 1. INTRODUCTION:

Engineering training is strongly conditioned by the demands of industrial, social, and technological development (De Araújo, Da Costa, Joseph, and Sánchez, 2020; Losada-Gutierrez, Espinosa, Santos-Perez, Marron-Romera, and Rodriguez-Ascariz, 2020; Oksana, Galstyan-Sargsyan, Amparo López-Jiménez, and Pérez-Sánchez, 2020; Oleksenko, 2020). The professional engineer must respond to the development that is intimately linked to the current and future potential of the country (Wang and Chiang, 2020). This implies that economic development depends on the quality of its professionals, which draws an enormous responsibility for higher education institutions (Camelo and González, 2004; Gómez-Llanos and Durán-Barroso, 2020). Within the field of electrical engineering, there are many critical areas for economic and social development, and it is possible to think of the electrical engineer as a cross-cutting professional for all types of industrial activity (Benešová and Tupa, 2017; Martínez, Montiel, and Martínez, 2018). One of these areas corresponds to the control and automation of processes, which goes hand in hand with skills in analyzing dynamic systems and the design of instrumentation and control systems (Martínez, Jacinto, and Montiel, 2019). These professional demands have led to the development of active training strategies that increase the performance in the training process of these future professionals (Tian and He, 2020). One of these strategies is peer assessment as a formative evaluation tool integrated into the professional training process that aims to stimulate critical thinking and the formation of a culture of self-learning (Bin Mubayrik, 2020; Cifrian, Andrés, Galán, and Viguri, 2020).

The education cannot be then to introduce concepts to the students. However, it must be oriented to a good performance of the future professional under any situation, including scenarios not contemplated in their formation process (Roca and Garcia-Valles, 2020). This implies that students become autonomous and aware of their training process (Suraratdecha and

Tayjasanant, 2020). Peer assessment is a strategy to self-reflect by students that can produce meaning in education (Ma, Yan, and Wang, 2020; To and Panadero, 2019). A meaningful learning process includes, in addition to cognitive change, the persistence over time of that change (Ospina and Galvis, 2017; Reynders, Lantz, Ruder, Stanford, and Cole, 2020). Since this permanence is linked to the prior knowledge of the student, it has been observed that the best strategies to develop these meaningful processes are those that invite learning through experience, i.e., active learning (Martínez, Montiel, and Jacinto, 2016; Moleko and Mosimege, 2020). Peer assessment is one of the key activities of active learning. In developing a peer assessment, the student has to analyze the material of his fellow student, synthesize the ideas of the student to understand his position and concepts and evaluate this information to produce an assessment of the process. Also, it is necessary to feedback to the student, an activity that strengthens the theoretical concepts evaluated and enhances the capacity for synthesis and apprehension. Studies have shown that peer assessment increases student motivation and commitment and encourages them to reflect on their training process (Verkade and Bryson-Richardson, 2013).

The student must learn to take ownership of his learning process. This means that he must take ownership of the learning process as an integral part of his development as a person, both socially and professionally. Learning is fundamental to development as an individual and has a strong impact on the development of society. However, an effective and meaningful learning process depends on the ability of the individual to awaken and maintain his or her motivation (Réka *et al*., 2015). The student must be able to orient his training process in such a way that a curious spirit is generated in him to question everything, investigate, read, write, speak with colleagues and experts, and in general develop any action that allows him to critically assimilate concepts (Lamon, Knowles, Hendy, Story, and Currey, 2020). These activities characterize active learning and learning by doing (Huang, Tseng, Jenq, and Ou, 2020). When developing these activities, the processes of analysis, synthesis, and evaluation of the information that is the basis of learning are motivated (Cardozo *et al*., 2020). On the other hand, passive learning is given when the student does not carry out these activities but remains the receiver of information provided by a teacher (Bell, 2020). This type of passive learning does not encourage critical thinking or analysis, which is why the process is less significant and has little impact on the development of the individual.

A self-directed student is one who can successfully control his learning process. This control involves defining what he wants to learn, how he will do this learning, and when. Developing these skills is not easy and implies the existence of a set of motivators. Research and experiences in educational processes have shown that the best motivators are born from the student himself (Forestier, Portelas, Mollard, and Oudeyer, 2020). This intrinsic motivation allows the student to develop self-projection skills, self-study, self-exploration, and in general, to answer the questions of what to learn, how, and when to do it (Réka *et al*., 2015). It is possible to identify some particular characteristics of a self-directed student, for example, his ability to define learning objectives. This is a consequence of his desire to improve and his capacity to evaluate his current state, the resources he has, and the resources he requires. It is also characterized by knowing his capacity to study, which methodology is the most appropriate for his process, and which people could help him to achieve his objectives.

## 2. MATERIALS AND METHODS:

To apply the study to the students, in addition to the data collection instrument (survey), a research protocol was designed with all the details of the study and an informed consent form that was shared with all the participants in the study and accepted by each of them before the application of the instrument. The Bioethics Committee approved these documents and the study of the Universidad Distrital Francisco José de Caldas (CIDC-0041-2021).

The study participants were selected from the last semesters of the program of Technology in Electricity of the Universidad Distrital Francisco José de Caldas. This academic program is developed over six semesters (three years), students belong to the fifth and sixth academic semester. 99% of the Technological Faculty students correspond to young people who recently graduated from their secondary education and come from locations close to the impact area of the technological campus (Villate and Jirón, 2004). This means that more than 85% of these young students come from the lowest social strata (Clavijo, 2018). The ages of the students in the study ranged from 18 to 22 years old, with 83.3% of males and 16.7% of females (Herrera, Jerez, and Vargas, 2013). The students develop the

courses of Dynamic Systems Analysis and Digital Circuits, which is why the area of dynamic systems was selected to evaluate the impact of the strategy. These courses correspond to a representative sample, so it is hoped that the results of the study can be extended to the entire campus community.

Of the total number of participating students, 31 were linked to the study during the first semester of 2020, and this first group was labeled as a control group. These students worked a distance training model without the use of peer evaluation and with a strategy that consisted of adapting the traditional academic processes to the distance video conferencing platform (Gómez, Montiel, and Martínez, 2020). The second group formed by 34 students joined the study during the second semester of 2020, and they maintained a strategy of distance training very similar to the one of the first control group, except that they implemented the peer evaluation approach. This second group was labeled a peer-assessment group. All students (from both the first and second groups) were organized into small groups of two to develop all academic activities (Bustami, Syafruddin, and Afriani, 2018).

The instruments used in this study were:

1. **Thematic oral presentation**. During five sessions with the students by videoconference, the professor presented the criteria for the analysis of dynamic systems, both at a continuous and discrete level. During these sessions, the material provided to the students included a list of the basic tools used in the modeling of different physical systems, details of their use, and a wide range of design examples developed step by step in synchrony with the students. Also, the students were made aware of how to verify these behaviors by simulation, and in the case of digital systems, ways to implement certain combinational circuits were established in Verilog. A video recording of these sessions was made and kept available to students throughout the academic semester.
2. **Peer-fed labs**. Each pair of students must present their results to their classmates through video conferencing every week to develop practical laboratory activity. These laboratory practices include mostly implementing and evaluating specific circuits but sometimes contain simulations, analysis of physical models, or performance analysis. During each presentation, the group receives feedback from both the teacher and the other students. The criteria for development and presentation are similar to all groups, which is why all students have strong criteria for delivering concepts from the work of their peers. At the end of each presentation, the strengths and weaknesses of each group are highlighted.
3. **Written evaluation**. The written evaluation is the classic instrument used in the courses to determine the academic performance of the students. However, the evaluation applied to students had variations that made it more appropriate to the content, methodology, and purpose of the study. For both groups (control and peer assessment), the assessment included items that examined the conceptual interpretation of the students and items that tested their abilities to analyze a given problem situation. In both cases, the work was developed by the pairs of students with the full freedom of action (without supervision) but with restricted development time. The difference in the application of the instrument was that for the control group, the assessment was carried out only by the teacher. In contrast, in the peer assessment group, the peer assessment was conducted by the peer groups under the supervision of the teacher. In the latter case, all students were provided with an evaluation guide instrument with the evaluation criteria and a guide to performing the peer feedback.
4. **Personalized external advice**. For the groups that considered it necessary, additional advisories were made available, requested at the students' discretion. The students clarified specific doubts related to the course and the strategy of peer evaluation. This instrument was used by 12% of the students in the study.

Participants in the peer assessment group were provided with an instrument with the minimum assessment criteria, indicating when an answer is correct, when it is incorrect, why certain answers are incorrect, and how to weigh the development of their peers (Jian-Wei, Chia-Wen, Chu-Ching, and Lung-Chun, 2017). This instrument also contained instructions on how to provide feedback to their peers, emphasizing that this feedback was always mandatory. Students were also instructed that the peer assessment activity was as important as the assessment developed, i.e., that it was part of the course performance grade. Each pair of students assessed the written test of two groups of

students, and two other groups assessed each group of students. The teacher-reviewed the evaluations of the students before giving them feedback, including his evaluation of the work developed by the students, both evaluated and evaluators. These documents were fed back to the students during a videoconference session, during which all the results were socialized. The control group students took a similar written test, but the evaluation and feedback were done only by the teacher. This activity was also developed during a videoconference session.

At the end of each semester, an individual test of overall student performance was conducted. This test was evaluated only by the teacher and was intended to measure the level of proficiency of the two groups and to identify the actual impact of the peer evaluation strategy (Gerald, 2018). The tests applied to both groups were similar in design and structure. They contemplated both conceptual elements of the dynamic systems and specific skills in the analysis and design of control schemes. Again, the test was designed and applied so that the student could use any resource at his or her disposal, with only restrictions on time and number of students (the test was the only individual tool applied in the course). A survey of the peer review group was also developed individually to determine the students' position on the use of this tool.

In the final stage of the study, the researchers performed a micro-analysis of the data collected during the year of the study. This micro-analysis was centered on the individual final tests developed by the students of the two groups. The results were carefully reviewed to identify recurrent errors in each group of students. These errors included misapplication and inconsistencies of concepts, erroneous analysis of certain dynamic models, and inadequate use of code structures in Verilog, regardless of their proper final functioning. The group of researchers developed specific rubrics to weigh the performance in these aspects. These rubrics, normalized in the range of zero to 100, were statistically processed by calculating mean values and applying the Student *t*-test (Alzaid, 2017). For the qualitative analysis, the survey results applied to the students of the peer evaluation group were used.

## 3. RESULTS AND DISCUSSION:

To observe the impact of the peer evaluation on student performance, we calculated descriptive statistics of the results collected from the final tests applied to the two groups (control group and peer evaluation group, Table 1). From these statistics, it can be concluded that all the characteristics evaluated in the final performance of the students showed a significant increase.

Table 2 shows the result of paired samples *t*-test on the features (Bogdanova, Sherstinova, Blinova, and Martynenko, 2017). For the first feature, a significant difference ($P = 0.044 < 0.05$) was obtained between the data of the two groups. This means that the results did not occur by chance and that the peer review strategy led to an improvement in the performance of the students in applying the concepts. In the other three characteristics, a similar result was obtained, the *P* values were low. Therefore the increase in performance concerning the inconsistency of concepts, analysis of dynamic systems, and adequate coding occurred due to the peer evaluation strategy used in the G2 group (peer assessment group). According to the results, our study confirms that there is a significant positive effect on student performance due to the use of peer assessment as part of student learning strategies.

From the analysis of the data, it is observed that the peer assessment group in this study had a positive effect on student performance attributable to the peer assessment strategy, particularly about the analysis and understanding of central concepts of dynamic systems analysis, which led the students in this group to improve their average evaluation by 21% with respect the control group. In terms of dynamic analysis and coding strategies, significant performance increases were also detected as a direct consequence of the strategy.

It was detected that during peer evaluation, students become more sensitive to their weaknesses and strengths, which leads to a critical self-analysis of their performance and a more significant learning process along with the development of the feedback from their peers. The student autonomously identifies the competencies he should strengthen and those in which he is highly competent and transfers this analysis to his peers.

In terms of qualitative analysis, a survey examined the student perceptions of the strategy's usefulness in improving their learning strategy, the contribution of feedback to their training

processes, the contribution to their motivational levels, the degree of satisfaction with the strategy, and considerations regarding the additional burden implied by the strategy. Figures 1 to 6 show the results of some of the most representative questions.

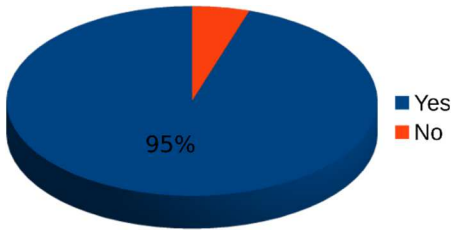


***Figure 1.*** Question: Is the workload adequate to achieve the learning outcomes? Yes or No

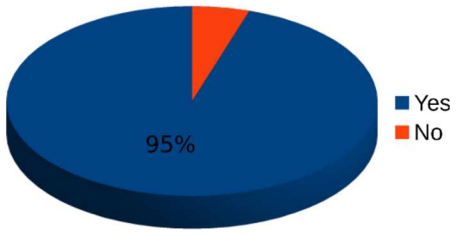


***Figure 2.*** Question: Does the quality of teaching help the student achieve learning outcomes? Yes or No

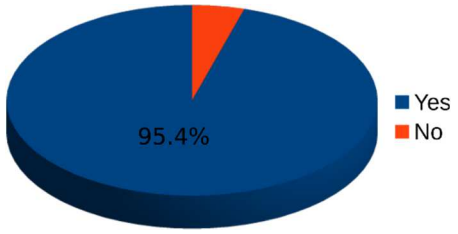


***Figure 3.*** Question: Am I motivated to achieve learning outcomes? Yes or No

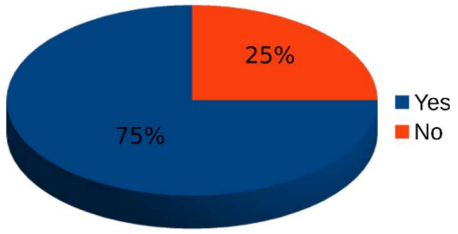


***Figure 4.*** Question: Feedback from my peers improved my learning? Yes or No

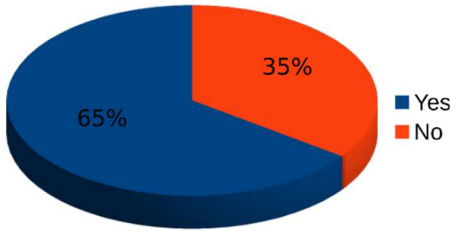


***Figure 5.*** Question: Do you consider that you require additional feedback from the teacher as part of the evaluation and feedback process? Yes or No

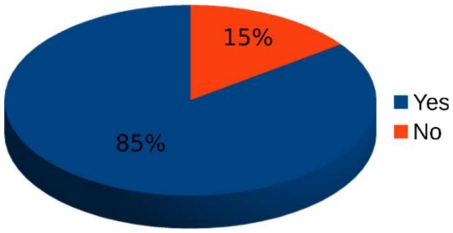


***Figure 6.*** Question: Was the information you received in the peer assessment useful to the course? Yes or No

From these results, it is evident that the peer assessment group students managed to develop some awareness and self-criticism regarding the strategy. While it was observed that students are aware of the increased work involved in developing the peer assessment, there is greater acceptance that the strategy brings many benefits in the sense that it allows strengthening specific weaknesses while at the same time socializing and enhancing strengths. This increased student work translates into more careful attention to concepts and strategies that improved academic performance, strengthened analytical and critical skills, and enhanced motivation in studying the course.

The analysis of the responses of the students shows that the peer evaluation strategy allowed the students to be more critical and responsible for their training process. The answers to the questions show a high degree of awareness of their capabilities and weaknesses, which they identified thanks to the contributions of their peers. The degree of responsibility placed on them by the teacher may make students concentrate more on their performance and the analysis and feedback they provide to their peers. This strengthens their academic capacity and their self-critical level of their professional training (they learn to control their academic progress). While it is true that a more in-depth study is needed to account for the level of additional dedication of the strategy hand in hand with the design of academic credits for a given academic course, it is valid to state at this point that the integrated design of a curriculum with the adoption of these techniques is presented as a promising strategy under an academic environment strongly impacted by social restrictions and isolation.

Another point that requires further study is related to the role of the teacher throughout the

peer evaluation process. Previous research has shown that although the evaluation developed by students in this model tends to be of a good level, the truth is that it is never as accurate and complete as the one developed by the teacher (Salehi, and Daryabar, 2014). This means that the teacher is a fundamental part of the strategy, and must be involved at every stage of the process. This means a greater degree of dedication, something that should also be considered in the design of the curriculum. Also, students should not feel that they are alone in the process (something that can be detected in the responses of the students), on the contrary, they should continuously feel the support of the teacher.

## 4. CONCLUSIONS:

This article presents a study applied to young undergraduate students in electrical engineering that sought to determine the effects of peer evaluation and feedback within the transitional model of distance learning. It aimed to identify the possible effects on specific parameters of training in the area of dynamic systems, and these parameters included the correct and consistent application of concepts of analysis of dynamic systems, the correct analysis of dynamics, and proper coding in Verilog. The student population under test was mainly male (a little more than 80%), between 18 and 22 years old, and belonging to the lowest social strata of the city. These characteristics are generalized in the Universidad Distrital Francisco José de Caldas student population, located in the city of Bogotá (Colombia). A total of 65 students participated, separated into two groups. A first control group developed a distance learning process characterized by adapting the face-to-face classes to a video conferencing platform. The second group used the same training strategy but added the technique of peer evaluation and feedback as part of the process. Both groups handled the same content and depth levels, developed during the same time frame (six months). There was no contact between the two groups, and pairs of students organized all academic work. The final performance of each group was weighted with the same tool to determine the difference in performance between the two groups. The analysis of these tests showed that in all the parameters analyzed, there was an increase in performance completely attributable to the strategy. In some cases, it was even weighted above 20%. It was also possible to identify a favorable acceptance of the strategy by the students, even though they consider that substantial additional work is required. Further studies should determine the true degree of incidence of the strategy on the time required by students to propose changes in the curriculum. It was also observed that there is a need to increase the training of students in the techniques of peer evaluation.

## 5. ACKNOWLEDGMENTS:

This work was supported by the Universidad Distrital Francisco José de Caldas, in part through CIDC, and partly by the Facultad Tecnológica. The views expressed in this paper are not necessarily endorsed by Universidad Distrital. The authors thank the research group ARMOS for supporting the development.

## 6. REFERENCES:

1. Alzaid, J. (2017). The Effect of Peer Assessment on the Evaluation Process of Students. International Education Studies, 10(6), 159-173.
2. Bell, R. (2020). Adapting to constructivist approaches to entrepreneurship education in the Chinese classroom. Studies in Higher Education, 45 (8), 1694–1710.
3. Benešvá, A., and Tupa, J. (2017). Requirements for Education and Qualification of People in Industry 4.0. Procedia Manufacturing, 11, 2195–2202.
4. Bin Mubayrik, H. (2020). New Trends in Formative-Summative Evaluations for Adult Education. SAGE Open, 10 (3).
5. Bogdanova, N., Sherstinova, T., Blinova, O., and Martynenko, G. (2017). Linguistic Features and Sociolinguistic Variability in Everyday Spoken Russian. Lecture Notes in Computer Science, 10458 (1), 503-511.
6. Bustami, Y., Syafruddin, D., and Afriani, R. (2018). The implementation of contextual learning to enhance biology students' critical thinking skills. Indonesian Journal of Science Education, 7(4), 451-457.
7. Camelo, G., and González, Y. (2004). Elaboración de un manual de procedimientos para las instituciones educativas distritales. Tekhnê, 1 (2), 25–33.
8. Cardozo, L., Azevedo, M., Carvalho, M., Costa, R., de Lima, P., and Marcondes, F. (2020). Effect of an active learning methodology combined with formative assessments on performance, test anxiety, and stress of university students.

Advances in physiology education, 44 (4), 744–751.
9. Cifrian, E., Andrés, A., Galán, B., and Viguri, J. (2020). Integration of different assessment approaches: Application to a project-based learning engineering course. Education for Chemical Engineers, 31, 62–75.
10. Clavijo, G. (2018). Universidad Distrital Francisco José de Caldas: sesenta años de historia institucional y académica 1951-2011. Editorial Universidad Distrital Francisco José de Caldas.
11. De Araújo, R., Da Costa, M., Joseph, B., and Sánchez, J. (2020). Developing professional and entrepreneurship skills of engineering students through problem-based learning: A case study in Brazil. International Journal of Engineering Education, 36 (1 A), 155–169.
12. Forestier, S., Portelas, R., Mollard, Y., and Oudeyer, P. (2020). Intrinsically Motivated Goal Exploration Processes with Automatic Curriculum Learning. arXiv:1708.02190 [cs].
13. Gerald, B. (2018). A Brief Review of Independent, Dependent, and One Sample t-test. International Journal of Applied Mathematics and Theoretical Physics, 4(2), 50-54.
14. Gómez, H., Montiel, H., and Martínez, F. (2020). Connectivity Characteristics and Level of Acceptance Linked to Online Learning by Higher Education Students During the Confinement Generated by the Covid-19 Pandemic. International Journal of Engineering Research and Technology (IJERT), 13(8), 1934-1939.
15. Gómez-Llanos, E., and Durán-Barroso, P. (2020). Learning design decisions in massive open online courses (Mooc) applied to higher education in civil-engineering topics. Sustainability (Switzerland), 12 (20), 1–13.
16. Herrera, S., Jerez, E., and Vargas, K. (2013). Formulación del plan de emergencias y contingencias para la Facultad Tecnológica de la Universidad Distrital Francisco José de Caldas. Tekhnê, 10(1), 42-69.
17. Huang, C., Tseng, H., Jenq, C., and Ou, L. (2020). Active learning of medical students in Taiwan: A realist evaluation. BMC Medical Education, 20 (1).
18. Jian-Wei, L., Chia-Wen, T., Chu-Ching, H., and Lung-Chun, C. (2017). Peer assessment with group awareness tools and effects on project-based learning. Interactive Learning Environments, 1-17.
19. Lamon, S., Knowles, O., Hendy, A., Story, I., and Currey, J. (2020). Active Learning to Improve Student Learning Experiences in an Online Postgraduate Course. Frontiers in Education, 5.
20. Losada-Gutierrez, C., Espinosa, F., Santos-Perez, C., Marron-Romera, M., and Rodriguez-Ascariz, J. (2020). Remote Control of a Robotic Unit: A Case Study for Control Engineering Formation. IEEE Transactions on Education, 63 (4), 246–254.
21. Ma, Z., Yan, X., and Wang, Q. (2020). Assessing individual contribution in collaborative learning through self- and peer-assessment in the context of China. Innovations in Education and Teaching International, 57 (3), 352–363.
22. Martínez, F., Jacinto, E., and Montiel, H. (2019). Neuronal Environmental Pattern Recognizer: Optical-by-Distance LSTM Model for Recognition of Navigation Patterns in Unknown Environments. In Y. Tan and Y. Shi (Eds.), Data Mining and Big Data (pp. 220–227). Singapore: Springer.
23. Martínez, F., Montiel, H., and Jacinto, E. (2016). Inductive Teaching and Problem-Based Learning as Significant Training Tools in Electrical Engineering. In (pp. 179–188).
24. Martínez, F., Montiel, H., and Martínez, F. (2018). Blueprints Obtention by means of Using Digital Image Processing Algorithms. International Journal of Engineering and Technology, 10 (4), 1129–1135.
25. Moleko, M., and Mosimege, M. (2020). Teachers' and learners' experiences for guiding effective teaching and learning of mathematics word problems. Issues in Educational Research, 30 (4), 1375–1394.
26. Oksana, P., Galstyan-Sargsyan, R., Amparo López-Jiménez, P., and Pérez-Sánchez, M. (2020). Transversal competences in engineering degrees: Integrating content and foreign language teaching. Education Sciences, 10 (11), 1–13.
27. Oleksenko, V. (2020). Pedagogical Conditions for Ensuring the Quality of Engineering Training in Ukraine in the 19th Century. Encounters in Theory and History of Education, 21, 213–230.
28. Ospina, Y., and Galvis, J. (2017). A novel design of an E-learning digital ecosystem.

Tekhnê, 14 (1), 55–60.
29. Réka, J., Kármen, D., Susana, F., Kinga, K., Edit, M., and Kinga, S. (2015). Implications of Motivational Factors Regarding the Academic Success of Full-time and Distance Learning Undergraduate Students: A Self-determination Theory Perspective. Procedia - Social and Behavioral Sciences, 187, 50–55.
30. Reynders, G., Lantz, J., Ruder, S., Stanford, C., and Cole, R. (2020). Rubrics to assess critical thinking and information processing in undergraduate STEM courses. International Journal of STEM Education, 7 (1).
31. Roca, N., and Garcia-Valles, M. (2020). Trainee Teacher Experience in Geoscience Education: Can We Do Better? Geoheritage, 12 (4).
32. Salehi, M., and Daryabar, B. (2014). Self- and peer assessment of oral presentations: Investigating correlations and attitudes. English for Specific Purposes World, 15(42), 1–12.
33. Suraratdecha, S., and Tayjasanant, C. (2020). Thai teachers' self-assessment and student perceptions on the practice of autonomy. Kasetsart Journal of Social Sciences, 41 (1), 46–52.
34. Tian, J., and He, G. (2020). The five-in-one teaching mode in the teaching of engineering courses. Computer Applications in Engineering Education, 28 (6), 1683–1695.
35. To, J., and Panadero, E. (2019). Peer assessment effects on the self-assessment process of first-year undergraduates. Assessment and Evaluation in Higher Education, 44 (6), 920–932.
36. Verkade, H., and Bryson-Richardson, R. (2013). Student acceptance and application of peer assessment in a final year genetics undergraduate oral presentation. Journal of Peer Learning (Online), 6 (1), 1–18.
37. Villate, C., and Jirón, M (2004). De Sierra Morena Alta a Candelaria La Nueva: 8 años de la Facultad Tecnológica. Editorial Universidad Distrital Francisco José de Caldas.
38. Wang, L., and Chiang, F. (2020). Integrating novel engineering strategies into STEM education: APP design and an assessment of engineering-related attitudes. British Journal of Educational Technology, 51 (6), 1938–1959.

***Table 1***. Descriptive statistics of the performance of the two groups (control group and peer assessment group) at the end of the academic training processes

| | Mean | | StDev | | Min | | Max | |
|---|---|---|---|---|---|---|---|---|
| **Misapplication of concepts** | G1 57.6 | G2 90.1 | G1 18.3 | G2 5.3 | G1 36.7 | G2 73.6 | G1 81.2 | G2 95.7 |
| **Inconsistencies in the concepts** | G1 83.4 | G2 92.6 | G1 10.8 | G2 10.1 | G1 74.3 | G2 79.6 | G1 95.8 | G2 97.1 |
| **Wrong dynamic analysis** | G1 71.2 | G2 92.4 | G1 15.9 | G2 3.5 | G1 54.4 | G2 82.9 | G1 88.9 | G2 99.6 |
| **Inadequate coding** | G1 92.5 | G2 98.3 | G1 2.52 | G2 0.9 | G1 89.2 | G2 97.3 | G1 93.7 | 100 |

G1 = Control group
G2 = Peer-assessment group

***Table 2.*** *T*-test of paired samples from the two groups

| | T Value | Degrees of Freedom | P Value |
|---|---|---|---|
| **Misapplication of concepts** | 2.831 | 63 | 0.044 |
| **Inconsistencies in the concepts** | 8.791 | 63 | 0.008 |
| **Wrong dynamic analysis** | 4.703 | 63 | 0.007 |
| **Inadequate coding** | 5.672 | 63 | 0.001 |

## APPENDIX

Survey form used with the students.

1. Course name:

2. Professor:

3. Level of effort you have put into the course

| | Deficient | Average | Satisfactory | Very Good | Excellent |
|---|---|---|---|---|---|
| | | | | | |

4. Knowledge acquired

| | Deficient | Average | Satisfactory | Very Good | Excellent |
|---|---|---|---|---|---|
| Level of skills or knowledge at the beginning of the course | | | | | |
| Level of skills or knowledge at the end of the course | | | | | |
| Level of skills or knowledge required to complete the course | | | | | |
| To what extent has the course contributed to improving your skills or knowledge? | | | | | |

5. Professor's skills and dedication

| | Strongly disagree | Disagree | Neutral | Agree | Strongly agree |
|---|---|---|---|---|---|
| The professor was an effective trainer | | | | | |
| The explanations were clear and well structured | | | | | |
| The professor stimulated the interest of the students | | | | | |
| The professor made good use of the teaching time | | | | | |
| The professor | | | | | |

| | | | | | |
|---|---|---|---|---|---|
| was attentive and helpful | | | | | |
| The grades were published early and contained valuable commentary | | | | | |

| |
|---|
| 6. The learning outcomes in the unit are clearly identified<br>Yes NO |
| 7. The learning experiences in the unit helped me achieve the course objectives<br>Yes NO |
| 8. The learning resources in this unit helped me achieve the course objectives<br>Yes NO |
| 9. The assessment tasks in this unit fairly assess my achievement of the learning outcomes<br>Yes NO |
| 10. Feedback on my work in this unit helped me to achieve the unit outcomes<br>Yes NO |
| 11. The workload for this unit is adequate to achieve the learning outcomes<br>Yes NO |
| 12. The quality of teaching in this unit helps me achieve the learning outcomes<br>Yes NO |
| 13. I am motivated to achieve the learning outcomes in this unit<br>Yes NO |
| 14. I make the most of the learning experiences in this unit<br>Yes NO |
| 15. The feedback from my peers enhanced my learning in this unit<br>Yes NO |
| 16. Overall, I am satisfied with the co-evaluation process developed by my peers<br>Yes NO |
| 17. Overall, I am satisfied with the co-evaluation process I developed<br>Yes NO |
| 18. I consider that the professor's distance lecture activity was effective in my learning process<br>Yes NO |
| 19. I consider that the laboratory activities through simulations were effective in my learning process<br>Yes NO |
| 20. I consider that the asynchronous video activity was effective in my learning process<br>Yes NO |
| 21. I consider that the co-evaluation activity was effective in my learning process<br>Yes NO |
| 22. During the co-evaluation of my peers I solved doubts related to the course contents<br>Yes NO |
| 23. If you have participated in the remote sessions (or listened to the recordings), did you find the content of the lectures useful?<br>Yes NO |

| |
|---|
| 24. Did you find that the use of live presentations (student presenting their academic work online) during the sessions was good for the student presenting their work?<br>Yes NO |
| 25. Did you find that the use of live presentations (the student presents his/her academic work online) during the sessions was good for the other students in the course?<br>Yes NO |
| 26. Have you found this co-assessment format to be effective in helping you meet the learning outcomes?<br>Yes NO |
| 27. Would you recommend this co-evaluation approach?<br>Yes NO |
| 28. Did the professor provide useful information for the co-assessment process?<br>Yes NO |
| 29. Considers that it requires additional feedback from the professor as part of the assessment and feedback process<br>Yes NO |
| 30. Did you find the co-assessment based sessions to be a challenge that developed additional skills related to the |

| |
|---|
| course?<br>Yes NO |
| 31. The information you provided in the co-assessment was useful for the course<br>Yes NO |
| 32. The information you received in the co-assessment was useful for the course<br>Yes NO |
| 33. The co-assessment activity meant unnecessary work, it did not add to the learning work already developed for the written test<br>Yes NO |

PERIÓDICO TCHÊ QUÍMICA
ARTIGO ORIGINAL

# DETERMINANDO ENXAQUECA COM FATORES DESENCADEANTES DE AURA PARA MELHORAR A PRÁTICA: UM ESTUDO TRANSVERSAL DA ARABIA SAUDITA

# DETERMINING MIGRAINE WITH AURA TRIGGER FACTORS TOWARD IMPROVING THE PRACTICE: A CROSS-SECTIONAL STUDY FROM SAUDI ARABIA

# تحديد عوامل إثارة نوبات الصداع النصفي المصحوب بهالة لتحسين الممارسة العملية:

دراسة مقطعية على المملكة العربية السعودية

ALSHAMRANI, Foziah Jabbar [1,2*]; ALMOHISH, Noor Mohammad [1]; ALMUAIGEL, Mohammed Faisal [1], ALRAMADHAN, Narjes Ali [3], ALJUMAH, Maryam Mohammad [3]

[1] Neurology Department, College of Medicine, Imam King Fahad University Hospital, Saudi Arabia

[2] Abdulrahman Bin Faisal University, Saudi Arabia

[3] Medical Intern, College of Medicine, King Faisal University, Saudi Arabia

** Corresponding author*
*e-mail: fshamrani@iau.edu.sa*

Received 11 November 2020; received in revised form 22 February 2021; accepted 10 March 2021

## RESUMO

**Introdução:** A cefaleia primária é uma das doenças mais comuns tratadas nas clínicas de neurologia. Globalmente, estima-se que a prevalência atual de transtorno de cefaleia em adultos sintomáticos, pelo menos uma vez no último ano, é de cerca de 50%. De acordo com o estudo do *Global Burden of Disease,* em 2015, a enxaqueca foi classificada como a terceira causa mais comum de deficiência em todo o mundo. Uma das enxaquecas significativas é a enxaqueca com aura, uma dor de cabeça frequente que ocorre após ou com distúrbios sensoriais. **Objetivo.** Este estudo teve como objetivo identificar e comparar os gatilhos em pacientes previamente diagnosticados com enxaqueca com aura (MwA) com aqueles que não foram identificados com enxaqueca com aura antes, mas diagnosticados de acordo com um questionário distribuído no Reino da Arábia Saudita (KSA). **Métodos:** Adultos com idade entre 18 e 50 anos foram selecionados aleatoriamente no Reino da Arábia Saudita para participar deste estudo transversal não intervencionista multicêntrico. Os dados do estudo foram coletados por meio de um questionário online usando os critérios de diagnóstico da Classificação Internacional de Distúrbios de Cefaléia 2018 e o questionário de cefaléia da Cleveland Clinic Canada. **Resultados e Discussão:** Dos 4.140 indivíduos potencialmente elegíveis, 302 não foram previamente diagnosticados com enxaqueca com aura, mas foram diagnosticados com um questionário (Grupo A), enquanto 71 participantes já foram diagnosticados (MwA) (Grupo B). Uma relação significativa foi encontrada entre MwA e estresse e ansiedade, distúrbios do sono, lugares barulhentos, exposição a muitas luzes, trabalho prolongado no computador, fome, jejum, estudo para exames e menstruação no Grupo A. O Grupo B experimentou todos os gatilhos anteriores além das mudanças climáticas, certos odores e o consumo de queijo, banana e cachorro-quente. **Conclusões:** Os fatores desencadeantes são comuns em indivíduos com MwA. O conhecimento desses gatilhos é essencial para prevenir as complicações graves de MwA, portanto, melhora a qualidade de vida dos pacientes.

**Palavras-chave**: *enxaqueca com aura, dor de cabeça, Reino da Arábia Saudita, dor de cabeça primária, fatores desencadeantes*

## ABSTRACT

**Background:** Primary headache is one of the most common disorders treated in neurology clinics. Globally, it has been estimated that the current prevalence of headache disorder in adults symptomatic, at least once within the last year, is about 50%. According to the Global Burden of Disease Study 2015, migraine was ranked as the third most common cause of disability worldwide. One of the significant migraines is migraine with aura, a frequent headache that occurs after or with sensory disturbances**. Aim**: This study aimed to identify and compare triggers in previously diagnosed patients with migraine with aura (MwA) to those who have not been identified with migraine with aura before but diagnosed according to a questionnaire survey distributed in the Kingdom of Saudi Arabia (KSA). **Methods:** Adults aged 18–50 years were randomly selected in the Kingdom of Saudi Arabia to

participate in this non-interventional, multicentre, cross-sectional study. The study data was collected via an online questionnaire using the diagnostic criteria of the International Classification of Headache Disorders 2018 and the Cleveland Clinic Canada headache questionnaire. **Results and Discussion:** Of the 4.140 potentially eligible individuals, 302 were not previously diagnosed with migraine with aura but were diagnosed with a questionnaire (Group A), while 71 participants were already diagnosed (MwA) (Group B). A significant relationship was found among MwA and stress and anxiety, sleep disturbance**,** noisy places, exposure to lots of lights, prolonged computer work, hunger, fasting, studying for exams, and menstruation in Group A. Group B experienced all of the previous triggers in addition to weather changes, certain odors, and the consumption of cheese, bananas, and hotdogs. **Conclusions:** The trigger factors are common in individuals with MwA. Awareness of these triggers is essential for preventing the severe complications of MwA, hence, enhance the quality of life of patients.

**Keywords**: *migraine with aura, headache, Kingdom of Saudi Arabia, primary headache, trigger factors*.

**الملخص البحثي:**

**مقدمة:** يعد الصداع الأولي أحد أكثر الامراض شيوعًا التي يتم علاجها في عيادات طب الأعصاب. على الصعيد العالمي ، تشير التقديرات إلى أن معدل الانتشار الحالي لمرض الصداع لدى البالغين الذين تظهر عليهم الأعراض ، مرة واحدة على الأقل خلال العام الماضي ، يبلغ حوالي 50٪. وفقًا لدراسة العبء العالمي للأمراض لعام 2015 ، تم تصنيف الصداع النصفي على أنه ثالث أكثر أسباب الإعاقة شيوعًا في جميع أنحاء العالم. يعد الصداع النصفي المصحوب بالهالة أحد أهم أنواع الصداع النصفي، وهو صداع متكرر يحدث بعد أو مع اضطرابات حسية.

**الهدف:**هدفت هذه الدراسة إلى تحديد ومقارنة المحفزات في المرضى الذين تم تشخيصهم سابقًا بالصداع النصفي المصحوب بالهالة مع أولئك الذين لم يتم تشخيصهم بالصداع النصفي المصحوب بالهالة من قبل ولكن تم تشخيصهم وفقًا لاستبيان تم توزيعه في المملكة العربية السعودية.

**الطريقة:** تم اختيار البالغين الذين تتراوح أعمارهم بين 18 و 50 عامًا بشكل عشوائي في المملكة العربية السعودية للمشاركة في هذه الدراسة المقطعية غير التدخلية متعددة المراكز. تم جمع بيانات الدراسة عبر استبيان عبر الإنترنت باستخدام معايير التشخيص الخاصة بالتصنيف العالمي لاضطرابات الصداع 2018 واستبيان كليفلاند كلينك كندا.

**النتيجة:**من بين 4.140 فردًا، لم يتم تشخيص 302 شخصًا سابقًا على أنهم مصابون بالصداع النصفي المصحوب بالهالة ، ولكن تم تشخيصهم عن طريق الاستبيان (المجموعة أ) ، بينما تم بالفعل مشاركة 71 مشاركًا بالاستبيان وهم مشخصين سابقاً بالصداع النصفي مع هالة (المجموعة ب). تم العثور على علاقة كبيرة بين الصداع النصفي المصحوب بالهالة والتوتر والقلق واضطراب النوم والأماكن الصاخبة والتعرض للكثير من الأضواء وعمل الكمبيوتر لفترات طويلة والجوع والصيام والدراسة للامتحانات والحيض في المجموعة الأولى. بالإضافة إلى التغيرات المناخية وبعض الروائح واستهلاك الجبن والموز والهوت دوج.

**الخاتمة:** العوامل المحفزة للصداع النصفي شائعة لدى الأفراد المصابين بـالصداع النصفي مع هالة. يعد الوعي بهذه المحفزات أمرًا ضروريًا لمنع المضاعفات الشديدة لـلصداع النصفي المصحوب بهالة، وبالتالي تحسين نوعية حياة المرضى.

## 1. INTRODUCTION:

A primary headache is one of the most common disorders treated in neurology clinics (Wöber and Wöber-Bingöl, 2010). Globally, it has been estimated that the current prevalence of headache disorder in adults symptomatic, at least once within the last year, is about 50%. Worldwide, half to three-quarters of adults aged 18-65 had a headache, and at least 30 percent of these individuals, reported migraines. A primary headache is diagnosed depending on the defined standards in the International Headache Society categorization (Zenebe *et al*., 2020 and Breslau *et al*., 2001). According to data published by the World Health Organisation, tension headaches are considered the most common headaches. However, migraine constitutes the primary reason behind a large number of visitors to the neurology clinic. Various headaches cohabit among some sick people who do not meet the diagnostic standards, while in some cases, they are concealing a secondary headache. Owing to this reason, consulting a doctor is recommended to apply the correct diagnosis and the suitable identified treatment (Andrasik *et al*., 1982). As a result, the case does not apply to all patients.

In respect of tension headache, which is considered the most common type of headache, it has resulted from muscular tension on both napes of the neck and the forehead in general. And usually concurrent with stress periods. Such headaches lead to continuous tension or pressure (Amiri *et al*., 2007; Wachholtz *et al*., 2017). It resembles a helmet in terms of its primarily occurrence on nape of the neck and the forehead, i.e., in both sides of the head. In many cases, palpation of the affected muscles might alleviate the pain. Generally speaking, the severity of the pain in tension headaches is frequently less disabling and reasonable than headache resulting from either migraine or secondary headaches

(Siegel *et al*., 2017; Dueland, 2015). In general, the pain starts throughout the day, but its intensity increases in the afternoon. However, it might become acute, and it might last for a couple of days (Dwyer, 2018; Blumenfeld and Siavoshi, 2018).

Recurrent or repeated episodes of headache distinguish between migraine or acute headache. The severity might differ in the different episodes, but might be acute, when the patient asks for medical care. In general, the pan starts with one or other part of the head (hemicranial) until it covers the entire head. It is usually vibrant such as heartbeats and might be associated with vomiting, nausea, and a discomfort that becomes worse with noise (phonophobia), smells (osmophobia), and light (photophobia), (Matar *et al*., 2015). The pain becomes worse with physical activity, enhances with rest, and might be caused by stress periods, climate changes, menstruation, fasting, some foods, hunger, or changes in sleep pattern (sleepless, or even more than usual) (Moghaddassi *et al*., 2016).

## 2. REVIEW OF LITERATURE

### 2.1. Migraine

It might be caused by genetic heritage because it is commonly acceptable to notice that such a disease is associated with a migraine family history. An aura usually precedes a migraine attack, but it may also occur during the attack. It may appear without a headache and last for only four hours or several days. It might be provided as aura migraine (20%) — preceded by sensory, visual, motor, speech, or motor symptoms, or as migraine without aura (80%). Aura migraine patients might suffer from headache episodes with no aura (Wöber and Wöber-Bingöl, 2010; Silberstein *et al*., 2016).

Migraine or severe headache is attributed to either recurrent or repeated episodes of headache. The severity might differ in the different episodes, but might be extreme, when the patient claims for medical care. In general, the pain starts with one or other side of the head (hemicranial) until it covers the entire head (Jackson *et al*., 2015). Its speed resembles heartbeat and may be associated with both vomiting and nausea, besides the feeling of discomfort that becomes worse with noise (phonophobia), smells (osmophobia), and light (photophobia). It may become worse when the patient does exercise. Still, it enhances when the person takes a rest and might be stimulated by stress periods, sleep pattern changes that s characterized by either taking insufficient amount of sleep or oversleeping, women period, fasting, climate changes, some foods, or hunger (Schain *et al*., 2017).

It is worth mentioning that chronic disease occurs when a patient suffers from severe headache that lasts more than fifteen days each month might have tension or migraine. To clarify, eight patients meet migraine standards (Barnes, 2015). Approximately a small proportion of patients, 2.5% their case changes from episodic to the chronic form. The following points clarify the underlying reasons that develop this chronic disease, namely non-modifiable reasons - low economic status, a history of head traumas, or being a Woman -, and modifiable factors, such as the existence of 'fibromyalgia' or other painful symptoms, obesity, an increased frequency of stress, abuse of analgesic, stress, medication, depression, anxiety, caffeine abuse (Levy *et al*., 2019; Jahromi *et al*., 2018).

### 2.2. Trigeminal autonomic cephalalgia

Various cases with common clinical characteristics are unified together: one-sided pain existed in the area nourished by the trigeminal nerve and independent cranial symptoms, such as red-eye, watery eyes, nasal packing, congestion, facial sweating, or flow of liquid from the nose or rhinorrhea (Ashina *et al*., 2015). They last for a short period and very severe headaches and have various episodes a day. The pain and the independent symptoms result from the activation of the trigeminal nerve and the parasympathetic nervous system due to the facial-trigeminal reflex in the brainstem or the pathological activation (Moghaddassi *et al*., 2016). The hypothalamus is the brain region that acts as a producer that enhances such reflex.

### 2.3. Migraine with Aura

Migraine headache, either with or without aura, is considered the most common type of primary headache. Migraine considers a complicated disorder that involve various pathophysiological mechanisms like hypothalamic dysfunction revealed by a chronobiologic dysregulation, and a probable hyperdopaminergic state. In general, it starts from childhood or adolescence and might last for a long time. According to World Health Organization (2001) roughly 2–15% of the population of the world is influenced by Migraine with aura (MwA) and Migraine without aura (MA). Migraine is a common neurological disorder that is preceded by an aura

in approximately 20–30% of migraine patients. Migraine without aura (MA) is a phenomenon whose manifestations coincide with a wave of cortical spreading depolarization/depression (CSD) through the cerebral cortex. It is considered the most frequent one. Incidence figures revealed that severe migraine is commonly found among women of child-bearing age, primarily because of MwA.

The determination of stimulating factors is commonly recommended as a primary strategy in the treatment of migraine. Several external and internal factors engaged in migraine attacks. Various studies are compatible with: fasting, lack of sleep, and stress as the most common stimulator factors. However, other factors should be considered, such as excessive caffeine consumption, hormonal factors in women, and alcohol usage (Roccella *et al*., 2019). Various stimulating factors might enhance headache attacks, such as milk and dairy products, sexual activity, head trauma, exhaustion, neck problems, traveling, posture, smoking, vegetables, nuts, and fruits. but there is not much scientific evidence on this issue (Hadjikhani and Vincent, 2019; Munjal *et al*., 2018). Identifying stimulating factors might enable health professionals to manage the migraine headache and enhance the patient's quality of life (Vianna-bell *et al*., 2019; Santangelo *et al*., 2018). It is significant for patients with migraines to be well educated about all stimulating factors of migraine and management (Sen *et al*., 2018). The health professional role in headache management might contain providing patients with information, headache history taking; and engaging with patients to make sure their compliance with their care program, complete an effect questionnaire, and to express and spread headache diaries (Lebedeva *et al*., 2018; Ghanizada and Al-karagholi, 2019; Hospitalario *et al*., 2020). Stimulating factors are significant in controlling migraine management because any negligence of these factors might reduce the frequency of headaches and increase patients' quality of life. Regardless of its significance, a minority of people aware of migraine stimulating factors in the Society (Frank *et al*., 2020; Yeh *et al*., 2018).

A widespread debilitating primary headache condition is called a migraine headache. It was ranked as the third most common cause of disability in both men and women under 50 years worldwide in the Global Burden of Disease Report 2015. Migraine patients with migraine without aura (MwoA) are usually characterized by unilateral position, pulsating quality, mild to extreme strength, which can be exacerbated by routine physical activity and are correlated with nausea/or photophobia and phonophobia. It presents as chronic headaches lasting from 4 to 72 hours. Migraine with aura is characterized mainly by repeated attacks lasting only minutes, is accompanied by unilateral, entirely reversible symptoms of the visual, auditory, or another central nervous system that typically develop progressively, followed by migraine-related headache and symptoms. Common migraine triggers include extended periods of fasting, hypoglycemia, sleep disturbances, psychological stresses, hormonal changes, and certain medications. It is essential to know the triggers for a migraine headache so that attacks can be prevented. If left untreated, migraines can lead to serious complications, including stroke. A large-scale prospective epidemiologic study of the association between migraine and stroke in women found a non-random association of severe headaches and migraines with stroke. Furthermore, another study showed that women with MwA who take combined hormonal contraception had a 6-fold increased risk of ischemic stroke (Mph *et al*., 2017),

The goal of this research was to identify trigger factors in patients previously diagnosed with MwA and compare them to patients in the Kingdom of Saudi Arabia (KSA). They were not diagnosed with MwA in the hospital but were diagnosed through the questionnaire.

## 3. MATERIALS AND METHODS:

This cross-sectional study included adults aged 18–50 years of both sexes who were randomly selected from the KSA population between 2018 and 2019. In total, 4.140 individuals were identified as potentially eligible study participants. Each individual was assessed for MwA Using the International Classification of Headache Disorders 2018 diagnostic guidelines and the type of the Cleveland Clinic Canada headache questionnaire (Appendix 1) with the comorbidity and secondary headache exclusion criteria at the start of the questionnaire. The patients were divided into two groups. The patients were divided into two groups. In group A, a total of 302 participants who were not MwA screened but whose health condition was diagnosed through questionnaire; And group B, a total of 71 participants patients with previous medical examination, who knew cases of MwA.

### 3.1. The Delphi approaches

The Delphi approach contains a questionnaire or interview schedule (Appendix 1) to a panel of 'informed people' in a particular field of application for taking their opinion or judgment on a specific issue. After that, the data are gathered, and another questionnaire (Appendix 1) is designed depending solely on the findings taken from the first application (Harteis and Hertramph, 2010). Such a second questionnaire will be given to each participant required (in respect of the first phases findings), to retake their previous opinion and return their answers to the researcher. The purpose behind repeating the phases is to arrive at the final conclusion, i.e., the consensus of opinion, or a point of diminishing returns might be reached. As a result, the Delphi technique considers a multistage approach in which every stage depends on the previous one's findings (Harteis and Hertramph, 2010). It resembles a highly organized meeting of experts, managed by a chairperson who is skilled in outlining the emotions of the meeting by clarifying the participants perspectives back to them in such a way that they enable them to improve further; the only variable is that the responses of the individuals are unfamiliar to one another (Harteis and Hertramph, 2010; James and Cathain, 2019). There is crucial evidence in the literature that in the first phase of any Delphi investigation, a wide discrepancy of person's perspective is typical. However, after several repetitions, the subjects of the study are inclined to intersect towards unanimous. Regarded this as almost unavoidable, taking into account the use of the feedback-response loop. A significant issue among researchers thinking to employ the Delphi technique lies in comprehending the meaning behind 'unanimous.' It is recommended that this should be commensurate with 51% agreement among participants.

### 3.2. Ethics

This study was approved by the university Institutional Review Board (IRB) and was conducted in alignment with the ethical principles of the 1975 Declaration of Helsinki (as revised in 2000). The respondents supplied informed written consent. A special code for data storage protected by a password was provided to every respondent for data management and protection. It guaranteed the privacy of all data. Employing the Windows Statistical Kit for Social Sciences, statistical research was performed. Employing the chi-squared test, also categorical variables were contrasted.

### 3.3. Instruments

Generally speaking, the study employed two tools, namely: The List of Trigger Factors of Migraine (LTFM) and the Personal Information Form (PIF) (Appendix 1). Concerning the contents of the second tool so-called 'PIF' contained the cure for patients with migraine, headache characteristics, and sociodemographic. The study recorded the following: lifestyle data, biographic data, headache characteristics, medication, and general medical history, and the patients were asked about potential trigger factors of migraine. The following issues were covered in respect of lifestyle data: sleep, physical activity, consumption of alcohol, chocolate, smoking habits, and caffeine. On the other hand, biographic data covered the following issues: gender, age, number of children, marital status, profession, and education level.

### 3.4. Data Analysis

To analyse the demographic characteristics, descriptive statistics were used. Besides, the use of SPSS is essential for both statistical analyses and calculations. Data were presented as standard deviation (SD), means, range, and median. The essential statistical tests were used on the data revealing a normal distribution. The percentage was employed for tackling the distribution of stimulating factors among patients with migraines. The Chisquare test was employed to define the precise relationships that occur between the parameters of gender, age, migraine types, and stimulating factors. As a result, the p values of $<0.05$ were considered as significant.

### 3.5. Other relevant information

This research focused on undiagnosed cases of MwA among Saudis. Many trigger factors are common across multiple studies, but they may differ from between countries; thus, it is important to identify them to prevent serious complications. A general description about demographics including all parameters Region: (Eastern province Northern province, Central province,Western province,Southern province) and, sex (male and femail), age (18-50), social status (Single and Married) , job (Students, Ordinary Employee,Shifts worker/night-time worker, Unemployed), and alcohol, smoke, drugs ,Beta-, propranolol, timolol, metoprolol, venlafaxine, amitriptyline, anticonvulsants, paracetamol and aspirin were also investigated.

Besides, trigger factors parameters as stress and anxiety, sleep, noisy place, lights, computer work, hungry, fasting, exams and menstruation were also investigated (supplementary material upon request).

## 4. RESULTS AND DISCUSSIONS:

### 4.1. Results

Of the 4.140 individuals enrolled in the study, 2.678 were excluded due to the presence of chronic disease or being on specific medication that could cause a secondary headache. A further 128 were excluded because a neurologist had already diagnosed them to have a primary headache other than MwA (Table 1).

In Group A, 302 participants have not previously been diagnosed with MwA by Questionnaire, they have MwA. In Group B, 71 participants had known cases of MwA and were diagnosed in hospital. The demographical data for both Groups A and B are shown in (Table 2). The Pearson correlation coefficient indicated a significant relationship between MwA in Group A, stress and anxiety, sleep disturbance**,** noisy places, exposure to lots of lights, prolonged computer work, hunger, fasting, studying for exams, and menstruation (Table 3). The Pearson correlation coefficient also revealed a significant relationship between MwA in Group B, studying for exams, stress and anxiety, sleep disturbance, noisy places, exposure to lots of lights, prolonged computer work, hunger, fasting, menstruation, weather changes, certain odors, and the consumption of cheese, bananas, and hotdogs (Table 4).

Concerning specific triggers for Group A, the Pearson correlation indicated no significant relationship with use of any drugs, being on a low-calorie diet, relaxation after a period of stress, weather changes, eating oranges, cheese, bananas, smoked fish, fast foods, hotdogs, chocolate, spicy foods, exposure to certain odors, smoking, sexual activity, drinking alcohol, decrease or increase the daily dose of caffeine, and exercise (all>0.05).

On the other hand, with Group B, the Pearson correlation indicated no significant relationship with use of drugs, being on a low-calorie diet, relaxation after a period of stress, eating oranges, smoked fish, fast foods, chocolate, spicy foods, smoking, sexual activity, drinking alcohol, decrease or increase daily dose of caffeine, and exercise (all p>0.05).

Among the 373 subjects, 28% percent reported using But it was diagnosed through a questionnaire. Group B, participants had a previous diagnosis of migraine with aura. When taking the drug, MwA lasted for only minutes in 53.9% of cases in group A and 70.4% of cases in group B, respectively.18% reported receiving emergency injections, and 28% reported using naproxen to treat their MwA (Figure 1). When medication is taken, the MwA only lasted for minutes in 53.9% of cases in Group A and 70.4% of cases in Group B, respectively (Figure 2).

In this study, the common triggers for MwA in the KSA in Group A are: stress and anxiety, sleep disturbances**,** noisy places, exposure to lots of lights, prolonged computer work, hunger, fasting, studying for exams, and menstruation; and in Group B, they are: Study for exams, stress and anxiety, sleep disturbances, noisy places, exposure to lots of lights, prolonged computer work, hunger, fasting, menstruation, certain odors, and eating cheese, bananas, and hotdogs. Based on the data, it appears that those diagnosed with MwA are more likely to be aware of their trigger factors than someone who is undiagnosed. Therefore, clinical diagnosis and awareness of MwA are crucial to avoid the trigger factors to prevent serious complications of MwA that can affect one's quality of life.

### 4.2. Discussion

This study identified some trigger factors for MwA in the KSA. Earlier studies have focused on migraines in general but have not differentiated between the trigger factors associated with MwA and those associated with MwoA. The patients were divided into two groups: Group A, which included patients who have not been diagnosed with MwA but were diagnosed by the questionnaire, and Group B, which included patients who have known cases of MwA.

This study found no significant relationship between MwA in Group A and eating any kind of food. Still, on the other hand, there was a significant relationship between MwA in Group B and the consumption of cheese, bananas, and hotdogs. Previous studies have identified chemical triggers for migraines Theobromine, phenolic amines, octopamine, nitrites, nitric oxide, allergenic proteins, linoleic and oleic fatty acids, onosodium glutamate, tartrazine, aspartame, histamine, tyramine, and sulphites, including tyramine, phenylethylamine, theobromine, In certain forms of foods which can lead to migraines, these chemical causes have been identified (Zencirci, 2010; Al-shimmery, 2010). There are

also food allergies in some patients, which may explain why some foods act as triggers for MwA, especially because there has been a correlation between migraines and food allergies.

In this study, 185 patients from Group A and 55 patients from Group B developed MwA when fasting, with a significant relationship between fasting and MwA in both groups. Previous studies have shown that headaches after fasting are more common in patients with a history of chronic migraine (Zencirci, 2010; Al-shimmery, 2010). Fasting leads to changes in serotonin and norepinephrine levels, hypoglycemia, and increased stress hormone levels. Migraines are rarely associated with insulin-induced hypoglycemia in patients with diabetes; therefore, the role of decreased blood glucose has been questioned (Health, 2018).

Menstruation is a leading trigger factor for some patients. In this study, Group A and Group B both showed a significant relationship between having MwA and menstruation. In the literature, reports are suggesting that hormonal changes and a decrease in plasma oestradiol are triggers for migraine (Bergh, Amery, Ph, and Waelkens, 1987),(Lebedeva *et al*., 2018). It was found that some patients are susceptible to MwA after sexual activity; however, there was no relationship between sexual activity and Group A and Group B, which is consistent with a previous finding that the prevalence of headache associated with sexual activity is more significant in patients with migraine. Some studies have shown that a low percentage of migraine patients consume alcohol due to previous experiences of alcohol acting as a trigger (Robbins *et al*., 1993; Sen *et al*., 2018). However, this study found no significant relationship with Group A or B; however, this may be due to the low number of patients who drink alcohol and not on a regular basis in our study.

It was observed no significant relationship between environmental triggers (weather and odors) and having MwA in Group A. On the other hand, Group B showed a significant relationship between environmental triggers. Previous research has suggested that patients who develop migraines after exposure to certain odors may have olfactory hypersensitivity (Biehl *et al*., 2007; Ghanizada and Al-karagholi, 2019). A total of 143 and 46 patients in Group A and Group B, respectively, developed MwA after exposure to certain odors. One study showed that after the provocation of MwA using natural trigger factors, no patient developed attacks following photostimulation alone.

The literature has reported an association between weather and migraine changes in some patients (Tafuri *et al*., 2015). This research further corroborates this as 122 and 61 patients in Group A and B, respectively, developed MwA after exposure to weather changes, with a significant relationship in Group B.

Environmental noise is an essential trigger in some patients who have MwA. This study found that 225 and 54 patients in Group A and Group B, respectively, developed MwA when they are in noisy places, which aligns with another study that reported an increased risk of migraine in adults who experienced severe annoyance as a result of traffic and neighborhood noise (Academy *et al*., 2013; Vianna-bell *et al*., 2019).

This study found no significant relationship between exercise and having MwA in Group A and Group B, with only 35 patients from Group A and 39 patients from Group B developing MwA. However, a previous study has suggested that MwA can be triggered by physical activity in some patients(Munjal *et al*., 2018)

There was also no significant relationship between water consumption in Group A and Group B and the development of MwA. Other researchers have shown that insufficient fluid intake could trigger MwA in some patients but could not explain the mechanism behind water intake and migraines (Silberstein *et al*., 2016). Furthermore, there was significant relationship between sleep disturbance in Group A and Group B developing MwA. Previous studies have recognized a relationship between sleep and migraines. For example, in one study, 527 subjects developed MwA. They reported sleep disturbance as a trigger finding as 272 patients from Group A and 59 patients from Group B noticed a relationship between MwA and sleep disturbance.

Previous research suggests the relationship between stress and migraine (Hauge, Kirchmann, and Olesen, 2010). In the present study, 234 patients from Group A and 60 patients from Group B reported stress and anxiety to trigger MwA, with a significant relationship found in Group A. There was no significant relationship between relaxation after a period of stress and having MwA in Group A and Group B.

In regards to medication, one study stated that acute medication tends to be more effective if administered early in the attack (Jia *et al*., 2017). While Group B patients are aware of their condition and may also be aware of their own trigger factors, they can take medication upon MwA onset, which may prevent its development.

However, Group A patients are not aware that they have a migraine so taking medication may be delayed.

The limitations of this study are the relatively small number of subjects who were diagnosed with MwA and small number of individuals who responded to certain triggers (e.g. drinking alcohol). Further studies are needed to examine each trigger factor individually with a larger sample size of patients with MwA in the Saudi population and compare it with MwoA.

## 5. CONCLUSIONS:

The recognition of headache stimulating factors in migraine patients might be an efficient strategy to avoid the improvement of migraine headaches from a global perspective. Patients treated for migraine are more prone to engage in disease self-management, implement promising findings, and have better life quality. The strategies of management strategies are available to deal with and avoid such headaches, and some headache sufferers achieve satisfactory management. Therefore, nurses and other health-care providers have to be prepared to evaluate and interfere in preventing or controlling the headache from patients with migraines, particularly those with MwA and MA. Medical staff might support patients to be well acquainted with all stimulating factors of migraine and management. The necessary self-management behavior is embedded in reducing headache stimulators to avoid migraine attacks, and patient-centered education has been revealed to manage acute disease efficiently.

## 6. REFERENCES:


1. Academy, A., Ac, F., Bb, N., and Kj, R. (2013). *Provocation of migraine with aura using natural trigger factors Paul R . Martin This information is current as of December 2 , 2013*. 27–28. https://doi.org/10.1212/01.wnl.0000440604.28014.b3
2. Al-shimmery, E. K. (2010). *Precipitating and Relieving Factors of Migraine Headache in 200 Iraqi Kurdish Patients*. *25*(3), 212–217. https://doi.org/10.5001/omj.2010.59
3. Amin, F. M., Hougaard, A., and Magon, S. (2017). *without aura : A resting-state fMRI study Altered thalamic connectivity during spontaneous attacks of migraine without aura : A resting-state fMRI study*. (August). https://doi.org/10.1177/0333102417729113
4. Andrasik, F., Blanchard, E. B., Arena, J. G., Teders, S. J., Teevan, R. C., and Rodichok, L. D. (1982). Psychological functioning in headache sufferers. *Psychosomatic Medicine*.
5. Barnes, N. P. (2015). Migraine headache in children. *BMJ Clinical Evidence*, *2015*.
6. Bergh, V. Van Den, Amery, W. K., Ph, D., and Waelkens, J. (1987). *Trigger Factors in Migraine : a Study Conducted by the Belgian Migraine Society*.
7. Biehl, K., Evers, S., and Frese, A. (2007). *Comorbidity of migraine and headache associated with sexual activity*. 1271–1273. https://doi.org/10.1111/j.1468-2982.2007.01381.x
8. Blumenfeld, A., and Siavoshi, S. (2018). The challenges of cervicogenic headache. *Current Pain and Headache Reports*, *22*(7), 47.
9. Breslau, N., Schultz, L. R., Stewart, W. F., Lipton, R., and Welch, K. M. A. (2001). Headache types and panic disorder: directionality and specificity. *Neurology*, *56*(3), 350–354.
10. Dueland, A. N. (2015). Headache and alcohol. *Headache: The Journal of Head and Face Pain*, *55*(7), 1045–1049.
11. Dwyer, B. (2018). Posttraumatic headache. *Seminars in Neurology*, *38*(06), 619–626. Thieme Medical Publishers.
12. Frank, F., Faulhaber, M., Messlinger, K., Accinelli, C., Peball, M., Schiefecker, A., Broessner, G. (2020). *Migraine and aura triggered by normobaric hypoxia*. https://doi.org/10.1177/0333102420949202
13. Ghanizada, H., and Al-karagholi, M. A. (2019). *PACAP27 induces migraine-like attacks in migraine patients*. (March 2020). https://doi.org/10.1177/0333102419864507
14. Hadjikhani, N., and Vincent, M. (2019). *Neuroimaging clues of migraine aura*. *2*.
15. Hansen, J. M., Hauge, A. W., Olesen, J., and Ashina, M. (2010). Calcitonin gene-related peptide triggers migraine-like attacks in patients with migraine with aura. *Cephalalgia*, *30*(10), 1179–1186.

16. Harteis, C., and Hertramph, H. (2010). *How Epistemic Beliefs Influence e-Learning in Daily Work-life*. (May 2014).

17. Hauge, A. W., Kirchmann, M., and Olesen, J. (2010). *Characterization of consistent triggers of migraine with aura*. *31*(4), 416–438. https://doi.org/10.1177/0333102410382795

18. Health, P. (2018). *Pediatric abdominal migraine : current perspectives on a lesser known entity*. 47–58.

19. Hospitalario, C., Santiago, U. De, Aguiar, P., Hospitalario, C., Santiago, U. De, and Leira, R. (2020). *Prolonged Migraine Stuttering Aura : Structural , Functional ,*. (March). https://doi.org/10.1111/head.13780

20. Jackson, J. L., Cogbill, E., Santana-Davila, R., Eldredge, C., Collier, W., Gradall, A., Kuester, J. (2015). A comparative effectiveness meta-analysis of drugs for the prophylaxis of migraine headache. *PloS One*, *10*(7), e0130733.

21. Jahromi, S. R., Abolhasani, M., Ghorbani, Z., Sadre-Jahani, S., Alizadeh, Z., Talebpour, M., Togha, M. (2018). Bariatric surgery promising in migraine control: a controlled trial on weight loss and its effect on migraine headache. *Obesity Surgery*, *28*(1), 87–96.

22. James, M., and Cathain, O. (2019). *Delphi consensus reached to produce a decision tool for SelecTing Approaches forRapid Reviews (TARR)*.

23. Jia, J., Ong, Y., and Felice, M. De. (2017). *Migraine Treatment : Current Acute Medications and Their Potential Mechanisms of Action*.

24. Lebedeva, E. R., Gurary, N. M., Gilev, D. V, Christensen, A. F., and Olesen, J. (2018). *Explicit diagnostic criteria for transient ischemic attacks to differentiate it from migraine with aura*. *38*(8), 1463–1470. https://doi.org/10.1177/0333102417736901

25. Levy, D., Labastida-Ramirez, A., and MaassenVanDenBrink, A. (2019). Current understanding of meningeal and cerebral vascular function underlying migraine headache. *Cephalalgia*, *39*(13), 1606–1622.

26. Matar, A. K., Kerem, N. C., Srugo, I., and Genizi, J. (2015). Primary headache in children and adolescents--diagnosis and treatment. *Harefuah*, *154*(12), 795–803.

27. Moghaddassi, M., Togha, M., Shahram, F., Hanif, H., Dadkhah, S., Jahromi, S. R., and Mozafari, M. (2016). Headache in Behcet's disease: types and characteristics. *Springerplus*, *5*(1), 1077.

28. Monica, L., Gorghiu, G., Lucian, R., Maria, A., and Bizoi, M. (2013). Delphi Study - A Comprehensive Method for Outlining Aspects and Approaches of Modern Science Education. *Procedia - Social and Behavioral Sciences*, *83*, 535–541. https://doi.org/10.1016/j.sbspro.2013.06.102

29. Mph, S. W. C., Mph, N. K. T., Monsour, M., Curtis, K. M., Whiteman, M. K., Marchbanks, P. A., and Mph, D. J. J. (2017). with migraines and risk of ischemic stroke. *The American Journal of Obstetrics and Gynecology*, *216*(5), 489.e1-489.e7. https://doi.org/10.1016/j.ajog.2016.12.019

30. Munjal, X. N., Safier, X. R., Cummings, X. D. D., and Zuccoli, X. G. (2018). *Time Course of Cerebral Perfusion Changes in Children with Migraine with Aura Mimicking Stroke*. 1751–1755.

31. Robbins, L., Clinic, H., Court, N., and Road, C. (1993). *Precipitating Factors in Migraine : A Retrospective Review of 494 Patients*. 15–17.

32. Roccella, M., Marotta, R., Operto, F. F., Smirni, D., Precenzano, F., Bitetti, I., Murabito, P. (2019). *NREM Sleep Instability in Pediatric Migraine Without Aura*. *10*(August), 1–6. https://doi.org/10.3389/fneur.2019.00932

33. Santangelo, G., Russo, A., Tessitore, A., Garramone, F., Marcuccio, L., Fornaro, I., and Trojano, L. (2018). *Prospective memory is dysfunctional in migraine without aura*. (February). https://doi.org/10.1177/0333102418758280

34. Schain, A. J., Melo-Carrillo, A., Strassman, A. M., and Burstein, R. (2017). Cortical spreading depression closes paravascular space and impairs glymphatic flow: implications for migraine headache. *Journal of Neuroscience*, *37*(11), 2904–2915.

35. Sen, S., Androulakis, X. M., Duda, V., Alonso, A., Chen, L. Y., Soliman, E. Z., Rosamond, W. D. (2018). *Migraine with visual aura is a risk factor for incident atrial fi brillation*. *0*. https://doi.org/10.1212/WNL.0000000000006650

36. Siegel, S., Carneiro, R. W., Buchfelder, M., Kleist, B., Grzywotz, A., Buslei, R., Kreitschmann-Andermahr, I. (2017). Presence of headache and headache types in patients with tumors of the sellar region—can surgery solve the problem? Results of a prospective single center study. *Endocrine*, *56*(2), 325–335.

37. Silberstein, S. D., Calhoun, A. H., Lipton, R. B., Grosberg, B. M., Cady, R. K., Dorlas, S., … Goadsby, P. J. (2016). Chronic migraine headache prevention with noninvasive vagus nerve stimulation: The EVENT study. *Neurology*, *87*(5), 529–538.

38. Tafuri, E., Santovito, D., Nardis, V. De, Marcantonio, P., Paganelli, C., Affaitati, G., … Paganelli, C. (2015). *Annals of Medicine MicroRNA profiling in migraine without aura : Pilot study MicroRNA profi ling in migraine without aura : Pilot study*. *3890*. https://doi.org/10.3109/07853890.2015.1071871

39. Vianna-bell, H., Florencio, L. L., Pinheiro, C. F., Dach, F., Bigal, M. E., and Bevilaqua-grossi, D. (2019). *Presence of vestibular symptoms and related disability in migraine with and without aura and chronic migraine*. *39*(1), 29–37. https://doi.org/10.1177/0333102418769948

40. Wachholtz, A. B., Malone, C. D., and Pargament, K. I. (2017). Effect of different meditation types on migraine headache medication use. *Behavioral Medicine*, *43*(1), 1–8.

41. Wöber, C., and Wöber-Bingöl, Ç. (2010). Triggers of migraine and tension-type headache. In *Handbook of clinical neurology* (Vol. 97, pp. 161–172). Elsevier.

42. Yeh, W. Z., Blizzard, L., and Taylor, B. V. (2018). *What is the actual prevalence of migraine ?* (January), 6–11. https://doi.org/10.1002/brb3.950

43. Zencirci, B. (2010). *Comparison of the effects of dietary factors in the management and prophylaxis of migraine*. 125–130.

44. Zenebe, Z. Y., Mehila, Z., Hanna, D., Redda, T.-H., Derya, U., Tayyar, Ş., Steiner, T. J. (2020). The prevalence of headache disorders in children and adolescents in Ethiopia: a schools-based study. *The Journal of Headache and Pain*, *21*(1).

***Table 1.*** *The frequency and percentage of normal people and participants with headache*

| | | Frequency | Percentage |
|---|---|---|---|
| Normal | | 961 | 65.7% |
| Unknown and diagnosed with migraine with aura by the questionnaire* | | 302 | 20.6% |
| Previously known case of headache | migraine with aura | 71 | 4.8% |
| | migraine without aura** | 61 | 4.1% |
| | Tension headache | 67 | 4.5% |
| Total | | 1462 | 100% |

* Group A, ** Group B

***Table 2.*** *Demographics in participants not previously diagnosed with Migraine with Aura but diagnosed by questionnaire (n=302) and participants previously diagnosed with Migraine with Aura (n=71)*

| Demographics | | Group A (n=302) | | Group B (n=71) | |
|---|---|---|---|---|---|
| | | Frequency | Percent | Frequency | Percent |
| Region | Eastern province | 92 | 30.5% | 29 | 40.8% |
| | Northern province | 43 | 14.2% | 11 | 15.5% |
| | Central province | 68 | 22.5% | 10 | 14.1% |
| | Western province | 64 | 21.2% | 14 | 19.7% |
| | Southern province | 35 | 11.6% | 7 | 9.9% |
| Sex | Male | 108 | 35.8% | 19 | 26.8% |
| | Female | 194 | 64.2% | 52 | 73.2% |
| Age | 18-25 | 163 | 54% | 36 | 50.7% |
| | 26-30 | 52 | 17.2% | 15 | 21.1% |
| | 31-35 | 41 | 13.6% | 6 | 8.5% |
| | 36-40 | 24 | 7.9% | 8 | 11.3% |
| | 41-45 | 14 | 4.6% | 2 | 2.8% |
| | 46-50 | 8 | 2.6% | 4 | 5.6% |
| Social status | Single | 190 | 61.3% | 37 | 52.1% |
| | Married | 112 | 37.1% | 34 | 47.9% |
| Job | Students | 142 | 47% | 32 | 45.% |
| | Ordinary Employee | 76 | 25.2% | 16 | 22.5% |
| | Shifts worker/night-time worker | 23 | 7.6% | 7 | 9.9% |
| | Unemployed | 61 | 20.2% | 16 | 22.5% |
| Drink Alcohol | Yes | 8 | 2.6% | 3 | 1.4% |

| | | | | | |
|---|---|---|---|---|---|
| | No | 294 | 97.4% | 68 | 95.8% |
| Are you a smoker? | Yes | 46 | 15.2% | 10 | 14.1% |
| | No | 256 | 84.8% | 71 | 85.9% |

***Table 3.*** *Trigger Factors for Group A participants (n = 302)*

| Trigger Factors | Number of patients who notes that | | P-values |
|---|---|---|---|
| | There is a relationship | No relationship | |
| Stress and anxiety | 234 (77.5%) | 68 (22.5%) | < 0.0001 |
| Sleep disturbance | 272 (90.1%) | 30 (9.9%) | < 0.0001 |
| When you are in a noisy place | 225 (74.5%) | 77 (25.5%) | < 0.0001 |
| When you see a lot of lights | 209 (69.2%) | 93 (30.8%) | < 0.0001 |
| Prolonged computer work | 229 (75.8%) | 73 (24.2%) | < 0.0001 |
| When you are hungry | 168 (55.6%) | 134 (44.4%) | 0.006 |
| When you are fasting | 185 (61.3%) | 117 (38.7%) | < 0.0001 |
| Study for exams | 139 (75.1%) | 46 (24.9%) | < 0.0001 |
| Menstruation | 130 (67%) | 64 (33%) | < 0.0001 |

***Table 4.*** *Trigger Factors for Group B participants (n = 71)*

| Trigger Factors | Number of patients who notes that | | P-values |
|---|---|---|---|
| | There is a relationship | No relationship | |
| Stress and anxiety | 60 (84.5%) | 11 (15.5%) | < 0.001 |
| Sleep disturbance | 59 (83.1%) | 12 (16.9%) | < 0.001 |
| Study for exams | 26 (81.3%) | 6 (18.8%) | < 0.001 |
| When you are in a noisy place | 54 (76.1%) | 17 (23.9%) | < 0.001 |
| When you see a lot of lights | 58 (81.7%) | 13 (18.3%) | < 0.001 |
| Weather changes | 61 (85.9%) | 10 (14%) | < 0.001 |
| When you eat cheese | 57 (80.3%) | 14 (19.7%) | < 0.001 |
| When you eat banana | 62 (87.3%) | 9 (12.7%) | < 0.001 |
| When you eat hotdog | 63 (88.7%) | 8 (11.3%) | < 0.001 |
| When you eat eggs | 56 (78.8%) | 8 (21.1%) | < 0.001 |
| Menstruation | 37 (71.2%) | 15 (28.8%) | < 0.002 |
| Prolonged computer work | 50 (70.4%) | 21 (29.6%) | < 0.001 |
| Certain odors | 46 (64.8%) | 25 (35.2%) | < 0.001 |
| When you are hungry | 49 (69%) | 22 (31%) | < 0.001 |
| When you are fasting | 55 (77.4%) | 16 (22.5%) | < 0.001 |

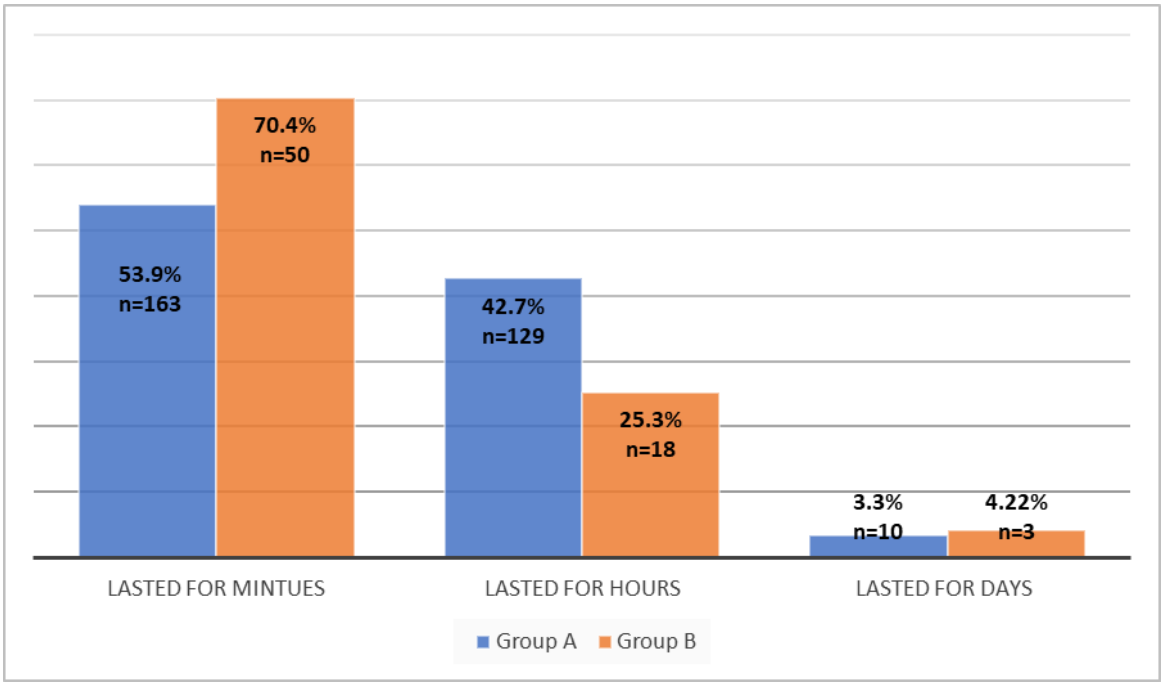


***Figure 1.*** *A comparison of headaches duration when a medication was used between groups A and B.Notes:* Group A, participants were not previously diagnosed with migraine with aura but diagnosed by reseach questionnaire. Group B, participants with a previous diagnosis of migraine with aura.

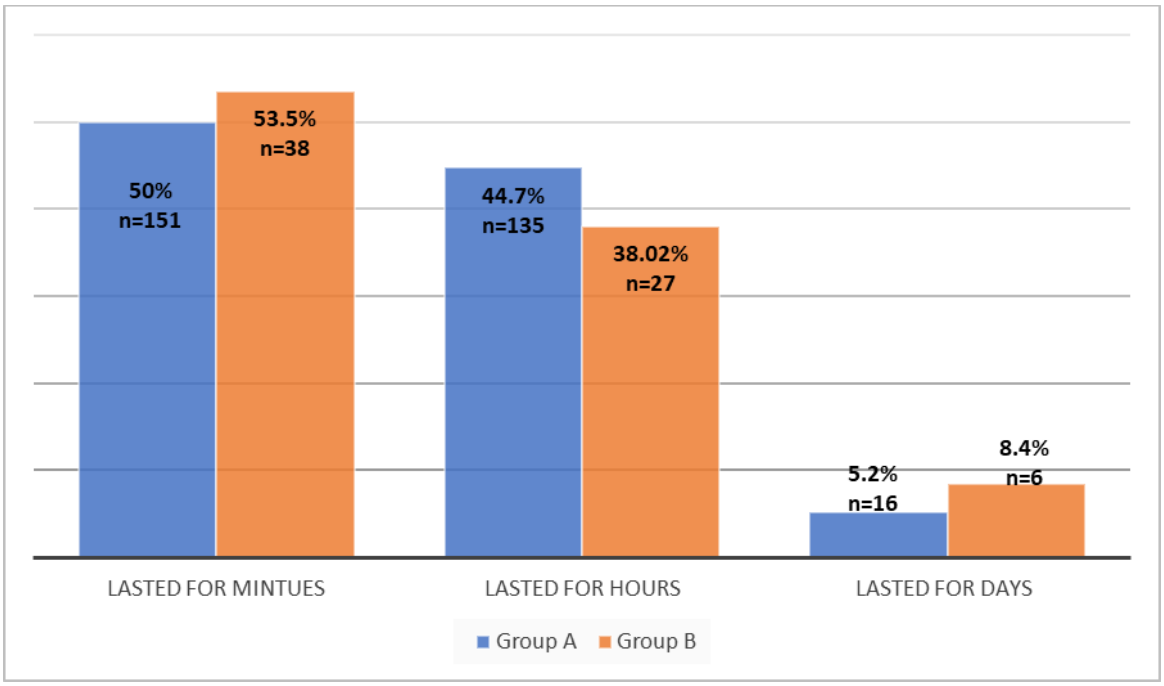


***Figure 2.*** *A comparison of headaches through medication was used between groups A and B. Notes: Group A, participants not previously diagnosed with migraines with aura but diagnosed by a research questionnaire. Group B, participants with a previous diagnosis of migraine with aura.*

**APPENDIX 1**

**Determining Migraine with Aura Trigger Factors, toward improving the practice: A cross-sectional study from Saudi Arabia**

**(Questionnaire)**

Do you agree to participate in this study? (all your information will be private)

- Yes
- No

Data collector name: …….

Region:

- Eastern province
- Northern province
- Central province
- Western province
- Southern province

Gender:

- Male
- Female

Age:

- 18-25
- 26-30
- 31-35
- 36-40
- 41-45
- 46-50

Social status:

- Single
- Married
- Divorced
- Widow

Your weight?

- My weight has been fairly stable (within 10 Ibs) in my adult life

- My weight has been increase over the years
- My weight has gradually declined over the years
- My weight tends to fluctuate up and down

Your height? ……

Do you diagnosed before in neurology clinic with any of the following?

- Migraine headache without aura
- Migraine headache with aura
- Tension headache
- No I didn't diagnosed before

Did you suffer from headaches when you were younger?

- Child
- Teenager
- 20s-40s year of age
- 50s - 60 year of age

Was there a precipitating event or trigger for your current headache problem?

- None known
- Specific stress (mention it below and when)
- Injury (mention the type of injury and when below)
- motor vehicle accident (mention when below)
- Illness (mention what type of illness and when below)
- Menarche (first period)
- Pregnancy (mention how many children do you have and in which pregnancy you developed the headache below)
- Birth control pills (mention what type and when you start using it below)
- Hormonal replacement therapy (mention for how long you are using it)
- Other (mention it)

Do you have first degree family history of chronic headaches?

- Yes
- No

If yes mention the relative relation ……

Job:

- Students
- Ordinary Employee

- Shifts worker/night time worker
- Unemployed

Mention your job or your college: …….

How many hours you work daily?

- 2-6 hours
- 6-8 hours
- More than 8 hours
- More than 12 hours

How many hours you sleep daily?

- Between 2-5 hours
- Between 6-8 hours
- More than 9 hours

What's the pattern of your sleep?

- Regular sleep pattern
- Delayed or insufficient sleep / insomnia (including Intermittent sleep pattern)

Approximately, How many cup of water you drink daily?

- 1-2
- 3-4
- 5-6
- 6-9
- More than 10

How many main meals you eat daily?

- 1
- 2
- 3
- More than 3

How many cup of tea or coffee you drink daily?

- Nothing
- From 1-2
- From 3-4
- More than 5

Are you smoker?

- Yes
- No

If yes, how many cigarrete per day? ……

Do you use any illegal drugs?

- Yes, daily
- Frequently
- No

Do you drink alcohol?

- Yes, daily
- Frequently
- No

If yes, how many glass per day?

How many times you go for exercise per weak?

- No attacks
- 1-5 attacks
- 6-12 attacks
- More than 12 attacks

Do you have any chronic diseases? (You can choose more than 1)

- Diabetes
- Hypertension
- Asthma
- Sinusitis (pressure on your forehead, behind your eyes, on your cheecks, nasal discharge, fever)
- IBS or any GI problems
- Autoimmune diseases
- Congenital diseases
- Thyroid problems
- Psychiatric problems
- Cardiac problems
- Neurological problems
- Vision problems (having refractive errors without correction? Dryness? )

If yes, mention it please ……

Do you use any medication for long term in the last 6 months?

- Contraceptive pills

- Steroid
- Medications to enhance Weight loss medications
- Antidiabetec medications
- Antihypertensive medications
- Antacid or PPI
- Thyroid medications
- Antihistamine
- Hormonal replacement therapy

Others? Mention it please ……

Is your headache?

- Transit, in attacks
- Persistent

For how long you have headache attacks?

- Less than 1 month
- Less than 6 months
- More than 6 months
- More than 1 year
- More than 2 years
- More than 3 years

Headaches typically begin:

- Gradually
- Suddenly
- Varies

They usually begin in the

- Night
- Evening
- Afternoon
- Morning

How long before they reach maximal intensity

- Minutes
- Hours

Headaches usually last (with medication)

- Minutes
- Hours

- Days

Headaches usually last (without medication)

- Minutes
- Hours
- Days

Approximately How many attacks you have in the last 6 months:

- 5-7 attacks
- More than 8 attacks
- More than 15 attacks
- Less than 3 attacks
- No attacks

During your last 5 attacks, the headache was localized as:

- Left side
- Right side
- May be either side right or left
- Temple
- Behind eye(s)
- Back of head
- Neck
- Bilateral headache
- Start unilateral then bilateral
- Localized more in your forehead like a band

Do you have any of the following symptoms before 5-50 minutes from starting of the headache attack?

- Mood changes
- Personality changes
- Change in appetite
- Neck pain
- Food cravings
- Fatigue
- Numbness in any parts of you body
- Weakness in any part of your body
- Since of pin or niddle moving from part of your body, tongue, or face
- Seeing zigzag figure near your eyes, or stars
- Seeing points moving in front of you
- Nausea / vomiting

- Dizziness or vertigo
- Partial loss of vision / blurry vision / blindness (circle applicable)
- Paralysis
- No, I don't have these

How you can prescribe the nature of your headache?

- Pulsating
- tightening
- Stabbing
- Throbbing
- Pressure
- Burning
- Dull ache
- None of the above (mention it)

Do you experience any of the following during the attack? (you can choose more than one):

- Nausea
- Vomiting
- Photophobia (sensitivity to light)
- Phonophobia (sensitivity to sounds)
- Strong smells/odors bother you
- Dizziness / lightheadedness / vertigo (circle applicable description)
- Numbness or tingling
- Increased sensitivity of Scalp / Hair / Ears
- Eye tears
- Difficulty concentrating
- Runny or stuffy nose
- Mood changes / irritability

During a headache, what makes you feel the most comfortable

- Lying down / sleeping
- Keeping physically active
- Massage your head
- Cold pack on your head/neck
- Being in a dark quiet room
- Pacing back-and-forth
- Tying something around your head
- Hot pack on your head/neck

Duration of your headache attacks last for:

- Less than 4 hours
- 4-72 hours
- More than 72 hours

How it affects your daily life?

- Aggravated by routine physical activity such as walking or climbing stairs
- NOT Aggravated by routine physical activity such as walking or climbing stairs

Does it prevent you from doing your job?

- Yes
- No

How sever you can rate your pain?

- Mild – moderate in intensity
- Moderate – sever

What are you doing usually to relive your attacks and it works with you?

- Taking paracetamol
- Taking ibuprophen
- Emergency injection

If you take paracetamol or ibuprophen mention how many tablets you need to relive your headache attack …….

Rate the following from (0 to 2): 0 means no relationship, 1 means sometimes you notice, 2 means you usually notice that this thing trigger your headache).

| **Triggers** | **0** | **1** | **2** |
|---|---|---|---|
| Stress and anxiety | | | |
| Sleep disturbance | | | |
| Study for exams | | | |
| Use any of the drugs mentioned above | | | |
| When you use low calorie diet | | | |
| When you in a noisy place | | | |

| | | | |
|---|---|---|---|
| When you see a lot of lights | | | |
| Relaxation after a period of stress | | | |
| Change in weather | | | |
| When you drink alcohol | | | |
| When you drink so much caffeine | | | |
| When you decrease your daily dose of caffeine | | | |
| When you increase your daily dose of caffeine | | | |
| When you eat hotdog | | | |
| When you are hungry | | | |
| When you eat fast food | | | |
| When you eat eggs | | | |
| When you eat spicy food | | | |
| When you eat smoked fish | | | |
| When you eat chocolate | | | |
| When you eat cheese, banana, orange | | | |
| Menstruation | | | |
| Exercise | | | |
| Prolonged computer work | | | |

| | | | |
|---|---|---|---|
| Certain oddrs | | | |
| Alcohol | | | |
| wine | | | |
| Sexual activity | | | |
| coughing | | | |
| Weather changes | | | |

Do you have any other triggers didn’t mention above?

- Yes
- No

If yes, mention it please …….

Thank you

PERIÓDICO TCHÊ QUÍMICA
ARTIGO ORIGINAL

# MICROBIOMA UTERINO EM MULHERES FÉRTEIS SAUDÁVEIS E NO CASO DE PATOLOGIA DO ENDOMÉTRIO EM FALHAS MÚLTIPLAS DOS PROGRAMAS DE FERTILIZAÇÃO IN-VITRO

# UTERINE MICROBIOME IN HEALTHY FERTILE WOMEN AND IN CASE OF ENDOMETRIUM PATHOLOGY IN MULTIPLE FAILURES OF IN-VITRO-FERTILIZATION PROGRAMS

# МИКРОБИОМ ПОЛОСТИ МАТКИ У ЗДОРОВЫХ ФЕРТИЛЬНЫХ ЖЕНЩИН И ПРИ ПАТОЛОГИИ ЭНДОМЕТРИЯ ПРИ МНОГОКРАТНЫХ НЕУДАЧАХ ПРОГРАММ ВРТ

BARINOVA, Victoria Vladislavovna[1,2*]; KUZNETSOVA, Natalya Borisovna[1,2]; BUSHTYREVA, Irina Olegovna[2]; OKSENYUK, Oksana Stanislavna[1]; SHATALOV, Alexander Evgenievich[1]

[1]Rostov-on-Don State Medical University, Rostov-on-Don, Russian Federation.

[2]Clinic of Professor Bushtyreva LLC, Rostov-on-Don, Russian Federation.

** Corresponding author*
*e-mail: victoria-barinova@yandex.ru*

Received 08 February 2021; received in revised form 28 February 2021; accepted 17 March 2021

## RESUMO

**Introdução:** Graças às novas tecnologias de diagnóstico, não há dúvida de que o útero não é mais considerado estéril. Um microbioma comprometido do endométrio pode ser uma razão significativa para parto prematuro, infertilidade, recorrência de perda de gravidez e falhas repetidas de implantação em programas de fertilização in-vitro. **Objetivo:** estudar as características do microbioma endometrial em mulheres saudáveis férteis e em mulheres com múltiplas falhas na fertilização in-vitro. **Materiais e métodos:** Para avaliar as diferenças na microbiota endometrial de 20 mulheres com infertilidade e experimentando várias tentativas malsucedidas de fertilização in vitro e 15 mulheres férteis saudáveis, o microbioma endometrial foi estudado usando um NGS de 16S rRNA. **Resultados e Discussão:** *Lactobacillus* (29,4%), *Comamonas* (16,8%) e *Mesorhizobium* (6,0%) foram os gêneros mais abundantes no grupo de pacientes férteis saudáveis, sendo *Lactobacillus* (33,3%), *Ralstonia* (7,9%) e *Pediococcus* (4,8%) eram abundantes principalmente no grupo de pacientes inférteis. A abundância relativa média de *Lactobacillus* não diferiu significativamente entre os grupos e compreendeu 33,3% no 1º grupo e 29,4% no 2º grupo. Abundância relativa média significativamente mais elevada de bactérias do gênero *Brevundimonas* e *Ralstonia* foi registrada no primeiro grupo. As mulheres férteis do 2º grupo tiveram uma abundância relativa média estatisticamente significativamente maior de *Acidovorax*, *Brevibacillus*, *Caulobacter*, *Comamonas*, *Delftia*, *Distigma*, *Pseudomonas*, *Schlegelella*, *Thermus*. **Conclusões:** Os dados apresentados confirmam que o endométrio não é um tecido estéril, apesar dos conceitos antigos sobre sua esterilidade. *Lactobacillus* são gêneros dominantes; no entanto, não há dominância absoluta de *Lactobacillus* acima de 90%. A abundância relativa média de *Lactobacillus* no microbioma uterino em pacientes férteis e pacientes com múltiplas falhas de fertilização in-vitro não diferiu.

**Palavras-chave**: *microbioma endometrial, infertilidade, fertilização in-vitro, fertilidade.*

## ABSTRACT

**Background:** Thanks to new diagnostic technologies, it is of no doubt that the uterus is no longer considered to be sterile. A disturbed microbiome of endometrium can be a significant reason for preterm birth, infertility, the recurrence of pregnancy loss, and repeated implantation failures in in-vitro-fertilization programs. **Aim:** Study the endometrial microbiome features in healthy fertile women and in women with multiple in-vitro-fertilization failures. **Methods:** To assess the differences in the endometrial microbiota of 20 women with infertility and experiencing multiple unsuccessful attempts of in-vitro-fertilization and 15 fertile, healthy women, endometrial microbiome was studied using an NGS of 16S rRNA. **Results and Discussion:** *Lactobacillus* (29.4%), *Comamonas* (16.8%), and *Mesorhizobium* (6.0%) were the most abundant genera in group of healthy fertile patients, and *Lactobacillus* (33.3%), *Ralstonia* (7.9%) and *Pediococcus* (4.8%) were most abundant in

the group of infertile patients. The mean relative abundance of *Lactobacillus* did not significantly differ between groups and comprised 33.3% in the group of infertile women and 29.4% in healthy fertile women. A considerably higher mean relative abundance of bacteria of the genus *Brevundimonas* and *Ralstonia* was recorded in the group of infertile women. The fertile women had a statistically significantly higher mean relative abundance of *Acidovorax, Brevibacillus, Caulobacter, Comamonas, Delftia, Distigma, Pseudomonas, Schlegelella,* and *Thermus*. **Conclusions:** The presented data confirm that endometrium is not a sterile tissue despite long-standing concepts concerning its sterility. *Lactobacillus* are dominant genera; however, there is no absolute dominance of *Lactobacillus* over 90%. The mean relative abundance of *Lactobacillus* in the uterine microbiome in fertile patients and patients with multiple in-vitro-fertilization failures did not differ.

**Keywords**: *endometrial microbiome, infertility, in-vitro-fertilization, fertility*

## АННОТАЦИЯ

**Введение:** Благодаря новым диагностическим методикам, в настоящий момент не возникает сомнения, что полость матки не является стерильной. Нарушенный микробиом эндометрия может являться значимой причиной преждевременных родов, привычного невынашивания беременности, бесплодия и повторных неудач имплантации в программах ВРТ. **Цель:** изучить особенности микробиома эндометрия у здоровых фертильных пациенток и у пациенток с многократными неудачами ВРТ. **Материалы и методы:** С целью оценки различий микробиома эндометрия у 20 женщин с бесплодием и многократными неудачными попытками ВРТ и у 15 фертильных здоровых женщин был изучен микробиом эндометрия путем секвенирования нового поколения гена 16S рРНК. **Результаты:** Самыми представленными в группе здоровых фертильных пациенток были роды *Lactobacillus* 29,4%, *Comamonas* 16,8% и *Mesorhizobium* 6,0%, а в группе бесплодных пациенток с многократными неудачами ЭКО – *Lactobacillus* 33,3%, *Ralstonia* 7,9% и *Pediococcus* 4,8%. При этом доля лактобактерий у пациенток первой группы значимо не отличалась от пациенток 2ой группы (33,3% и 29,4% соответственно). В группе женщин с бесплодием и многократными неудачными попытками ЭКО регистрировалась достоверно более высокая относительная представленность бактерий рода *Brevundimonas* и *Ralstonia*. При этом у фертильных женщин 2ой группы регистрировалась статистически значимо более высокая представленность *Acidovorax*, *Brevibacillus*, *Caulobacter*, *Comamonas*, *Delftia*, *Distigma*, *Pseudomonas*, *Schlegelella*, *Thermus*. **Заключение:** Представленные данные подтверждают концепцию нестерильности эндометрия и существования маточного микробиома. Лактобактерии являются доминирующим родом в составе маточного микробиома, однако не абсолютно доминирующим, т.е. не более 90%. При этом доля лактобактерий у фертильных пациенток и у пациенток с многократными неудачами ВРТ значимо не отличалась.

**Ключевые слова:** микробиом эндометрия, бесплодие, ЭКО, фертильность.

## 1. INTRODUCTION:

The endometrium has always been considered sterile in nonpregnant, pregnant women and postpartum women, as proven by cultural method diagnostics (Butler, 1958). Indeed, premature deliveries, recurrent miscarriage, and repeated implant failures in artificial reproductive technologies are known to be associated with the presence of highly concentrated microbial products, endotoxins, or infection process within the endometrium (Fox, *et al*., 2015; Drbohlav *et al*., 1998; Hernandes, *et al*., 2020; Cicinelli *et al*., 2014).

It is difficult to imagine that the endometrium can remain a colonization-free zone at the same time as being near various microorganisms of the lower reproductive system, as well as with sperm – which may carry bacteria.

The ascending path through the uterine cervix is considered the main source of bacterial existence within the endometrium (Mitchell *et al*., 2015). As an example, experimental models have shown that the labeled particles, identical to sperm cells (microaggregates of the human-derived protein albumin), may pass through the cervical canal to the womb within several minutes in cases of nonpregnant women (Zervomanolakis *et al*., 2007; Kunz, *et al.,* 1997). In this manner, the uterine peristaltic contractions, which facilitate the entry of sperm into the uterine cavity, may perform bacterial insemination within the endometrium. Simultaneously, the anatomical constitution of cervix and the cervical mucus protect the womb from vaginal bacteria. Due to this fact, data has shown a rapidly declining relative and absolute *lactobacillus* abundance in the lower third, middle third and upper third parts of the endometrium. Therefore, the ‘higher’ the definite part the womb

is, the lower the relative abundance of *lactobacillus* there (Mitchell *et al*., 2015), i.e. concentration of *lactobacillus* is less in the bottom of the uterus than near the cervical canal. Thus, it is obvious to conclude that the endometrium cannot be considered as sterile tissue.

Recent research in this field, with the implementation of molecular technology, has proven the existence of residential microflora within the human endometrium and its potential influence on the reproduction of women (Benner *et al.,* 2018). In particular, with the processes of ovum implantation and the outcomes of pregnancies (Marchesi and Ravel, 2015; Fang *et al*., 2016; Franasiak *et al*., 2016; Yan *et al.,* 2016).

The most commonly discussed hypothesis is the 'lactobacillary' and 'non-lactobacillary' microbiome in the endometrium (Moreno *et al*., 2016). This means that the dominance of *lactobacillus* (relative abundance is more than 90%) within the microbiota contents of the endometrium was generally associated with a successful implantation and a high frequency of live-borns in patients having undergone in-vitro-fertilization (Moreno *et al*., 2016; Kyono *et al*., 2018; Walther-Antonio *et al*., 2016). Consequently, it can be concluded that potentially increasing the relative abundance of *lactobacillus* by up to 90% or more in women with a non-*lactobacillus* microflora within the endometrium could lead to frequent successful implantations in infertile patients and can later be associated with a 'healthy' uterine microbiome.

Unfortunately, numerous scientific publications and the accumulated scientific material do not allow forming a solid understanding of what normal and a dysbiotic uterine microbiome is by now or explain how to correct in case of abnormality (Wee *et al*., 2018; Verstraelen *et al*., 2016; Tao *et al*., 2017; Miles *et al*., 2017; Pelzer *et al*., 2018; Chen *et al*., 2017).

This study aimed to assess the uterine microbiome in women with infertility who have experienced numerous failed attempts of in-vitro-fertilization and healthy fertile women without an obstetric or gynecological history who had at least one successful vaginal delivery.

## 2. MATERIALS AND METHODS:

### 2.1. Study Design

The study included 35 women divided into two groups (Table 1). All patients were examined at the Department of Obstetrics and Gynecology № 1 of the Federal State Budgetary Educational Institution of Higher Education, Rostov State Medical University, and Ministry of Health of Russia (Rostov-on-Don, Russia). Patients of both groups were comparable in body mass index, age of menarche, duration of the menstrual cycle and duration of menstruation itself, and age.

Group I included 20 women with infertility due to various origins and multiple unsuccessful in-vitro-fertilization attempts (two or more attempts), aged 20 to 42 years. All of these women underwent frozen embryo transfer protocols after preparation of endometrium with estrogens and progesterone. Only one embryo was transferred to the uterus, and preimplantation genetic testing was performed on all embryos before transfer. The exclusion criteria included any uterine pathology, along with congenital malformations, uterine fibroids, polyps, uterine synechia, and uterine manipulations within the last six months, as well as the presence of an IUD within the last six months, any systemic inflammatory disease or severe extragenital pathology, or the use of systemic antibiotic therapy in the last three months.

Group II consisted of 15 healthy women from 20 to 42 years old without any complaints, without burdened obstetric or gynecological history, who'd had at least one vaginal birth in the anamnesis. In addition to the criteria for group I, the exclusion criteria also included surgical abortions, pregnancy losses, non-developing pregnancies, and uterine cavity curettages in the postpartum period, together with a history of cesarean section.

### 2.2. Ethics

Each study participant completed an written informed consent. The local ethics committee of the Rostov State Medical University of the Russian Ministry of Health approved this study.

### 2.3. Sample collection

All samples of endometrium were collected between 22 to 24 days of the regular menstrual cycle. To avoid contamination with microorganisms from the vagina or cervical canal, and to obtain exclusive data on the species composition of the uterine cavity, a

catheter for transferring the embryo into the uterine cavity was used to collect the material, consisting of an 'outer hard part' and an 'inner soft part' (Figure 1). After visualization of the cervix, using a sterile gauze swab moistened with chlorhexidine solution, mucus was removed from the surface of the cervix, then the cervix was processed. The catheter for transferring embryos into the uterine cavity was carefully inserted into the cervical canal without touching the walls of the vagina. In contrast, the inner soft part of the catheter was completely inserted into the outer one. In this way, bacterial contamination of the cervical canal was avoided.

After entering the uterine cavity, the inner catheter was carefully pushed out from the outer one into the uterine fundus area. The material was taken from the fundus to study the microbiome of the uterus, then the inner catheter was again placed in the outer part, and the entire system was removed from the cervical canal and vagina. A sample of endometrial flora was placed in an Eppendorf tube with a special transport medium 'transport medium with mucolytic' (Federal Budget Institution of Central Epidemiological Research, Rospotrebnadzor, Moscow, Russia), the medium was kept at +4°C until DNA isolation.

The total DNA was isolated using the Ribo-prep kit (FBSI Central Research Institute of Epidemiology, Rospotrebnadzor, Russia) according to the manufacturer's protocol. This proprietary method is based on cell lysis with a guanidine thiocyanate (GuSCN) and a Triton X-100-based lysis buffer, followed by DNA precipitation and washing with isopropanol-based buffers. DNA is finally diluted in 10 mM Tris-HCl (pH = 8.0).

Libraries of 16S rRNA gene fragments were prepared according to '16S Metagenomic Sequencing Library Preparation' (Part No. 15044223 Rev. B) of Illumina. 5 ng of total DNA was amplified for 25 cycles using the primers recommended in the protocol for the V3 and V4 regions of the 16S rRNA bacteria gene and the ready-made mixture for PCR KAPA HiFi HotStart ReadyMix (2X) (Roche Diagnostics, Switzerland). The resulting DNA fragments were purified using AMPure XP beads paramagnetic particles (Beckman Coulter, USA). To carry out indexing PCR, 5 ng of DNA after the first round of amplification was subjected to eight amplification cycles using tag-coded primers from the Nextera XT Index Kit (Illumina, USA) and the KAPA HiFi HotStart ReadyMix (2X) PCR mixture (Roche Diagnostics, Switzerland). The obtained libraries of gene fragments were purified using paramagnetic particles, combined with an equimolar ratio, and sequenced on a MiSeq system (Illumina, United States) in a 2 * 151 paired end-sequencing mode.

### 2.4. Data analysis

The data analysis obtained during the sequencing of gene fragment libraries was carried out using a pipeline implemented in the R v.3.6 programming languages (R Core Team, 2014) and Python. At the first stage of the pipeline, the primer sequences were removed from the beginning of reads. Reads that did not contain primers were also removed. Then, the last 25 nucleotides of the reads were removed as low quality, and the obtained data were processed using the DADA2 protocol to detect exact sequence variants. After determining the exact variants of the sequences, forward and reverse readings were combined by concatenation, and the resulting sequences were used for Bayesian taxonomic classification (Wang *et al*., 2007) using the SILVA v132 reference database (Quast *et al*., 2013). Species identification was performed using the DADA2 full match algorithm using the SILVA v132 database sequences pre-processed with custom scripts to match the analysis.

### 2.5. Statistical analysis

The Shapiro–Wilk test was used to check the clinical and demographic characteristics of patients in the studied groups for normal distribution (Table 1). The concentrations of the studied microorganisms are not of a normal distribution and are significantly rarefied; therefore, they are presented as medians (Table 2). The nonparametric Mann–Whitney test was used to compare quantitative indicators in groups. The differences were considered statistically significant at the $p < 0.05$ level. The calculations were performed in R (version 3.2, R Foundation for Statistical Computing, Vienna, Austria).

## 3. RESULTS AND DISCUSSION:

The clinical and demographic characteristics of both patient groups are presented in Table 1. A study of the endometrial microbiome by sequencing made it possible to identify microorganisms belonging to 19 types, 26 classes, 89 families, 257 genera, and 366

different species by taxonomic classification. A comparison between groups was carried out at the taxonomic level of genera.

According to the genera level between the two groups, statistically, significant differences were revealed in the relative abundance of the following genera of microorganisms: *Acidovorax, Brevibacillus, Brevundimonas, Caulobacter, Comamonas, Delftia, Distigma, Pseudomonas, Ralstonia, Schlegelella,* and *Thermus*. In the group of women with infertility and repeated unsuccessful in-vitro-fertilization attempts, a significantly higher abundance of bacteria of the genus *Brevundimonas* (0.065 – 0; 0.38 in the Group I and 0 [0; 0] in the Group II) and *Ralstonia* (0.21 [0; 1.2] in the Group I and 0 [0; 0.12] in the Group II) was identified.

At the same time, the fertile women of Group II had a statistically significantly higher abundance of *Acidovorax* (0 [0; 1.33] in the Group I and 2.1 [0.75; 3.44] in the Group II), *Brevibacillus* (0 [0; 0] in Group I and 0.11 [ 0; 0.3] in Group II), *Caulobacter* (0 [0; 0.28] in Group I and 0.54 [0.15; 1.07] in Group II, respectively), *Comamonas* (0.01 [0; 6.37] in Group I and 7.44 [4.15; 18.2] in Group II), *Delftia* (0.025 [0; 1.26] in Group I and 2.4 [0.81; 4.11] in Group II), *Distigma* (0 [0; 0.22] in Group I and 0.64 [0.11; 1.22] in Group II, respectively), *Pseudomonas* (0 [0; 0.12] in the Group I and 0.48 [0.01; 2.26] in the Group II), *Schlegelella* (0 [0; 0.72] in the Group I and 1.18 [0.29; 2.14] in the Group II), *Thermus* (0 [ 0; 2.63] in the Group I and 2.57 [1.05; 5.62] in the Group II) (Table 2).

When analyzing the average relative abundance of bacterial genera, the most represented in the group of healthy fertile patients were *Lactobacillus* 29.4%, Comamonas 16.8% and Mesorhizobium 6.0%, and in the group of infertile patients with multiple in-vitro-fertilization failures – *Lactobacillus* 33.3%, Ralstonia 7.9%, and Pediococcus 4.8% (Figures 2, 3 and 4).

Meanwhile, the abundance of *Lactobacillus* in Group I patients did not differ significantly from the abundance of Lactobacilli in patients of Group II (33.3% and 29.4%, respectively). Also, it is not possible to make confident conclusions about the dominance of *Lactobacillus* over 90% in the composition of the uterine microbiome in healthy women, as Moreno claims from his observations (Moreno *et al*., 2016; Kyono *et al*., 2018). The category 'other microorganisms' included various microorganisms whose relative abundance in the microbiome was less than 1%. In patients of group I, 'other' microorganisms accounted for 18.7%, and 14.4% in Group II – 14.4%, respectively. Also, unclassified microorganisms – that is, those that could not be identified or whose genome is absent in the known databases – accounted for 10.5% in Group I and 7.5% in Group II. In general, it can be argued that the endometrial microbiome is quite diverse both in healthy fertile patients and in patients with multiple in-vitro-fertilization failures, which may be directly related to the place of collection of material for the microbiome study – namely, the uterine fundus. After all, the 'higher' the locus of material sampling in the female reproductive system, the lower the abundance of *Lactobacillus*. However, despite the diversity of microorganisms, attention was drawn to the almost complete absence (less than 1%) in fertile patients and the presence of the following genera of microorganisms in infertile women with in-vitro-fertilization failures: *Streptococcus* (3.2% in Group I), *Ralstonia* (7,9% in Group I), *Pediococcus* (4.8% in Group I), *Clostridium* (4.0% in Group I). At the same time, bacteria registered in fertile patients but not detected in significant proportions (more than 1%) in patients with infertility were *Acinetobacter* (1.7% in Group II), *Anaerobacillus* (1.3% in Group II), *Cupriavidus* (1.1% in Group II), *Curvibacter* (2.0% in Group II), *Delftia* (2.8% in Group II), *Paucibacter* (1.3% in Group II), *Prevotella* (1.7% in Group II), *Shlegella* (1.3% in Group II).

This research had many limitations. First, the sample size – 20 patients from Group I and 15 from Group II – may not represent population abundance as a whole but may indicate some trends for further study. Therefore, the results obtained require other studies carried out using larger cohorts of patients.

Another limitation of this study was the lack of negative control samples. In scientific papers devoted to studying the microbiome of biotopes of complex localizations, increasing attention is devoted both to the presence of control samples and their negative values. If the endometrial microbiota exists, then it is present in very low concentrations. Therefore, its molecular characteristics are influenced by background DNA contamination from extraction kits and reagents for PCR sequencing (Salter *et al*., 2014; Weyrich *et al.,* 2019). For this reason, contaminating DNA can account for a significant part, if not all, of the recorded molecular microbial signatures within the endometrium. It is,

therefore, imperative that endometrial microbiota studies include technical controls for potential sources of background DNA contamination (Salter *et al*., 2014), as well as a detailed presentation of the microbial profiles of these controls (Eisenhofer *et al.*, 2019). Most of the studies available to date do not include control samples, or the data on their microbial profile is insufficiently presented. When sequencing the control samples of nutrients or transport medium or air from the operating room, the number of reads should be hundreds of times less than the number of reads of material from the endometrium. Potential microbial contamination is possible from extraction kits, culture medium, and air, which can greatly affect the interpretation of the identified microorganisms' clinical significance. The role of negative control samples, therefore, is of paramount importance. This, however, increases research costs by almost three times, which further complicates work planning.

The third limitation was the method of material sampling for research – which was the transcervical approach. In most endometrial microbiome studies currently available, the sampling was carried out transcervically, possibly associated with the contamination of endometrial samples by microbes or microbial molecular signals from the vagina and cervical canal. In most studies to date, in which material for sequencing has been collected via transcervical access, the lactobacillary microflora characteristic of the vaginal microbiome was noted. At the same time, in studies where the material was collected in a transabdominal way, the variety of microorganisms was higher. Thus, Chen *et al.* used 16S rRNA sequencing to assess the microbiome of both the lower and upper sections of the female reproductive tract. This showed that, for the upper sections, the average proportion of *Lactobacillus* is only 1.7% (fallopian tubes). In the endometrium, the relative abundance of *Lactobacillus* was 30.6%, but *Acinetobacter* (9.1%), *Pseudomonas* (9.1%), *Vagococcus* (7.3%), *Sphingobium* (5.0%) and *Comamonadaceae* (4.9%) were widely abundant (Chen *et al*., 2017). Walther-Antonio *et al*. examined ten women after hysterectomy associated with benign neoplasms. In the myometrium and endometrium, *Lactobacillus* was found in extremely low proportions. The most represented in the endometrium were *Shigella* and *Barnesiella* (Walther-Antonio *et al*., 2016). In contrast, in a study that obtained material from the middle third of the endometrium after hysterectomy, there was also no dominance of *Lactobacillus* (Winters *et al*., 2019), and the endometrial bacterial profiles were mainly abundant with *Acinetobacter, Pseudomonas, Comamonadaceae* and *Cloacibacterium*. It turns out, therefore, that in all studies in which the method of sampling was transcervical, the predominance of *Lactobacillus* in the composition of the uterine microbiome was reported and, as with other sample obtaining methods, the microbiome was more variable.

The significance of the presented research lies in several positions. First, the presented data confirms the concept of endometrial non-sterility and the existence of the uterine microbiome as a whole (Altmäe *et al.*, 2018; Baker *et al.,* 2018). Unambiguously, sequencing makes it possible to detect the presence of bacteria in the endometrium, but the results of the analysis itself do not allow for quantifying this presence. That is, it is impossible to judge the level of bacteria found in a particular sample.

Statistically significant differences between groups were obtained in the following genera of microorganisms: *Acidovorax, Brevibacillus, Brevundimonas, Caulobacter, Comamonas, Delftia, Distigma, Pseudomonas, Ralstonia, Schlegelella,* and *Thermus*. However, their average relative representation in the uterine microbiome composition was less than 1%; therefore, the question of their influence on the implantation processes of a fertilized egg is debatable.

Presented data confirm the current concept of the dominance of *Lactobacillus* in the uterine microbiome. Considering the anatomical proximity of the uterine cavity and endometrium with the main source of *Lactobacillus* in the reproductive system – with the vagina – and the existence of peristaltic uterine contractions, contributing to the capture of *Lactobacillus* from the vagina and the ascending pathway of their entry into the uterine cavity, the dominance of *Lactobacillus* becomes an understandable and logical fact. Various data on the percentage of *Lactobacillus* in the microbiome can be explained by the 'area' of sampling of the material for study: the closer to the area of the cervical canal, the higher the percentage of *Lactobacillus*; the closer to the area of the fundus, the less its percentage (Winters *et al.,* 2019).

Besides, the presented data refutes the theory of lactobacillary and non-lactobacillary microbiome in the genesis of fertilized egg implantation failures. According to the presented

data, the proportion of *Lactobacillus* in fertile patients and in patients with multiple in-vitro-fertilization failures did not differ significantly and amounted to 33.3% and 29.4%, respectively. This may be due to the area of sampling – in this study, this is the bottom of the uterus, e.g. the most distant from the source of *Lactobacillus* – the vagina – the locus of the uterus. Therefore, the dominance of *Lactobacillus* cannot be considered as a factor determining the absolute success of implantation. Besides, the relative abundance of *Lactobacillus* – over 50% in the microbiome – was recorded in only 5 out of 15 women from the group of fertile patients. In 7 out of 20 women from the group of women with in-vitro-fertilization failures (Figure 4). The absolute dominance of *Lactobacillus* – more than 90% – was noted in a total of three women out of the entire sample (35 patients), which does not correlate with Moreno's data (Moreno *et al*., 2016).

In all likelihood, it is not only the relative abundance of *Lactobacillus* that affects implantation success, as it is necessary to search for those pathogenic microorganisms that trigger a cascade of inflammatory reactions in the endometrium, thereby determining the implantation impairment. It is important to study the microbiome of the endometrium, together with markers of chronic endometritis, via a histological and immunochistochemical examination of the endometrium during biopsy (Agostinis *et al.,* 2018; Zhang *et al.,* 2019). The mechanisms providing a positive result during implantation of a fertilized egg are more subtle and include not only the influence of certain pathogenic microorganisms and their endotoxins but also the local immune response of the endometrium. In this regard, it is more expedient to study the composition of the endometrial microbiome in close connection with immunohistochemistry markers of chronic endometritis. Moreover, it is important to include in diagnostic algorithms an assessment of the functional state of the endometrium (dopplerometry of the uterine spiral arteries) and to assess tissue morphology during biopsy (; Liu Y *et al., 2018;*).

According to the presented data, in the group of women with infertility and repeated unsuccessful in-vitro-fertilization attempts, a significantly higher relative abundance of bacteria of the genus *Brevundimonas* and *Ralstonia* were recorded, and in fertile women of the second group, a statistically significant higher abundance of *Acidovorax, Brevibacillus, Caulobacter, Comamonas, Delftia, Distigma, Pseudomonas, Schlegelella,* and *Thermus* were recorded. Whether this statistically significant difference is of clinical importance or not remains unclear as, firstly, the average relative abundance of these bacterial genera was less than 1%. Secondly, all these microorganisms are opportunistic and lead to the development of the disease only under concomitant circumstances.

The most abundant in the group of healthy fertile patients were *Lactobacillus, Comamonas* and *Mesorhizobium*. While in the group of infertile patients with multiple in-vitro-fertilization failures *Lactobacillus, Ralstonia* and *Pediococcus* were most abundant. Regarding *Lactobacillus*, their biological role in the microbiota composition is more or less clear. As for *Comamonas*, this genus belongs to conditionally pathogenic microorganisms stable in the external environment and are characteristic of the gastrointestinal tract (Khalki *et al*., 2016). *Mesorhizobium* are also conditionally pathogenic microorganisms that occur in nature as a symbiont of plants, but there are several reports of their involvement in the development of peritonitis (Krishnan *et al*., 2016). *Ralstonia* are generally characteristic of such an econiche as water and are able to survive in conditions of low nutrient supply. In humans, they are involved in the occurrence of osteomyelitis and meningitis (Ryan and Adley, 2014). *Pediococcus* is a lactic acid-producing bacteria used as probiotics. The role of all these genera of microorganisms in the uterine microbiome composition remains insufficiently studied to date (Porto *et al*., 2017).

There are many interesting perspectives to potentially improve endometrial dysbiosis: among them is fecal transplantation, vaginal microbiota transplantation, and the administration of pro-and prebiotics (DeLong *et al.*, 2019; Lev-Sagie *et al.,* 2019; Quaranta *et al.,* 2019; Stallmach *et al*., 2019). All these methods have been discussed but are worth further investigation.

## 4. CONCLUSIONS:

The present study confirms that even such hard-to-reach locus as the endometrium are not sterile. The endometrium is not such a 'densely populated' biotope as, for example, the intestine, and the concentration of bacteria here is negligible. Still, one cannot ignore the role of detected microorganisms in the genesis of recurrent implantation failures. The most abundant genera, seen both in fertile and infertile

women with repeated implantation failures, was *Lactobacillus*. There was no significant difference in the mean relative abundance of *Lactobacillus* between two groups.

Infertile women with repeated in-vitro-fertilization failures and repeated impaired implantation had significantly higher mean relative abundance of bacteria of the genus *Brevundimonas* and *Ralstonia*. The fertile women had a statistically significantly higher mean relative abundance of *Acidovorax*, *Brevibacillus*, *Caulobacter*, *Comamonas*, *Delftia*, *Distigma*, *Pseudomonas*, *Schlegelella*, and *Thermus*. But the abundance of all these genera was very low. Thus, it is unclear whether such low concentrations can have clinical effects and influence implantation process.

Knowledge of the composition of the endometrial microbiome supports the need to develop algorithms for correcting dysbiosis. In this case, it is crucial to consider the pathways of microorganisms entering the uterine – ascending from the vagina, hematogenous from the intestine, and oral cavity. All this provides broad prospects for further research.

## 5. ACKNOWLEDGMENTS:

The authors are grateful to the staff of the genetic laboratory of Serbalab LLC, St. Petersburg: Mikhail Vladimirovich Aseev, Vasilisa Valerievna Dudurich, Dmitry Evgenievich Polev, and Yuri Alexandrovich Barbitov. This work was carried out within the framework of grant No. 19-75-00006 ‘Role of the uterine microbiome in the genesis of reproductive losses and in-vitro-fertilization failure’ of the Russian Science Foundation.

## 6. REFERENCES:

1. Agostinis, C.; Mangogna, A.; Bossi, F.; Ricci, G.; Kishore, U.; Bulla, R. Uterine Immunity and Microbiota: A Shifting Paradigm. Front. Immunol. 2019, 10, 2387. Altmäe, S. Uterine Microbiota: A Role Beyond Infection. EMJ Reprod. Heal. 2018, 6, 70–75.
2. Altmäe, S. Commentary: Uterine Microbiota: Residents, Tourists, or Invaders? Front. Immunol. 2018, 9, 1874.
3. Baker, J.M.; Chase, D.M.; Herbst-Kralovetz, M.M. Uterine Microbiota: Residents, Tourists, or Invaders? Front. Immunol. 2018, 9, 208.
4. Benner, M.; Ferwerda, G.; Joosten, I.; van der Molen, R.G. How uterine microbiota might be responsible for a receptive, fertile endometrium. Hum. Reprod. Update 2018, 24, 393–415.
5. Butler, B. (1958). Value of endometrial cultures in sterility investigation. *Fertility and Sterility*, 9, 269–273.
6. Chen, C., Song, X., Wei, W., Huanzi Zhong, Juanjuan Dai, Zhou Lan, Fei Li, Xinlei Yu, Qiang Feng, Zirong Wang, Hailiang Xie, Xiaomin Chen, Chunwei Zeng, Bo Wen, Liping Zeng, Hui Du, Huiru Tang, Changlu Xu, Yan Xia, Huihua Xia, Huanming Yang, Jian Wang, Jun Wang, Lise Madsen, Susanne Brix, Karsten Kristiansen, Xun Xu, Junhua Li, Ruifang Wu, Huijue Jia (2017). The microbiota continuum along the female reproductive tract and its relation to uterine-related diseases. *Nature Communications*, 8, 875. https://doi.org/10.1038/s41467-017-00901-0
7. Cicinelli, E., Matteo M., Tinelli R., Vincenzo Pinto, Marinaccio M., Indraccolo U., Dominique De Ziegler, Resta L.. (2014). Chronic endometritis due to common bacteria is prevalent in women with recurrent miscarriage as confirmed by improved pregnancy outcome after antibiotic treatment. *Reproductive* Science, 21, 640–647. https://doi.org/10.1177/1933719113508817
8. DeLong, K.; Zulfiqar, F.; Hoffmann, D.E.; Tarzian, A.J.; Ensign, L.M. Vaginal Microbiota Transplantation: The Next Frontier. J. Law. Med. Ethics 2019, 47, 555–567.
9. Drbohlav, P., Hálková, E., Masata, J., J Rezácová, V Cerný, D Rossová. (1998). The effect of endometrial infection on embryo implantation in the IVF and ET program. *Czech Gynaecology*, 63, 181–185. https://doi.org/10.1038/s41598-019-46173-0
10. Eisenhofer, R.; Minich, J.J.; Marotz, C.; Cooper, A.; Knight, R.; Weyrich, L.S. Contamination in Low Microbial Biomass Microbiome Studies: Issues and Recommendations. Trends Microbiol. 2019, 27, 105–117.
11. Fang, R.L., Chen, L-X., Shu, W-S., Shu-

Zhong Yao,1 Si-Wen Wang,3 and Yu-Qing Chen (2016). Barcoded sequencing reveals diverse intrauterine microbiomes in patients suffering with endometrial polyps. *American Journal of Translational Research*, *8*(3), 1581–1592.

12. Fox, C.; Eichelberger, K. Maternal microbiome and pregnancy outcomes. Fertil. Steril. 2015, 104, 1358–1363.
13. Franasiak, J.M., Werner, M.D., Juneau C.R., X. Tao, J. Landis, Y. Zhan, N. R. Treff, and R. T. Scott. (2016). Endometrial microbiome at the time of embryo transfer: next-generation sequencing of the 16S ribosomal subunit. *Journal of Assisted Reproduction and Genetics*, 33, 129–136. https://doi.org/10.1007/s10815-015-0614-z
14. Hernandes, C.; Silveira, P.; Rodrigues Sereia, A.F.; Christo, A.P.; Mendes, H.; Valter de Oliveira, L.F.; Podgaec, S. Microbiome Profile of Deep Endometriosis Patients: Comparison of Vaginal Fluid, Endometrium and Lesion. Diagnostics 2020, 10, 163.
15. Khalki, H., Deham, H., Taghouti, A., Yahyaoui G., Mahmoud M. (2016). Appendicite à *Comamonas testosteroni* (*Comamonas testosteroni* appendicitis). *Medecine et maladies infectieuses*, *46*(3), 168-170. https://doi.org/10.1016/j.medmal.2015.12.009
16. Krishnan, A., Raby, E., Puttagunta, H., Leung M.,Thomas M. (2016). Mesorhizobium peritonitis: The first reported case. *Nephrology*, *22*(1), 96. https://doi.org/10.1111/nep.12716
17. Kunz, G.; Beil, D.; Deiniger, H.; Einspanier, A.; Mall, G.; Leyendecker, G. The uterine peristaltic pump. Normal and impeded sperm transport within the female genital tract. Adv. Exp. Med. Biol. 1997, 424, 267–277.
18. Kyono, K., Hashimoto, T., Nagai, Y., Sakuraba, Y. (2018). Analysis of endometrial microbiota by 16S ribosomal RNA gene sequencing among infertile patients: a single-center pilot study. *Reproductive Medicine and Biology*, 17, 297–306. https://doi.org/10.1002/rmb2.12105
19. Lev-Sagie, A.; Goldman-Wohl, D.; Cohen, Y.; Dori-Bachash, M.; Leshem, A.; Mor, U.; Strahilevitz, J.; Moses, A.E.; Shapiro, H.; Yagel, S., Elinav E. Vaginal microbiome transplantation in women with intractable bacterial vaginosis. Nat. Med. 2019, 25, 1500–1504.
20. Liu, Y., Wong, K.K.W., Ko, E.Y.L, Chen X., Huang J., Tsui S., Li T., Chim S.S.C. (2018). Systematic comparison of bacterial colonization of endometrial tissue and fluid samples in recurrent miscarriage patients: implications for future endometrial microbiome studies. *Clinical Chemistry*, 64, 1743–1752. https://doi.org/10.1373/clinchem.2018.289306
21. Marchesi, J.R., Ravel, J. (2015). The vocabulary of microbiome research: a proposal. *Microbiome*, 3, 31. https://doi.org/10.1186/s40168-015-0094-5
22. Miles, S.M., Hardy, B.L., Merrell, D.S. (2017). Investigation of the microbiota of the reproductive tract in women undergoing a total hysterectomy and bilateral salpingo-oopherectomy. *Fertility and Sterility*, *107*(3), 813–820.e811. https://doi.org/10.1016/j.fertnstert.2016.11.028
23. Mitchell, C.M., Haick, A., Nkwopara, E., Garcia R., Rendi M., Agnew K., Fredricks D., Eschenbach D. (2015). Colonization of the upper genital tract by vaginal bacterial species in nonpregnant women. *American Journal* of *Obstetrics and Gynecology*, *212*(5), 611–619. https://doi.org/10.1016/j.ajog.2014.11.043
24. Moreno, I., Codoñer, F.M., Vilella, F., Valbuena, D., Martinez-Blanch, J.F., Jimenez-Almazán, J., Alonso, R., Alamá, P., Remohí, J., Pellicer, A., Ramon, D., Simon, C. (2016). Evidence that the endometrial microbiota has an effect on implantation success or failure. *American Journal of Obstetrics and Gynecology*, 215, 684–703. https://doi.org/10.1016/j.ajog.2016.09.075
25. Pelzer, E.S., Willner, D., Buttini, M., Huygens, F. (2018). A role for the endometrial microbiome in dysfunctional menstrual bleeding. *Antonie Van*

*Leeuwenhoek*, 111, 933–943. https://doi.org/10.1007/s10482-017-0992-6

26. Porto, M.C.W., Kuniyoshi, T.M., Azevedo, P.O., Vitolo M., R P S Oliveira. (2017). Pediococcus spp.: An important genus of lactic acid bacteria and pediocin producers. *Biotechnology Advances*, *35*(3), 361–374. https://doi.org/10.1016/j.biotechadv.2017.03.004
27. Stallmach, A.; Steube, A.; Grunert, P.; Hartmann, M.; Biehl, L.M.; Vehreschild, M.J.G.T. Fecal Microbiota Transfer. Dtsch. Arztebl. Int. 2020, 117, 31–38.
28. Quaranta, G.; Sanguinetti, M.; Masucci, L. Fecal Microbiota Transplantation: A Potential Tool for Treatment of Human Female Reproductive Tract Diseases. Front. Immunol. 2019, 10, 2653
29. Quast, C., Pruesse, E., Yilma, P. Gerken J., Schweer T., Yarza P., Peplies J., Glöckner F.O. (2013). The SILVA ribosomal RNA gene database project: improved data processing and web-based tools. *Nucleic Acids Research*, 41(Database issue), 590–596. https://dx.doi.org/10.1093%2Fnar%2Fgks1219
30. Ryan, M.P., Adley, C.C. (2014). Ralstonia spp.: emerging global opportunistic pathogens. *European Journal of Clinical Microbiology & Infectious Diseases*, *33*(3), 291-304. https://doi.org/10.1007/s10096-013-1975-9
31. Salter, S.J., Cox, M.J., Turek, E.M., Calus S.T., Cookson, W.O., Moffatt M.F., Turner P., Parkhill P., Loman N.J. Walker A.W. (2014). Reagent and laboratory contamination can critically impact sequence-based microbiome analyses. *BMC Biology*, 12, 87. https://doi.org/10.1186/s12915-014-0087-z
32. Tao, X., Franasiak, J.M., Zhan, Y., Richard T. Scott I, Rajchelb J., Bedard J., Newby R. Jr., Scott R.T., Treff N., Chu T. (2017). Characterizing the endometrial microbiome by analyzing the ultra-low bacteria from embryo transfer catheter tips in IVF cycles: Next generation sequencing (NGS) analysis of the 16S ribosomal gene. *Human Microbiome Journal*, 3, 15–21. https://doi.org/10.1016/j.humic.2017.01.004
33. Verstraelen, H., Vilchez-Vargas, R., Desimpel, F., Jauregui R., Nele Vankeirsbilck, Weyers S,, Verhelst R., De Sutter P., Pieper D.H., Van De Wiele T.. (2016). Characterization of the human uterine microbiome in nonpregnant women through deep sequencing of the V1-2 region of the 16S rRNA gene. *PeerJ*, 19(4), e1602. https://doi.org/10.7717/peerj.1602
34. Walther-Antonio, M., Chen, J., Multinu, F., Multinu F., Hokenstad A., Distad T., Cheek E.H., Keeney G.L., Creedon D., Nelson H., Mariani A., Chia N. (2016). Potential contribution of the uterine microbiome in the development of endometrial cancer. *Genome Medicine*, 8, 122. https://doi.org/10.1186/s13073-016-0368-y
35. Wang, Q, Garrity, G.M., Tiedje, J.M., Cole J.R. (2007). Naive Bayesian classifier for rapid assignment of rRNA sequences into the new bacterial taxonomy. *Applied and Environmental Microbiology*, *73*(16), 5261–5267. https://doi.org/10.1128/AEM.00062-07
36. Wee, B.A., Thomas, M., Sweeney, E.L., Francesca D., Samios F.M., Ravel J., Gajer P., Myers G., Timms P., Allan J.A., Huston W.A. (2018). A retrospective pilot study to determine whether the reproductive tract microbiota differs between women with a history of infertility and fertile women. *Australian and New Zealand Journal of Obstetrics and Gynaecology*, 58, 341–348. https://doi.org/10.1111/ajo.12754
37. Weyrich, L.S.; Farrer, A.G.; Eisenhofer, R.; Arriola, L.A.; Young, J.; Selway, C.A.; Handsley-Davis, M.; Adler, C.J.; Breen, J.; Cooper, A. Laboratory contamination over time during low-biomass sample analysis. Mol. Ecol. Resour. 2019, 19, 982–996.
38. Winters, A.D., Romero, R., Gervasi, M., Gomez-Lopez N.,Tran M.R., Garcia-Flores V., Pacora P., Jung E., Sonia S. Hassan, Hsu C.D., Theis K.R.. (2019). Does the endometrial cavity have a molecular microbial signature? Scientific Reports, 9, 9905.

https://doi.org/10.1038/s41598-019-46173-0

39. Yan S.F., Liu X.Y., Cheng Y.F., Li Z.Y., Ou J., Wang W., Li F.Q. Relationship between intrauterine bacterial infection and early embryonic developmental arrest. Chin Med J (Engl) 2016; 129:1455–8.

40. Zervomanolakis, I., Ott, H.W., Hadziomerovic, D., V Mattle, B E Seeber, I Virgolini, D Heute, S Kissler, G Leyendecker, L Wildt. (2007). Physiology of upward transport in the human female genital tract. *Annals of the New York Academy of Sciences*, 1101, 1–20. https://doi.org/10.1196/annals.1389.032

41. Zhang, Y.; Xu, H.; Liu, Y.; Zheng, S.; Zhao, W.; Wu, D.; Lei, L.; Chen, G. Confirmation of chronic endometritis in repeated implantation failure and success outcome in IVF-ET after intrauterine delivery of the combined administration of antibiotic and dexamethasone. Am. J. Reprod. Immunol. 2019, 82, e13177.

***Table 1.*** *Clinical and demographic characteristics of patients in the surveyed groups*

| Index | Group I (infertile) N=20 | p-value (Shapiro–Wilk test) in the Group I | Group II (Fertile women) N=15 | p-value (Shapiro–Wilk test) in the Group II | p-value (Mann–Whitney test) |
|---|---|---|---|---|---|
| **Age** | 33.3 (3.8) | 0.99 | 32 (6.26) | 0.16 | 0.06 |
| **BMI** | 23.8 (4.51) | 0.32 | 21.3 (1.99) | 0.79 | 0.08 |
| **Menarche** | 12.9 (1.19) | 0.14 | 13.5 (0.74) | 0.25 | 0.3 |
| **Length of the menstrual cycle** | 27.2 (2.43) | 0.37 | 30.9 (8.83) | 0.19 | 0.3 |
| **Duration of menstruation** | 4.67 (1.18) | 0.14 | 4.57 (0.84) | 0.16 | 0.06 |
| **Number of in-vitro-fertilization procedures** | 4,72 (2,11) | - | - | - | - |
| **Number of births in history** | - | - | 2,14 (0,75) | - | - |

*Note*: The data in the table is given as mean and standard deviation. Differences were considered statistically significant at $p < 0.05$.

***Table 2.*** *Comparison of the mean abundance of the most common genera of microorganisms in the endometrial microbiome of women in Group I (infertile patients with repeated IVF failures) and Group II (healthy fertile women without a burdened obstetric-gynecological history), only statistically significant differences*

| Index | Median [Lower quartile; Upper quartile] | | Mean p |
|---|---|---|---|
| | Group I (infertile) N=20 | Group II (Fertile women) N=15 | |
| Acidovorax | 0 [0; 1.33] | 2.1 [0.75; 3.44] | 0,009 |
| Brevibacillus | 0 [0; 0] | 0.11 [0; 0.3] | 0,01 |
| Brevundimonas | 0.065 [0; 0.38] | 0 [0; 0] | 0,03 |
| Caulobacter | 0 [0; 0.28] | 0.54 [0.15; 1.07] | 0,03 |
| Comamonas | 0.01 [0; 6.37] | 7.44 [4.15; 18.2] | 0,02 |
| Delftia | 0.025 [0; 1.26] | 2.4 [0.81; 4.11] | 0,004 |
| Distigma | 0 [0; 0.22] | 0.64 [0.11; 1.22] | 0,02 |
| Pseudomonas | 0 [0; 0.12] | 0.48 [0.01; 2.26] | 0,03 |
| Ralstonia | 0.21 [0; 1.2] | 0 [0; 0.12] | 0,02 |
| Schlegelella | 0 [0; 0.72] | 1.18 [0.29; 2.14] | 0,02 |
| Thermus | 0 [0; 2.63] | 2.57 [1.05; 5.62] | 0,009 |

*Note*: in the table, mean values are presented as Median [Lower quartile; Upper quartile]; comparison was carried out using the Mann–Whitney test. Differences were considered statistically significant at $p < 0.05$.

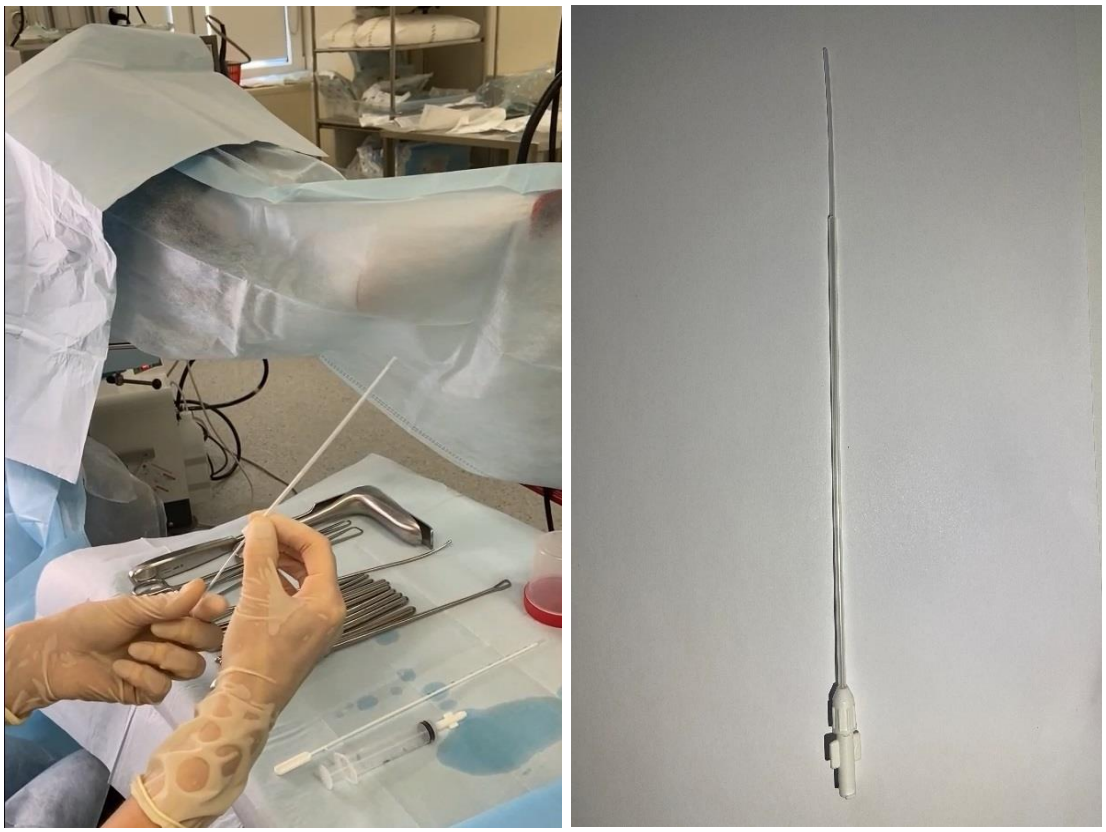

***Figure 1.*** *A sampling of microbiome of endometrium using double-sheathed catheter for embryo transfer to avoid contamination with microorganisms from the vagina or cervical canal and to obtain data exclusively on the species composition of the uterine cavity.*

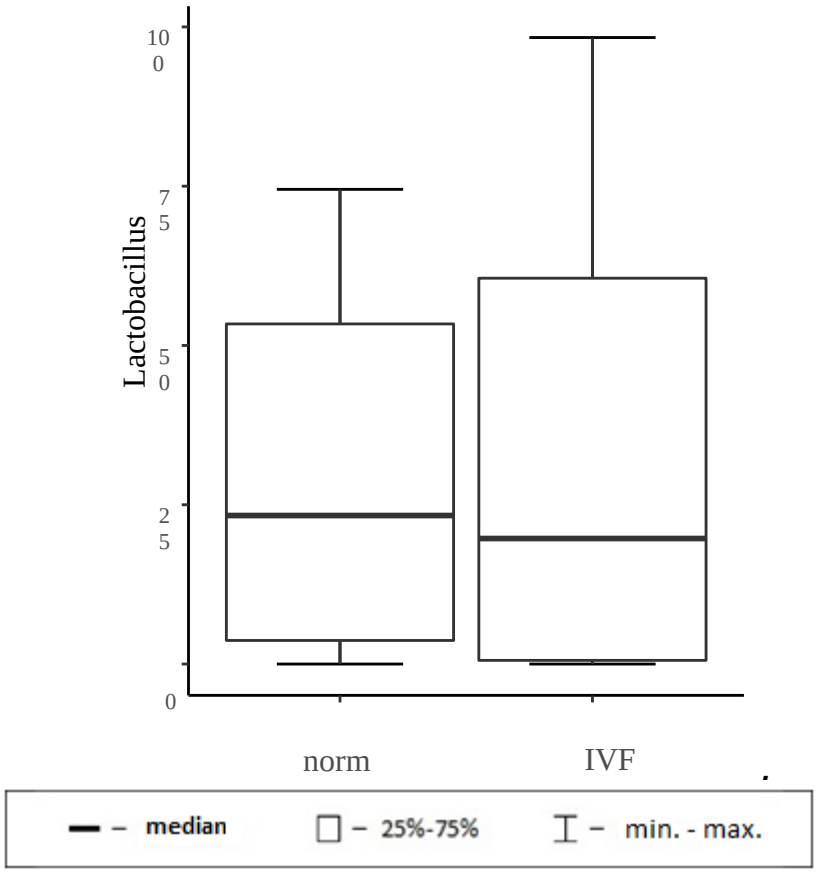


***Figure 2.*** *Boxplot of relative abundance of Lactobacillus in groups I and II in the composition of the endometrial microbiota. The bold line within the box is drawn to the median of each group, the bottom and top of the box to the 25th and 75th percentiles, respectively. The whiskers are drawn to the 10th and 90th percentiles.*

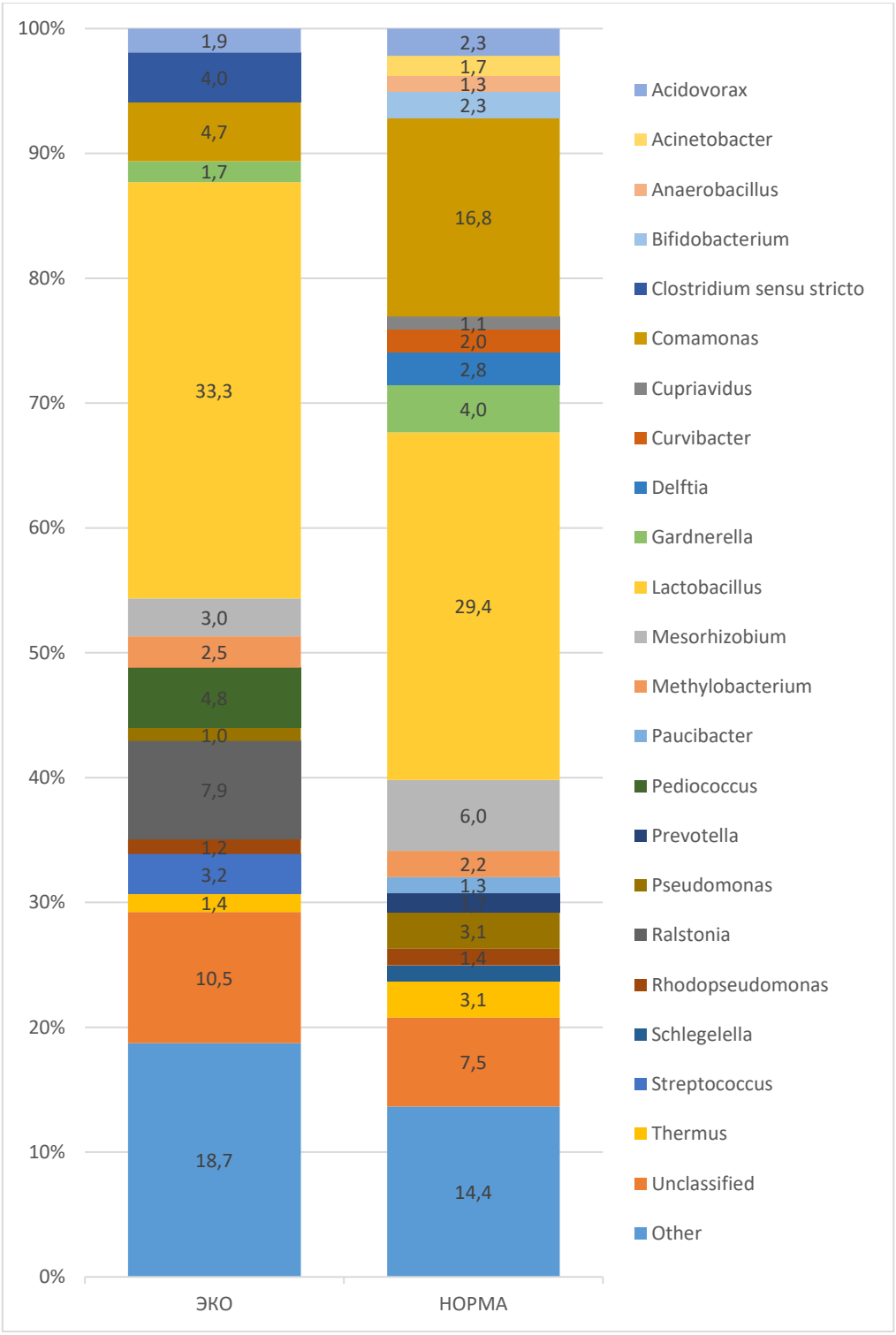


***Figure 3.*** *The mean relative abundance of the most common genera of microorganisms in the endometrial microbiome of women in group I (infertile patients with repeated in-vitro-fertilization failures) and group II (healthy fertile women without a burdened obstetric-gynecological history) 'Other' bacteria include various bacteria whose average proportion was less than 1%.*

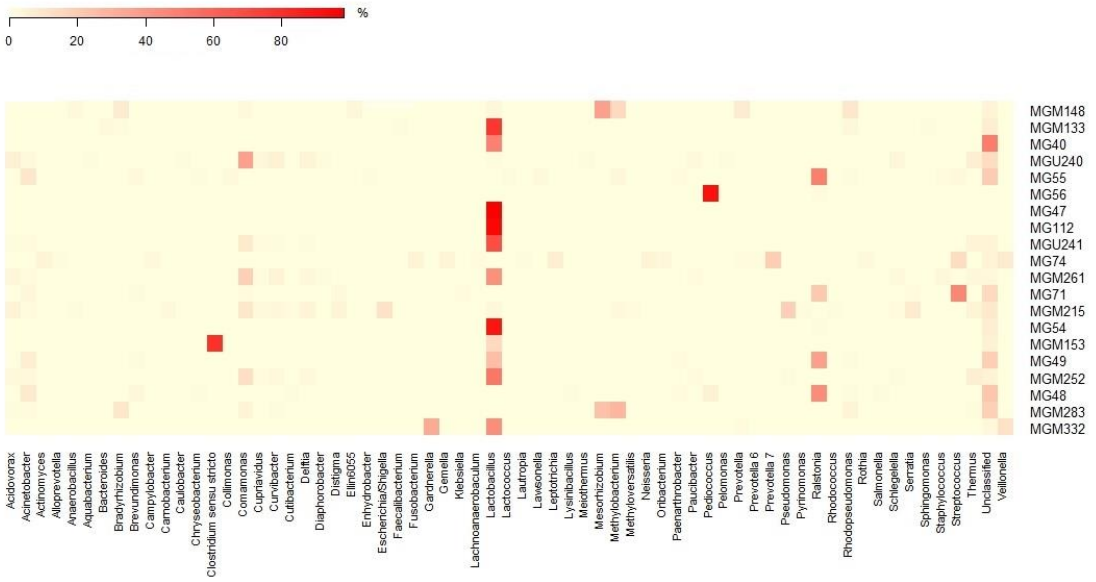


a

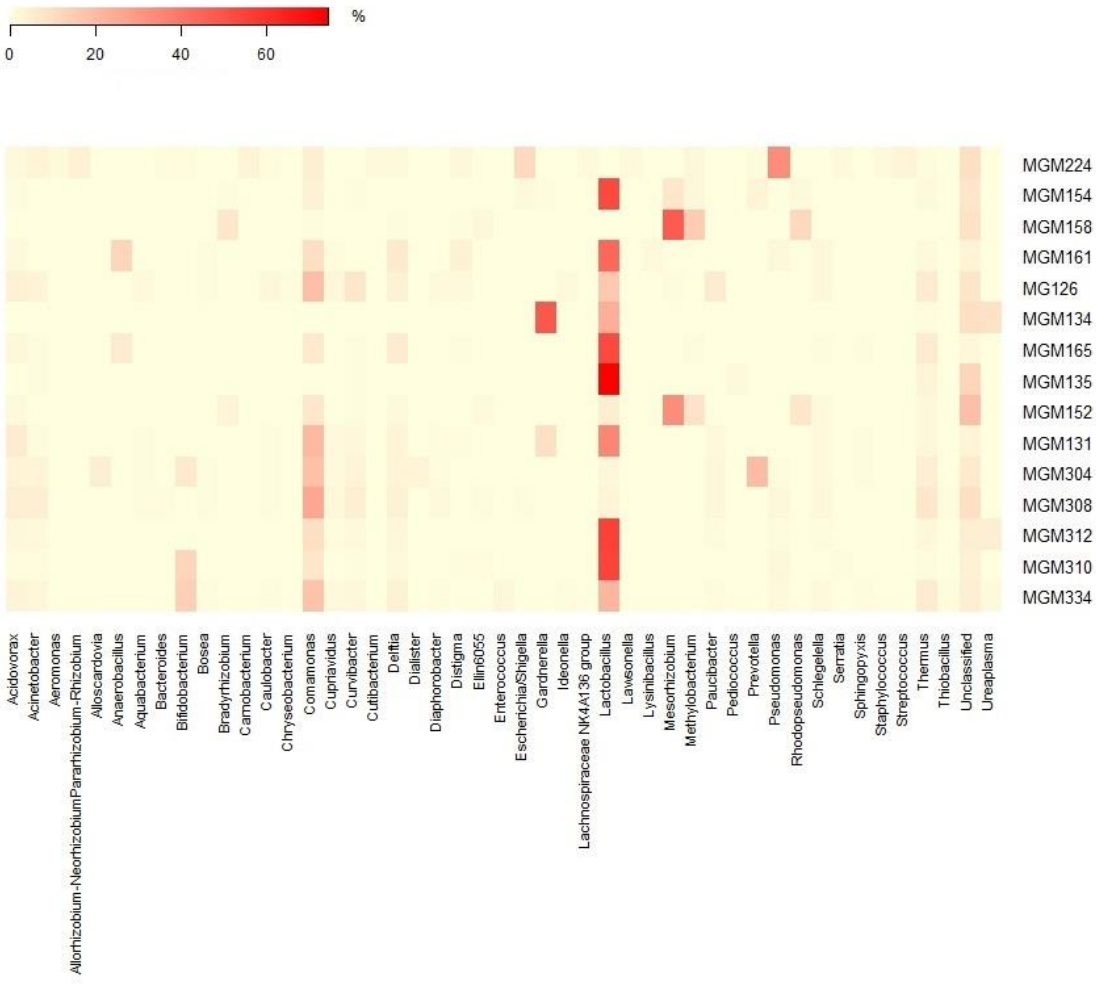


b

***Figure 4.*** *Heat map of the mean relative abundance of bacteria in patients of group I (infertile patients with repeated in-vitro-fertilization failures) (a) and group II (healthy fertile women without burdened obstetric and gynecological history) (b). The figures show the genera of bacteria, whose relative abundance in the microbiome was 1% and higher.*

## INSTRUCTIONS FOR AUTHORS

We ask authors always to visit the online instructions for the use of the latest instructions available. Manuscripts must be submitted using the template available on the Journal's website.

## PREPARATION OF MANUSCRIPTS



---

## 1. PREPARATION OF MANUSCRIPTS (TEMPLATE):

Please, observe the following points in preparing manuscripts. Papers not conforming strictly to these instructions may be returned to their authors for appropriate revision or may be delayed in the review process.

**READABILITY:** Manuscripts should be written in clear, concise, and grammatically correct English (British or American English throughout). The editors can not undertake wholesale revisions of poorly written papers. Every paper must be free of unnecessary jargon and readable by any specialist in the related field. The Abstract should be written in an explanatory style that will be comprehensible to readers who are not experts in the subject matter.

**PROOFREADING:** Please proofread carefully for both errors and inconsistencies in the following: spelling (especially of scientific terminology, proper names, and foreign words), mathematical notation, numerical values in tables and text, and accuracy of quotations. The Journal will evaluate the file seeking English grammatical issues, correctness, clarity, and engagement errors. There will be a tolerance of up to 100 errors in all manuscripts. In case more errors were found, editors will allow the authors to resubmit again and, in case these errors persist, a proofreading fee will be charged.

**GENERAL FORMAT:** The completed paper has to be written in English and submitted as a **Word document only** using the template of the Journal. Page size: A4, line spacing: single, font type: Arial. Please leave headers and footers unchanged since the editors should fill it. Please check guidelines for accurate information based on all different categories (review articles and technical notes). A single file of the whole manuscript should then be submitted through TCHE QUIMICA JOURNAL's e-mail (journal.tq@gmail.com) along with the COVER LETTER. ***The Journal no longer accepts submissions in any other form than by E-MAIL*** (journal.tq@gmail.com).

**FORMAT FOR INITIAL SUBMISSION:** Title, Author(s), Abstract (maximum 300 words), Keywords (at least 3, maximum 6), Main text (Introduction, Review of Literature, Definitions (if any), Materials and Methods or Methodology, or Development, or Background, Results and Discussion or Findings, Conclusions), Acknowledgements (if any), References, Appendix (if any). This structure of

the main text is not obligatory, but the paper must be logically presented. Footnotes should be avoided. The main text must be written with font size 11, justify. Within each main section, three levels of subheadings are available, and the titles must be bold, bold, and italic, italic, respectively. The manuscript should contain the whole text, figures, tables, and explanations. For more details, please check the template of the Journal.

## 2. THE FIRST PAGE OF THE MATERIAL SHOULD BE AS FOLLOWS:

**TITLE:** PORTUGUESE, ENGLISH, and the third language if the author's native language is not English or Portuguese. The editors can provide the title in Portuguese for those whose Portuguese is not the first language. It should be brief and informative. The title should reflect essential aspects of the article, in a preferably concise form of not more than 100 characters and spaces: font size 12, capital letters, center alignment.

**BY-LINE:** Names (size 12, Arial, small capital) of the authors. No inclusion of scientific titles is necessary. In the case of two or more authors, place their names in the same row, separate them with a semicolon (;) and please indicate the corresponding author with * in superscript. The corresponding author should be the one submitting the article online and an e-mail given (only one e-mail) below the addresses of all authors. Authors from different institutions must be labeled with numbers in superscript after the names. The affiliation of the authors should also be given (size 10).

**ABSTRACT:** PORTUGUESE, ENGLISH, and a third language if the author's native language is not English or Portuguese. The editors can provide the title in Portuguese for those whose Portuguese is not the first language. Required for all manuscripts in which the problem, the principal results, and conclusions are summarized. The abstract must be self-explanatory, preferably typed in one paragraph, and limited to 300 words. It should not contain formulas, references, or abbreviations. The name ABSTRACT should be written in capital letters, Arial, size 12, bold, left alignment. The Abstract should be written font Arial, size 10, justify.

**KEYWORDS:** PORTUGUESE, ENGLISH, and a third language if the author's native language is not English or Portuguese. The editors can provide the title in Portuguese for those whose Portuguese is not the first language. Authors should provide appropriate and short keywords that encapsulate the principal topics of the paper. *The maximum number of keywords is 5* not including items appearing in the title. The keywords should be supplied, indicating the scope of the paper. Size 10, italic, justify, only the word Keywords must be bold, left alignment.

The authors should include Abbreviations and Nomenclature listings when necessary.

## 3. THE CENTRAL TEXT PART OF THE MATERIAL SHOULD BE AS FOLLOWS:

The words Introduction, Review of Literature, Definitions (if any), Materials and Methods or Methodology, or Development, or Background, Results and Discussion of Findings, Conclusions must be written in capital letters, Arial, font size 12, left alignment, bold.

**INTRODUCTION:** The introduction must clearly state the problem, the reason for doing the work, the hypotheses or theoretical predictions under consideration, and the essential background. It should not contain equations or mathematical notation. A brief survey of the relevant literature so that

a non-specialist reader could understand the significance of the presented results. A good introduction should ideally have 3-5 well-explained paragraphs and should finishing pointing out the AIM of the study.

**MATERIALS AND METHODS OR METHODOLOGY, OR DEVELOPMENT, OR BACKGROUND**: Provide sufficient details to the reader to understand how the study was performed. The technical description of methods should be given when such methods are new. It is generally recommended that the materials and methods should be written in the past tense, preferably in the passive voice. In this section, ethical approval, study dates, number of subjects, groups, evaluation criteria, exclusion criteria and statistical methods should be described sequentially. The following questions should be absolutely provided: the beginning, and termination dates of the study period; number of subjects/patients/experimental animals etc. enrolled in the study; has the approval of the ethics committee been obtained? Study design (prospective, retrospective or other); still additional features of the study design (cross-sectional) should be indicated. Apart from this, other types of study designs (randomized, double-blind, placebo-controlled or double-blind, parallel control etc.) should be revealed. Before you finish your manuscript, ask yourself the following questions about your Materials and Methods section to ensure that you have included all important information. Is there sufficient detail so that the experiments can be reproduced? Is there excess information that could be removed without affecting the interpretation of the results? Are all the appropriate controls mentioned? Are all appropriate citations included? Is the source of each reagent listed? The Materials and Methods section is a vital component of any manuscript. This section of the report gives a detailed account of the procedure that was followed in completing the experiment(s) discussed in the paper. Such an account is very important, not only so that the reader has a clear understanding of the experiment, but a well written Materials and Methods section also serves as a set of instructions for anyone desiring to replicate the study in the future. Considering the importance of "reproducible results" in science, it is very relevant why this second application is so vital. Some general rules for Methods sections are:

- It should be clear from the Methods section how all of the data in the Results section were obtained.
- The study system should be clearly described. In medicine, for example, researchers need to specify the number of study subjects; how, when, and where the subjects were recruited, and that the study obtained appropriate ‘informed consent’ documents; and what criteria subjects had to meet to be included in the study.
- In most cases, the experiments should include appropriate controls or comparators. The conditions of the controls should be specified.
- The outcomes of the study should be defined, and the outcome measures should be objectively validated.
- The methods used to analyze the data must be statistically sound.
- For qualitative studies, an established qualitative research method (e.g. grounded theory is often used in sociology) must be used as appropriate for the study question.
- If the authors used a technique from a published study, they should include a citation and a summary of the procedure in the text. The method also needs to be appropriate to the present experiment.
- All materials and instruments should be identified, including the supplier’s name and location.
- The Methods section should not have information that belongs in another section (such as the Introduction or Results).
- You may suggest if additional experiments would greatly improve the quality of the manuscript. Your suggestions should be in line with the study’s aims. Remember that almost any study could be strengthened by further experiments, so only suggest further work if you believe that the manuscript is not publishable without it.

**RESULTS AND DISCUSSION OR FINDINGS**: Results should be presented concisely. Also, point out the significance of the results, and place the results in the context of other work and theoretical

background. The results and discussion sections are one of the challenging sections to write. It is important to plan this section carefully as it may contain a large amount of scientific data that needs to be presented in a clear and concise fashion. The purpose of a Results section is to present the key results of your research. Results and discussions can either be combined into one section or organized as separate sections. Use subsections and subheadings to improve readability and clarity. Number all tables and figures with descriptive titles. Present your results as figures and tables and point the reader to relevant items while discussing the results. This section should highlight significant or interesting findings along with P values for statistical tests. Be sure to include negative results and highlight potential limitations of the paper. The results and discussion section of your research paper should include the following: Findings; Comparison with prior studies; Limitations of your work; Casual arguments; Speculations; Deductive arguments.

Sources:

https://www.ref-n-write.com/trial/research-paper-example-writing-results-discussion-section-academic-phrasebank-vocabulary/

https://www.ncbi.nlm.nih.gov/pmc/articles/PMC4548564/

**CONCLUSION:** Summarize the data discussed in the Results and Discussion or Findings section showing the relevance of the work and how different it is from other researches. Also, point out the benefits and improvements that can be observed to develop new science standards that can change something in the related field.

**ACKNOWLEDGMENTS:** (if any) These should be placed in a separate paragraph at the end of the text, immediately before the list of references. It may include funding information too.

**REFERENCES:** References should be cited in the text using the **name-and-year system (Author, year) (APA FORMAT).** Alternatively, the author's surname may be integrated into the text, followed by the year of publication in parentheses. **Examples:** Grasslands are regarded as important foraging areas for many insectivores in Europe, such as birds (Vichery, 2001; Barnet et al., 2004), bats (Guttinger, 1997) or amphibians and reptiles (Langton and Burton, 1997). However, the knowledge of the overall arthropod availability in such grasslands is scarce, since many studies about insect populations concentrate on extensive grasslands on poor, dry or wet soils include only few species or systematic groups (Ellgsen *et al*., 1997; Gibson *et al*., 1992; Hansel and Plachter, 2004; Manhart *et al*., 2004; Kruess and Tscharntke, 2002a, b; Wingerden *et al*., 1992; Sjodin, 2007a, b; Perner *et al*., 2005). Carbon dioxide produced by the combustion of biodiesel can be recycled by photosynthesis, thereby minimizing the impact of biodiesel combustion on the greenhouse effect (Korbitz, 1999; Agarwal and Das, 2001).

- *Cite only essential resources, avoid citing unpublished material. References to papers "in press" must mean that the article has been accepted for publication. At the end of the paper list references alphabetically by the last name of the first author. Please, list only those references that are cited in the text and prepare this list as an automatically numbered list. The word References with size 12, bold, capital letters, left alignment*

---

## 4. GUIDELINES FOR REFERENCES:

- **The Journal uses the APA (American Psychological Association) FORMAT CITATION as follows**:

**Author's surname, initial(s). (Date Published). Title of Source. Location of publisher: publisher. Retrieved from URL**

**Author Rules:**

1. **Initials are separated and ended by a period.**

   Examples: Goldani, E.
   De Boni, L.A.B.

2. **Multiple authors are separated by commas and an ampersand.**

   Examples: Goldani, E. & De Boni, L.A.B.
   Goldani, E., De Boni, L.A.B. & Casanova, K.

3. **Multiple authors with the same surname and initial: add their name in square brackets.**

   Example: Goldani, E. [Eduardo]

**Date Rules:**

1. **Date refers to date of publishing**
2. **If the date is unknown 'n.d' is used in its place.**

   Example: De Boni, L.A.B (n.d)

**Title Rules:**

1. **The format of this changes depending on what is being referenced**

**Publisher Rules:**

1. **If in the US: the city and two letter state code must be stated.**

   Examples: San Diego, CA
   Houston, TX
   New York, NY

2. **If not in the US: the city and country must be stated.**

   Examples: Sydney, Australia
   Lisbon, Portugal
   Rome, Italy

**Retrieved from URL:** This is used if the source is an online source

**GENERAL RULE FOR ACADEMIC PAPERS:**

Author's surname, initial(s). Year of publication after the name of the authors (between parentheses). Title of the paper. Name of the journal in italic, number of the edition also in italic, volume between parentheses and finally initial and final page, and, if the case, retrieved from (what website) or DOI

For example:

1. Nikolaeva, L.P., Cherdantsev DV., Titiv K.S. (2017). Characteristics of bone marrow stem cells in patients with complicated diabetes mellitus. *The Russian biotherapeutic journal, 16*(1): 47-50.
2. Mitchell, J.A. (2017). Citation: Why is it so important. *Mendeley Journal, 67*(2), 81-95. Retrieved

from https://www.mendeley.com/reference-management/reference-manager

3. Karthiga, N., Rajendran, S., Prabhakar, P., Rathish, R.J. (2015). Corrosion inhibition by plant extracts - An overview. *Int. J. Nano. Corr. Sci. Eng, 2*(4):31-49.
4. Akbulut, S., and Bayramoglu, M.M. (2013). The Trade and Use of Some Medical and Aromatic Herbs in Turkey. *Ethno Med, 7*(2): 67-77.

✓ **The Journal recommend to visit the websites below for a more detailed information.**

**< https://www.mendeley.com/guides/apa-citation-guide >**
**< https://libguides.murdoch.edu.au/APA6/all >**
**< https://aut.ac.nz.libguides.com/APA6th/referencelist >**

---

## 5. FIGURES:

The number of pictures (including graphs, diagrams, etc.) should not exceed 10 and should be submitted either in JPG or PNG formats. All photographs, charts, and diagrams should be numbered consecutively (e.g., Figure 1, Figure 2, Figure 3,…..) in the order in which they are referred in the text. Caption must appear below the figure (size 11, bold, italic) and should be sufficiently detailed to enable us to understand apart from the text. Explanation of lettering and symbols should be also given in the caption and only exceptionally in the figures. Figures should be of good quality and preferably in black and white. (Color figures will appear in the downloadable files, but all papers will be printed in black and white.) Scanned figures should be at a resolution of 800 dpi/bitmap for line graphs. Diagrams containing chemical structures should be of high graphical quality and always be of the same size so that they can be uniformly reduced. Figures should have a maximum width of one Journal column (8.5 cm) to be inserted on the body of the text so that they can be applied to the standards of the Journal. If the figures exceed 8.5 cm, they will be placed at the end of the article. Also, authors may be requested to submit each figure also as an image file in one of the following formats: jpg or png. For pictures, graphs, diagrams, tables, etc., identical to material already published in the literature, authors should seek permission for publication from the companies or scientific societies holding the copyrights and send it to the editors of Tche Quimica Journal along with the final form of the manuscript.

---

## 6. TABLES:

Tables should be self-explanatory. They should be mentioned in the text, numbered consecutively (e.g., Table 1, Table 2, Table 3,....), and accompanied by a title at the top (size 11, bold, italic). Please insert all the tables in the text and do not enclose huge tables that can not fit within the page margins.

---

## 7. MATHEMATICAL EXPRESSIONS:

In general, minimize unusual typographical requirements, use solidus, built-up fractions. Avoid lengthy equations that will take several lines (possibly by defining the terms of the equation in separate displays). For drawing equations, please use the Equation Editor of Word, if possible. Make subscripts and superscripts clear. Display only those mathematical expressions that must be numbered for later reference or that need to be emphasized. The equations displayed should be consecutively numbered throughout the paper. The numbers should be placed in parentheses on the right of the equation, e.g. (Eq. 1).

---

## 8. SUPPLEMENTARY MATERIAL:

Any Supplementary material (other figures, tables, diagrams, etc.) should be placed at the end of the manuscript and indicated (APPENDIX, for example). A single.PDF - document, including the supplementary material, should be submitted.

**Editors may ask authors to split off part of the manuscript at any time of the editing process, presenting it as supplementary material.**

---

## ARTICLE PROCESSING CHARGES (APC)

## PUBLICATION FEES (1), ADDITIONAL FEES FOR PUBLICATION (2), DISCOUNTS (3), AND FREE PUBLICATION OPPORTUNITIES (4)

Authors are required to pay a publication fee to share in the costs of production. The fee will be asked **if, and only if, the article is accepted for publication**. Once full payment has been made (PayPal, Bank Transfer, or Western Union Services), the paper will be published at the Ahead of Print and scheduled for the next available issue. All waivers (and the publication fee requests) are **applied to the accepted papers after successful peer-review only**.

Please observe the flowchart below to understand how the Journal works.

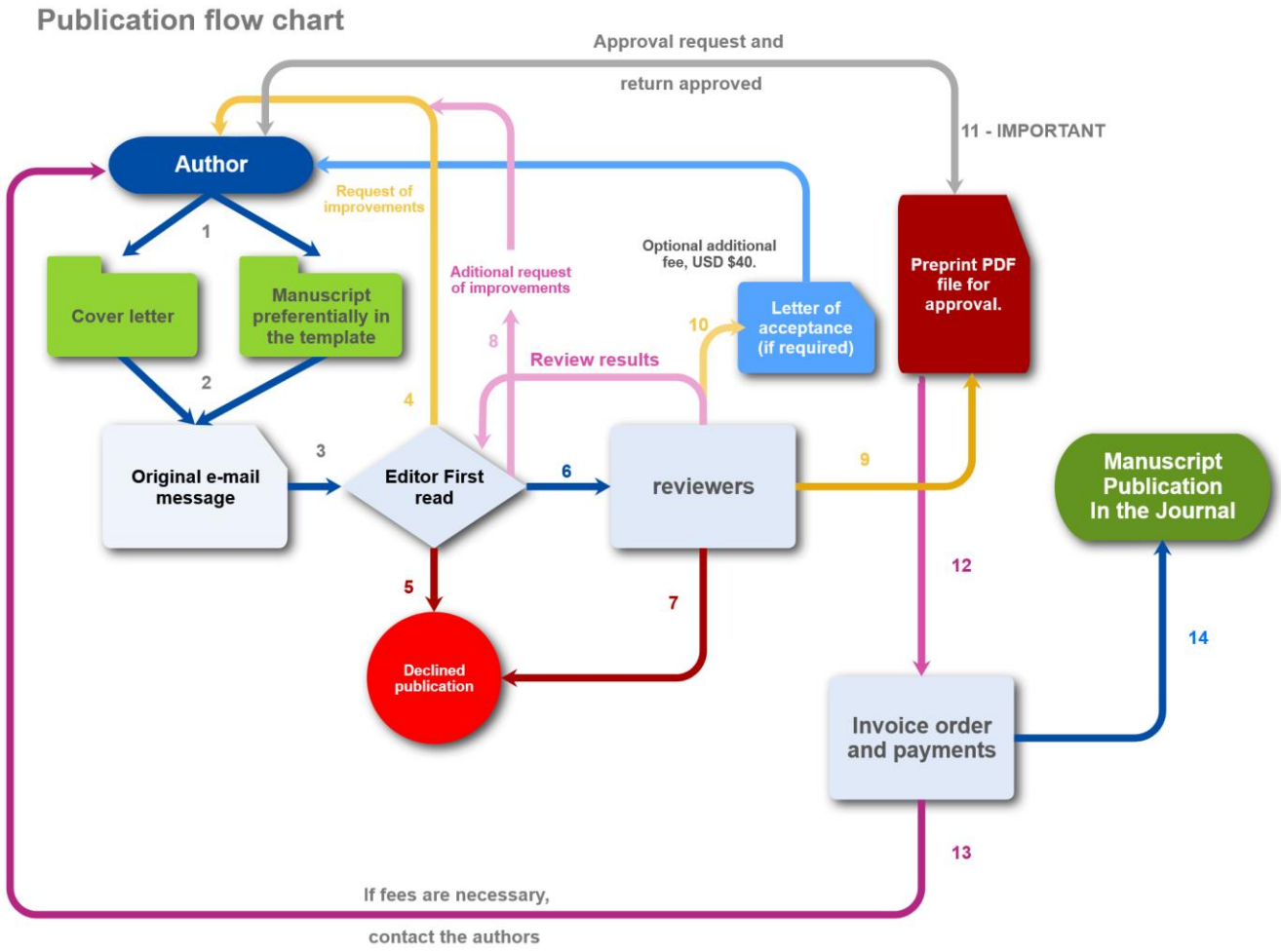

## 1. PUBLICATION FEES

*Brazilian authors, USD 200

*Other countries income groups:

High income and ***Israel, India, Pakistan, United Kingdom, China, France, United States, Russia, North Korea, and Iran*** (nuclear-capable countries) - USD 300

Upper middle-income USD 250

Lower middle-income USD 120

Lower middle income (Heavily indebted poor countries (HIPC)) USD 100

Low-income USD 100

Low income (Heavily indebted poor countries (HIPC)) USD 80

- ✓ (*) Classification according to the World Bank list of economies (June 2020). Please check https://datahelpdesk.worldbank.org/knowledgebase/articles/906519-world-bank-country-and-lending-groups

## 2. ADDITIONAL FEES FOR PUBLICATION

### *a) Proofreading and/or plagiarism*

If the submitted manuscript has more than 100 grammatical errors or plagiarism greater than 5%, **an additional fee of USD 200** will be charged. This fee does not guarantee publication of the manuscript and is non-refundable.

### *b) Changing PDF pre-printing files*

After the final verification of the manuscript and the generation of the PDF pre-print file, **a fee of USD 100** will be charged to authors who wish to make any changes. For each new change, the fee is charged again.

### *c) Acceptance Letter for article publication*

The acceptance letter is an **optional service** of the Journal. If the authors need a document to prove that their article has been peer-reviewed and accepted for publication, they may request, upon payment of **an additional fee of USD 40**, an acceptance letter for publication of the article.

NOTE 1: THE LETTER OF ACCEPTANCE may be issued **if, and only if,** the article has undergone a complete peer-review and is considered ACCEPTED for publication. Letters will NOT be issued for newly sent articles that have not yet been appropriately evaluated and peer-reviewed.

NOTE 2: The Journal does not agree with the trade-in documents that can attest to the publication of articles that have not gone through peer-review due process and are legitimately considered approved for publication in the subsequent edition.

NOTE 3: Bearing in mind that the pre-printing PDF is generally already considered as proof of publication, authors must, via e-mail, justify the request for a letter of acceptance for purposes of general registration by the Journal.

***d) Formatting the manuscript according to the template of the Journal***

The use of the template is mandatory. All authors must submit their papers according to the official model of the Journal available at www.journal.tchequimica.com (Downloads >> Templates and Instructions). In case the authors do not have time or proper conditions to execute the formatting of the manuscript, we can provide all the adaptation to the template of the Journal. However, this is an **optional service,** and **an extra fee of USD 80** will be charged on top of the Article Processing Charges.

If there is no need, additional fees are not charged.

## 3. DISCOUNTS

a) **50% discount** for authors who support other journals from the team (*Southern Brazilian Journal of Chemistry* - this is a 100% free journal), ***with 1 manuscript approved*** for publication;

b) **100% discount** for authors who support other journals from the team (*Southern Brazilian Journal of Chemistry* - this is a 100% free journal), ***with 2 manuscripts approved*** for publication;

c) **Volume discount.** If you are an author/collaborator of the Journal that has ***published with us 4 manuscripts*** (paid your full corresponded price), your fifth manuscript will be free of charge. Later the counting cycle restart.

## 4. FREE PUBLICATION OPPORTUNITIES

a) Young scientists that are publishing the first manuscript of their career. **Requirements:** Copy of the curriculum without publications; maximum of 2 authors; one manuscript previously accepted in the ***Southern Brazilian Journal of Chemistry*** (the manuscript may be from the author or from colleagues, provided that the extra purpose of the collaboration is notified at the time of submission), or two manuscripts previously accepted in the ***Journal of Law, Public Policies, and Human Sciences*** (manuscripts may be from the author or from colleagues, provided that the extra purpose of the collaboration is notified at the time of submission). (Last revision of the rule: 15$^{th}$ of October 2020);

b) All personal related to the production of the journals, from Brazil and abroad;

c) Longtime collaborators. Authors who have published four (4) articles with us during the past decade will be rewarded with one (1) free publication. After that, this cycle starts again, that is, for every five (5) articles published, one will be free of publication fees. Thank you for choosing and trusting the Journal to publish your research.

d) Paper considered by the Editors of high quality, priority, and relevance for the development of the society shall pay no fees. Note that this condition is a small recognition prize, not something that you may request. Thank you for your comprehension.

***Thank you very much for choosing Tche Quimica Journal to publish your paper! We would be happy if you consider the Journal to submit any further paper in the near future***.

Kind Regards,

Editorial Team

Dr. Luis Alcides Brandini De Boni

Dr. Eduardo Goldani